GIS as a tool for studying temporal and spatial patterns in Norwegian ecosystems across disciplines and scales

by

Vegar Bakkestuen

Dissertation presented for the degree of Doctor Philosophia

Natural History Museum

Faculty of Mathematics and Natural Sciences

University of Oslo

Series of dissertations submitted to the
Faculty of Mathematics and Natural Sciences, University of Oslo
Nr. 836

ISSN 1501-7710

Cover: Inger Sandved Anfinsen.
Printed in Norway: AiT e-dit AS, Oslo, 2009.

Produced in co-operation with Unipub AS.
The thesis is produced by Unipub AS merely in connection with the
thesis defence. Kindly direct all inquiries regarding the thesis to the copyright
holder or the unit which grants the doctorate.

Unipub AS is owned by
The University Foundation for Student Life (SiO)

Contents

Preface

The research on which this thesis is based was carried out in the working environments of NINA (Norwegian Institute for Nature Research), NHM-UiO (Natural History Museum, University of Oslo) and for a short period INBio (Instituto Nacional de Biodiversidad) in Costa Rica. The thesis is a product of the diverse research interests among very good colleagues, formerly and present, and students, at these institutions. They are far too many to mention by names, but to all of you: Go raibh mile maith agaibh!

I especially wish to thank Lars Erikstad, who introduced me to GIS in early stages of my research career, for full support in many ways throughout these years of hard work. Furthermore, everlasting supportive secretaries Gerd Aarsand, Narinder Mercy, Sissel Vadstein and Elisabeth Aronsen at the different institutions are thanked for innumerable practical and administrative efforts, directly related to this thesis as well as to everyday work. Constructive comments on an earlier version of the synthesis were given by Dag Hessen, Jogeir Stokland, Lars Erikstad, Trine Bekkby and Rune Halvorsen. This thesis could hardly have been written without the contribution from Rune Halvorsen. Among very many things, he showed me how to write science, which I think was the most difficult part throughout this process. So a big thank to you, Rune!

At the end I wish to thank all supportive friends who stood behind me the ten years or so it took me to finally reach this big milestone. Special thanks are due to my ever supporting family, both to those beloved that passed away before I managed to complete the work and to the few ones I have left. Last but not least, my thanks go to my wife Elin, for long time patiently waiting to get her husband back.

Vegar Bakkestuen

Mai 2008, Hamar, Norway

Abstract

As a starting point GIS (geographical information systems) seem intuitively to be a practical tool for biologists performing ecological research. GIS conveniently stores, explores, analyses and visualizes biological/ecological/environmental observations. A thorough exploration of the opportunities offered by GIS was made in twelve different Norwegian ecological studies. These studies span scales from the regional at which biogeographical patterns can be studied, to centimetre-scales at which the fates of small (bryophyte) individuals may be followed. They encompass different ecosystems – marine, freshwater and terrestrial. They target animal, fungi and plants. More than 300 vascular plant species, 150 bryophytes species, 50 lichen species, 150 fungi species and 100 zooplankton species were included in the studies in addition to two species of butterflies and one seal species.

GIS was an efficient tool for handling variation in data properties in all studies that opened many new opportunities. The most promising new scientific results from the GIS analyses were perhaps the least-cost path modelling for actual movement and dispersal of organisms in a landscape, the development of objective, step-less models for biogeographical variation and spatial prediction modelling of species occurrence and diversity patterns. However, concern is raised that the rather high user threshold of GIS software [and the recurrent needs for data programming (scripting)] prevents many scientists from using GIS in their own ecological research.

The importance of being able to address different spatial and temporal scales in all kinds of ecological research is also discussed. Scale is easily handled in GIS. Most notably, two of the most critical questions in spatial pattern analysis can be analysed through geostatistical GIS tools: determination of the appropriate scale to conduct the analysis; and to assess the nature (and strength) of the spatial structure. A two-stage strategy, comprising biogeographical analysis of the distributions of species by use of sampling units that span the main regional gradients, and a local ecological approach to the abundance variation of the species, seems to be a most fruitful analytic strategy.

This study also underpins the everlasting need for including baseline investigations (identification of patterns of variation in species composition, followed by ecological interpretation) in ecological studies irrespective of scale, environment and species. The included monitoring approaches showed condiderable variation occurs over short time periods, even in apparently stable ecosystems. Monitoring projects are therefore important

for the understanding of important processes and present condition in ecosystems. Both baseline investigations and monitoring projects is this thesis is thus crucial for be one of the main targets for ecological research in coming years: prediction of what will happen to species and ecosystems under different environmental (including climate) change scenarios. In this context, GIS seems an inevitably important tool.

List of papers

Papers included in this dissertation:

PAPER 1: Bakkestuen, V., Erikstad, L., & Halvorsen, R. 2008. Step-less models for regional environmental variation in Norway. Journal of Biogeography 35: 1906-1922.

PAPER 2: Bakkestuen, V., Aarrestad, P.A., Stabbetorp, O.E., Erikstad, L. & Eilertsen, 0. 2008. Vegetation composition, gradients and environment relationships of birch forest in six monitoring reference areas in Norway. Sommerfeltia 33 (in press)

PAPER 3: Bakkestuen, V., Halvorsen, R. & Heegaard, E. 2008. Disentangling complex fine-scaled ecological patterns by path modeling, using GLMM and GIS. Journal of Vegetation Science (in press)

PAPER 4: Bekkby, T., Erikstad, L., Bakkestuen, V. & Bjørge, A. 2002. A landscape ecological approach to coastal zone applications. Sarsia 87: 396-408.

PAPER 5: Bekkby, T., Rinde, E., Erikstad, L., Bakkestuen, V., Longva, O., Christensen, O., Isæus, M. & Isachsen, P.E. 2008. Spatial probability modelling of eelgrass Zostera marina L. distribution on the West coast of Norway. ICES Journal of Marine Science 65: 1093-1101.

PAPER 6: Bendiksen, E., Økland, R.H., Høiland, K., Eilertsen, O. & Bakkestuen, V. 2005. Relationships between macrofungi, vegetation and environmental factors in boreal coniferous forests in the Solhomfjell area, Gjerstad, S Norway. Sommerfeltia 30: 1-125.

PAPER 7: Hessen, D.O., Faafeng, B.A., Smith, V.H., Bakkestuen, V. & Walseng, B. 2006. Extrinsic and intrinsic controls of zooplankton diversity in lakes. Ecology 87: 433-443.

PAPER 8: Hessen, D.O., Bakkestuen, V. & Walseng, B. 2007. Energy input and zooplankton diversity. Ecography 30: 749-758.

PAPER 9: Økland, R. H. & Bakkestuen, V. 2004. Fine-scale spatial patterns in populations of the clonal moss Hylocomium splendens partly reflect structuring processes in the boreal forest floor. Oikos 106: 565-575.

PAPER 10: Økland, T., Bakkestuen, V., Økland, R.H. & Eilertsen, O. 2004. Changes in forest understory vegetation in Norway related to long-term soil acidification and climatic change. Journal of Vegetation Science 15: 437-448.

PAPER 11: Sutcliffe, O.L., Bakkestuen*, V., Fry, G.L.A. & Stabbetorp., O.E. 2003. Modelling the benefits of farmland restoration: Methodology and application to butterfly movement. Landscape and Urban Planning 63: 15-31.

PAPER 12: Wollan, A. K., Bakkestuen, V., Kauserud, H., Gulden., G & Halvorsen, R. 2008. Modelling and predicting fungal distribution patterns using herbarium data. Journal of Biogeography 35: 2298-2310.

*Corresponding author

Introduction

Variation in nature occurs on all spatial scales, from global and biogeographical to the very finest at which we observe the distributions of individuals. The patterns we observe are likely to be structured over a spectrum of scales, by broad to finer-scaled factors, brought about by a multitude of processes. The ultimate target of ecological studies is to understand why individuals, species, habitats and ecosystems are found at certain points in time and space. Although this target is not truly achievable, because of the complexity of nature, the search for general ecological rules that are invariant of scales and organisms will continue to be a main operational target for ecological research.

All ecological systems are spatially heterogeneous, exhibiting considerable complexity and variability in time and space. Understanding ecosystems implies disentangling of complexity and multi-scale relations (e.g. Cale & Hobbs 1994, Gustafson 1998) and therefore contains major elements of interdisciplinary integration across scales. The choice of scale(s) is difficult for several reasons: (1) understanding the relationships across scales, (2) availability of data across scales, (3) costs of achieving relevant data, and (4) availability of relevant methods to analyse patterns. Individuals and species experience the environment on specific scale intervals and respond to environmental variability individually (Gleason 1926). Thus, no description of the variability of the environment makes sense without reference to the particular range of scales that are relevant to the organisms or processes being examined (Levin 1992). This is the key to scaling and interdisciplinary integration: sorting variation into signal and noise on different scales.

Most natural environmental variation is more or less gradual in space, forming complex gradients (Whittaker 1967). Species composition varies along these complex gradients to form ecoclines consisting of parallel gradual changes in both environmental and species composition (Whittaker et al. 1973). Hence, changes of complex gradients, at all scales, bring about changes of fundamental life conditions for individuals, populations and ecosystems at the corresponding scales, from local via regional to global. Our ability to predict changes in nature due to, for example, climate change, is dependent on our ability to understand these relationships across scales and disciplines (Wiens 1989).

In search for general patterns and rules across scales and disciplines I present results of twelve different studies, encompassing micro-scale variation in bryophyte populations at the scale level of individuals, to biogeographic patterns of nature variation

(Fig. 1). This dissertation includes study species from the animal, fungi and plant kingdoms, in addition to studies of abiotic environmental variation alone, including climate. These studies have been performed in terrestrial, freshwater and marine systems. Many of the studies deal with ecosystem dynamics as parts of monitoring programs which aim at predicting patterns elsewhere in space and/or ahead in time. The most important tool used in this interdisciplinary approach is the availability of a geographical information system, GIS. The GIS is a working environment where all species and different scales can be represented in an efficient way on a standard platform. A formidable array of different GIS layers and tools form the basis for this thesis.

The main aims of this thesis can be summarized in three points:

(1) The launch: To discuss the importance of baseline investigations for monitoring of ecosystems.

(2) The voyages: To explore the opportunities offered by time series and monitoring endeavours.

(3) The final frontier (Where No Man Has Gone Before): To add new knowledge, i.e. to explore the potential for predicting patterns and distributions of ecosystems and species in time and space.

Furthermore, two specific aims related to scale issues and methodology should be added:

(4) Scale: To discuss the importance of understanding and tackling scale relationships in ecological studies.

(5) Dimension: To assess the role of GIS in ecological studies.

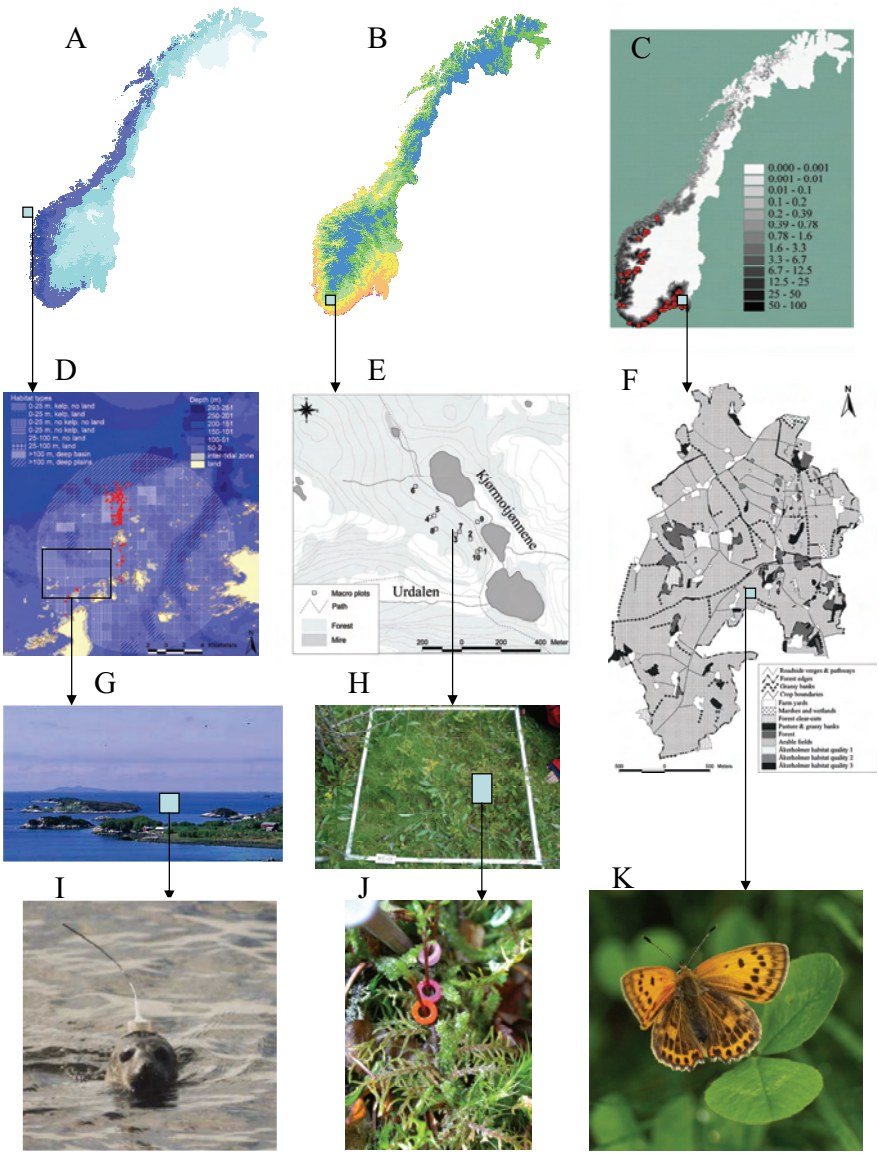

Fig. 1. Overview of different studies in the thesis and how they relate in space and scale. A: Step-less model of bioclimatic regional vegetation variation in Norway showing a gradient from coast to inland and from oceanic/humid to continental areas (PAPER 1). B: Step-less model of bioclimatic regional vegetation variation in Norway showing a gradient from north to south and from high to low altitudes (PAPER 1). C: Predicted distribution of

a fungi species, *Amanita phalloides*, based on predictors from PAPER 1 (PAPER 12). D: Marine habitat types and behaviour observations of harbour seal pups (*Phoca vitelina*) (PAPERS 4 and 5). E: Reference area for the environmental - vegetation/fungi relationship studies and monitoring (PAPERS 2, 6 and 10), and sampling station for zooplankton studies (PAPERS 7 and 8). F: Study area for butterfly movements investigations (PAPER 11) G: Study area for marine investigations (photo Trine Bekkby) (PAPERS 4 and 5). H: Sample plot for vegetation registrations (photo Per Arild Aarrestad) (PAPER 2 and 10). I: Radio tracking of harbour seal pup (photo Trine Bekkby) (PAPER 4). J: Non destructive tagging of *Hylocomium splendens* shoots using PVC rings (photo Rune Halvorsen) (PAPERS 3 and 9) and K: Tracking of the butterfly species *Lycaena virgaureae* (female) using permanent water proof pen (photo Kristin Vigander) (PAPER 11).

Study area: Norway

This thesis comprises studies from the entire mainland and the adjacent coastal areas of Norway, reaching from 58° to 71° north and from 4° to 31° east, from the sea bottom to 2469 m above sea level. The strong bioclimatic variation makes Norway ideal for studying variation in biological patterns in time and space. Norway has a long coastline, high mountains that create a partly rain-shadowed inland, varied geology and topography and thus encompassing extensive variation along several ecological and bioclimatic gradients within rather restricted geographic areas (Moen 1999).

Geologically, Norway is situated at the western fringe of the Baltic shield, where it borders onto Precambrian rocks and the Caledonian mountain range which is dominated by sedimentary, more or less metamorphic, bedrock (Sigmond 1985). The surficial (mostly glacial, marine and glacifluvial, but locally collovial, periglacial and organic) deposits are normally thin and discontinuous. However, in the eastern parts of Norway these deposits may locally be thick. Continuous till cover occurs both in northern and southern Norway. Marine clays are found locally along the coast up to about 220 m above sea level (the upper Weichselian marine limit; Hafsten 1983). Landform varies from gently undulating terrain to rugged forms typically with dramatic glacially sculptured elements such as fjords, U-valleys and cirques (Holtedahl 1960, Rudberg 1960). Terrain relief increases westwards (towards the coast).

The two main bioclimatic gradients in Norway are (1) the temperature-related gradient, traditionally divided into 'zones' – temperature decreases with increasing latitude and elevation,; and (2) the gradient from strongly oceanic (and humid) to slightly continental (and arid) climates, traditionally divided into 'sections' – oceanicity decreases from west to east, humidity also from sea level to high altitudes (Moen 1999). All eight temperature-related (vegetation) zones commonly recognised in North Europe (from nemoral to high alpine) occur in Norway, and zones from the nemoral to the middle boreal occur further north in Norway than in any other part of the World (Moen 1999). The oceanic west coast has small annual temperature amplitudes and high rainfall all seasons. The maximum annual precipitation occurs in mid-fjord districts (often up to 3500 mm, with local maximum values of 6000 mm). The continental interior of Norway has high annual temperature amplitudes with hot, dry summers and cold winters; annual precipitation below 300 mm locally occurs.

Human activities have influenced Norwegian ecosystems since the end of the last ice age, and practically all areas below the timberline have been strongly influenced. Additionally, areas in the low-alpine vegetation zone have been considerably modified through mountain summer farming and domestic grazing (Bryn & Daugstad 2001). Time since the last glaciation and land upheaval, i.e. ecosystem age, land use changes and immigration patterns have also given rise to important spatial gradients.

The launch: establishing the baseline

Biogeographical patterns and gradients

The current expert view of bioclimatic regional vegetation variation in Norway, i.e. the division of the country into zones and sections (see descriptions above), was substantiated by applying objective multivariate methods to 54 climatic, topographical, hydrological and geological variables, represented as raster-formatted GIS layers (PAPER 1). This study, which will be called PCA Norway in the rest of this dissertation, provides a baseline for many of the other studies, as knowledge of the most important broad-scale environmental gradients (see definition in PAPER 1) is important for understanding biogeographical variation in Norway (Moen 1999).

The PCA Norway analyses disclose potential for improvement of the current expert-based classifications into vegetation zones and sections, as exemplified by the proposal in PAPER 1 to displace the nemoral zone from the southern tip of Norway towards the east and north along the South Norwegian coast. The PCA Norway results provide a fine-resolution, continuous parameterisation (termed step-less models) of the complex gradients underlying the bioclimatic zones and sections, thus demonstrating that objective methods may be used to test and improve manual classifications at all scales. The step-less models of environmental variation produced by the PCA Norway approach may successfully be used as predictor variables for species and ecosystem distribution modelling (see examples below).

One example of utilization of PCA Norway is given in PAPER 12. Both the environmental variables included in PCA Norway as well as secondary derived variables, such as area cover of main ecosystems (e.g. mires, forests, alpine heaths, and agricultural land), were used to explore distribution patterns for nine selected fungal species based upon herbarium data. GLM (logistic regression) analyses were used to relate species occurrence in a 5×5 km grid covering Norway to 75 environmental predictor variables. Variables related to temperature and radiation were most frequently included in the GLM models, and between 27 and 60 percent of the variation in species occurrence was accounted for by significant predictors.

Another example of use of the step-less models produced by PCA Norway is provided by PAPER 8, in which regional species richness patterns of zooplankton in

Norway were analyzed and discussed. Important contributing variables (GIS layers) identified by PCA Norway were superimposed on the 1891 lakes from all over the Norwegian mainland. Multivariate analysis (PCA) indicated that maximum monthly temperature and energy input (solar radiation) were the best predictors of species richness for this group of species. This was also confirmed by stepwise, linear regression analysis. Nevertheless, both the PCA analysis and the linear regression models left a large fraction of the variance unexplained, probably due to lake-specific properties such as catchment influence, variation in lake productivity, food-web structure, immigration history and dispersal limitations and other, more or less stochastic effects.

PAPER 8 was a follow-up of PAPER 7, in which an independent and smaller set (336 Norwegian lakes) of data on zooplankton species presence, latitude, altitude, lake area, mean depth, chlorophyll a (a measure of production) and fish community structure was analysed without access to the regional PCA Norway data, but based upon in-situ measurements of environmental variables. The main differences between PAPERS 7 and 8 were the number of observations, that local site measurements were available in the smaller data sets (and that, in general, the selection of variables differed between the two data sets), and differences with respect to taxonomic resolution. Such differences are typical for ecological data: large data sets (in terms of number of observations) can be generated from maps and survey data, while specific environmental predictors such as element concentrations in water and soil are expensive in terms of collection and analysis costs, and hence possible to obtain for small (or medium-sized) data sets only. In the smaller data set (PAPER 7), lake productivity, in terms of phosphorus concentration and algal biomass, was the most important predictor of zooplankton richness. These variables were not available regionally as GIS layers in PAPER 8. This demonstrates the limitation of large data sets, in which all the relevant variables are rarely at hand and a large amount of variation in observed patterns is usually left unexplained. As discussed later, I propose a two-step approach when large regional data sets are available and in-situ measurements are sparse. The step-less models of regional gradients provided by the PCA Norway approach in PAPER 1 may be used to put species richness and distribution patterns into a biogeographical context. Restricted data sets with (in-situ) measurements of environmental factors at sampling sites are ideal to establish local ecoclinal gradients. Nevertheless, despite the large number of variables included in PAPER 7, the predictive power of multiple regression models was moderate (<50% of the variance explained), pointing to a

potentially important role of within-lake properties, stochasticity, dispersal or yet unknown factors for zooplankton diversity in lakes.

PAPERS 7 and 8 pointed to temperature and temperature-related variables as the major determinants of species richness (see also Walseng et al. 2006). Similarly, PAPER 12 indicated that temperature-related variables were the most important factors for fungal distribution. This suggests that climatic, temperature-related, factors are more important that precipitation-related factors for species distributions, contrary to the ranking of the two regional complex gradients in PCA Norway where humidity and continentality came out as the principal component. However, this merely shows that the biological response does not have to be predictable in terms of scaling of gradients in physical or other units (Økland 1992). There are, however, also many examples of species dependency on the oceanity-continentality gradient, in PAPER 12 as well, so that the ranking of the importance of these two regional complex gradients may differ among species groups (see Pedersen 1990). As discussed in PAPER 1 these two complex gradients may form one composite complex gradient within restricted areas.

Local patterns and gradients

The segregation between regional (biogeographic) and local variation is taken place where study areas 'extent' see PAPER 1) become fairly homogenous with respect to the step-less zone and section gradients defined in PAPER 1. The semi-variogram for step-less zone and sections models in PAPER 1 (Fig. 7) indicate that the range of spatially structured variation of the step-less model (i.e. the range in which zone and section can be predicted by knowledge of spatial position) is up to 160 km. However, the semi-variance rises steadily from the shortest distance (10 km) which indicates that the distance interval at which local patterns and ecoclines gain dominance over biogeographical patterns is below 10 km. Based upon studies of agricultural landscapes, Økland et al. (2006) suggest that this shift actually takes place at distances of ca. 500 m in SE Norway.

Local ecoclines to a large extent arise because of topographic variation (PAPERS 4, 5, 6, 10; Ahti et al. 1968, Økland & Bendiksen 1985). Main vegetation gradients as well as plant richness patterns are closely related to topography (Stoutjesdijk & Barkman 1992, Økland & Eilertsen 1993, Fransson 2003), because topography controls the distribution of nutrients and water availability in boreal ecosystems (Økland 1996). The investigation of forest-floor vegetation variation within six *Vaccinium myrtillus* dominated birch-forest

sites (PAPER 2) showed that terrain variation (from dry sites on top of hills to valley bottoms) explained the primary coenocline in all areas. This moisture-topography related ecocline (see Økland & Eilertsen 1993) consisted of intercorrelated variables such as soil moisture, pH, Ca, K and S, in accordance with the local gradient structure found in bilberry dominated spruce forest (Økland 1996, see also PAPER 10), spruce-pine forest (Økland & Eilertsen 1993) and alpine systems (Økland & Bendiksen 1985). Tree influence, topographic position and soil depth were other factors influencing species composition in birch forest (PAPER 2).

In PAPER 6, the macrofungal species composition and its relationships to ecological factors and 'green vegetation' were investigated in a boreal coniferous forest area (the same area as studied by Økland & Eilertsen 1993; one of the 17 areas included in PAPER 10). The first fungal coenocline was found to correspond to the main coenocline for vegetation, comprising the variation from pine to spruce dominated forests; from ridge via slope to valley bottom. While macro-scale topographic variables were relatively more strongly correlated with the vegetational coenocline, soil pH and nitrogen content were more strongly correlated with the fungal coenocline. The correspondence between ordination results obtained for fungi and plants demonstrates (1) that distributional patterns of macrofungi and plants within forests to a large extent (but not completely) are caused by the same major environmental complex-gradients and (2) that the same field and analytic methods are applicable to both groups of organisms.

To compare important local ecoclines relevant for sessile contra highly mobile organisms is difficult. Especially in a fragmented landscape, movement and dispersal capacity are important factors in determining which species are able to persist. To examine the role of landscape structure and pattern on movement, a model to predict the 'least-cost' pathway a species would take through an agricultural landscape matrix between habitat fragments was developed in PAPER 11. This was done by assigning friction values to different habitat types. The model was validated by using empirical data on inter-patch movement for two butterfly species. As a measure of the ecological distance between habitat patches, the least-cost path model, was a better predictor of butterfly movement than Euclidean distance between patches. This approach differs fundamentally from the ones used for sessile plants and demonstrates the importance in ecology of a toolbox well equipped with a diversity of approaches and analytic strategies. Knowing the cost of moving between favourable habitats is an important step in understanding the ecology of moving organisms (animals) on a local scale.

Many of the local gradients that are relevant in terrestrial ecosystems (PAPERS 2, 6 and 10) are also important in marine systems (PAPERS 4 and 5). For instance, topography is important in terrestrial ecosystems and also to large extent structures marine ecosystems via light attenuation and slope (substrate stability) (PAPER 5). Our knowledge of terrestrial and marine systems differs strongly mainly because the availability of species and explanatory data is widely different, reflecting the practical difficulties and costs involved in obtaining such data. As will be discussed later, spatial prediction of occurrence and distributions from environmental data is an important tool in marine ecology.

Managing deep sea ecosystems requires tools that facilitate integration of data from a variety of sources for efficient analysis and presentation. PAPER 4 is one of the first applications of GIS to the Norwegian coastal ecosystems, integrating information on bathymetry, terrain variation and wind conditions into a georeferenced model.

Micro-scale patterns

The significance of population biology for understanding fine-scale plant patterns (coenclines and ecoclines) has been recognised for decades (van der Maarel 1984). Spatial patterns of important population or individual characteristics are expected to reflect structuring ecosystem processes to the extent that populations with strikingly different spatial patterns most likely have been structured by different processes. PAPERS 3 and 9 represent GIS-based approaches to very fine-scaled plant patterns, i.e. bryophyte demography (*Hylocomium splendens*) data which have been placed into a well-defined micro-scale ecological framework. Demography plots, 25 × 25 cm, situated in seven of the monitoring sites, were used for PAPER 10. PAPER 3 applies a methodological approach with conceptual path models, GLMM and GIS that proved useful for disentangling complex ecological relationships.

More specifically, PAPER 3 shows that micro-topography is a potentially important predictor of bryophyte demography in general and of performance and fate of individuals in particular. Most likely this is a result of the very same moisture-topography related ecocline discussed under local patterns and gradients, which is relevant over a considerable span of spatial scales. Micro-topography contributed to explaining bryophyte performance by four different mechanisms (PAPER 3): (1) a direct effect of slope on the segment's (functional individual's) vertical position in the carpet; (2–3) direct effects of both slope and convexity on fates of individuals via controls on risk of burial; and (4) an indirect

effect of convexity on branching pattern via a direct effect on size. No indication of a direct effect of terrain on branching was found.

In PAPER 9, the issue of how large an amount of variation in demography that can be explained on a spatial scale of individuals is addressed. Few studies of spatial patterns in plant assemblages in general and bryophyte assemblages in particular have been performed, and patterns have only vaguely been linked with process. The study presented in PAPER 9 uses a subsample of 21 plots also included in PAPER 3 to describe fine-scaled spatial variation in size. All *Hylocomium splendens* segments in the investigated plots were followed for a 10-year period and their size (dry mass, estimated from in situ measurements) and fate (terminated or ramifying) were recorded annually. For about one half of the populations, size and termination of segments could be assigned to a specific spatial pattern. The predicted outcome could be explained by one of three main structuring processes: (1) negative spatial dependence on the scale of individuals (below 2 cm), indicative of negative interactions, (2) positive spatial dependence on the scale of individuals, indicative of positive interactions and (3) positive spatial dependence on broader scales, indicative of structuring by environmental factors or patchy disturbance. Patterns (i) and (iii) were observed both for size and terminated segments more often than expected. Fractal dimension profiles for size obtained separately for each year revealed temporal patterns of spatial structure that tended to be invariant over years. Negative spatial dependence of size, possibly due to large size difference between buried segments and other segments during self thinning, was typical of populations rapidly growing in number. Positive spatial dependence with a range of influence by the spatial process of 4–8 cm was observed in plots with sparse bryophyte cover and high cover of deciduous litter. This is most likely caused by accumulation of litter in depressions between shoots or groups of shoots.

The results in PAPER 9 accord with those of previous studies (Mack and Harper 1977, Mithen et al. 1984, Silander & Pacala 1985, Wagner & Radosevich 1998, Molofsky 1999), demonstrating that the neighbourhood of plant interactions, the plant's eye view (Turkington and Harper 1979), is of comparable size to that of 'individuals', or even smaller. This implies that a mean-field description of the boreal forest floor, as well as of most other communities, obtained by averaging over large lots or sets of large plots, will be insufficient and perhaps misleading if one aims at understanding the processes shaping the community (Purves & Law 2002). Furthermore, our results lend support to the conclusion of Purves & Law (2002) that consequences of fine-scale spatial structure are

potentially profound, calling for development of a theoretical and empirical framework for plant community dynamics with local spatial structure as its core.

PAPERS 3 and 9 directly address the important question of how much of the variation observed in nature can be explained in terms of explanatory variables on different scales (PAPER 3), interactions between variables (PAPER 9) and the amount of stochasticity (i.e. 'noise'). It seems that a relative large amount of variation is left unexplained both on the very fine, the local and the regional (biogeographical) scales (see PAPERS 3, 7, 8 and 9), especially when large and complicated data sets are analysed. Further analyses are needed to tell if the variation so far left unexplained may actually have an ecological explanation, and/or if it is a result of uncoordinated and unpredictable events ('noise').

The voyages: the importance of time series and monitoring endeavours

No ecosystem is static, and temporal changes may occur rapidly, e.g. under the current climatic change regime. Monitoring is important for documenting and understanding such changes. In fact, baseline investigations performed at only point in time are likely to fail to provide an adequate understanding of an ecosystem in which the temporal dimension is important. Furthermore, time (history) has proven increasingly important towards finer scales, i.e. as determinant of population or individual characteristics at a given time (see PAPERS 3 and 9). The fact that samples like those in the zooplankton studies (PAPERS 7 and 8) are actually snap-shots is likely to 'explain' some of the unexplained variance in the observed patterns, since the zooplankton communities show seasonal and interannual variation in species composition and species number. Hence, community dynamics is a source of random variation, 'noise', in species composition.

Monitoring of ground vegetation in boreal forests (PAPER 2 and 10) started in the late 1980s, before the tendency for winters and autumns to be milder and less snow-rich, which we have seen in many later years. Recent results from monitoring in boreal forests reveal two patterns of biodiversity changes that may be related to broad-scale impacts: (1) the abundance of several vascular plant species declined in the 1990s in spruce forests on richer soils in the southern part of the country, most likely due to long-distance airborne pollution, and (2) bryophyte growth (cover and annual biomass production) has increased considerably. Furthermore, rodent cycles influence population characteristics, as demonstrated for *Hylocomium splendens* in PAPER 3 and 9; rodent population peaks cause an immediate decline in *Hylocomium* population sizes due to grazing and unrooting, followed by regeneration of small shots the coming years (PAPER 3, also see Rydgren et al. 2007). Patterns brought about by these structuring processes give an important temporal dimension to the ecosystems in question, which can not be captured by one baseline investigation. However, they are revealed by re-analysis of permanent monitoring plots.

The pattern of vascular plant changes is interpreted as a time-delayed response of long-lived, mainly clonal, populations to acidified soils resulting from deposition of long-distance airborne pollutants. The pattern of bryophyte changes, with reference to the close

link between climatic conditions for growth and abundance changes for *Hylocomium splendens* established in previous demographic studies (Økland 1997, Rydgren et al 2007), is related to climatic conditions favourable for bryophyte growth. PAPER 10 concludes that many forest understorey plants are sensitive indicators of environmental change, and that the concept used for intensive monitoring of Norwegian forests (Lawesson et al. 2000) enables early detection of changes in vegetation brought about by broad-scale, regional, impact factors.

PAPER 10 confirms that monitoring enables early detection of vegetation changes related to long-distance airborne pollutants and other broad-scale impact factors, such as varying and changing climatic conditions. Important reasons for success in this respect were: (1) selection of reference areas minimally influenced by successions after local disturbances (e.g. wildfire, previous timber harvests and burn-and-slash cultivation), as such successions tend to obscure changes due to regional impact factors such as deposited airborne pollutants and climatic change; (2) establishment of plots in each reference area along the main local complex gradients in a standardized manner ensures a comparable range of variation to be included from all areas (e.g. the 'richer' *Picea abies* dominated forests, which, if not included in the study, would have left the declining abundance of moderately nutrient-demanding vascular plants in Norwegian *Picea* forests undetected); (3) a sampling scheme facilitating analysis of univariate as well as multivariate patterns of change; and (4) supplementary plant demography studies conducted in permanent vegetation plots, e.g. the parallel demographic study of *Hylocomium splendens* (i.e. PAPER 3 and 9). Monitoring of change in single-species abundances, species number and species composition in permanent 1-m^2 plots in Norwegian boreal forests confirms previous assumptions that the forest understorey vegetation contains a large set of indicators sensitive to changes in environmental conditions.

Monitoring is the only way to document changes that occur in ecosystems. As will be discussed in the next section, monitoring also has an important function in verifying prediction models.

The final frontier ('where no man has gone before')

Prediction of species distributions through niche modelling (Peterson & Vieglais 2001, Elith et al. 2006, Stokland et al. 2008) has become a state-of-the-art approach among conservation ecologists in recent years (since 2000), and is an example of novel use of GIS modelling tools. Niche modelling may be used to take the step from results based on static analyses to projections and predictions for the future, including construction of scenarios. The niche modelling studies included in this thesis do, however, only address predictions in space. PAPER 1 provides a successful example of regional modelling of biogeographical patterns with high precision, using regional environmental GIS strata. Furthermore, PAPER 1 opens for the possibility that also the distribution of single species richness (PAPER 7) and of land-cover types may be modelled with acceptable accuracy. Such models can further facilitate selection of intensive monitoring plots based on stratification, parameterization of representativeness and analysis of rareness.

PAPER 12 demonstrates that temperature is a key factor governing the distribution of macrofungi. These organisms are therefore likely to respond to global climate change. In PAPER 12 we demonstrate that ecological and biogeographical research on macrofungi may fruitfully be carried out on herbarium material (e.g. for conservational purposes), as fungal data in museum herbaria, collected over long periods of time, probably represent the best available source of presence data, especially at large/regional scales (also see Kauserud et al. 2008). Methods that handle data of the presence-only type are particularly useful for fungi since obtaining reliable absence data is time consuming (and burdened with much stochasticity) because their ephemeral fruit bodies can often be spotted only for a few days in occasional years. In PAPER 12 we observed a good fit between observed and predicted potential distributions, and most deviations between observations and predictions were possible to explain. Together with generally very high AUC values of Maxent models used in PAPER 12, this lends credibility to the material, the methods, and to the choice of scale for this regional study (5×5 km).

Another type of prediction is presented in PAPER 11, where GIS least cost path tools were used to predict influences on dispersal under different scenarios. As a measure of the ecological distance between habitat patches, the least-cost path model was a better

predictor of butterfly movement than Euclidean distance. The model proved useful for ranking of management scenarios, and thus has potential as a decision-support tool. Results indicate that removal of all infrastructure from within arable fields will significantly reduce rates of inter-patch movement while restoration of all boundaries between arable fields as grassy banks will increase the connectivity between sub-populations. Planners widely recommend using corridors to connect fragments of remnant habitats, despite relatively little empirical evidence is available in support of the view that dispersal of individuals is enhanced by this practice. The modelling results in PAPER 11 do, however, show that important aspects of species movement and survival can be expressed in models suitable for area planning and management.

PAPER 4 demonstrates that information on depth and wind exposure derived from a digital terrain model can be combined in a rule-based approach to predict the distribution of kelp forest dominated by *Laminaria hyperborea*. Interestingly, the predictions improved detection of kelp forests although they deviated from information provided by kelp harvesters. Inclusion of information about sea-bed sediments further improved the predictive ability of the model. This approach enabled more correct decisions concerning kelp forest harvesting and restoration. Integrating the kelp forest prediction model with information on depth and the presence of slopes, islands and georeferenced data on the behaviour of the harbour seal *Phoca vitulina*, the kelp forest prediction model of PAPER 4 could be expanded to a prediction model of harbour seal habitat selection.

Based on modelled or measured geophysical variables, a predictive spatial distribution model for the eelgrass, *Zostera marina,* was established in PAPER 5. This model was implemented in GIS and a model-based map of the probability of finding *Z. marina* was developed. The Akaike information criterion (AIC) and the predictive modelling extension GRASP in S-Plus were used to develop the model. The analyses largely confirmed results of previous studies, that the probability of finding *Z. marina* is high in shallow, gently sloping sheltered sites close to the coast.

Predictive models contribute to a better understanding of the factors and processes structuring the distribution of marine habitats. Furthermore, such models provide useful tools for management and research. The main reason for this is that they are quantitatively and objectively defined, and that the results can be easily visualized as an occurrence probability map that is easy to understand by the various stakeholders.

With increasing rarity of a species, however, the risk that prediction models fail to reveal true patterns increases because models become increasingly vulnerable to

peculiarities of the sampling and the data, including 'false absences'. For rare species 'false absences' may significantly reduce the quality of a model, while the high number of occurrences for common species counteracts the effect of a few relatively lower number of 'false absences' (Engler et al. 2004). On the other hand, however, rare species with a restricted distribution often attract considerable attention by field biologists, resulting in a more representative picture of the actual distribution than can be expected for widespread common species, which are often considered as too trivial for representative collecting to be worthwhile. With increasing representativity of recorded distributions, however, higher proportions of variation are explained and goodness-of-fit increases (e.g. as indicated by higher AUCs). Then better maps of potential distribution can generally be expected.

Several pitfalls exist in prediction modelling. Maxent and other modelling tools are generally prone to overfitting when the numbers of explanatory variables are high (S.J. Phillips, personal communication). This was clearly demonstrated in a preliminary analysis for PAPER 12 in which all the 75 explanatory variables were included. Maxent then produced maps of potential distributions almost like blueprints of the recorded distributions. The alternative strategy used in PAPER 12, to restrict Maxent to variables included selected as independently significant in GLM models, seems beneficial in terms of realism and usefulness of predictive maps.

Including other still unavailable explanatory variables, such as edaphic and biotic factors (see Stokland et al. 2008) and information on the spatial distribution of 'nature types', e.g. at the ecosystem scale and complexity level in the new system of nature types in Norway (Halvorsen et al. 2008a, 2008b), in prediction models, may improve the explanatory power of distribution models. However, at the same time, the risk of overfitting increases.

The results from the terrestrial modelling approaches (PAPERS 1, 7 and 12) demonstrate the paramount importance of the choice of scale ('grain'; Dungan et al. 2002) in biogeographic modelling studies. Good predictive models result when the grain (grid cell size) provides an adequate resolution of the variation in the environmental variables that govern the distributions of the species in question. Thus, 1×1 to 10×10 km cell sizes represent regional gradients in temperature, precipitation and oceanity well, but do not capture substrate and other factors of a local, edaphic type. In the local modelling approaches, data of higher quality and higher resolution are needed to improve predictions.

As a result of the shift in relative importance of local vs. regional gradients around 250–750 m grain size, as suggested in PAPER 1 and by Økland et al. (2006), fine scale

prediction of species occurrences must be modelled in two steps: (1) a biogeographical approach that places the species into a setting of the main regional gradients (see PAPER 1); and (2) a local approach that uses more fine-scaled map information (perhaps also aerial photographs) to locate potential sites for the species along the main local complex gradients within the suitable grid cells found in step (1).

The importance of understanding scale relationships in ecological studies

'Scale' is used with many different meanings in ecology, including the size of the investigation area which can be defined as 'extent', whereas 'grain' is defined as the size of individual sample units (Wiens 1989, Gustafson 1998, Dungan et al. 2002). Several important issues are related to scale. We can not generalise outside the extent without having to postulate that the same processes and scale relationships operate in the area outside. Neither can a particular data set be used to discover patterns at scales finer than the grain. We are often forced to increase grain if we shall increase the size of the investigation area because computation time increases nonlinearly with increasing data-set size. This implies that macro-scale patterns are often captured at the expense of local and micro-scale variation. With constant extent, an increase in grain will normally lower the spatial variance. With constant grain, an increase in extent will normally increase the variance. This implies that the question of up- and downscaling represents a major challenge in understanding relationships of complex systems (see also Quattrochi & Goodchild 1997).

Complex ecosystem structure is typically represented by categorical maps or by a collection of samples taken at specific spatial locations (point data). An example of a categorical map is the division of Norway into vegetation regions by Moen (1999), which was taken as a basis for quantitative analysis in PAPER 1. Alternatively, geostatistical analysis of point data assumes that the system is spatially continuous, making fewer assumptions about the nature of spatial structure. Gustafson (1998) reviews the two techniques and concludes that pattern analysis techniques (the use of categorical maps) are most useful when applied and interpreted in the context of the organism(s) and ecological processes of interest at the appropriate scales (which as he points out can be unknown). Point data analysis, however, can answer two of the most critical questions in spatial pattern analysis: (1) what is the appropriate scale to conduct the analysis, and (2) what is the nature (and strength) of the spatial structure? Geostatistical analysis has become a standard tool for interpretation of spatial patterns of organisms, of the numerous environmental factors to which they respond, and of the joint spatial dependence between organisms and their environment (PAPER 10, Rossi et al. 1992). Geostatistics and other

statistical methods are important for the whole potential in digital spatial data analysis to be utilised. Observed values for variables used in ecological studies are often correlated in space (and time); spatial structures can emerge from different sources, such as measurement errors, continuity effects including spatial heterogeneity and spatially dependent processes and mechanisms (Haining 1990). In the future, designing of mapping and monitoring systems and the choice of indicators in a way that makes the data suitable for geostatistical analysis will be important. PAPER 1 exemplifies an approach that transforms categorical maps into step-less models which can be analysed with geostatistical methods.

For multidisciplinary integration of data, terrain variables are important on a wide range of scales both because of their availability and their ecological relevance (see PAPERS 1, 3, 4, 5, 6 and 12). We have noted see that elevation and terrain data are important on all scales although linked to different ecological complex gradients. Above 250–750 m linear scale resolution, terrain is a main driver of bio(climatic)geographic patterns. Below this threshold, terrain structures determine the most important vegetation gradients (PAPER 2, PAPER 10) down to the finest scales, where terrain influences individuals (PAPER 3). This important multi-scale relationship of terrain is important for linking data over a wide spectrum of scales and from different disciplines. Improved understanding of how knowledge based on data at one spatial scale is connected with knowledge based on data at other scales is important for integration of data across scales and disciplines. This is fundamental for utilising spatial data in monitoring programs and in the process of acquiring information from ground truthing. This is also fundamental for natural resource management in a realistic spatial context.

In combination with GIS, the use of information from remotely sensed strata, including aerial photographs, has become increasingly popular in integrated studies of ecological patterns on scales in which other data are of limited availability. It is, in this context, important to stress that field validation is always important. Segmentation and classification of aerial photographs and high resolution satellite maps have potentials to become important for pattern identification on scales within grain sizes of 1–50 m, i.e. where other spatial environmental data is limited. It is important, then, specifically to take into account the uncertainty that is acceptable at different scales.

In PAPER 8, the predictive power of the ‘metabolic scaling laws’ for species richness was tested in search for a scaling relationship totally different from that approached in the other studies in the thesis. A universal law for species richness was

proposed by regressing ln of species richness on the inverse of the temperature (in Kelvin), corrected for the activation energy (eV) as predicted by the Boltzmann constant. A significant, negative slope for ln richness over temperature, given as 1/kT, was found. The slope, 0.78, was however slightly higher than the range of slopes predicted from the scaling law (0.60–0.70). We conclude that this hypothesis should be further tested.

The studies included in this dissertation show that by looking at Norway through grids of different spatial resolutions, an important threshold of grain size occurs somewhere between 100 m and 1 km [250–750 m suggested by Økland et al. (2006)]. This boundary zone manifests itself in several ways: variation between grains larger than this will mostly reflect regional biogeographic gradients, while smaller grains will reflect local topographic, edaphic and hydrological gradients. Furthermore, regional analysis with smaller grains than 1 km is impracticable with standard computer power. This calls for at least two separate analyses to establish knowledge of a community, population or an individual at a given time in space. (1) a biogeographical analysis of distribution of the species, by use of sampling units that spans the main regional gradients (see PAPER 1), and (2) a local ecological approach to the abundance variation of the species, that uses smaller observation units and fine scaled map information (perhaps derived from aerial photographs) to locate suitable smaller sampling units. Several of the studies (PAPERS 1, 3, 4, 5, 6 and 12) demonstrate that terrain should always be included in both terrestrial and marine modelling approaches.

The dimensions: On the use of GIS in ecological studies

With this thesis I intend to demonstrate that GIS can be a useful tool in most field ecological studies. The value of using GIS tools is well documented in several ways, in many of the individual papers. The demonstrated usefulness contrasts the fact that GIS is still not commonly used by ecologists.

There are many reasons why the threshold for users to implement GIS in ecological studies may be experienced as high. Firstly, access to GIS software and relevant map data is often expensive. Secondly, even though the principles of GIS are easy to understand, using the tool is complicated, tedious and requires skills not normally included in the biology curriculum as a basic element. Thirdly, and what I consider the main obstacle for becoming a successful GIS analyst of ecological data, is learning the programming language of a GIS software. Although many pre-programmed routines exist in the software itself or as free downloadable programs (scripts or extensions) on the Internet, surprisingly many situations occur when 'on the fly' programming is needed. In fact only PAPERS 6 and 7 in this thesis does not include any 'on the fly' GIS programming at all. Programming may include preparation of data for analyses (as exemplified by PAPER 3), but is most often needed to have new ecologically relevant functions implemented into the GIS analyses. Lastly, there is a lack of knowledge among students and researchers of the opportunities in ecological analyses and modelling offered by GIS. GIS is of more use if it is included in an ecological study from the planning stage and implemented thereafter (see PAPER 1).

GIS is used as a visualization tool in all papers. The most important GIS analyzing tools used are as followed: Overlay analysis and neighbourhood statistics (used in PAPERS 1, 3, 4, 5, 8, 9, 11 and 12); geostatistical tools (used in PAPERS 1, 2 and 9); least cost path analysis (used in PAPER 11); prediction tools (used in PAPERS 4, 5 and 12); interpolation tools (used in PAPERS 1, 2, 3, 4, 5, 8, 11 and 12), and terrain modelling tools (used in PAPERS 1, 3, 4, 5, 8, 10, 11 and 12).

References

Ahti, T., Hämet-Ahti, L. & Jalas, J. 1968. Vegetation zones and their sections in north western Europe. - Annales Botanici Fennici 5: 169-204.

Bryn, A. & Daugstad, K. 2001. Summer farming in the subalpine birch forest. In F.E. Wielgolaski (ed.) Nordic mountain birch ecosystem pp. 307-315. - UNESCO Man and Biosphere Series 27.

Cale, P.G. & Hobbs, R.J. 1994. Landscape heterogeneity indices: problems of scale and applicability, with particular reference to animal habitat description. - Pacific Conservation Biology 1(1): 183-193.

Dungan, J.L. Perry, J.N., Dale, M.R.T., Legendre, P., Citron-Pousty, S., Fortin, M.-J., Jakomulska, A., Miriti, M. & Rosenberg, M.S. 2002. A balanced view of scale in spatial statistical analysis. - Ecography 25: 626-640.

Elith, J.C.H., Anderson, R.P., Dudı´k, M., Ferrier, S., Guisan, A., Hijmans, R.J., Huettmann, F., Leathwick, J.R., Lehmann, A., Li, J., Lohmann, L.G., Loiselle, B.A., Manion, G., Moritz, C., Nakamura, M., Nakazawa, Y., Overton, J. McC., Peterson, A.T., Phillips, S.J., Richardson, K.S., Scachetti-Pereira, R., Schapire, R.E., Soberón, J., Williams, S., Wisz, M.S. & Zimmermann, N.E. 2006. Novel methods improve prediction of species' distributions from occurrence data. Ecography 29: 129-151.

Erikstad, L., Lindblom, I., Jerpåsen, G., Hanssen, M.A., Bekkby, T., Stabbetorp, O.E. & Bakkestuen, V. 2007. Environmental value assessment in a multidisciplinary EIA setting. - Environmental Impact Assessment Review 28: 131-143

Fransson, S. 2003. Bryophyte vegetation on cliffs and screes in Western Värmland, Sweden. - Acta Phytogeographica Suecica 86: 1-95.

Gleason H.A. 1926. The individualistic concept of the plant association. - Bulletin of the Torrey Botanical Club 53:7-26

Gustafson, E.J. 1998. Quantifying landscape spatial pattern: What is the state of the art? - Ecosystems 1(2): 143-156.

Hafsten, U. 1983. Shore-level changes in South Norway during the last 13,000 years, traced by biostratigraphical methods and radiometric dating. - Norsk Geografisk Tidsskrift (Norwegian Journal of Geography) 37: 63-79.

Haining, R. 1990. Spatial data analysis in the Social and Environmental Science. - Cambridge University Press, Cambridge 1-409.

Halvorsen, R., Andersen, T., Blom, H.H., Elvebakk, A., Elven, R., Erikstad, L., Gaarder, G., Moen, A., Mortensen, P.B., Norderhaug, A., Nygaard, K., Thorsnes, T. & Ødegaard, F. 2008. Naturtyper i Norge - et nytt redskap for å beskrive variasjonen i naturen. - Naturtyper i Norge Bakgrunnsdokument 1 (versjon 0.1): 1-17 (www.artsdatabanken.no) (in Norwegian)

Halvorsen, R., Andersen, T., Blom, H.H., Elvebakk, A., Elven, R., Erikstad, L., Gaarder, G., Moen, A., Mortensen, P.B., Norderhaug, A., Nygaard, K., Thorsnes, T. & Ødegaard, F. 2008. Naturtyper i Norge - teoretisk grunnlag, prinsipper for inndeling og definisjoner. - Naturtyper i Norge Bakgrunnsdokument 2 (versjon 0.1): 1-121 (www.artsdatabanken.no) (in Norwegian)

Holtedahl, O. 1960. Geology of Norway. - Norges Geologiske Undersøkelse (NGU) 208: 1-540. (in Norwegian)

Kauserud, H., Stige, L.C., Vik, J.O., Økland, R.H., Høiland, K. & Stenseth, N.C. 2008. Mushroom fruiting and climate change. - Proceedings of the National Academy of Sciences of the United States of America (PNAS) 105: 3811-3814.

Lawesson, J.E., Eilertsen, O., Diekmann, M., Reinikainen, A., Gunnlaugsdottir, E., Fosaa, A.M., Carøe, I., Skov, F., Groom, G., Økland, T., Økland, R., Andersen, P.N. & Bakkestuen, V. 2000. A concept for vegetation studies and monitoring in the Nordic countries. - TemaNord 2000. 515: 1-124

Levin, S.A. 1992. The problem of pattern and scale in ecology. - Ecology 73(6): 1943-1967.

Mack, R.N. & Harper, J.L. 1977. Interference in dune annuals: spatial pattern and neighborhood effects. - Journal of Ecology 65: 345 -363.

Mithen, R., Harper, J.L. & Weiner, J. 1984. Growth form and mortality of individual plants as a function of 'available area'. - Oecologia 62: 57-60.

Moen, A. 1999. National atlas of Norway. Vegetation. - Norwegian Mapping Authority, Hønefoss. 1-200.

Molofsky, J. 1999. The effect of nutrients and spacing on neighbour relations in Cardamine pensylvanica . - Oikos 84: 506-514.

Økland, R.H. 1992. Studies in SE Fennoscandian mires: relevance to ecological theory. - Journal of Vegetation Science 3: 279-284.

Økland, R.H. 1997. Population biology of the clonal moss Hylocomium splendens in Norwegian boreal spruce forests. III. Six-year demographic variation in two areas. - Lindbergia 22: 49-68.

Økland, R.H. & Bendiksen, E. 1985. The vegetation of the forest-alpine transition in the Grunningsdalen area, Telemark, SE Norway. - Sommerfeltia 2: 1-224.

Økland, R.H. & Eilertsen, O. 1993. Vegetation-environment relationships of boreal coniferous forests in the Solhomfjell area, Gjerstad, S Norway. - Sommerfeltia 16: 1- 254.

Økland, R.H., Bratli, H., Dramstad, W.E., Edvardsen, A., Engan, G., Fjellstad, W., Heegaard, E., Pedersen, O., & Solstad, H. 2006. Scale-dependent importance of environment, land use and landscape structure for species richness and composition of SE Norwegian modern agricultural landscapes. - Landscape Ecology 21: 969-987.

Økland, T. 1996. Vegetation-environment relationships of boreal spruce forest in ten monitoring reference areas in Norway. - Sommerfeltia 22: 1-349.

Peterson, A.T. & Vieglais, D.A. 2001. Predicting species invasions using ecological niche modeling. - BioScience 51: 363-371.

Purves, D.W. & Law, R. 2002. Fine-scale spatial structure in a grassland community: quantifying the plant's eye view. - Journal of Ecology 90: 121-129.

Quattrochi, D.A. & Goodchild M.F. (Eds) 1997. Scale in remote sensing and GIS. - CRC Press, Inc., Town. 1-406.

Rossi, R.E., Mulla, D.J., Journel A.G., & Franz, E.H. 1992. Geostatistical tools for modeling and interpreting ecological spatial dependence. - Ecological Monographs 62: 277-314.

Rudberg, S. 1960. Geology and morphology. In: A. Sømme (ed.) A geography of Norden pp. 31-47. - Cappelen, Oslo.

Rydgren, K., Økland, R.H., Picó, F.X. & de Kroon, H. 2007. Moss species benefits from breakdown of cyclic rodent dynamics in boreal forests. - Ecology 88: 2320-2329.

Sigmond, E.M.O. 1985. Brukerveiledning til Berggrunnskart over Norge. Nasjonalatlas for Norge. - Statens kartverk, Hønefoss. (in Norwegian).

Silander, J.A. Jr & Pacala, S.W. 1985. Neighborhood predictors of plant performance. - Oecologia 66: 256-263.

Stokland, J.N., Bakkestuen, V., Bekkby, T., Rinde, E., Skarpaas, O., Sverdrup-Thygeson, A., Yoccoz, N.G. & Halvorsen, R. 2008. Prediksjonsmodellering av arters og naturtypers utbredelse og forekomst: utfordringer og potensiell bruksverdi i Norge. - NatHist. Mus. Univ. Oslo Publ. 1: in press (in Norwegian)

Stoutjesdijk, P. & Barkman, J.J. 1992. Microclimate, vegetation and fauna. - Opulus Press, Uppsala.

Turkington, R. & Harper, J.L. 1979. The growth, distribution and neighbour relationships of *Trifolium repens* in a permanent pasture. II. Inter- and intra-specific contact. – Journal of Ecology 67: 219-230.

van der Maarel, E. 1984. Dynamics of plant populations from a synecological viewpoint. In: Dirzo R, Sarukhan J (eds) Perspectives in plant population ecology pp. 66-82. Sinauer Associates. Sunderland Massachusetts.

Wagner, R.G. & Radosevich, S.R. 1998. Neighborhood approach for quantifying interspecific competition in coastal Oregon forests. - Ecological Applications 8: 779-794.

Walseng, B., Hessen, D.O., Halvorsen, G. & Schartau, A.K. 2006. Major contribution from littoral crustaceans to zooplankton species richness in lakes. - Limnology and Oceanography 51: 2600-2606.

Whittaker R.H. 1967. Gradient analysis of vegetation. - Biological Review 42: 207-264

Wiens, J.A. 1989. Spatial scaling in ecology. - Functional Ecology 3: 385-397.

Paper 1

This article is removed.

Paper 2

sommerfeltia

33

V. Bakkestuen, P. A. Aarrestad, O. E. Stabbetorp, L. Erikstad & O. Eilertsen

Vegetation composition, gradients and environment relationships of birch forest in six reference areas in Norway.

2008

SOMMERFELTIA 33 (2008)

Bakkestuen, V., Aarrestad, P.A., Stabbetorp, O.E., Erikstad, L. & Eilertsen, O. 2008. Vegetation composition, gradients and environment relationships of birch forest in six reference areas in Norway. - Sommerfeltia 33: 1 – XXX. Oslo.

Terrestrial Monitoring of boreal birch forest ecosystems (TOV) was initiated in 1989 by the Directorate for Nature Management. The programme has a multidisciplinary approach and integrates studies of precipitation, soil water, soil, understorey vegetation composition, lichens on birch trunks, population studies of birds and mammals and environmental pollutants in plants and animals. Here we present studies of forest floor vegetation at establishment, which supplements and complements two studies established in boreal coniferous forests in 1988: 'The effect of acid precipitation on forest and forest understorey vegetation in Gjerstad, South Norway' and 'Vegetational and environmental monitoring of boreal spruce forest in ten reference areas', the latter initiated by the Norwegian Institute of Land Inventory (NIJOS) as part of a forest health monitoring programme.

The reference areas were selected to span regional gradients in climatic conditions and deposition of airborne pollutants, in old-growth bilberry-dominated birch forest in Norway. Ten macro plots in each reference area were located to span differences in nutrient and soil moisture conditions, terrain features, etc. by a sampling design similar to the one used in coniferous forests. Fifty 1 m^2 meso sample plots, randomly chosen within the ten macro plots, were subjected to vegetation analysis, using frequency in subplots as well as percent cover as species abundance measures.

The main vegetational gradients were found by parallel use of DCA and GNMDS ordination methods; the results of which were subjected to environmental interpretation by means of non-parametric correlation and split-plot GLM analyses. Both ordination methods gave to large degree similar, interpretable, vegetation gradients. The most important ecoclines were related to variation in nutrient conditions, best expressed by pH, Ca, K and S. Tree influence, topographic (un)favourability, soil moisture and soil depth were other factors which were correlated with one of the two main vegetation gradients (ecoclines).

The main vegetational gradients and environmental/climatic/geographical complex gradients in the total data set were found by DCA and subsequent interpretation of axes The main complex gradient corresponded to the variation in the vegetation from sites with low pH and low content of nutrients (low concentrations of macro nutrients like C, Ca, Mn, S and Total N) and high loss of ignition to vice versa. The second gradient corresponded to variation in the vegetation from sites with high effective temperature sums at low latitudes and high soil concentrations of Mn and S, to sites with opposite characteristics. Most of the variation (> 80%) in the vegetation compositions could be ascribed to the between macro plots scale level, leaving a small residual variation on the between area and in the plots within macro plot scale level.

Keywords: *Betula*; Biodiversity; Boreal birch forest; Bryophyte; Climate; DCA; Ecology; Environment, Gradient; Lichens; Monitoring; Norway; Ordination; PCA; Permanent plots; Vascular plants; Vegetation.

Vegar Bakkestuen. Dept. of Botany, Natural History Museum, University of Oslo, P.O. Box 1172 Blindern, NO–0318 Oslo, Norway.

Vegar Bakkestuen, Odd Egil Stabbetorp and Lars Erikstad. Norwegian Institute of Nature Gaustadalléen 21, N-0349 Oslo, Norway.

Per Arild Aarrestad. Norwegian Institute for Nature Research, Tungasletta 2, N-7485 Trondheim, Norway

Odd Eilertsen, Norwegian Forest and Landscape Institute, Postboks 115, N-1431 Ås

.

CONTENTS

INTRODUCTION

Acid rain has been one of the major impact factors on the South Norwegian environment since the 1970s (Anonymous 2006). The problem has for a large part been linked to deposition of long distance airborne sulphur, to which areas in south-western Norway dominated by Precambrian rocks with low buffer capacity have been regarded as the most vulnerable. In the 1970s and 1980s the main focus was on freshwater systems and fish populations, but concern for terrestrial systems originated soon after. In later years, airborne sulphur pollution has declined and some improvement of the environmental status has been reported for Norwegian ecosystems (http://www.miljostatus.no).

There has been an ongoing discussion regarding what impact acid rain has had on understorey vegetation and soil conditions. Possible damages to forest vegetation were first addressed around 1985 when vegetation changes that might be related to 'acid rain' were first recorded (Wittig & Neite 1985, Falkengren-Grerup 1986). As a response to this, several Norwegian projects were initiated with the aim to study possible changes in forest floor vegetation composition and chemical variables, like OPS (*'Overvåkingsprogram for skogskader',* [Norwegian monitoring programme for forest damage]) (Hylen & Larsson 2007) and ICP Forest (Intensive forest monitoring) (Andreassen et al. 2006). The first projects addressing ground vegetation in Norwegian boreal forests were 'The effect of acid precipitation on forest and forest understorey vegetation in Gjerstad, South Norway' (R. Økland & Eilertsen 1993) and 'Vegetational and environmental monitoring of boreal spruce forest' (T. Økland 1996). These monitoring projects were both initiated in 1988 and are still running (Framstad 2008).

The main methodological framework for vegetation monitoring in Norway (Lawesson et al. 2000) and also for this study (also see Bakkestuen & Erikstad 2002) was established during the initial phases of ground vegetation monitoring. The framework was designed for early detection of vegetation changes related to long-distance airborne pollutants and other broad-scale impact factors, such as climatic change. A few important success factors were assumed to be: (1) Selection of reference areas that were minimally influenced by successions after local disturbances, e.g. wildfire, previous timber harvests and burn-and-slash cultivation. Such successions tend to obscure changes due to regional impact factors such as deposited airborne pollutants and climatic change. (2) Establishment of plots in each reference area along the main local complex gradients in a standardized way that ensured a comparable range of variation due to local environmental factors to be included from all areas. (3) Comprehensive sampling of environmental variables that in some way might have an effect on the species composition (R. Økland 1990). In practice collection of environmental variables was restricted to measurements of chemical characteristics in soil, e.g. organic matter content (humus) and chemical properties such as pH, C, N and exchangeable cations and physical characteristics such as relative elevation, soil depth, inclination, slope etc. Furthermore, data on biological characteristics such as e.g. the cover of different vegetation layers and species richness of different groups were also

collected. (4) Use of two different species abundance measurements, subplot frequency and percentage cover, which ensured that demands for observer independence were fulfilled (by the subplot frequency method) while at the same time facilitating detection of temporal changes for frequent species (with high subplot frequency; see Aarrestad et al 2008). (5) A sampling scheme that facilitated analysis of univariate as well as multivariate patterns of change. (6) Supplementary plant demography studies conducted in permanent vegetation plots, e.g. a parallel demography study (see R. Økland 1995, 2000).

The monitoring project 'TOV' (terrestrial monitoring) was initiated one year after the corresponding activities in boreal coniferous forests, i.e. in 1989, with focus on birch forest ecosystems as a supplement to the two monitoring programmes in coniferous forests (Løbersli 1989). Unlike the coniferous forest investigations, TOV is a larger multidisciplinary project that integrates studies of precipitation, soil water, soil chemical and physical properties, ground vegetation species composition, lichens on birch trunks, population studies of birds and mammals, and direct monitoring of environmental pollutants in plants and animals, into one monitoring approach.

Six reference areas for intensive monitoring of ground vegetation in birch forest were established between 1990 and 1993 (five of these in mountain birch forests). The first four reference areas, established in 1990–1992, were designed to cover a small part of the local floristic variation in the vegetation. Only species-poor bilberry-dominated birch forests sites were included, and the vegetation gradients identified by ordination methods were accordingly short in terms of compositional turnover (Brattbakk et al. 1991, 1992, Brattbakk 1993). However, the first results from the boreal coniferous forests monitoring projects indicated that changes due to airborne pollutants mainly occurred in more species-rich bilberry-dominated vegetation types (R. Økland 1994). It was thus decided to change the design of birch forest monitoring to cover roughly the same amount of variation in vegetation and environmental factors as in coniferous forests (i.e. include variation along a nutrient gradient from oligotrophic to medium eutrophic vegetation and a soil moisture gradient from dry to moist soil), and hence to make adjustments to the sampling design of the first four reference areas. The two areas established in 1993 were established according to the new protocol. The three long-term monitoring studies in Norwegian boreal forests were then thus methodologically co-ordinated with respect to: (1) the range of within-area environmental conditions sampled; (2) selection of areas with few and/or small signs of human-induced successions; (3) plot size; (4) interval between re-analyses; (5) species abundance measures; (6) environmental variables recorded at the start; and (7) analysis of vegetation-environment relationships at establishment (see T. Økland et al. 2001, 2004).The focus of this publication is to present the results of the baseline investigations of vegetation-environment relationships in the six reference areas after adjustment of methodology in 1993, i.e. results of field work performed in the period 1993–1997.

Even if TOV, as well as the two sister projects in coniferous forests, as a monitoring program, was basically designed to reveal effects of acid rain, the design and the long duration of the program

underpins it importance in a more general monitoring context. In addition, the results from these studies have contributed, and will continue to contribute to increased understanding of the most important structuring processes in boreal forests (R. Økland & Eilertsen 1993, T. Økland 1996). The sub-alpine vegetation types between the boreal spruce forest and the alpine region have a considerable vertical distribution in Fennoscandia (Hämet-Ahti 1963, Wielgolaski 1997), and they are considered to be of great importance for biodiversity with high conservation value (Odland et al. 1992). It is a national task for Norway, due to its geographical position, to monitor the eventual change of these ecosystems, which are unique in a European context. The last years focus on biodiversity and climate change issues makes these birch forest investigations even more interesting because the monitoring concept makes it possible to study possible changes in amount and cover of field- and ground layer species along the zonal and sectional (i.e. regional) gradients (see Moen 1999).

The aims of this study is to identify variation in ground vegetation composition ('ecoclines') in six birch forests in Norway by use of multivariate statistical methods; and to interpret these ecoclines in terms of environmental variation. These two aims serve the main objective to understand the vegetation-environment relationships of boreal birch forests. This knowledge will be foundation for interpretation of eventually vegetation changes in the ongoing monitoring project.

THE STUDY AREAS

The six reference areas for monitoring boreal birch forest vegetation in Norway are Lund, Møsvatn, Gutulia, Åmotsdalen, Børgefjell and Dividalen, listed from south to north in Norway (Fig. 1 and Table 1). They were all located in areas protected by law (except Lund). The areas were selected in order to span the gradient in deposition of long-range transboundary air pollutants from south-southwest to the north of the country. The six areas cover the main climatic and geographical variation of (middle) and north boreal birch forest in Norway. Most of the reference areas are situated in forests developed by natural regeneration with minor human influence ('naturskog' according to Rolstad et al. 2002). However, grazing pressure by sheep and domestic reindeer have, in some areas, brought about vegetation changes in direction of semi-natural vegetation. The reference areas comprise a comparable range of variation in natural vegetation, e.g. lichen-dominated, bilberry dominated, small fern and tall herb dominated vegetation, related to local variation in soil moisture and soil richness.

The reference area in Børgefjell was established in 1990 (Brattbakk et al. 1991) and methodically revised in 1995 (Eilertsen & Stabbetorp 1997). Lund was established in 1991 (Brattbakk et al. 1992) and the sampling revised in 1996 (Stabbetorp et al. 1999). Åmotsdalen was established in 1991 (Brattbakk et al. 1992), revised in 1994/96 (Bakkestuen et al. 1999a). Møsvatn was established in 1992 (Brattbakk 1993) and revised in 1994/97 (Bakkestuen et al. 1999b). Gutulia and Dividalen were established in 1993 (Eilertsen & Often 1994, Eilertsen & Brattbakk 1994).

Fig. 1. Map of Norway showing the localisation of the 6 monitoring reference areas.

Table 1. Monitoring areas: geographical position, climate and background information. UTM (Universal Transverse Mercator) is according to the World Geodetic System (WGS84). The monitoring areas of Lund, Møsvatn and Åmotsdalen belong to zone 32W, Gutulia and Børgefjell belong to 33W and Dividalen is situated in zone 34W. Vegetation zones, sections and terminology are according to Moen (1999). Mean annual precipitation is estimated from 1961–90 normals (Førland 1993) for stations close to each study area, also taking topographic position and altitude (cf. Sjørs 1948, Førland 1979) into account. Temperature is based upon 1961–90 normals (Aune 1993) for stations close to each area, adjusted for altitude according to Laaksonen (1976). * refers to month with lowest mean normal temperature 1961–90 (January in most cases, occasionally February).

Reference area	County	Municipality	Lat. (EN)	Long. (EE)	UTM grid reference	Vegetation zone	Vegetation section	Altitude (m)	Area (km^2)	Annual precipitation (mm)	Temperature (EC)			First analysed (year)
											Year	Jan.*	Jul.	
Lund	Rogaland	Lund	58°33′	6°26′	LK 50,92	Middle Boreal	Western (O2)	350-420	0.1	2100	6.4	–1.1	14.7	1996
Møsvatn	Telemark	Tinn	59°51-52′	8°17′	MM 60,35	Northern Boreal	Slightly western (O1)	1000-1050	0.3	810	0.8	–8.4	11.4	1997
Gutulia	Hedmark	Engerdal	62°01-03	12°09-11′	UJ 48-53,80-87	Northern Boreal	Transitional (OC)	770-865	5	700	–0.3	–12.0	11.4	1993
Åmotsdalen	Sør-Trøndelag	Oppdal	62°28′	9°28′	NQ 21-23,25-27	Northern Boreal	Transitional (OC)	900-925	1	500	0.7	–8.0	10.5	1996
Børgefjell	Nord-Trøndelag	Røyrvik	65°01-7′	12°44-56′	VN 44-45,15	Northern Boreal	Slightly western (O1)	520-580	0.8	1100	1.4	–8.3	12.1	1995
Dividalen	Troms	Målselv	68°40-45′	19°36-49′	DB 50-51,22	Northern Boreal	Kontinental (C)	385-615	2	300	0.8	–9.4	12.8	1993

GEOLOGY

Precambrian bedrock dominates in all reference areas. however, to variable extents influenced by tectonic movements and metamorphosis linked to the Caledonian mountain formations (Sigmond et al. 1984).

In the Lund area the bedrock consists of gneiss rich in biotite (mica), which give rise to soils relatively poor in mineral nutrients, while the bedrock in the Møsvatn area consists of metarhyolite and metamorphic tuffs belonging to the Rjukan group, which give rise to soils slightly richer in mineral nutrients (Dons & Jorde 1978, Dons et al. 1990).

In Åmotsdalen the Precambrian rocks consist of metamorphic shales rich in quartzitic and granitic materials, feldspar and with elements of deformed basal conglomerates (Krill 1987). The bedrock of Gutulia belongs to the Kvitvola nappe unit (Nystuen & Trømborg 1972, Nystuen 1979), which consists of deformed and metamorphic sandstones rich in quartz and feldspar, normally producing nutrient poor soils. Locally more mica-rich rocks outcrops give rise.to soils somewhat richer in mineral nutrients.

In the Børgefjell area the bedrock is dominated by granites and granitic gneisses poor in mineral nutrients, but with some gneisses richer in feldspar minerals. The investigation area in Dividalen has a higher geodiversity, situated on three main geological units (Osland 1974). The lowest lying part consists of an autochtonous, locally metamorphic granite or granitic gneiss with veins of dark mica and amphibole. The steep intermediate area consists of conglomerate, clay schists and sandstones, in some places with thin zones of limestone. At higher altitudes, the bedrock belongs to a nappe complex, locally with zones with shattered mica rich rocks and marble. The Dividalen reference area is thus very different from the other areas with bedrocks that give rise to soils richer in base minerals, i.e. with high values of pH, Ca and Mg.

QUATERNARY DEPOSITS, LANDFORMS AND TOPOGRAPHY

The Lund reference area is situated 320–420 m a.s.l. in a relatively steep mountain side facing north-east. One of the investigated sites is situated on a gravel deposit between two small lakes. The mountain side varies between even slopes and small gully-like depressions with periodic small streams. In the upper parts, where the terrain is less steep, small fens occur, but most of the mountain side is well drained with a thin layer of till, often with a high block content and with considerable variation in the size of the stone blocks.

The Møsvatn reference area is situated between the high mountains on the Hardangervidda mountain plateau and the deep valleys south of this. The monitoring area (1000–1050 m a.s.l.) is located on the north and east slopes of a small hill, above a mire surrounded by a mountain meadow landscape. The till deposits are thin and discontinuous and contain several bedrock outcrops. In the northern low-lying parts of this reference area the till has a very high content of blocks, compared with the rest of the area.

The Åmotsdalen reference area (900–925 m a.s.l.) is situated on kame terraces and till deposits on the south facing slopes of the valley. Glacifluvial sandy deposits dominate the lower parts of the area. The glacifluvial deposits are linked to a glacier directed drainage system which extends up the valley to passpoints to the west and north-west in the mountains (Sollid et al. 1980a, 1980b). At higher altitudes, thin and discontinuous deposits of till dominate together with mires and bedrock outcrops.

In the Gutulia reference area (770–865 m a.s.l.) till dominates with variable thickness, normally thin at higher altitudes and thicker in the mountain slopes and the valleys. The till contains some limestone and dolomite erratics, originating from sedimentary rocks found between the Precambrian basement and the nappe rocks above.

The Børgefjell reference area is situated between 520 and 580 m a.s.l. A coarse till deposit dominates the area, which contains few bedrock outcrops partly situated on the east slopes of a U-shaped valley, one on weakly convex terrain in between mires and the other on a medium steep valley side.

The Dividalen reference area extents across a wide U-shaped valley in the lower part of the valley side, between 385 and 615 m a.s.l. Glacifluvial deposits are found at middle levels in the valley side. These are linked to a glacier directed drainage system going up the valley to pass points towards the east. Block-rich tills dominate the valley floor. The till is also rich in clay and consolidated, which does not favour drainage. The terrain is therefore locally paludified. At higher elevations the till cover is thin and discontinuous.

CLIMATE

The reference areas span a geographical gradient from south to north Norway with major differences in tempeartures and precipitation (Table 1). The southernmost area, Lund, differed stromgly from the other areas (Table 1). Lund has the highest summer temperature (> 11.5 °C) and the winter temperature is rather mild (> –1.4 °C) (Førland 1993). The other areas have lower summer temperatures, ranging between 11.4 and 8.0 °C. Gutulia has the lowest

winter temperature (–11.4 °C). Lund is also the area with far the highest precipitation while Dividalen to the north has the lowest mean annual precipitation.

VEGETATION ZONES AND SECTIONS

The six reference areas span natural climatic and geographical gradients of Norwegian birch forests (Table 1, Fig. 1) as well as gradients in deposition of major long-distance airborne pollutants (Tørseth & Semb 1997, Aas et al. 2002). The areas span almost the entire oceanicity gradient from the markedly oceanic section (O2) at Lund to the slightly continental section (C1) at Dividalen (terminology of vegetation zones and sections in accordance with Moen 1999). All areas are situated in the north boreal vegetation zone, except Lund which is situated in the lower part of the middle boreal zone, close to the more termophilous south boreal zone (Table 1).

HISTORICAL BACKGROUND OF BOREAL BIRCH FOREST INVESTIGATIONS

Boreal birch forests have been described from central and southern parts of Norway by e.g. Nordhagen (1928, 1943), Mork & Heiberg (1936), Dahl (1957), Aune (1973) and Moen (1990). Several associations in the hierarchical plant sociological system (Braun-Blanquet 1928, 1965, Dierschke 1994) have been proposed by Nordhagen (1943), Kielland-Lund (1972, 1973, 1981) and Aune (1973). Overviews of the relations of birch forests to syntaxonomy have been given by Vevle (1986), Dahl (1986), Kielland-Lund (1994) and Fremstad (1997). Relevés and vegetation descriptions from birch forests spread over Norway have been used to classify the boreal birch forests into vegetation types by Fremstad (1997). These vegetation types are, to a large extent, based on environmental gradients (climate, soil related and long-term human impact). R. Økland & Bendiksen (1985) classified upper boreal and middle boreal vegetation types on poor soils in the Grunningsdalen area in Telemark according to positions along the complex gradient topographic moisture–snow cover into xeric, subxeric, submesic and mesic series. This accord with Finnish studies, e.g. Kalela (1961), Hämet Ahti (1963) and Kielland Lund (1967, 1973, 1981). However, counting the mentioned studies above as well, hardly any environment-vegetation relationships studies using gradient analyses techniques (sensu R. Økland 1990) has been performed in Fennoscandian boreal birch forests. This knowledge gap has been one of the main drivers to complete this monograhy.

AREA HISTORY AND INFLUENCE OF GRAZING

Lund

The Lund reference area is not protected by law, but privately owned. It is situated just outside the Førland/Sletthei landscape Protection area (Fig. 2). The investigated area is located far from built-up areas and only to a small degree influenced by human activity (Brattbakk et al. 1992, Stabbetorp et al. 1999). A sheepwalk occurs in the main valley, Urdalen, and heathland has periodically been burnt on ridges in the vicinity of the reference area until recently. The sheep have access to the investigated area. However, no visual signs of grazing have been recorded from the reference area. The area is used for hunting elk and deer, but it is not heavily used for recreation.

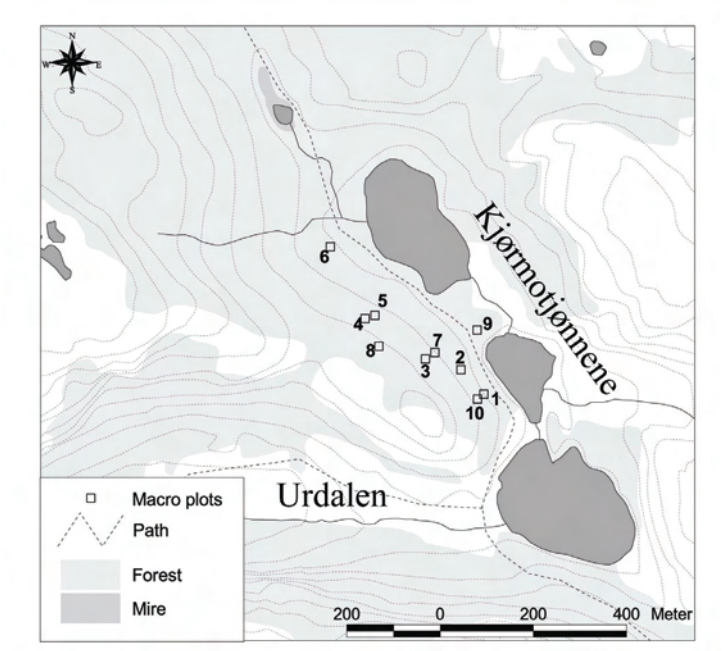

Fig. 2. Map of the reference area Lund with positions of macro plots 1–10. Based on digital N50 maps from the Norwegian Mapping Authority. Map sheet Ørsdalsvatnet 1312 III.

Møsvatn

The reference area is situated on Merakkhaugen on privately owned land within the Møsvatn-Austfjell Landscape Protection Area, protected by law since 1993 (Fig. 3). Summer farming has earlier been common in the area, but at the time of analysis only took place in Hjerdalen (Brattbakk 1993). Today there is a weak grazing pressure by cattle and sheep in and around the investigated plots, and frequent cutting of woods have been observed. Merakkhaugen is visited by some hikers, and in autumn the area is often used by people collecting berries, especially cloudberry. However, it is assumed that the investigated area, due to its position in the north facing slope away from the main pathways, is more protected from grazing, wood cutting and human trampling than the surrounding areas (Bakkestuen et al. 1999a, Bakkestuen & Erikstad 2002).

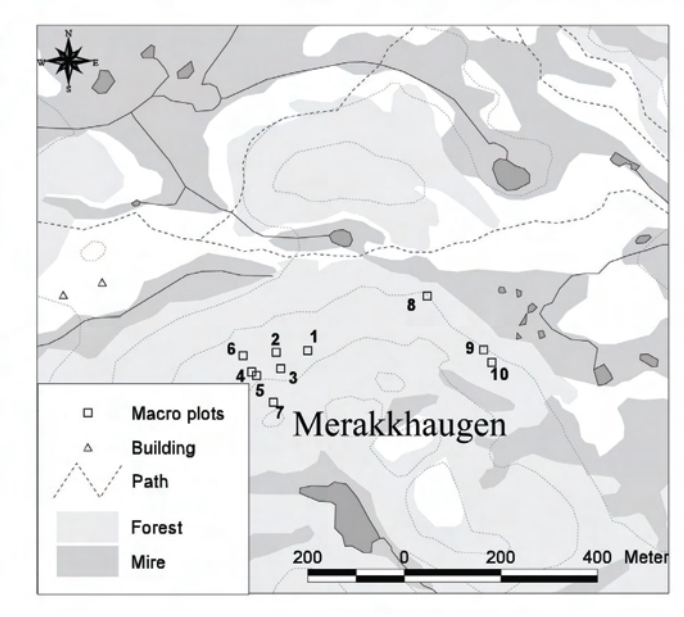

Fig. 3. Map of the reference area Møsvatn with positions of macro plots 1–10. Based on digital N50 maps from the Norwegian Mapping Authority. Map sheet Frøystul 1514 I.

Gutulia

The investigated area (Fig. 4) is state owned land, protected as a part of the Gutulia National Park since 1968. Summer farming was performed regularly in Gutulia until 1949 (Kielland-Lund 1972, Wold 1989). Later on, to restore some of the original mountain dairy farming environment, the pasture has been grazed again by cattle for some years. Only a small area

within the investigation area is considered to be influenced by grazing for the last hundred years (O. Vangen pers. medd, Eilertsen & Often 1994). However, the influence from grazing by domesticated reindeer was at the time of analysis significant in the whole area, particularly above the tree limit, where also the trampling effect is largest. The national park is also much visited by tourists and hikers, but these mainly follow the main tracks outside the reference area. According to Godal & Hauge (1964) and Ø. Aas (1989) there has been some wood cutting in Gutulia and at least four forest fires have occurred in historical times (Wold 1989). However, traces of forest fires were most abundant in pine forests in the area.

Two other vegetation monitoring projects have been established in Gutulia. Boreal coniferous forests are monitored in Gutulia as one of the ten reference areas in 'Vegetational and environmental monitoring of boreal spruce forest' by the Norwegian forest and landscape institute (formerly NIJOS; T. Økland 1993, 1996). The coniferous forest sites are situated just to the south-east of the birch forest reference area. In 1992, NIJOS also established a monitoring project within low alpine vegetation in Gutulia (Rydgren 1994) which has, however, so far not been re-analysed

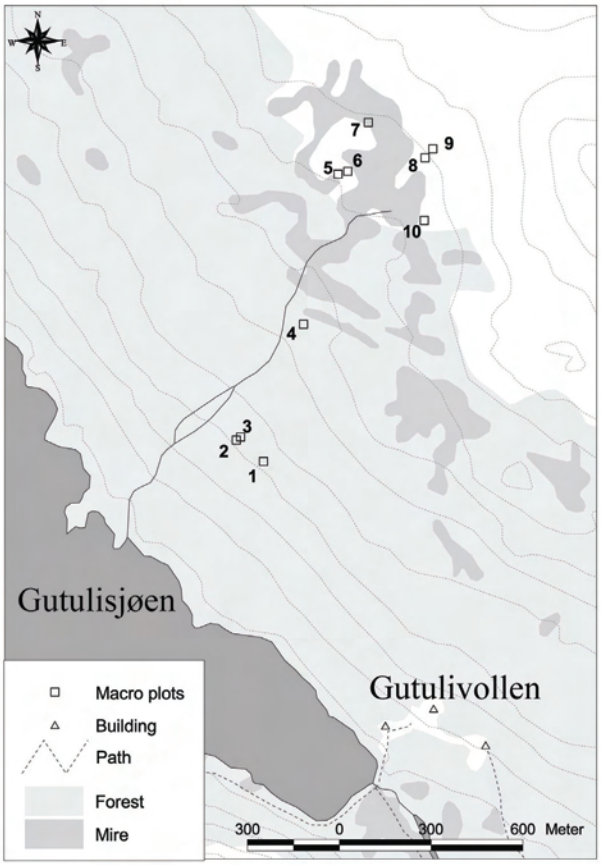

Fig. 4. Map of the reference area Gutulia with positions of macro plots 1–10. Based on digital N50 maps from the Norwegian Mapping Authority. Map sheet Elgå 1719 IV.

Åmotsdalen

The investigated area is privately owned, but from 2002 included in the Åmotsdalen Landscape Protection Area (Fig. 5). Five summer farms have occured in the vicinity of the reference area, while none of these were still in active use at the time of the investigation (Brattbakk et al. 1992). The forests close to the summer farms have earlier been considerably affected by grazing by cattle and sheep, and by removal of shrubs to improve the grazing land. Furthermore they have been affected by wood cutting and hay harvesting. However, the reference area is situated in the least affected parts of the forests, and at the time of analysis the vegetation appeared only slightly affected by grazing. A tourist path runs through the area, but it is not much in use. Some sheepwalks were observed in the investigation area during fieldwork in 1996 (Bakkestuen et al. 1999b).

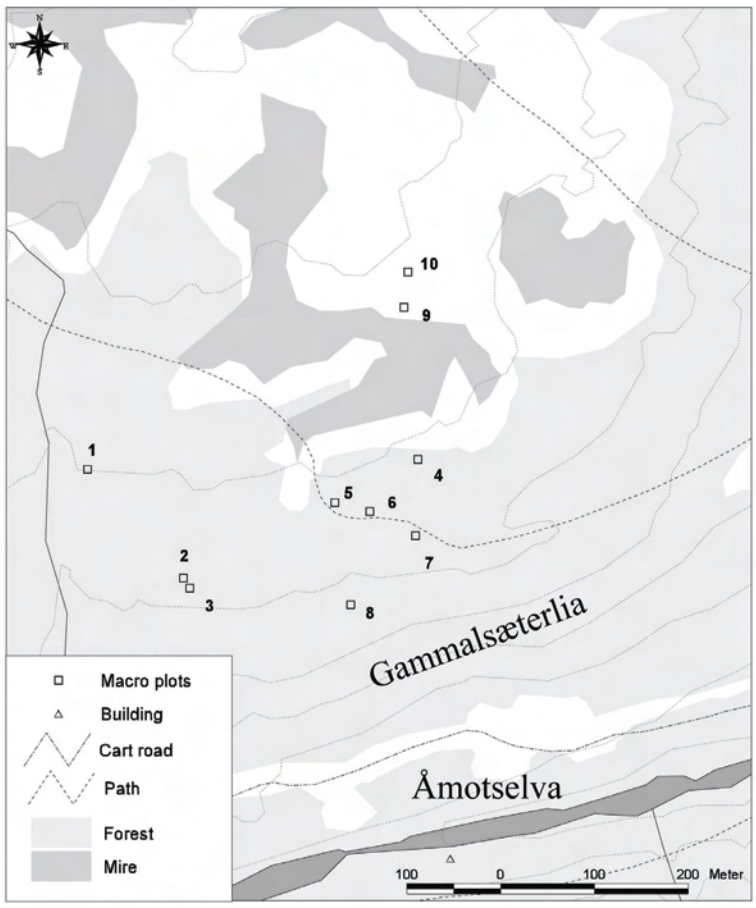

Fig. 5. Map of the reference area Åmotsdalen with positions of macro plots 1–10. Based on digital N50 maps from the Norwegian Mapping Authority. Map sheet Snøhetta 1519 IV.

Børgefjell

The investigated area (Fig. 6) is state owned land and protected as a part of Børgefjell National Park since 1963. A sámi camp is situated close to the reference area, and the whole area was influenced by summer grazing by domestic reindeer. By 1996 the number of reindeer was estimated to be approximately two thousand individuals (Eilertsen & Stabbetorp 1997), and the vegetation in the reference area was likely to be affected by the grazing pressure. Snow scooters were extensively used also within the borders of the national park. Few signs of wood cutting occurred in the area, and no signs of hay harvesting and grazing of

farm animals could be observed. No summer farms exist (or have existed) in the area; just some privately owned cottages and a tourist cottage were present. Hikers get access to the area by a taxi boat across the lake Store Namsvatn. This has resulted in a low but continuous flow of hikers into the area, but this activity seemed not to have any significant influence on the vegetation in the monitored area.

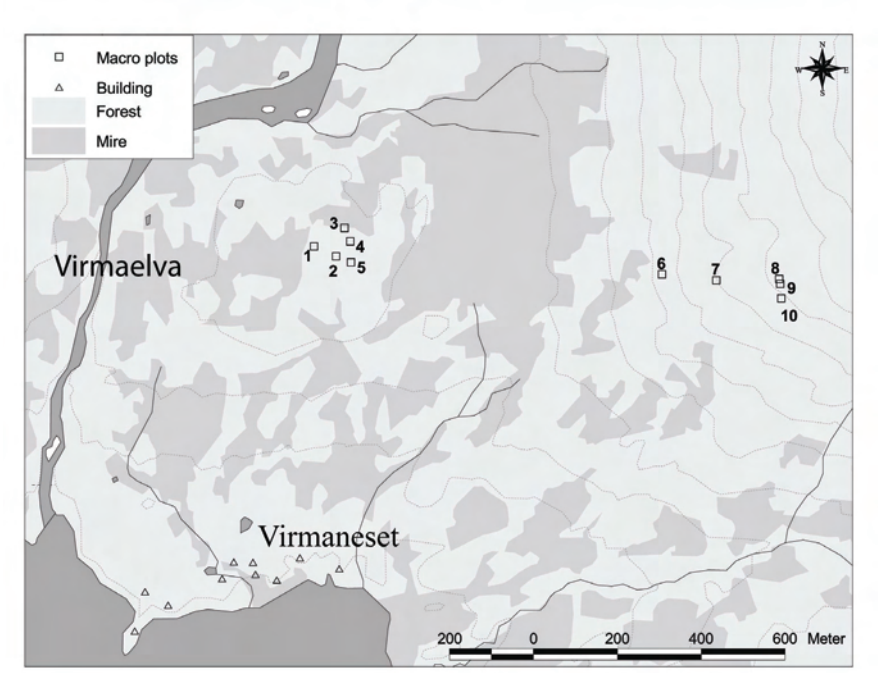

Fig. 6. Map of the reference area Børgefjell with positions of macro plots 1–10. Based on digital N50 maps from the Norwegian Mapping Authority. Map sheet Børgefjellet 1925 IV.

Dividalen

The investigated area is state owned land and is protected as a part of Dividalen National Park since 1971. The National Park is used in the summer by the Swedish sámi villages (sidas) of Lainiovouma and Saarivuoma (Eilertsen & Brattbakk 1994). The area south of Skaterdalen have been utilized by the reindeer management of Saarivuoma (Kalstad 1974). No summer farms have existed in the area and the only traces of fellings in the investigation area occurred along Hagembekken (Fig. 7). Three hiker cabins were situated in the national park, and the area was much visited by locals and tourists. Some human impact occurred along the main tracks, but the major part of the national park is little affected by trampling. Previously there has been military activity in the area (Munch 1974).

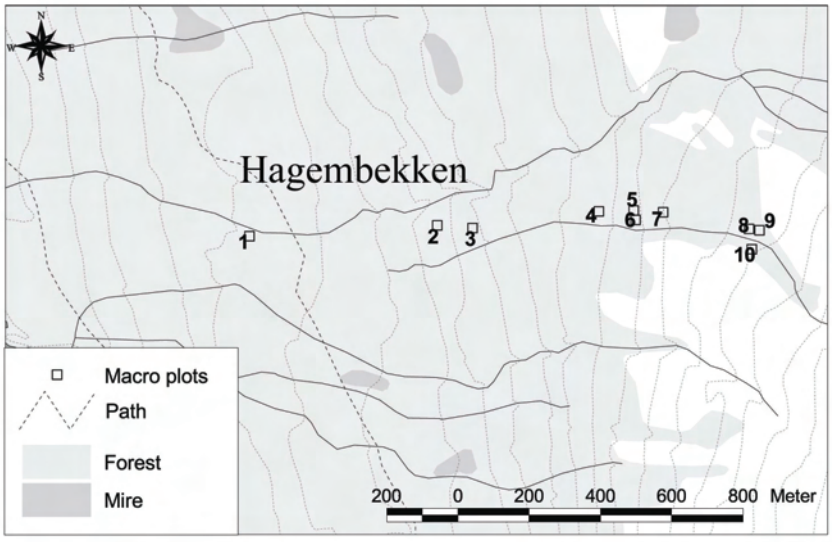

Fig. 7. Map of the reference area Dividalen with positions of macro plots 1–10. Based on digital N50 maps from the Norwegian Mapping Authority. Map sheet Altevatn 1532 II.

MATERIAL AND METHODS

Data were collected from Gutulia and Dividalen in 1993, from Børgefjell in 1995, from Lund and Åmotsdalen in 1996 and from Møsvatn in 1997. These data represents the first analyses of each of the six reference areas with common methodology (see below).

SAMPLING DESIGN

Early phase methodology

When the first four reference areas (Børgefjell in 1990, Lund in 1991, Åmotsdalen in 1991, and Møsvatn in 1992) were established, sites of slightly variable shape and size (approximately 50 m^2) were placed subjectively in homogenous bilberry-dominated birch forests. The vegetation was at that time analysed in sample plots subjectively distributed along transects within each site. At Børgefjell 10 sites were established, with 10 0.5×0.5 m sample plots in each site, 100 in total (Brattbakk et al. 1991). At Lund six sites were established with 6 to 10 1×1 m sample plots in each site, 50 sample plots in total (Brattbakk et al. 1992), while at Åmotsdalen and Møsvatn 10 sites each containing five 1×1 m sample plots were established (Brattbakk et al. 1992, Brattbakk 1993). All sample plots were permanently marked.

New methodology

In 1993 it was decided to include vegetation over a wider range of variation in soil moisture, soil mineral nutrient richness and microclimate within each reference area. In Gutulia and Dividalen, established in 1993, a restricted random sampling procedure was used.

Ten macro plots, each 5×10 m, were placed subjectively in each reference area in order to represent the main floristical and ecological gradients within the birch forest. Five meso plots for vegetation analysis, each 1×1 m, were randomly distributed within each of the macro plots. A meso plot was rejected if containing a tree taller than 2 m or if more than 20% of the plot was covered by stones or fallen tree logs. All plots were placed at least one meter from to the nearest plot to avoid trampling destruction of the vegetation within the plots. The corners of the macro plots and the lower left corner of each meso plot were marked by wooden poles. All corners of the meso plot were permanently marked with subterranean eloxed aluminium tubes. This restricted random sampling procedure is regarded as an optimal compromise between objectivity and time consumption in vegetation monitoring (cf. R. Økland 1990, T. Økland 1996).

Adjustment of early methodology

The field sampling design used in Børgefjell, Lund, Åmotsdalen and Møsvatn reference areas 1990–92 was changed before first re-analysis (in Børgefjell in 1995, in Lund and Åmotsdalen in 1996, and in Møsvatn in 1997).

Thirty of the original sample plots from each reference area were retained, while 20 new 1×1 m sample plots (meso plots) were established within four new macro plots, using the same methods as described for Gutulia and Dividalen. The new macro plots were subjectively positioned within the birch forest of each reference area, to ensure that all 1×1m sample plots together represented the main floristical and ecological gradients within the reference area.

At Børgefjell the original 0.5×0.5 m sample plots were expanded to 1×1 m plots. After adjustment all reference area contains fifty 1×1 m sample plots (meso plots) for vegetation analyses distributed within 10 macro plots (or sites). The total number of meso plots within the TOV birch forest monitoring programme is therefore 300.

RECORDING OF VEGETATION IN THE SAMPLE PLOTS

Each of the 300 meso plots (50 in each reference area) was divided into 16 equally large 0.0625 m^2 subplots. Presence/absence of all species of vascular plants, bryophytes and macrolichens was recorded in each subplot and frequency in subplots calculated as a measure of abundance. A species was recorded as present when any part of the plant was positioned within (over) the subplot. The percentage cover of every species was estimated within each 1×1 m meso plot as an additional measure of abundance. An aluminium frame of 1×1 m was used for exact delineation of subplots.

RECORDING OF ENVIRONMENTAL VARIABLES

A total of 38 explanatory variables including local topography, forest structure, soil properties and regional climatic and geographic variables, were measured or calculated for each of the 300 plots. A summary of explanatory variables with abbreviations is given in Table 2. The term 'explanatory' is used in the statistical meaning of the word to indicate the variables' potential for explaining variation in other data sets (e.g. R. Økland et al. 2001). Causal relationships are discussed *a posteriori* by taking correlations with the explanatory variables as well as other relevant material into account.

Thirty-one local environmental variables were recorded in each reference area at specific scales (macro or meso plot). A local macro plot variable is considered to represent the

entire area around (and encompassing) a meso plot, recorded for a 5×5 m around each plot or for the entire macro plot. Meso plot variables represent the area within the 1×1 m plot.

Table 2. Environmental variables; abbreviation, unit of measurement and potential range of scale. Mmol: millimoles, ddu: day-degree unit.

Abbrev.	Variable	Unit	Pot. range
Local macro plot variables			
Ma Slo	Macro plot slope	°	0-90
Ma Asp	Macro plot aspect unfavourability	°, recalc	0-180
Ma HI	Macro plot heat index		–∞-+∞
Ma Ter	Macro plot terrain form		–2 - +2
Ma Une	Macro plot terrain unevenness		0-5
TBA	Tree basal area	m^3/ha	0-∞
Local meso plot variables			
Me Slo	Meso plot slope	°	0-90
Me Asp	Meso plot aspect unfavourability	°, recalc	0-180
Me HI	Meso plot heat index		–∞-+∞
Me Ter	Meso plot terrain form		–2-+2
Me Une	Meso plot terrain unevenness		1-5
Smi	Minimum soil depth	cm	0-105
Sme	Medium soil depth	cm	0-105
Sma	Maximum soil depth	cm	0-105
Mme	Soil moisture	%	0-100
LOI	Loss-on-ignition	%	0-100
Total N	Kjeldahl nitrogen	mmol(+)/kg/LOI	0-∞
$pH_{(H2O)}$	pH (H_20 – extraction)		0-14
$pH_{(CaCl2)}$	pH ($CaCl_2$ – extraction)		0-14
H	Exchangeable hydrogen	mmol/kg/LOI	0-∞
Al	NH_4NO_3 extractable aluminium	mmol/kg/LOI	0-∞
C	NH_4NO_3 extractable carbon	mmol/kg/LOI	0-∞
Ca	NH_4NO_3 extractable calsium	mmol/kg/LOI	0-∞
Fe	NH_4NO_3 extractable iron	mmol/kg/LOI	0-∞
K	NH_4NO_3 extractable potassium	mmol/kg/LOI	0-∞
Mg	NH_4NO_3 extractable magnesium	mmol/kg/LOI	0-∞
Mn	NH_4NO_3 extractable manganese	mmol/kg/LOI	0-∞
Na	NH_4NO_3 extractable sodium	mmol/kg/LOI	0-∞
P	NH_4NO_3 extractable phosphorous	mmol/kg/LOI	0-∞
S	NH_4NO_3 extractable sulphour	mmol/kg/LOI	0-∞
Zn	NH_4NO_3 extractable zink	μmol/kg/LOI	0-∞
Regional parameters			
Prec.	Annual precipitation	mm	0-∞
T	Mean annual temperature	°C	0-∞
ETS	Effective temperature sum	ddu	0-∞

Tamm's H	Tamm's humidity index	mm	0-∞
Lat.	Latitude	°	–90-90
Long.	Longitude	°C	–180-180
Alt.	Altitude	m	

Local macro plot variables

All macro plot variables, except tree basal area, were measured for each meso plot in a 5×5 m area with the meso plot in the centre. *Macro plot slope* (Ma Slo), representative for the 5×5 m area, was measured by a clinometer The aspect of the 5×5 m area was measured by a 360 ° compass; values were read off to nearest degree. *Macro plot aspect unfavourability* (Ma Asp) expressed as deviation from SSW [202.5 °, cf. T. Økland (1990, 1996), R. Økland & Eilertsen (1993)], was calculated from the aspect measurements. SSW is considered to be the most favourable aspect (Dargie 1984, Heikkinen 1991) due to high incoming radiation at times of day with high temperatures. The *Macro plot heat index* (Ma HI), similar to Parker's index (Parker 1988) was calculated by the following formula:

Ma Hi = tan (Ma Slo) × cos (Ma Asp)

Increasing Ma Hi values reflects increasing solar radiation.

Macro plot terrain form (Ma Ter) was estimated subjectively on a scale from –2 to +2; where –2 indicates a distinctly concave recession in the terrain, –1 indicates a weak concavity, 0 corresponds to an even surface or a balance between concave and convex micro-forms (at scales considerably finer than the macro plot), +1 indicates a weak convexity and +2 indicates a distinct convex ridge or protruding land form at the relevant scale. *Macro plot unevenness* (Ma Une) was estimated subjectively on a scale from 1 to 5, where 1 represents an even surface and 5 represents a surface with many convex and/or concave parts, with high relative altitude differences.

Tree basal area (TBA) was measured at breast height at each meso plot by means of a relascope. The basal area expresses the tree density (m^2/ha) around the plot and thus reflects the supply of light to the understorey vegetation.

Local meso plot variables

Meso plot slope (Me Slo) was measured by placing a clinometer on the metal frame, adjusted to fit the slope of the terrain. The aspect was measured by a 360 ° compass. *Meso plot aspect unfavourability* (Me Asp) was calculated in the same way as for macro plot unfavourability (see above). *Meso plot heat index* (Me HI) was calculated as for macro plot heat index:

Me HI = tan (Me Slo) × cos (Me Asp)

Increasing Me Hi values reflects increasing solar radiation.

Microtopographic indices were calculated from assessments within each of the 16 subplots within the meso plot. The terrain form was assessed on the scale from –2 to +2 for each subplot, where –2 represents a distinct concave terrain and +2 a distinct convex terrain (on the rekevant scale). The mean value for the 16 subplots was termed *meso plot terrain form* (Me Ter), while the variance provides an estimation of the unevenness in the meso plot, *the meso plot terrain unevenness* (Me Une).

Meso plot soil depth was measured by recording the soil depth at eight fixed sites; two on each side of the meso plot approximately ten cm outside the plot. The following three variables were derived: *Minimum soil depth* (Smi), *median soil depth* (Sme) and *maximum soil depth* (Sma).

Soil moisture (Mme) was determined in a volumetric bulk sample collected from the upper 5 cm of the soil, 10 cm outside the meso plot, using a 100 cm^3 metallic soil corer with a lower cutting egde. All samples from one reference area were collected on the same day, after a period of some days without rainfall, with the aim of representing median soil moisture conditions (cf. T. Økland 1990, R. Økland & Eilertsen 1993). The samples were stored in tightly sealed polythene bags. The samples were weighed fresh and oven-dried at 110°C to constant weight, and the water content was calculated as weight percentage of fresh soil and used as a measure for soil moisture.

Soil samples were collected from the upper 5 cm of the humus layer (Oh) for chemical analyses. If the humus layer was less than 5 cm thick, the whole layer was sampled. Several subsamples were collected outside the border of each meso plot and the subsamples were mixed in order to counteract fine-scale spatial variation in physical and chemical properties of the humus. All samples from one reference area were collected on the same day and oven-dried at 25°C as soon as possible after sampling.

The soil samples were analysed at the Norwegian Forest and Landscape Institute according to methods described in Ogner et al. (1991). *Loss on ignition* (LOI) was determined by ignition in muffle furnace at 590°C and expressed as weight percentage of dry soil. Digestible organic nitrogen and NH_4 was analysed by the *Kjeldahl-nitrogen* method (Total N). *pH* was analysed by H_2O extraction, (pH_{H2O}) and $CaCl_2$ extraction (pH_{CaCl2}). *Ammonium nitrate extractable elements* (Al, C, Ca, Fe, K, Mg, Mn, Na, P, S, Zn) were analysed by a simultaneous ICP technique (Inductively-Coupled Plasma Emission Spectroscopy) and *exchangeable acidity/hydrogen* (H) by titration of an ammonium nitrate extract. The

concentrations of extractable elements and Kjeldahl nitrogen were expressed as fractions of loss on ignition as recommended by T. Økland (1988).

Regional climatic and geographical variables

Seven region-scale, climatic and geographical variables (regional variables) were used in the numerical and statistical analyses of the total dataset, comparing the reference areas. *Mean annual precipitation* (Prec.) [normal period 1961–90; Førland (1993)] and *mean annual temperature* (T) [Aune (1993), corrected for altitude according to Laaksonen (1976)] were taken from the nearest weather observation stations. For some reference areas, several weather stations were combined to produce an integrated estimate of precipitation and temperature. *Effective temperature sum* (ETS) according to Laaksonen (1979) and *Tamm's index of humidity* (Tamm's H) (Tamm 1959) were calculated for each macro plot. *Latitude* (Lat.) and *longitude* (Long.) for each reference area and *altitude* (Alt.) for each macro plot were taken from digital N50 maps from the Norwegian Mapping Authority.

NUMERICAL AND STATISTICAL ANALYSES OF DATA SETS FROM EACH REFERENCE AREA

Data manipulation: transformation of variables

For all variables (Tables 2), skewness and kurtosis standardised by division with their expected standard deviations, $(6/n)^{0.5}$ (Sokal & Rohlf 1995), were calculated. Acceptable homogeneity of variances (homoscedasticity) was achieved by transforming all variables to zero skewness [transformation formulae of R. Økland *et al,* (2001) were used]:

$$y'_{kj} = e^{c_k x_{kj}} \quad (1)$$

$$y'_{kj} = \ln(c_k + x_{kj}) \quad (2)$$

$$y'_{kj} = \ln[c_k + \ln(c_k + x_{kj})] \quad (3)$$

where x_{kj} is the original value of variable k in plot j and c_k is a variable-specific parameter determined so that the transformed variable $Y' = \{y_{kj}'\}$ has zero skewness. Eq. (1) was applied to left-skewed variables (standardised skewness < 0), eq. (2) to right-skewed variables and eq. (3) was applied to right-skewed variables for which no value of c_k could be found by eq. (2)

that resulted in standardised skewness = 0. After transformation, all variables Y' were ranged to obtain new variables $Y = \{y_{kj}\}$ on a 0–1 scale:

$$y_{kj} = [y'_{kj} - \min(y'_{kj})]/[\max(y'_{kj}) - \min(y'_{kj})] \quad (4)$$

Ordination of vegetation-sample plot matrices

Detrended Correspondence Analysis (DCA; Hill 1979, Hill & Gauch 1980) ordination was used to extract the main gradients of the frequency in subplot abundance data sets from the six reference areas. The calculations were performed by means of CANOCO 4.5 (ter Braak 1987b, 1990, ter Braak & Smilauer 1998, 2002). Detrending by segments and non-linear rescaling options were used to avoid arch and edge effects of corresponding correspondence analysis (CA) ordinations (R. Økland 1990). The DCA ordination axes are scaled in standard deviation (S.D.) units.

Global Non-metric Multidimensional Scaling, GNMDS (Kruskal 1964a, 1964b) was used to ordinate frequency in subplots data sets from each reference area. GNMDS were run using R Version 2.4.1 (Anonymous 2004a), including packages *vegan* Version 1.9–13 (Oksanen 2007, Oksanen et al. 2007) and *MASS*, the latter included in package cluster *stats* (Anonymous 2004b), using functions *vegdist*, *initMDS*, *isoMDS* and *postMDS*, with options: dimensionality = 2; dissimilarity measure = percentage dissimilarity (Bray-Curtis), standardized by division with species maxima: minimum number of starting configurations = 100, of which one was the DCA; maximum number of iterations = 1000; stress reductions ratio for stopping iteration procedure = 0.99999. Solutions were not accepted unless reached from at least two different starting configurations.

The degree of correspondence between the axes obtained by DCA and GNMDS was tested by calculating Kendall's rank correlation coefficients between scores along the first two DCA axes and the two GNMDS axes. The GNMDS ordination axes were overall very strongly correlated (see results from each reference area) with the corresponding DCA axes. We therefore present only the DCA ordination results which have advantage (over GNMDS) that the ordination axes are scaled in standard deviation (S.D.) units (e.g. R. Økland 1990).

All ordination diagrams were made by ArcView 3.2 (Anonymus1999a).

Methods for correlating ordination axis with environmental data and interpretation of ordination results

DCA ordinations were interpreted by split-plot GLM analysis (Crawley 2002) combined with Kendall's rank correlation coefficient τ calculated between plot scores along DCA axes and environmental variables. Parallel use of these two methods has proved useful because scale-

dependent vegetation-environment relationships are revealed and relationships are evaluated by use of appropriate degrees of freedom (Auestad et al 2008, Liu et al. 2008).

GLM was chosen because it allows flexible handling of data over a wide range of statistical properties (Venables & Ripley 2002). By split-plot analysis each axis, the ordination plot score was used as response variable and one or more environmental variables were used as predictors. The aov function of R version 2.4.1 was used with identity link function and normal errors (Anonymous 2004a). Statistical inference was obtained by considering species (plot) as nested within macro plot. The parameters of SSexpl/SSmacro plot (fraction of variation explained by variable at the macro plot), model coefficient r, F (measurement of fit between predictor and response variables at a given hierarchical level) and P value for F (for a test of no relationship against the two-tailed alternative) were used to determine the contributions of the measured environmental variables to explaining variation in species composition.

Correlation analyses were performed between pairs of local explanatory variables and between these variables and the DCA-ordination sample plot scores. Kendall's τ was used (Conover 1980) as a measure of correlation in both analyses. Kendall's τ is a non-parametric measure (it only takes the ranks of variables into account), recommended by Fenstad et al. (1977) whenever the underlying distribution is unknown (or conditions of homogeneous variances and normal distribution of errors not expected to be satisfied). Kendall's τ and the corresponding statistical test of deviation from 0 were performed in SPSS 11.0 (Anonymous 1999b).

Ordination of environmental data by means of PCA

PCA (Principal Component Analysis) ordination (Pearson 1901, ter Braak & Prentice 1988) was run on a correlation matrix (on centred and standardised transformed variables and conjugate variables), using the 31 local variables from each reference area. Correlation biplot scaling of axes was used to optimise the fit of angles between variable vectors to inter-variable correlations. The resulting PCA axes summarise the correlation structure between the environmental variables. All PCA analyses were performed by means of CANOCO 4.5

Distributions of species abundances in the DCA ordination

Frequencies in subplots for species that occur in more than 5 meso plots were plotted onto the meso plot positions in the DCA ordination diagram for each reference area. This gives valuable information about the autecology of each species (T. Økland 1996). The resulting diagrams were used to make isoline diagrams for environmental variables. Isolines were constructed by block kriging interpolation using kriging interpolation version 3.2 for ArcView

3.2 (Anonymous 1999a). Plot scores in the two-dimensional space spanned by ordination axes 1 and 2 were used as geographic co-ordinates and an isotropic semi-variance analysis of the transformed explanatory variable was performed, using an active lag of 4 S.D. units and steps of 0.25 S.D. units. Interpolation was performed from a grid with cell size of 0.25×0.25 S.D. units. Goodness-of-fit of the three-dimensional surface (and the isolines) was assessed by a cross-validation, jackknifing procedure (Anonymous 1998) whereby r^2 was calculated between the original and the predicted values for the variable. Interpolations were made by use of 12 neighbouring plots. After analysis, the fitted values for the explanatory variable were de-ranged and back transformed to the original scale. De-ranging was performed by solving

$$y_{kj} = \frac{y'_{kj} - \min(y'_{kj})}{\max(y_{kj}) - \min(y_{kj})}$$

for y_{kj}', and back-transformation was performed by solving (1)–(3) for y_{kj}:

$$y'_{kj} = e^{c_k x_{kj}}\ ;\ z_{kj} = \frac{\ln(y'_{kj})}{c_k} \qquad (5)$$

$$y'_{kj} = \ln(c_k + x_{kj})\ ;\ z_{kj} = e^{y'_{kj}} - c_k \qquad (6)$$

$$y'_{kj} = \ln[c_k + \ln(c_k + x_{kj})]\ ;\ z_{kj} = e^{e^{y'_{kj}} - c_k} - c_k \qquad (7)$$

Isolines were smoothed by using a B-spline function (Pavlidis 1982) and visualised as a line theme in ArcView 3.2 (Anonymous 1999a) to fit the de-ranged and back-transformed interpolated values.

NUMERICAL AND STATISTICAL ANALYSES OF THE TOTAL DATA SET FROM ALL REFERENCE AREAS

DCA ordination of the total data set

DCA was performed on the total data set consisting of 300 meso plots from the six reference areas. The same options were used as in the DCA of the data from each reference area.

A second DCA ordination of the total data set was also performed, using 7 covariables for the regional climatic/geographical environmental variables not shared with the local environmental variables (C | E in the terminology used for variation partitioning; see below). These covariables were found as follows:

A Canonical Correspondence Analyses, CCA (ter Braak 1986, 1987a), with the 31 local environmental variables as covariables and the seven regional environmental variables as explanatory variables, was performed on the total data set. The resulting (maximally constrained) seven CCA axes (with sample scores that are linear combinations of the environmental variables, cf. Palmer 1993) sort the variation in species composition that is exclusively attributable to climatic/geographical variables ({C | E}) on axes of decresing importance for variation in species composition.

DCA ordinations of the total data set were interpreted by split-plot GLM analysis (Crawley 2002) combined with Kendall's rank correlation coefficient τ calculated between plot scores along DCA axes and environmental variables.

The DCA ordination with covariables was used to study regional variation in the response of vegetation to main complex-gradients, cf. T. Økland (1996). For selected species, occurrences were plotted at meso-plot positions by using different symbols for each reference area.

NOMENCLATURE

The nomenclature of vascular plants follows Lid & Lid (2005). *Alchemilla* spp. may include several species of the genus, except *A. alpina*. *Dryopteris expansa* agg. may include *Dryopteris expansa* (C.Presl.) Fraser-Jenk. & Jermy, *D. dilatata* (Hoffm.) A. Gray, and *D. carthusiana* (Vill.) H.P.Fuchs. *Euphrasia* spp. and *Taraxacum* spp. may include several species. *Hieracium* is identified to the section level.

The nomenclature of bryophytes follows Frisvoll et al. (1995). *Bryum* spp. is determined to the genus level. *Dicranum fuscescens* agg. may include *D. flexicaule* Brid. and *D. fuscescens* Sm. *Hypnum cupressiforme* agg. may include *H. andoi* A.J.E.Sm., *H.*

cupressiforme Hedw., *H. jutlandicum* Holmen & Warncke and *H. resupinatum* Spruce. *Plagiothecium laetum* includes also *P. denticulatum* (Hedw.) Schimp. and *P. laetum* var. *secundum* (Lindb.) Frisv. et al. (= *P. curvifolium* Schlieph.). *Rhytidiadelphus squarrosus* agg. includes *R. squarrosus* (Hedw.) Warnst. and *R. subpinnatus* (Lindb.) T.Kop. *Chiloscyphus coadunatus* refers to *C. coadunatus* var. *rivularis* (Raddi) Frisv. et al. (= *Lophocolea bidentata* (L.) Dum.). *Scapania* spp. may include several species of the genus. *Lophozia ventricosa* agg. may include *L. silvicola* Buch, *L. ventricosa* (Dicks.) Dum. and *L. longiflora* (Nees) Schiffn.

The nomenclature of lichens follows Krog et al. (1994). *Cladonia arbuscula* agg. may include *C. arbuscula* (Wallr.) Flot. and *C. mitis* Sandst. *Cladonia chlorophaea* agg. may include *C. chlorophaea* (Flörke ex Sommerf.) Spreng., *C. cryptochlorophaea* Asah., *C. grayi* Merr. ex Sandst., *C. fimbriata* (L.) Fr., *C. merochlorophaea* Asah., and *C. pyxidata* (L.) Hoffm. *Cladonia coccifera* agg. may include *C. borealis* S.Stenroos, *C. coccifera* (L.) Willd., and *C. pleurota* (Flörke) Schaer. *Cladonia coniocraea* agg. may include *C. coniocraea* (Flörke) Spreng. and *C. ochrochlora* Flörke.

RESULTS

LUND REFERENCE AREA

Correlations between environmental variables

There were strong pairwise correlations between several of the topographical variables, between topographical and chemical variables and between soil chemical variables (Table 3).

Macro and meso plot slope and heat indices were negatively correlated. Macro and meso plot aspect unfavourability were negatively correlated with heat indices and positively with macro plot terrain unevenness and meso plot slope. Macro plot slope was further positively correlated with median and maximum soil depth. The topographical variables terrain unevenness and terrain form and tree basal area, however, hardly showed significant correlations with other variables.

Macro and meso plot slope and the macro plot heat index were also positively correlated to pH, C and Mn and negatively correlated with Ca, Mg, Zn, P and soil moisture. Soil moisture was positively correlated with LOI, Ca, Mg and Na and negatively correlated with pH. LOI was positively correlated with Ca, Mg, P and Zn.

pH showed an unexpected, positive, correlation with variables reflecting soil acidity such as exchangeable hydrogen (H) and extractable Fe and Al concentrations, and was negatively correlated with concentrations of elements that are typically abundantly present in base-rich soils, such as Ca and Mg. Ca, Mg, P and Zn were, however, positively correlated with each other and negatively correlated with H.

Table 3. Lund: Kendall's rank correlation coefficients τ between 31 environmental variables in the 50 sample plots (lower triangle), with significance probabilities (upper triangle). Statistically significant correlations (P<0.05) in bold face. Names of explanatory variables abbreviated in accordance with Table 2.

	1	2	3	4	5	6	7	8	9	10	11	12	13	14	15	16	17	18	19	20	21	22	23	24	25	26	27	28	29	30	31
01 Ma Slo	*	0.050	**0.000**	0.518	0.752	0.149	**0.000**	0.090	**0.000**	0.453	0.125	0.861	**0.032**	**0.009**	**0.012**	**0.003**	0.084	**0.000**	**0.001**	0.090	**0.002**	**0.000**	**0.007**	**0.001**	0.052	**0.003**	**0.000**	0.068	**0.003**	**0.000**	**0.002**
02 Ma Asp	0.201	*	**0.000**	0.588	**0.016**	0.633	**0.014**	**0.000**	**0.002**	0.092	0.833	0.073	**0.008**	0.906	0.113	0.400	0.129	**0.000**	**0.000**	0.252	**0.034**	0.987	0.232	0.946	**0.000**	0.102	0.893	0.390	0.071	0.232	**0.017**
03 Ma HI	**–0.815**	**–0.383**	*	0.697	0.611	0.160	**0.000**	**0.032**	**0.000**	0.620	0.319	0.827	**0.011**	**0.031**	**0.025**	**0.014**	0.076	**0.000**	**0.000**	0.203	**0.002**	**0.002**	**0.009**	**0.008**	0.235	**0.003**	**0.000**	0.120	**0.004**	**0.000**	**0.002**
04 Ma Ter	0.072	–0.061	–0.043	*	0.432	0.448	0.541	0.098	0.874	0.922	0.584	0.485	0.639	0.406	0.163	0.104	0.659	0.951	0.895	0.143	0.104	0.724	**0.011**	**0.050**	0.491	0.258	0.322	0.791	0.331	0.406	0.197
05 Ma Une	–0.035	**0.267**	–0.055	–0.095	*	0.887	0.765	**0.038**	0.297	0.597	0.478	0.205	0.357	0.693	0.281	0.297	0.210	0.847	0.930	0.258	0.668	0.557	0.456	0.895	0.098	0.386	0.357	0.772	0.732	0.169	0.655
06 TBA	–0.151	0.051	0.145	0.087	–0.016	*	0.172	0.617	0.201	0.385	0.741	0.081	0.339	0.980	0.754	0.754	0.441	0.334	0.352	0.537	0.393	0.365	0.606	0.339	0.347	0.953	0.431	0.832	0.106	0.629	0.806
07 Me Slo	**0.595**	**0.252**	**–0.545**	0.068	0.033	–0.142	*	**0.017**	**0.000**	0.853	0.113	0.707	0.161	0.237	**0.029**	**0.024**	0.167	**0.000**	**0.002**	0.379	0.064	**0.009**	0.099	0.062	0.113	**0.038**	**0.000**	0.530	**0.033**	**0.001**	**0.038**
08 Me Asp	0.169	**0.368**	**–0.211**	–0.182	**0.225**	0.052	**0.238**	*	**0.000**	0.249	0.639	0.253	**0.024**	0.416	0.052	0.292	0.688	0.104	0.082	0.277	0.592	0.763	0.332	0.412	0.284	0.558	0.141	0.241	0.987	0.627	0.503
09 Me HI	**–0.563**	**–0.315**	**0.552**	0.017	–0.113	0.131	**–0.807**	**–0.430**	*	0.788	0.092	0.924	**0.031**	0.209	0.207	0.062	0.328	**0.000**	**0.001**	0.719	0.122	**0.039**	0.328	0.106	0.380	**0.032**	**0.000**	0.520	**0.036**	**0.002**	**0.047**
10 Me Ter	–0.077	0.175	0.050	–0.011	–0.059	–0.092	0.019	0.117	–0.027	*	0.414	0.674	0.490	0.192	0.239	0.297	0.429	0.173	0.134	0.289	0.614	0.490	0.827	0.126	0.219	0.699	0.072	0.274	0.775	0.736	0.219
11 Me Une	0.153	0.021	–0.098	–0.060	0.077	–0.034	0.158	0.046	–0.165	–0.083	*	0.307	0.063	0.960	0.311	0.477	0.770	0.379	0.657	0.053	0.311	0.980	0.114	0.327	0.610	0.189	0.231	0.231	0.353	0.719	0.427
12 Smi	–0.019	0.193	–0.023	–0.082	0.147	–0.192	–0.040	0.120	–0.010	0.045	–0.107	*	**0.000**	0.076	0.066	**0.009**	0.513	0.979	0.530	**0.012**	0.246	**0.008**	0.226	0.194	**0.002**	0.333	**0.016**	0.708	**0.050**	0.155	**0.007**
13 Sme	**0.214**	**0.268**	**–0.251**	–0.051	0.100	–0.099	0.140	**0.222**	**–0.212**	0.070	–0.183	**0.416**	*	**0.000**	0.841	0.907	0.960	0.241	0.248	0.056	0.066	0.713	0.063	0.349	0.357	**0.011**	0.713	**0.040**	**0.009**	0.292	**0.045**
14 Sma	**0.262**	0.012	**–0.213**	0.092	0.043	0.003	0.118	–0.080	–0.124	–0.133	0.005	0.187	**0.397**	*	0.175	0.054	0.061	**0.043**	0.095	**0.003**	**0.002**	**0.021**	**0.010**	**0.004**	0.073	**0.004**	0.763	**0.004**	**0.003**	**0.027**
15 Mme	**–0.248**	0.159	**0.219**	–0.153	0.116	0.032	**–0.217**	0.191	0.123	0.119	0.099	0.192	0.020	–0.134	*	**0.000**	0.162	**0.008**	**0.020**	0.457	**0.026**	**0.000**	**0.014**	**0.000**	**0.010**	**0.007**	**0.003**	**0.004**	**0.044**	**0.002**	0.288
16 LOI	**–0.293**	0.085	**0.241**	–0.178	0.113	–0.032	**–0.224**	0.103	0.182	0.105	0.070	**0.274**	–0.011	–0.190	**0.527**	*	0.162	**0.001**	**0.001**	0.099	**0.000**	**0.000**	**0.000**	**0.000**	**0.006**	**0.000**	**0.002**	**0.000**	**0.001**	**0.000**	**0.028**
17 Total N	0.171	0.153	–0.174	0.048	–0.135	0.079	0.137	–0.039	–0.096	0.080	–0.029	–0.068	0.005	0.185	–0.136	–0.136	*	**0.000**	**0.000**	**0.020**	**0.001**	**0.000**	**0.004**	0.189	**0.003**	**0.006**	0.587	0.345	0.110	**0.000**	**0.021**
18 pH_{H2O}	**0.355**	**0.381**	**–0.416**	0.007	0.021	–0.100	**0.366**	0.160	**–0.357**	0.138	0.087	–0.003	0.115	**0.200**	**–0.262**	**–0.316**	**0.355**	*	**0.000**	**0.005**	**0.000**	**0.000**	**0.000**	**0.004**	0.808	**0.000**	**0.018**	**0.020**	**0.000**	**0.000**	**0.000**
19 pH_{CaCl2}	**0.318**	**0.357**	**–0.382**	–0.015	0.010	–0.096	**0.315**	0.172	**–0.328**	0.152	0.044	–0.066	0.114	0.165	**–0.228**	**–0.325**	**0.357**	**0.834**	*	**0.039**	**0.000**	**0.000**	**0.001**	**0.003**	0.621	**0.000**	**0.014**	**0.029**	**0.000**	**0.000**	**0.000**
20H	0.168	0.115	–0.124	0.160	0.122	–0.063	0.087	–0.107	–0.035	0.107	–0.190	**0.263**	0.187	**0.297**	–0.073	–0.161	**0.228**	**0.278**	**0.203**	*	**0.000**	0.106	**0.000**	**0.000**	0.345	**0.000**	**0.040**	0.162	**0.000**	**0.002**	**0.000**
21 Al	**0.301**	**0.214**	**–0.306**	0.178	–0.046	–0.088	0.184	–0.053	–0.151	0.051	–0.099	0.121	0.181	**0.312**	**–0.218**	**–0.384**	**0.314**	**0.527**	**0.495**	**0.629**	*	**0.003**	**0.000**	**0.000**	0.694	**0.000**	0.993	**0.004**	**0.000**	**0.000**	**0.000**
22 C	**0.348**	0.002	**–0.305**	0.039	–0.063	0.093	**0.260**	–0.030	**–0.202**	–0.070	–0.002	**–0.278**	0.036	**0.228**	**–0.370**	**–0.517**	**0.345**	**0.342**	**0.390**	0.158	**0.290**	*	**0.010**	**0.000**	**0.000**	**0.001**	**0.000**	**0.001**	**0.021**	**0.000**	**0.042**
23 Ca	**–0.268**	–0.120	**0.255**	**–0.278**	0.080	–0.053	–0.164	0.095	0.096	–0.022	0.155	–0.127	–0.182	**–0.252**	**0.241**	**0.342**	**–0.278**	**–0.367**	**–0.330**	**–0.577**	**–0.693**	**–0.251**	*	**0.000**	0.861	**0.000**	0.694	**0.005**	**0.000**	**0.000**	**0.000**
24 Fe	**0.325**	–0.007	**–0.260**	**0.214**	0.014	0.098	0.185	–0.080	–0.158	–0.154	–0.096	–0.136	0.092	**0.280**	**–0.394**	**–0.616**	0.128	**0.283**	**0.288**	**0.358**	**0.504**	**0.558**	**–0.451**	*	**0.024**	**0.000**	**0.037**	**0.000**	**0.000**	**0.000**	**0.001**
25 K	0.193	**–0.207**	–0.116	0.075	–0.179	0.096	0.157	–0.105	–0.086	–0.124	0.050	**–0.329**	–0.090	0.177	**–0.251**	**–0.270**	**0.288**	0.024	0.048	–0.092	–0.038	**0.447**	–0.017	**0.220**	*	0.967	**0.032**	0.139	0.238	**0.001**	0.553
26 Mg	**–0.298**	–0.164	**0.290**	–0.124	0.094	–0.006	**–0.205**	–0.057	**0.210**	–0.039	0.129	–0.101	**–0.248**	**–0.280**	**0.264**	**0.433**	**–0.269**	**–0.498**	**–0.459**	**–0.450**	**–0.693**	**–0.316**	**0.703**	**–0.458**	–0.004	*	0.311	**0.000**	**0.000**	**0.000**	**0.000**
27 Mn	**0.396**	–0.014	**–0.388**	–0.108	–0.099	–0.081	**0.350**	0.145	**–0.344**	–0.181	0.118	**–0.252**	–0.036	–0.030	**–0.293**	**–0.296**	0.053	**0.232**	**0.242**	**–0.200**	0.001	**0.388**	0.038	**0.203**	**0.210**	–0.099	*	**0.034**	0.770	**0.017**	0.900
28 Na	–0.181	0.086	0.152	–0.029	–0.031	–0.022	–0.062	0.115	0.063	0.110	0.118	0.039	**–0.202**	**–0.285**	**0.283**	**0.430**	–0.092	**–0.229**	**–0.214**	–0.136	**–0.278**	**–0.336**	**0.272**	**–0.389**	–0.144	**0.402**	**–0.207**	*	**0.002**	**0.007**	**0.029**
29 P	**–0.293**	–0.181	**0.285**	–0.106	–0.037	0.166	**–0.212**	–0.002	**0.205**	–0.029	0.091	**–0.205**	**–0.258**	**–0.297**	**0.197**	**0.318**	–0.156	**–0.547**	**–0.486**	**–0.546**	**–0.698**	**–0.226**	**0.561**	**–0.466**	0.115	**0.607**	–0.029	**0.296**	*	**0.000**	**0.000**
30 S	**0.413**	0.120	**–0.380**	0.091	–0.148	0.050	**0.343**	0.048	**–0.304**	0.034	–0.035	–0.148	0.103	**0.290**	**–0.300**	**–0.401**	**0.546**	**0.500**	**0.517**	**0.300**	**0.445**	**0.597**	**–0.438**	**0.422**	**0.311**	**–0.471**	**0.233**	**–0.265**	**–0.378**	*	**0.001**
31 Zn	**–0.311**	**–0.241**	**0.309**	–0.141	0.048	–0.025	**–0.205**	–0.066	**0.193**	–0.124	0.078	**–0.281**	**–0.197**	**–0.218**	0.104	**0.215**	**–0.226**	**–0.442**	**–0.402**	**–0.496**	**–0.647**	**–0.198**	**0.602**	**–0.334**	0.058	**0.611**	0.012	**0.213**	**0.561**	**–0.337**	*

PCA ordination of environmental variables

The first PCA axis accounted for 31.6 % (eigenvalue of 0.316) of the variance in the matrix of standardised transformed environmental variables, and the second axis for 15.5 % (eigenvalue of 0.155).

pHH2O, pHCaCl2, extractable Al, S, Fe and C, exchangeable H and macro plot slope obtained high loadings on PCA axis 1 (Fig. 8). Low loadings were obtained by extractable Mg, P, Ca and Zn, LOI and macro- and meso plot heat indices. This negative correlation between the two groups of variables was consistent with the pairwise rank correlation values of the variables in Table 3. Several of the topographical variables that were significantly correlated with the variables mentioned above also had a similar distribution pattern in the PCA ordination duiagram.

Macro plot aspect unfavourablility, minimum soil depth and soil moisture obtained high loadings on PCA axis 2 while extractable K, Fe, Mn and C obtained low loadings.

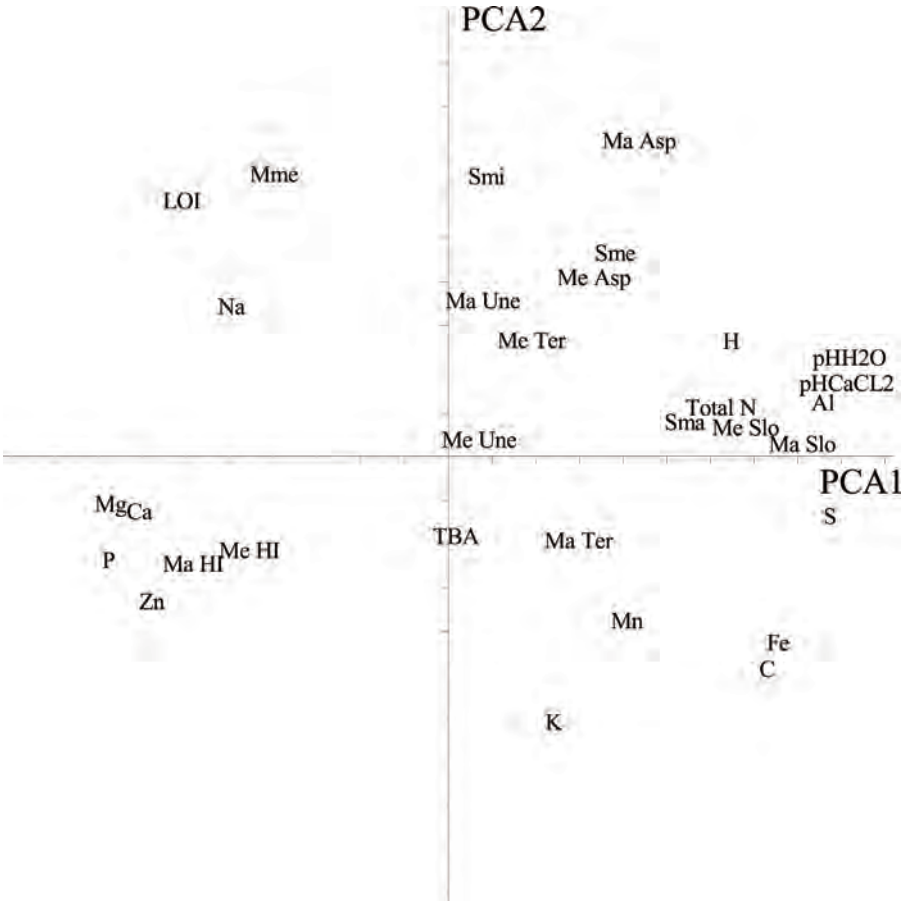

Fig. 8. Lund: PCA ordination of 31 environmental variables. Abbreviations in accordance with Table 2, axes 1 (horizontal) and 2 (vertical). Positions of variables in the ordination space give the head of variable vectors. Tickmarks indicate 0.1 units along both axes.

DCA ordination

The gradient length of DCA axis 1 was 2.37 S.D. units, and the length of DCA axis 2 was 1.15 S.D. units. The eigenvalue of the first axis was 0.230. The next three axes had decreasing eigenvalues of 0.126, 0.073 and 0.046, respectively.

The sample plots were distributed relatively evenly in the DCA ordination diagram, although slightly more plots were located on the left hand side (Fig. 9). Two plots were somewhat separated from the other plots on the right hand side of the diagram. These plots were removed, and a new DCA ordination was performed on the remaining 48 sample plots. As the new ordination did not change the overall distribution pattern of sample plots in the diagram, we decided to use the ordination of all sample plots for further analyses.

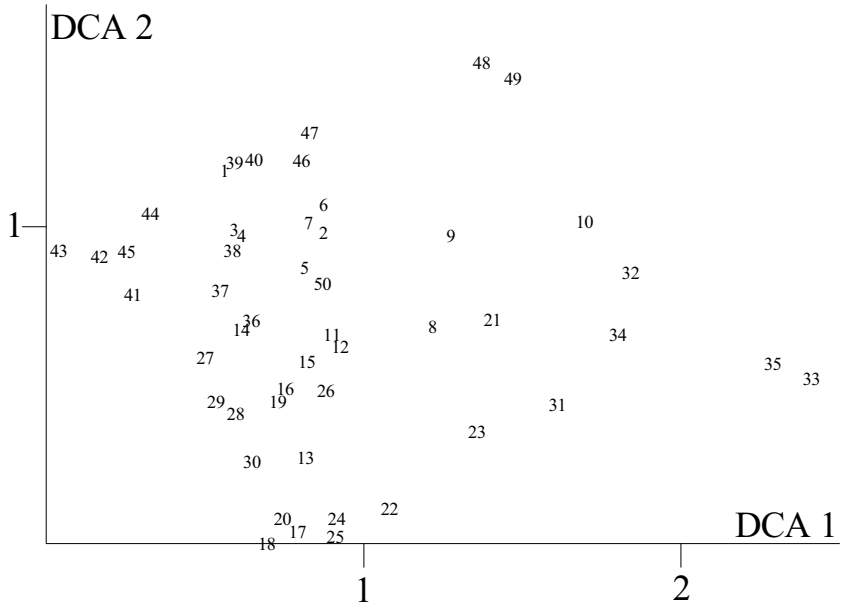

Fig. 9. Lund: DCA ordination diagram of 50 meso plots, axes 1 (horizontal) and 2 (vertical). Meso plot number are plotted just right of the sample plot positions. Scaling of axes in S.D. units.

GNMDS ordination

The GNMDS ordination diagram (Fig. 10) was visually similar with the DCA diagram (Fig. 8b), although plot 43 obtained a higher score along axis 2 in the GNMDS ordination. The correlation between GNMDS axis 1 and DCA axis 1 was $\tau = 0.784$ and for GNMDS axis 2 and DCA axis 2 $\tau = 0.628$ (both $P < 0.001$).

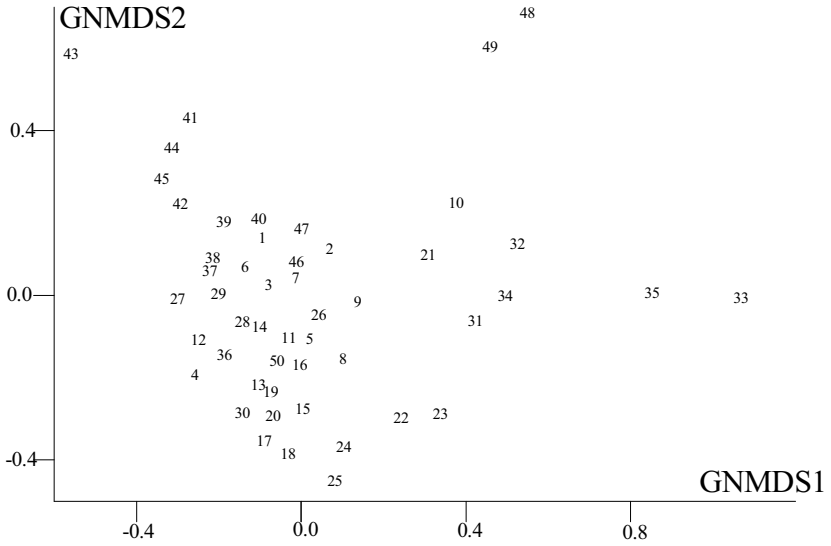

Fig. 10. Lund: GNMDS ordination biplot diagram of 50 plots (indicated by their number).

Split-plot GLM analysis of relationships between ordination axes and environmental variables

Variation (in plot scores) along DCA axis 1 was partitioned with 84.49 % at the macro-plot scale (i.e. between macro plots) and 15.51 % at the (between) meso plot scale within macro plots (Table 4). For the second ordination axis, 78.76 % of the variation was explained at the macro-plot scale and 21.24 % at the meso plot scale (Table 5)

At the macro-plot scale, eleven environmental variables were significantly (at the $\alpha = 0.05$ level) related to DCA 1 while five variables (also at the $\alpha = 0.05$ level) were related to DCA 2. At the plot scale level, nine environmental variables were significantly related to DCA 1 and two variables to DCA 2 (Tables 4 and 5).

At the macro-plot scale, soil concentrations of Ca, Mg, P and Zn decreased significantly along DCA 1 while pH and the concentrations of Total N, H and Al, macro plot aspect unfavourability and meso plot terrain form increased. At the plot scale, many of these variables showed the same tendencies. Predictors with additional significant relationship at the plot scale were meso plot unevenness which decreased (at the $\alpha = 0.05$ level) while medium soil depth (Sme) increased. Macro plot aspect unfavourability, meso plot terrain form and the concentration of Zn were, however, not significantly related to DCA 2 on the plot scale.

At the macro-plot scale, DCA 2 was positively related to the concentration of K and negatively related to aspect unfavourability, soil moisture, loss on ignition and the

concentration of Na in soil. At the plot scale, DCA axis 2 was significantly negatively related to meso plot slope and significantly positively related to meso plot heat index (Table 5).

Table 4. Lund: Split-plot GLM analysis and Kendall's nonparametric correlation coefficient τ between DCA 1 and 31 environmental variables (predictor) in the 50 plots. df_{resid}: degrees of freedom for the residuals; *SS*: total variation; *FVE*: fraction of total variation attributable to a given scale (macro plot or plot); SS_{expl}/SS: fraction of the variation attributable to the scale in question, explained by a variable; *r*: model coefficient (only given when significant at the α = 0.05 level, otherwise blank); *F*: *F* statistic for test of the hypothesis that $r = 0$ against the two-tailed alternative. Split-plot GLM relationships significant at level α = 0.05, *P*, *F*, *r* and SS_{expl}/SS, and Kendall's nonparametric correlation coefficient $|\tau| \geq 0.30$ are given in bold face. Numbers and abbreviations for names of environmental variables are in accordance with Table 2.

Predictor	Dependent variable = DCA 1 (*SS* = 12.1733)								Correlation between predictor and DCA 1
	Error level								
	Macro plot df_{resid} = 8 $SS_{macro\ plot}$ = 10.2848 *FVE* = 0.8449 of *SS*				Plot within macro plot df_{resid} = 39 SS_{plot} = 1.88852 *FVE* = 0.1551 of *SS*				Total
	$SS_{expl}/SS_{macro\ plot}$	*r*	*F*	*P*	SS_{expl}/SS_{plot}	*r*	*F*	*P*	τ
Ma Slo	0.2219		2.2815	0.1694	0.0084		0.3302	0.5688	0.270
Ma Asp	**0.4466**	**0.9461**	**6.4551**	**0.0346**	0.0098		0.3866	0.5377	**0.400**
Ma HI	0.2699		2.9570	0.1238	0.0105		0.4142	0.5236	**–0.337**
Ma Ter	0.0011		0.0084	0.9293	0.0208		0.8292	0.3681	–0.125
Ma Une	0.0367		0.3050	0.5958	0.0212		0.8430	0.3642	0.099
TBA	0.0214		0.1747	0.6870	0.0481		1.9706	0.1683	–0.086
Me Slo	0.2717		2.9843	0.1223	0.0033		0.1294	0.7210	**0.322**
Me Asp	0.2464		2.6161	0.1444	0.0107		0.4236	0.5190	0.294
Me HI	0.2440		2.5821	0.1467	0.0000		0.0003	0.9955	–0.293
Me Ter	**0.4894**	**3.0151**	**7.6669**	**0.0243**	0.0010		0.0382	0.8460	0.210
Me Une	0.0055		0.0441	0.8389	**0.1737**	**–0.3918**	**8.1997**	**0.0067**	–0.080
Smi	0.3257		3.8641	0.0849	0.0815		3.4594	0.0705	0.239
Sme	0.1569		1.4890	0.2571	**0.1256**	**0.4043**	**5.6031**	**0.0230**	0.218
Sma	0.1183		1.0738	0.3304	0.0352		1.4224	0.2402	0.056
Mme	0.0013		0.0102	0.9222	0.0022		0.0862	0.7706	–0.096
LOI	0.0008		0.0065	0.9379	0.0002		0.0076	0.9308	–0.053
Total N	**0.5568**	**2.0410**	**10.050**	**0.0132**	0.0001		0.0055	0.9410	0.273
$pH_{(H2O)}$	**0.6956**	**2.2347**	**18.283**	**0.0027**	**0.1753**	**0.5774**	**8.2895**	**0.0064**	**0.511**
pH_{CaCl2}	**0.7261**	**2.2714**	**21.208**	**0.0017**	**0.1588**	**0.5124**	**7.3636**	**0.0098**	**0.500**
H	**0.5077**	**2.3715**	**8.2486**	**0.0208**	**0.1406**	**0.4577**	**6.3826**	**0.0157**	–0.298
Al	**0.5783**	**1.9645**	**10.972**	**0.0107**	0.0706		2.9642	0.0931	**0.309**
C	0.0551		0.4670	0.5137	0.0092		0.3604	0.5518	0.184
Ca	**0.5188**	**–2.3164**	**8.6251**	**0.0188**	**0.0964**	**–0.3769**	**4.1628**	**0.0481**	–0.251
Fe	0.0015		0.0123	0.9146	0.0002		0.0061	0.9384	0.290
K	0.0193		0.1570	0.7023	**0.1399**	**–0.5058**	**6.3454**	**0.0160**	–0.082
Mg	**0.5321**	**–2.3242**	**9.0990**	**0.0167**	**0.1211**	**–0.4074**	**5.3728**	**0.0258**	–0.293
Mn	0.0117		0.0948	0.7660	0.0030		0.1187	0.7323	0.228
Na	0.0084		0.0682	0.8006	0.0421		1.7140	0.1981	–0.091
P	**0.4680**	**–1.9429**	**7.0384**	**0.0291**	**0.1497**	**–0.4073**	**6.8654**	**0.0125**	–0.298
S	0.3645		4.5884	0.0646	0.0433		1.7644	0.1918	**0.309**

Zn	**0.8342**	**–2.4589**	**40.254**	**0.0002**	0.0213	0.848	0.3628	**–0.339**

Table 5. Lund: Split-plot GLM analysis and Kendall's nonparametric correlation coefficient τ between DCA 2 and 31 environmental variables (predictor) in the 50 plots. df_{resid}: degrees of freedom for the residuals; *SS*: total variation; *FVE*: fraction of total variation attributable to a given scale (macro plot or plot); SS_{expl}/SS: fraction of the variation attributable to the scale in question, explained by a variable; *r*: model coefficient (only given when significant at the α = 0.05 level, otherwise blank); *F*: *F* statistic for test of the hypothesis that $r = 0$ against the two-tailed alternative. Split-plot GLM relationships significant at level α = 0.05, *P*, *F*, *r* and SS_{expl}/SS, and Kendall's nonparametric correlation coefficient $|\tau| \geq 0.30$ are given in bold face. Numbers and abbreviations for names of environmental variables are in accordance with Table 2.

Predictor	Dependent variable = DCA 2 (*SS* = 12.1733)								Correlation between predictor and DCA 2
	Error level								
	Macro plot df_{resid} = 8 $SS_{macro\ plot}$ = 5.5784 *FVE* = 0.7876 of *SS*				Plot within macro plot df_{resid} = 39 SS_{plot} = 1.50473 *FVE* = 0.2124 of *SS*				Total
	$SS_{expl}/SS_{macro\ plot}$	*r*	*F*	*P*	SS_{expl}/SS_{plot}	*r*	*F*	*P*	τ
Ma Slo	0.1084		0.9730	0.3528	0.0303		1.2184	0.2764	0.170
Ma Asp	**0.4576**	**–0.7053**	**6.7504**	**0.0317**	0.0139		0.5497	0.4629	**–0.381**
Ma HI	0.0008		0.0068	0.9365	0.0298		1.1990	0.2802	–0.075
Ma Ter	0.1384		1.2846	0.2899	0.0070		0.2753	0.6028	0.133
Ma Une	0.2716		2.9830	0.1224	0.0086		0.3392	0.5637	–0.297
TBA	0.0186		0.1517	0.7070	0.0029		0.1128	0.7387	–0.051
Me slo	0.0774		0.6710	0.4364	**0.1128**	**–0.0650**	**4.9587**	**0.0318**	0.054
Me Asp	0.2764		3.0565	0.1185	0.0585		2.4240	0.1276	–0.255
Me HI	0.0055		0.0446	0.8380	**0.1966**	**0.5199**	**9.5450**	**0.0037**	0.053
Me Ter	0.0280		0.2301	0.6443	0.0037		0.1448	0.7056	–0.092
Me Une	0.0646		0.5526	0.4785	0.0060		0.2358	0.6300	0.019
Smi	0.1121		1.0100	0.3443	0.0045		0.1770	0.6763	–0.148
Sme	0.1349		1.2472	0.2965	0.0000		0.0011	0.9742	–0.158
Sma	0.2085		2.1079	0.1846	0.0013		0.0515	0.8217	0.135
Mme	**0.5780**	**–1.0537**	**10.958**	**0.0107**	0.0357		1.4454	0.2365	**–0.402**
LOI	**0.4372**	**–0.9283**	**6.2146**	**0.0376**	0.0394		1.6016	0.2132	**–**0.291
Total N	0.0303		0.2496	0.6308	0.0063		0.2455	0.6230	0.179
$pH_{(H2O)}$	0.0164		0.1337	0.7241	0.0000		0.0000	0.9770	0.030
pH_{CaCl2}	0.0040		0.0320	0.8625	0.0011		0.0430	0.8368	–0.012
H	0.0895		0.7867	0.4010	0.0023		0.0909	0.7646	0.063
Al	0.1066		0.9545	0.3572	0.0167		0.6642	0.4200	0.104
C	0.3010		3.4446	0.1006	0.0463		1.8942	0.1766	0.213
Ca	0.2323		2.4207	0.1584	0.0027		0.1039	0.7490	–0.149
Fe	0.3904		5.1225	0.0535	0.0406		1.6495	0.2066	0.179
K	**0.5131**	**1.6687**	**8.4307**	**0.0198**	0.0146		0.5776	0.4518	**0.358**
Mg	0.1925		1.9078	0.2046	0.0109		0.4315	0.5151	–0.215
Mn	0.0696		0.5981	0.4615	0.0041		0.1614	0.6900	0.136
Na	**0.4694**	**–1.6676**	**7.0773**	**0.0288**	0.0024		0.0928	0.7623	0.087
P	0.1185		1.0755	0.3300	0.0441		1.8010	0.1874	–0.040
S	0.2200		2.2570	0.1714	0.0362		1.4643	0.2335	–0.040
Zn	0.0566		0.4804	0.5079	0.0124		0.4916	0.4874	–0.064

Correlations between DCA ordination axes and environmental variables

Eight environmental variables had correlations with DCA axis 1 and three with DCA axis 2 at the $|\tau| > 0.3$ level (Tables 4 and 5). The two measures of pH ($pH_{(H2O)}$, $\tau = 0.511$ and $pH_{(CaCl2)}$, $\tau = 0.500$) were best correlated with the first DCA axis (Fig. 15), while soil moisture ($\tau = -0.402$) was the variable most strongly correlated with DCA 2 (Fig. 14).

Other strong correlations with DCA 1 and 2 at the $|\tau| > 0.3$ level which are visualised in isodiagram figures are macro plot aspect ($\tau = -0.400$, Fig. 11), macro plot heat index ($\tau = -0.337$, Fig. 12), meso plot slope ($\tau = -0.322$, Fig. 13) and the concentrations of Al ($\tau = -0.303$, Fig. 16), K ($\tau = 0.358$ with DCA 2, Fig. 17), S ($\tau = 0.309$, Fig. 18) and Zn ($\tau = -0.339$, Fig. 19).

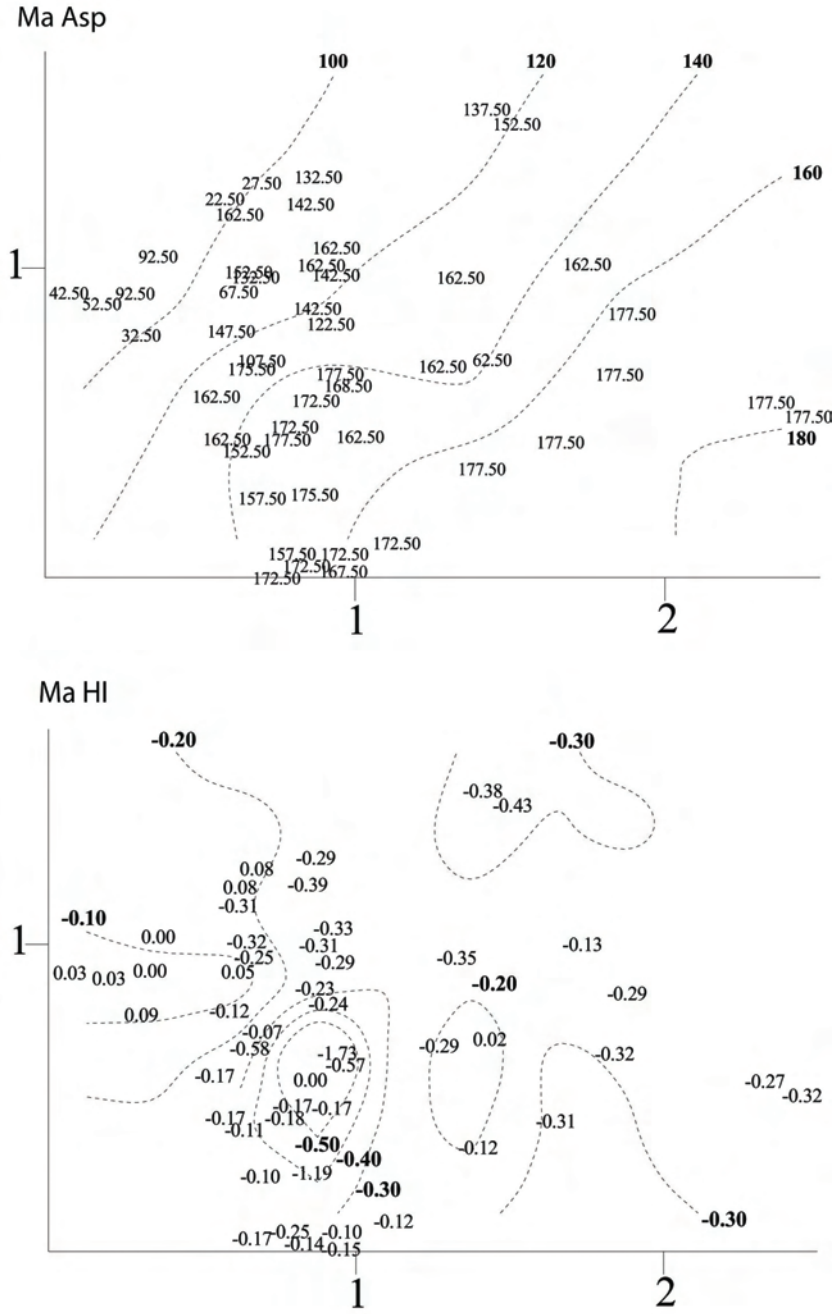

Figs 11-12. Lund: isolines for environmental variables in the DCA ordinations of 50 meso plots, axes 1 (horizontal) and 2 (vertical). Values for the environmental variables are plotted onto the meso plots' positions. Scaling in S.D. units. Fig. 11. Ma Asp (R^2 = 0.491). Fig. 12. Ma HI (R^2 = 0.573). R^2 refers to the coefficient of determination between original and smoothened values as interpolated from the isolines. Names of environmental variables in accordance with Table 2.

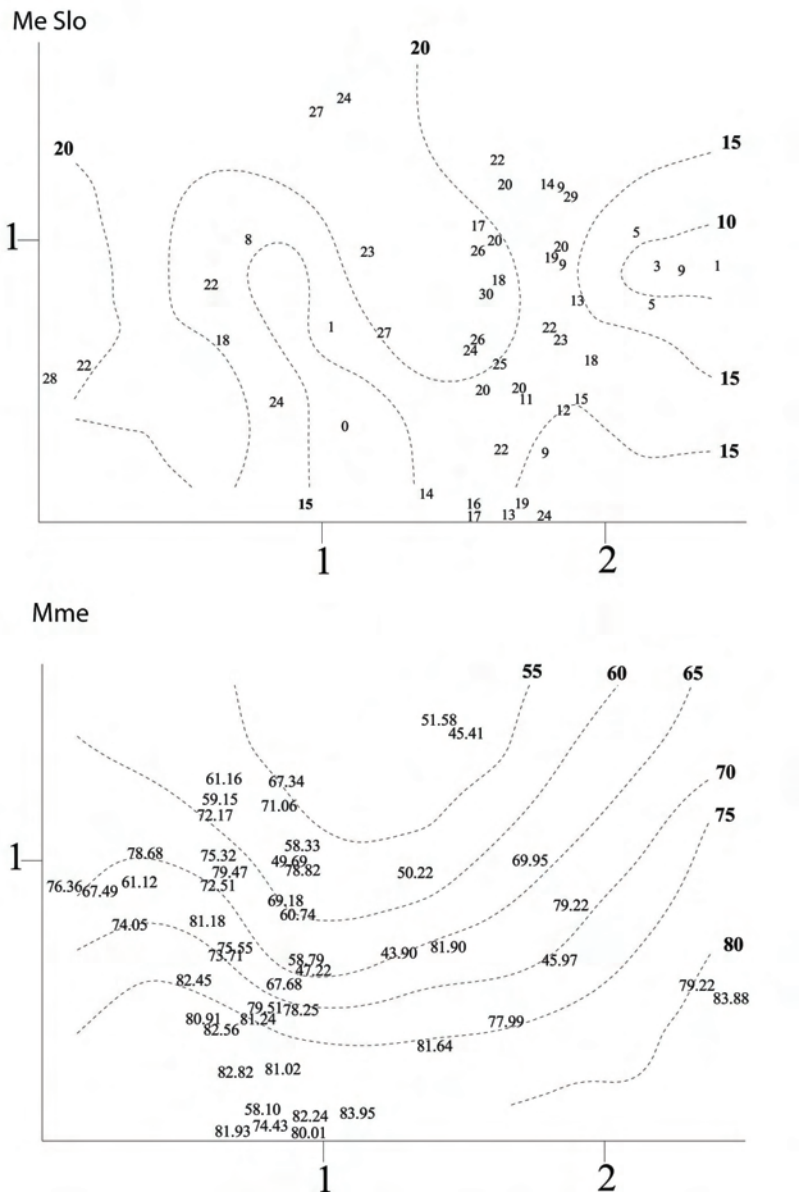

Figs 13-14. Lund: isolines for environmental variables in the DCA ordinations of 50 meso plots, axes 1 (horizontal) and 2 (vertical). Values for the environmental variables are plotted onto the meso plots' positions. Scaling in S.D. units. Fig. 13. Me Slo (R^2 = 0.493). Fig. 14. Mme (Soil moisture) (R^2 = 0.503). R^2 refers to the coefficient of determination between original and smoothened values as interpolated from the isolines. Names of environmental variables in accordance with Table 2.

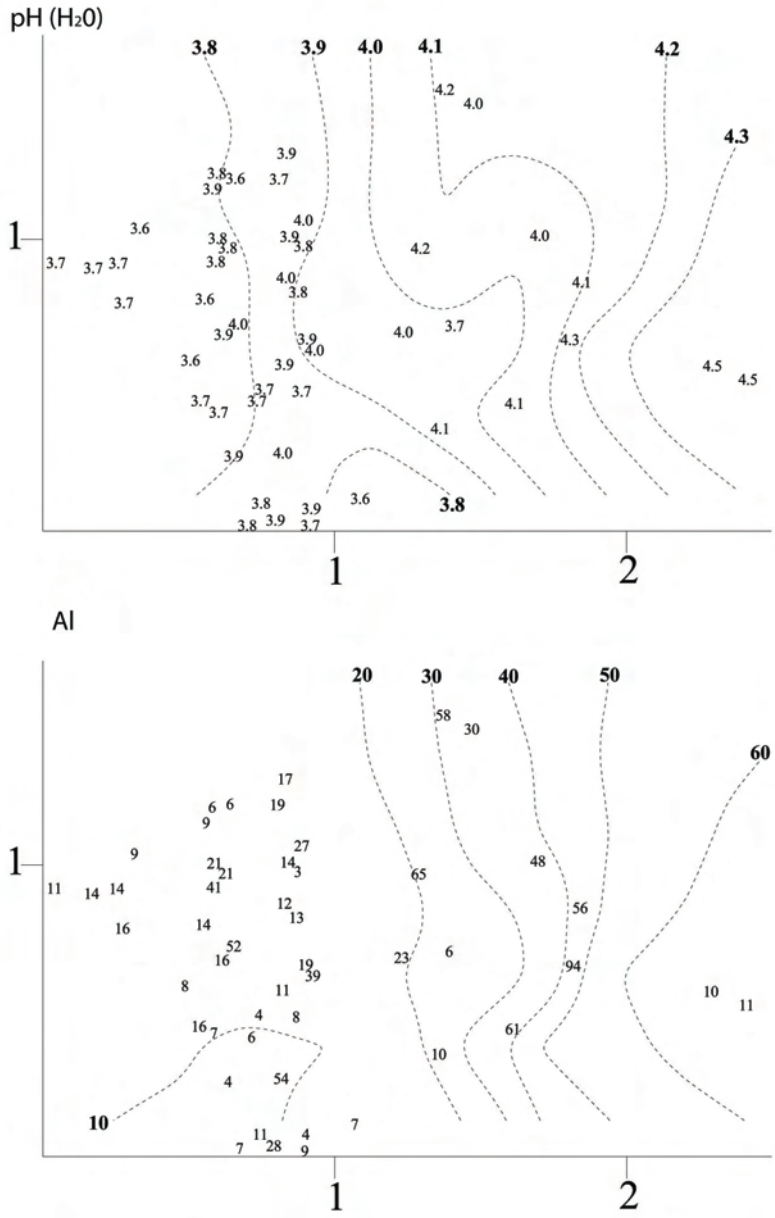

Figs 15-16. Lund: isolines for environmental variables in the DCA ordinations of 50 meso plots, axes 1 (horizontal) and 2 (vertical). Values for the environmental variables are plotted onto the meso plots' positions. Scaling in S.D. units. Fig. 15. $pH_{(H2O)}$ ($R^2 = 0.605$). Fig. 16. Al ($R^2 = 0.508$). R^2 refers to the coefficient of determination between original and smoothened values as interpolated from the isolines. Names of environmental variables in accordance with Table 2.

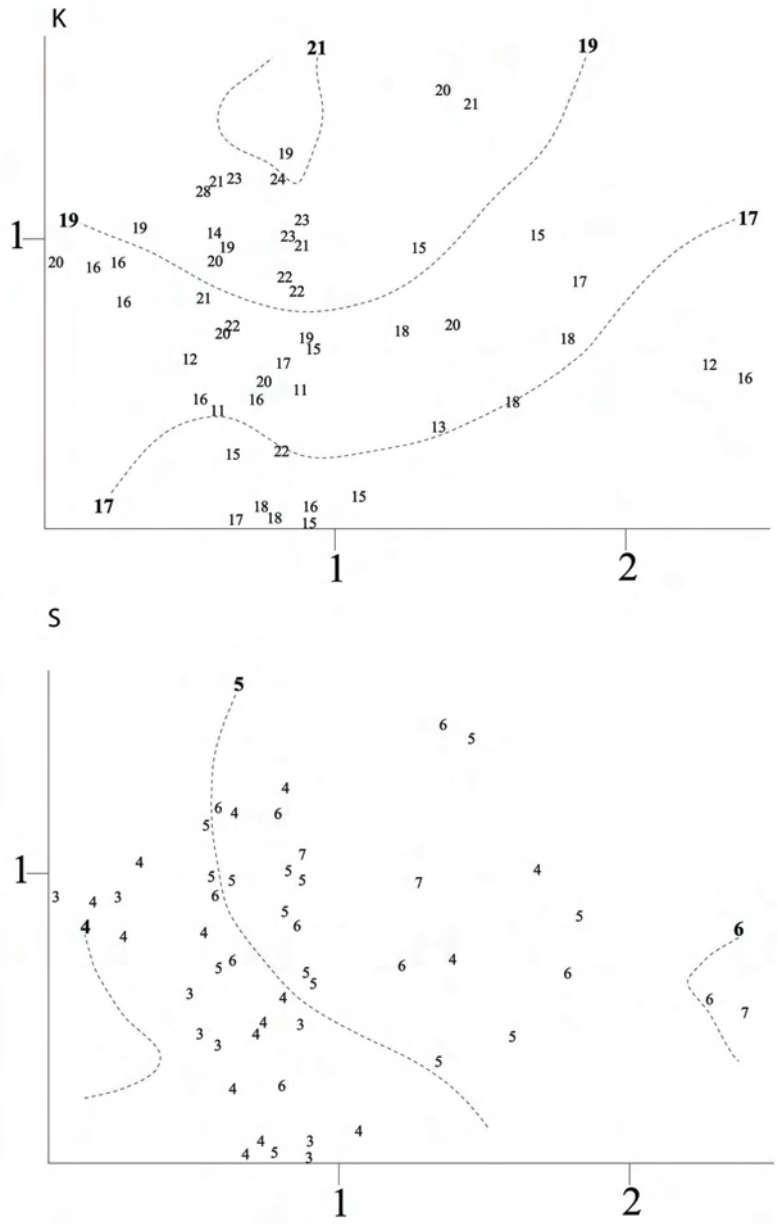

Figs 17-18. Lund: isolines for environmental variables in the DCA ordinations of 50 meso plots, axes 1 (horizontal) and 2 (vertical). Values for the environmental variables are plotted onto the meso plots' positions. Scaling in S.D. units. Fig. 17. K (R^2 = 0.437). Fig. 18. Al (R^2 = 0.564). R^2 refers to the coefficient of determination between original and smoothened values as interpolated from the isolines. Names of environmental variables in accordance with Table 2.

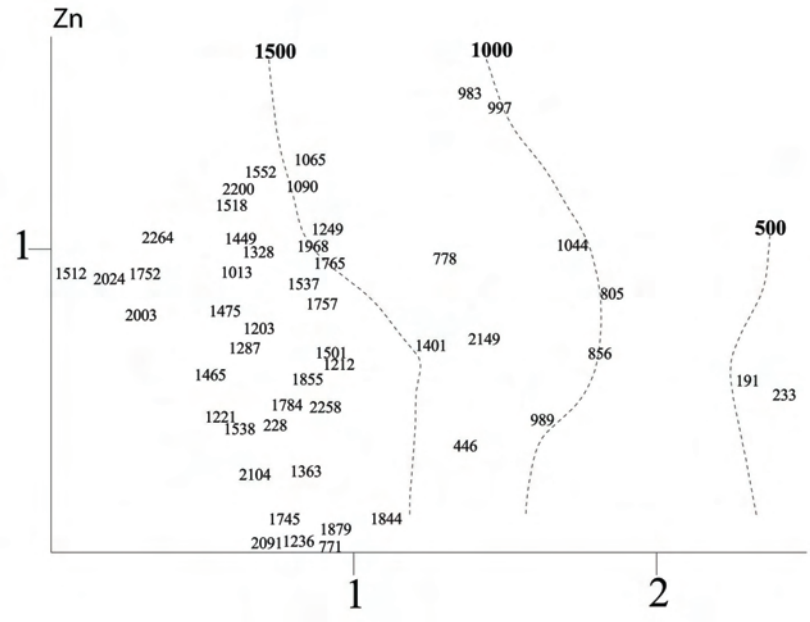

Fig. 19. Lund: isolines for environmental variables in the DCA ordinations of 50 meso plots, axes 1 (horizontal) and 2 (vertical). Values for the environmental variables are plotted onto the meso plots' positions. Scaling in S.D. units. Fig. 19. Zn (R^2 = 0.585). R^2 refers to the coefficient of determination between original and smoothened values as interpolated from the isolines. Names of environmental variables in accordance with Table 2.

Frequent species

A total of 69 species were recorded within the fifty 1×1m meso sample plots: 35 vascular plants, 19 mosses, 15 liverworts (and no lichens). The most frequent species were (the sum of subplot frequencies in brackets): *Vaccinium myrtillus* (779 out of 800), *Avenella flexuosa* (744), *Vaccinium vitis-idaea* (543), *Trientalis europaea* (452), *Maianthemum bifolium* (386), *Pleurozium schreberi* (363), *Dicranum majus* (339), *Polytrichastrum formosum* (311), *Rhytidiadelphus loreus* (278), and *Plagiothecium undulatum* (271).

The distribution of species abundance in the DCA ordination

Common species with wide ecological amplitude were *Vaccinium myrtillus* (Fig. 22), *Maianthemum bifolium* (Fig. 29), *Trientalis europaea* (Fig. 35) and *Avenella flexuosa* (Fig. 37).

Species restricted to the left hand side of the ordination diagram and which hence showed optimum in sample plots with low pH values were *Calluna vulgaris* (Fig. 21),

Chamaepericlymenum suecicum (Fig. 26), *Linnaea borealis* (Fig. 28), *Lycopodium annotinum* (Fig. 29) and *Melampyrum pratense* (Fig. 31). The mosses *Dicranum scoparium* (Fig. 42), *Hylocomium splendens* (Fig. 44) and *Pleurozium schreberi* (Fig. 48) also showed preference for low DCA axis 1 values.

Agrostis capillaris (Fig. 36), *Diplophyllum taxifolium* (Fig. 55) and to some extent *Blechnum spicant* (Fig. 25), *Phegopteris connectilis* (Fig. 32) and *Potentilla erecta* (Fig. 33), situated at the right hand side of the DCA diagram, showed preferences for sites with higher pH.

Plagiothecium laetum (Fig. 46) and *Calypogeia muelleriana* (Fig. 52) had lower frequencies in the subplots, but seemed not to vary systematically along first two DCA axes. Most of the other species had their optimum distribution at low to medium DCA axis 1 scores.

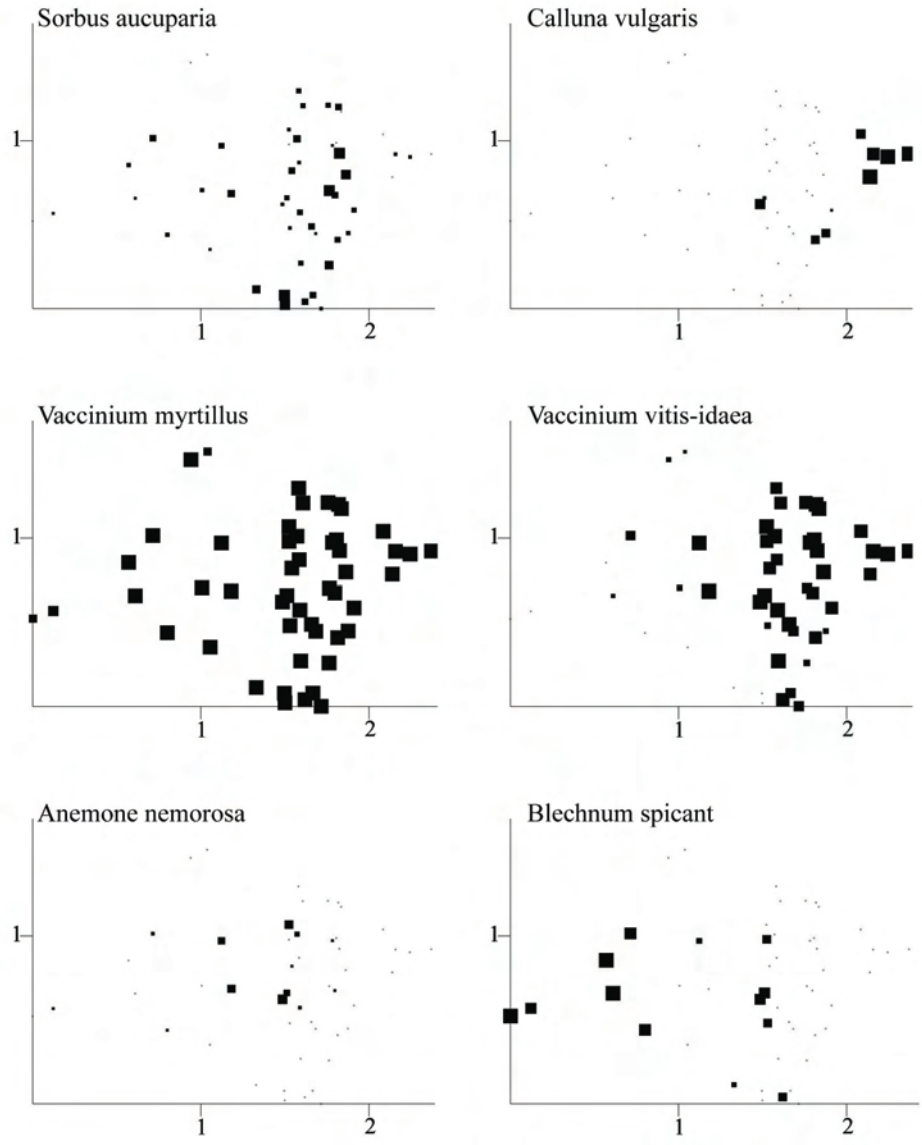

Figs 20-25. Lund: distributions of species abundances in the DCA ordination of 50 sample plots, axes 1 (horizontal) and 2 (vertical). Frequency in subplots for each species in each meso plot proportional to quadrate size. Scaling in S.D. units. Fig. 20. *Sorbus aucuparia*. Fig. 21. *Calluna vulgaris*. Fig. 22. *Vaccinium myrtillus*. Fig. 23. *Vaccinium vitis-idaea*. Fig. 24. *Anemona nemorosa*. Fig. 25. *Blechnum spicant*.

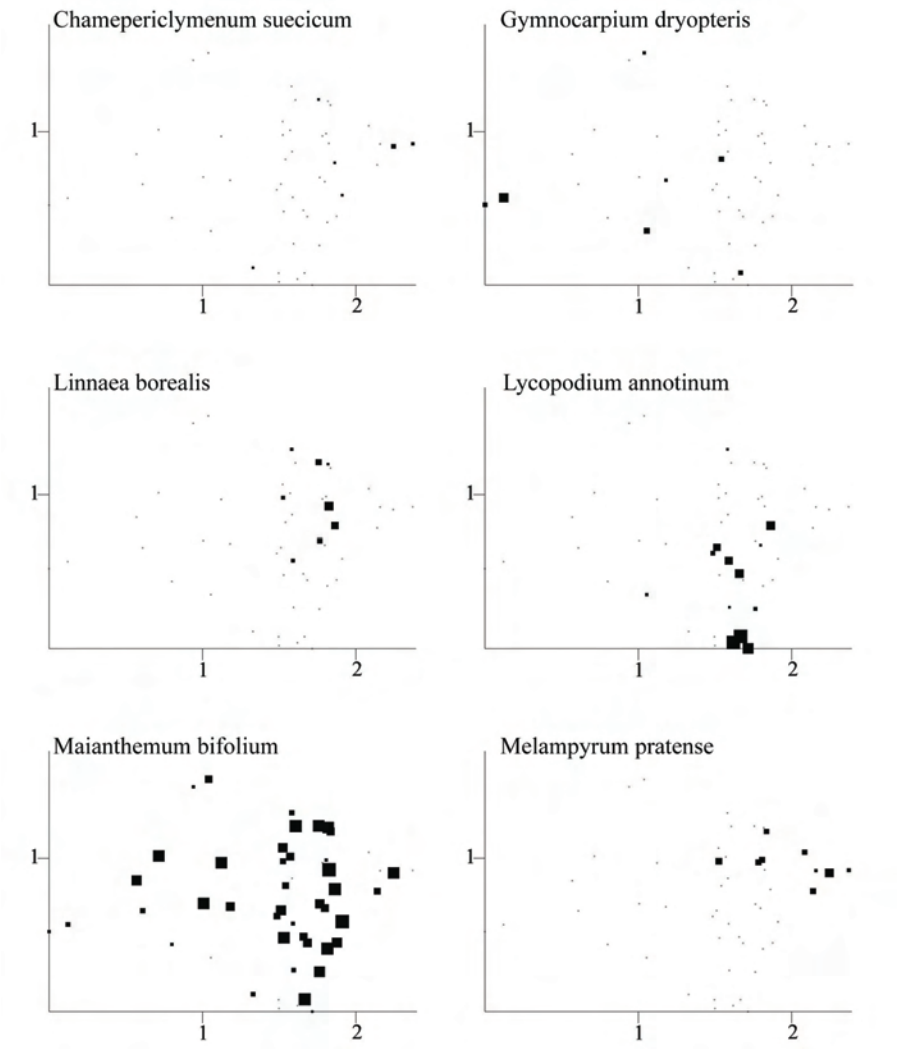

Figs 26-31. Lund: distributions of species abundances in the DCA ordination of 50 sample plots, axes 1 (horizontal) and 2 (vertical). Frequency in subplots for each species in each meso plot proportional to quadrate size. Scaling in S.D. units. Fig. 26. *Chamepericlymenum suecicum* (syn. *Cornus suecica*). Fig. 27.*Gynmocarpium dryopteris*. Fig. 28. *Linnaea borealis*. Fig. 29. *Lycopodium annotinum*. Fig. 30. *Maianthemum bifolium*. Fig. 31. *Melampyrum pratense*.

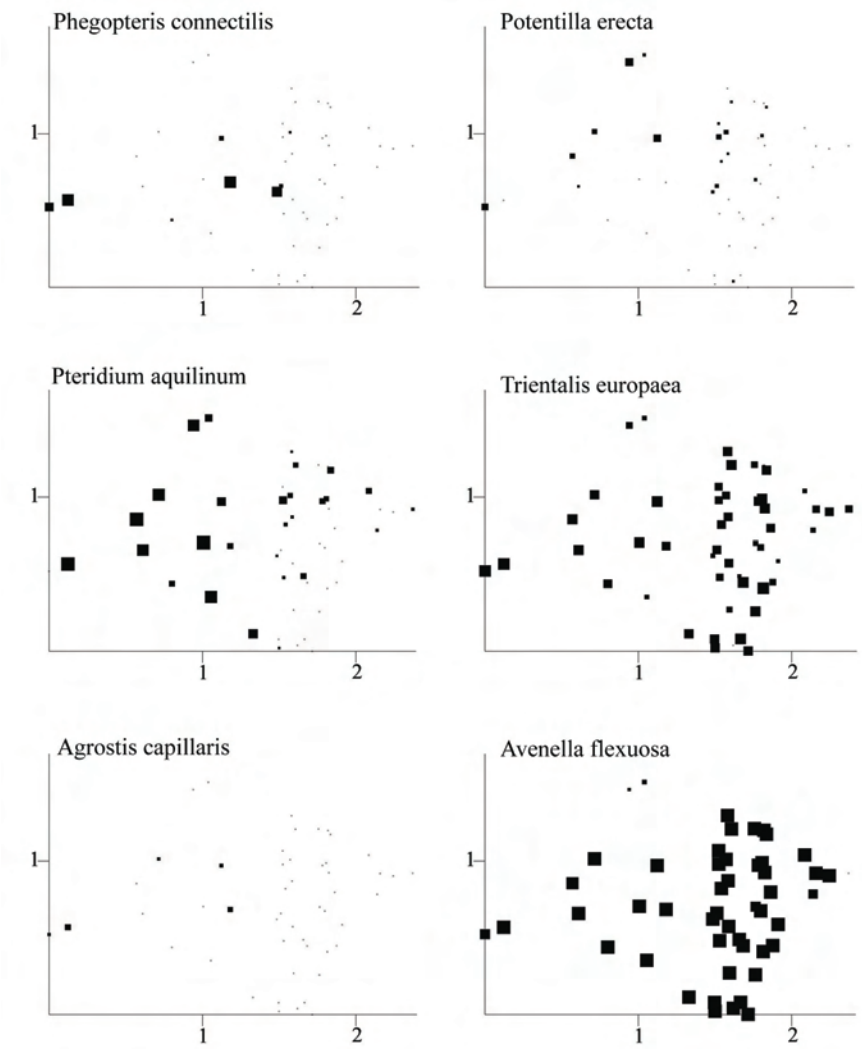

Figs 32-37. Lund: distributions of species abundances in the DCA ordination of 50 sample plots, axes 1 (horizontal) and 2 (vertical). Frequency in subplots for each species in each meso plot proportional to quadrate size. Scaling in S.D. units. Fig. 32. *Phegopteris connectilis*. Fig. 33. *Potentilla erecta*. Fig. 34. *Pteridium aquilinum*. Fig. 35. *Trientalis europaea*. Fig. 36. *Agrostis capillaris*. Fig. 37. *Avenella flexuosa* (syn. *Deschampsia flexuosa*).

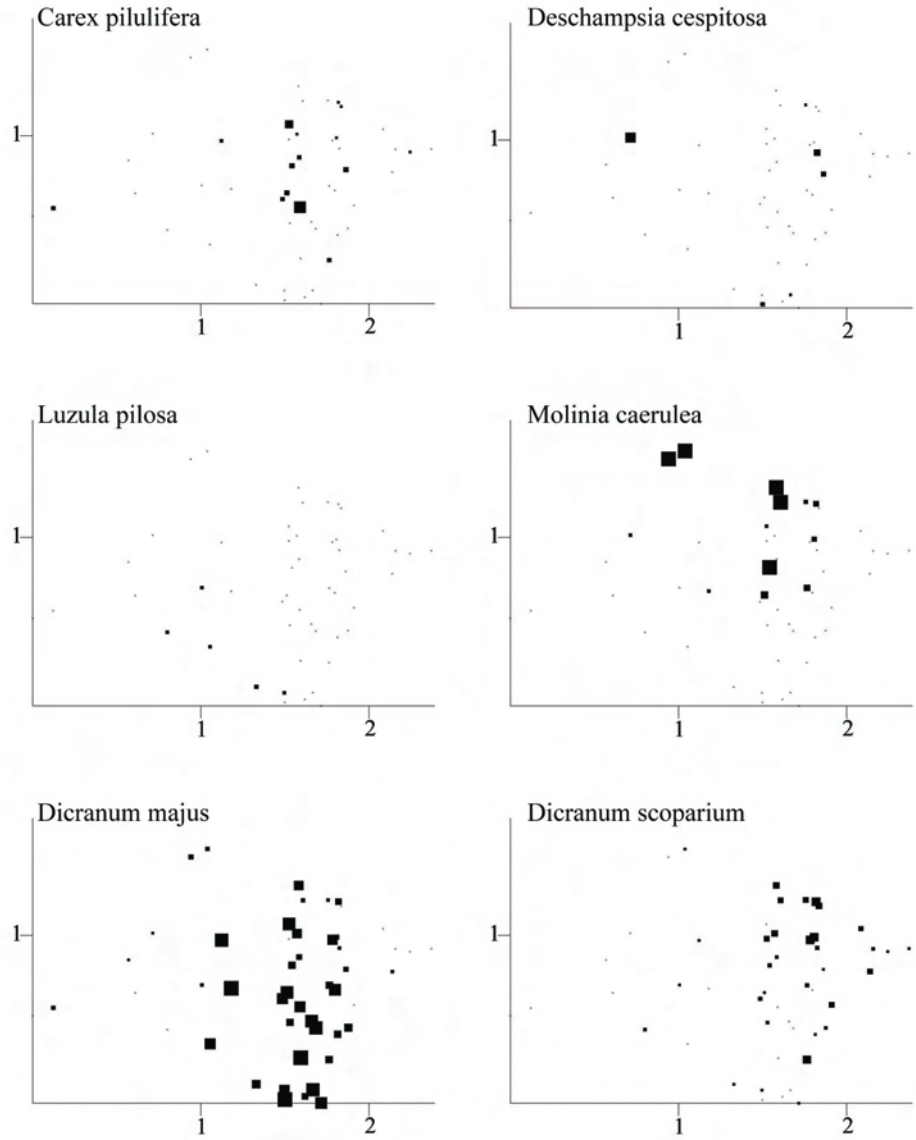

Figs 38-43. Lund: distributions of species abundances in the DCA ordination of 50 sample plots, axes 1 (horizontal) and 2 (vertical). Frequency in subplots for each species in each meso plot proportional to quadrate size. Scaling in S.D. units. Fig. 38. *Carex pilulifera.* Fig. 39. *Deschampsia cespitosa*. Fig. 40. *Luzula pilosa*. Fig. 41. *Molinia caerulea*. Fig. 42. *Dicranum majus*. Fig. 43. *Dicranum scoparium*.

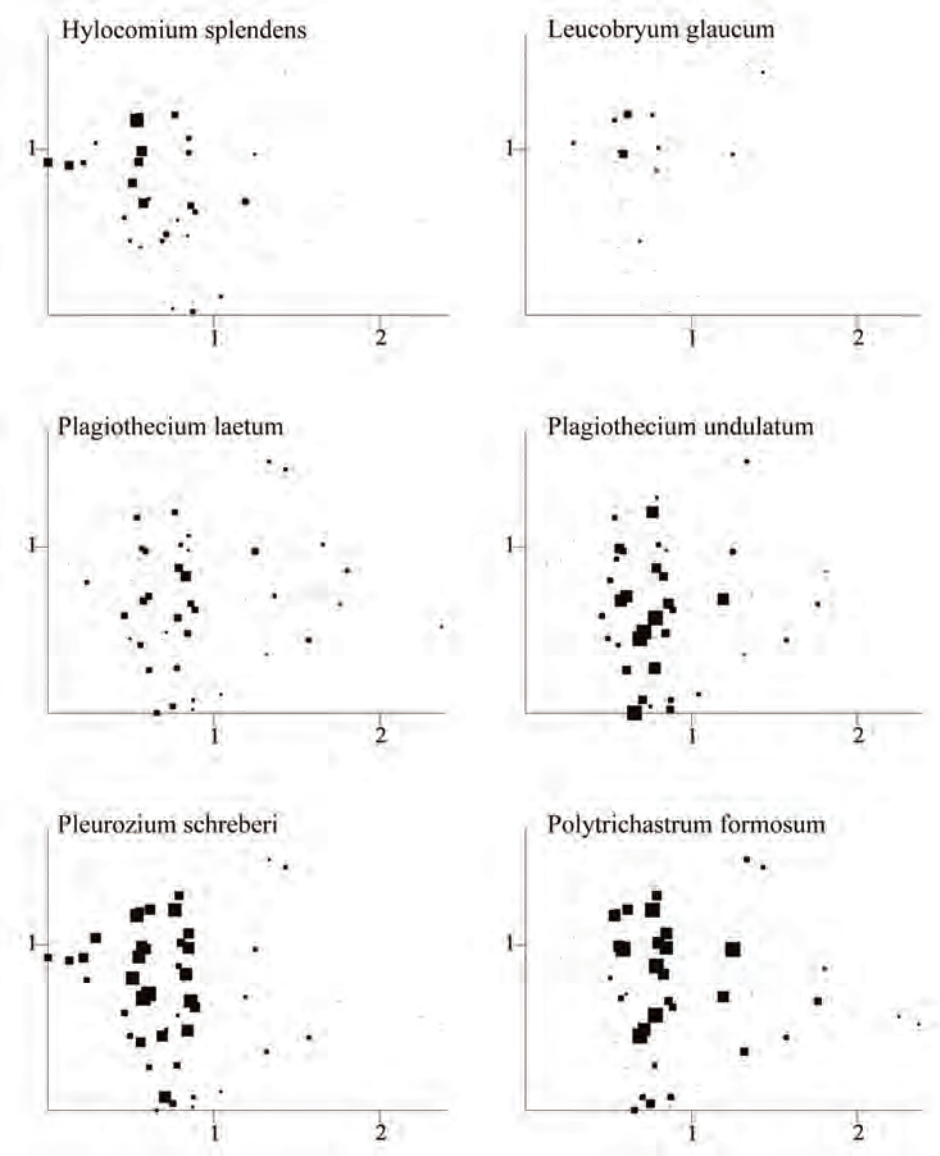

Figs 44-49. Lund: distributions of species abundances in the DCA ordination of 50 sample plots, axes 1 (horizontal) and 2 (vertical). Frequency in subplots for each species in each meso plot proportional to quadrate size. Scaling in S.D. units. Fig. 44. *Hylocomium splendens*. Fig. 45. *Leucobryum glaucum*. Fig. 46. *Plagiothecium laetum*. Fig. 47. *Plagiothecium undulatum*. Fig. 48. *Pleurozium schreberi*. Fig. 49. *Polytrichastrum formosum*.

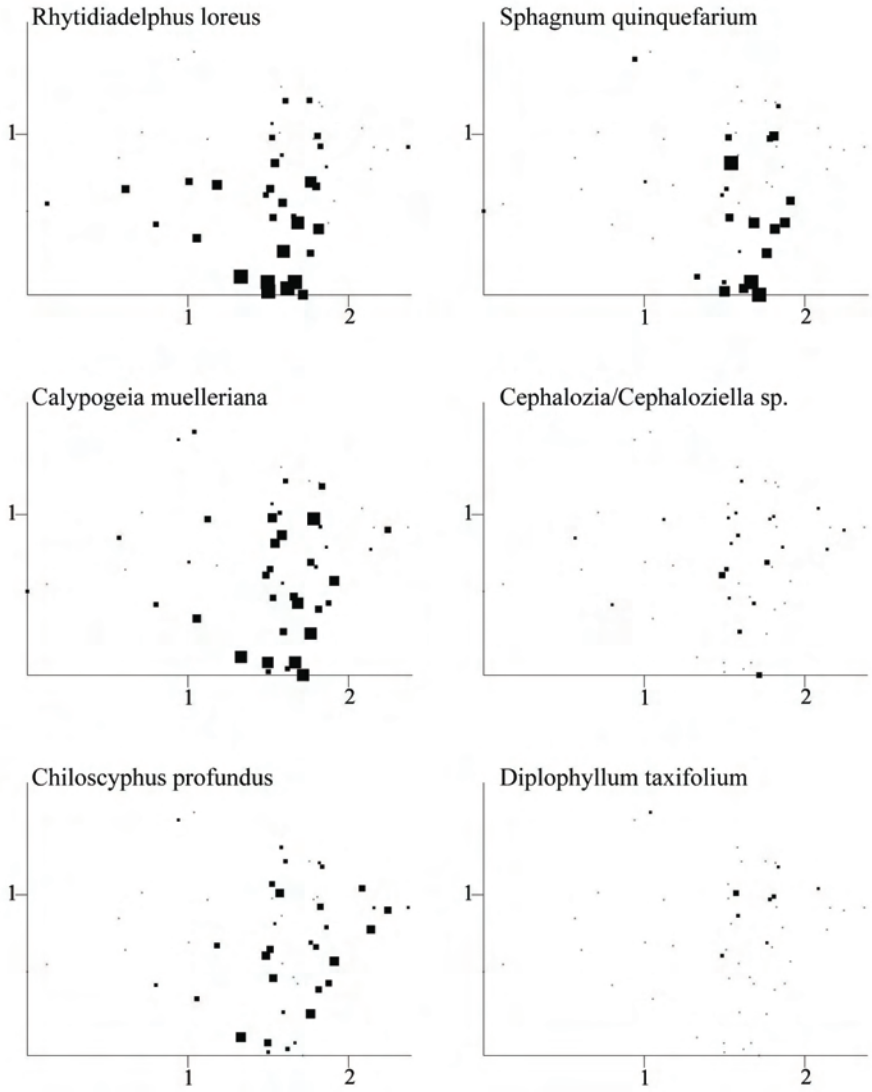

Figs 50-55. Lund: distributions of species abundances in the DCA ordination of 50 sample plots, axes 1 (horizontal) and 2 (vertical). Frequency in subplots for each species in each meso plot proportional to quadrate size. Scaling in S.D. units. Fig. 50. *Rhytidiadelphus loreus*. Fig. 51. *Sphagnum quinquefarium*. Fig. 52. *Calypogeia muelleriana*. Fig. 53. *Cephalozia/Cephaloziella sp.* Fig. 54. *Chiloscyphus profundus*. Fig. 55. *Diplophyllum taxifolium*.

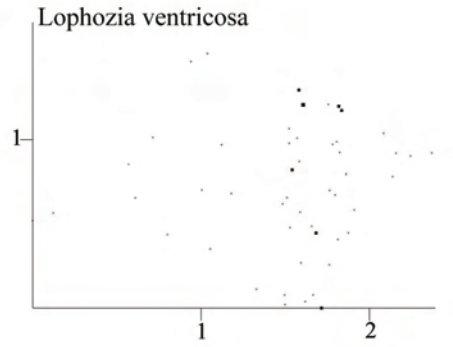

Fig. 56. Lund: distributions of species abundances in the DCA ordination of 50 sample plots, axes 1 (horizontal) and 2 (vertical).Frequency in subplots for each species in each meso plot proportional to quadrate size. Scaling in S.D. units. Fig. 56. *Lophozia ventricosa*.

MØSVATN REFERENCE AREA

Correlations between environmental variables

There were strong pairwise correlations between several of the topographical variables, between soil chemical variables and between topographical and chemical variables related to soil richness (Table 6).

Macro and meso plot slopes and heat indices were negatively correlated, and slopes were positively correlated with meso plot terrain form. Tree basal area (tree biomass) was positively correlated with macro plot slope, macro plot heat index and macro plot aspect unfavourability.

LOI was negatively correlated with soil pH and with concentrations of all extractable elements, except P, and positively correlated with exchangeable H. In general, element concentrations were pairwise positively correlated, and all were negatively correlated with exchangeable H.

Tree basal area, macro plot and meso plot slope and heat indices were correlated with chemical variables that were related to a gradient in soil nutrient richness. They were positively (except heat indices) correlated with total nitrogen, extractable Ca, Mg, Na and K and with pH, and negatively correlated (except heat indices) with LOI and exchangeable H. Minimum soil depth was positively correlated with soil acidity (H) and negatively correlated with pH while maximum soil depth was positively correlated with pH.

Macro plot terrain form and terrain unevenness showed no significant correlations with soil chemical variables. However, the meso plot terrain form was negatively correlated with soil pH and extractable concentrations of Ca and Na, while meso plot terrain unevenness was positively correlated with soil pH.

Soil moisture was not significantly correlated with topographical variables and heat index. However, it was positively correlated with extractable Na and Al and negatively correlated with extractable P, K and Zn.

Table 6. Møsvatn: Kendall's rank correlation coefficients τ between 31 environmental variables in the 50 sample plots (lower triangle), with significance probabilities (upper triangle). Statistically significant correlations (P<0.05) in bold face. Names of explanatory variables abbreviated in accordance with Table 2.

	1	2	3	4	5	6	7	8	9	10	11	12	13	14	15	16	17	18	19	20	21	22	23	24	25	26	27	28	29	30	31
01 Ma Slo	*	**0.004**	**0.000**	0.910	**0.028**	**0.007**	**0.000**	0.085	**0.000**	**0.000**	**0.038**	**0.014**	0.274	0.148	0.564	**0.011**	**0.021**	**0.001**	**0.001**	**0.002**	**0.042**	**0.004**	**0.000**	0.404	0.057	0.128	**0.002**	**0.000**	**0.000**	**0.000**	0.803
02 Ma Asp	**0.323**	*	**0.000**	0.415	0.177	**0.028**	**0.022**	**0.000**	**0.000**	**0.004**	0.091	0.657	0.345	**0.002**	0.515	**0.002**	**0.000**	**0.004**	**0.004**	**0.004**	0.471	**0.000**	**0.000**	0.145		**0.006**	**0.002**	**0.000**	0.096	**0.000**	0.560
03 Ma HI	**–0.713**	**–0.658**	*	0.524	0.052	**0.003**	**0.000**	**0.001**	**0.000**	**0.000**	0.081	0.141	0.953	**0.016**	0.880	**0.002**	**0.005**	**0.000**	**0.000**	**0.000**	0.501	**0.000**	**0.000**	0.749	**0.001**	**0.013**	**0.000**	**0.000**	**0.040**	**0.000**	0.987
04 Ma Ter	–0.012	–0.089	0.067	*	0.892	0.430	0.097	0.551	0.318	0.094	0.722	0.958	0.748	0.077	0.515	0.537	0.993	0.800	0.660	0.953	0.472	0.452	0.886	0.571	0.339	0.062	0.966	0.472	0.899	0.365	0.441
05 Ma Une	**0.238**	0.145	–0.200	0.014	*	0.195	0.113	0.118	**0.020**	0.489	**0.001**	0.084	0.100	0.880	0.177	0.445	0.156	0.314	0.247	0.486	0.540	0.217	0.250	0.237	0.318	0.656	0.445	0.137	0.369	0.085	0.980
05 TBA	**0.294**	**0.237**	**–0.308**	0.082	0.133	*	0.091	**0.046**	**0.007**	0.109	**0.028**	0.262	0.424	0.415	0.496	**0.010**	**0.001**	**0.000**	**0.000**	**0.001**	0.668	**0.004**	**0.000**	0.326	**0.003**	**0.026**	**0.000**	**0.004**	0.211	**0.000**	0.769
07 Me Slo	**0.585**	**0.247**	**–0.470**	–0.174	0.163	0.174	*	0.207	**0.000**	**0.000**	0.181	0.177	0.584	**0.001**	0.794	**0.001**	0.187	**0.000**	**0.000**	**0.000**	0.980	**0.011**	**0.000**	0.539	**0.010**	**0.011**	**0.000**	**0.001**	0.150	**0.001**	0.085
08 Me Asp	0.188	**0.589**	**–0.351**	0.063	0.161	**0.206**	0.131	*	**0.000**	0.352	**0.013**	0.727	0.349	0.077	0.953	**0.003**	**0.003**	**0.013**	**0.020**	0.058	0.404	**0.013**	**0.036**	0.108	**0.016**	**0.016**	0.054	**0.025**	**0.044**	**0.001**	0.846
09 Me HI	**–0.493**	**–0.439**	**0.503**	0.102	**–0.232**	**–0.268**	**–0.666**	**–0.489**	*	**0.002**	**0.016**	0.200	0.251	**0.003**	0.834	**0.000**	**0.002**	**0.000**	**0.000**	**0.000**	0.900	**0.002**	**0.000**	0.732	**0.007**	**0.007**	**0.000**	**0.000**	**0.046**	**0.000**	0.437
10 Me Ter	**–0.415**	**–0.312**	**0.420**	0.176	–0.071	–0.165	**–0.403**	–0.097	**0.317**	*	0.106	0.054	0.573	0.148	0.226	0.122	0.148	**0.031**	**0.048**	**0.017**	0.220	0.220	**0.012**	0.801	0.470	0.207	0.051	**0.001**	**0.034**	**0.036**	0.973
11 Me Une	**0.221**	0.179	–0.177	0.037	**0.321**	**0.222**	0.136	**0.254**	**–0.238**	–0.164	*	**0.002**	0.687	0.411	0.402	0.155	**0.018**	**0.037**	**0.036**	0.284	**0.032**	0.323	0.276	0.180	0.815	0.725	0.269	0.056	**0.006**	0.052	0.366
12 Smi	**–0.279**	–0.050	0.160	0.006	–0.186	–0.121	–0.146	–0.038	0.135	0.209	**–0.332**	*	**0.003**	0.302	0.206	**0.009**	0.059	**0.000**	**0.000**	0.077	**0.004**	0.166	0.072	0.615	0.690	0.456	**0.019**	**0.018**	**0.000**	0.061	0.080
13 Sme	–0.117	0.100	–0.006	–0.033	–0.166	0.081	0.056	0.095	–0.114	0.057	0.040	**0.318**	*	**0.018**	**0.033**	0.967	0.847	0.508	0.446	0.808	**0.011**	0.694	0.669	0.147	0.206	0.272	0.913	0.530	**0.007**	0.586	0.238
14 Sma	0.154	**0.323**	**–0.244**	–0.182	–0.015	0.082	**0.334**	0.180	**–0.295**	–0.147	0.082	–0.110	**0.237**	*	0.900	**0.002**	**0.006**	**0.008**	**0.004**	0.125	0.388	0.069	**0.029**	0.706	0.125	0.834	**0.011**	0.089	0.212	**0.002**	0.847
15 Mme	0.061	0.068	–0.015	–0.066	0.135	–0.068	0.026	–0.006	0.020	–0.122	0.082	–0.133	**–0.211**	–0.012	*	0.139	0.225	0.541	0.467	0.219	**0.000**	0.089	0.362	0.130	**0.040**	0.067	0.201	**0.022**	**0.001**	0.598	**0.009**
16 LOI	**–0.268**	**–0.318**	**0.311**	0.063	–0.076	**–0.258**	**–0.344**	**–0.305**	**0.406**	0.156	–0.140	**0.274**	0.004	**–0.311**	0.144	*	**0.000**	**0.000**	**0.000**	**0.000**	0.622	**0.000**	**0.000**	0.447	**0.000**	**0.000**	**0.000**	**0.005**	**0.027**	**0.000**	**0.018**
17 Total N	**0.244**	**0.423**	**–0.283**	0.001	0.141	**0.325**	0.133	**0.305**	**–0.303**	–0.146	**0.233**	–0.199	0.019	**0.270**	0.118	**–0.398**	*	**0.000**	**0.000**	**0.003**	**0.011**	**0.001**	**0.000**	0.311	**0.049**	0.281	**0.000**	**0.001**	**0.000**	**0.000**	0.336
18 pH_{H2O}	**0.364**	**0.304**	**–0.357**	–0.026	0.101	**0.407**	**0.354**	**0.251**	**–0.411**	**–0.218**	**0.206**	**–0.369**	–0.066	**0.263**	–0.060	**–0.622**	**0.502**	*	**0.000**	**0.000**	0.757	**0.000**	**0.000**	0.259	**0.000**	**0.001**	**0.000**	**0.001**	**0.001**	**0.000**	0.083
19 pH_{CaCl2}	**0.360**	**0.307**	**–0.357**	–0.045	0.116	**0.378**	**0.352**	**0.236**	**–0.400**	**–0.200**	**0.207**	**–0.368**	–0.076	**0.284**	–0.071	**–0.630**	**0.492**	**0.946**	*	**0.000**	0.732	**0.000**	**0.000**	0.266	**0.000**	**0.001**	**0.000**	**0.001**	**0.002**	**0.000**	0.064
20H	**–0.323**	**–0.302**	**0.391**	–0.006	–0.069	**–0.345**	**–0.369**	–0.191	**0.369**	**0.240**	–0.106	0.186	0.024	–0.151	0.120	**0.453**	**–0.288**	**–0.614**	**–0.613**	*	**0.004**	**0.000**	**0.000**	**0.021**	**0.000**	**0.000**	**0.000**	**0.017**	0.670	**0.000**	**0.003**
21 Al	**0.215**	0.076	–0.068	–0.073	0.061	0.043	–0.003	0.084	–0.012	–0.124	**0.211**	**–0.306**	**–0.251**	0.085	**0.360**	–0.048	**0.249**	0.030	0.034	**0.280**	*	0.371	0.457	**0.000**	**0.016**	**0.000**	0.157	**0.002**	**0.000**	0.498	**0.000**
22 C	**0.308**	**0.383**	**–0.359**	0.077	0.123	**0.290**	**0.256**	**0.250**	**–0.305**	–0.124	0.097	–0.146	0.039	0.179	–0.166	**–0.554**	**0.334**	**0.512**	**0.517**	**–0.471**	–0.087	*	**0.000**	0.296	**0.000**	**0.000**	**0.000**	**0.013**	0.719	**0.000**	**0.000**
23 Ca	**0.457**	**0.397**	**–0.499**	–0.015	0.115	**0.459**	**0.457**	**0.211**	**–0.429**	**–0.252**	0.107	–0.190	0.042	**0.215**	–0.089	**–0.510**	**0.404**	**0.657**	**0.645**	**–0.652**	–0.073	**0.535**	*	0.201	**0.000**	**0.000**	**0.000**	**0.000**	0.201	**0.000**	**0.033**
24 Fe	0.088	0.153	–0.032	0.058	0.118	–0.098	–0.062	0.162	0.034	–0.025	0.132	–0.053	–0.143	–0.037	0.148	–0.074	0.099	–0.111	–0.109	**0.224**	**0.442**	0.102	–0.125	*	0.477	0.732	0.080	0.178	**0.005**	0.940	0.993
25 K	0.201	**0.351**	**–0.323**	0.097	0.100	**0.297**	**0.258**	**0.242**	**–0.262**	–0.073	0.023	–0.042	0.125	0.151	**–0.200**	**–0.471**	**0.192**	**0.450**	**0.461**	**–0.473**	**–0.236**	**0.691**	**0.566**	–0.069	*	**0.000**	**0.000**	0.072	0.173	**0.000**	**0.000**
26 Mg	0.161	**0.288**	**–0.249**	0.190	0.044	**0.223**	**0.256**	**0.244**	**–0.264**	–0.127	0.035	0.078	0.108	0.021	–0.179	**–0.362**	0.105	**0.334**	**0.333**	**–0.497**	**–0.345**	**0.517**	**0.502**	0.033	**0.558**	*	**0.000**	0.252	0.148	**0.004**	**0.000**
27 Mn	**0.326**	**0.324**	**–0.376**	–0.004	0.076	**0.357**	**0.388**	0.194	**–0.385**	–0.196	0.109	**–0.246**	–0.011	**0.252**	–0.125	**–0.582**	**0.355**	**0.750**	**0.767**	**–0.691**	–0.138	**0.587**	**0.683**	–0.171	**0.579**	**0.447**	*	**0.002**	0.139	**0.000**	**0.000**
28 Na	**0.515**	**0.394**	**–0.491**	–0.073	0.148	**0.291**	**0.340**	**0.227**	**–0.372**	**–0.344**	0.188	**–0.248**	–0.062	0.168	**0.223**	**–0.277**	**0.334**	**0.330**	**0.319**	**–0.233**	**0.301**	**0.242**	**0.433**	0.131	0.176	0.112	**0.296**	*	**0.000**	**0.000**	0.118
29 P	**–0.382**	–0.174	**0.206**	0.013	–0.090	–0.125	–0.144	**–0.203**	**0.195**	**0.213**	**–0.269**	**0.419**	**0.267**	–0.123	**–0.326**	**0.216**	**–0.378**	**–0.322**	**–0.307**	0.042	**–0.620**	–0.035	–0.125	**–0.273**	0.133	0.141	–0.144	**–0.450**	*	0.083	**0.005**
30 S	**0.422**	**0.516**	**–0.509**	–0.092	0.172	**0.354**	**0.332**	**0.347**	**–0.441**	**–0.212**	0.191	–0.197	0.054	**0.313**	–0.051	**–0.496**	**0.425**	**0.529**	**0.535**	**–0.393**	0.066	**0.618**	**0.561**	0.007	**0.538**	**0.282**	**0.571**	**0.425**	-0.169	*	0.362
31 Zn	–0.026	0.061	0.002	0.078	–0.003	–0.029	0.173	0.020	–0.076	–0.003	–0.089	0.184	0.117	0.019	**–0.254**	**–0.231**	–0.094	0.170	0.181	**–0.295**	**–0.433**	**0.367**	**0.208**	0.001	**0.427**	**0.549**	**0.342**	–0.153	**0.275**	0.089	*

PCA ordination of environmental variables

The first PCA axis accounted for 40.6 % (eigenvalue of 0.406) of the variance in the matrix of standardised transformed environmental variables, and the second axis accounted for 14.6 % (eigenvalue of 0.146).

pH_{H2O}, $pH_{CaCl)}$ and extractable S, Mn, Ca and C obtained the highest loadings on PCA axis 1, while loss on ignition, exchangeable H and macro- and meso plot heat indices obtained low loadings (Fig. 57). Extractable Al and soil moisture obtained low loadings on PCA axis 2, while extractable P and Zn obtained high loadings.

The PCA results were consistent with the correlation matrix of the environmental variables, showing that pH, Ca, Mn and several of the topgraphical indices (not heat indices) with high loadings on axis 1 were highly positively correlated, and that variables in this group was negatively correlated with loss on ignition, extractable H and heat indices. Thus the environmental data from the Møsvatn reference area reflects an important gradient in soil nutrient richness and base status.

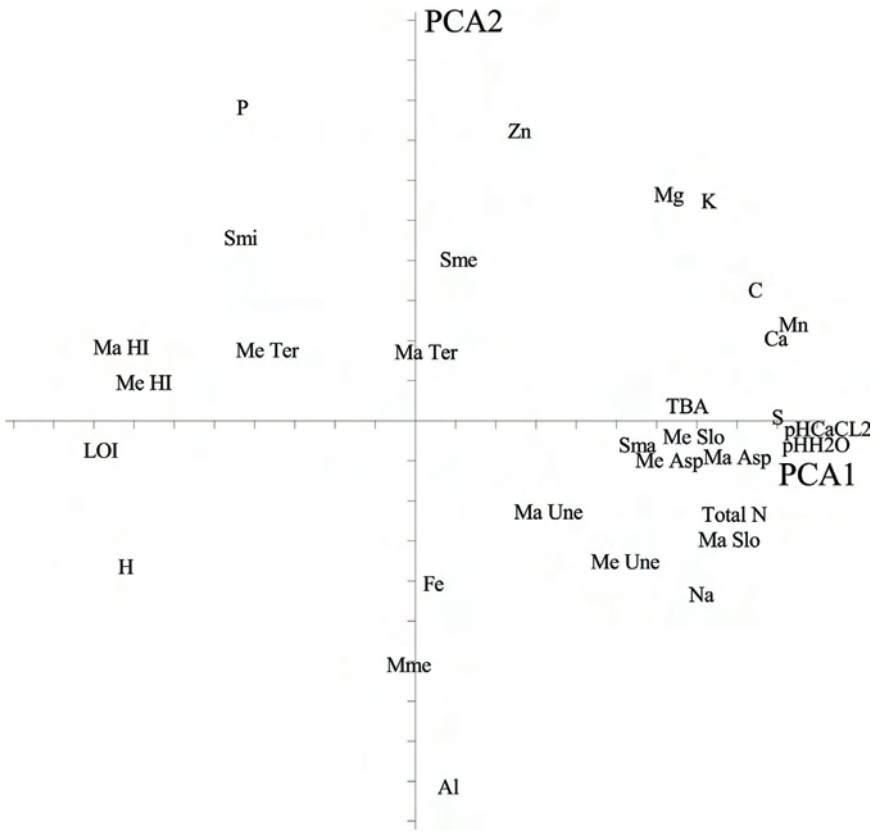

Fig. 57. Møsvatn: PCA ordination of 31 environmental variables. Abbreviations in accordance with Table 2. Positions of variables in the ordination space give the head of variable vectors. Tickmarks indicate 0.1 units along both axes.

DCA ordination

The gradient length of the two first DCA axes was 4.53 and 1.88 S.D. units, and the eigenvalues were 0.554 and 0.140, respectively. Meso plot 35 made up an outlier along the first axis. A second DCA ordination was obtained by removing this plot from the analysis, and a new ordination was performed. However, the relative positions of the remaining plots in the diagram did not change, nor was the main pattern along the axes affected. All plots were therefore used in further analyses.

The first axis represented a high proportion of the structured variation in the material while, consequently, the remaining axes captured smaller amounts of variation. Variation along DCA axis 2 was mainly restricted to sample plots to the right in the ordination diagram, i.e. with high DCA 1 scores (Fig. 58).

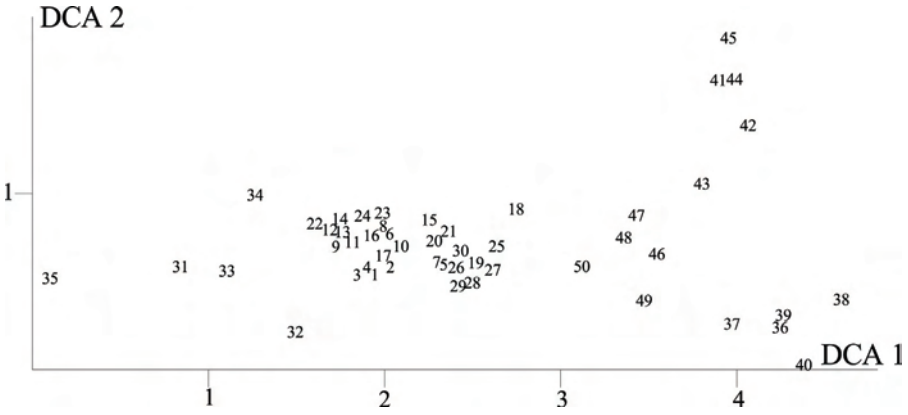

Fig. 58. Møsvatn: DCA ordination diagram of 50 meso plots, axes 1 (horizontal) and 2 (vertical). Meso plot number are plotted just right of the sample plot positions. Scaling of axes in S.D. units.

GNMDS ordination

The GNMDS ordination diagram (Fig. 59) was visually similar to the DCA diagram (Fig. 58), although plot 35 was separated somewhat from all other plots both along the first and the second ordination axis. The correlation between GNMDS 1 and DCA 1 was $\tau = 0.953$, and the correlation between GNMDS 2 and DCA 2 was $\tau = 0.407$ (both $P < 0.001$).

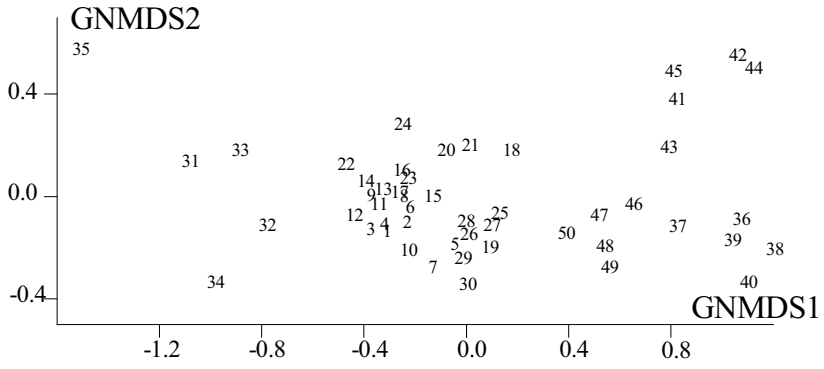

Fig.59. Møsvatn: GNMDS ordination biplot diagram of 50 meso plots (indicated by their number).

Split-plot GLM analysis of relationships between ordination axes and environmental variables

Variation (in plot scores) along DCA axis 1 was partitioned with 93.62 % at the macro-plot scale (i.e. between macro plots) and 6.38 % at the (between) meso plot scale within macro plots (Table 7). For the second ordination axis, 82.00 % of the variation was explained at the macro-plot scale and 18.00 % at the meso plot scale (Table 8)

At the macro-plot scale, twenty-two environmental variables were significantly (at the $\alpha = 0.05$ level) related to DCA 1 while no variable (also at the $\alpha = 0.05$ level) was related to DCA 2. At the plot scale level, four environmental variables were significantly related to DCA 1 and one variable to DCA 2 (Tables 7 and 8).

At the macro-plot scale, most of the significant variables increased along DCA 1; exceptions were heat indices, meso plot terrain form, minimum soil depth, LOI and the concentrations of H and P in soil which decreased. Significant relationships were found for four variables at the plot scale (Table 7).

At the macro-plot scale, DCA 2 was only significant positively correlated with median soil depth at the plot scale level. No other significant relationships were detected (at the $\alpha = 0.05$ level) (Table 8).

Table 7 Møsvatn: Split-plot GLM analysis and Kendall's nonparametric correlation coefficient τ between DCA 1 and 31 environmental variables (predictor) in the 50 plots. df_{resid}: degrees of freedom for the residuals; *SS*: total variation; *FVE*: fraction of total variation attributable to a given scale (macro plot or plot); SS_{expl}/SS: fraction of the variation attributable to the scale in question, explained by a variable; *r*: model coefficient (only given when significant at the $\alpha = 0.05$ level, otherwise blank); *F*: *F* statistic for test of the hypothesis that $r = 0$ against the two-tailed alternative. Split-plot GLM relationships significant at level $\alpha = 0.05$, *P*, *F*, *r* and SS_{expl}/SS, and Kendall's nonparametric correlation coefficient $|\tau| \geq 0.30$ are given in bold face. Numbers and abbreviations for names of environmental variables are in accordance with Table 2.

Predictor	Dependent variable = DCA 1 (*SS* = 50.8559)							Correlation between predictor and DCA 1
	Error level							
	Macro plot $df_{resid} = 8$ $SS_{macro\ plot} = 47.6090$ *FVE* = 0.9362 of *SS*				Plot within macro plot $df_{resid} = 39$ $SS_{plot} = 3.24690$ *FVE* = 0.0638 of *SS*			Total
	$SS_{expl}/SS_{macro\ plot}$	*r*	*F*	*P*	SS_{expl}/SS_{plot}	*r*	*F*	*P*	τ

Ma Slo	**0.4611**	**2.6769**	**6.8448**	**0.0308**	0.0007		0.0273	0.8696	**0.388**
Ma Asp	**0.4985**	**2.6061**	**7.9514**	**0.0225**	0.0283		1.1350	0.2933	**0.441**
Ma HI	**0.7252**	**–4.6325**	**21.2480**	**0.0017**	0.0075		0.2942	0.5906	**–0.433**
Ma Ter	0.1041		0.9297	0.3632	0.0411		1.6733	0.2034	–0.128
Ma Une	0.1335		1.2323	0.2992	0.0065		0.2554	0.6161	0.131
TBA	**0.6836**	**4.0763**	**17.2840**	**0.0032**	0.0008		0.0310	0.8610	**0.617**
Me Slo	**0.5123**	**4.1573**	**8.4031**	**0.0199**	0.0386		1.5677	0.2180	**0.379**
Me Asp	0.0902		0.7930	0.3992	0.0213		0.8508	0.3620	0.035
Me HI	**0.7630**	**–4.7897**	**25.7500**	**0.0294**	0.0565		0.0291	0.8655	**–0.426**
Me Ter	**0.6624**	**–7.2123**	**15.6980**	**0.0042**	0.0026		0.1031	0.7499	–0.250
Me Une	**0.5105**	**6.6347**	**8.3436**	**0.0203**	0.0220		0.8777	0.3546	0.177
Smi	**0.5935**	**–4.3949**	**11.6790**	**0.0091**	0.0213		0.8494	0.3624	–0.297
Sme	0.0000		0.0000	0.9968	0.0168		0.6650	0.4198	–0.002
Sma	**0.6022**	**5.6671**	**12.1090**	**0.0083**	0.0009		0.0338	0.8551	**0.364**
Mme	0.0142		0.1150	0.7433	0.0643		2.6806	0.1096	0.047
LOI	**0.6560**	**–3.0244**	**15.2590**	**0.0045**	0.0002		0.0093	0.9237	**–0.499**
Total N	**0.8349**	**5.7496**	**40.4630**	**0.0002**	0.0043		0.1695	0.6829	**0.500**
$pH_{(H2O)}$	**0.9084**	**4.0510**	**79.3780**	**0.0000**	0.0076		0.2995	0.5873	**0.716**
pH_{CaCl2}	**0.9198**	**3.9279**	**91.7770**	**0.0000**	0.0027		0.1053	0.7473	**0.726**
H	**0.7214**	**–4.6122**	**20.7130**	**0.0019**	**0.1006**	**–0.6547**	**4.3636**	**0.0433**	**–0.536**
Al	0.0470		0.3944	0.5475	0.0500		2.0534	0.1598	0.105
C	**0.6319**	**3.5272**	**13.7320**	**0.0060**	0.0026		0.1011	0.7522	**0.491**
Ca	**0.8994**	**5.1352**	**71.5000**	**0.0000**	**0.0981**	**0.7604**	**4.2421**	**0.0462**	**0.675**
Fe	0.0238		0.1948	0.6706	0.0318		1.2798	0.2648	–0.045
K	**0.5455**	**4.2784**	**9.6034**	**0.0147**	**0.0987**	**0.5387**	**4.2692**	**0.0455**	**0.450**
Mg	0.2609		2.8233	0.1314	0.0432		1.7621	0.1921	**0.324**
Mn	**0.8145**	**3.2564**	**35.1220**	**0.0004**	**0.0989**	**0.6429**	**4.2791**	**0.0453**	**0.636**
Na	**0.7596**	**4.3704**	**25.2840**	**0.0010**	0.0018		0.0684	0.7950	**0.458**
P	**0.4529**	**–2.7878**	**6.6221**	**0.0330**	0.0335		1.3539	0.2517	**–0.313**
S	**0.9355**	**4.8181**	**116.130**	**0.0000**	0.0316		1.2736	0.2660	**0.602**
Zn	0.0003		0.0023	0.9626	0.0781		3.3024	0.0769	0.099

Table 8. Møsvatn: Split-plot GLM analysis and Kendall's nonparametric correlation coefficient τ between DCA 2 and 31 environmental variables (predictor) in the 50 plots. df_{resid}: degrees of freedom for the residuals; *SS*: total variation; *FVE*: fraction of total variation attributable to a given scale (macro plot or plot); SS_{expl}/SS: fraction of the variation attributable to the scale in question, explained by a variable; *r*: model coefficient (only given when significant at the $\alpha = 0.05$ level, otherwise blank); *F*: *F* statistic for test of the hypothesis that $r = 0$ against the two-tailed alternative. Split-plot GLM relationships significant at level $\alpha = 0.05$, *P*, *F*, *r* and SS_{expl}/SS, and Kendall's nonparametric correlation coefficient $|\tau| \geq 0.30$ are given in bold face. Numbers and abbreviations for names of environmental variables are in accordance with Table 2.

Predictor	Dependent variable = DCA 2 (*SS* = 5.8257)								Correlation between predictor and DCA 2
	Error level								
	Macro plot $df_{resid} = 8$ $SS_{macro\ plot} = 4.7768$ *FVE* = 0.8200 of *SS*				Plot within macro plot $df_{resid} = 39$ $SS_{plot} = 1.04892$ *FVE* = 0.1800 of *SS*				Total
	$SS_{expl}/$	*r*	*F*	*P*	$SS_{expl}/$	*r*	*F*	*P*	τ

	$SS_{macro\ plot}$			SS_{plot}			
Ma Slo	0.0033	0.0269	0.8737	0.0172	0.6837	0.4133	–0.170
Ma Asp	0.2392	2.5146	0.1515	0.0010	0.0373	0.8480	0.298
Ma HI	0.0582	0.4948	0.5018	0.0084	0.3337	0.5668	–0.122
Ma Ter	0.2876	3.2288	0.1101	0.0215	0.8554	0.3607	0.230
Ma Une	0.0942	0.8324	0.3882	0.0008	0.0320	0.8590	0.026
TBA	0.0075	0.0605	0.8118	0.0570	2.3596	0.1326	–0.066
Me slo	0.0118	0.0956	0.7651	0.0047	0.1859	0.6688	–0.102
Me Asp	0.0018	0.0145	0.9072	0.0215	0.8574	0.3602	0.151
Me HI	0.0010	0.0082	0.9299	0.0178	0.7071	0.4055	–0.148
Me Ter	0.0129	0.1049	0.7543	0.0127	0.5013	0.4831	–0.014
Me Une	0.0318	0.2628	0.6220	0.0035	0.1373	0.7130	0.051
Smi	0.0054	0.0433	0.8404	0.0009	0.0348	0.8530	0.140
Sme	0.0164	0.1331	0.7247	**0.0967**	**0.2233**	**4.1768**	**0.0478**	0.199
Sma	0.0264	0.2168	0.6539	0.0600	2.4888	0.1227	–0.035
Mme	0.0031	0.0253	0.8776	0.0236	0.9424	0.3377	–0.027
LOI	0.0002	0.0017	0.9680	0.0123	0.4863	0.4897	0.055
Total N	0.0001	0.0010	0.9758	0.0327	1.3171	0.2581	–0.001
$pH_{(H2O)}$	0.0012	0.0098	0.9236	0.0068	0.2665	0.6086	–0.080
pH_{CaCl2}	0.0036	0.0293	0.8683	0.0105	0.4145	0.5234	–0.096
H	0.1858	1.8250	0.2137	0.0000	0.0000	0.9978	–0.068
Al	0.1121	1.0102	0.3443	0.0011	0.0433	0.8363	–0.193
C	0.1594	1.5166	0.2531	0.0012	0.0471	0.8293	0.064
Ca	0.0819	0.7138	0.4227	0.0002	0.0063	0.9374	0.056
Fe	0.0512	0.4317	0.5296	0.0000	0.0005	0.9830	0.045
K	0.1305	1.2002	0.3052	0.0028	0.1094	0.7426	0.125
Mg	0.2825	3.1495	0.1139	0.0273	1.0937	0.3021	0.234
Mn	0.0370	0.3071	0.5946	0.0062	0.2422	0.6254	0.017
Na	0.0377	0.3137	0.5908	0.0733	3.0835	0.0869	0.035
P	0.0011	0.0088	0.9277	0.0025	0.0995	0.7541	0.127
S	0.0790	0.6866	0.4314	0.0080	0.3138	0.5786	0.035
Zn	0.2082	2.1031	0.1850	0.0330	1.3296	0.2559	0.172

Correlations between DCA ordination axes and environmental variables

Twenty of the 31 measured variables were strongly correlated with DCA axis 1 ($|\tau| > 0.300$), while no variables were equally strongly correlated with DCA 2 (Table 7). $pH_{(CaCl2)}$ (τ = 0.726, Fig. 69), $pH_{(H2O)}$ (τ = 0.716), extractable Ca (τ = 0.675, Fig. 72) and Mn (τ = 0.636, Fig. 75) and tree basal area (τ = 0.617, Fig. 63) were best correlated with DCA axis 1, while meso plot aspect unfavourablility (τ = 0.298) was the variable most strongly correlated with DCA 2).

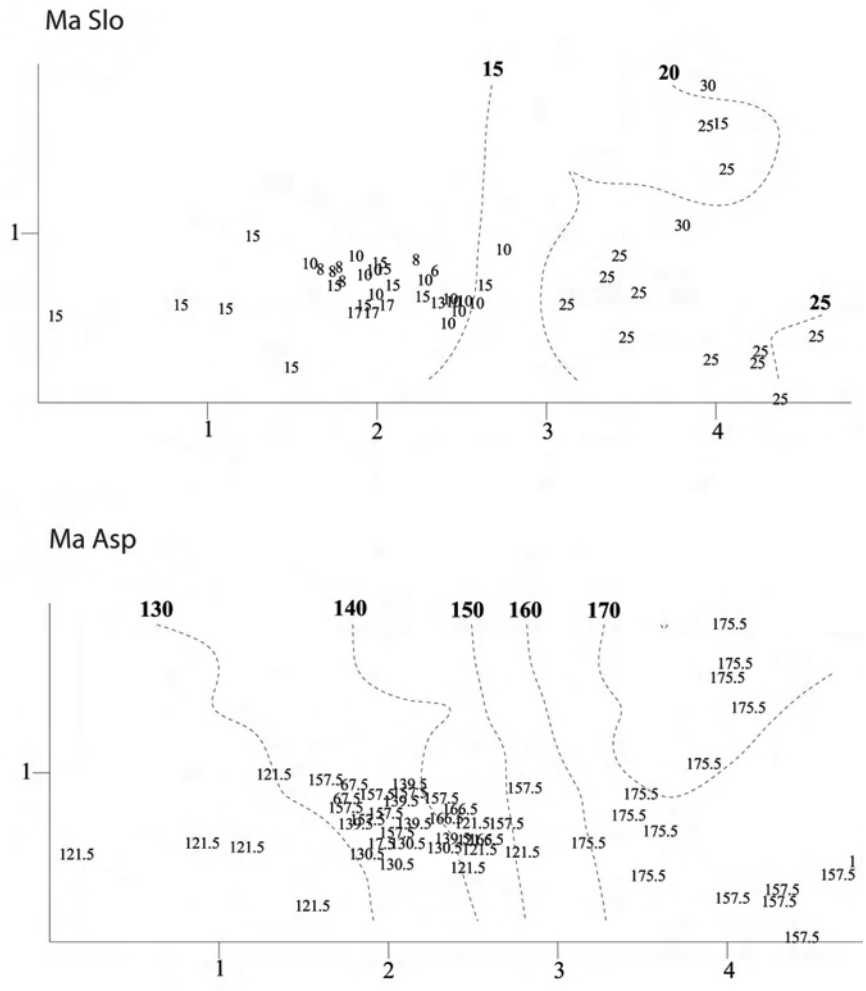

Figs 60-61. Møsvatn: isolines for environmental variables in the DCA ordinations of 50 meso plots, axes 1 (horizontal) and 2 (vertical). Values for the environmental variables are plotted onto the meso plots' positions. Scaling in S.D. units. Fig. 58. Ma Slo (R^2 = 0.648). Fig. 59. Ma Asp (R^2 = 0.615). R^2 refers to the coefficient of determination between original and smoothened values as interpolated from the isolines. Names of environmental variables in accordance with Table 2.

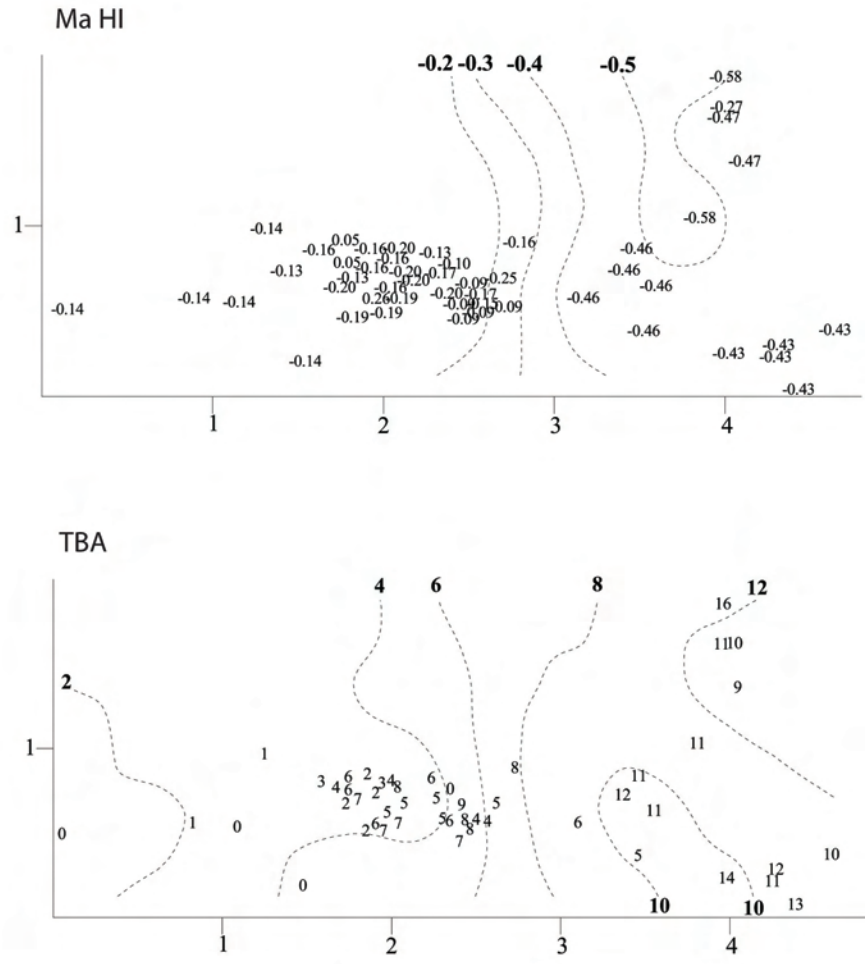

Figs 62-63. Møsvatn: isolines for environmental variables in the DCA ordinations of 50 meso plots, axes 1 (horizontal) and 2 (vertical). Values for the environmental variables are plotted onto the meso plots' positions. Scaling in S.D. units. Fig. 62. Ma HI (R^2 = 0. 684). Fig. 63. TBA (R^2 = 0.507). R^2 refers to the coefficient of determination between original and smoothened values as interpolated from the isolines. Names of environmental variables in accordance with Table 2.

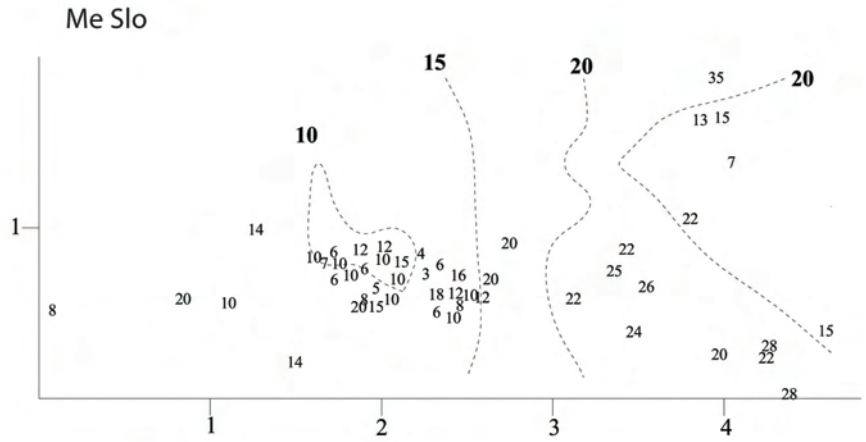

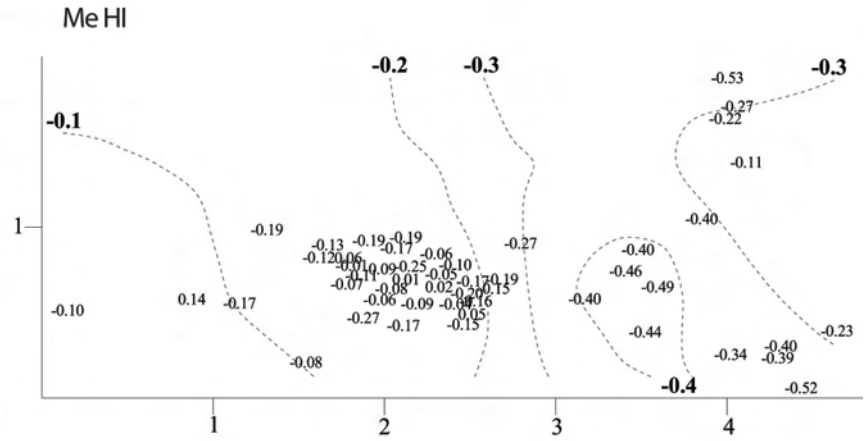

Figs 64-65. Møsvatn: isolines for environmental variables in the DCA ordinations of 50 meso plots, axes 1 (horizontal) and 2 (vertical). Values for the environmental variables are plotted onto the meso plots' positions. Scaling in S.D. units. Fig. 64. Me Slo (R^2 = 0.643). Fig. 65. Me HI (R^2 = 0.748). R^2 refers to the coefficient of determination between original and smoothened values as interpolated from the isolines. Names of environmental variables in accordance with Table 2.

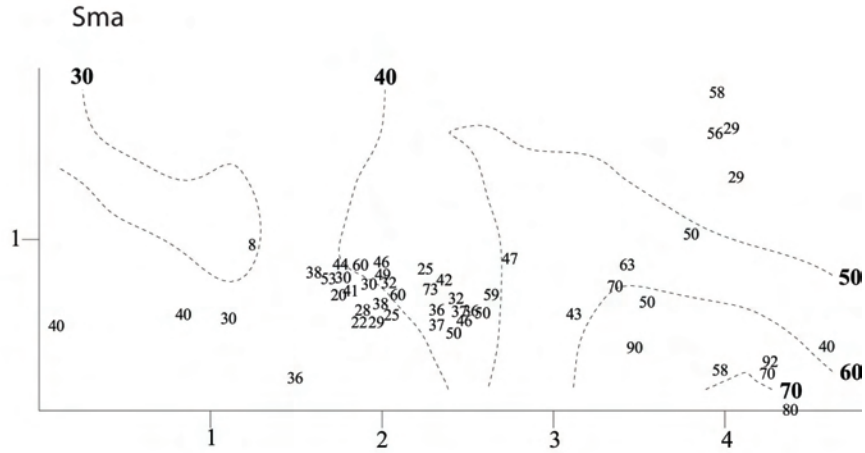

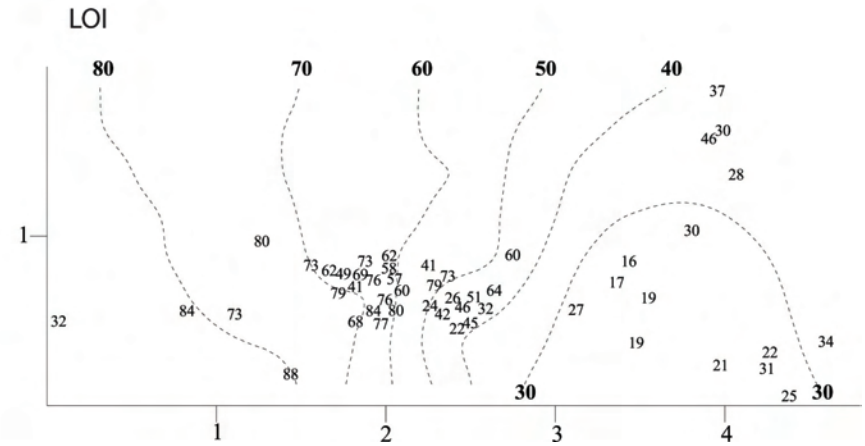

Figs 66-67. Møsvatn: isolines for environmental variables in the DCA ordinations of 50 meso plots, axes 1 (horizontal) and 2 (vertical). Values for the environmental variables are plotted onto the meso plots' positions. Scaling in S.D. units. Fig. 66. Sma (R^2 = 0.583). Fig. 67. LOI (R^2 = 0.707). R^2 refers to the coefficient of determination between original and smoothened values as interpolated from the isolines. Names of environmental variables in accordance with Table 2.

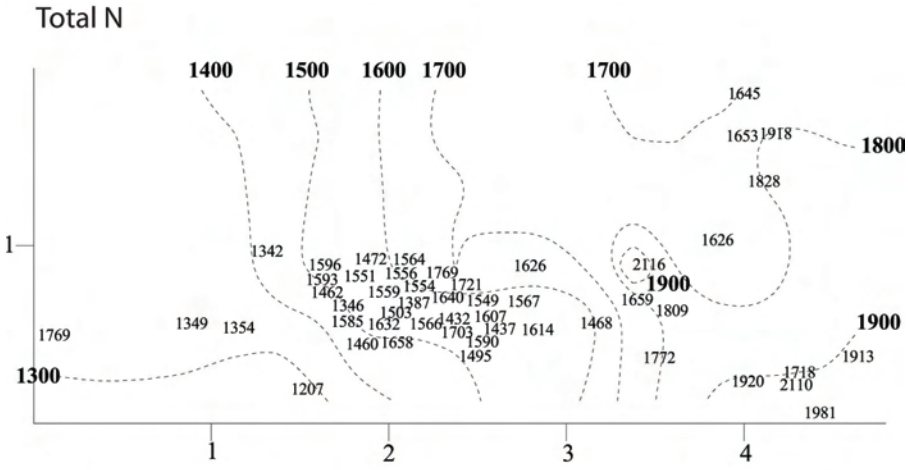

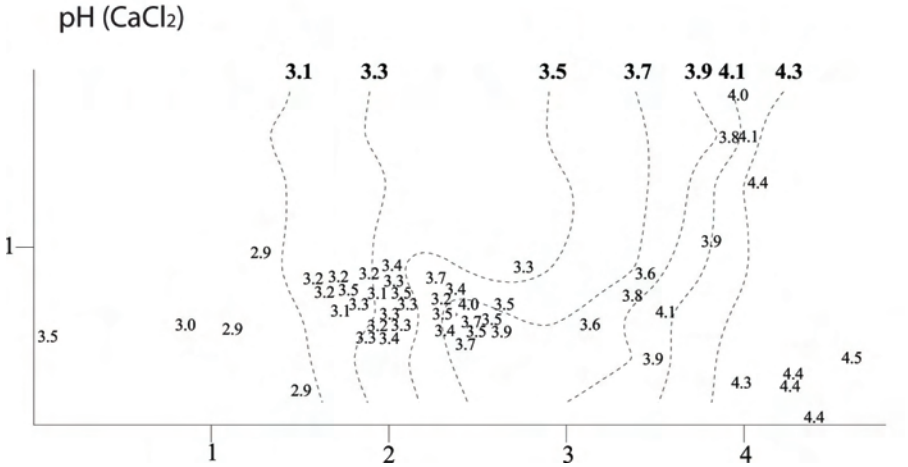

Figs 68-69. Møsvatn: isolines for environmental variables in the DCA ordinations of 50 meso plots, axes 1 (horizontal) and 2 (vertical). Values for the environmental variables are plotted onto the meso plots' positions. Scaling in S.D. units. Fig. 68. Total N (R^2 = 0.738). Fig. 69. $pH_{(CaCl2)}$ (R^2 = 0.837). R^2 refers to the coefficient of determination between original and smoothened values as interpolated from the isolines. Names of environmental variables in accordance with Table 2.

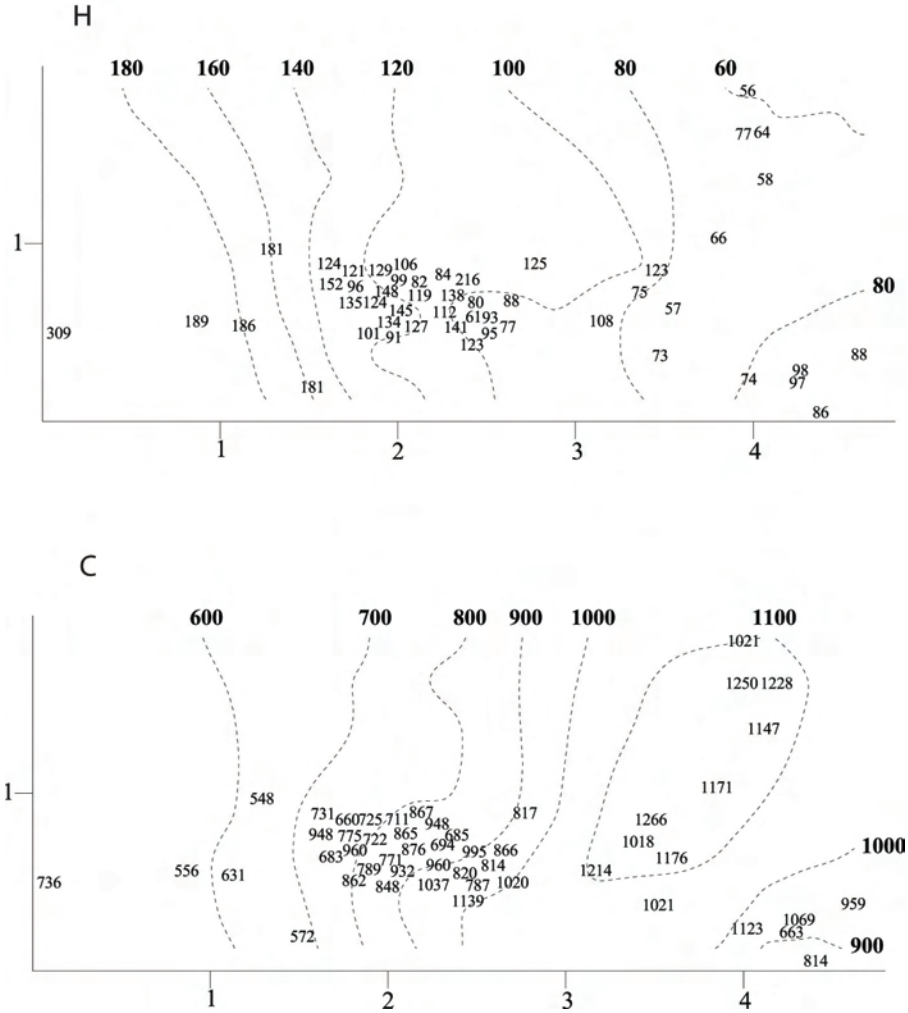

Figs 70-71. Møsvatn: isolines for environmental variables in the DCA ordinations of 50 meso plots, axes 1 (horizontal) and 2 (vertical). Values for the environmental variables are plotted onto the meso plots' positions. Scaling in S.D. units. Fig. 70. H (R^2 = 0.750). Fig. 71. C (R^2 = 0.753). R^2 refers to the coefficient of determination between original and smoothened values as interpolated from the isolines. Names of environmental variables in accordance with Table 2.

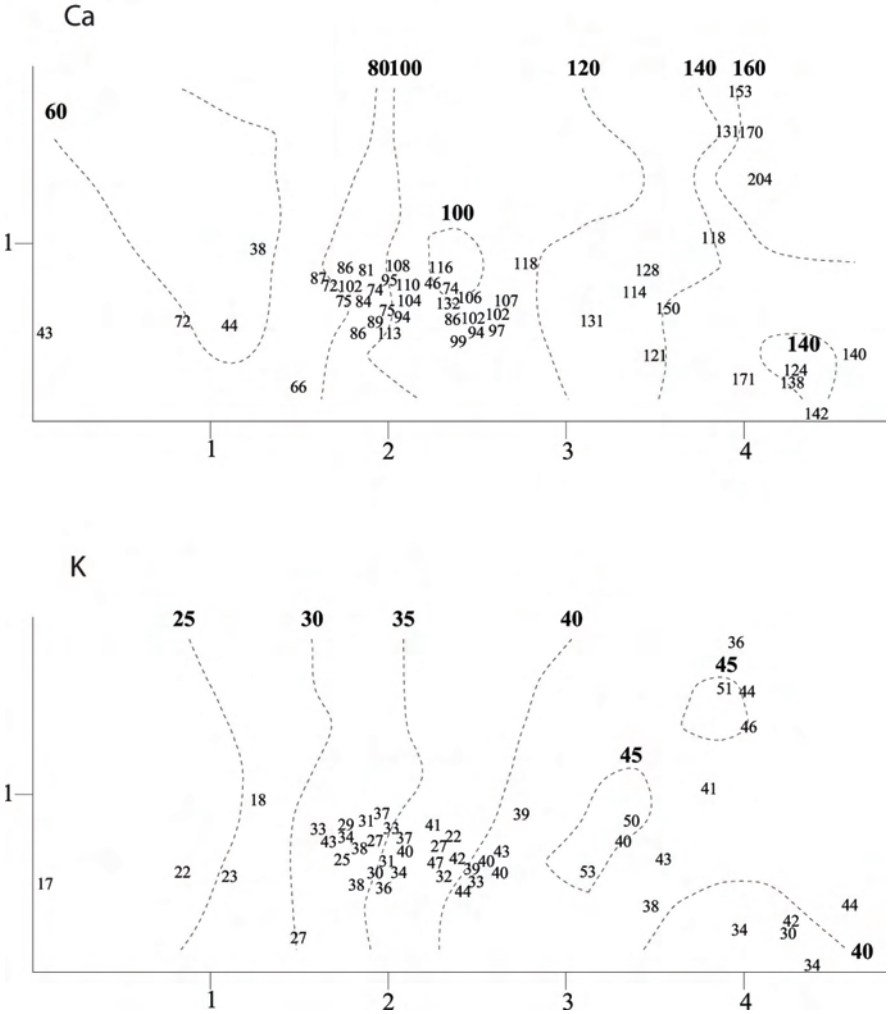

Figs 72-73. Møsvatn: isolines for environmental variables in the DCA ordinations of 50 meso plots, axes 1 (horizontal) and 2 (vertical). Values for the environmental variables are plotted onto the meso plots' positions. Scaling in S.D. units. Fig. 72. Ca (R^2 = 0.803). Fig. 73. K (R^2 = 0.669). R^2 refers to the coefficient of determination between original and smoothened values as interpolated from the isolines. Names of environmental variables in accordance with Table 2.

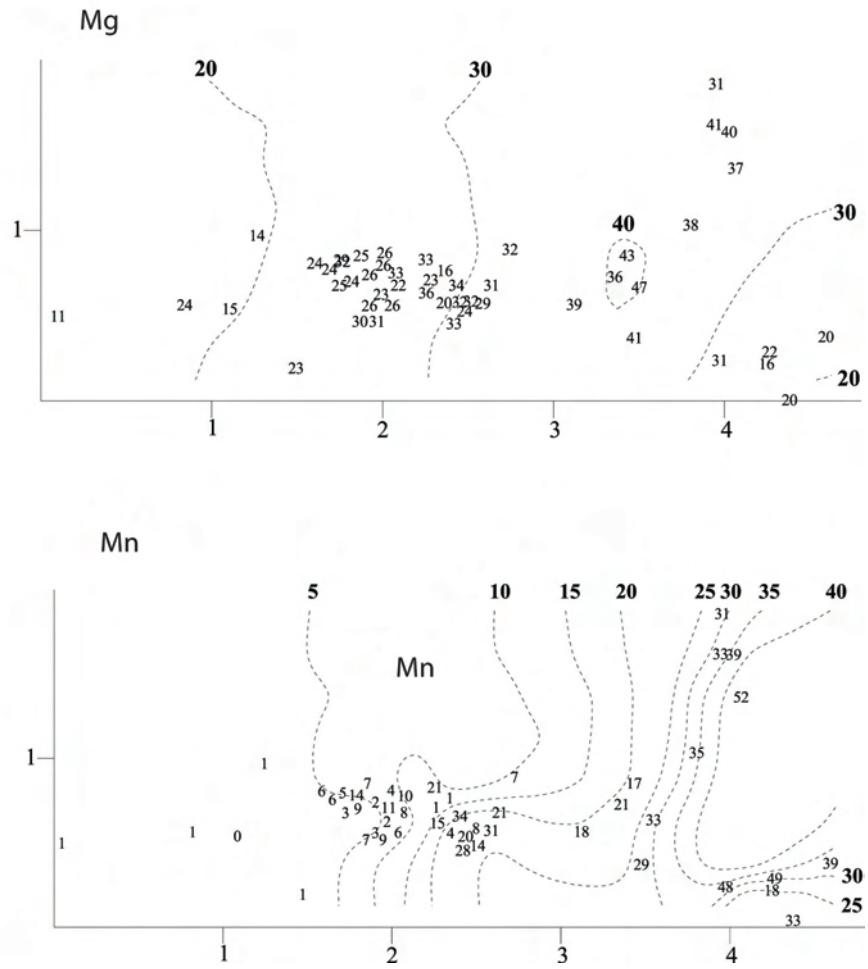

Figs 74-75. Møsvatn: isolines for environmental variables in the DCA ordinations of 50 meso plots, axes 1 (horizontal) and 2 (vertical). Values for the environmental variables are plotted onto the meso plots' positions. Scaling in S.D. units. Fig. 74. Mg (R^2 = 0.618). Fig. 75. Mn (R^2 = 0.771).R^2 refers to the coefficient of determination between original and smoothened values as interpolated from the isolines. Names of environmental variables in accordance with Table 2.

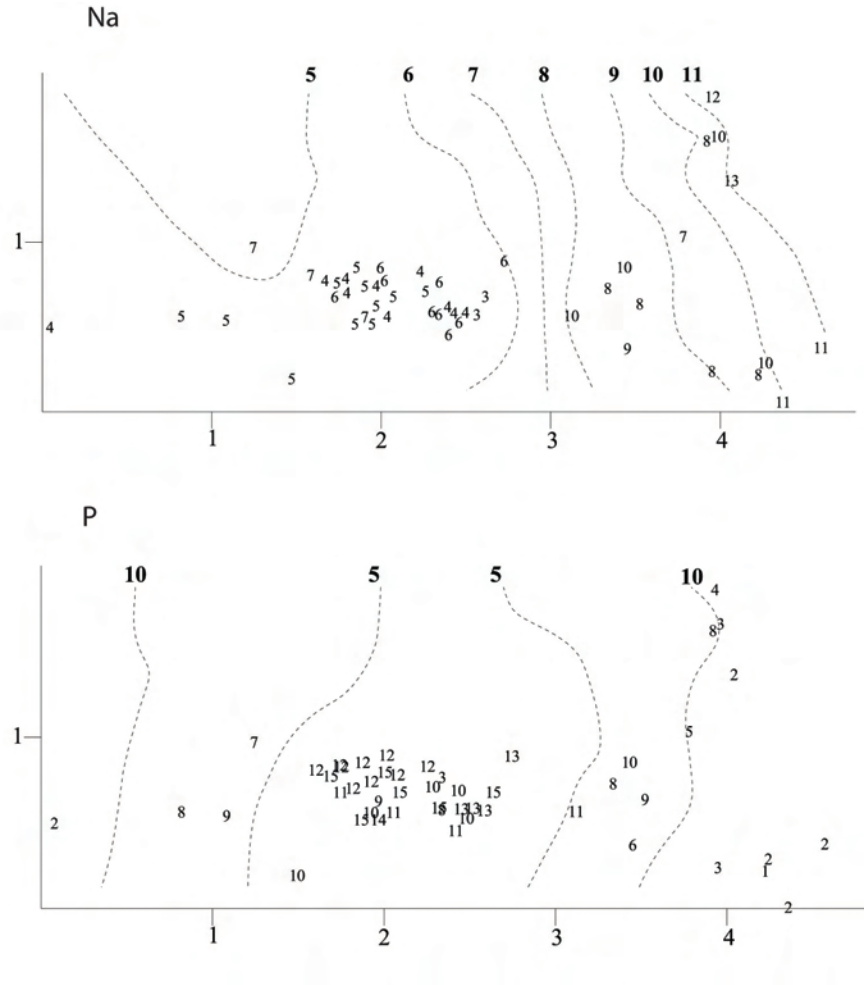

Figs 76-77. Møsvatn: isolines for environmental variables in the DCA ordinations of 50 meso plots, axes 1 (horizontal) and 2 (vertical). Values for the environmental variables are plotted onto the meso plots' positions. Scaling in S.D. units. Fig. 76. Na (R^2 = 0.743). Fig. 77. P (R^2 = 0.569). R^2 refers to the coefficient of determination between original and smoothened values as interpolated from the isolines. Names of environmental variables in accordance with Table 2.

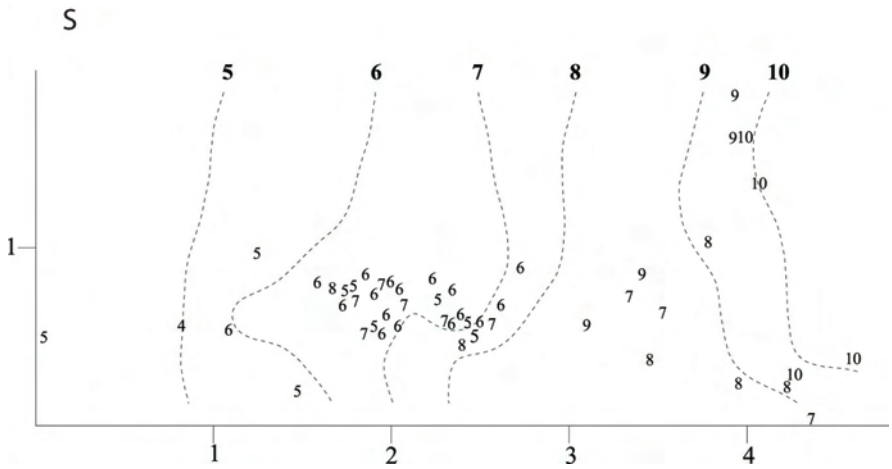

Fig. 78. Møsvatn: isolines for environmental variables in the DCA ordinations of 50 meso plots, axes 1 (horizontal) and 2 (vertical). Values for the environmental variables are plotted onto the meso plots' positions. Scaling in S.D. units. Fig. 78. S (R^2 = 0.776). R^2 refers to the coefficient of determination between original and smoothened values as interpolated from the isolines. Names of environmental variables in accordance with Table 2.

Frequent species

A total of 124 species were recorded within the fifty 1 × 1 m meso plots: 61 vascular plants, 25 mosses, 19 liverworts and 19 lichens. The most frequent species were (the sum of subplot frequencies in brackets): *Avenella flexuosa* (717 out of 800), *Barbilophozia lycopodioides* (691), *Vaccinium myrtillus* (663), *Vaccinium vitis-idaea* (452), *Empetrum nigrum* (443), *Trientalis europaea* (376), *Pleurozium schreberi* (347), *Hylocomium splendens* (312), *Vaccinium uliginosum* (298), and *Brachythecium reflexum* (295).

The distribution of species abundance in the DCA ordination

Forty seven of the total 124 species occurred in 5 or more of the sample plots (Figs 79-125).

Only *Vaccinium myrtillus* (Fig. 82) occurred abundantly in most of the sample plots, demonstrating a wide ecological amplitude. *Empetrum nigrum* (Fig. 81), *Vaccinium uliginosum* (Fig. 83) and *Vaccinium vitis-idaea* (Fig. 84) also had relatively wide ecological amplitudes, but were absent from the extreme right-hand situated plots in the DCA ordination diagram with favourable soil nutrient status. *Solidago virgaurea* (Fig. 97), *Trientalis europaea* (Fig. 98), *Avenella flexuosa* (Fig. 100), *Brachythecium reflexum* (Fig. 103) and *Barbilophozia lycopodioides* (Fig. 115) were only absent from plots with very low DCA 1 scores, i.e. the plots with the most acid and nutrient-poor soils.

Species with more narrow amplitudes in the material, which showed preferences for plots with higher pH and higher concentrations of nutrients, were *Geranium sylvaticum* (Fig. 85), *Phegopteris connectilis* (Fig. 94), *Ranunculus acris* (Fig. 95), *Rumex acetosa* (Fig. 96), *Milium effusum* (Fig. 102) and *Mnium spinosum* (Fig. 108).

Cladonia arbuscula (Fig. 119), *C. rangiferina* (Fig. 124) and *C. stellaris* (Fig. 125) were restricted to the left-hand side of the ordination diagram and thus occurred in sample plots with low slope, low tree basal area, low soil nutrient status and high LOI values (on ridges with scattered trees).

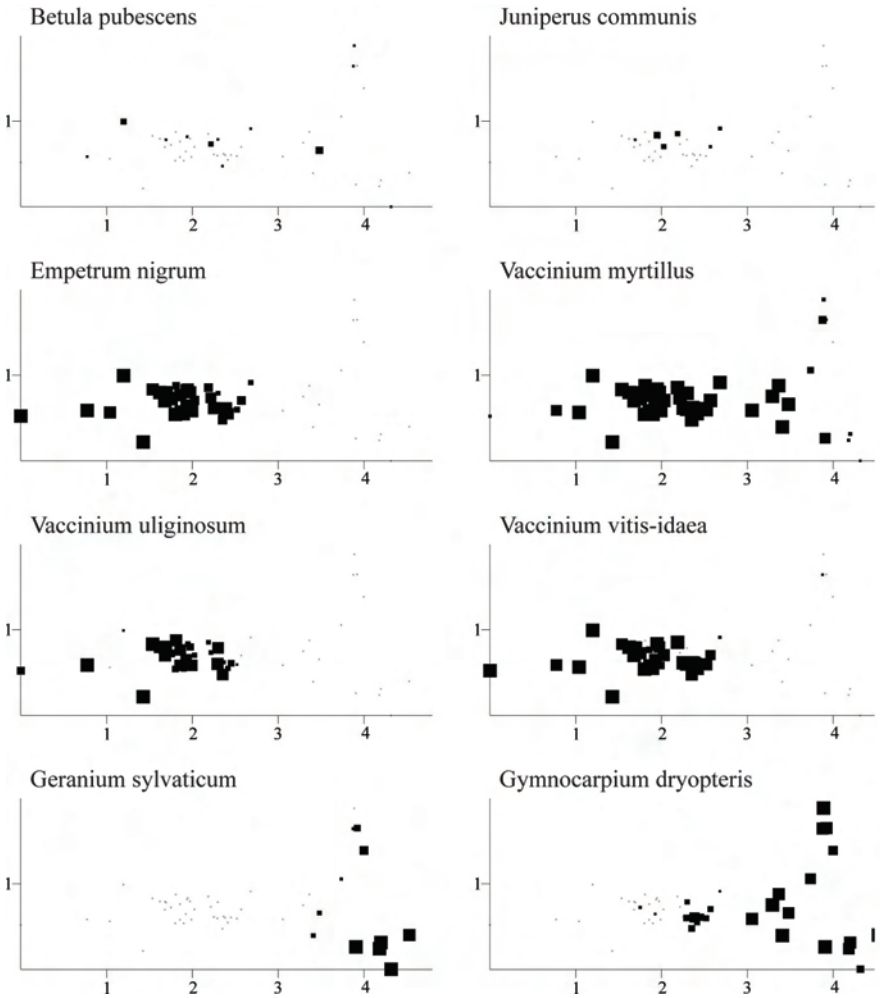

Figs 79-86. Møsvatn: distributions of species abundances in the DCA ordination of 50 sample plots, axes 1 (horizontal) and 2 (vertical). Frequency in subplots for each species in each meso plot proportional to quadrate size. Scaling in S.D. units. Fig. 79. *Betula pubescens*. Fig. 80. *Juniperus communis*. Fig. 81. *Empetrum nigrum*. Fig. 82. *Vaccinium myrtillus*. Fig. 83. *Vaccinium uliginosum*. Fig. 84. *Vaccinium vitis-idaea*. Fig. 85. *Geranium sylvaticum*. Fig. 86. *Gymnocarpium dryopteris*.

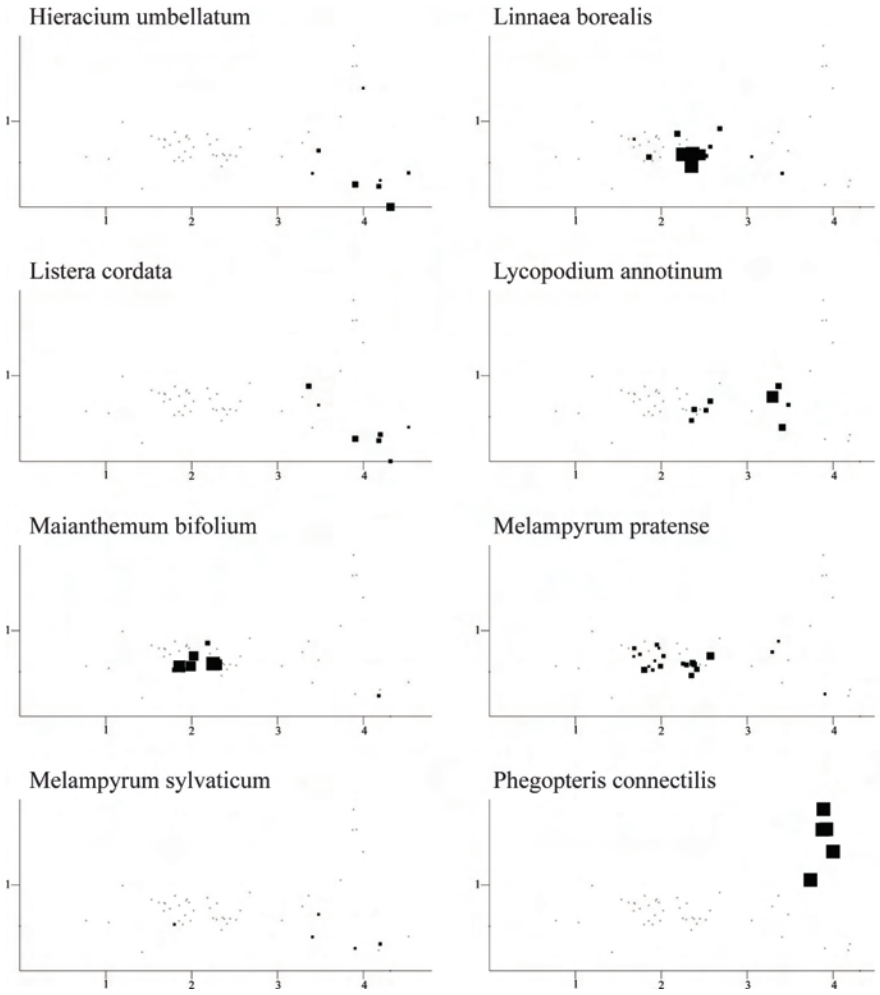

Figs 87-94. Møsvatn: distributions of species abundances in the DCA ordination of 50 sample plots, axes 1 (horizontal) and 2 (vertical). Frequency in subplots for each species in each meso plot proportional to quadrate size. Scaling in S.D. units. Fig. 87. *Hieracium umbellatum*. Fig. 88. *Linnaea borealis*. Fig. 89.*Listera cordata*. Fig. 90. *Lycopodium annotinum*. Fig. 91. *Maianthemum bifolium*. Fig. 92. *Melampyrum pratense*. Fig. 93. *Melampyrum sylvaticum*. Fig. 94. *Phegopteris connectilis*.

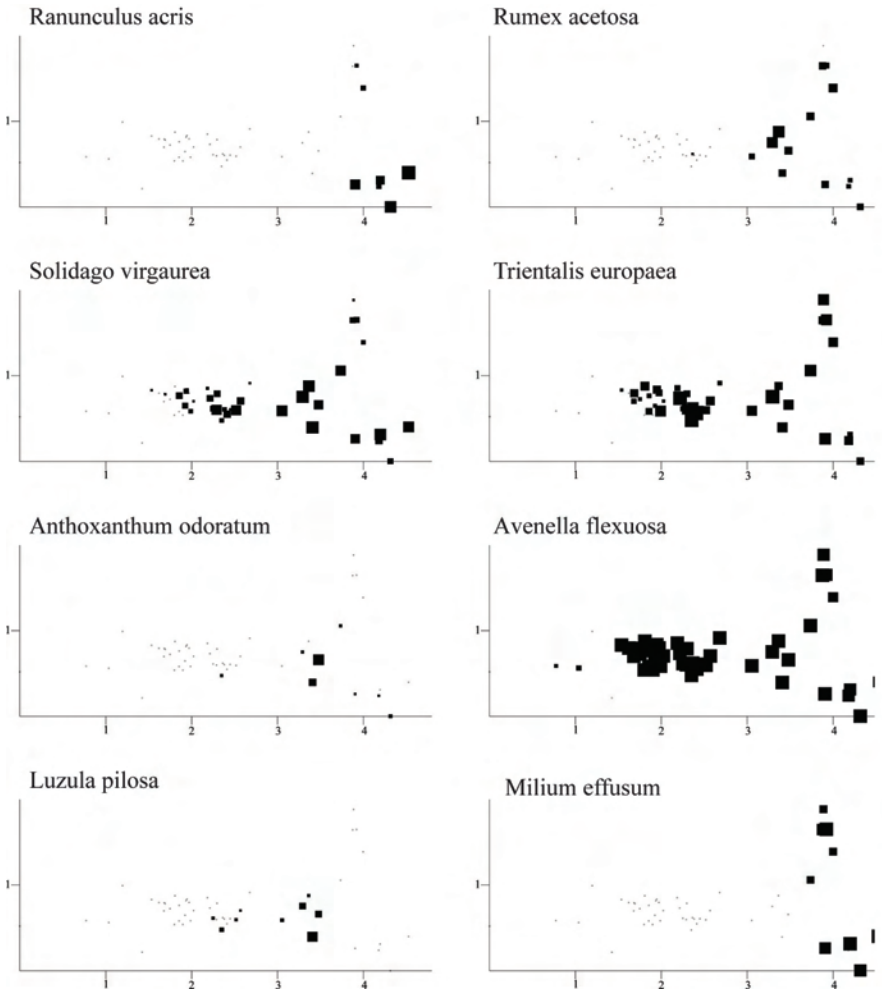

Figs 95-102. Møsvatn: distributions of species abundances in the DCA ordination of 50 sample plots, axes 1 (horizontal) and 2 (vertical). Frequency in subplots for each species in each meso plot proportional to quadrate size. Scaling in S.D. units. Fig. 95. *Ranunculus acris*. Fig. 96. *Rumex acetosa*. Fig. 97. *Solidago virgaurea*. Fig. 98. *Trientalis europaea*. Fig. 99. *Anthoxanthum odoratum*. Fig. 100. *Avenella flexuosa* (syn. *Deschampsia flexuosa)*. Fig. 101. *Luzula pilosa*. Fig. 102. *Milium effusum*.

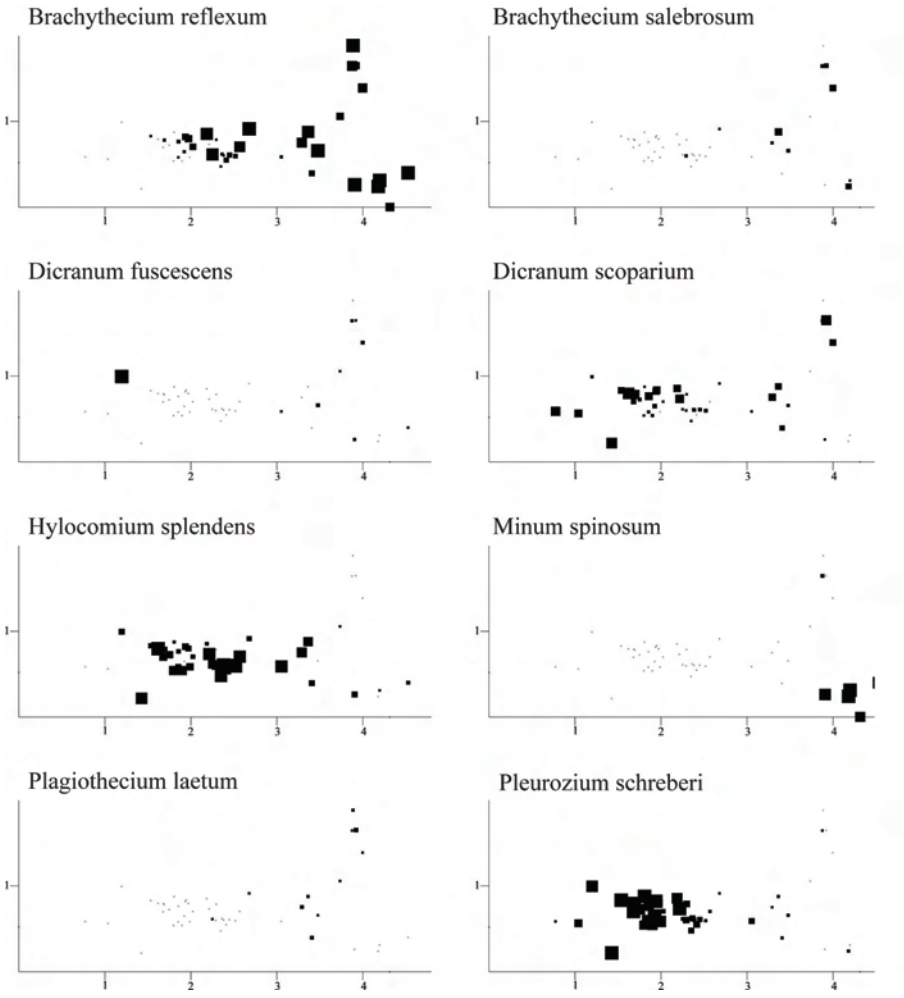

Figs 103-110. Møsvatn: distributions of species abundances in the DCA ordination of 50 sample plots, axes 1 (horizontal) and 2 (vertical). Frequency in subplots for each species in each meso plot proportional to quadrate size. Scaling in S.D. units. Fig. 103. *Brachythecium reflexum*. Fig. 104. *Brachythecium salebrosum*. Fig. 105. *Dicranum fuscescens*. Fig. 106. *Dicranum scoparium.* Fig. 107. *Hylocomium splendens.* Fig. 108. *Mnium spinosum*. Fig. 109. *Plagiothecium laetum*. Fig. 110. *Pleurozium schreberi*.

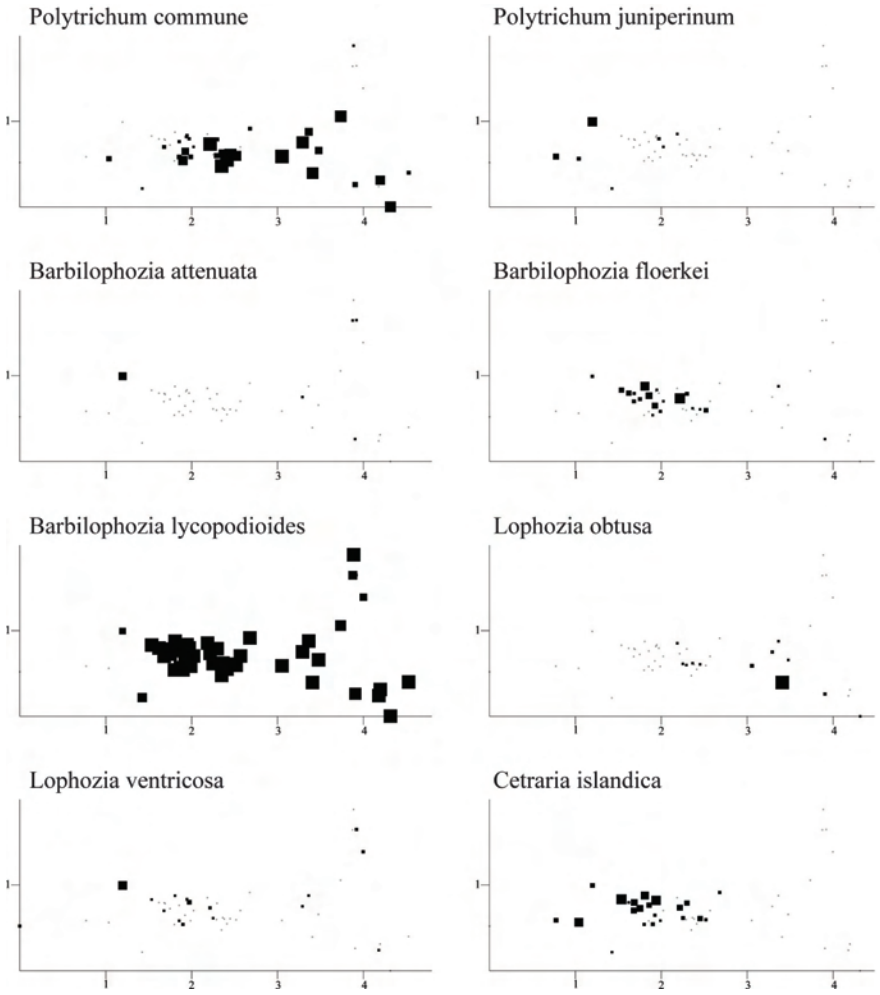

Figs 111-118. Møsvatn: distributions of species abundances in the DCA ordination of 50 sample plots, axes 1 (horizontal) and 2 (vertical). Frequency in subplots for each species in each meso plot proportional to quadrate size. Scaling in S.D. units. Fig. 111. *Polytrichum commune*. Fig. 112. *Polytrichum juniperinum*. Fig. 113. *Barbilophozia attenuata*. Fig. 114. *Barbilophozia floerkei*. Fig. 115. *Barbilophozia lycopodioides*. Fig. 116. *Lophozia obtusa*. Fig. 117. *Lophozia ventricosa*. Fig. 118. *Cetraria islandica*.

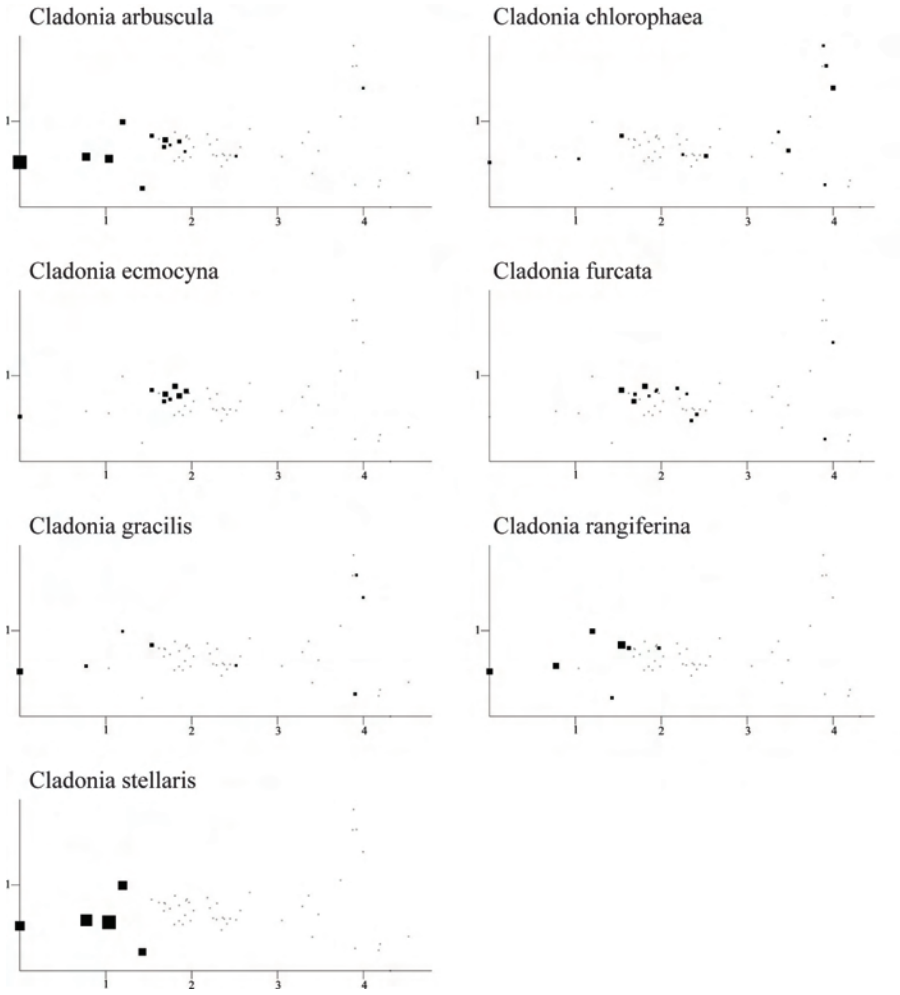

Figs 119-125. Møsvatn: distributions of species abundances in the DCA ordination of 50 sample plots, axes 1 (horizontal) and 2 (vertical). Frequency in subplots for each species in each meso plot proportional to quadrate size. Scaling in S.D. units. Fig. 119. *Cladonia arbuscula*. Fig. 120. *Cladonia chlorophaea*. Fig. 121. *Cladonia ecmocyna*. Fig. 122. *Cladonia furcata.* Fig. 123. *Cladonia gracilis*. Fig. 124. *Cladonia rangiferina*. Fig. 125. *Cladonia stellaris.*

GUTULIA REFERENCE AREA

Correlations between environmental variables

Macro and meso plot slope were negatively correlated with heat indices, tree basal area, soil moisture and soil pH, and negatively correlated with soil depth, loss on ignition and exchangeable H (Table 9). Tree basal area was positively correlated with soil pH. Soil depth (Smi, Sme and Sma) was, in general, negatively correlated with concentrations of extractable elements that reflected soil richness (e.g. Ca, Mg, K and Na) and with pH, and positively correlated with loss on ignition and soil acidity (exchangeable H).

Soil moisture was positively correlated with soil pH, extractable P, C, Ca, K, Mg, Mn and Zn and negatively correlated with loss on ignition and soil acidity. Loss on ignition was, in turn, positively correlated with soil acidity and negatively correlated with variables reflecting soil nutrient richness. Variables reflecting soil nutrient richness (pH, P, N, Ca, Mg, Na, K, Mn) were, in general, internally positively correlated, each of these were negatively correlated with soil acidity (exchangeable H and extractable Al). Thus the Gutulia reference area showed variation in soil nutrient richness and base status with the most acidic plots situated in rather flat areas with deeper soils characterized by high loss on ignition, and the more base rich plots on steeper slopes with higher biomass of trees.

Table 9. Gutulia: Kendall's rank correlation coefficients τ between 31 environmental variables in the 50 sample plots (lower triangle), with significance probabilities (upper triangle). Statistically significant correlations (P<0.05) in bold face. Names of explanatory variables abbreviated in accordance with Table 2.

	1	2	3	4	5	6	7	8	9	10	11	12	13	14	15	16	17	18	19	20	21	22	23	24	25	26	27	28	29	30	31
01 Ma Slo	*	0.474	**0.000**	0.072	**0.001**	**0.019**	**0.000**	0.069	**0.000**	**0.003**	0.053	**0.027**	**0.009**	**0.022**	**0.023**	**0.000**	0.317	**0.000**	**0.000**	**0.000**	0.132	**0.005**	0.193	**0.004**	**0.003**	0.101	**0.000**	0.562	0.243	**0.002**	0.137
02 Ma Asp	0.073	*	**0.002**	0.104	0.599	0.743	0.170	**0.000**	**0.001**	0.190	0.978	0.338	0.187	0.580	0.175	0.841	0.492	0.873	0.860	0.675	0.627	0.603	0.513	0.461		0.365	0.197	0.241	0.867	0.451	0.140
03 Ma HI	**–0.789**	**–0.309**	*	0.326	**0.006**	**0.032**	**0.000**	**0.000**	**0.000**	**0.017**	0.167	**0.004**	**0.001**	**0.007**	**0.006**	**0.000**	0.094	**0.000**	**0.000**	**0.000**	**0.046**	**0.010**	0.222	**0.001**	**0.001**	**0.025**	**0.000**	0.203	0.241	**0.003**	**0.016**
04 Ma Ter	0.205	–0.182	–0.109	*	0.503	0.885	0.527	0.241	0.589	**0.000**	0.302	0.554	0.522	0.672	0.353	0.907	0.950	0.725	0.626	0.836	0.392	0.353	0.794	0.698	0.268	0.252	0.978	0.185	0.168	0.646	0.123
05 Ma Une	**–0.387**	0.058	**0.301**	–0.083	*	0.083	**0.000**	0.873	**0.011**	0.405	**0.000**	0.177	0.068	**0.033**	**0.012**	**0.002**	0.323	**0.001**	**0.001**	**0.000**	0.089	**0.012**	0.092	**0.001**	**0.011**	0.281	**0.004**	0.516	0.124	**0.004**	0.551
05 TBA	**0.241**	0.033	**–0.214**	0.016	–0.193	*	0.147	0.440	0.125	0.459	0.553	**0.030**	0.051	0.378	0.597	**0.000**	**0.029**	**0.000**	**0.000**	**0.000**	0.147	**0.007**	0.860	0.795	**0.008**	0.744	**0.000**	0.230	0.055	**0.000**	0.455
07 Me Slo	**0.693**	0.139	**–0.632**	0.072	**–0.393**	0.148	*	0.368	**0.000**	0.120	0.296	**0.044**	**0.009**	**0.013**	**0.034**	**0.001**	0.674	**0.004**	**0.002**	**0.006**	0.275	**0.047**	0.410	**0.024**	**0.018**	0.214	**0.001**	0.614	0.401	**0.008**	0.338
08 Me Asp	0.183	**0.707**	**–0.354**	–0.130	0.018	0.077	0.090	*	**0.000**	0.915	0.964	0.678	0.356	0.993	0.225	0.913	0.288	0.987	0.973	0.669	0.436	0.669	0.821	0.456	0.427	0.273	0.446	0.273	0.874	0.874	0.110
09 Me HI	**–0.648**	**–0.325**	**0.760**	–0.060	**0.279**	–0.153	**–0.662**	**–0.446**	*	0.076	0.365	0.168	0.058	0.104	0.072	**0.021**	0.336	**0.035**	**0.025**	**0.039**	0.336	0.219	0.303	0.060	0.080	0.143	**0.006**	0.311	0.900	0.072	0.225
10 Me Ter	**0.334**	–0.145	**–0.263**	**0.503**	–0.102	0.083	0.175	–0.012	–0.194	*	0.675	0.986	0.993	0.859	0.206	0.454	**0.042**	0.612	0.471	0.476	0.113	0.618	0.206	**0.028**	0.776	0.310	0.476	0.075	0.165	0.762	0.708
11 Me Une	–0.219	0.003	0.152	–0.129	**0.566**	–0.067	–0.118	0.005	0.100	–0.052	*	0.677	1.000	0.957	0.139	0.164	0.609	0.082	0.106	0.063	0.108	0.193	0.446	**0.001**	0.087	0.686	0.212	0.328	0.121	0.355	0.726
12 Smi	**–0.232**	–0.099	**0.290**	0.068	0.154	**–0.226**	**–0.210**	–0.042	0.141	0.002	0.048	*	**0.000**	**0.000**	**0.000**	**0.000**	0.729	**0.000**	**0.000**	**0.000**	**0.014**	**0.000**	**0.003**	**0.001**	**0.000**	**0.000**	**0.000**	0.654	**0.008**	**0.000**	**0.000**
13 Sme	**–0.266**	–0.132	**0.323**	0.072	0.202	–0.197	**–0.263**	–0.092	0.187	–0.001	0.000	**0.792**	*	**0.000**	**0.000**	**0.000**	0.880	**0.000**	**0.000**	**0.000**	**0.007**	**0.000**	**0.003**	**0.001**	**0.000**	**0.000**	**0.000**	0.854	**0.005**	**0.000**	**0.000**
14 Sma	**–0.233**	–0.055	**0.264**	0.047	**0.234**	–0.089	**–0.252**	–0.001	0.160	–0.020	0.006	**0.706**	**0.728**	*	**0.000**	**0.000**	0.482	**0.000**	**0.000**	**0.000**	**0.005**	**0.000**	**0.001**	**0.001**	**0.000**	**0.000**	**0.000**	0.828	**0.003**	**0.000**	**0.000**
15 Mme	**0.229**	0.134	**–0.268**	–0.102	**–0.275**	0.053	**0.212**	0.119	–0.176	0.138	–0.163	**–0.437**	**–0.497**	**–0.504**	*	**0.000**	**0.024**	**0.000**	**0.001**	**0.000**	**0.000**	**0.000**	**0.028**	**0.000**	**0.000**	**0.000**	**0.001**	0.114	**0.000**	**0.020**	**0.000**
16 LOI	**–0.424**	–0.020	**0.368**	–0.013	**0.341**	**–0.455**	**–0.319**	–0.011	**0.225**	–0.082	0.153	**0.530**	**0.512**	**0.417**	**–0.365**	*	0.498	**0.000**	**0.000**	**0.000**	0.252	**0.000**	0.296	**0.002**	**0.000**	**0.046**	**0.000**	0.795	0.281	**0.000**	**0.003**
17 Total N	–0.100	–0.068	0.164	0.007	–0.108	**0.218**	–0.042	–0.104	0.094	**–0.222**	0.056	0.035	0.015	0.069	**–0.220**	–0.066	*	0.215	0.181	0.417	**0.000**	0.598	0.900	**0.010**	0.553	**0.006**	0.398	**0.001**	**0.001**	**0.022**	**0.005**
18 pH_{H2O}	**0.376**	0.016	**–0.345**	0.039	**–0.367**	**0.435**	**0.293**	–0.002	**–0.207**	0.056	–0.192	**–0.587**	**–0.545**	**–0.466**	**0.343**	**–0.748**	0.121	*	**0.000**	**0.000**	0.085	**0.000**	**0.008**	**0.001**	**0.000**	**0.004**	**0.000**	0.920	0.228	**0.000**	**0.000**
19 pH_{CaCl2}	**0.399**	0.017	**–0.351**	0.054	**–0.355**	**0.455**	**0.315**	0.003	**–0.220**	0.079	–0.178	**–0.592**	**–0.565**	**–0.472**	**0.326**	**–0.764**	0.131	**0.942**	*	**0.000**	0.128	**0.000**	**0.008**	**0.001**	**0.000**	**0.005**	**0.000**	0.763	0.209	**0.000**	**0.000**
20H	**–0.357**	–0.041	**0.353**	0.023	**0.391**	**–0.380**	**–0.272**	–0.042	**0.202**	–0.078	0.204	**0.599**	**0.580**	**0.508**	**–0.407**	**0.667**	–0.079	**–0.834**	**–0.832**	*	**0.004**	**0.000**	**0.002**	**0.000**	**0.000**	**0.000**	**0.000**	0.927	**0.022**	**0.000**	**0.000**
21 Al	–0.151	–0.048	**0.195**	0.094	0.186	0.145	–0.109	–0.076	0.094	–0.173	0.177	**0.249**	**0.268**	**0.275**	**–0.456**	0.112	**0.381**	–0.169	–0.149	**0.285**	*	**0.003**	**0.000**	**0.000**	**0.000**	**0.000**	0.139	0.096	**0.000**	0.398	**0.000**
22 C	**0.283**	0.051	**–0.250**	–0.102	**–0.275**	**0.267**	**0.198**	0.042	–0.120	0.055	–0.143	**–0.533**	**–0.535**	**–0.514**	**0.389**	**–0.453**	0.051	**0.584**	**0.606**	**–0.610**	**–0.293**	*	**0.001**	**0.004**	**0.000**	**0.000**	**0.000**	0.304	**0.001**	**0.000**	**0.000**
23 Ca	0.131	–0.065	–0.119	–0.029	–0.184	0.018	0.082	–0.022	–0.101	0.138	–0.084	**–0.304**	**–0.292**	**–0.313**	**0.215**	–0.102	–0.012	**0.261**	**0.261**	**–0.304**	**–0.429**	**0.339**	*	**0.000**	**0.000**	**0.000**	0.051	0.477	**0.001**	0.069	**0.000**
24 Fe	**–0.286**	–0.073	**0.312**	–0.043	**0.372**	0.026	**–0.225**	–0.073	0.184	**–0.240**	**0.376**	**0.347**	**0.343**	**0.333**	**–0.512**	**0.298**	**0.251**	**–0.340**	**–0.320**	**0.429**	**0.634**	**–0.283**	**–0.350**	*	**0.000**	**0.000**	**0.002**	**0.039**	**0.000**	0.139	**0.000**
25 K	**0.296**	0.129	**–0.339**	–0.122	**–0.279**	**0.263**	**0.237**	0.078	–0.171	0.031	–0.188	**–0.671**	**–0.633**	**–0.595**	**0.473**	**–0.513**	–0.058	**0.638**	**0.626**	**–0.700**	**–0.399**	**0.711**	**0.396**	**–0.422**	*	**0.000**	**0.000**	0.834	**0.000**	**0.000**	**0.000**
26 Mg	0.165	0.089	**–0.219**	–0.126	–0.118	–0.033	0.124	0.108	–0.143	0.111	–0.044	**–0.418**	**–0.417**	**–0.435**	**0.396**	**–0.195**	**–0.269**	**0.282**	**0.275**	**–0.391**	**–0.646**	**0.406**	**0.603**	**–0.460**	**0.525**	*	**0.008**	0.707	**0.000**	**0.036**	**0.000**
27 Mn	**0.367**	0.128	**–0.430**	0.003	**–0.318**	**0.414**	**0.336**	0.075	**–0.269**	0.078	–0.137	**–0.589**	**–0.586**	**–0.463**	**0.319**	**–0.696**	0.082	**0.771**	**0.788**	**–0.729**	–0.144	**0.528**	0.190	**–0.301**	**0.624**	**0.260**	*	0.744	0.168	**0.000**	**0.000**
28 Na	–0.058	–0.116	0.124	–0.146	0.071	0.119	–0.050	–0.108	0.099	–0.195	0.108	–0.046	–0.018	–0.021	–0.154	0.025	**0.318**	0.010	0.029	0.009	0.162	0.100	0.069	**0.202**	0.020	–0.037	–0.032	*	0.207	0.060	0.795
29 P	0.117	0.017	–0.115	–0.152	–0.168	–0.191	0.084	–0.016	–0.012	0.152	–0.171	**–0.270**	**–0.278**	**–0.293**	**0.456**	–0.105	**–0.316**	0.118	0.123	**–0.223**	**–0.736**	**0.316**	**0.337**	**–0.510**	**0.386**	**0.548**	0.135	–0.123	*	0.178	**0.000**
30 S	**0.316**	0.075	**–0.294**	–0.051	**–0.314**	**0.380**	**0.267**	0.016	–0.176	–0.033	–0.102	**–0.494**	**–0.530**	**–0.458**	**0.228**	**–0.530**	**0.223**	**0.635**	**0.651**	**–0.592**	–0.082	**0.633**	0.177	–0.144	**0.576**	**0.205**	**0.618**	0.184	0.131	*	**0.001**
31 Zn	0.149	0.146	**–0.236**	–0.170	–0.065	0.074	0.096	0.157	–0.119	0.041	–0.038	**–0.528**	**–0.512**	**–0.480**	**0.496**	**–0.295**	**–0.277**	**0.343**	**0.357**	**–0.442**	**–0.569**	**0.584**	**0.419**	**–0.376**	**0.605**	**0.691**	**0.393**	–0.025	**0.546**	**0.334**	*

PCA ordination of environmental variables

The first two PCA axes accounted for 46.6% and 14.5% of the variance in the matrix of standardised transformed environmental variables, respectively (the corresponding eigenvalues were 0.466 and 0.145).

Lowest loadings on PCA axis 1 as well as loadings close to zero on PCA axis 2 were obtained by median, minimum and maximum soil depth, loss on ignition, and exchangeable H, S and Mn (Fig. 126). High loadings on this axis and loadings close to zero on PCA axis 2 were obtained by extractable C, K, P and Zn and $pH_{(H2O)}$ and $pH_{(CaCl2)}$. Extractable Mg and Ca obtained relatively high loadings on PCA axis 1 together with macro and meso plot slope, while soil concentrations of Fe, macro plot heat index and macro plot unevenness obtained low loadings.

Total N and extractable Al obtained high loadings on PCA axis 2, while extractable P and Mg obtained low loadings.

The PCA ordination results were thus consistent with the correlation matrix in Table 9, emphasising importance of soil nutrient richness and topography for the environmental structure in the Gutulia reference area.

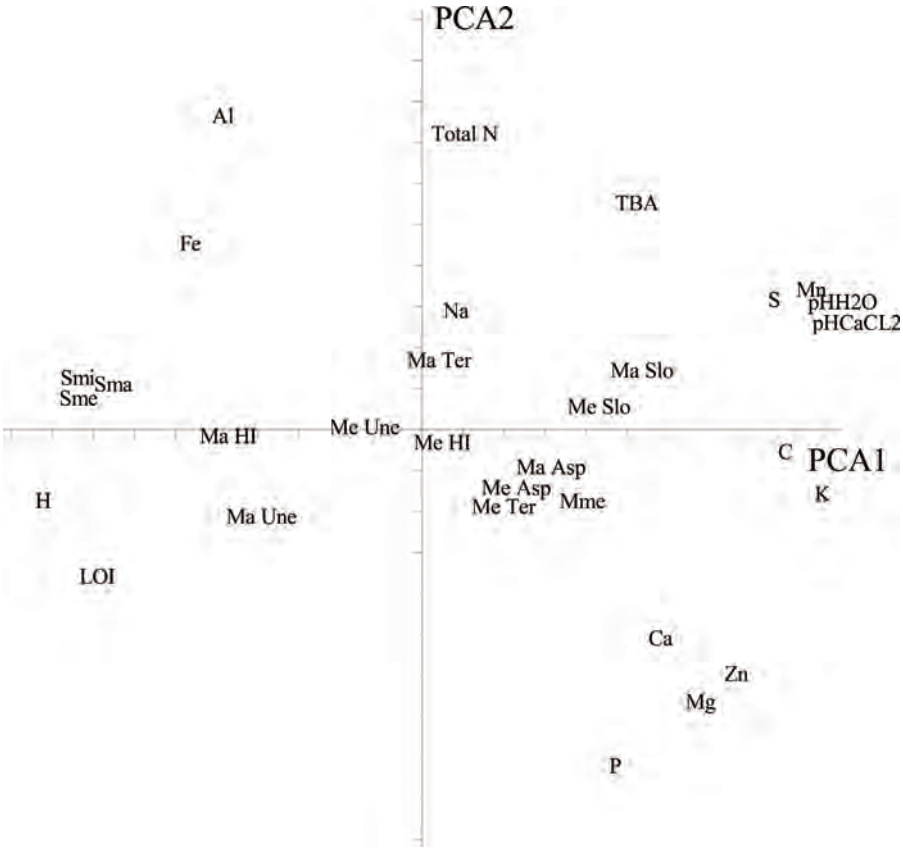

Fig. 126. Gutulia: PCA ordination of 31 environmental variables. Abbreviations in accordance with Table 2, axes 1 (horizontal) and 2 (vertical). Positions of variables in the ordination space give the head of variable vectors. Tickmarks indicate 0.1 units along both axes.

DCA ordination

The gradient length of the two first DCA axes was 2.76 and 1.62 S.D. units with eigenvalues of 0.404 and 0.136 respectively, showing that the first axis was particularly important.

The sample plots were relatively evenly distributed along DCA axis 1, but dispersion along DCA axis 2 was largest among plots with DCA axis 1 values less than 1.4 S.D. units (Fig. 127).

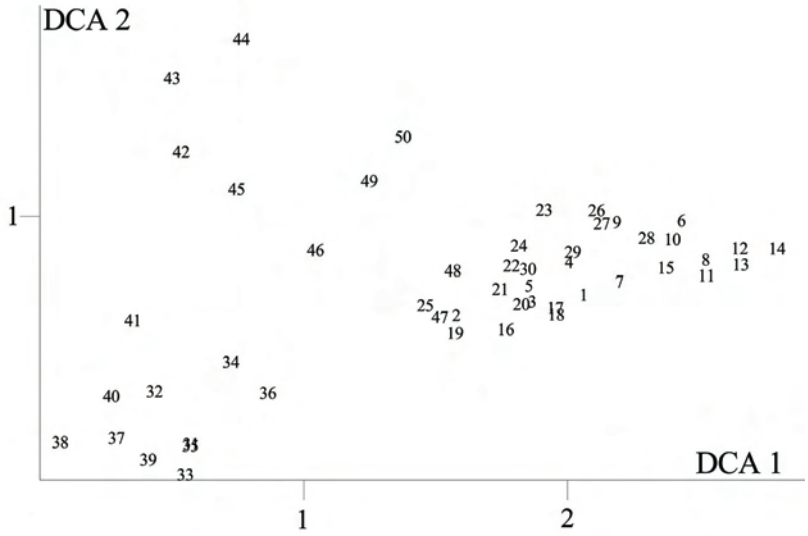

Fig. 127. Gutulia: DCA ordination diagram of 50 meso plots, axes 1 (horizontal) and 2 (vertical). Meso plot number are plotted just right of the sample plot positions. Scaling of axes in S.D. units.

GNMDS ordination

The GNMDS ordination diagram (Fig 128) showed good visual similarity to the DCA diagram (Fig 127). The correlation between GNMDS axis 1 and DCA axis 1 was $\tau = 0.917$ and between GNMDS axis 2 and DCA axis 2 $\tau = 0.342$.

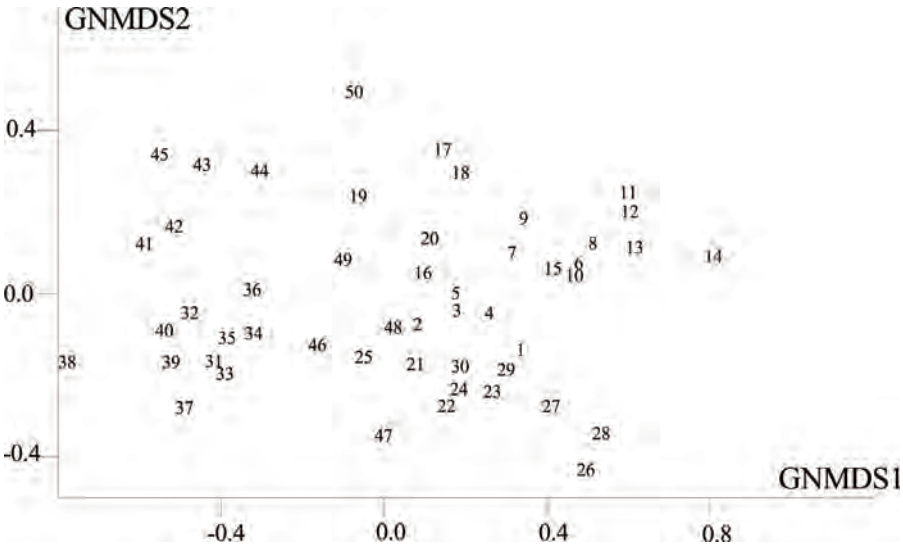

Fig.128. Gutulia: GNMDS ordination biplot diagram of 50 meso plots (indicated by their number).

Split-plot GLM analysis of relationships between ordination axes and environmental variables

Variation (in plot scores) along DCA axis 1 was partitioned with 95.35 % at the macro-plot scale (i.e. between macro plots) and 4.65 % at the (between) meso plot scale within macro plots (Table 10). For the second ordination axis, 77.50 % of the variation was explained at the macro-plot scale and 22.50 % at the plot scale (Table 11)

At the macro-plot scale, eleven environmental variables were significantly (at the α = 0.05 level) related to DCA 1 while two variables (also at the α = 0.05 level) were related to DCA 2. At the plot scale level, no environmental variables were significantly related to both DCA 1 and DCA 2 (Tables 10 and 11).

At the macro-plot scale, tree basal area and both pH measures and soil concentrations of Total N, C, K, Mn and S increased significantly along DCA 1, while soil concentration of H, loss on ignition and median soil depth decreased (Table 10).

At the macro-plot scale, DCA 2 was only significant (positively) related to the concentration of Total N and Na (Table 11).

Table 10. Gutulia: Split-plot GLM analysis and Kendall's nonparametric correlation coefficient τ between DCA 2 and 31 environmental variables (predictor) in the 50 plots. df_{resid}: degrees of freedom for the residuals; *SS*: total variation; *FVE*: fraction of total variation attributable to a given scale (macro plot or plot); SS_{expl}/SS: fraction of the variation attributable to the scale in question, explained by a variable; *r*: model coefficient (only given when significant at the $\alpha = 0.05$ level, otherwise blank); *F*: *F* statistic for test of the hypothesis that $r = 0$ against the two-tailed alternative. Split-plot GLM relationships significant at level $\alpha = 0.05$, *P*, *F*, *r* and SS_{expl}/SS, and Kendall's nonparametric correlation coefficient $|\tau| \geq 0.30$ are given in bold face. Numbers and abbreviations for names of environmental variables are in accordance with Table 2.

Predictor	Dependent variable = DCA 1 (*SS* = 29.2643)							Correlation between predictor and DCA 1
	Error level							
	Macro plot df_{resid} = 8 $SS_{macro\ plot}$ = 27.9043 *FVE* = 0.9535 of *SS*				Plot within macro plot df_{resid} = 39 SS_{plot} = 1.36000 *FVE* = 0.0465 of *SS*			Total
	$SS_{expl}/SS_{macro\ plot}$	*r*	*F*	*P*	SS_{expl}/SS_{plot}	*r*	*F*	*P*	τ
Ma Slo	0.0553		0.4679	0.5133	0.0009		0.0347	0.8533	0.217
Ma Asp	0.0023		0.0181	0.8963	0.0002		0.0060	0.9387	–0.046
Ma HI	0.0619		0.5279	0.4882	0.0002		0.0077	0.9304	–0.188

Ma Ter	0.0047		0.0381	0.8500	0.0341	1.3776	0.2476	–0.049
Ma Une	0.2292		2.3785	0.1616	0.0147	0.5807	0.4506	–0.297
TBA	**0.5716**	**2.9582**	**10.6740**	**0.0114**	0.0008	0.0329	0.8571	**0.365**
Me Slo	0.0246		0.2016	0.6654	0.0510	2.0951	0.1558	0.133
Me Asp	0.0116		0.0937	0.7673	0.0195	0.7764	0.3836	0.024
Me HI	0.0844		0.7378	0.4154	0.0004	0.0176	0.8953	–0.102
Me Ter	0.0578		0.4910	0.5034	0.0084	0.3290	0.5695	–0.035
Me Une	0.0227		0.1855	0.6780	0.0901	3.8621	0.0565	–0.137
Smi	0.3935		5.1903	0.0522	0.0000	0.0006	0.9799	**–0.430**
Sme	**0.4095**	**–1.747**	**5.5481**	**0.0463**	0.0528	2.1723	0.1485	**–0.403**
Sma	0.3352		4.0344	0.0795	0.0217	0.8646	0.3582	–0.271
Mme	0.1321		1.2176	0.3019	0.0139	0.5497	0.4629	0.169
LOI	**0.5269**	**–1.873**	**8.9093**	**0.0175**	0.0003	0.0130	0.9099	**–0.451**
Total N	**0.4169**	**2.2566**	**5.7199**	**0.0437**	0.0041	0.1622	0.6893	0.295
$pH_{(H2O)}$	**0.7113**	**2.1803**	**19.7090**	**0.0022**	0.0084	0.3288	0.5697	**0.568**
pH_{CaCl2}	**0.7125**	**2.0798**	**19.8230**	**0.0021**	0.0024	0.0945	0.7601	**0.575**
H	**0.6636**	**–2.061**	**15.7810**	**0.0041**	0.0003	0.0102	0.9201	**–0.553**
Al	0.0054		0.0435	0.8400	0.0019	0.0755	0.7849	–0.053
C	**0.6654**	**2.7013**	**15.9080**	**0.0040**	0.0124	0.4908	0.4877	**0.558**
Ca	0.2347		2.4533	0.1559	0.0012	0.0451	0.8330	0.221
Fe	0.0180		0.1468	0.7116	0.0132	0.5204	0.4750	–0.112
K	**0.4409**	**2.2281**	**6.3085**	**0.0363**	0.0088	0.3466	0.5594	**0.487**
Mg	0.0773		0.6702	0.4367	0.0208	0.8285	0.3683	0.189
Mn	**0.5906**	**1.8420**	**11.5410**	**0.0094**	0.0001	0.0055	0.9413	**0.451**
Na	0.3533		4.3706	0.0700	0.0004	0.0156	0.9013	0.269
P	0.0025		0.0200	0.8910	0.0003	0.0105	0.9188	0.030
S	**0.8087**	**2.6093**	**33.8220**	**0.0004**	0.0101	0.3984	0.5316	**0.605**
Zn	0.1602		1.5260	0.2518	0.0019	0.0740	0.7870	0.288

Table 11. Gutulia: Split-plot GLM analysis and Kendall's nonparametric correlation coefficient τ between DCA 2 and 31 environmental variables (predictor) in the 50 plots. df_{resid}: degrees of freedom for the residuals; *SS*: total variation; *FVE*: fraction of total variation attributable to a given scale (macro plot or plot); SS_{expl}/SS: fraction of the variation attributable to the scale in question, explained by a variable; *r*: model coefficient (only given when significant at the $\alpha = 0.05$ level, otherwise blank); *F*: *F* statistic for test of the hypothesis that $r = 0$ against the two-tailed alternative. Split-plot GLM relationships significant at level $\alpha = 0.05$, *P*, *F*, *r* and SS_{expl}/SS, and Kendall's nonparametric correlation coefficient $|\tau| \geq 0.30$ are given in bold face. Numbers and abbreviations for names of environmental variables are in accordance with Table 2.

Predictor	Dependent variable = DCA 2 (*SS* = 6.0188)							Correlation between predictor and DCA 2
	Error level							
	Macro plot $df_{resid} = 8$ $SS_{macro\ plot} = 4.6643$ *FVE* = 0.7750 of *SS*				Plot within macro plot $df_{resid} = 39$ $SS_{plot} = 1.35446$ *FVE* = 0.2250 of *SS*			Total
	$SS_{expl}/SS_{macro\ plot}$	*r*	*F*	*P*	SS_{expl}/SS_{plot}	*r*	*F*	*P*	τ
Ma Slo	0.3389		4.1007	0.0774	0.0275		1.1011	0.3005	–0.102
Ma Asp	0.0472		0.3967	0.5464	0.0003		0.0099	0.9214	–0.109

Ma HI	0.2968		3.3759	0.1035	0.0142	0.5604	0.4586	0.159
Ma Ter	0.0342		0.2837	0.6088	0.0302	1.2132	0.2774	0.039
Ma Une	0.0231		0.1893	0.6750	0.0010	0.0409	0.8408	0.094
TBA	0.0021		0.0171	0.8992	0.0051	0.2015	0.6560	0.023
Me slo	0.3579		4.4591	0.0677	0.0334	1.3460	0.2530	–0.182
Me Asp	0.0718		0.6189	0.4541	0.0127	0.5003	0.4836	–0.042
Me HI	0.3162		3.6994	0.0906	0.0010	3.6994	0.0906	0.092
Me Ter	0.1452		1.3585	0.2774	0.0291	1.1710	0.2859	–0.057
Me Une	0.0245		0.2007	0.6660	0.0075	0.2954	0.5899	0.074
Smi	0.0295		0.2431	0.6352	0.0109	0.4303	0.5157	0.001
Sme	0.0342		0.2834	0.6089	0.0692	2.9001	0.0965	0.033
Sma	0.0869		0.7613	0.4083	0.0612	2.5422	0.1189	0.099
Mme	0.0264		0.2172	0.6536	0.0078	0.3070	0.5827	–0.200
LOI	0.0057		0.0456	0.8363	0.0142	0.5625	0.4578	0.032
Total N	**0.4236**	**0.9300**	**5.8802**	**0.0415**	0.0215	0.8551	0.3608	0.299
$pH_{(H2O)}$	0.0006		0.0048	0.9464	0.0356	1.4406	0.2373	0.028
pH_{CaCl2}	0.0005		0.0043	0.9493	0.0123	0.4852	0.4902	0.039
H	0.0017		0.0139	0.9090	0.0010	0.0373	0.8478	–0.017
Al	0.0316		0.2611	0.6232	0.0079	0.3106	0.5805	0.048
C	0.0013		0.0106	0.9207	0.0356	1.4410	0.2372	0.104
Ca	0.1056		0.9449	0.3595	0.0090	0.3557	0.5543	0.242
Fe	0.0555		0.4697	0.5125	0.0078	0.3046	0.5842	0.133
K	0.0307		0.2537	0.6280	0.0002	0.0069	0.9345	–0.006
Mg	0.0004		0.0028	0.9589	0.0297	1.1946	0.2811	0.048
Mn	0.0001		0.0009	0.9769	0.0135	0.5340	0.4693	–0.074
Na	**0.4173**	**1.4811**	**5.7294**	**0.0436**	0.0078	0.3071	0.5826	**0.367**
P	0.0146		0.1188	0.7392	0.0058	0.2268	0.6366	–0.074
S	0.0206		0.1681	0.6926	0.0003	0.0130	0.9096	0.056
Zn	0.0077		0.0617	0.8102	0.0079	0.3114	0.5800	0.020

Correlations between DCA axes and environmental variables

Extractable S (Fig. 139), pH measuresments [$pH_{(CaCl2)}$ (Fig. 133)], extractable C (Fig. 135) and exchangeable H (negatively related to the axis; Fig. 134) showed the highest correlations with DCA axis 1 (Table 15). A total of 11 out of 31 of the measured variables had a correlation $|\tau| > 0.300$ (Figs 129-139). Variables related to high soil nutrient richness were positively correlated while loss on ignition and exchangeable H were negatively correlated with this axis.

Only one variable, extractable Na (Fig. 138), had a correlation higher than $|\tau| > 0.300$ with DCA axis 2.

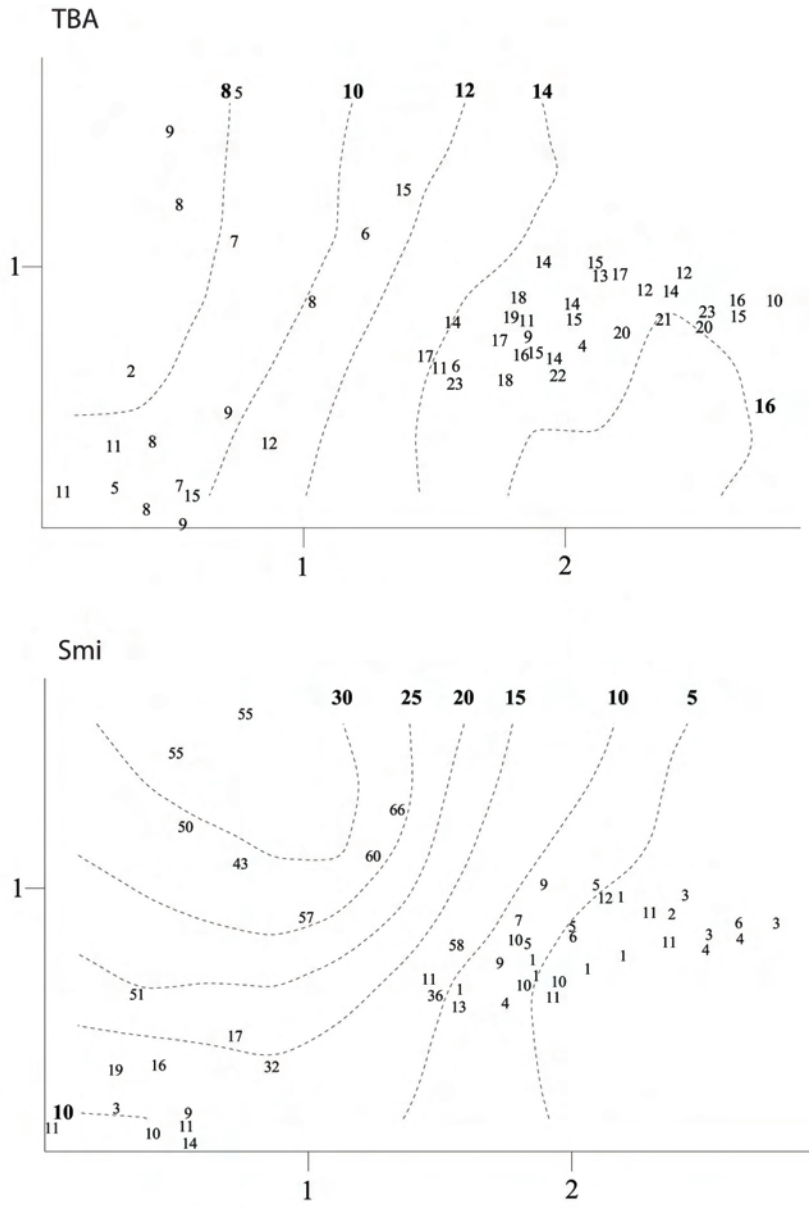

Figs 129-130. Gutulia: isolines for environmental variables in the DCA ordinations of 50 meso plots, axes 1 (horizontal) and 2 (vertical). Values for the environmental variables are plotted onto the meso plots' positions. Scaling in S.D. units. Fig. 129. TBA (R^2 = 0.611). Fig. 130. Smi (R^2 = 0.658). R^2 refers to the coefficient of determination between original and smoothened values as interpolated from the isolines. Names of environmental variables in accordance with Table 2.

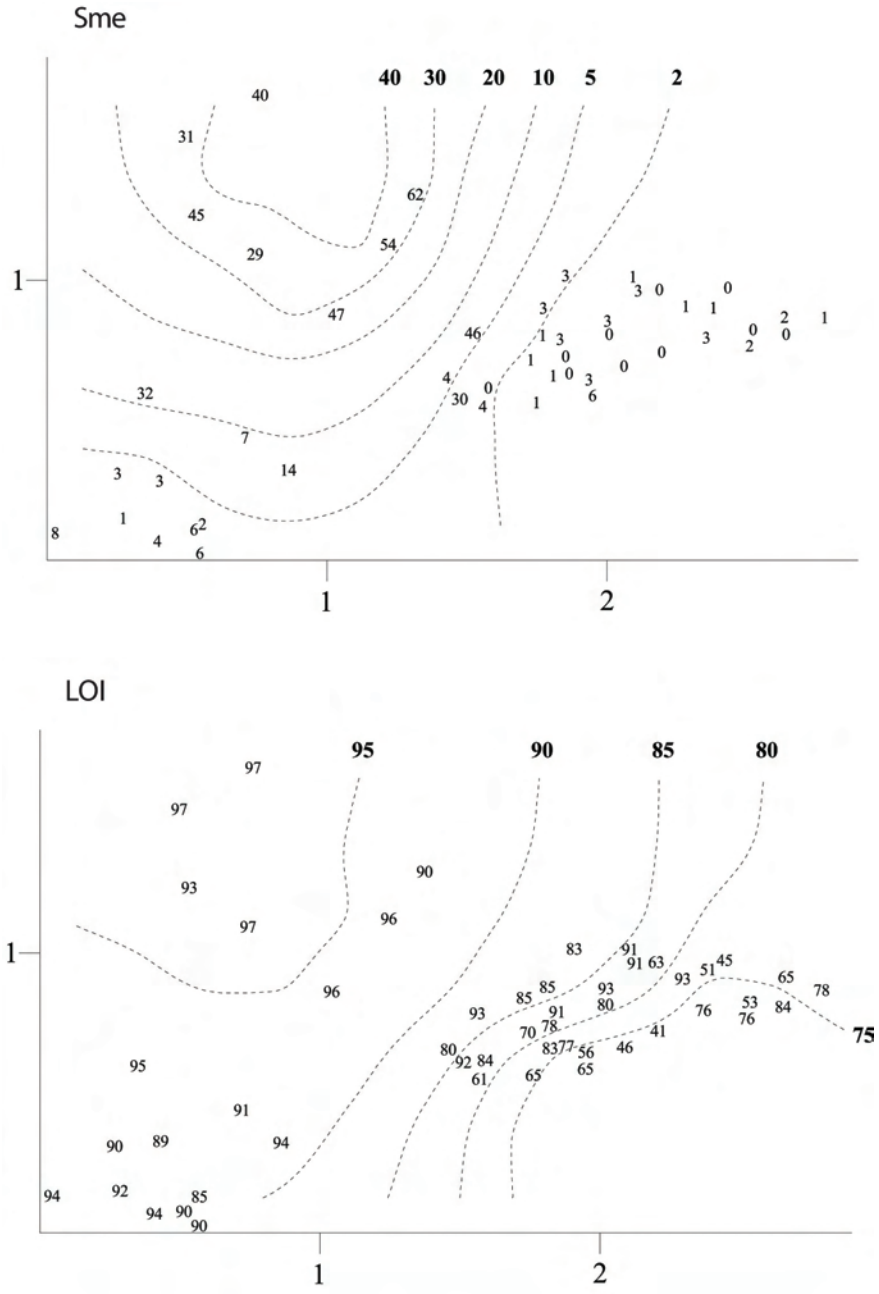

Figs 131-132. Gutulia: isolines for environmental variables in the DCA ordinations of 50 meso plots, axes 1 (horizontal) and 2 (vertical). Values for the environmental variables are plotted onto the meso plots' positions. Scaling in S.D. units. Fig. 131. Sme (R^2 = 0.691). Fig. 132. LOI (R^2 = 0.681). R^2 refers to the coefficient of determination between original and smoothened values as interpolated from the isolines. Names of environmental variables in accordance with Table 2.

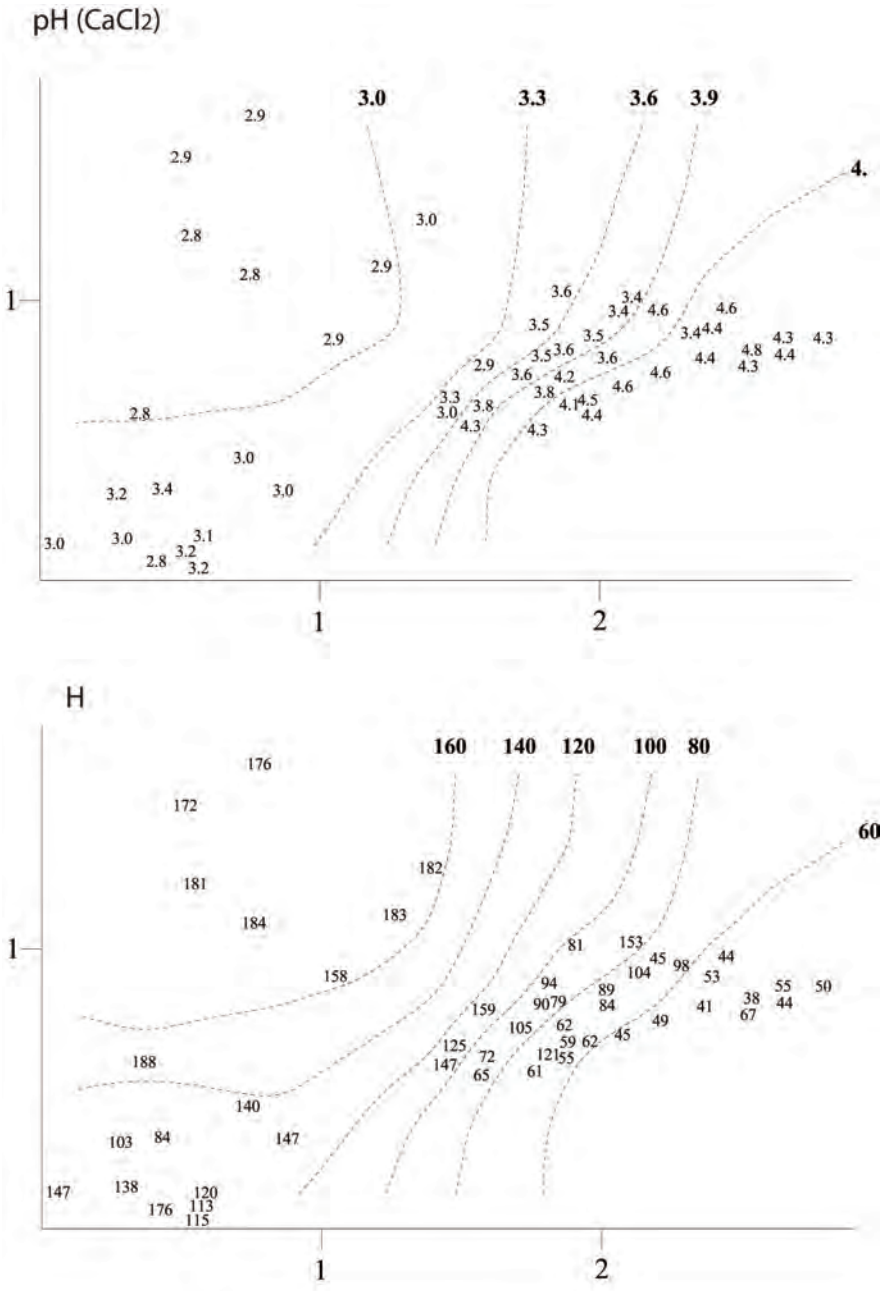

Figs 133-134. Gutulia: isolines for environmental variables in the DCA ordinations of 50 meso plots, axes 1 (horizontal) and 2 (vertical). Values for the environmental variables are plotted onto the meso plots' positions. Scaling in S.D. units. Fig. 133. pH ($CaCl_2$) (R^2 = 0.852). Fig. 134. H (R^2 = 0.785). R^2 refers to the coefficient of determination between original and smoothened values as interpolated from the isolines. Names of environmental variables in accordance with Table 2.

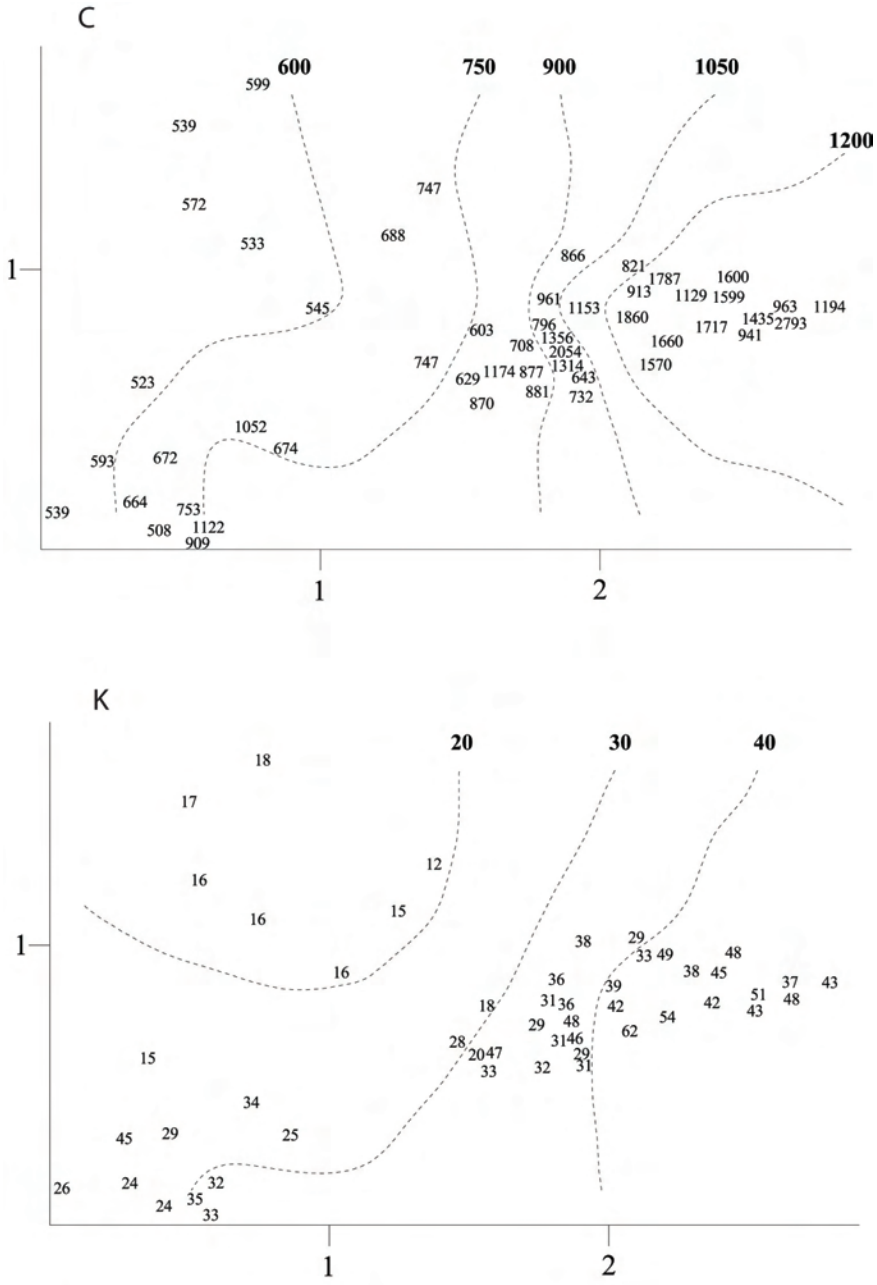

Figs 135-136. Gutulia: isolines for environmental variables in the DCA ordinations of 50 meso plots, axes 1 (horizontal) and 2 (vertical). Values for the environmental variables are plotted onto the meso plots' positions. Scaling in S.D. units. Fig. 135. C (R^2 = 0.714). Fig. 136. K (R^2 = 0.726). R^2 refers to the coefficient of determination between original and smoothened values as interpolated from the isolines. Names of environmental variables in accordance with Table 2.

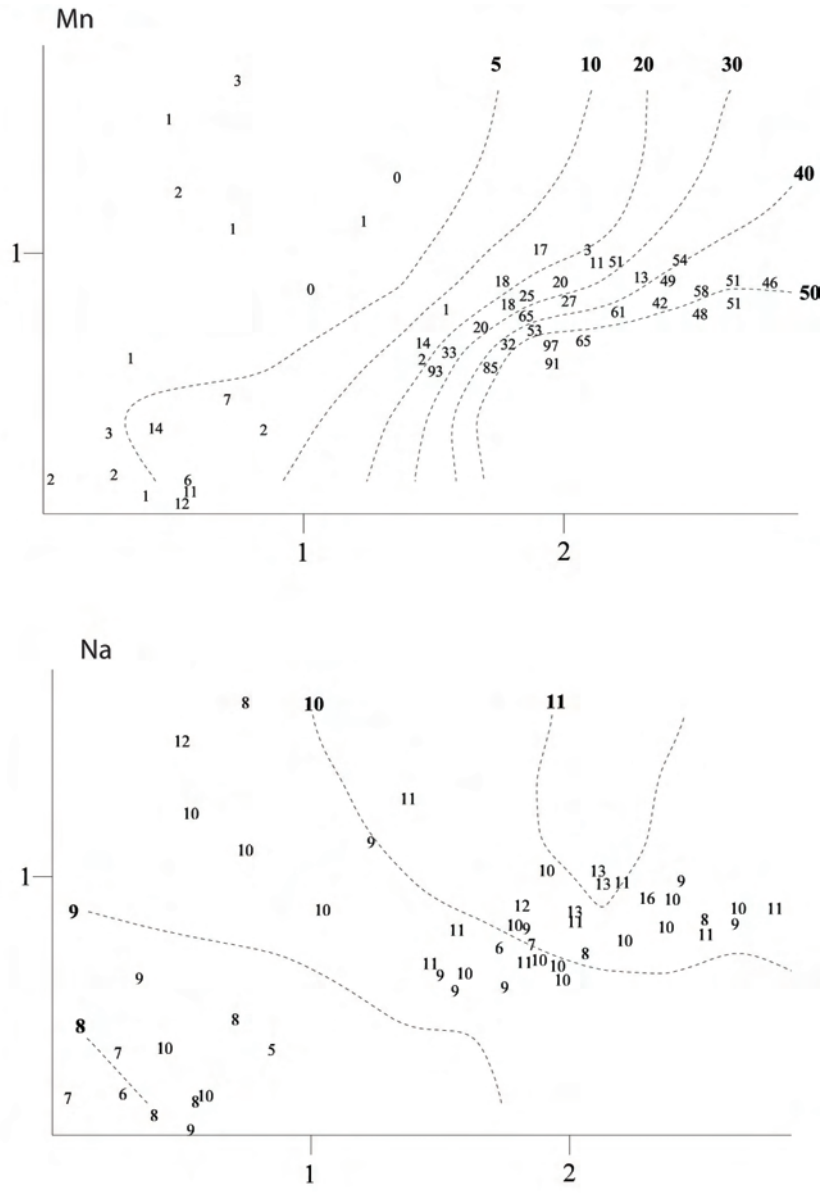

Figs 137-138. Gutulia: isolines for environmental variables in the DCA ordinations of 50 meso plots, axes 1 (horizontal) and 2 (vertical). Values for the environmental variables are plotted onto the meso plots' positions. Scaling in S.D. units. Fig. 136. Mn (R^2 = 0.812). Fig. 137. Na (R^2 = 0.666). R^2 refers to the coefficient of determination between original and smoothened values as interpolated from the isolines. Names of environmental variables in accordance with Table 2.

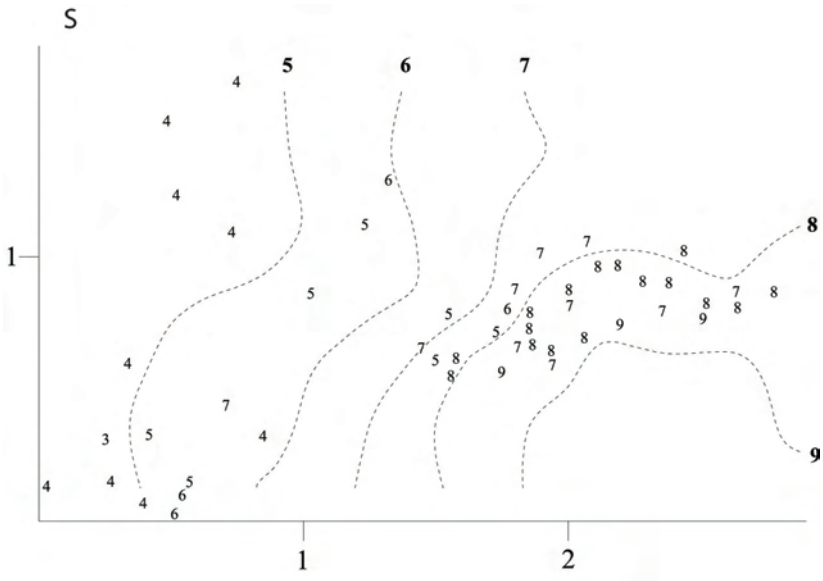

Fig. 139. Gutulia: isolines for environmental variables in the DCA ordinations of 50 meso plots, axes 1 (horizontal) and 2 (vertical). Values for the environmental variables are plotted onto the meso plots' positions. Scaling in S.D. units. Fig. 139. S (R^2 = 0.815). R^2 refers to the coefficient of determination between original and smoothened values as interpolated from the isolines. Names of environmental variables in accordance with Table 2.

Frequent species

A total of 87 species were recorded within the fifty 1 × 1 m meso sample plots: 41 vascular plants, 19 mosses, 11 liverworts and 16 lichens. The most frequent species (the sum of subplot frequencies in brackets) are: *Vaccinium myrtillus* (786 out of 800), *Avenella flexuosa* (766), *Vaccinium vitis-idaea* (674), *Barbilophozia lycopodioides* (534), *Dicranum scoparium* (473), *Trientalis europaea* (352), *Pleurozium schreberi* (315), *Empetrum nigrum* (286), *Melampyrum pratense* (267) and *Gymnocarpium dryopteris* (251).

The distribution of species abundance in the DCA ordination

Fifty seven of the totally 87 species occurred in 5 or more of the sample plots (Figs 140–196). *Vaccinium myrtillus* (Fig. 145), *Vaccinium vitis-idaea* (Fig. 147), *Avenella flexuosa* (Fig. 162) and *Dicranum scoparium* (Fig. 169) had wide ecological amplitudes and were highly abundant in most of the sample plots. *Barbilophozia lycopodioides* (Fig. 179) also had a relatively wide distribution, although it was rather rare in plots with low axis 1 scores and high axis 2 scores that were poor in soil nutrients, acidic, and situated on relatively deep and soils.

Species restricted to high DCA axis1 scores, preferring soils with high pH values and high concentrations of extractable C, Ca, K, Mn and S, were *Juniperus communis* (Fig. 141), *Gymnocarpium dryopteris* (Fig. 148), *Linnaea borealis* (Fig. 149), *Melampyrum sylvaticum* (Fig. 152), *Oxalis acetosella* (Fig. 153), *Rumex acetosa* (Fig. 156), *Solidago virgaurea* (Fig. 157*), Anthoxanthum odoratum* (Fig. 159), *Carex vaginata* (Fig. 160), *Deschampsia cespitosa* (Fig. 161), *Luzula pilosa* (Fig. 164), *Milium effusum* (Fig. 165), *Brachythecium salebrosum* (Fig. 168), *Plagiothecium laetum* (Fig. 171), *Rhodobryum roseum* (Fig. 176) and *Lophozia obtusa* (Fig. 182).

Species restricted to sample plots with lower soil pH and less nutrient-rich soils were *Betula nana* (Fig. 140), *Eriophorum vaginatum* (Fig. 163), *Cetraria islandica* (Fig. 185), *Cladonia arbuscula* (Fig. 186), *Cladonia bellidiflora* (Fig.187), *Cladonia crispata* (Fig. 191), *Cladonia gracilis* (Fig. 193), *Cladonia rangiferina* (Fig. 194) and *Cladonia uncialis* (Fig 196). Of these *Betula nana* and *Eriophorum vaginatum* had their main occurrence at high DCA axis 2 scores, on deep soils, while the *Cladonia* species were restricted to low DCA 2 scores, preferring a thin soil layer.

Melampyrum pratense (Fig. 151) and *Trientalis europaea* (Fig. 158) seemed to occur irrespective to pH and concentration of C, H, K, Mn, Na and S (cf. Fig. 133-139).

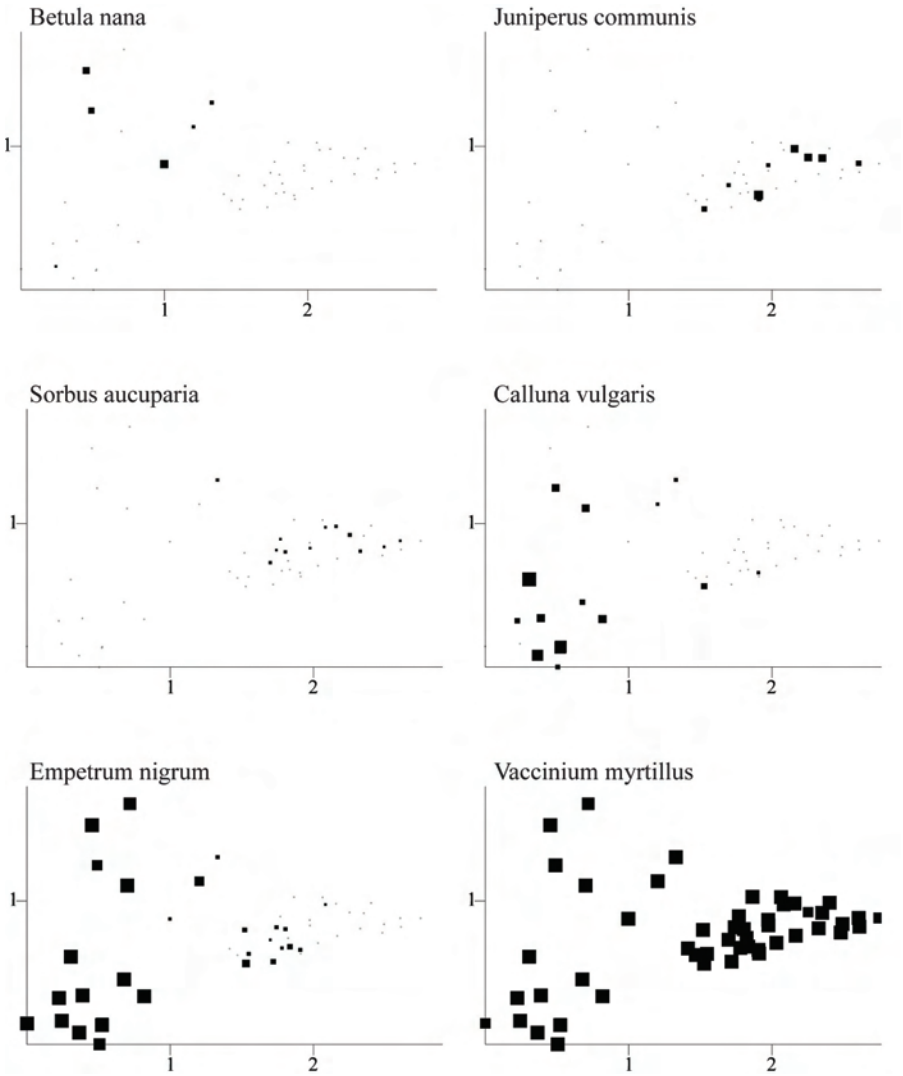

Figs 140-145. Gutulia: distributions of species abundances in the DCA ordination of 50 sample plots, axes 1 (horizontal) and 2 (vertical). Frequency in subplots for each species in each meso plot proportional to quadrate size. Scaling in S.D. units. Fig. 140. *Betula nana*. Fig. 141. *Juniperus communis*. Fig. 142. *Sorbus aucuparia*. Fig. 143. *Calluna vulgaris*. Fig. 144. *Empetrum nigrum*. Fig. 145. *Vaccinium myrtillus*.

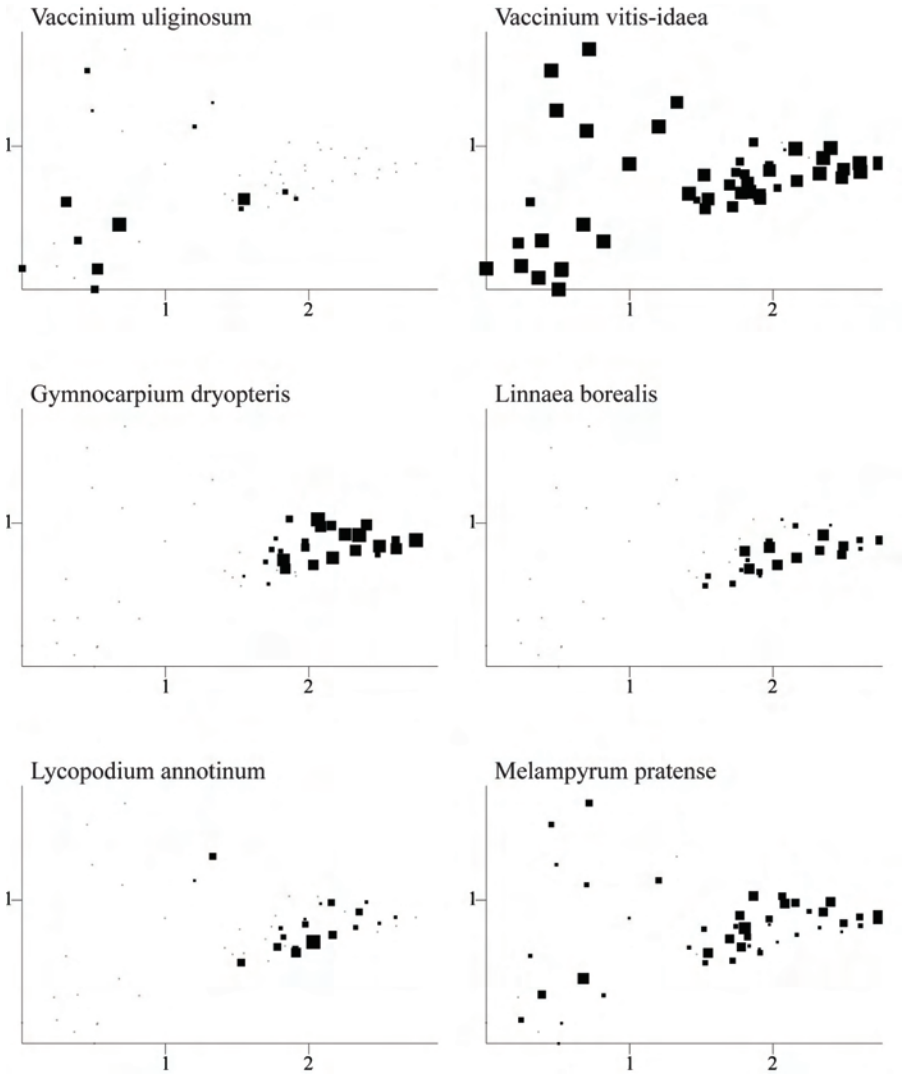

Figs 146-151. Gutulia: distributions of species abundances in the DCA ordination of 50 sample plots, axes 1 (horizontal) and 2 (vertical). Frequency in subplots for each species in each meso plot proportional to quadrate size. Scaling in S.D. units. Fig. 146. *Vaccinium uliginosum*. Fig. 147. *Vaccinium vitis-idaea*. Fig. 148. *Gymnocarpium dryopteris*. Fig. 149. *Linnaea borealis*. Fig. 150. *Lycopodium annotinum*. Fig. 151. *Melampyrum pratense.*

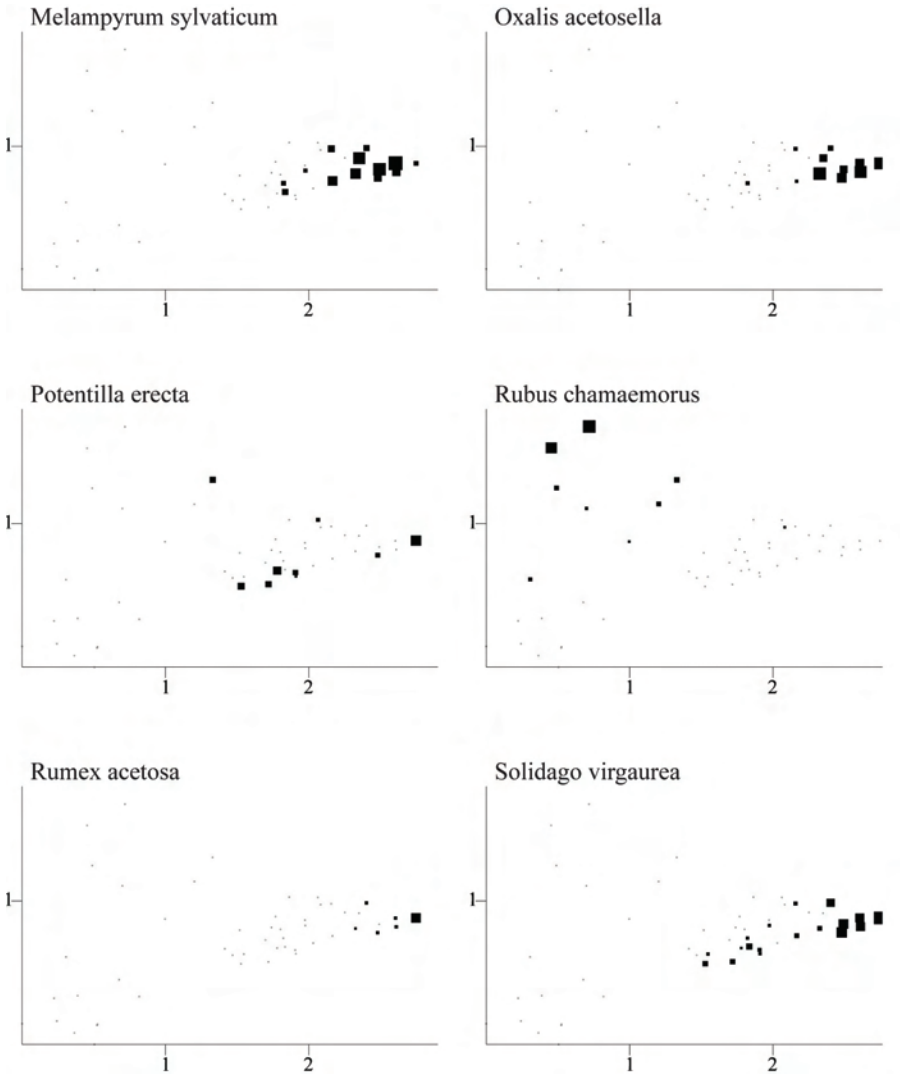

Figs 152-157. Gutulia: distributions of species abundances in the DCA ordination of 50 sample plots, axes 1 (horizontal) and 2 (vertical). Frequency in subplots for each species in each meso plot proportional to quadrate size. Scaling in S.D. units. Fig. 152. *Melampyrum sylvaticum.* Fig. 153. *Oxalis acetosella*. Fig. 154. *Potentilla erecta*. Fig. 155. *Rubus chamaemorus*. Fig. 156. *Rumex acetosa*. Fig. 157. *Solidago virgaurea.*

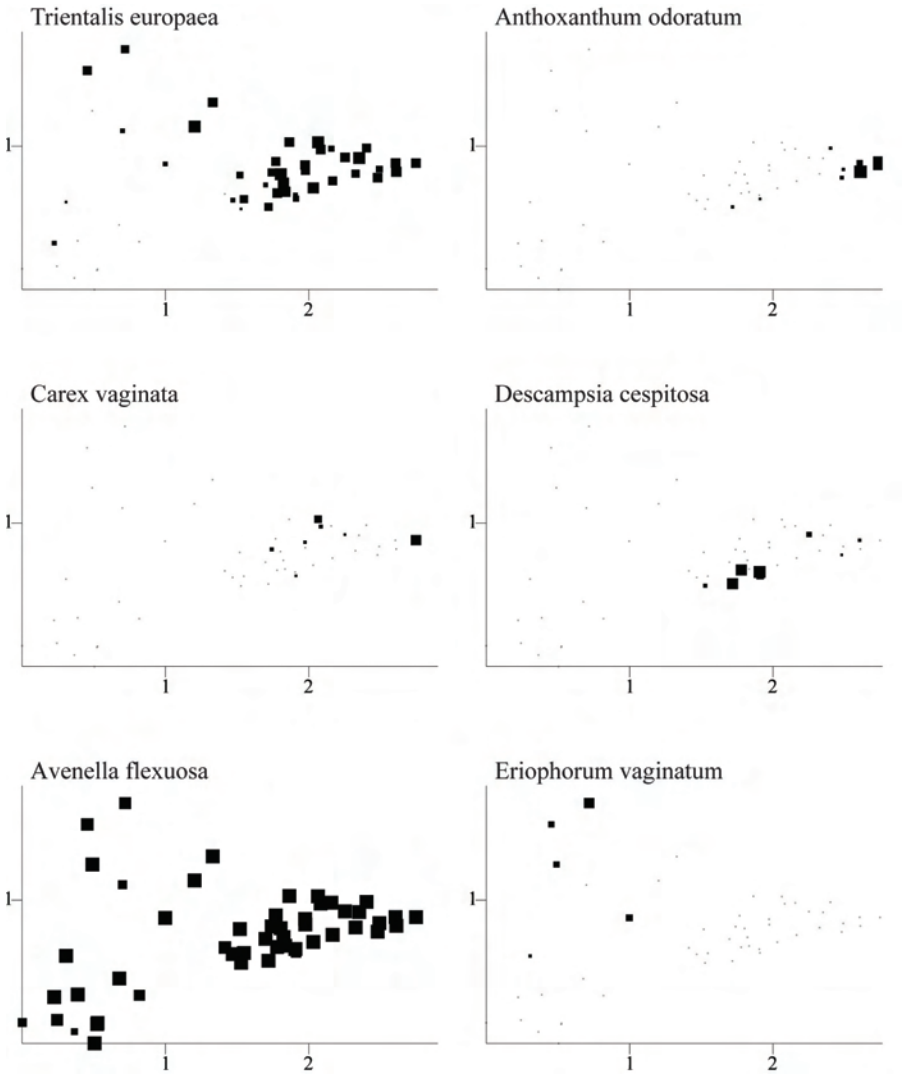

Figs 158-163. Gutulia: distributions of species abundances in the DCA ordination of 50 sample plots, axes 1 (horizontal) and 2 (vertical). Frequency in subplots for each species in each meso plot proportional to quadrate size. Scaling in S.D. units. Fig. 158. *Trientalis europaea*. 159. *Anthoxanthum odoratum*. Fig. 160. *Carex vaginata*. Fig. 161. *Deschampsia cespitosa*. Fig. 162. *Avenella flexuosa* (syn. *Deschampsia flexuosa*). Fig. 163. *Eriophorum vaginatum*.

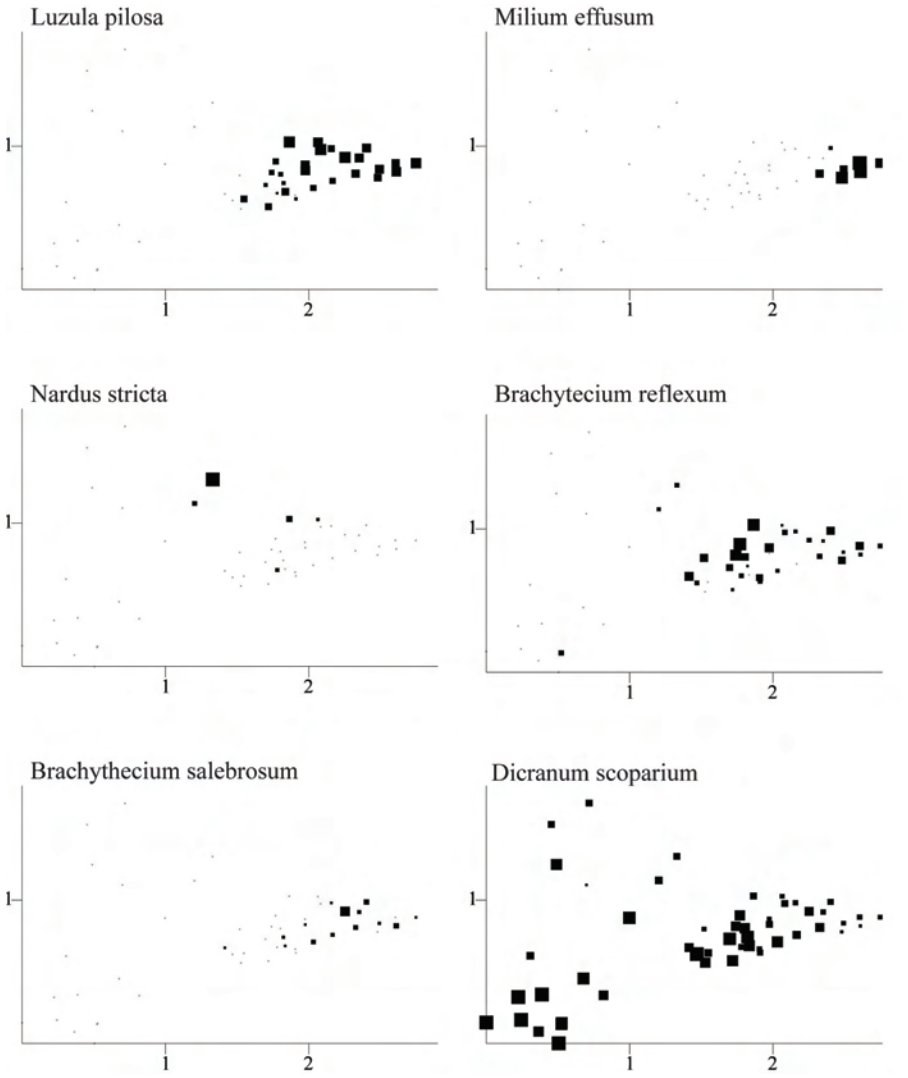

Figs 164-169. Gutulia: distributions of species abundances in the DCA ordination of 50 sample plots, axes 1 (horizontal) and 2 (vertical). Frequency in subplots for each species in each meso plot proportional to quadrate size. Scaling in S.D. units. Fig. 164. *Luzula pilosa*. Fig. 165. *Milium effusum*. Fig. 166. *Nardus stricta*. Fig. 167. *Brachythecium reflexum.* Fig. 168. *Brachythecium salebrosum.* Fig. 169. *Dicranum scoparium.*

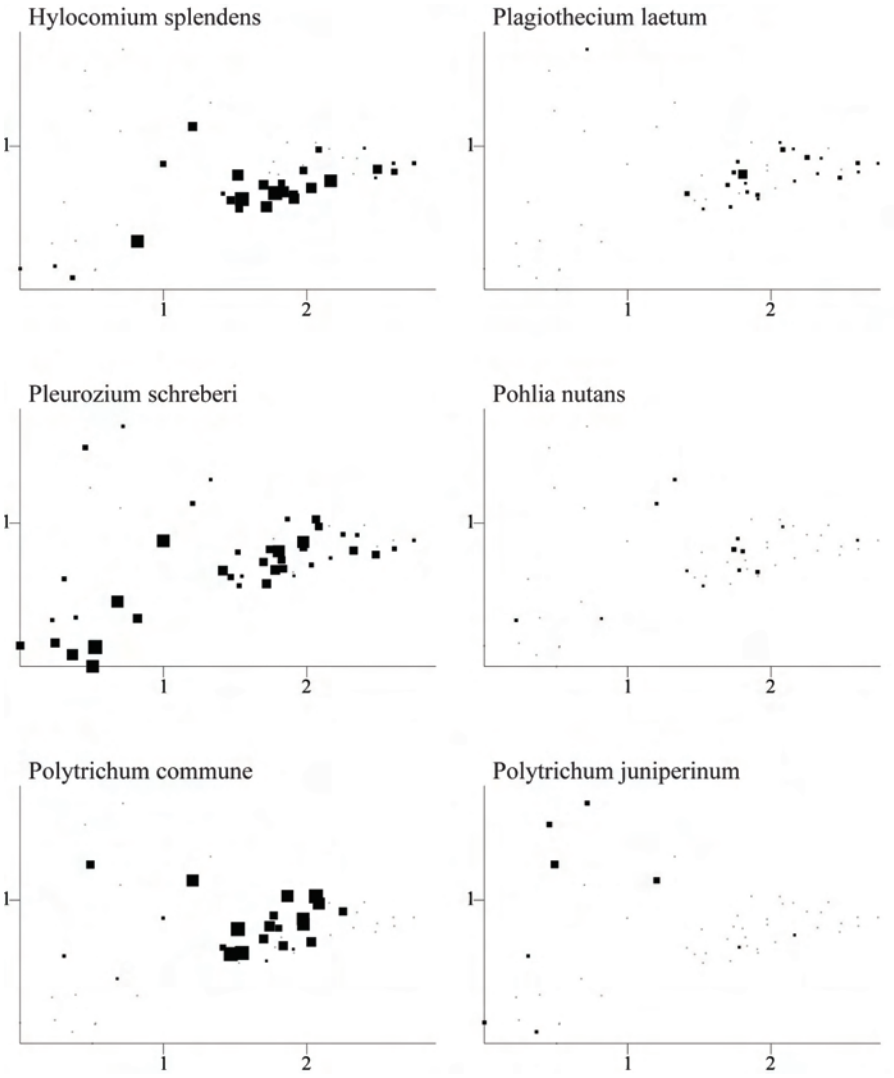

Figs 170-175. Gutulia: distributions of species abundances in the DCA ordination of 50 sample plots, axes 1 (horizontal) and 2 (vertical). Frequency in subplots for each species in each meso plot proportional to quadrate size. Scaling in S.D. units. Fig. 170. *Hylocomium splendens.* Fig. 171. *Plagiothecium laetum.* Fig. 172. *Pleurozium schreberi*. Fig. 173. *Pohlia nutans*. Fig. 174. *Polytrichum commune*. Fig. 175. *Polytrichum juniperinum*.

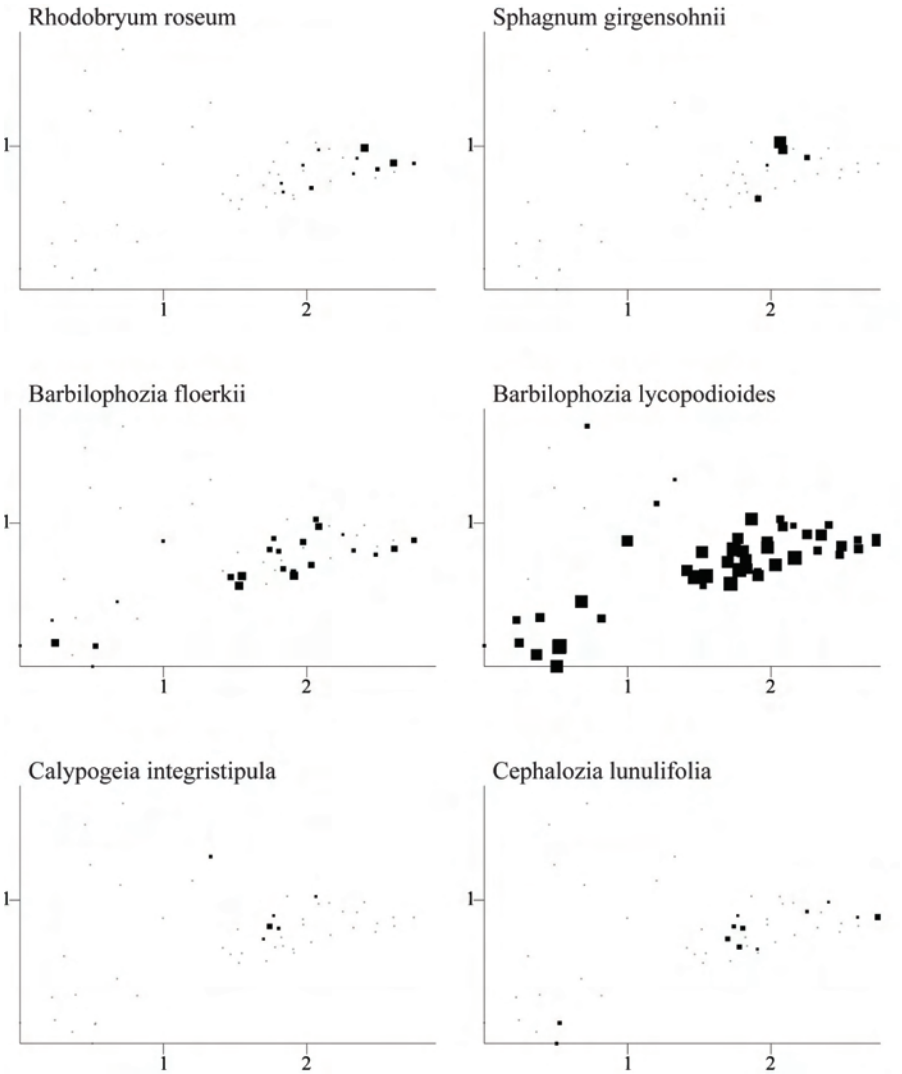

Figs 176-181. Gutulia: distributions of species abundances in the DCA ordination of 50 sample plots, axes 1 (horizontal) and 2 (vertical). Frequency in subplots for each species in each meso plot proportional to quadrate size. Scaling in S.D. units. Fig. 176. *Rhodobryum roseum*. Fig. 177. *Sphagnum girgensohnii.*. Fig. 178. *Barbilophozia floerkii*. Fig. 179. *Barbilophozia lycopodioides*. Fig. 180. *Calypogeia integristipula*. Fig. 181. *Cephalozia lunulifolia.*

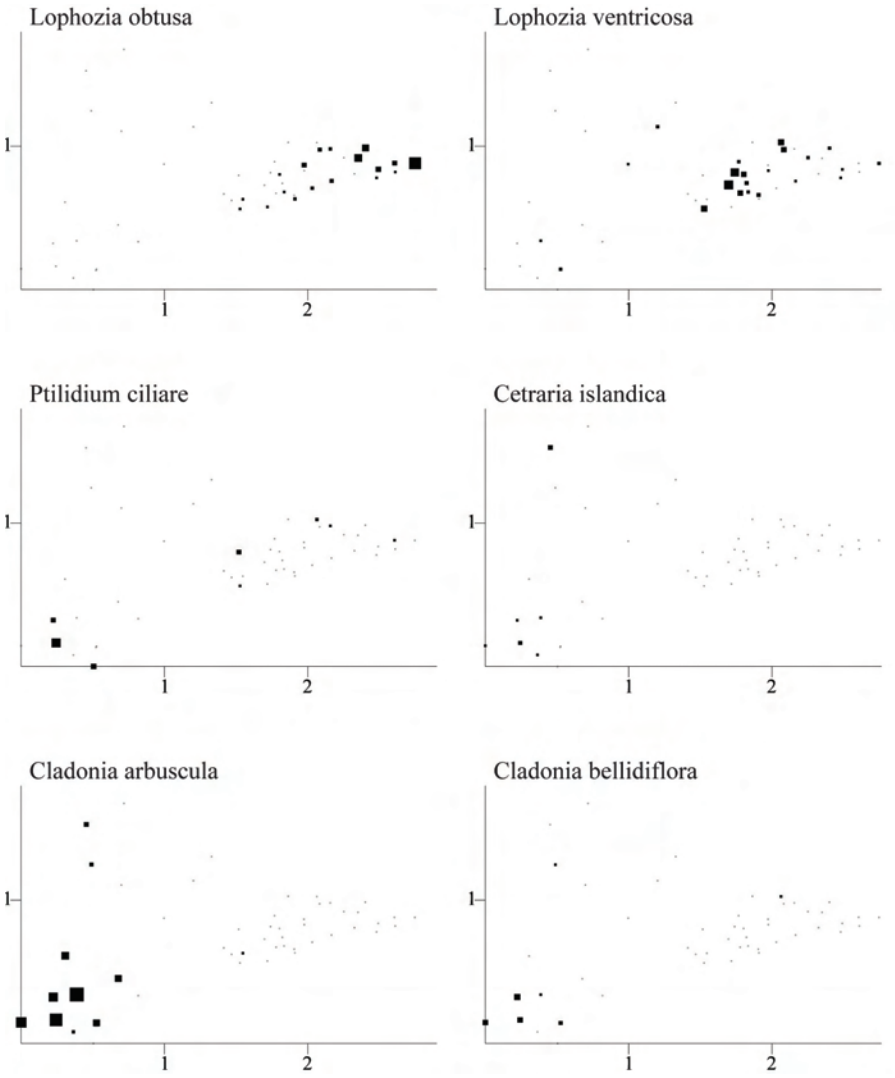

Figs 182-187. Gutulia: distributions of species abundances in the DCA ordination of 50 sample plots, axes 1 (horizontal) and 2 (vertical). Frequency in subplots for each species in each meso plot proportional to quadrate size. Scaling in S.D. units. Fig. 182. *Lophozia obtusa*. Fig. 183. *Lophozia ventricosa*. Fig. 184. *Ptilidium ciliare*. Fig. 185. *Cetraria islandica*. Fig. 186. *Cladonia arbuscula*. Fig. 197. *Cladonia bellidiflora*.

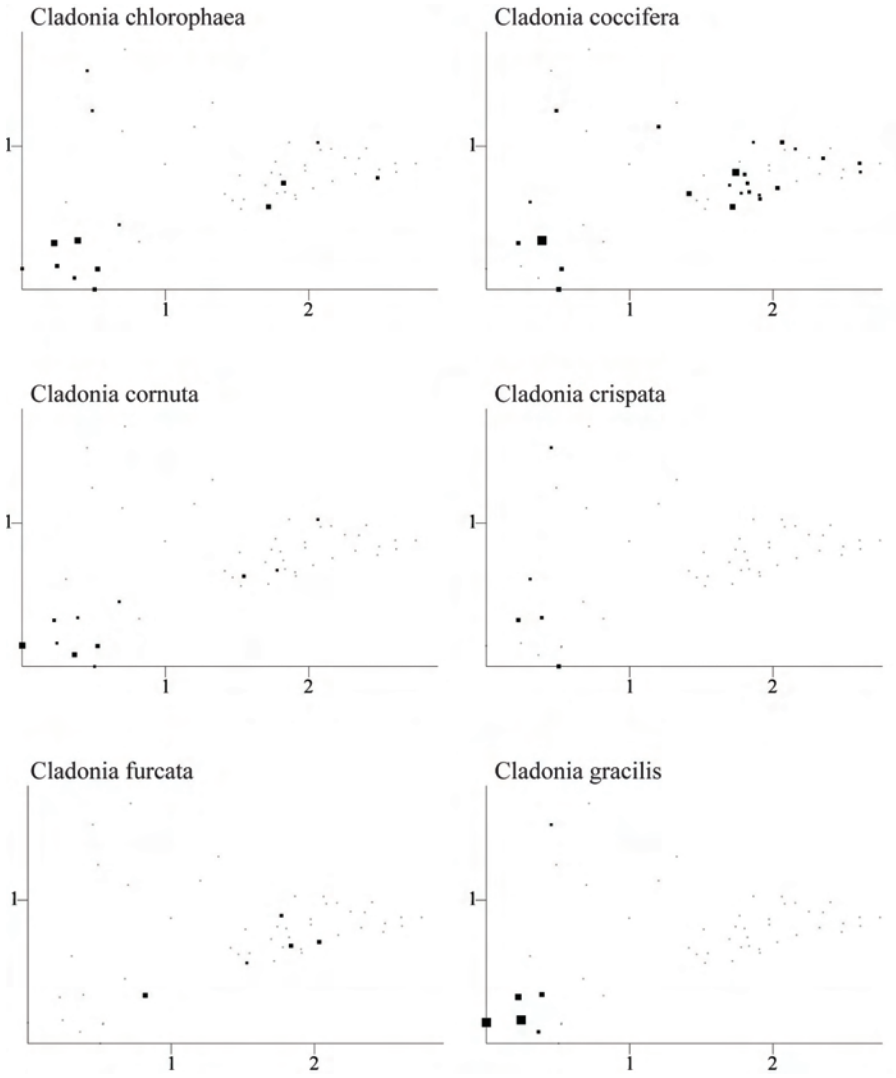

Figs 188-193. Gutulia: distributions of species abundances in the DCA ordination of 50 sample plots, axes 1 (horizontal) and 2 (vertical). Frequency in subplots for each species in each meso plot proportional to quadrate size. Scaling in S.D. units. Fig. 188. *Cladonia chlorophaea*. Fig. 189. *Cladonia coccifera*. Fig. 190. *Cladonia cornuta*. Fig. 191. *Cladonia crispata*. Fig. 192. *Cladonia furcata*. Fig. 193. *Cladonia gracilis*.

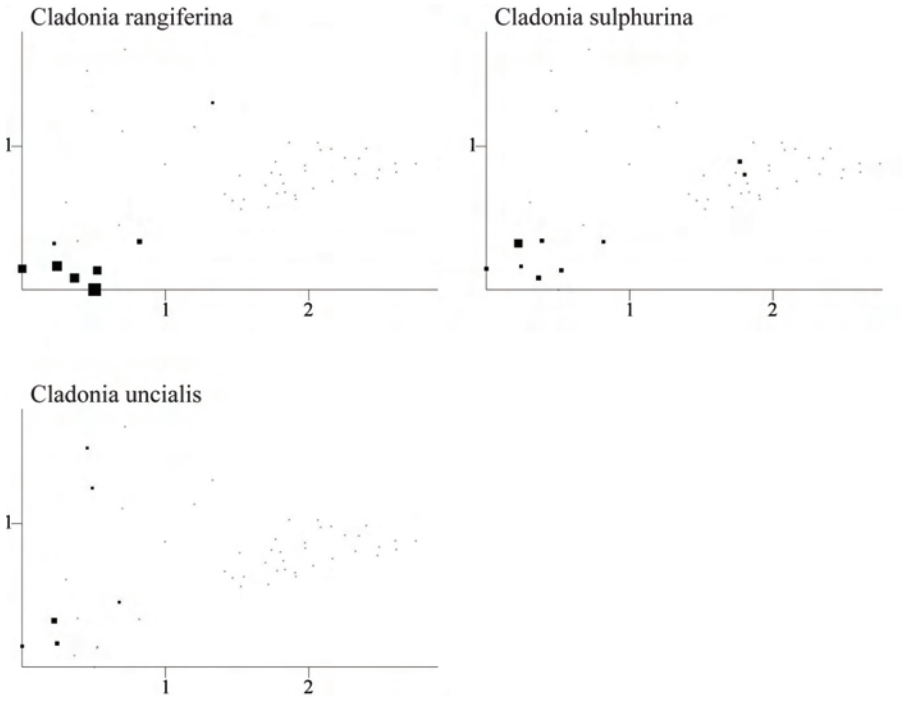

Figs 194-196. Gutulia: distributions of species abundances in the DCA ordination of 50 sample plots, axes 1 (horizontal) and 2 (vertical). Frequency in subplots for each species in each meso plot proportional to quadrate size. Scaling in S.D. units. Fig. 194. *Cladonia rangiferina*. Fig. 195. *Cladonia sulphurina*. Fig. 196. *Cladonia uncialis*.

Correlations between environmental variables

There were strong pairwise correlations between several of the topographical variables, between soil chemical variables and between topographical and chemical variables related to soil nutrient richness and soil moisture (Table 12).

Macro plot slope was positively correlated with macro and meso plot aspect unfavourability and negatively correlated with macro plot heat index and macro plot terrain form. Meso plot slope was positive correlated with macro plot aspect unfavourability and negative correlated with meso plot heat index. In general meso plot slope was positively correlated with soil chemical variables that reflected soil nutrient status (e.g. Ca concentrations and pH) and negatively correlated with soil acidity (H and Fe) and high LOI. Meso plot heat index was negatively correlated with soil variables related to a gradient in soil nutrient richness (e.g. pH, Ca and K).

Tree basal area was negatively correlated with LOI and H and positively correlated with pH and most extractable elements. Median, minimum and maximum soil depths were internally positively correlated, but not strongly correlated with other variables. Soil moisture and LOI were negatively correlated with pH and most other extractable elements, and positively correlated with each other. pH was positively correlated with total N, C, Ca, K, Mg, Mn and Zn and negatively correlated with H and Fe. Extractable P was negatively correlated with soil moisture, total N, pH, Na and Zn, and positively correlated with LOI and C.

Table 12. Åmotsdalen: Kendall's rank correlation coefficients τ between 31 environmental variables in the 50 sample plots (lower triangle), with significance probabilities (upper triangle). Statistically significant correlations (P<0.05) in bold face. Names of explanatory variables abbreviated in accordance with Table 2.

	1	2	3	4	5	6	7	8	9	10	11	12	13	14	15	16	17	18	19	20	21	22	23	24	25	26	27	28	29	30	31
01 Ma Slo	*	**0.009**	**0.022**	**0.020**	0.488	0.298	0.124	**0.003**	0.806	0.655	0.767	0.536	0.604	0.531	**0.010**	0.660	0.520	0.653	0.886	0.407	0.436	**0.020**	0.709	0.058	0.310	0.648	0.748	0.111	0.108	0.397	0.352
02 Ma Asp	**0.278**	*	**0.000**	0.744	0.322	0.141	**0.000**	0.264	**0.000**	0.442	0.316	0.717	0.353	0.556	0.080	**0.011**	0.749	**0.000**	**0.000**	**0.001**	0.267	0.096	**0.003**	**0.000**		0.226	**0.000**	0.501	0.178	**0.021**	**0.008**
03 Ma HI	**–0.236**	**0.539**	*	0.051	0.137	0.164	**0.001**	0.164	**0.000**	0.885	0.546	0.592	0.096	0.867	**0.004**	**0.015**	0.547	**0.002**	**0.001**	**0.001**	0.384	**0.040**	**0.036**	**0.002**	0.088	0.503	**0.000**	0.676	0.349	0.082	0.145
04 Ma Ter	**–0.273**	0.038	0.218	*	0.472	0.971	0.771	0.346	0.821	0.660	0.545	0.759	0.737	0.167	0.312	0.377	0.321	0.986	0.864	0.732	0.843	0.134	0.665	0.665	0.386	0.417	0.377	0.271	0.843	0.074	0.885
05 Ma Une	0.079	–0.110	–0.162	–0.089	*	0.473	**0.016**	0.206	**0.003**	**0.005**	**0.044**	0.287	0.432	**0.002**	0.586	0.351	0.079	0.867	0.792	0.738	0.586	0.660	0.574	0.316	0.765	0.449	0.493	0.471	0.860	**0.047**	0.260
05 TBA	–0.111	0.154	0.142	0.004	–0.081	*	0.185	**0.012**	0.100	0.650	**0.000**	0.686	0.565	0.886	**0.000**	**0.008**	0.381	**0.022**	**0.008**	**0.021**	0.089	**0.002**	**0.040**	0.578	**0.001**	0.066	**0.001**	0.960	0.625	**0.003**	**0.030**
07 Me Slo	0.165	**0.633**	**0.353**	–0.034	**–0.272**	0.140	*	0.719	**0.000**	0.979	0.257	0.606	0.767	0.642	0.137	**0.008**	0.973	**0.000**	**0.000**	**0.001**	0.362	**0.013**	**0.005**	**0.000**	**0.018**	0.218	**0.000**	0.076	0.589	**0.000**	**0.007**
08 Me Asp	**0.319**	0.119	–0.144	0.111	0.144	**–0.269**	0.039	*	**0.011**	0.966	0.470	0.052	**0.009**	0.185	**0.025**	0.252	0.993	0.159	0.086	**0.039**	0.321	0.120	0.832	0.641	**0.041**	0.703	0.091	0.063	0.183	0.401	0.953
09 Me HI	0.025	**0.480**	**0.394**	–0.025	**–0.322**	0.168	**0.747**	**–0.265**	*	0.946	0.294	0.530	0.116	0.162	**0.009**	**0.008**	0.953	**0.000**	**0.000**	**0.000**	0.099	**0.002**	**0.003**	**0.000**	**0.006**	0.212	**0.000**	0.874	0.795	**0.001**	**0.016**
10 Me Ter	–0.048	–0.081	0.015	0.051	**–0.315**	–0.048	0.003	–0.005	0.007	*	0.523	0.939	0.384	0.122	0.491	0.677	0.137	0.825	0.939	0.296	**0.011**	0.218	0.391	0.546	0.108	0.502	0.546	0.381	0.082	0.715	**0.032**
11 Me Une	0.031	–0.102	–0.060	–0.068	**0.220**	**–0.394**	–0.116	0.075	–0.104	–0.066	*	0.185	0.363	**0.020**	0.089	0.188	**0.013**	0.200	0.138	0.183	0.280	0.095	**0.025**	0.769	0.167	0.089	0.152	0.782	0.744	0.051	0.072
12 Smi	–0.064	–0.037	–0.053	0.034	0.116	–0.041	0.053	0.201	–0.062	–0.008	0.131	*	**0.000**	**0.000**	0.621	0.575	0.913	0.744	0.893	0.887	0.682	0.744	0.694	0.319	0.821	0.379	0.645	**0.003**	0.080	0.280	0.821
13 Sme	0.055	–0.096	–0.168	–0.038	0.087	–0.060	–0.031	**0.278**	–0.159	–0.091	–0.092	**0.413**	*	0.074	0.096	0.400	0.491	0.075	**0.043**	0.069	0.501	0.364	0.093	0.135	0.687	0.674	0.064	**0.033**	0.459	0.853	0.355
14 Sma	–0.065	–0.060	–0.017	0.155	**0.335**	–0.015	–0.048	0.137	–0.138	–0.158	**0.230**	**0.461**	0.180	*	0.927	0.172	0.731	0.547	0.503	0.564	0.874	0.887	0.900	0.821	0.303	0.106	0.953	**0.011**	0.288	0.245	0.706
15 Mme	**0.266**	–0.176	**–0.282**	–0.113	–0.059	**–0.353**	–0.151	**0.231**	**–0.256**	0.070	0.168	0.049	0.167	–0.009	*	**0.000**	0.744	**0.006**	**0.001**	**0.000**	**0.000**	**0.000**	**0.000**	**0.040**	**0.000**	**0.004**	**0.000**	**0.032**	**0.007**	**0.026**	**0.006**
16 LOI	0.045	**–0.257**	**–0.240**	–0.099	–0.101	**–0.268**	**–0.270**	0.118	**–0.262**	0.042	0.130	–0.055	0.084	–0.134	**0.344**	*	**0.026**	**0.000**	**0.000**	**0.000**	0.225	**0.001**	**0.000**	**0.000**	**0.000**	**0.000**	**0.000**	**0.049**	**0.037**	**0.000**	**0.044**
17 Total N	–0.066	–0.032	0.059	0.111	–0.190	0.089	–0.003	0.001	0.006	0.151	**–0.244**	0.011	–0.069	0.034	–0.032	**–0.218**	*	**0.004**	**0.007**	0.541	**0.012**	0.808	0.143	0.770	0.457	0.408	0.195	**0.009**	**0.003**	**0.004**	0.757
18 pH_{H2O}	0.046	**0.352**	**0.312**	–0.002	–0.018	**0.232**	**0.364**	–0.146	**0.368**	0.023	–0.127	–0.032	–0.179	0.059	**–0.270**	**–0.634**	**0.280**	*	**0.000**	**0.000**	0.847	**0.010**	**0.000**	**0.000**	**0.001**	**0.000**	**0.000**	0.130	**0.004**	**0.000**	**0.020**
19 pH_{CaCl2}	0.015	**0.355**	**0.324**	0.019	–0.029	**0.268**	**0.376**	–0.177	**0.397**	0.008	–0.147	–0.013	**–0.204**	0.066	**–0.329**	**–0.654**	**0.264**	**0.907**	*	**0.000**	0.340	**0.001**	**0.000**	**0.000**	**0.000**	**0.000**	**0.000**	0.216	**0.025**	**0.000**	**0.009**
20H	0.085	**–0.322**	**–0.333**	–0.038	0.036	**–0.234**	**–0.354**	**0.212**	**–0.407**	0.106	0.131	–0.014	0.182	–0.057	**0.486**	**0.522**	–0.060	**–0.520**	**–0.585**	*	**0.000**	**0.000**	**0.000**	**0.000**	**0.000**	**0.000**	**0.000**	0.967	0.213	**0.006**	**0.000**
21 Al	0.080	–0.112	–0.085	–0.022	–0.059	–0.172	–0.093	0.102	–0.162	**0.258**	0.107	0.040	0.067	0.016	**0.438**	0.118	**0.246**	–0.019	–0.093	**0.437**	*	**0.000**	**0.000**	**0.005**	**0.000**	**0.000**	**0.002**	**0.005**	**0.000**	0.874	**0.000**
22 Ca	**–0.238**	0.168	**0.202**	0.167	–0.048	**0.309**	**0.252**	–0.160	**0.308**	–0.125	–0.164	–0.032	–0.091	–0.014	**–0.551**	**–0.326**	0.024	**0.252**	**0.329**	**–0.468**	**–0.440**	*	**0.000**	**0.015**	**0.000**	**0.001**	**0.000**	0.389	**0.002**	**0.000**	**0.000**
23 Fe	0.038	**0.296**	**0.205**	0.048	–0.061	**0.208**	**0.287**	–0.022	**0.292**	–0.087	**–0.220**	–0.039	–0.169	0.012	**–0.383**	**–0.396**	0.143	**0.476**	**0.536**	**–0.626**	**–0.386**	**0.394**	*	**0.000**	**0.000**	**0.000**	**0.000**	0.328	0.353	**0.028**	**0.001**
24 C	–0.195	**–0.435**	**–0.297**	0.048	0.108	–0.056	**–0.446**	0.048	**–0.419**	0.061	–0.029	0.098	0.150	0.022	**0.200**	**0.370**	–0.029	**–0.439**	**–0.456**	**0.535**	**0.275**	**–0.238**	**–0.458**	*	**0.001**	**0.001**	**0.000**	0.245	0.847	0.103	**0.017**
25 K	–0.104	0.191	0.167	0.096	0.032	**0.333**	**0.240**	**–0.210**	**0.272**	–0.163	–0.136	0.022	–0.040	0.101	**–0.473**	**–0.368**	0.073	**0.324**	**0.385**	**–0.491**	**–0.411**	**0.667**	**0.391**	**–0.313**	*	**0.000**	**0.000**	0.757	**0.005**	**0.000**	**0.000**
26 Mg	0.047	0.122	0.066	0.090	0.082	0.186	0.125	–0.039	0.123	–0.068	–0.168	0.086	–0.042	0.159	**–0.278**	**–0.461**	0.081	**0.368**	**0.418**	**–0.544**	**–0.360**	**0.313**	**0.553**	**–0.327**	**0.427**	*	**0.000**	0.162	0.645	**0.026**	**0.000**
27 Mn	0.033	**0.470**	**0.397**	0.099	–0.074	**0.345**	**0.451**	–0.174	**0.473**	–0.061	–0.141	–0.045	–0.185	0.006	**–0.406**	**–0.592**	0.127	**0.617**	**0.678**	**–0.639**	**–0.298**	**0.476**	**0.536**	**–0.530**	**0.535**	**0.425**	*	0.622	0.913	**0.000**	**0.000**
28 Na	0.163	0.068	–0.041	0.123	–0.078	–0.005	0.180	0.191	0.016	0.089	0.027	**0.290**	**0.214**	**0.249**	**0.210**	**–0.192**	**0.256**	0.148	0.121	–0.004	**0.275**	–0.084	–0.096	–0.113	0.030	0.136	0.048	*	**0.000**	**0.000**	0.719
29 P	–0.165	–0.135	–0.092	–0.022	0.019	0.050	–0.055	–0.137	0.025	–0.177	–0.032	–0.172	–0.074	–0.104	**–0.264**	**0.203**	**–0.293**	**–0.283**	**–0.220**	–0.122	**–0.577**	**0.308**	0.091	–0.019	**0.272**	0.045	–0.011	**–0.365**	*	0.488	**0.039**
30 S	–0.087	**0.232**	0.171	0.199	**–0.215**	**0.297**	**0.355**	–0.086	**0.318**	0.037	–0.192	0.106	0.019	0.114	**–0.218**	**–0.375**	**0.282**	**0.365**	**0.393**	**–0.269**	–0.016	**0.455**	**0.215**	–0.159	**0.494**	**0.218**	**0.443**	**0.353**	0.068	*	**0.026**
31 Zn	0.096	**0.266**	0.143	–0.016	0.122	**0.220**	**0.276**	–0.006	**0.238**	**–0.218**	–0.178	–0.022	0.093	0.037	**–0.269**	**–0.197**	–0.030	**0.227**	**0.254**	**–0.352**	**–0.396**	**0.358**	**0.331**	**–0.233**	**0.407**	**0.340**	**0.353**	0.035	**0.202**	**0.218**	*

PCA ordination of environmental variables

The first two PCA axes accounted for 34.6% and 12.4% of the variance in standardised transformed environmental variables, respectively (eigenvalues of 0.346 and 0.124).

$pH_{(H2O)}$, $pH_{(CaCl2)}$, Ca, K and Mn obtained high loadings along PCA axis 1 together with extractable C, macro plot aspect unfavourability, macro and meso plot slope and meso plot heat index, while low loadings were obtained by H, Fe, meso plot heat index and soil moisture (Fig. 197). These two groups of variables were negatively correlated with each other.

Extractable P obtained high loading on PCA axis 2, while Na, Al and soil moisture obtained low loadings.

The PCA results were consistent with the correlation matrix of the environmental variables, showing that variables related to soil richness and soil moisture made up the strongest environmental complex gradients in the Åmotsdalen reference area.

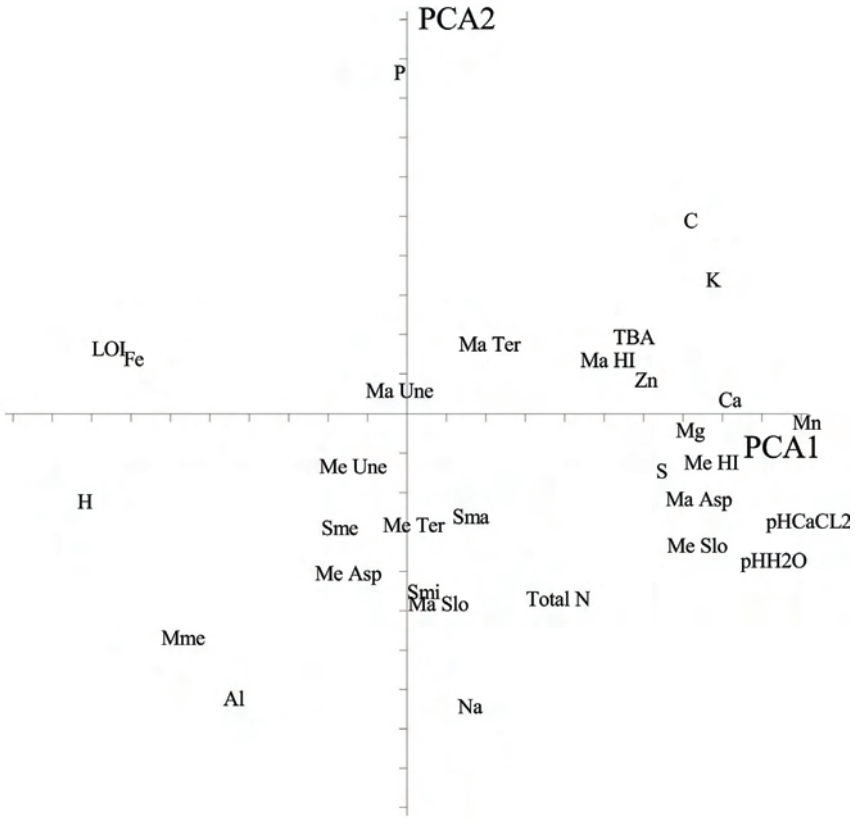

Fig. 197. Åmotsdalen: PCA ordination of 31 environmental variables. Abbreviations in accordance with Table 2), axes 1 (horizontal) and 2 (vertical). Positions of variables in the ordination space give the head of variable vectors. Tickmarks indicate 0.1 units along both axes.

DCA ordination

The gradient length of the two first DCA axes was 3.54 and 1.79 S.D. units, and the eigenvalues were 0.519 and 0.106, respectively. Accordingly, the only strong gradient in species composition was DCA 1. The plots partly segregated into two groups; one group with 40 samples occurred to the left in the DCA diagram (DCA 1 scores between 0 and 1.9 S.D. units on axis 1), while the remaining 10 plots occurred to the right (2.5–3.5 S.D. units) (Fig. 198).

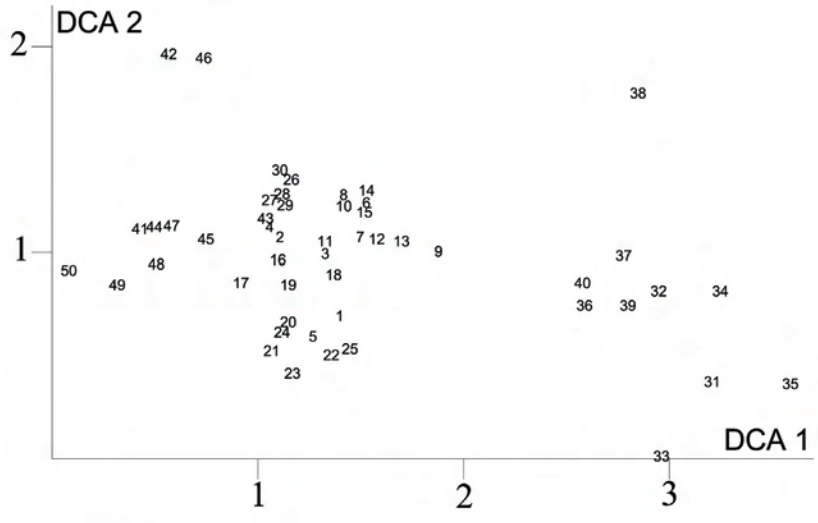

Fig. 198. Åmotsdalen: DCA ordination diagram of 50 meso plots, axes 1 (horizontal) and 2 (vertical). Meso plot number are plotted just right of the sample plot positions. Scaling of axes in S.D. units.

GNMDS ordination

The GNMDS ordination diagram (Fig 199) was visually similar to the DCA diagram (Fig 190a). The correlation between GNMDS axis 1 and DCA axis 1 was $\tau = 0.931$ and the correlation between GNMDS axis 2 and DCA axis 2 was $\tau = 0.620$.

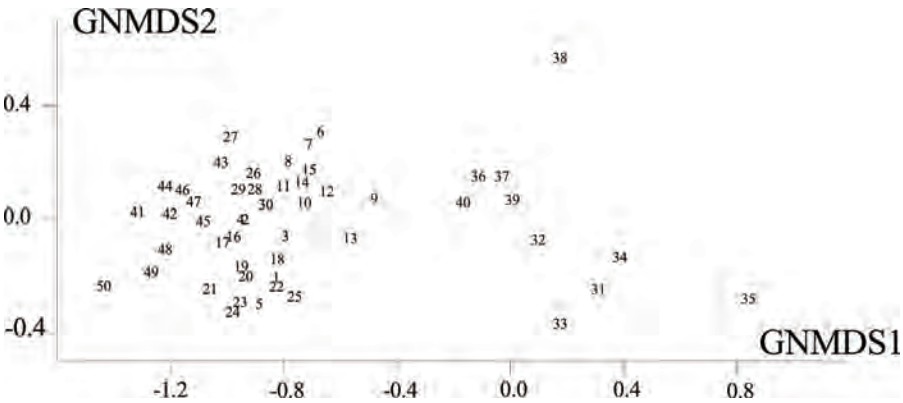

Fig.199. Åmotsdalen: GNMDS ordination biplot diagram of 50 meso plots (indicated by their number).

Split-plot GLM analysis of relationships between ordination axes and environmental variables

Variation (in plot scores) along DCA axis 1 was partitioned with 96.03 % at the macro-plot scale (i.e. between macro plots) and 3.97 % at the (between) meso plot scale within macro plots (Table 13). For the second ordination axis, 56.03 % of the variation was explained at the macro-plot scale and 43.97 % at the plot scale (Table 14).

At the macro-plot scale, eight environmental variables were significantly (at the α = 0.05 level) related to DCA 1 while three variables (also at the α = 0.05 level) were related to DCA 2. At the plot scale level, five environmental variables were significantly related to DCA 1 and two variables to DCA 2 (Tables 13 and 14).

At the macro-plot scale, tree basal area, pH and soil concentrations of Total N, Ca, Mn, and S increased significantly along DCA 1 while loss on ignition decreased. Predictors with significant relationship (positive) to this axis on the plot scale were maximum soil depth, soil moisture, pH measures and soil concentrations of Al.

At the macro-plot scale, DCA 2 was positively related to minimum soil depth and negatively related to macro plot terrain form and the concentration of Mn in soil. At the plot scale, DCA axis 2 was significantly negatively related to macro plot slope and positively correlated to soil concentration of Na (Table 14).

Table 13. Åmotsdalen: Split-plot GLM analysis and Kendall's nonparametric correlation coefficient τ between DCA 1 and 31 environmental variables (predictor) in the 50 plots. df_{resid}: degrees of freedom for the residuals; *SS*: total variation; *FVE*: fraction of total variation attributable to a given scale (macro plot or plot); SS_{expl}/SS: fraction of the variation attributable to the scale in question, explained by a variable; *r*: model coefficient (only given when significant at the $\alpha = 0.05$ level, otherwise blank); *F*: *F* statistic for test of the hypothesis that $r = 0$ against the two-tailed alternative. Split-plot GLM relationships significant at level $\alpha = 0.05$, *P*, *F*, *r* and SS_{expl}/SS, and Kendall's nonparametric correlation coefficient $|\tau| \geq 0.30$ are given in bold face. Numbers and abbreviations for names of environmental variables are in accordance with Table 2.

Predictor	Dependent variable = DCA 1 (*SS* = 34.3416)						Correlation between predictor and DCA 1
	Error level						
	Macro plot df_{resid} = 8 $SS_{macro\ plot}$ = 32.9770 *FVE* = 0.9603 of *SS*			Plot within macro plot df_{resid} = 39 SS_{plot} = 1.36464 *FVE* = 0.0397 of *SS*			Total
	$SS_{expl}/SS_{macro\ plot}$	*r*	*F*	*P*	SS_{expl}/SS_{plot}	*r*	*F*	*P*	τ
Ma Slo	0.2773		3.0701	0.1178	0.0812		3.4454	0.0710	–0.041
Ma Asp	0.0285		0.2351	0.6408	0.0192		0.7627	0.3878	0.166
Ma HI	0.1310		1.2061	0.3041	0.0017		3.6437	0.0927	0.148

Ma Ter	0.3714		4.7258	0.0614	0.0184		0.7295	0.3983	0.147
Ma Une	0.0371		0.3082	0.5939	0.0264		1.0563	0.3104	–0.09
TBA	**0.4875**	**2.7191**	**7.6086**	**0.0247**	0.0000		0.0001	0.9935	0.257
Me Slo	0.3861		5.0319	0.0552	0.0002		0.0096	0.9226	0.208
Me Asp	0.0045		0.0365	0.8533	0.0043		0.1686	0.6836	–0.135
Me HI	0.3129		3.6437	0.0927	0.0000		0.0009	0.9930	–0.248
Me Ter	0.0517		0.4364	0.5274	0.0041		0.1618	0.6897	0.045
Me Une	0.2576		2.7753	0.1343	0.0026		0.1010	0.7523	–0.22
Smi	0.0191		0.1557	0.7034	0.0209		0.8327	0.3671	0.088
Sme	0.0776		0.6734	0.4356	0.0121		0.4778	0.4935	–0.065
Sma	0.0951		0.8407	0.3860	**0.1008**	**0.3049**	**4.3729**	**0.0431**	0.123
Mme	0.1495		1.4064	0.2697	**0.1043**	**0.3367**	**4.5427**	**0.0394**	–0.235
LOI	**0.6934**	**–2.4254**	**18.0930**	**0.0028**	0.0019		0.0757	0.7847	**–0.536**
Total N	**0.5493**	**3.7831**	**9.7483**	**0.0142**	0.0630		2.6229	0.1134	**0.361**
$pH_{(H2O)}$	**0.7879**	**2.8417**	**29.7260**	**0.0006**	**0.1581**	**0.5362**	**7.3260**	**0.0100**	**0.572**
pH_{CaCl2}	**0.7507**	**2.5896**	**24.0870**	**0.0012**	**0.1604**	**0.6187**	**7.4522**	**0.0095**	**0.590**
H	0.2968		3.3771	0.1034	0.0015		0.0583	0.8104	**–0.387**
Al	0.0000		0.0000	0.9965	**0.1050**	**0.4716**	**4.5746**	**0.0388**	–0.047
C	0.1925		1.9072	0.2046	0.0367		1.4857	0.2302	0.297
Ca	**0.4048**	**2.6665**	**5.4417**	**0.0480**	0.0055		0.2173	0.6437	**0.407**
Fe	0.2194		2.2483	0.1721	0.0705		2.9584	0.0934	0.240
K	0.3225		3.8073	0.0868	0.0082		0.3240	0.5725	**0.409**
Mg	0.3895		5.1030	0.0538	0.0290		1.1634	0.2874	**0.423**
Mn	**0.6383**	**2.2069**	**14.1160**	**0.0056**	0.0451		1.8438	0.1823	**0.594**
Na	0.2159		2.2022	0.1761	0.0361		1.4605	0.2341	0.206
P	0.3249		3.8497	0.0854	0.0807		3.4217	0.0719	–0.227
S	**0.5611**	**3.1651**	**10.2280**	**0.0127**	0.0412		1.6741	0.2033	**0.477**
Zn	0.1902		1.8793	0.2076	0.0266		1.0677	0.3078	0.214

Table 14. Åmotsdalen: Split-plot GLM analysis and Kendall's nonparametric correlation coefficient τ between DCA 2 and 31 environmental variables (predictor) in the 50 plots. df_{resid}: degrees of freedom for the residuals; *SS*: total variation; *FVE*: fraction of total variation attributable to a given scale (macro plot or plot); SS_{expl}/SS: fraction of the variation attributable to the scale in question, explained by a variable; *r*: model coefficient (only given when significant at the $\alpha = 0.05$ level, otherwise blank); *F*: *F* statistic for test of the hypothesis that $r = 0$ against the two-tailed alternative. Split-plot GLM relationships significant at level $\alpha = 0.05$, *P*, *F*, *r* and SS_{expl}/SS, and Kendall's nonparametric correlation coefficient $|\tau| \geq 0.30$ are given in bold face. Numbers and abbreviations for names of environmental variables are in accordance with Table 2.

Predictor	Dependent variable = DCA 2 (*SS* = 6.8792)								Correlation between predictor and DCA 2
	Error level								
	Macro plot $df_{resid} = 8$ $SS_{macro\ plot} = 3.8547$ *FVE* = 0.5603 of *SS*				Plot within macro plot $df_{resid} = 39$ $SS_{plot} = 3.02452$ *FVE* = 0.4397 of *SS*				Total
	$SS_{expl}/$	*r*	*F*	*P*	$SS_{expl}/$	*r*	*F*	*P*	τ

	$SS_{macro\ plot}$				SS_{plot}				
Ma Slo	0.3067		3.5387	0.0967	**0.1704**	**–1.258**	**8.0085**	**0.0073**	–0.073
Ma Asp	0.0106		0.0856	0.7772	0.0364		1.4717	0.2324	–0.247
Ma HI	0.6403		14.244	0.0054	0.0129		0.5098	0.4795	–0.260
Ma Ter	**0.6765**	**–2.1084**	**16.7320**	**0.0035**	0.0275		1.1025	0.3002	–0.112
Ma Une	0.2552		2.7419	0.1363	0.0000		0.0011	0.9740	0.145
TBA	0.1339		1.2370	0.2983	0.0638		2.6599	0.1110	–0.182
Me slo	0.3133		3.6499	0.0925	0.0004		0.0153	0.9023	–0.259
Me Asp	0.0106		0.0856	0.7773	0.0415		1.6880	0.2015	–0.063
Me HI	0.3842		4.9904	0.0559	0.0245		0.9801	0.3283	–0.258
Me Ter	0.0209		0.1710	0.6901	0.0038		0.1473	0.7032	–0.057
Me Une	0.1369		1.2687	0.2927	0.0039		0.1531	0.6977	0.176
Smi	**0.4365**	**1.1815**	**6.1975**	**0.0376**	0.0382		1.5504	0.2205	0.22
Sme	0.2872		3.2238	0.1103	0.0479		1.9638	0.1690	0.213
Sma	0.3009		3.4433	0.1006	0.0293		1.1752	0.2850	0.217
Mme	0.3035		3.4854	0.0989	0.0871		3.7220	0.0610	**0.304**
LOI	0.1425		1.3298	0.2821	0.0000		0.0016	0.9680	0.205
Total N	0.2089		2.1126	0.1842	0.0862		3.6790	0.0625	–0.002
$pH_{(H2O)}$	0.2511		2.6822	0.1401	0.0019		0.0755	0.7849	–0.241
pH_{CaCl2}	0.2819		3.1400	0.1143	0.0028		0.1086	0.7435	–0.269
H	0.2490		2.6520	0.1421	0.0183		0.7268	0.3991	0.289
Al	0.1730		1.6735	0.2319	0.0272		1.0908	0.3027	0.254
C	0.2866		3.2141	0.1108	0.0000		0.0013	0.9715	–0.245
Ca	0.2705		2.9670	0.1233	0.0428		1.7432	0.1944	**–0.407**
Fe	0.3879		5.0707	0.0544	0.0230		0.9193	0.3436	**0.433**
K	0.1437		1.3431	0.2799	0.0061		0.2401	0.6269	–0.161
Mg	0.0471		0.3952	0.5471	0.0192		0.7622	0.3880	–0.184
Mn	**0.4339**	**–0.6221**	**6.1308**	**0.0384**	0.0610		2.5347	0.1194	**–0.387**
Na	0.0754		0.6527	0.4425	**0.2264**	**0.9904**	**11.4150**	**0.0017**	0.231
P	0.0042		0.0339	0.8584	0.0000		0.0007	0.9785	–0.059
S	0.0567		0.4810	0.5076	0.0618		2.5672	0.1172	–0.008
Zn	0.0267		0.2198	0.6517	0.0165		0.6553	0.4231	–0.097

Correlations between DCA ordination axes and environmental variables

The variables most strongly positively correlated with DCA axis 1 (Table 13) were soil extractable Mn ($\tau = 0.594$, Fig. 210) and $pH_{(CaCl2)}$ ($\tau = 0.590$, Fig 203), while loss on ignition ($\tau = –0.536$, Fig. 201) and exchangeable hydrogen (Fig. 204) were negatively correlated with this axis. Other variables that were positively correlated ($\tau > 0.300$) with DCA axis 1 were Total N (Fig. 202), Ca (Fig. 206), K (Fig. 208), Mg (Fig. 209), and S (Fig. 211). No variables, except LOI and H (Fig. 204), had equally strong negative correlations.

Fe ($\tau = 0.433$, Fig. 207) and soil moisture ($\tau = 0.304$, Fig. 200) had the strongest positive correlations with DCA axis 2. Extractable Ca (Fig. 206) and Mn (Fig. 210) were the only variables that were negatively correlated with DCA axis 2 at the $|\tau| > 0.300$ level. None of the topographical variables were significantly correlated with the first two DCA axes.

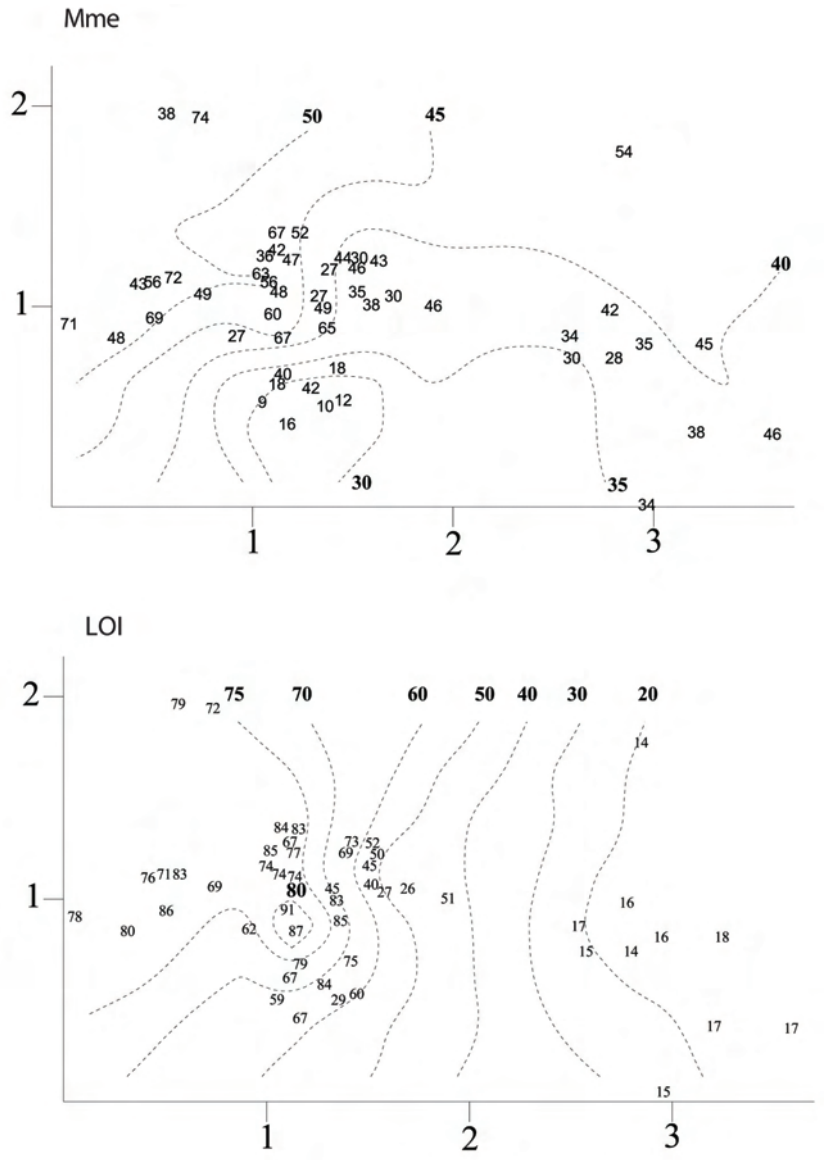

Figs 200-201. Åmotsdalen: isolines for environmental variables in the DCA ordinations of 50 meso plots, axes 1 (horizontal) and 2 (vertical). Values for the environmental variables are plotted onto the meso plots' positions. Scaling in S.D. units. Fig. 200. Mme (Soil moisture) (R^2 = 0.503). Fig. 201. LOI (R^2 = 0.771). Names of environmental variables in accordance with Table 2.

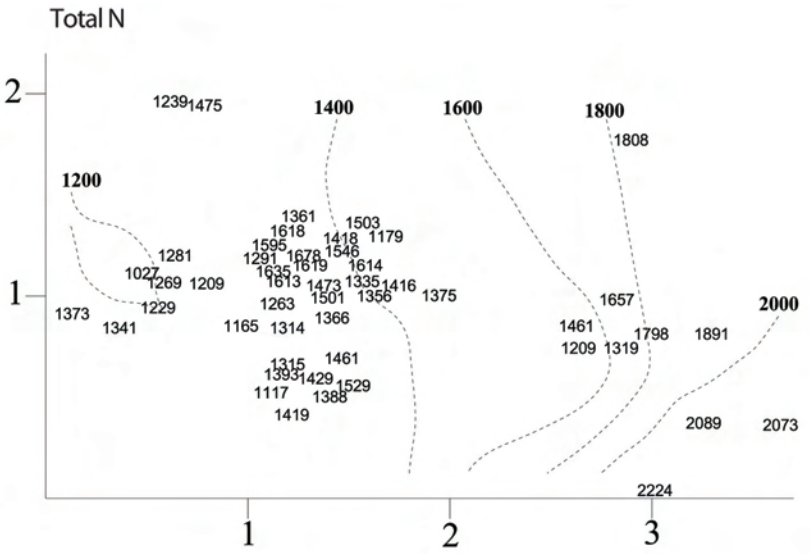

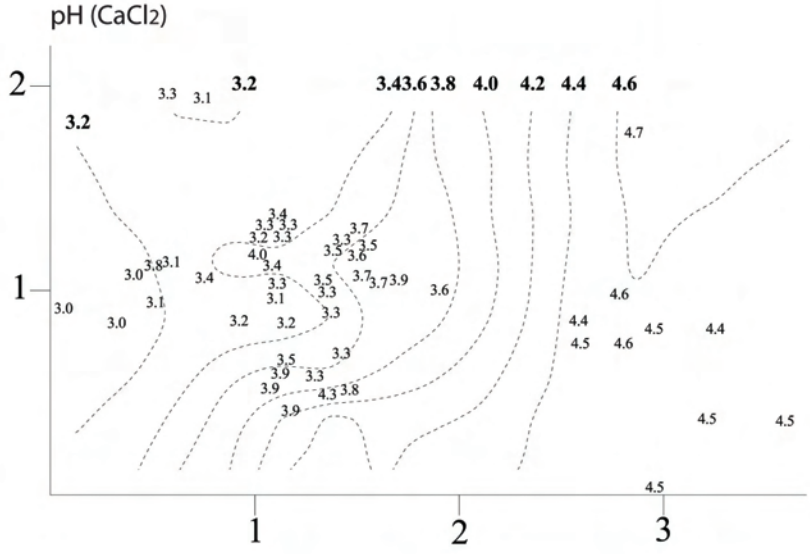

Figs 202-203. Åmotsdalen: isolines for environmental variables in the DCA ordinations of 50 meso plots, axes 1 (horizontal) and 2 (vertical). Values for the environmental variables are plotted onto the meso plots' positions. Scaling in S.D. units. Fig. 202. Total N ($R^2 = 0.694$). Fig. 203. $pH_{(CaCl2)}$ ($R^2 = 0.787$). R^2 refers to the coefficient of determination between original and smoothened values as interpolated from the isolines. Names of environmental variables in accordance with Table 2.

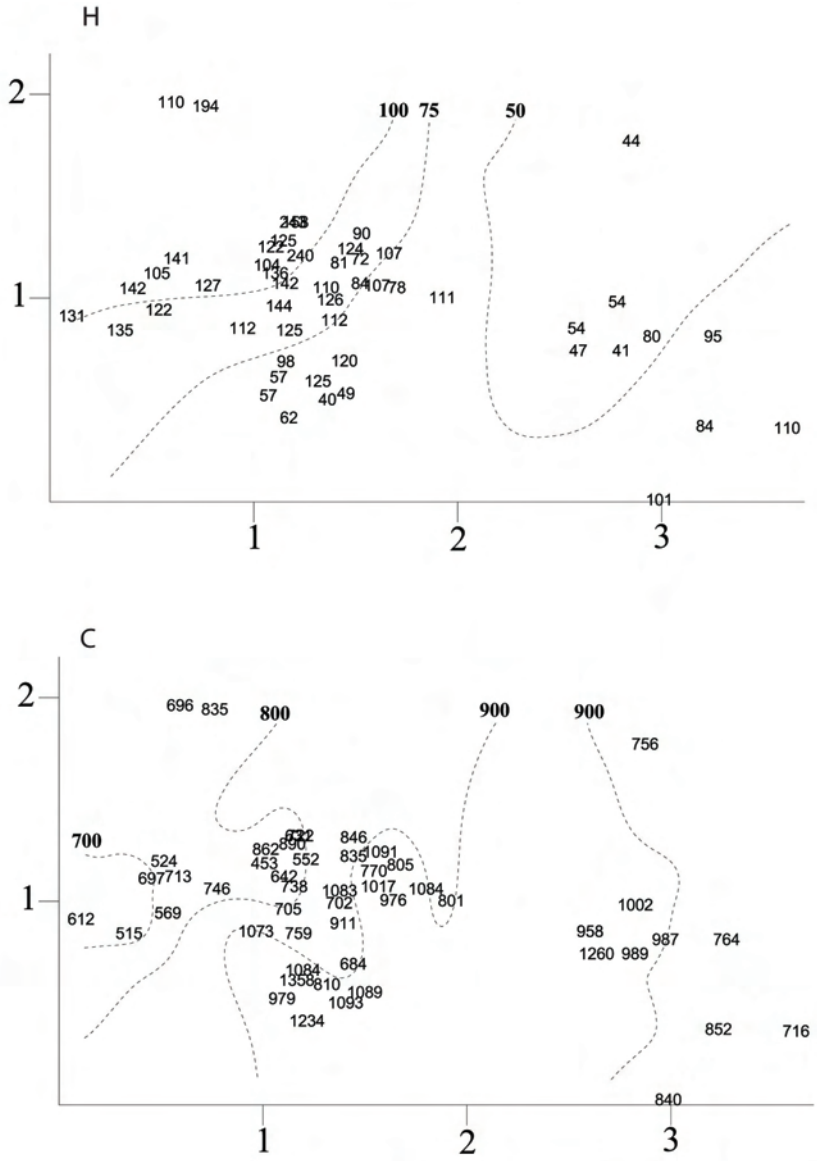

Figs 204-205. Åmotsdalen: isolines for environmental variables in the DCA ordinations of 50 meso plots, axes 1 (horizontal) and 2 (vertical). Values for the environmental variables are plotted onto the meso plots' positions. Scaling in S.D. units. Fig. 204. H (R^2 = 0.693). Fig. 205. C (R^2 = 0.675). R^2 refers to the coefficient of determination between original and smoothened values as interpolated from the isolines. Names of environmental variables in accordance with Table 2.

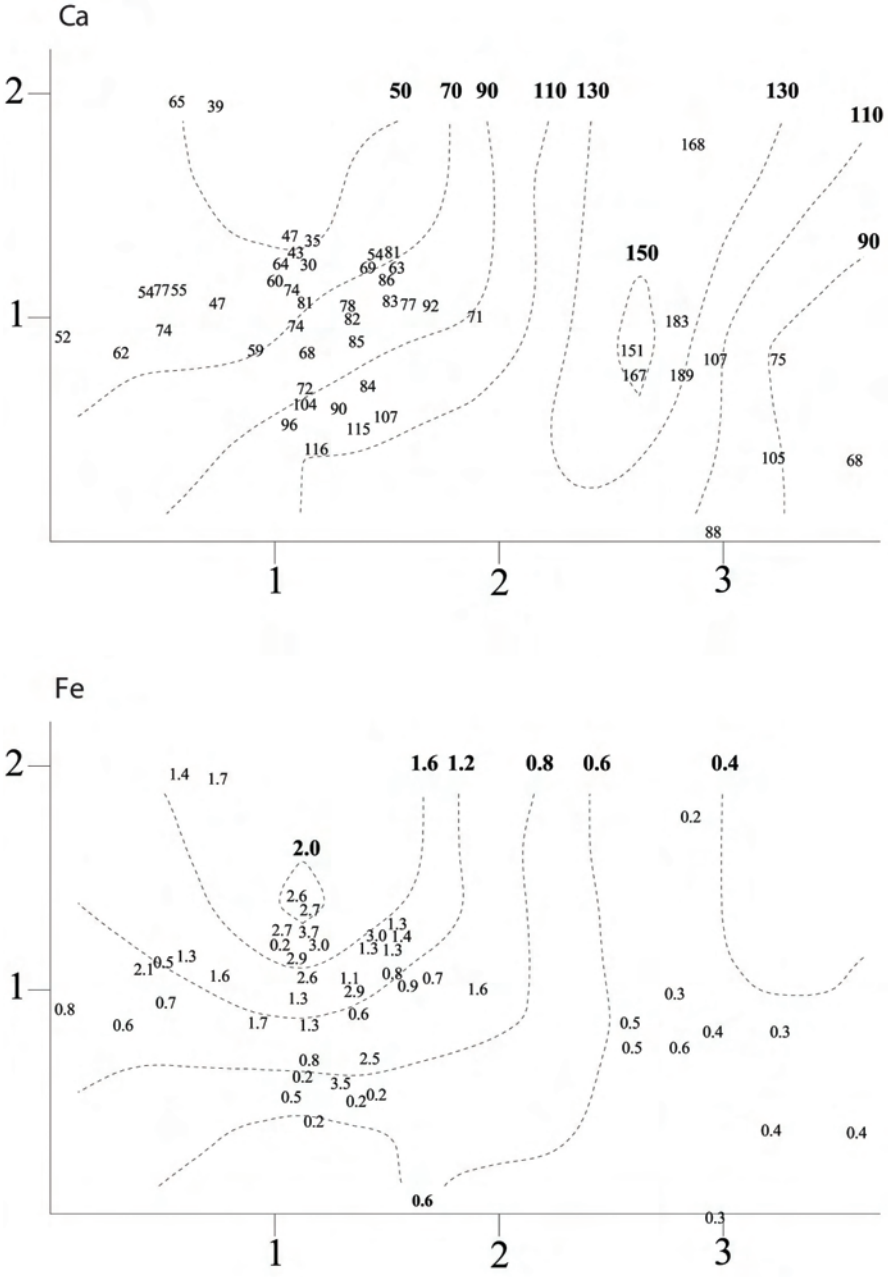

Figs 206-207. Åmotsdalen: isolines for environmental variables in the DCA ordinations of 50 meso plots, axes 1 (horizontal) and 2 (vertical). Values for the environmental variables are plotted onto the meso plots' positions. Scaling in S.D. units. 206. Ca (R^2 = 0.824). Fig. 207. Fe (R^2 = 0.557). Fig. R^2 refers to the coefficient of determination between original and smoothened values as interpolated from the isolines. Names of environmental variables in accordance with Table 2.

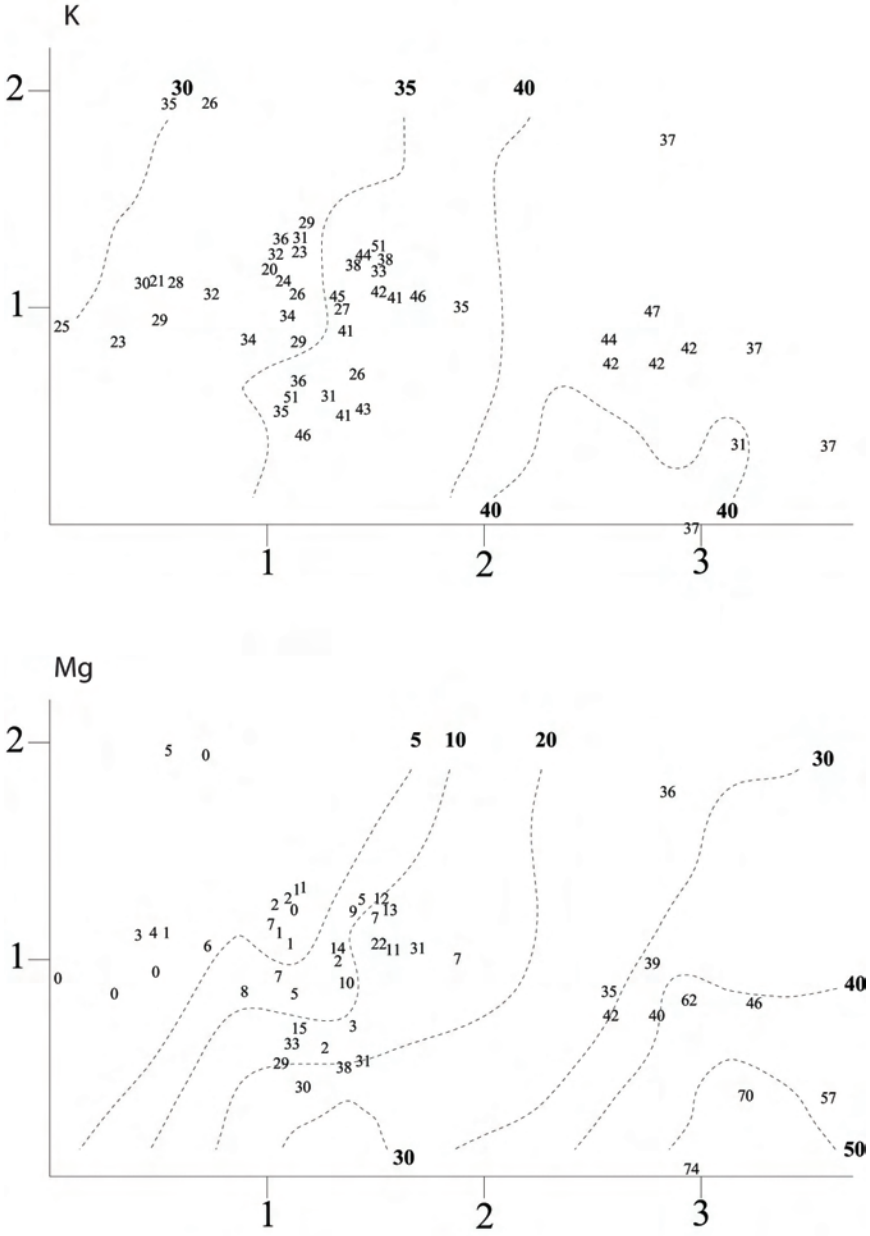

Figs 208-209. Åmotsdalen: isolines for environmental variables in the DCA ordinations of 50 meso plots, axes 1 (horizontal) and 2 (vertical). Values for the environmental variables are plotted onto the meso plots' positions. Scaling in S.D. units. Fig. 196. K (R^2 = 0.366). Fig. 197. Mg (R^2 = 0.778). R^2 refers to the coefficient of determination between original and smoothened values as interpolated from the isolines. Names of environmental variables in accordance with Table 2.

.

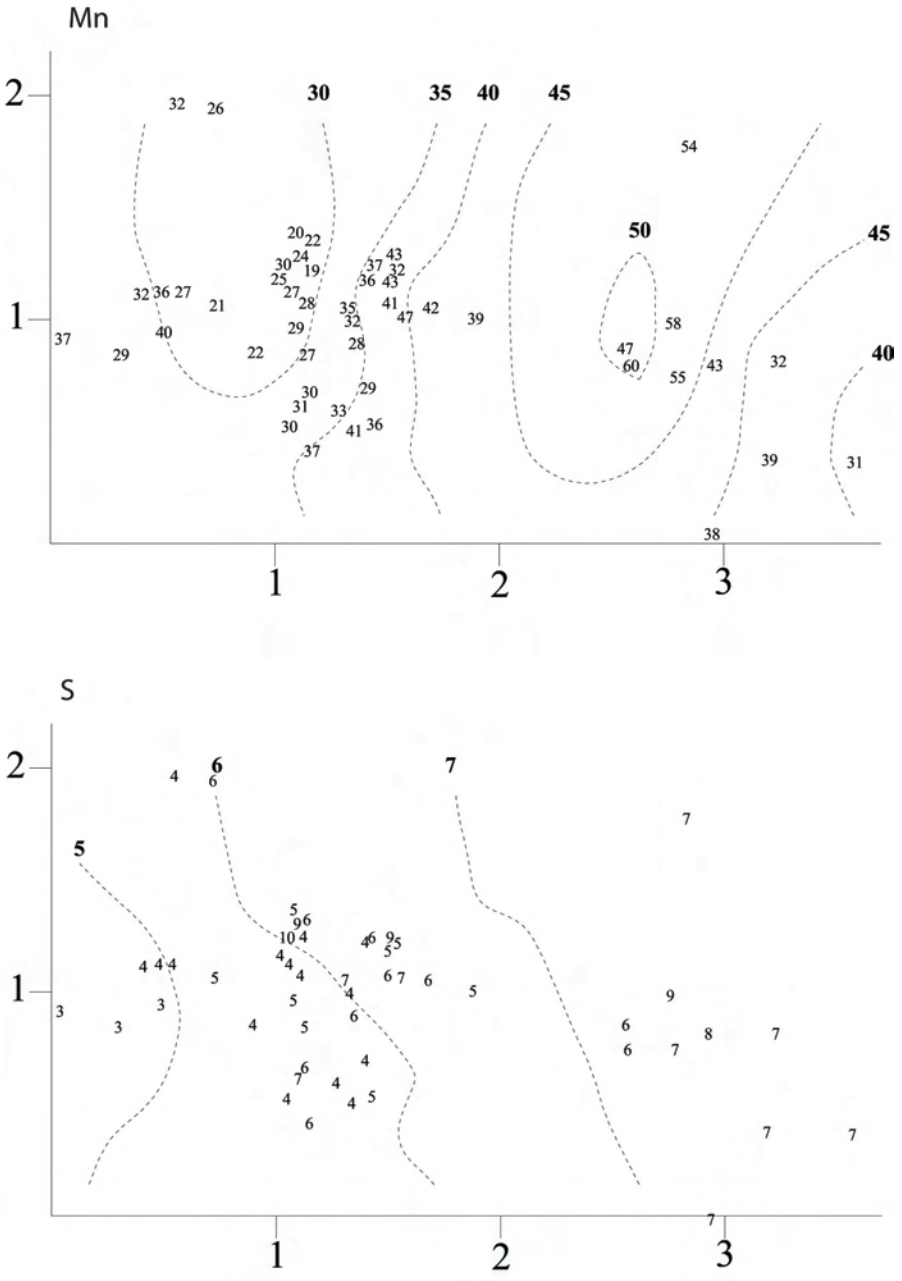

Figs 210-211. Åmotsdalen: isolines for environmental variables in the DCA ordinations of 50 meso plots, axes 1 (horizontal) and 2 (vertical). Values for the environmental variables are plotted onto the meso plots' positions. Scaling in S.D. units. Fig. 210. Mn (R^2 = 0.821). Fig. 211. S (R^2 = 0.821). R^2 refers to the coefficient of determination between original and smoothened values as interpolated from the isolines. Names of environmental variables in accordance with Table 2.

Frequent species

A total of 90 species were recorded within the 50 meso plots: 53 vascular plants, 14 mosses, 9 liverworts and 14 lichens. The most frequent species were (the sum of subplot frequencies in brackets): *Vaccinium myrtillus* (761 out of 800), *Avenella flexuosa* (743), *Vaccinium vitis-idaea* (724), *Empetrum nigrum* spp. *hermaphroditum* (607), *Polytrichum commune* (520), *Calluna vulgaris* (439), *Pleurozium schreberi* (363), *Barbilophozia lycopodoides* (367), *Trientalis europaea* (331) and *Chamaepericlymenum suecicum* (315).

The distribution of species abundance in the DCA ordination

Forty-seven of the total 90 species occurred in 5 or more of the sample plots (Figs 212–258).

Vaccinium myrtillus (Fig .217), *Vaccinium vitis-idaea* (Fig. 219), *Avenella flexuosa* (Fig. 241) and *Polytrichum commune* (Fig. 250) had wide ecological amplitudes and were highly abundant in most of the sample plots.

Many species were mainly restricted to the right part of the DCA ordination diagram (high DCA axis 1 scores), showing preferences for soils with high values of pH, extractable elements (e.g. Ca, K, Mg, Mn) and total N and low values of loss-on-ignition. Examples of such species were *Deschampsia cespitosa* (Fig. 240) and *Rhytidiadelphus squarrosus* (Fig. 253), mainly restricted to the driest sites (lower right part of the DCA ordination diagram), while *Alchemilla alpina* (Fig. 220), *Bistorta vivipara* (Fig. 221) *Geranium sylvaticum* (Fig. 223), *Gymnocarpium dryopteris* (Fig. 224), *Maianthemum bifolium* (Fig. 227), *Orthilia secunda* (Fig. 229), *Oxalis acetosella* (Fig. 230), *Pyrola minor* (Fig. 232), *Ranunculus acris* (Fig. 221), *Veronica officinalis* (Fig. 236) and *Agrostis capillaris* (Fig. 237) were more or less present in both the lower and upper right part of the DCA ordination diagram. *Rhodobryum roseum* (Fig. 252) had its optimum for intermediate to high DCA axis 1 and axis 2 scores.

Examples of species mainly restricted to sample plots with low values of pH, extractable elements and higher loss on ignition (the left part of the DCA ordination diagram) were *Betula nana* (Fig. 212), *Vaccinium uliginosum* (Fig. 218), *Dicranum fuscescens* (Fig. 245), *Ptilidium ciliare* (Fig. 256), *Cladonia chlorophaea* (Fig. 257) and *Cladonia rangiferina* (Fig. 258). Of these *Betula nana* occupied the most moist plots at high DCA axis 2 scores. Species such as *Calluna vulgaris* (Fig. 214), *Empetrum nigrum* (Fig. 215), *Dicranum scoparium* (Fig. 247), *Hylocomium splendens* (Fig. 248), *Pleurozium schreberi* (Fig. 249) and *Barbilophozia lycopodioides* (Fig. 254) also preferred less nutrient-rich soils in the left part of DCA axis 1.

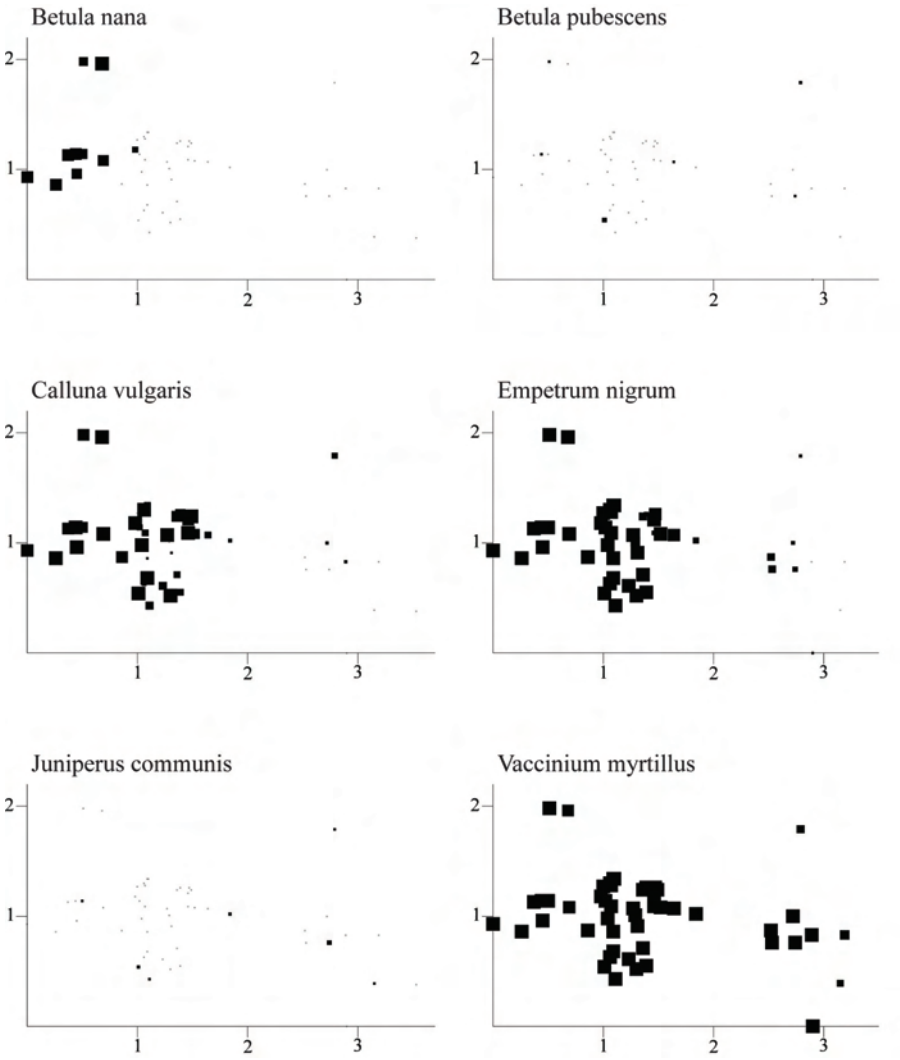

Figs 212-217. Åmotsdalen: distributions of species abundances in the DCA ordination of 50 sample plots, axes 1 (horizontal) and 2 (vertical). Frequency in subplots for each species in each meso plot proportional to quadrate size. Scaling in S.D. units. Fig. 212. *Betula nana*. Fig. 213. *Betula pubescens*. Fig. 214. *Calluna vulgaris*. Fig. 215. *Empetrum nigrum*. Fig. 216. *Juniperus communis*. Fig. 217. *Vaccinium myrtillus*.

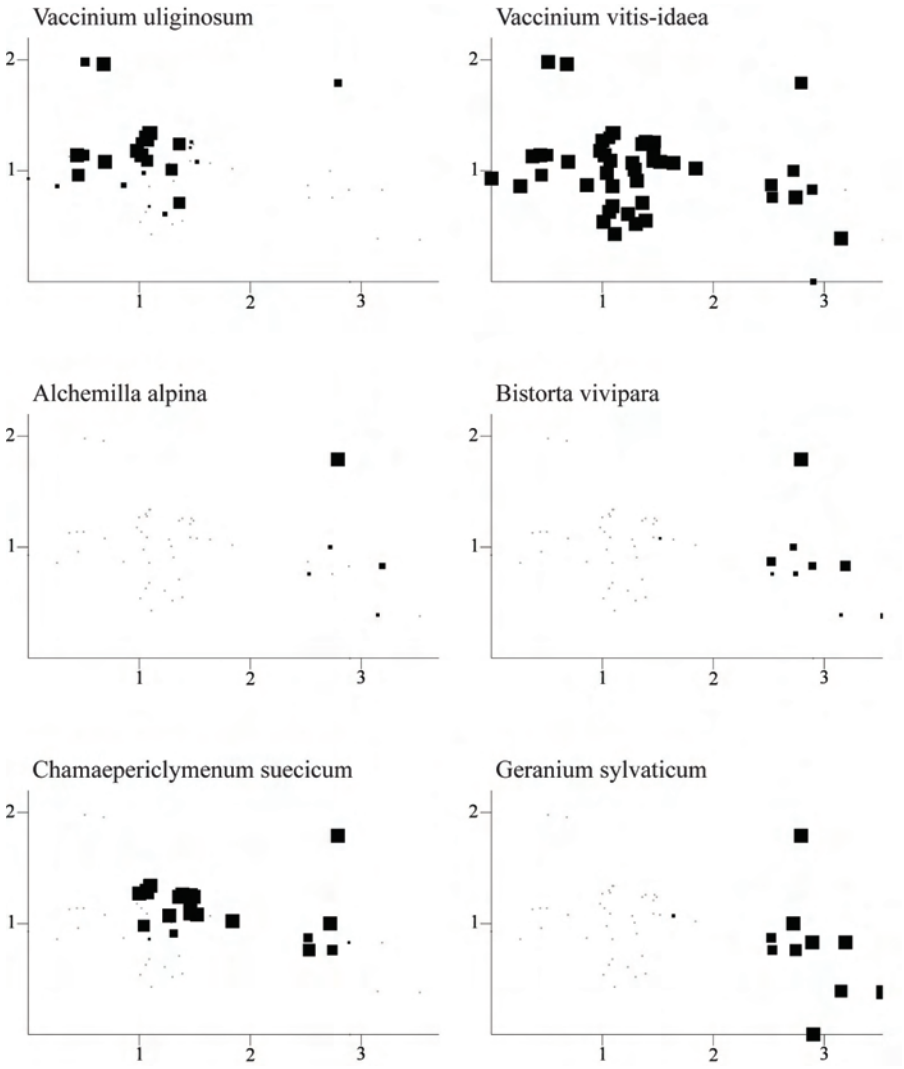

Figs 218-223. Åmotsdalen: distributions of species abundances in the DCA ordination of 50 sample plots, axes 1 (horizontal) and 2 (vertical). Frequency in subplots for each species in each meso plot proportional to quadrate size. Scaling in S.D. units. Fig. 218. *Vaccinium uliginosum*. Fig. 219. *Vaccinium vitis-idaea*. Fig. 220. *Alchemilla alpina*. Fig. 221. *Bistorta vivipara*. Fig. 222. *Chamaepericlymenum suecicum* (syn. *Cornus suecica*). Fig. 223. *Geranium sylvaticum*.

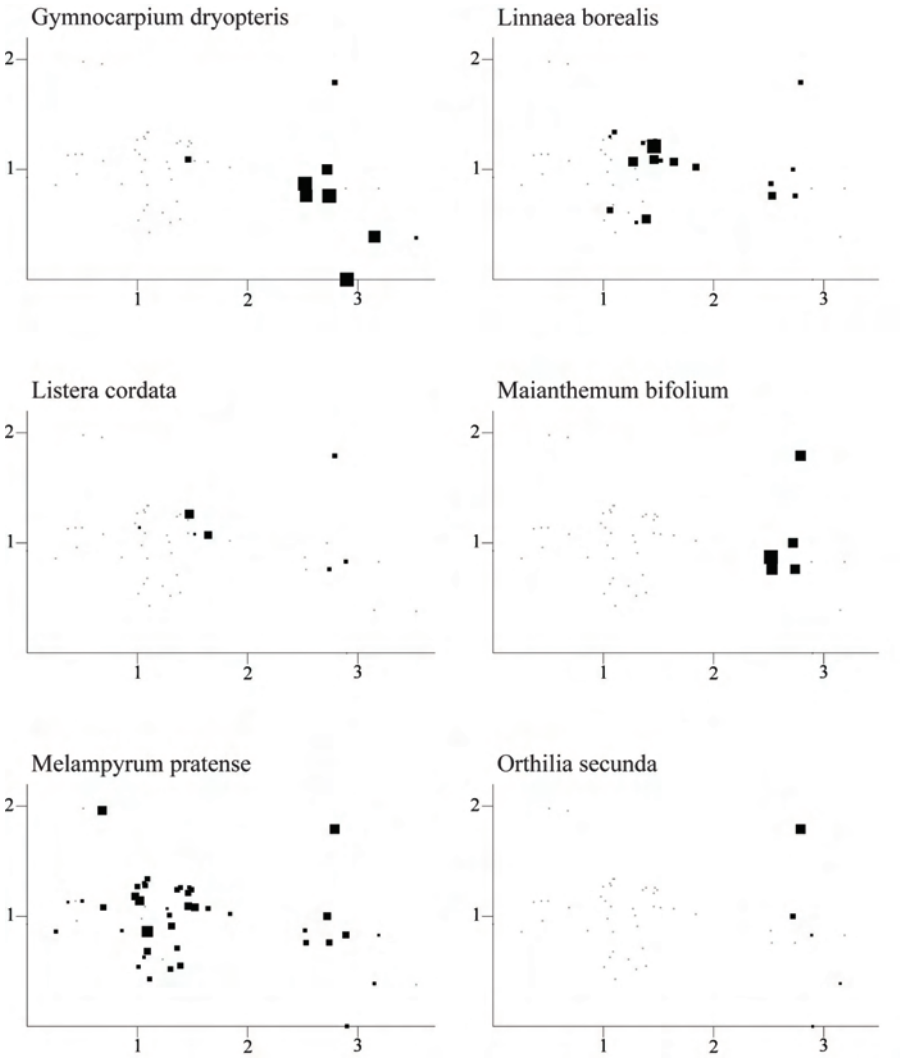

Figs 224-229. Åmotsdalen: distributions of species abundances in the DCA ordination of 50 sample plots, axes 1 (horizontal) and 2 (vertical). Frequency in subplots for each species in each meso plot proportional to quadrate size. Scaling in S.D. units. Fig. 224. *Gymnocarpium dryopteris*. Fig. 225. *Linnaea borealis*. Fig. 226. *Listera cordata*. Fig. 227. *Maianthemum bifolium*. Fig. 228. *Melampyrum pratense*. Fig. 229. *Orthilia secunda*.

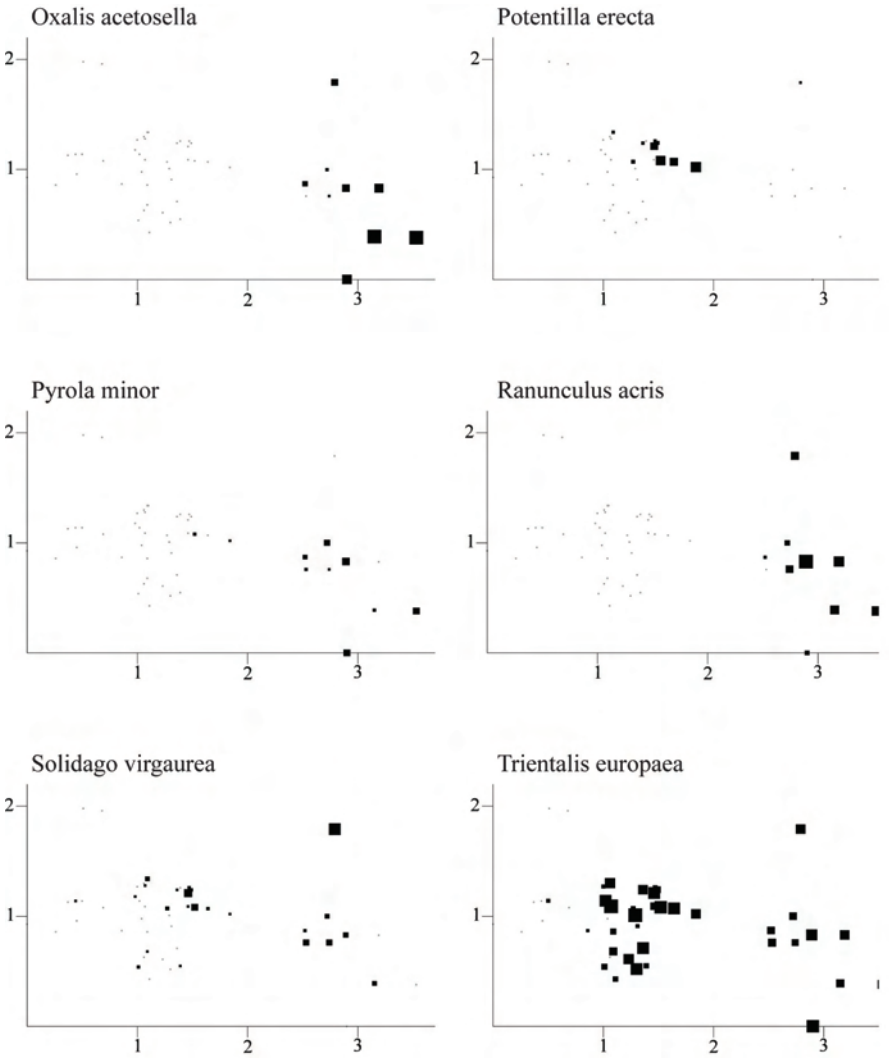

Figs 230-235. Åmotsdalen: distributions of species abundances in the DCA ordination of 50 sample plots, axes 1 (horizontal) and 2 (vertical). Frequency in subplots for each species in each meso plot proportional to quadrate size. Scaling in S.D. units. Fig. 230. *Oxalis acetosella*. Fig. 231. *Potentilla erecta*. Fig. 232. *Pyrola minor*. Fig. 233. *Ranunculus acris*. Fig. 234. *Solidago virgaurea*. Fig. 235. *Trientalis europaea*.

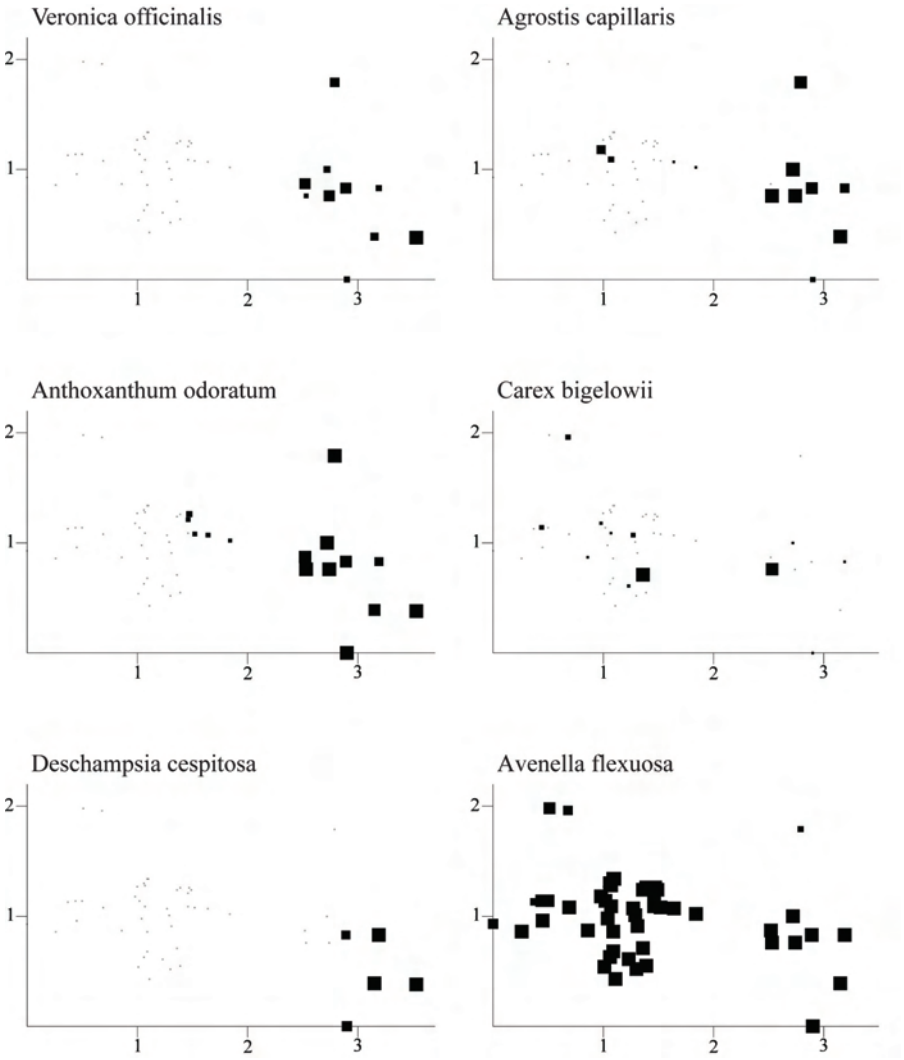

Figs 236-241. Åmotsdalen: distributions of species abundances in the DCA ordination of 50 sample plots, axes 1 (horizontal) and 2 (vertical). Frequency in subplots for each species in each meso plot proportional to quadrate size. Scaling in S.D. units. Fig. 236. *Veronica officinalis*. Fig. 237. *Agrostis caplillaris*. Fig. 238. *Anthoxanthum odoratum*. Fig. 239. *Carex bigelowii*. Fig. 240. *Deschampsia cespitosa*. Fig. 241. *Avenella flexuosa* (syn, *Deschampsia flexuosa*).

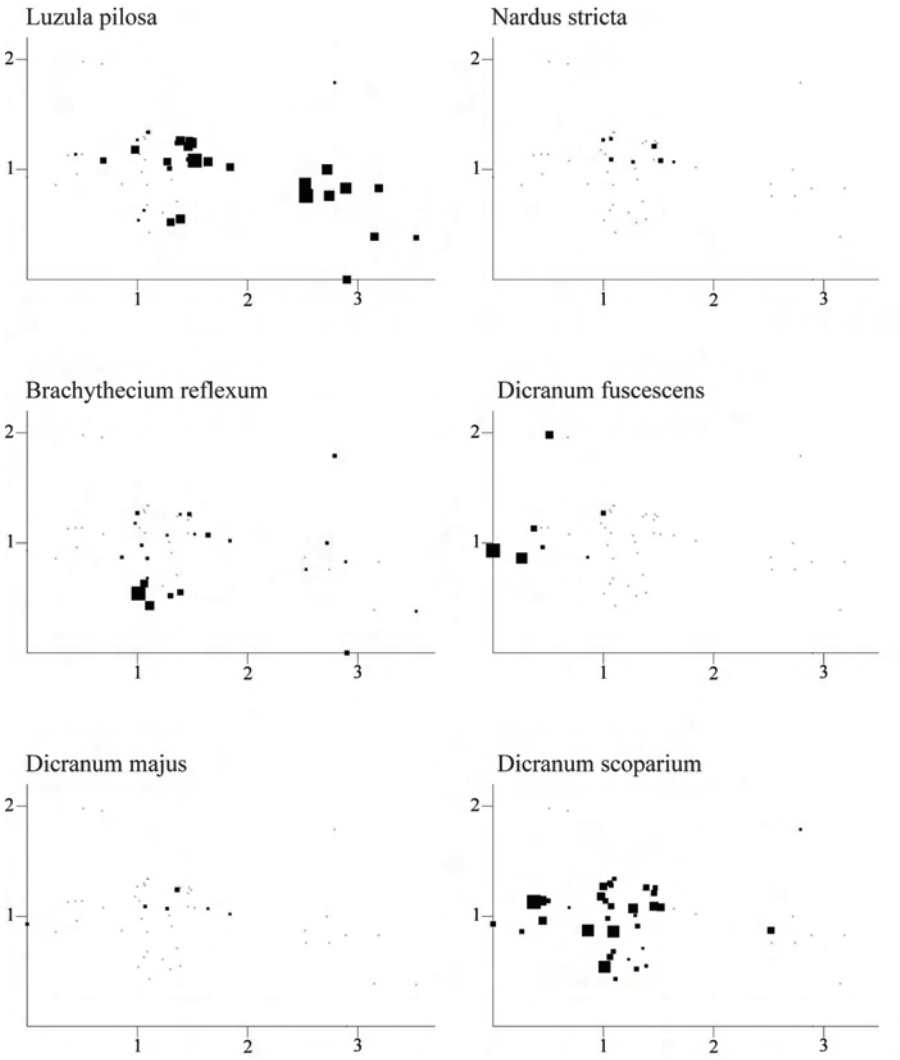

Figs 242-247. Åmotsdalen: distributions of species abundances in the DCA ordination of 50 sample plots, axes 1 (horizontal) and 2 (vertical). Frequency in subplots for each species in each meso plot proportional to quadrate size. Scaling in S.D. units. Fig. 242. *Luzula pilosa*. Fig. 243. *Nardus stricta*. Fig. 244. *Brachythecium reflexum*. Fig. 245. *Dicranum fuscescens*. Fig. 246. *Dicranum majus.* Fig. 247. *Dicranum scoparium.*

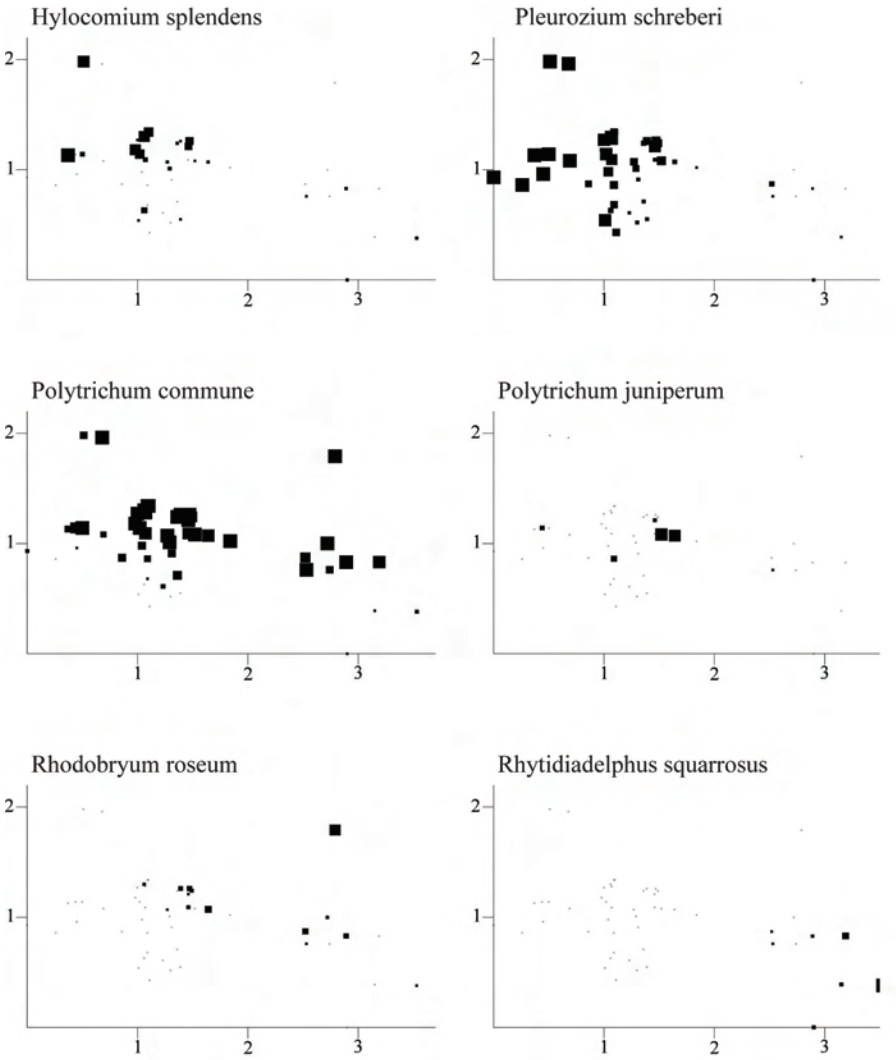

Figs 248-253. Åmotsdalen: distributions of species abundances in the DCA ordination of 50 sample plots, axes 1 (horizontal) and 2 (vertical). Frequency in subplots for each species in each meso plot proportional to quadrate size. Scaling in S.D. units. Fig. 248. *Hylocomium splendens.* Fig. 249. *Pleurozium schreberi*. Fig. 250. *Polytrichum commune*. Fig. 251. *Polytrichum juniperinum*. Fig. 252. *Rhodobryum roseum*. Fig. 253. *Rhytidiadelphus squarrosus*.

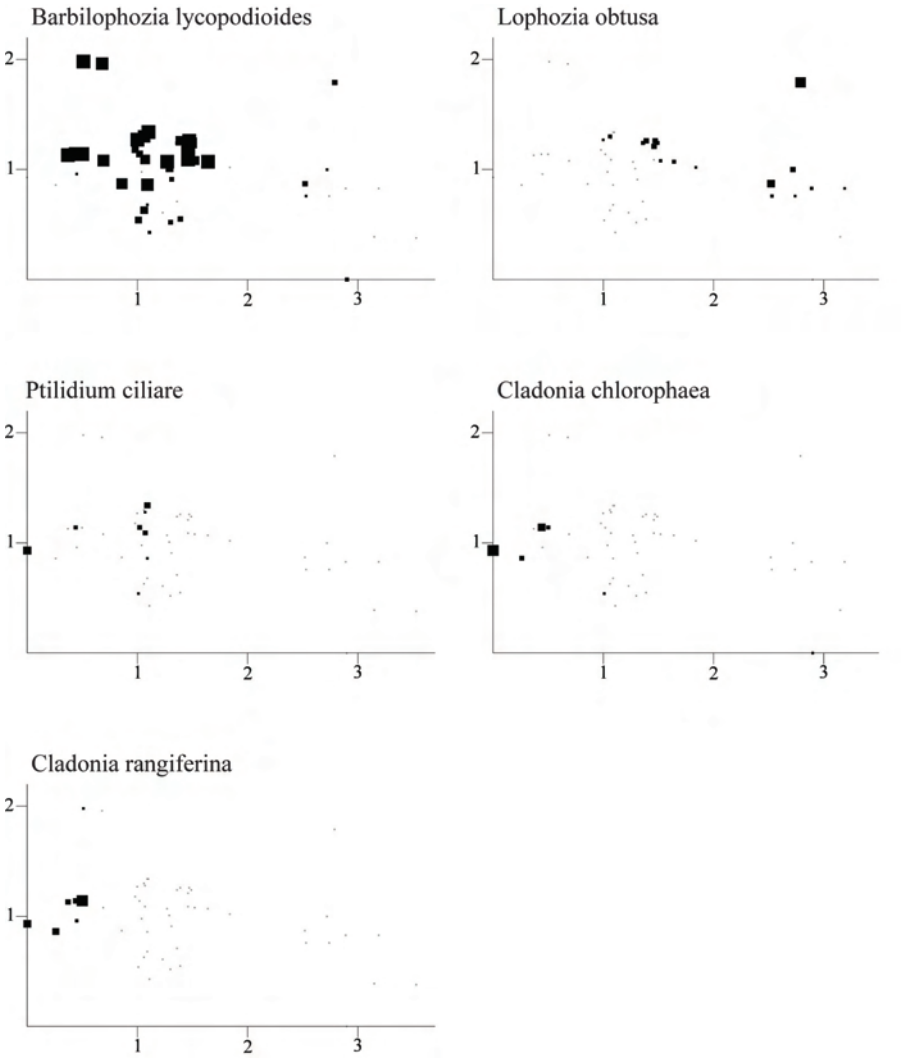

Figs 254-258. Åmotsdalen: distributions of species abundances in the DCA ordination of 50 sample plots, axes 1 (horizontal) and 2 (vertical). Frequency in subplots for each species in each meso plot proportional to quadrate size. Scaling in S.D. units. 254. *Barbilophozia lycopodioides*. Fig. 255. *Lophozia obtusa*. 256. *Ptilidium ciliare*. Fig. 257. *Cladonia chlorophaea*. Fig. 258. *Cladonia rangiferina*.

BØRGEFJELL REFERENCE AREA

Correlations between environmental variables

Many variables had strong pairwise correlations (Table 15). Macro and meso plot slope were negatively correlated with soil moisture, loss on ignition, exchangeable H and extractable Al, and positively correlated with variables reflecting soil nutrient richness, such as pH, P, Ca, Mg and K. Macro plot slope was also positively correlated with tree basal area which also was positively correlated with pH and extractable cations. Soil depth (Sme and Sma) was, in general, negatively correlated with extractable elements that reflected soil richness and positively correlated with LOI and soil acidity (H and low pH values). Soil moisture was positively correlated with LOI, and both were negatively correlated with soil nutrient richness variables. Variables reflecting soil nutrient richness (pH, P, N, Ca, Mg, Na, K, Mn) were positively correlated with each other and negatively correlated with soil acidity (exchangeable H and extractable Al).

Thus the Børgefjell reference area shows variation from soils poor in nutrients, high acidity and high loss on ignition on rather flat sites to plots richer in soil nutrients with denser forests on steeper slopes.

Table 15. Børgefjell: Kendall's rank correlation coefficients τ between 31 environmental variables in the 50 sample plots (lower triangle), with significance probabilities (upper triangle). Statistically significant correlations (P<0.05) in bold face. Names of explanatory variables abbreviated in accordance with Table 2.

	1	2	3	4	5	6	7	8	9	10	11	12	13	14	15	16	17	18	19	20	21	22	23	24	25	26	27	28	29	30	31
01 Ma Slo	*	0.364	**0.022**	0.178	0.083	**0.015**	**0.000**	0.702	0.171	0.212	**0.003**	**0.046**	0.086	**0.014**	**0.001**	**0.000**	0.103	**0.000**	**0.001**	**0.015**	**0.000**	**0.000**	**0.006**	0.377	**0.000**	0.932	**0.000**	0.946	**0.001**	**0.000**	**0.000**
02 Ma Asp	0.100	*	**0.000**	**0.035**	0.388	0.979	0.421	**0.001**	**0.000**	0.421	0.511	**0.031**	0.290	0.212	0.785	0.658	0.413	0.523	0.591	0.506	0.609	0.385	0.785	0.306		0.178	0.539	**0.007**	**0.050**	0.291	0.184
03 Ma HI	**0.245**	**–0.697**	*	0.264	0.539	0.292	**0.040**	**0.000**	**0.000**	0.891	**0.012**	0.577	0.680	0.960	0.124	0.198	0.256	0.556	0.933	0.550	0.693	0.396	0.128	0.573	0.926	0.124	0.405	**0.008**	0.181	0.833	0.705
04 Ma Ter	0.154	**0.241**	–0.125	*	0.435	0.344	0.232	**0.021**	0.184	**0.006**	0.552	0.087	0.618	0.772	0.100	**0.046**	0.495	0.517	0.740	0.875	0.753	0.178	0.463	0.442	**0.031**	0.421	0.263	0.196	**0.021**	0.074	0.104
05 Ma Une	–0.204	–0.102	–0.071	0.096	*	0.536	0.097	0.540	0.848	0.956	**0.000**	0.802	0.742	0.230	**0.002**	**0.027**	0.701	0.053	0.149	0.130	**0.007**	**0.019**	0.559	0.112	**0.045**	0.622	**0.003**	0.235	0.250	0.083	0.093
05 TBA	**0.263**	–0.003	0.111	–0.107	–0.072	*	0.158	0.605	0.635	0.725	0.392	0.704	1.000	0.325	**0.032**	**0.007**	**0.000**	**0.000**	**0.001**	**0.000**	**0.005**	**0.001**	**0.013**	0.973	**0.012**	0.685	**0.009**	**0.015**	0.150	**0.000**	**0.016**
07 Me Slo	**0.636**	0.086	**0.213**	0.133	–0.190	0.148	*	0.308	**0.007**	0.207	**0.007**	**0.012**	0.076	**0.037**	**0.004**	**0.000**	0.282	**0.021**	0.056	0.126	**0.003**	**0.000**	**0.023**	0.626	**0.000**	0.638	**0.000**	0.724	**0.010**	**0.003**	**0.000**
08 Me Asp	–0.040	**0.361**	**–0.372**	**0.253**	0.069	–0.054	–0.104	*	**0.000**	0.404	0.174	0.726	0.762	0.846	0.476	0.873	0.782	0.626	0.669	0.873	0.913	0.574	0.518	0.913	0.182	0.693	0.645	0.435	0.092	0.294	0.681
09 Me HI	0.142	**–0.459**	**0.583**	–0.144	–0.021	0.048	**0.271**	**–0.626**	*	0.946	0.091	0.511	0.847	0.591	0.222	0.307	0.462	0.757	0.676	0.651	0.841	0.973	0.203	0.676	0.639	0.482	0.558	0.071	0.277	0.639	0.789
10 Me Ter	0.136	0.088	0.015	**0.315**	0.007	–0.038	0.134	0.088	–0.007	*	0.333	0.315	0.284	0.885	0.845	0.188	0.547	0.248	0.598	0.899	0.715	0.273	0.535	0.593	0.288	0.792	0.177	0.355	0.182	0.288	0.079
11 Me Une	**–0.306**	0.068	**–0.257**	–0.065	**0.470**	–0.088	**–0.271**	0.136	–0.167	–0.100	*	0.281	0.244	0.056	**0.001**	**0.008**	0.834	0.112	0.106	0.265	**0.002**	**0.013**	**0.019**	**0.030**	**0.016**	0.927	**0.008**	0.183	0.288	0.064	**0.029**
12 Smi	**–0.219**	**–0.237**	0.060	–0.196	0.030	0.041	**–0.269**	0.037	–0.068	–0.110	–0.112	*	**0.000**	0.308	0.151	0.260	0.707	0.135	0.172	0.252	0.484	0.183	0.632	0.374	0.365	0.946	0.098	0.194	0.239	0.356	**0.028**
13 Sme	–0.180	–0.111	0.042	–0.054	–0.037	0.000	–0.180	0.030	0.019	–0.111	–0.116	**0.400**	*	**0.000**	0.180	0.076	0.076	**0.042**	**0.049**	**0.016**	**0.029**	**0.013**	**0.044**	0.054	**0.011**	**0.005**	**0.007**	0.987	**0.001**	**0.039**	**0.002**
14 Sma	**–0.258**	–0.132	0.005	0.032	0.136	–0.102	**–0.214**	–0.020	0.054	–0.015	0.191	0.108	**0.351**	*	**0.004**	**0.015**	0.250	**0.044**	**0.036**	**0.045**	**0.000**	**0.002**	**0.006**	**0.002**	**0.012**	**0.002**	0.529	**0.004**	**0.008**	**0.001**
15 Mme	**–0.337**	–0.028	–0.155	–0.177	**0.346**	**–0.219**	**–0.290**	0.071	–0.119	–0.020	**0.325**	0.149	0.132	**0.285**	*	**0.000**	0.353	**0.000**	**0.000**	**0.000**	**0.004**	**0.000**	**0.000**	0.658	**0.000**	0.173	**0.000**	0.509	**0.002**	**0.000**	**0.000**
16 LOI	**–0.474**	–0.046	–0.130	**–0.215**	**0.245**	**–0.272**	**–0.361**	0.016	–0.100	–0.135	**0.261**	0.117	0.175	**0.243**	**0.598**	*	**0.039**	**0.000**	**0.000**	**0.000**	**0.000**	**0.000**	**0.000**	0.296	**0.000**	**0.046**	**0.000**	0.320	**0.000**	**0.000**	**0.000**
17 Total N	0.169	0.085	–0.115	0.074	0.043	**0.355**	0.108	0.028	–0.072	0.062	–0.021	–0.039	–0.175	–0.115	–0.091	**–0.202**	*	**0.000**	**0.000**	**0.000**	**0.010**	**0.000**	**0.004**	0.770	**0.000**	**0.000**	**0.003**	**0.001**	**0.000**	**0.000**	**0.009**
18 pH_{H2O}	**0.407**	0.066	0.060	0.070	–0.216	**0.451**	**0.233**	–0.049	0.030	0.119	–0.157	–0.156	**–0.202**	**–0.202**	**–0.474**	**–0.627**	**0.428**	*	**0.000**	**0.000**	**0.000**	**0.000**	**0.000**	0.713	**0.000**	**0.015**	**0.000**	**0.041**	**0.000**	**0.000**	**0.000**
19 pH_{CaCl2}	**0.344**	0.056	–0.009	0.036	–0.161	**0.341**	0.193	–0.043	0.041	0.054	–0.160	–0.142	**–0.195**	**–0.210**	**–0.424**	**–0.592**	**0.426**	**0.822**	*	**0.000**	**0.000**	**0.000**	**0.000**	0.238	**0.000**	**0.002**	**0.000**	0.259	**0.000**	**0.000**	**0.000**
20H	**–0.251**	–0.069	0.060	0.017	0.168	**–0.395**	–0.154	0.016	0.044	0.013	0.109	0.118	**0.238**	**0.200**	**0.360**	**0.478**	**–0.482**	**–0.712**	**–0.709**	*	**0.000**	**0.000**	**0.000**	0.093	**0.000**	**0.000**	**0.000**	0.075	**0.000**	**0.000**	**0.000**
21 Al	**–0.372**	–0.053	–0.040	0.034	**0.300**	**–0.288**	**–0.294**	0.011	–0.020	–0.038	**0.312**	0.073	**0.215**	**0.365**	**0.280**	**0.437**	**–0.252**	**–0.397**	**–0.408**	**0.476**	*	**0.000**	**0.000**	**0.000**	**0.000**	**0.004**	**0.000**	0.610	**0.000**	**0.000**	**0.000**
22 C	**0.536**	0.090	0.086	0.145	**–0.261**	**0.350**	**0.375**	0.056	0.003	0.113	**–0.244**	–0.138	**–0.246**	**–0.310**	**–0.551**	**–0.740**	**0.376**	**0.694**	**0.682**	**–0.538**	**–0.517**	*	**0.000**	0.103	**0.000**	**0.001**	**0.000**	0.874	**0.000**	**0.000**	**0.000**
23 Ca	**0.286**	–0.028	0.154	0.079	–0.065	**0.252**	**0.228**	–0.064	0.124	0.064	**–0.231**	–0.050	**–0.198**	**–0.307**	**–0.388**	**–0.453**	**0.278**	**0.455**	**0.490**	**–0.479**	**–0.412**	**0.435**	*	**0.023**	**0.000**	**0.002**	**0.000**	0.553	**0.008**	**0.000**	**0.000**
24 Fe	–0.091	0.106	–0.057	0.083	0.176	0.003	–0.049	0.011	–0.041	0.055	**0.213**	0.092	0.190	**0.273**	0.043	0.102	–0.029	–0.036	–0.116	0.164	**0.509**	–0.159	**–0.221**	*	**0.010**	0.072	**0.034**	**0.015**	**0.018**	0.311	**0.001**
25 K	**0.450**	0.118	0.009	**0.232**	**–0.223**	**0.255**	**0.356**	0.133	–0.046	0.109	**–0.238**	–0.094	**–0.251**	**–0.314**	**–0.468**	**–0.654**	**0.342**	**0.540**	**0.574**	**–0.464**	**–0.603**	**0.740**	**0.404**	**–0.252**	*	**0.000**	**0.000**	0.927	**0.000**	**0.000**	**0.000**
26 Mg	0.009	0.139	–0.155	0.087	–0.055	0.041	0.047	0.039	–0.069	0.027	–0.009	–0.007	**–0.276**	**–0.250**	–0.133	**–0.195**	**0.442**	**0.238**	**0.303**	**–0.388**	**–0.282**	**0.314**	**0.308**	–0.176	**0.394**	*	**0.006**	0.173	**0.000**	**0.000**	**0.007**
27 Mn	**0.511**	0.063	0.084	0.121	**–0.326**	**0.266**	**0.365**	–0.046	0.057	0.139	**–0.261**	–0.172	**–0.264**	**–0.309**	**–0.546**	**–0.752**	**0.293**	**0.699**	**0.676**	**–0.549**	**–0.515**	**0.802**	**0.424**	**–0.207**	**0.690**	**0.270**	*	0.670	**0.000**	**0.000**	**0.000**
28 Na	–0.007	**0.279**	**–0.267**	0.140	0.132	**0.248**	–0.035	0.078	–0.177	0.095	0.131	–0.134	–0.002	–0.063	0.064	0.097	**0.336**	**0.200**	0.111	–0.174	0.050	0.016	0.058	**0.238**	–0.009	0.133	–0.042	*	0.980	0.380	0.564
29 P	**0.350**	**0.203**	–0.135	**0.249**	–0.128	0.147	**0.258**	0.168	–0.106	0.137	–0.105	–0.122	**–0.327**	**–0.284**	**–0.296**	**–0.453**	**0.360**	**0.397**	**0.433**	**–0.358**	**–0.455**	**0.556**	**0.259**	**–0.231**	**0.701**	**0.422**	**0.535**	0.002	*	**0.000**	**0.000**
30 S	**0.473**	0.109	0.021	0.192	–0.192	**0.357**	**0.297**	0.104	–0.046	0.109	–0.182	–0.096	**–0.203**	**–0.265**	**–0.500**	**–0.680**	**0.424**	**0.729**	**0.738**	**–0.569**	**–0.433**	**0.835**	**0.443**	–0.099	**0.762**	**0.342**	**0.739**	0.086	**0.584**	*	**0.000**
31 Zn	**0.501**	0.138	0.038	0.175	–0.186	**0.245**	**0.408**	0.041	0.026	0.181	**–0.215**	**–0.228**	**–0.306**	**–0.322**	**–0.424**	**–0.551**	**0.256**	**0.461**	**0.457**	**–0.381**	**–0.572**	**0.641**	**0.350**	**–0.313**	**0.714**	**0.265**	**0.646**	–0.056	**0.638**	**0.603**	*

PCA ordination of environmental variables

The first two PCA axes accounted for 37.3% and 14.3% of the variance in the matrix of standardised transformed environmental variables, respectively (eigenvalues of 0.373 and 0.143).

$pH_{(H2O)}$, $pH_{(CaCl2)}$, extractable C, K, Mn, S and Zn obtained the highest loadings on PCA axis 1 while loss on ignition, extractable Al, exchangeable H and soil moisture (Mme) obtained low values on the same axis (Fig. 259). Macro and meso plot slope, tree aspect, total N and extractable Ca, Mg and P also had relatively high loadings on PCA axis 1.

Macro and meso plot heat indices obtained the highest loadings on PCA axis 2 while macro and meso plot aspect unfavourability indices obtained the lowest loadings

The strong correlations between variables related to soil nutrient richness and slope steepness, and between soil acidity, LOI and soil moisture, are consistent with the correlation matrix of the environmental variables in Table 15.

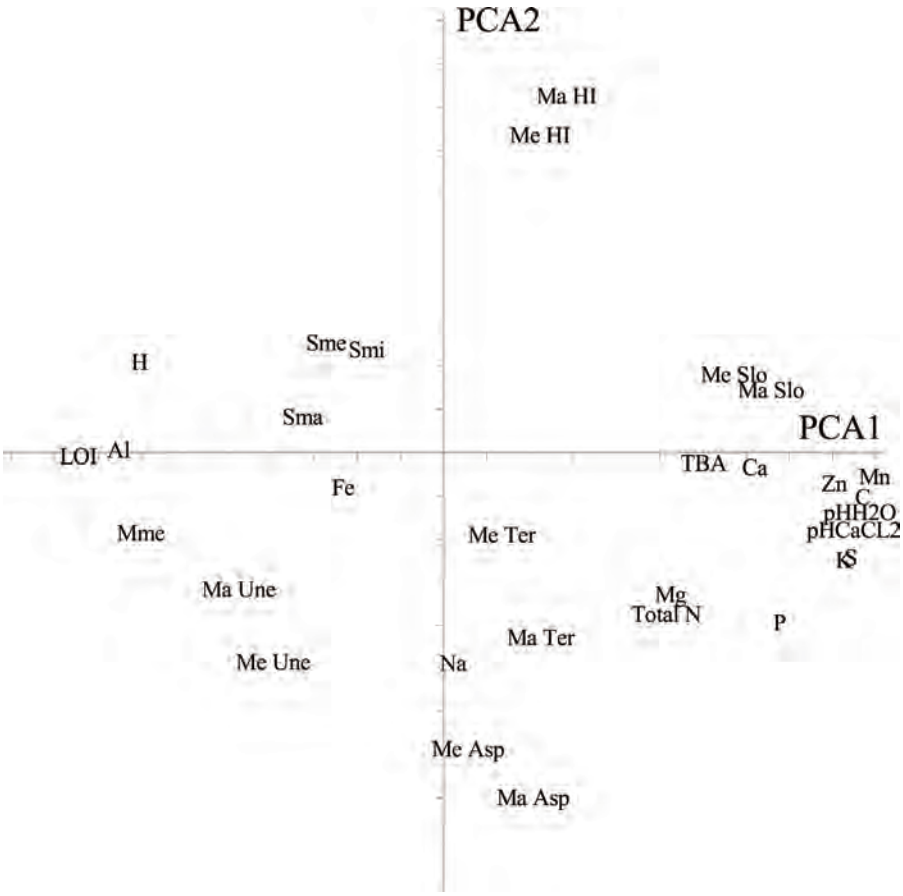

Fig. 259. Børgefjell: PCA ordination of 31 environmental variables. Abbreviations in accordance with Table 2, axes 1 (horizontal) and 2 (vertical). Positions of variables in the ordination space give the head of variable vectors. Tickmarks indicate 0.1 units along both axes.

DCA ordination

The gradient length of the first two DCA axes was 2.54 and 1.79 S.D. units with eigenvalues of 0.316 and 0.168, respectively. The sample plots segregated into four relatively diustinct clusters along the two first axes (Fig. 260). The first cluster, consisting of five sample plots (from macro plot 7) had low DCA axis 1 values (> 0.8 S.D. units) and medium high DCA axis 2 values. The next cluster, which also had the highest number of sample plots, occupied the middle of the diagram. The last two clusters were located at the right-hand side of the diagram and only these two clusters segregated along the second axis.

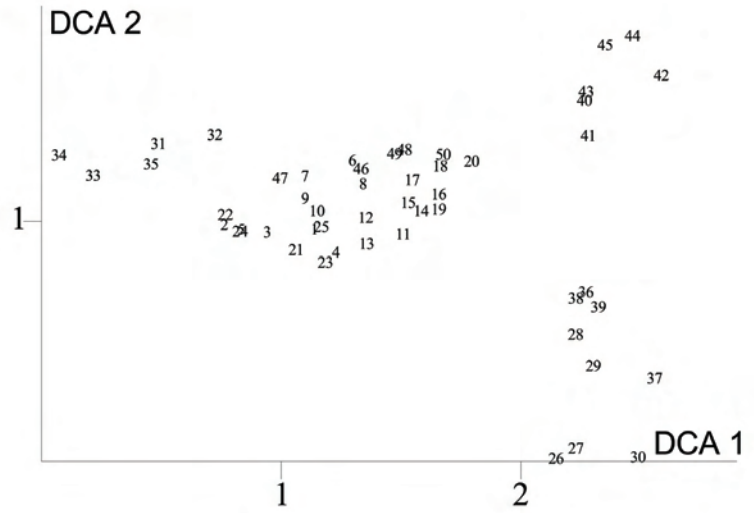

Fig. 260. Børgefjell: DCA ordination diagram of 50 meso plots, axes 1 (horizontal) and 2 (vertical). Meso plot number are plotted just right of the sample plot positions. Scaling of axes in S.D. units.

GNMDS ordination

The GNMDS ordination diagram (Fig 261) showed good visual similarity with the DCA diagram (Fig 260).The correlation between GNMDS axis 1 and DCA axis 1 was $\tau = 0.855$ and the correlation between GNMDS axis 2 and DCA axis 2 was $\tau = 0.631$.

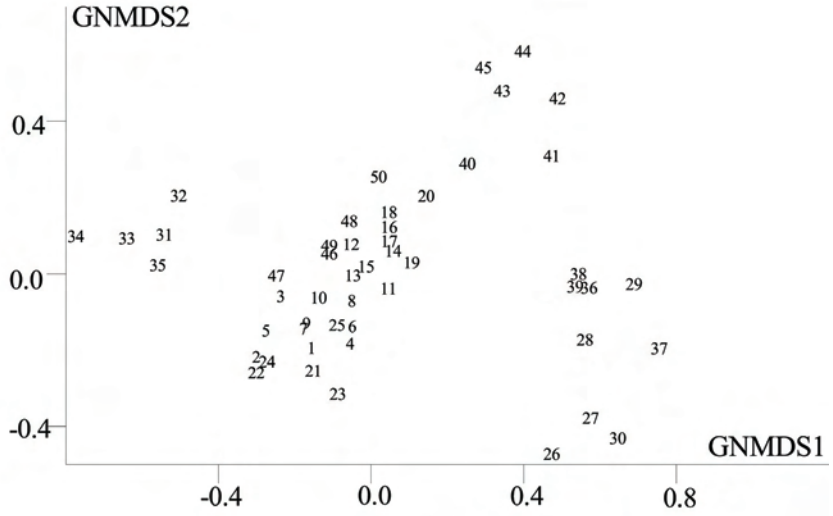

Fig.261. Børgefjell: GNMDS ordination biplot diagram of 50 sample plots (indicated by their number).

Split-plot GLM analysis of relationships between ordination axes and environmental variables

The variation (in plot scores) along DCA axis 1 was partitioned with 94.38 % at the macro-plot scale (i.e. between macro plots) and 5.62 % at the (between) meso plot scale within macro plots (Table 16). For the second ordination axis, 83.37 % of the variation was explained at the macro-plot scale and 16.63 % at the plot scale (Table 17)

At the macro-plot scale, seven environmental variables were significantly (at the $\alpha = 0.05$ level) related to DCA 1 while five variables (also at the $\alpha = 0.05$ level) were related to DCA 2. At the plot scale scale, nine environmental variables were significantly related to DCA 1 and two variables to DCA 2 (Tables 16 and 17).

At the macro-plot scale, soil concentrations of Total N, C and S, pH and tree basal area increased significantly (at the $\alpha = 0.05$ level) along DCA 1 while the concentration of H decreased. At the plot scale, macro and meso plot slope, macro plot heat index and soil concentrations of C, Ca, K, P and S increased while the concentration of Al decreased.

At the macro-plot scale, DCA 2 was positively related to the concentration of Zn and negatively related to meso plot unevenness, maximum soil depth, soil moisture and loss on ignition. At the plot scale, DCA axis 2 was significantly positively related to tree basal area and negatively related to minimum soil depth (at the $\alpha = 0.05$ level) (Table 17).

Table 16. Børgefjell: Split-plot GLM analysis and Kendall's nonparametric correlation coefficient τ between DCA 1 and 31 environmental variables (predictor) in the 50 plots. df_{resid}: degrees of freedom for the residuals; *SS*: total variation; *FVE*: fraction of total variation attributable to a given scale (macro plot or plot); SS_{expl}/SS: fraction of the variation attributable to the scale in question, explained by a variable; *r*: model coefficient (only given when significant at the $\alpha = 0.05$ level, otherwise blank); *F*: *F* statistic for test of the hypothesis that $r = 0$ against the two-tailed alternative. Split-plot GLM relationships significant at level $\alpha = 0.05$, *P*, *F*, *r* and SS_{expl}/SS, and Kendall's nonparametric correlation coefficient $|\tau| \geq 0.30$ are given in bold face. * No within macro plot variation. Numbers and abbreviations for names of environmental variables are in accordance with Table 2.

Predictor	Dependent variable = DCA 1 (*SS* = 20.9353)								Correlation between predictor and DCA 1
	Error level								
	Macro plot $df_{resid} = 8$ $SS_{macro\ plot} = 19.7589$ *FVE* = 0.9438 of *SS*				Plot within macro plot $df_{resid} = 39$ $SS_{plot} = 1.17638$ *FVE* = 0.0562 of *SS*				Total
	$SS_{expl}/SS_{macro\ plot}$	*r*	*F*	*P*	SS_{expl}/SS_{plot}	*r*	*F*	*P*	τ
Ma Slo	0.1245		1.1379	0.3172	**0.1934**	**0.4761**	**9.3517**	**0.0040**	0.248
Ma Asp	0.0189		0.1539	0.7051	*	*	*	*	0.060
Ma HI	0.0107		0.0862	0.7765	**0.1878**	**2.8563**	**9.0161**	**0.0046**	–0.045
Ma Ter	0.0009		0.0074	0.9335	0.0229		0.9149	0.3447	0.055
Ma Une	0.0153		0.1240	0.7338	0.0003		0.0131	0.9096	–0.030
TBA	**0.4038**	**1.4490**	**5.4194**	**0.0483**	0.0199		0.7935	0.3785	**0.448**
Me Slo	0.1159		1.0492	0.3357	**0.0979**	**0.2335**	**4.2309**	**0.0464**	0.201
Me Asp	0.2404		0.0800	0.0985	0.0122		2.6560	0.1112	0.096
Me HI	0.0186		0.1517	0.7071	0.0074		0.2898	0.5934	–0.049
Me Ter	0.0853		0.7465	0.4127	0.0135		0.5350	0.4689	0.027
Me Une	0.0316		0.2614	0.6230	0.0548		2.2609	0.1407	–0.081
Smi	0.0010		0.0082	0.9302	0.0013		0.0525	0.8200	0.012
Sme	0.0843		0.7364	0.4158	0.0044		0.1731	0.6796	–0.109
Sma	0.0483		0.4061	0.5418	0.0052		0.2020	0.6556	–0.136
Mme	0.0643		0.5501	0.4795	0.0022		0.0867	0.7700	–0.190
LOI	0.2273		2.3533	0.1636	0.0365		1.4792	0.2312	**–0.360**
Total N	**0.8972**	**2.8637**	**69.8410**	**0.0000**	0.0088		0.3453	0.5602	**0.639**
$pH_{(H2O)}$	**0.6472**	**2.6795**	**14.6780**	**0.0050**	0.0227		0.9071	0.3467	**0.560**
pH_{CaCl2}	**0.7237**	**3.1055**	**20.9500**	**0.0018**	0.0318		1.2810	0.2646	**0.562**
H	**0.7863**	**–3.1976**	**29.4330**	**0.0006**	0.0111		0.4395	0.5113	**–0.546**
Al	0.2055		2.0688	0.1883	**0.1172**	**–0.5758**	**5.1772**	**0.0285**	–0.265
C	**0.4007**	**1.7924**	**5.3498**	**0.0495**	**0.1928**	**0.6805**	**9.3154**	**0.0041**	**0.509**
Ca	0.3404		4.1294	0.0766	**0.1067**	**0.3177**	**4.6599**	**0.0371**	0.298
Fe	0.0073		0.0592	0.8140	0.0000		0.0001	0.9910	–0.063
K	0.2928		3.3120	0.1063	**0.3075**	**1.0645**	**17.3140**	**0.0002**	**0.520**
Mg	0.3097		3.5887	0.0948	0.0565		2.3363	0.1345	0.288
Mn	0.2837		3.1692	0.1129	0.0015		0.0571	0.8123	**0.412**
Na	0.1702		1.6405	0.2361	0.0142		0.5599	0.4588	0.210
P	0.3580		4.4607	0.0677	**0.1432**	**0.8311**	**6.5174**	**0.0147**	**0.447**
S	**0.5827**	**2.2077**	**11.1710**	**0.0102**	**0.1079**	**0.5103**	**4.7160**	**0.0360**	**0.582**
Zn	0.1823		1.7835	0.2185	0.0899		3.8512	0.0569	**0.404**

Table 17. Børgefjell: Split-plot GLM analysis and Kendall's nonparametric correlation coefficient τ between DCA 2 and 31 environmental variables (predictor) in the 50 plots. df_{resid}: degrees of freedom for the residuals; *SS*: total variation; *FVE*: fraction of total variation attributable to a given scale (macro plot or plot); SS_{expl}/SS: fraction of the variation attributable to the scale in question, explained by a variable; *r*: model coefficient (only given when significant at the $\alpha = 0.05$ level, otherwise blank); *F*: *F* statistic for test of the hypothesis that $r = 0$ against the two-tailed alternative. Split-plot GLM relationships significant at level $\alpha = 0.05$, *P*, *F*, *r* and SS_{expl}/SS, and Kendall's nonparametric correlation coefficient $|\tau| \geq 0.30$ are given in bold face. * No within macro plot variation. Numbers and abbreviations for names of environmental variables are in accordance with Table 2.

Predictor	Dependent variable = DCA 2 (*SS* = 7.5495)								Correlation between predictor and DCA 2
	Error level								
	Macro plot $df_{resid} = 8$ $SS_{macro\ plot} = 6.2941$ *FVE* = 0.8337 of *SS*				Plot within macro plot $df_{resid} = 39$ $SS_{plot} = 1.25535$ *FVE* = 0.1663 of *SS*				Total
	$SS_{expl}/SS_{macro\ plot}$	*r*	*F*	*P*	SS_{expl}/SS_{plot}	*r*	*F*	*P*	τ
Ma Slo	0.3104		3.6006	0.0943	0.0089		0.3491	0.5580	0.229
Ma Asp	0.0006		0.0051	0.9446	*	*	*	*	–0.005
Ma HI	0.1631		1.5587	0.2472	0.0096		0.3793	0.5416	0.271
Ma Ter	0.0038		0.0306	0.8656	0.0018		0.0687	0.7946	0.053
Ma Une	**0.4209**	**–0.6629**	**5.8159**	**0.0424**	0.0477		1.9543	0.1700	–0.271
TBA	0.0330		0.2729	0.6155	**0.1474**	**0.7126**	**6.7451**	**0.0132**	0.224
Me slo	0.3182		3.7328	0.0894	0.0034		0.1343	0.7160	0.277
Me Asp	0.0663		0.5679	0.4727	0.0712		0.0476	0.8285	–0.136
Me HI	0.1266		1.1595	0.3130	0.0012		0.0717	0.7903	0.185
Me Ter	0.0483		0.4061	0.5417	0.0016		2.3695	0.1318	0.066
Me Une	0.3249		3.8495	0.0854	0.0741		3.1197	0.0852	–0.218
Smi	0.0611		0.5206	0.4911	**0.1217**	**–0.2805**	**5.4028**	**0.0254**	–0.195
Sme	0.1170		1.0600	0.3333	0.0896		3.8400	0.0572	–0.091
Sma	**0.4261**	**–2.3678**	**5.9403**	**0.0407**	0.0002		0.0080	0.9292	–0.165
Mme	**0.6029**	**–4.5734**	**12.1440**	**0.0083**	0.0134		0.5310	0.4705	**–0.411**
LOI	**0.4099**	**–0.8743**	**5.5572**	**0.0462**	0.0411		1.6700	0.2039	**–0.427**
Total N	0.1320		1.2167	0.3021	0.0046		0.1819	0.6721	–0.140
$pH_{(H2O)}$	0.0763		0.6612	0.4397	0.0294		1.1814	0.2837	0.286
pH_{CaCl2}	0.0535		0.4523	0.5202	0.0877		3.7489	0.0601	0.186
H	0.0214		0.1745	0.6871	0.0683		2.8601	0.0988	–0.149
Al	0.3909		5.1344	0.0532	0.0004		0.0176	0.8953	–0.262
C	0.2515		2.6875	0.1398	0.0778		3.2891	0.0774	**0.337**
Ca	0.2633		2.8596	0.1293	0.0529		2.1775	0.1481	0.252
Fe	0.1586		1.5076	0.2544	0.0018		0.0692	0.7939	–0.019
K	0.3201		3.7662	0.0883	0.0447		1.8245	0.1846	0.280
Mg	0.0334		0.2765	0.6133	0.0218		0.8700	0.3567	–0.016
Mn	0.3438		4.1910	0.0748	0.0117		0.4614	0.5010	**0.411**
Na	0.2244		2.3153	0.1666	0.0002		0.0059	0.9392	–0.066
P	0.1159		1.0491	0.3357	0.0042		0.1634	0.6882	0.115
S	0.1125		1.0143	0.3434	0.0561		2.3197	0.1358	0.244
Zn	**0.4495**	**1.1885**	**6.5323**	**0.0339**	0.0023		0.0915	0.7640	0.278

Correlations between DCA ordination axes and environmental variables

Thirteen out of the 31 environmental variables were correlated with DCA axis 1 or/and DCA axis 2 at the $|\tau| > 0.300$ level (Tables 16 and 17). Total N ($\tau = 0.639$, Fig. 265), extractable S ($\tau = 0.582$, Fig. 272), pH [pH_{H2O} ($\tau = 0.562$, Fig. 266)] and exchangeable H ($\tau = –0.546$, Fig. 267) were most strongly correlated with DCA axis 1. The only two variables that were correlated with DCA axis 2 at the $|\tau| > 0.300$ level were soil moisture ($\tau = –0.411$, Fig. 263) loss on ignition ($\tau = –0.427$, Fig. 264), extractable Mn ($\tau = 0.411$, Fig. 270) and extractable C ($\tau = 0.337$, Fig. 268).

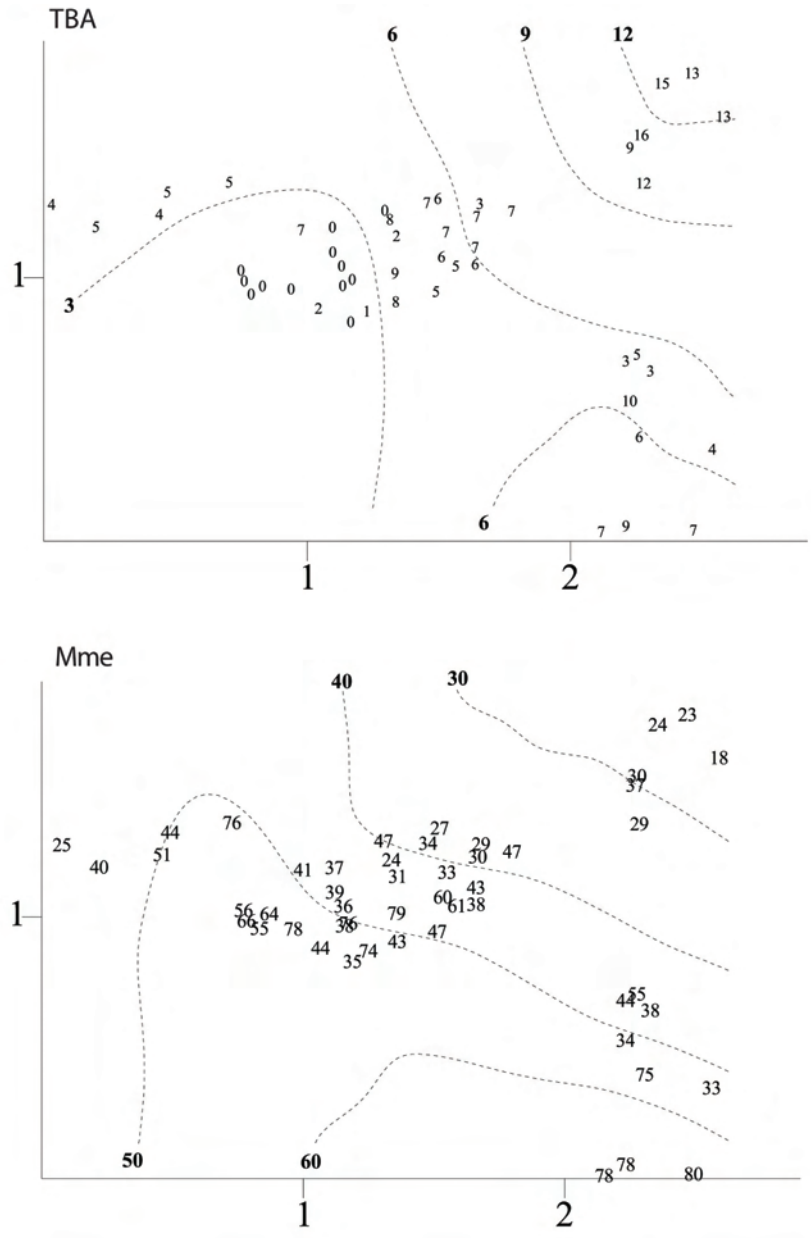

Figs 262-263. Børgefjell: isolines for environmental variables in the DCA ordinations of 50 meso plots, axes 1 (horizontal) and 2 (vertical). Values for the environmental variables are plotted onto the meso plots' positions. Scaling in S.D. units. Fig. 262. TBA ($R^2 = 0.719$). Fig. 249. Mme (Soil moisture) ($R^2 = 0.603$). R^2 refers to the coefficient of determination between original and smoothened values as interpolated from the isolines. Names of environmental variables in accordance with Table 2.

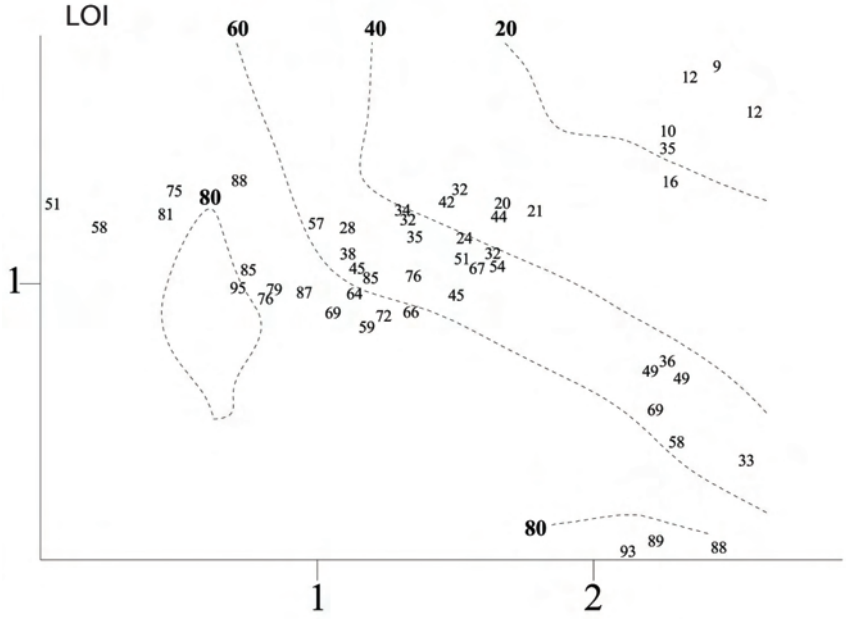

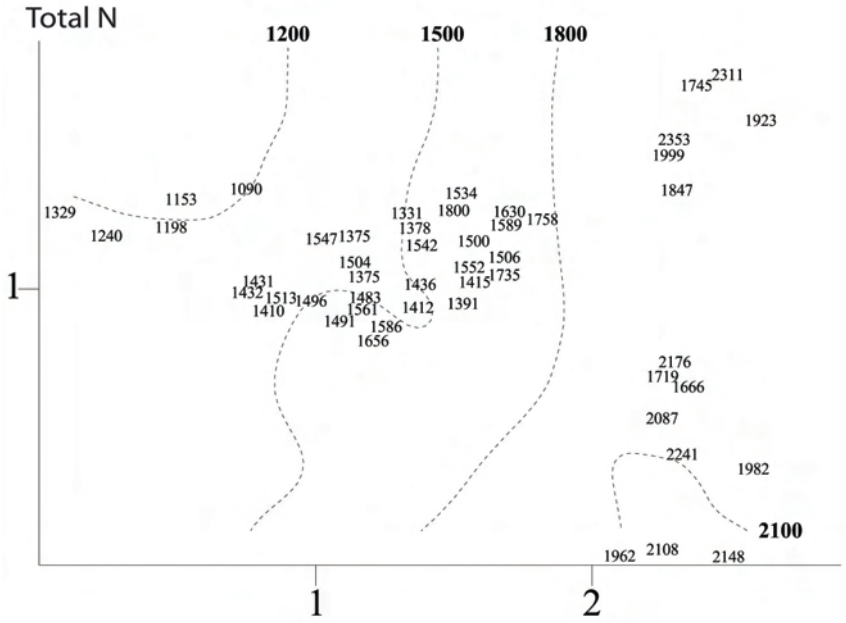

Figs 264-265. Børgefjell: isolines for environmental variables in the DCA ordinations of 50 meso plots, axes 1 (horizontal) and 2 (vertical). Values for the environmental variables are plotted onto the meso plots' positions. Scaling in S.D. units. Fig. 264. LOI (R^2 = 0.794). Fig. 265. Total N. C (R^2 = 0.839). R^2 refers to the coefficient of determination between original and smoothened values as interpolated from the isolines. Names of environmental variables in accordance with Table 2.

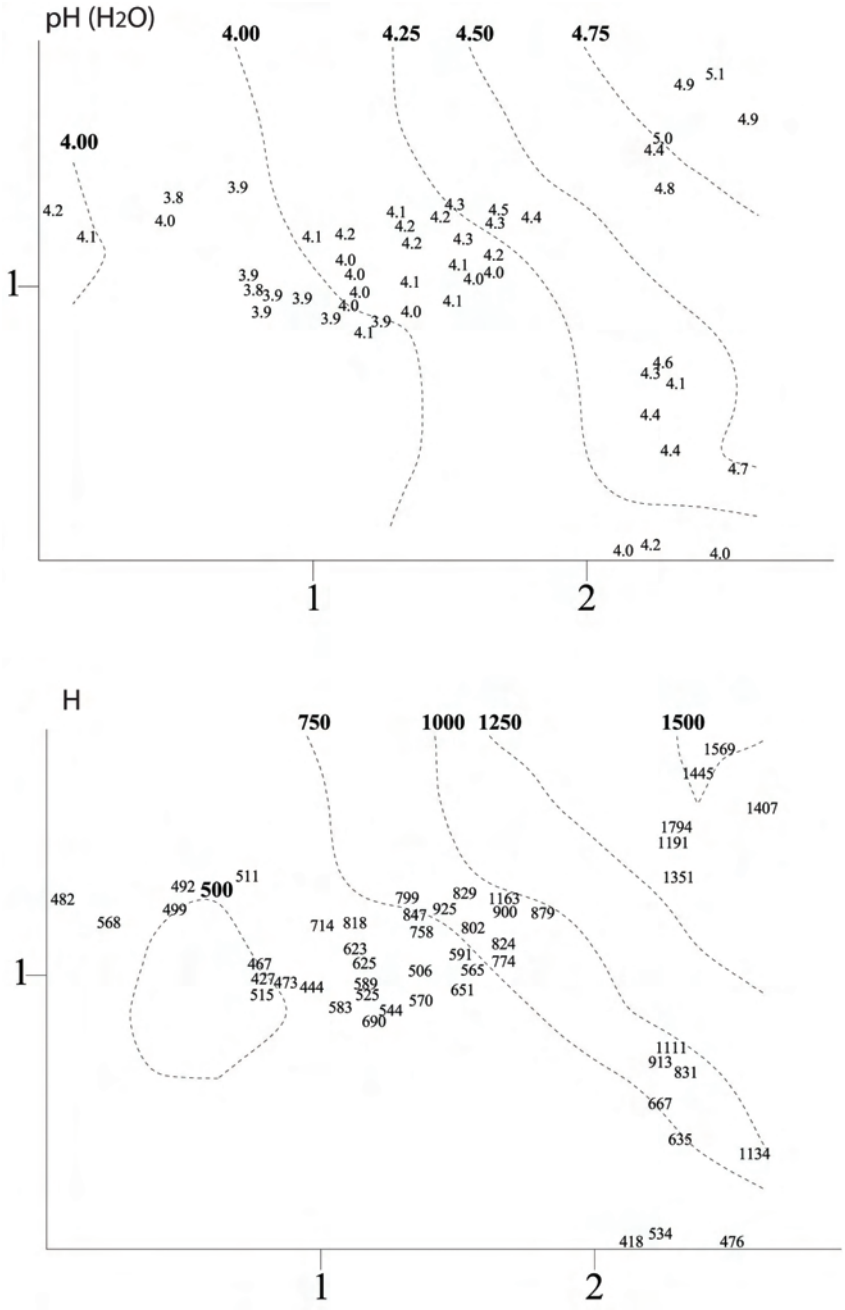

Figs 266-267. Børgefjell: isolines for environmental variables in the DCA ordinations of 50 meso plots, axes 1 (horizontal) and 2 (vertical). Values for the environmental variables are plotted onto the meso plots' positions. Scaling in S.D. units. Fig. 266. $pH_{(H2O)}$ (R^2 = 0.792). Fig. 267. H (R^2 = 0.760). R^2 refers to the coefficient of determination between original and smoothened values as interpolated from the isolines. Names of environmental variables in accordance with Table 2.

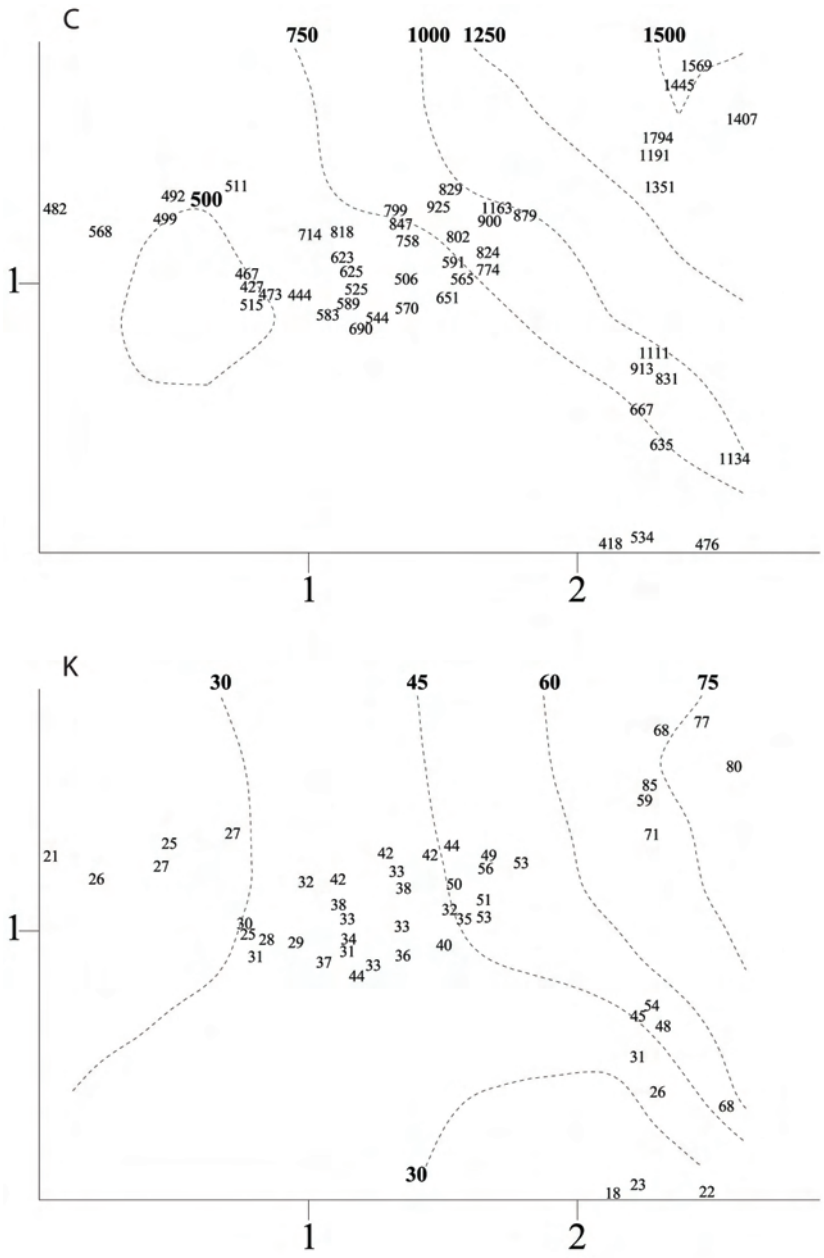

Figs 268-269. Børgefjell: isolines for environmental variables in the DCA ordinations of 50 meso plots, axes 1 (horizontal) and 2 (vertical). Values for the environmental variables are plotted onto the meso plots' positions. Scaling in S.D. units. Fig. 268. C (R^2 = 0.799). Fig. 269. K (R^2 = 0.830). R^2 refers to the coefficient of determination between original and smoothened values as interpolated from the isolines. Names of environmental variables in accordance with Table 2.

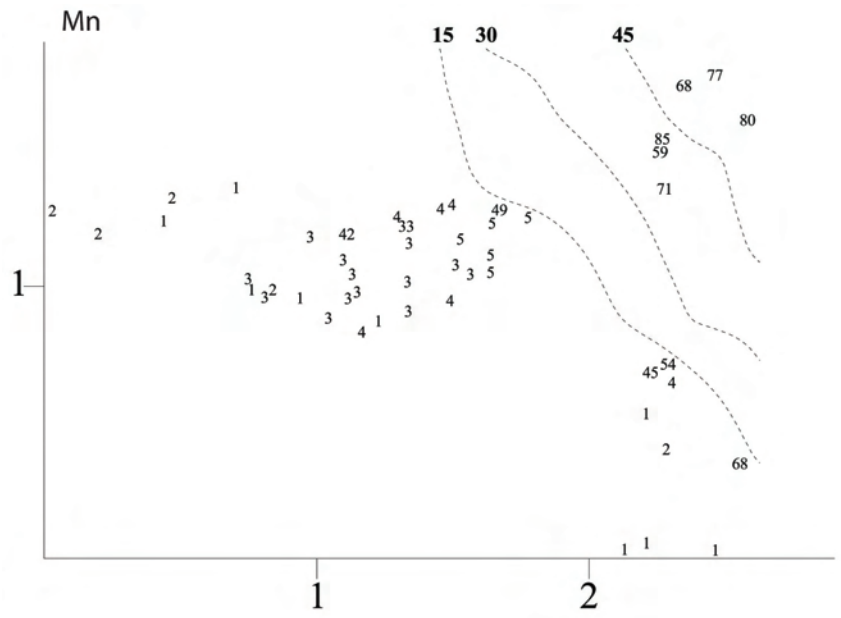

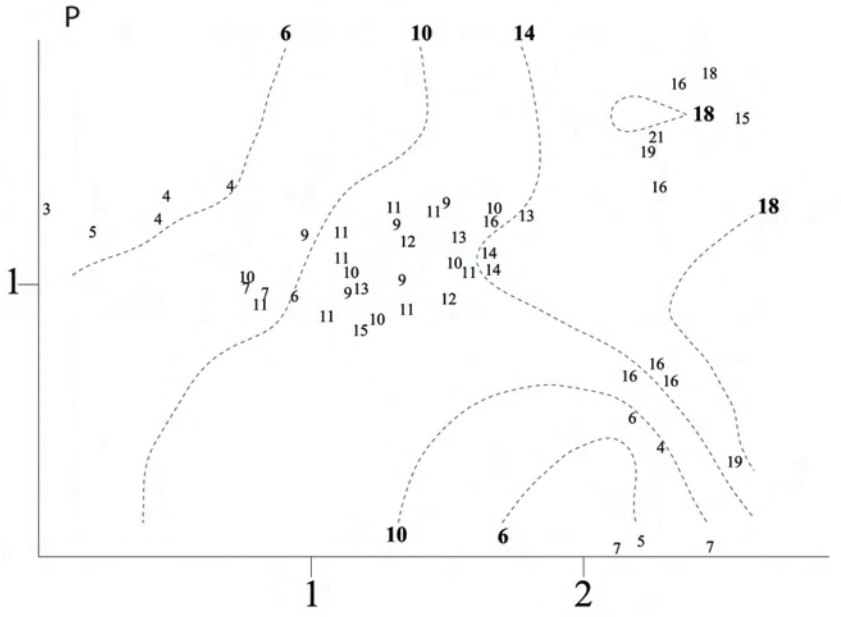

Figs 270-271. Børgefjell: isolines for environmental variables in the DCA ordinations of 50 meso plots, axes 1 (horizontal) and 2 (vertical). Values for the environmental variables are plotted onto the meso plots' positions. Scaling in S.D. units. Fig. 270. Mn (R^2 = 0.761). Fig. 271. P (R^2 = 0.729). R^2 refers to the coefficient of determination between original and smoothened values as interpolated from the isolines. Names of environmental variables in accordance with Table 2.

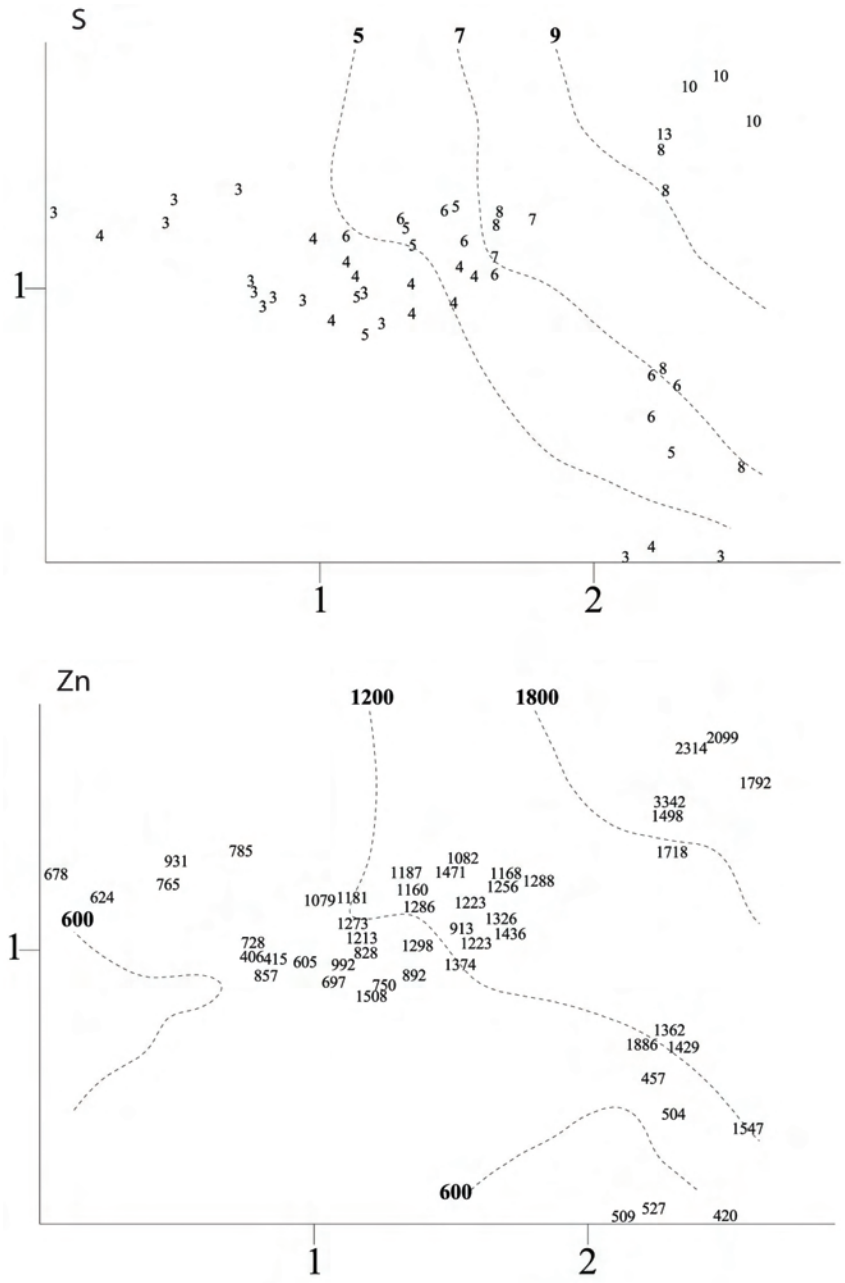

Figs 272-273. Børgefjell: isolines for environmental variables in the DCA ordinations of 50 meso plots, axes 1 (horizontal) and 2 (vertical). Values for the environmental variables are plotted onto the meso plots' positions. Scaling in S.D. units. Fig. 272. S (R^2 = 0.803). Fig. 273. Zn (R^2 = 0.710). R^2 refers to the coefficient of determination between original and smoothened values as interpolated from the isolines. Names of environmental variables in accordance with Table 2.

Frequent species

A total of 80 species were recorded within the fifty 1 × 1 m meso sample plots: 40 vascular plants, 17 mosses, 13 liverworts and 24 lichens. The most frequent species (the sum of subplot frequencies in brackets) were: *Vaccinium myrtillus* (783 out of 800), *Avenella flexuosa* (755), *Barbilophozia lycopodioides* (724), *Chamaepericlymenum suecicum* (695), *Empetrum nigrum* (583), *Dicranum scoparium* (547), *Pleurozium schreberi* (542), *Brachythecium reflexum* (481), *Vaccinium vitis-idaea* (378) and *Gymnocarpium dryopteris* (343).

The distribution of species abundance in the DCA ordination

Forty-seven of the totally 80 species occurred in 5 or more of the sample plots (Figs 274–320).

Examples of species with wide ecological amplitude were *Vaccinium myrtillus* (Fig. 279), *Chamaepericlymenum suecicum* (Fig. 283), *Avenella flexuosa* (Fig. 294) and partly *Barbilophozia lycopodioides* (Fig. 307), which all were abundant in most of the sample plots.

Species restricted to plots in the left part of the DCA ordination diagram, reflecting soils with low pH values and low amounts of total N, S, K, C, P and Mn, were *Calluna vulgaris* (Fig. 277), *Cladonia arbuscula* (Fig. 312), *Cladonia rangiferina* (Fig. 319) and *Cladonia uncialis* (Fig. 320), and partly *Empetrum nigrum* (Fig. 278) and *Pleurozium schreberi* (Fig.302). The lichen species *Cladonia arbuscula*, *C. rangiferina* and *C. uncialis* were also mainly restricted to high DCA axis 2 scores, typically having dry soil (cf. Fig. 263).

In contrast *Cicerbita alpina* (Fig. 282) and *Brachythecium salebrosum* (Fig. 297) and to some extent *Gymnicarpium dryopteris* (Fig. 285) were mostly restricted to sample plots with high pH values and high concentrations of total N, S, K, C, P and Mn. Species with optimum at high DCA axis 1 values differed with respect to distribution along DCA axis 2. *Dryopteris expansa* (Fig. 284) and to some extent *Plagiothecium* sp. (Fig 301) showed preference for the lower right-hand corner of the diagram, reflecting affinities to slightly moister soils. *Hieracium* sect. *Hieracium* (Fig. 286), *Polygonatum verticillatum* (Fig. 290) and *Anthoxanthum odoratum* (Fig 293) are examples of species that occurred mostly in the upper right-hand corner of the diagram, reflecting affinities to slightly drier soils.

Lycopodium annotinum (Fig. 287) was with one exception restricted to the central cluster in the DCA ordination diagram.

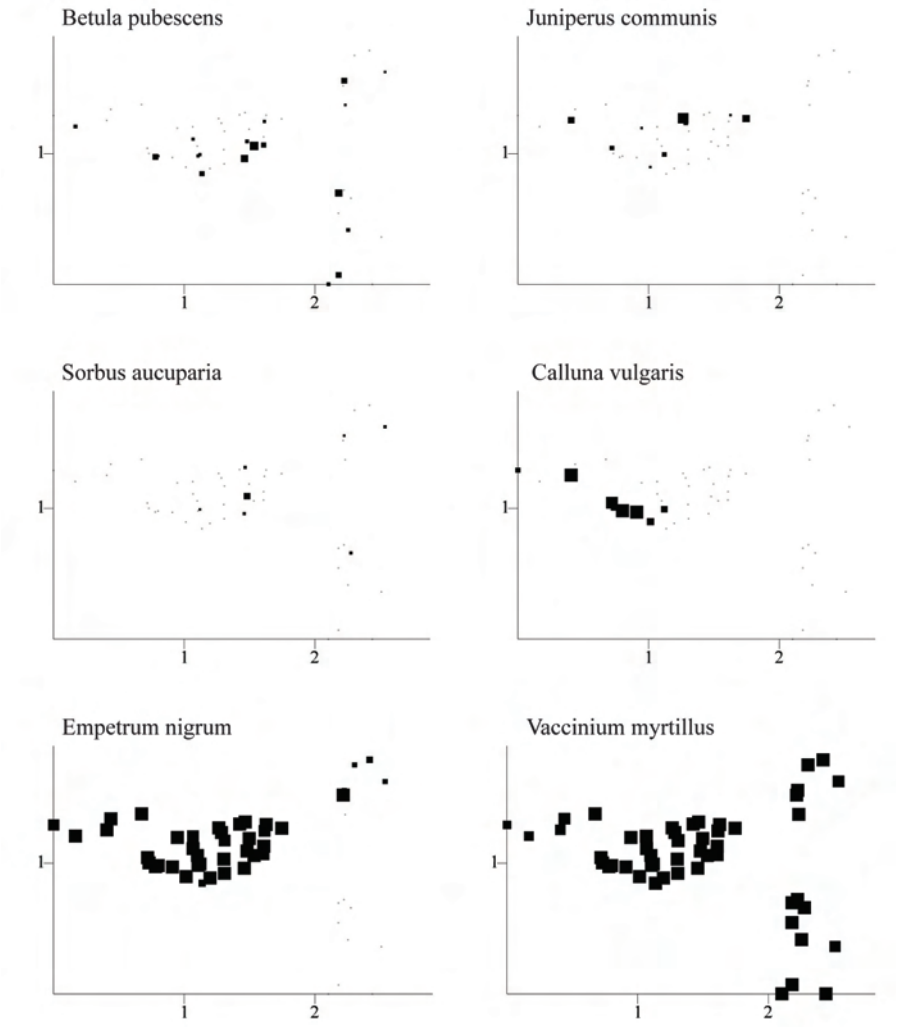

Fig. 274-279. Børgefjell: distributions of species abundances in the DCA ordination of 50 sample plots, axes 1 (horizontal) and 2 (vertical). Frequency in subplots for each species in each meso plot proportional to quadrate size. Scaling in S.D. units. Fig. 274. *Betula pubescens*. Fig. 275. *Juniperus communis*. Fig. 276. *Sorbus aucuparia*. Fig. 277. *Calluna vulgaris*. Fig. 278. *Empetrum nigrum*. Fig. 279. *Vaccinium myrtillus*.

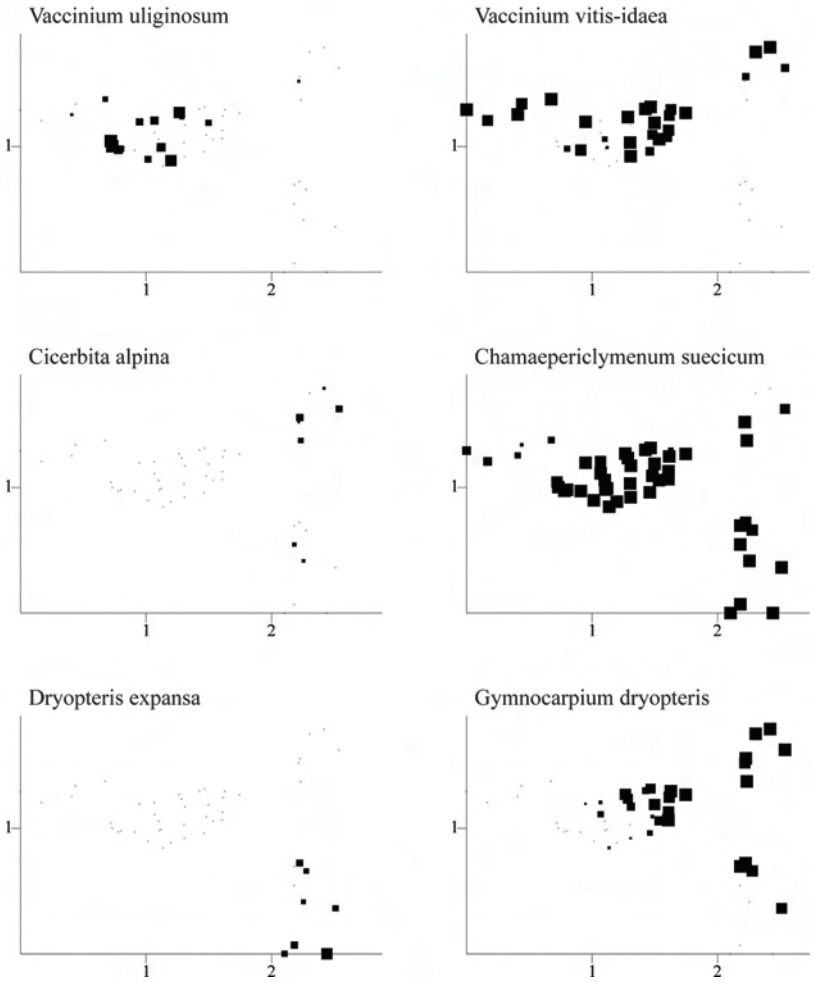

Figs 280-285. Børgefjell: distributions of species abundances in the DCA ordination of 50 sample plots, axes 1 (horizontal) and 2 (vertical). Frequency in subplots for each species in each meso plot proportional to quadrate size. Scaling in S.D. units. Fig. 280. *Vaccinium uliginosum*. Fig. 281. *Vaccinium vitis-idaea*. Fig. 282. *Cicerbita alpina*. Fig. 283. *Chamaepericlymenum suecicum* (syn. *Cornus suecica*). Fig. 284. *Dryopteris expansa*. Fig. 285. *Gymnocarpium dryopteris*.

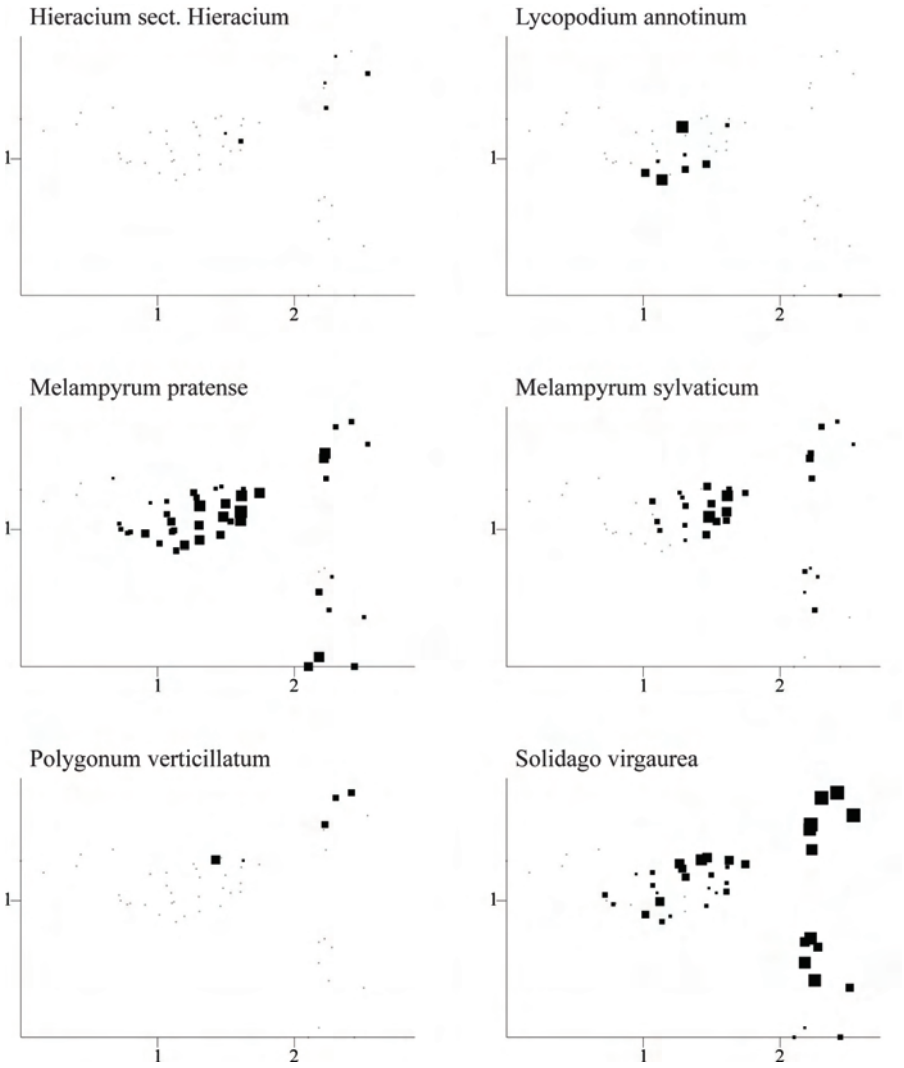

Figs 286-291. Børgefjell: distributions of species abundances in the DCA ordination of 50 sample plots, axes 1 (horizontal) and 2 (vertical). Frequency in subplots for each species in each meso plot proportional to quadrate size. Scaling in S.D. units. Fig. 286. *Hieracium* sect. *Hieracium*. Fig. 287. *Lycopodium annotinum*. Fig. 288. *Melampyrum pratense.* Fig. 289. *Melampyrum sylvaticum.* Fig. 290. *Polygonatum verticillatum*. Fig. 291. *Solidago virgaurea*.

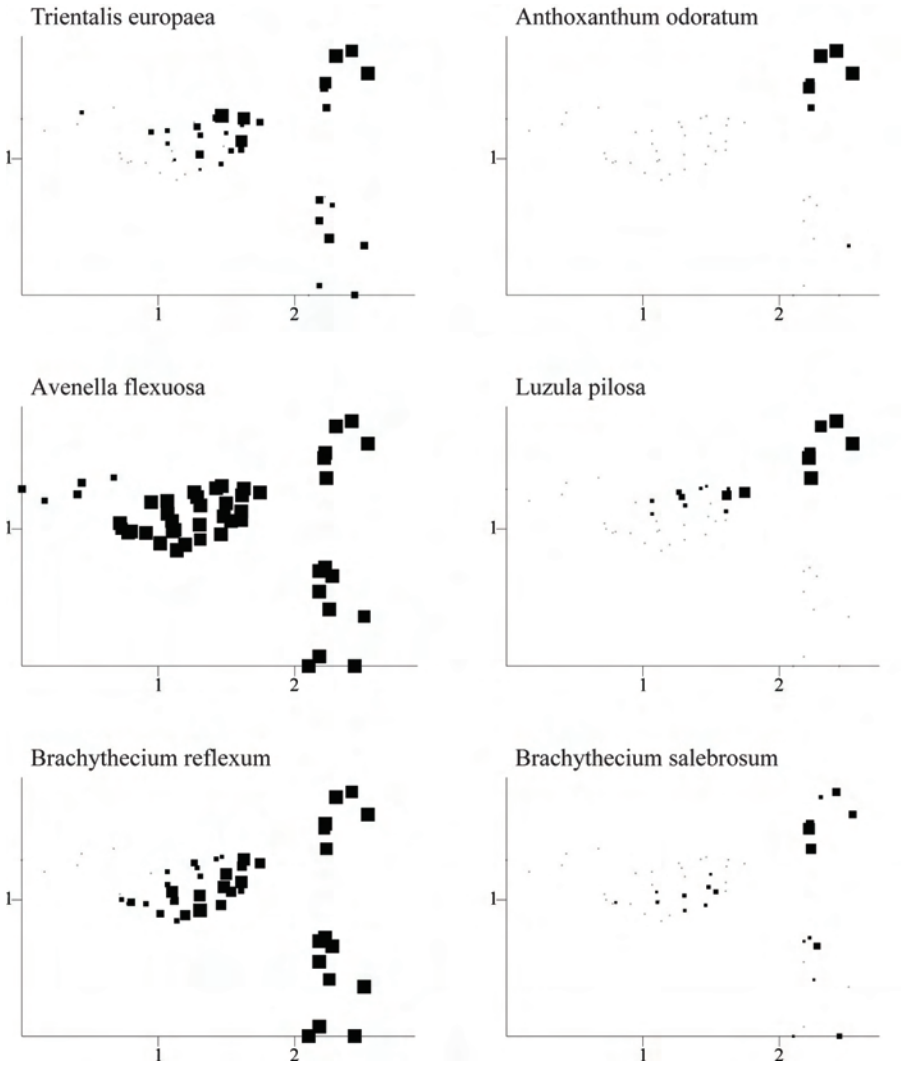

Figs 292-297. Børgefjell: distributions of species abundances in the DCA ordination of 50 sample plots, axes 1 (horizontal) and 2 (vertical). Frequency in subplots for each species in each meso plot proportional to quadrate size. Scaling in S.D. units. Fig. 292. *Trientalis europaea*. 293. *Anthoxanthum odoratum*. Fig. 294. *Avenella flexuosa* (syn. *Deschampsia flexuosa*). Fig. 295. *Luzula pilosa*. Fig. 296. *Brachythecium reflexum*. Fig. 297. *Brachythecium salebrosum*

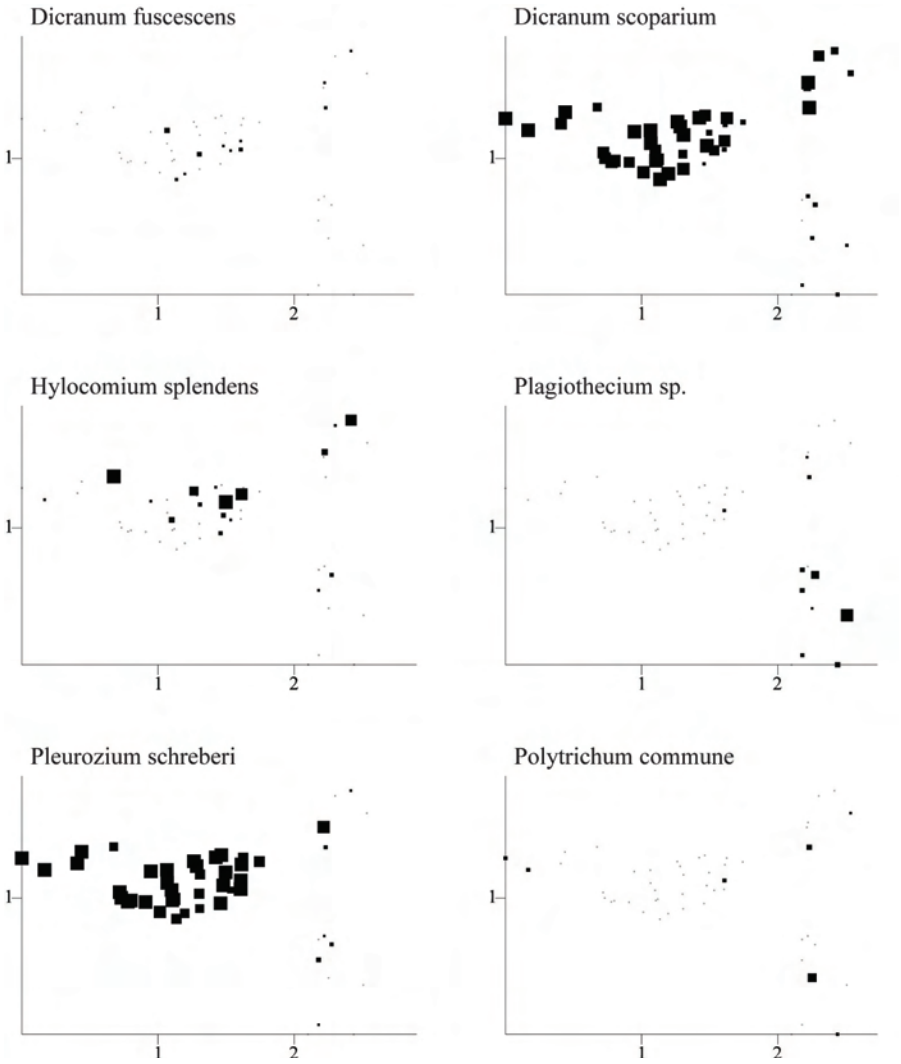

Figs 298-303. Børgefjell: distributions of species abundances in the DCA ordination of 50 sample plots, axes 1 (horizontal) and 2 (vertical). Frequency in subplots for each species in each meso plot proportional to quadrate size. Scaling in S.D. units. Fig. 298. *Dicranum fuscescens.* Fig. 299. *Dicranum scoparium.* Fig. 300. *Hylocomium splendens.* Fig. 301. *Plagiothecium* sp. Fig. 302. *Pleurozium schreberi*. Fig. 303. *Polytrichum commune*.

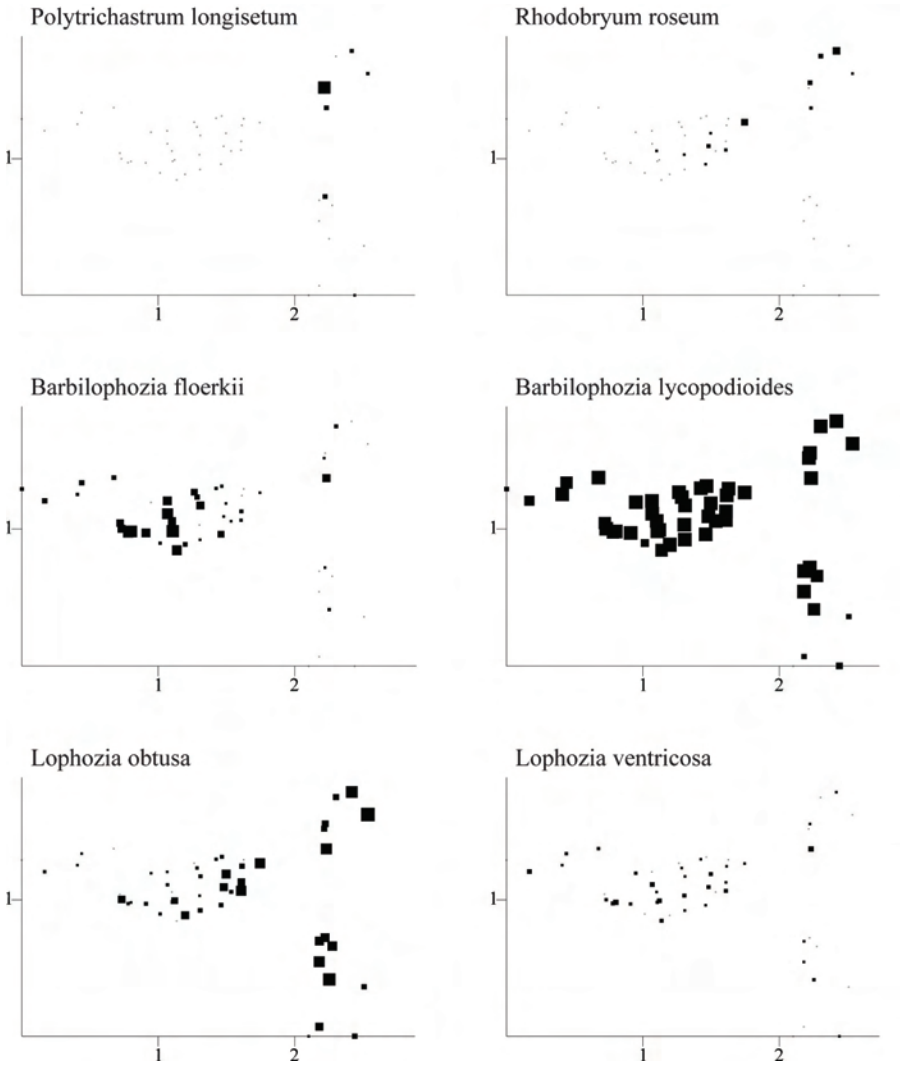

Figs 304-309. Børgefjell: distributions of species abundances in the DCA ordination of 50 sample plots, axes 1 (horizontal) and 2 (vertical). Frequency in subplots for each species in each meso plot proportional to quadrate size. Scaling in S.D. units. Fig. 304. *Polytrichastrum longisetum*. Fig. 305. *Rhodobryum roseum*. Fig. 306. *Barbilophozia floerkii*. Fig. 307. *Barbilophozia lycopodioides*. Fig. 308. *Lophozia obtusa*. Fig. 309. *Lophozia ventricosa*.

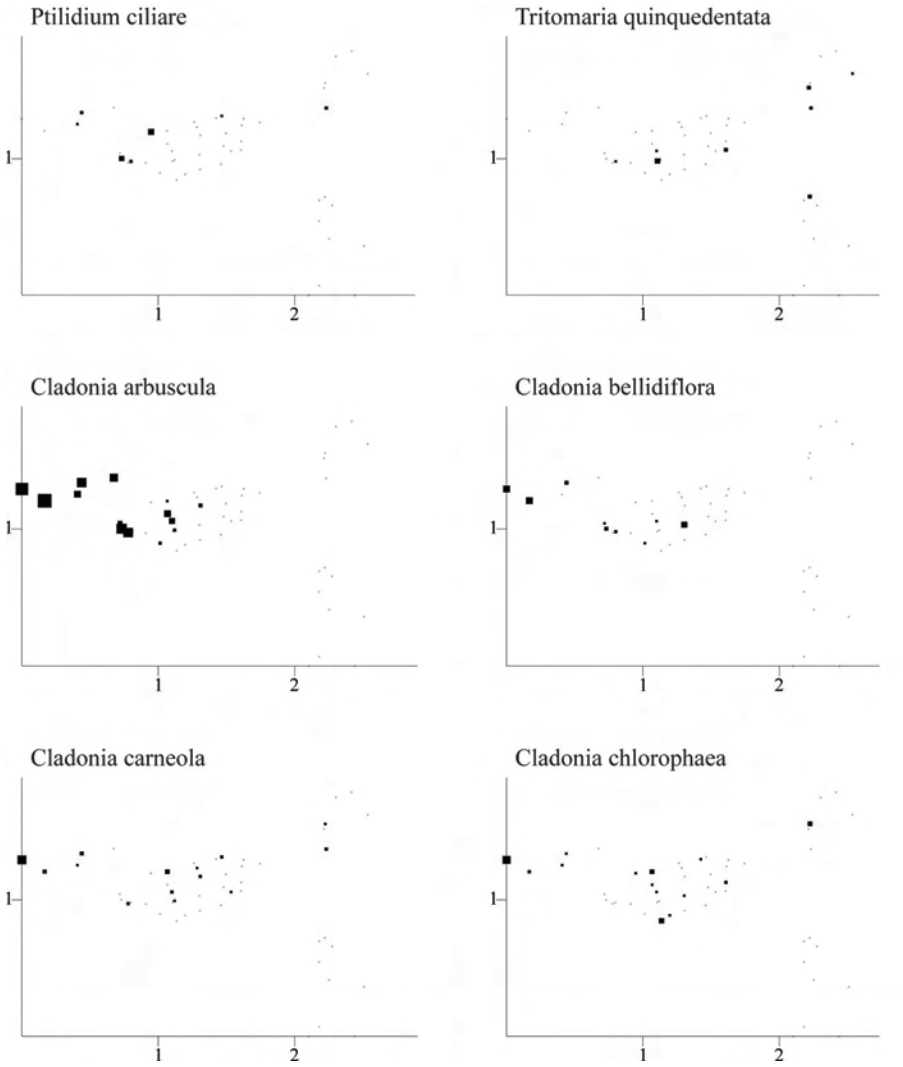

Figs 310-315. Børgefjell: distributions of species abundances in the DCA ordination of 50 sample plots, axes 1 (horizontal) and 2 (vertical). Frequency in subplots for each species in each meso plot proportional to quadrate size. Scaling in S.D. units. Fig. 310 *Ptilidium ciliare*. Fig. 311. *Tritomaria quinquedentata.* Fig. 312. *Cladonia arbuscula*. Fig. 313. *Cladonia bellidiflora*. Fig. 314. *Cladonia carneola.* Fig. 315. *Cladonia chlorophaea.*

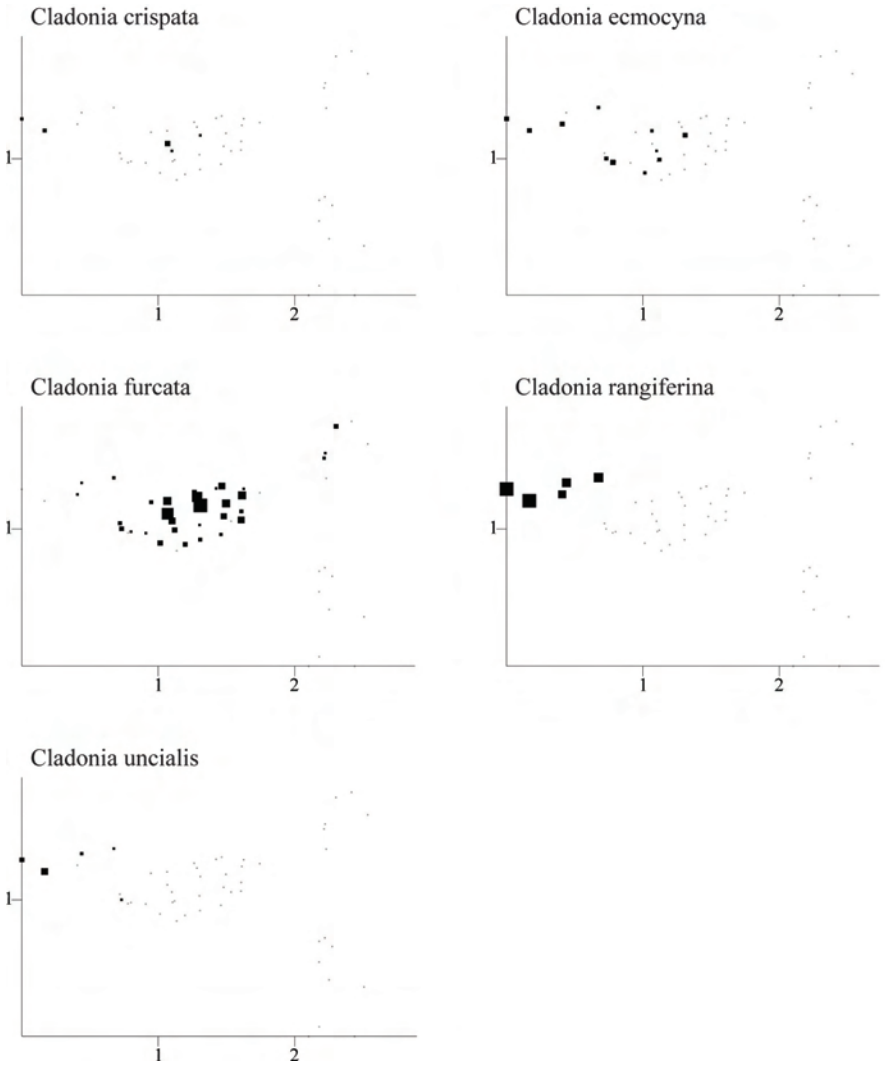

Figs 316-320. Børgefjell: distributions of species abundances in the DCA ordination of 50 sample plots, axes 1 (horizontal) and 2 (vertical). Frequency in subplots for each species in each meso plot proportional to quadrate size. Scaling in S.D. units. Fig. 316. *Cladonia crispata*. Fig. 317. *Cladonia ecmocyna.* Fig. 318. *Cladonia furcata*. Fig. 319. *Cladonia rangiferina*. Fig. 320. *Cladonia uncialis*.

DIVIDALEN REFERENCE AREA

Correlations between environmental variables

There were strong pairwise correlations between several of the topographical variables, between topographical variables and soil variables and between soil variables (Table 18).

Macro plot slope was negatively correlated with aspect unfavourabilites and positively correlated with heat indices. Both macro plot and meso plot terrain form and terrain unevenness were positively correlated with soil moisture. Tree basal area was positively correlated with macro plot aspect unfavourability and the heat index. Loss on ignition was negatively correlated with aspect, soil pH, total N, extractable C and Ca, and positively correlated with soil moisture and exchangeable H. Soil pH was positively correlated with total N, extractable C, Ca, Mn, S and Zn and negatively correlated with extractable Al, K, Mg, P and exchangeable H.

Table 18. Dividalen: Kendall's rank correlation coefficients τ between 31 environmental variables in the 50 sample plots (lower triangle), with significance probabilities (upper triangle). Statistically significant correlations (P<0.05) in bold face. Names of explanatory variables abbreviated in accordance with Table 2.

	1	2	3	4	5	6	7	8	9	10	11	12	13	14	15	16	17	18	19	20	21	22	23	24	25	26	27	28	29	30	31
01 Ma Slo	*	**0.000**	**0.000**	0.327	0.595	**0.000**	0.536	**0.003**	**0.000**	0.227	0.321	**0.022**	0.345	0.726	**0.001**	0.347	**0.035**	0.932	0.966	0.832	0.298	**0.006**	0.654	0.125	0.548	**0.038**	**0.003**	**0.000**	0.741	0.167	0.678
02 Ma Asp	**–0.418**	*	**0.000**	0.380	**0.000**	**0.020**	**0.023**	**0.000**	**0.000**	0.065	**0.001**	0.971	0.816	0.197	0.402	**0.025**	0.354	0.649	0.675	0.748	0.074	0.901	0.643	**0.001**		0.433	0.164	0.412	0.544	0.544	**0.032**
03 Ma HI	**0.595**	**–0.880**	*	0.661	**0.008**	**0.002**	**0.031**	**0.000**	**0.000**	0.215	**0.008**	0.612	0.427	0.223	0.743	0.155	0.913	0.893	0.913	0.980	**0.017**	0.309	0.966	**0.001**	**0.010**	0.705	**0.017**	0.833	0.396	0.216	0.073
04 Ma Ter	0.122	–0.114	0.054	*	**0.002**	0.262	0.077	0.648	0.719	**0.000**	**0.007**	0.051	0.262	0.317	**0.025**	0.273	0.607	0.621	0.509	0.734	0.056	**0.021**	0.915	0.467	**0.006**	0.225	0.093	0.778	**0.024**	**0.049**	0.101
05 Ma Une	–0.062	**–0.455**	**0.305**	**0.424**	*	0.879	1.000	**0.002**	0.336	**0.002**	**0.000**	0.330	0.376	1.000	**0.000**	**0.001**	**0.004**	0.605	0.618	0.789	0.581	**0.000**	0.605	0.310	0.200	0.130	**0.036**	**0.000**	0.373	0.101	0.061
05 TBA	**0.460**	**–0.258**	**0.329**	0.136	–0.017	*	0.774	0.095	**0.000**	0.261	0.567	**0.032**	0.722	0.186	0.304	0.329	0.053	0.469	0.567	0.637	0.906	0.092	0.391	0.556	0.814	0.381	0.106	**0.023**	0.337	0.814	0.724
07 Me Slo	–0.077	**0.294**	**–0.261**	0.251	0.000	0.035	*	0.205	0.236	0.206	0.865	**0.008**	0.790	0.801	0.886	0.475	0.380	0.554	0.513	0.380	**0.032**	0.159	0.791	**0.029**	**0.010**	**0.023**	**0.015**	**0.026**	0.116	0.063	0.639
08 Me Asp	**–0.330**	**0.759**	**–0.644**	–0.058	**–0.367**	–0.181	0.160	*	**0.000**	0.244	**0.031**	0.363	0.471	0.251	0.462	0.051	0.914	0.572	0.609	0.591	0.628	0.641	0.802	**0.020**	0.223	0.616	0.591	0.530	0.774	0.173	0.290
09 Me HI	**0.419**	**–0.543**	**0.568**	–0.043	0.108	**0.503**	–0.140	**–0.699**	*	0.877	0.806	0.068	0.382	0.315	0.388	0.694	0.117	0.795	0.795	0.719	0.552	0.053	0.477	0.057	0.280	0.795	0.086	0.487	0.508	0.062	0.808
10 Me Ter	0.148	–0.235	0.149	**0.497**	**0.414**	0.134	0.176	–0.146	–0.018	*	**0.000**	0.329	0.908	0.233	**0.025**	0.418	0.054	0.174	0.140	0.281	0.256	**0.037**	0.365	0.802	0.178	0.248	0.086	0.714	0.218	0.059	0.576
11 Me Une	0.113	**–0.380**	**0.299**	**0.352**	**0.510**	–0.064	–0.022	**–0.252**	0.027	**0.487**	*	0.692	0.154	0.219	**0.044**	0.310	**0.003**	0.331	0.297	0.506	0.451	**0.023**	0.214	0.575	0.462	0.834	0.220	0.262	0.484	0.220	0.310
12 Smi	**–0.242**	0.004	–0.053	–0.236	0.112	**–0.222**	**–0.318**	0.098	–0.184	–0.116	0.044	*	**0.002**	1.000	0.973	0.297	0.072	0.220	0.173	0.253	**0.002**	0.853	0.801	**0.011**	**0.001**	**0.005**	0.067	**0.006**	0.067	0.737	0.297
13 Sme	0.099	–0.025	0.082	–0.135	–0.101	–0.036	–0.032	0.077	–0.088	0.014	–0.157	**0.315**	*	0.486	0.110	0.650	0.788	0.155	0.098	0.246	**0.000**	0.062	0.246	**0.008**	**0.000**	0.429	**0.002**	0.290	0.075	0.089	0.439
14 Sma	–0.044	0.167	–0.149	0.143	0.000	–0.161	–0.036	0.146	–0.119	–0.167	–0.161	0.000	–0.084	*	0.972	0.808	0.315	0.972	0.972	0.862	0.426	0.703	0.755	0.253	0.315	0.253	0.510	0.917	0.556	0.703	0.467
15 Mme	**–0.344**	–0.090	–0.033	**0.264**	**0.549**	–0.103	0.017	–0.077	–0.085	**0.259**	**0.218**	–0.003	–0.159	–0.004	*	**0.001**	**0.005**	0.152	0.132	0.245	**0.046**	**0.000**	0.103	0.219	**0.011**	0.598	**0.000**	**0.000**	0.304	0.080	0.457
16 LOI	–0.097	**–0.241**	0.144	–0.129	**0.372**	–0.098	–0.084	–0.206	0.039	0.094	0.110	0.105	–0.045	–0.029	**0.322**	*	**0.000**	**0.000**	**0.000**	**0.000**	0.610	**0.000**	**0.000**	0.173	0.213	0.058	**0.000**	**0.026**	**0.016**	**0.000**	**0.000**
17 Total N	**0.217**	0.099	0.011	–0.061	**–0.323**	0.195	0.103	0.011	0.154	–0.223	**–0.322**	–0.180	0.027	0.118	**–0.277**	**–0.523**	*	**0.000**	**0.000**	**0.000**	0.296	**0.000**	**0.000**	0.509	0.281	0.096	**0.000**	**0.042**	**0.012**	**0.000**	**0.000**
18 pH_{H2O}	0.009	0.049	–0.014	–0.058	–0.058	0.073	–0.070	0.060	0.026	–0.158	–0.105	0.124	0.142	–0.004	–0.140	**–0.476**	**0.481**	*	**0.000**	**0.000**	**0.001**	**0.000**	**0.000**	0.114	**0.016**	**0.000**	**0.000**	0.245	**0.008**	**0.000**	**0.000**
19 pH_{CaCl2}	0.004	0.045	–0.011	–0.078	–0.056	0.058	–0.077	0.054	0.026	–0.171	–0.113	0.137	0.165	–0.004	–0.147	**–0.462**	**0.464**	**0.957**	*	**0.000**	**0.001**	**0.000**	**0.000**	0.136	**0.010**	**0.000**	**0.000**	0.228	**0.012**	**0.000**	**0.000**
20H	–0.022	–0.034	0.003	0.040	0.030	–0.047	0.103	–0.057	–0.035	0.125	0.072	–0.115	–0.115	–0.020	0.113	**0.425**	**–0.445**	**–0.854**	**–0.846**	*	**0.001**	**0.004**	**0.000**	0.157	0.106	**0.000**	**0.000**	0.148	**0.001**	**0.000**	**0.000**
21 Al	–0.107	0.191	**–0.242**	0.225	0.061	–0.012	**0.251**	0.051	–0.058	0.132	0.081	**–0.314**	**–0.360**	0.094	**0.195**	0.050	–0.102	**–0.332**	**–0.333**	**0.311**	*	0.051	**0.040**	**0.000**	**0.000**	**0.000**	**0.000**	0.757	**0.004**	0.134	0.587
22 C	**0.285**	0.013	0.103	**–0.271**	**–0.452**	0.170	–0.165	–0.049	0.190	**–0.241**	**–0.246**	–0.019	0.186	–0.045	**–0.407**	**–0.412**	**0.487**	**0.345**	**0.365**	**–0.285**	–0.190	*	**0.000**	0.993	**0.000**	0.184	**0.000**	**0.005**	0.266	**0.000**	**0.002**
23 Ca	0.046	0.050	–0.004	0.013	–0.057	0.086	–0.031	0.026	0.070	–0.105	–0.134	0.025	0.115	0.037	–0.159	**–0.481**	**0.553**	**0.777**	**0.765**	**–0.752**	**–0.200**	**0.363**	*	0.587	0.114	**0.000**	**0.000**	0.587	**0.001**	**0.000**	**0.000**
24 Fe	0.158	**–0.371**	**0.346**	–0.086	0.113	0.059	**–0.256**	**–0.245**	0.187	0.029	0.061	**0.256**	**0.264**	–0.135	–0.120	0.133	–0.064	0.155	0.146	–0.138	**–0.696**	0.001	0.053	*	**0.001**	**0.001**	**0.005**	0.328	**0.005**	0.808	0.069
25 K	–0.062	**0.222**	**–0.261**	**0.321**	0.143	0.024	**0.303**	0.128	–0.106	0.156	0.079	**–0.334**	**–0.370**	0.118	**0.247**	0.122	–0.105	**–0.237**	**–0.251**	0.158	**0.442**	**–0.484**	–0.154	**–0.334**	*	**0.001**	**0.000**	0.980	**0.000**	**0.000**	0.682
26 Mg	**0.213**	0.084	–0.038	0.143	–0.168	0.088	**0.265**	0.053	–0.026	0.134	0.023	**–0.283**	–0.079	0.135	–0.051	0.185	–0.162	**–0.548**	**–0.551**	**0.515**	**0.391**	–0.130	**–0.499**	**–0.322**	**0.339**	*	**0.001**	**0.000**	0.437	**0.006**	**0.017**
27 Mn	**0.309**	–0.149	**0.241**	–0.198	**–0.234**	0.163	**–0.284**	–0.057	0.169	–0.199	–0.132	0.184	**0.308**	–0.078	**–0.365**	**–0.393**	**0.373**	**0.525**	**0.537**	**–0.471**	**–0.481**	**0.621**	**0.435**	**0.275**	**–0.523**	**–0.336**	*	0.207	0.328	**0.000**	**0.018**
28 Na	**–0.395**	–0.088	–0.021	–0.033	**0.448**	**–0.229**	**–0.260**	–0.066	–0.068	–0.042	0.121	**0.278**	–0.105	–0.012	**0.474**	**0.218**	**–0.198**	0.114	0.118	–0.141	–0.030	**–0.277**	0.053	0.096	0.002	**–0.388**	–0.123	*	0.353	0.887	0.874
29 P	–0.034	–0.065	0.086	**–0.266**	–0.099	–0.097	–0.184	0.030	–0.065	–0.143	–0.076	0.184	0.177	–0.069	–0.100	**0.234**	**–0.244**	**–0.258**	**–0.246**	**0.316**	**–0.278**	0.109	**–0.329**	**0.272**	**–0.412**	0.076	0.096	–0.091	*	0.380	**0.000**
30 S	0.142	–0.065	0.125	**–0.232**	–0.182	0.024	–0.217	–0.143	0.184	–0.219	–0.132	0.034	0.169	–0.045	–0.171	**–0.345**	**0.453**	**0.458**	**0.495**	**–0.414**	–0.146	**0.636**	**0.496**	–0.024	**–0.375**	**–0.269**	**0.509**	–0.014	–0.086	*	**0.000**
31 Zn	–0.043	**0.229**	–0.181	0.193	–0.208	0.036	0.055	0.111	–0.024	–0.065	–0.110	–0.105	–0.077	0.086	–0.073	**–0.580**	**0.525**	**0.522**	**0.511**	**–0.528**	0.053	**0.296**	**0.623**	–0.177	0.040	**–0.233**	**0.231**	0.016	**–0.478**	**0.383**	*

PCA ordination of environmental variables

The first two PCA axes accounted for 30.3% and 17.5% of the variance in the matrix of standardised transformed environmental variables, respectively (eigenvalues of 0.303 and 0.175).

$pH_{(H2O)}$ and $pH_{(CaCl2)}$ obtained the highest loadings on PCA axis 1, together with extractable C, Ca, Mn, S and Zn and total N (Fig. 321). Low loadings were among others obtained by exchangeable H, extractable Mg and loss on ignition.

Extractable P obtained highest loadings on PCA axis 2 while extractable Zn and macro plot terrain form obtained low loadings.

The PCA results were thus consistent with the correlation matrix of the environmental variables, showing that soil pH and exchangeable H had a central position in the correlation structure of the variables.

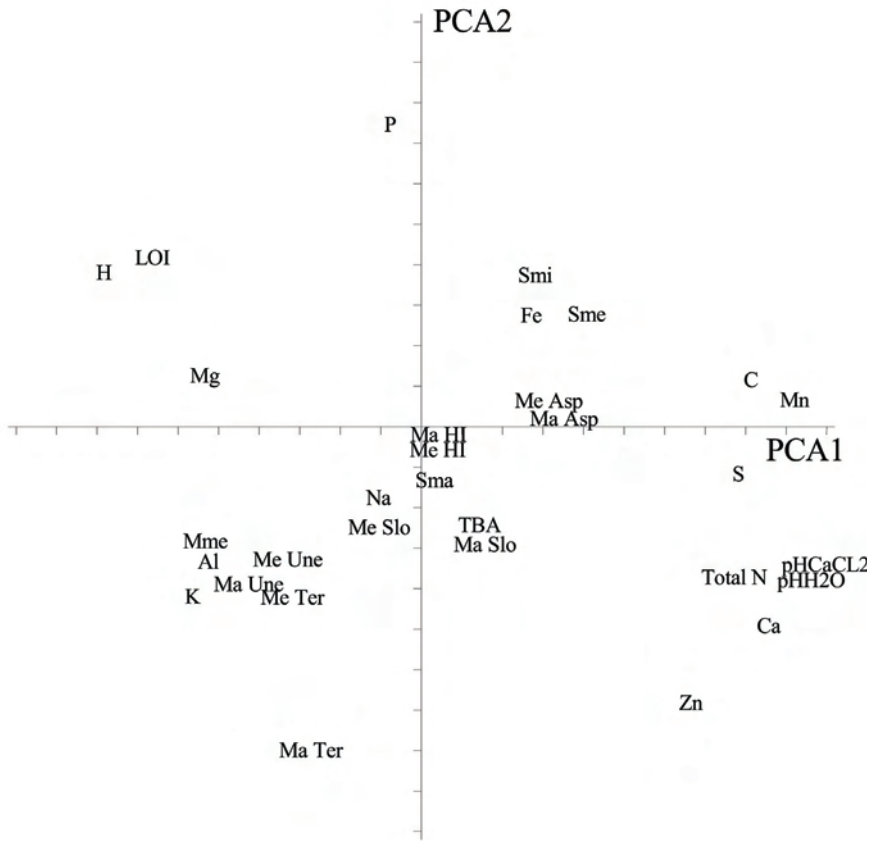

Fig.321. Dividalen: PCA ordination of 31 environmental variables. Abbreviations in accordance with Table 2, axes 1 (horizontal) and 2 (vertical). Positions of variables in the ordination space give the head of variable vectors. Tickmarks indicate 0.1 units along both axes.

DCA ordination

The gradient length of the first two DCA axes was 3.0 and 1.8 S.D. units with eigenvalues of 0.517 and 0.119, respectively, showing that the first axis by far was the strongest gradient in species composition. The sample plots segregated into two main clusters along the first DCA axis. One cluster, consisted of 40 sample plots with DCA 1 scores < 2 S.D. units, while the other (consisting of plots in macro plots 8 and 9) formed a tight group of sample plots with DCA axis 1 scores > 2.6 S.D. units (Fig. 322). The latter cluster showed almost no variation along DCA axis 2.

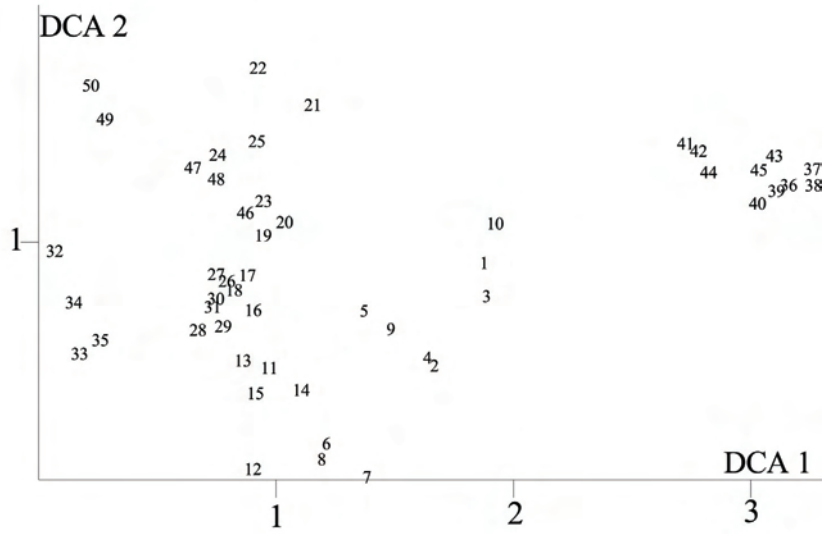

Fig. 322. Dividalen: DCA ordination diagram of 50 meso plots, axes 1 (horizontal) and 2 (vertical). Meso plot number are plotted just right of the sample plot positions. Scaling of axes in S.D. units.

GNMDS ordination

The GNMDS ordination diagram (Fig 323) had acceptable visual similarity with the DCA diagram (Fig 322), although some differences along the second axes were visible. The correlation between GNMDS axis 1 and DCA axis 1 was $\tau = 0.786$ and the correlation between GNMDS axis 2 and DCA axis 2 was $\tau = 0.393$.

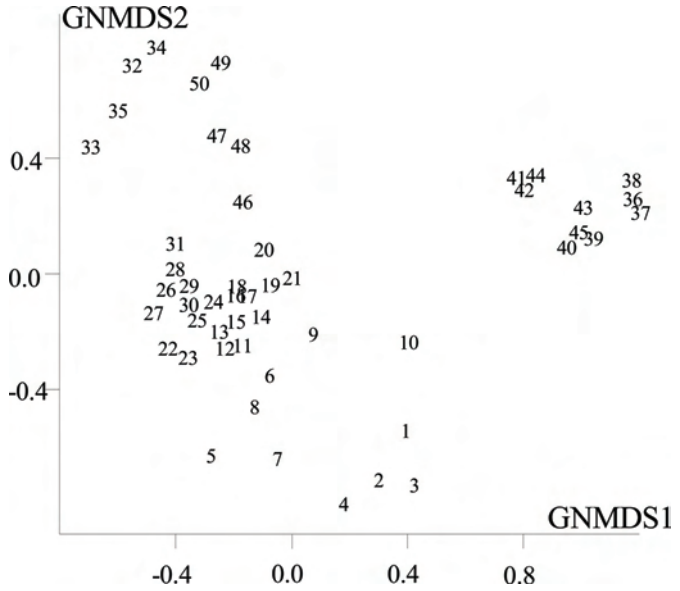

Fig.323. Dividalen: GNMDS ordination biplot diagram of 50 meso plots (indicated by their number). Names of variables are abbreviated in accordance with Table 2.

Split-plot GLM analysis of relationships between ordination axes and environmental variables

Variation (in plot scores) along DCA axis 1 was partitioned with 96.72 % at the macro-plot scale (i.e. between macro plots) and 3.28 % at the (between) meso plot scale within macro plots (Table 19). For the second ordination axis, 80.94 % of the variation was explained at the macro-plot scale and 19.06 % at the plot scale (Table 20)

At the macro-plot scale, ten environmental variables were significantly (at the $\alpha = 0.05$ level) related to DCA 1 while two variables (also at the $\alpha = 0.05$ level) were related to DCA 2. At the plot scale level, eleven environmental variables were significantly related to DCA 1 and seven variables were significantly related to DCA 2 (Tables 19 and 20).

At the macro-plot scale, pH and soil concentrations of Total N, C, Ca, Mn, S and Zn increased significantly along DCA 1 while concentrations of H and loss on ignition decreased. At the plot scale, many of these variables showed the same tendencies. Soil concentrations of K and Mg were the only additional significant predictors (both negatively related to the axis) while loss on ignition, however, was not significantly related to DCA 1 on the plot scale.

At the macro-plot scale, DCA 2 was positively related to the concentration of Zn and negatively related to P. At the plot scale, DCA axis 2 was significantly negatively related to loss on ignition and soil concentrations of H, Mg and P. Variables significantly positively related to DCA 2 at the plot scale were pH and soil concentrations of Ca and Zn (Table 20).

Table 19. Dividalen: Split-plot GLM analysis and Kendall's nonparametric correlation coefficient τ between DCA 1 and 31 environmental variables (predictor) in the 50 plots. df_{resid}: degrees of freedom for the residuals; *SS*: total variation; *FVE*: fraction of total variation attributable to a given scale (macro plot or plot); SS_{expl}/SS: fraction of the variation attributable to the scale in question, explained by a variable; *r*: model coefficient (only given when significant at the $\alpha = 0.05$ level, otherwise blank); *F*: *F* statistic for test of the hypothesis that $r = 0$ against the two-tailed alternative. Split-plot GLM relationships significant at level $\alpha = 0.05$, *P*, *F*, *r* and SS_{expl}/SS, and Kendall's nonparametric correlation coefficient $|\tau| \geq 0.30$ are given in bold face. * No within macro plot variation. Numbers and abbreviations for names of environmental variables are in accordance with Table 2.

Predictor	Dependent variable = DCA 1 (*SS* = 44.0948)								Correlation between predictor and DCA 1
	Error level								
	Macro plot $df_{resid} = 8$ $SS_{macro\ plot} = 42.6490$ *FVE* = 0.9672 of *SS*				Plot within macro plot $df_{resid} = 39$ $SS_{plot} = 1.44584$ *FVE* = 0.0328 of *SS*				Total
	$SS_{expl}/SS_{macro\ plot}$	*r*	*F*	*P*	SS_{expl}/SS_{plot}	*r*	*F*	*P*	τ
Ma Slo	0.1295		1.1895	0.3072	*	*	*	*	0.069
Ma Asp	0.0001		0.0008	0.9786	0.0018		0.0690	0.7942	–0.090
Ma HI	0.0469		0.3939	0.5477	0.0018		0.0690	0.7942	0.135
Ma Ter	0.0089		0.0721	0.7951	*	*	*	*	–0.150
Ma Une	0.0754		0.6527	0.4425	0.0000		0.0003	0.9863	–0.010
TBA	0.0849		0.7426	0.4139	0.0054		0.2134	0.6467	–0.251
Me Slo	0.1423		1.3274	0.2825	0.0007		0.0281	0.8677	0.024
Me Asp	0.0010		0.0079	0.9313	0.0244		0.9760	0.3293	–0.036
Me HI	0.0376		0.3128	0.5913	0.0003		0.0102	0.9200	0.088
Me Ter	0.0426		0.3561	0.5672	0.0048		0.1876	0.6673	–0.134
Me Une	0.0453		0.3791	0.5552	0.0084		0.3323	0.5676	–0.034
Smi	0.0009		0.0071	0.9349	0.0468		1.9147	0.1743	0.186
Sme	0.1517		1.4303	0.2660	0.0157		0.6203	0.4357	0.194
Sma	0.0849		0.7426	0.4139	0.0871		3.7209	0.0610	–0.061
Mme	0.2193		2.2471	0.1722	0.0255		1.0199	0.3188	–0.120
LOI	**0.5221**	**–2.3527**	**8.7413**	**0.0182**	0.0348		1.4043	0.2432	**–0.334**
Total N	**0.6667**	**3.5942**	**16.005**	**0.0039**	**0.1473**	**0.6576**	**6.7371**	**0.0132**	**0.363**
$pH_{(H2O)}$	**0.6429**	**2.7107**	**14.406**	**0.0053**	**0.2272**	**0.8335**	**11.469**	**0.0016**	**0.618**
pH_{CaCl2}	**0.6549**	**2.6664**	**15.183**	**0.0045**	**0.2447**	**0.8509**	**12.638**	**0.0010**	**0.637**
H	**0.6298**	**–2.9630**	**13.608**	**0.0061**	**0.1854**	**–0.7888**	**8.8745**	**0.0049**	**–0.621**
Al	0.0863		0.7556	0.4100	0.0196		0.7803	0.3825	–0.252
C	**0.6245**	**3.3661**	**13.305**	**0.0065**	**0.1354**	**0.5572**	**6.1087**	**0.0179**	**0.429**
Ca	**0.7473**	**3.0154**	**23.6600**	**0.0012**	**0.3507**	**1.1397**	**21.0680**	**0.0000**	**0.680**
Fe	0.0006		0.0048	0.9465	0.0137		0.5416	0.4662	0.076
K	0.2229		2.2947	0.1683	**0.1044**	**–0.4686**	**4.5447**	**0.0394**	–0.298
Mg	0.2640		2.8692	0.1287	**0.2134**	**–0.9498**	**10.5780**	**0.0024**	**–0.535**
Mn	**0.6089**	**2.4474**	**12.4550**	**0.0077**	**0.1777**	**0.5649**	**8.4292**	**0.0060**	**0.533**
Na	0.0075		0.0604	0.8120	0.0001		0.0045	0.9468	0.102
P	0.1350		1.2481	0.2963	0.0678		2.8382	0.1000	–0.159
S	**0.8128**	**5.0199**	**34.7330**	**0.0004**	**0.2289**	**0.6457**	**11.5760**	**0.0016**	**0.554**
Zn	**0.5117**	**2.2557**	**8.3818**	**0.0200**	**0.2877**	**0.9038**	**15.7530**	**0.0003**	**0.424**

Table 20. Dividalen: Split-plot GLM analysis and Kendall's nonparametric correlation coefficient τ between DCA 2 and 31 environmental variables (predictor) in the 50 plots. df_{resid}: degrees of freedom for the residuals; *SS*: total variation; *FVE*: fraction of total variation attributable to a given scale (macro plot or plot); SS_{expl}/SS: fraction of the variation attributable to the scale in question, explained by a variable; *r*: model coefficient (only given when significant at the $\alpha = 0.05$ level, otherwise blank); *F*: *F* statistic for test of the hypothesis that $r = 0$ against the two-tailed alternative. Split-plot GLM relationships significant at level $\alpha = 0.05$, *P*, *F*, *r* and SS_{expl}/SS, and Kendall's nonparametric correlation coefficient $|\tau| \geq 0.30$ are given in bold face. * No within macro plot variation. Numbers and abbreviations for names of environmental variables are in accordance with Table 2.

Predictor	Dependent variable = DCA 2 (*SS* = 9.3501)								Correlation between predictor and DCA 2
	Error level								
	Macro plot $df_{resid} = 8$ $SS_{macro\ plot} = 7.5677$ *FVE* = 0.8094 of *SS*				Plot within macro plot $df_{resid} = 39$ $SS_{plot} = 1.78235$ *FVE* = 0.1906 of *SS*				Total
	$SS_{expl}/SS_{macro\ plot}$	*r*	*F*	*P*	SS_{expl}/SS_{plot}	*r*	*F*	*P*	τ
Ma Slo	0.0106		0.0857	0.7771	*	*	*	*	–0.010
Ma Asp	0.1484		1.3944	0.2716	0.0055		0.2169	0.6440	0.254
Ma HI	0.2026		2.0330	0.1917	0.0055		0.2169	0.6440	–0.275
Ma Ter	0.0812		0.7073	0.4248	*	*	*	*	0.200
Ma Une	0.0402		0.3353	0.5785	0.0171		0.6796	0.4147	–0.121
TBA	0.1528		1.4430	0.2640	0.0000		0.0001	0.9908	0.241
Me slo	0.0002		0.0015	0.9704	0.0189		0.7528	0.3909	0.031
Me Asp	0.0468		0.3925	0.5484	0.0115		0.4546	0.5041	0.104
Me HI	0.0516		0.4357	0.5278	0.0053		0.2059	0.6525	–0.081
Me Ter	0.0102		0.0825	0.7813	0.0217		0.8650	0.3581	0.112
Me Une	0.0524		0.4425	0.5246	0.0818		3.4758	0.0698	–0.057
Smi	0.2173		2.2209	0.1745	0.0006		0.0249	0.8753	–0.229
Sme	0.1090		0.9790	0.3514	0.0073		0.2864	0.5956	–0.127
Sma	0.1528		1.4430	0.2640	0.0447		1.8270	0.1843	0.045
Mme	0.0011		0.0085	0.9287	0.0397		1.6127	0.2116	–0.048
LOI	0.2681		2.9302	0.1253	**0.2251**	**–0.6875**	**11.3300**	**0.0017**	**–0.314**
Total N	0.3507		4.3204	0.0713	0.0035		0.1355	0.7148	**0.301**
$pH_{(H2O)}$	0.1560		1.4786	0.2587	**0.1222**	**0.6787**	**5.4304**	**0.0251**	0.260
pH_{CaCl2}	0.1263		1.1564	0.3136	0.0904		3.8740	0.0562	0.247
H	0.1944		1.9300	0.2022	**0.1210**	**–0.7075**	**5.3666**	**0.0259**	**–0.304**
Al	0.1634		1.5631	0.2465	0.0252		1.0093	0.3213	0.224
C	0.0012		0.0095	0.9247	0.0336		1.3571	0.2511	0.027
Ca	0.2636		2.8641	0.1290	**0.1637**	**0.8646**	**7.6354**	**0.0087**	**0.331**
Fe	0.3111		3.6119	0.0939	0.0047		0.1843	0.6700	–0.296
K	0.3092		3.5802	0.0951	0.0547		2.2555	0.1412	0.297
Mg	0.0019		0.0155	0.9040	**0.2114**	**–1.0498**	**10.4550**	**0.0025**	–0.032
Mn	0.0088		0.0711	0.7965	0.0048		0.1868	0.6680	–0.048
Na	0.0002		0.0014	0.9712	0.0224		0.8919	0.3508	–0.051
P	**0.7898**	**–1.6488**	**30.0590**	**0.0006**	**0.3768**	**–0.9903**	**23.5800**	**0.0000**	**–0.607**
S	0.0856		0.7485	0.4121	0.0005		0.0181	0.8937	0.153
Zn	**0.6320**	**1.0560**	**13.7390**	**0.0060**	**0.1190**	**0.6455**	**5.2697**	**0.0272**	**0.509**

Correlations between DCA ordination axes and environmental variables

Eleven out of the 31 measured environmental variables were correlated with either DCA axis 1, DCA axis 2 or both at the $|\tau| > 0.300$ level (Table 21). Exctractable Ca ($\tau = 0.680$, Fig. 329), pH [pH ($CaCl_2$) ($\tau = 0.637$, Fig. 326)] and exchangeable H ($\tau = –0.621$, Fig. 327), S ($\tau = 0.554$, Fig. 332), Mg ($\tau = –0.535$, Fig. 330) and Mn ($\tau = 0.533$, Fig. 331) were the variables best correlated with DCA axis 1. The variables that were best correlated with DCA axis 2 were extractable P ($\tau = –0.607$, Fig. 332) and Zn ($\tau = –0.509$, Fig. 334).

Dividalen was the only reference area in which the macro plots were distributed along an altitudinal gradient. Thus correlation coefficients were also calculated between DCA scores and the altitude of each sample plot. Altitude was highly significantly correlated with DCA axis 2 ($\tau = 0.563$).

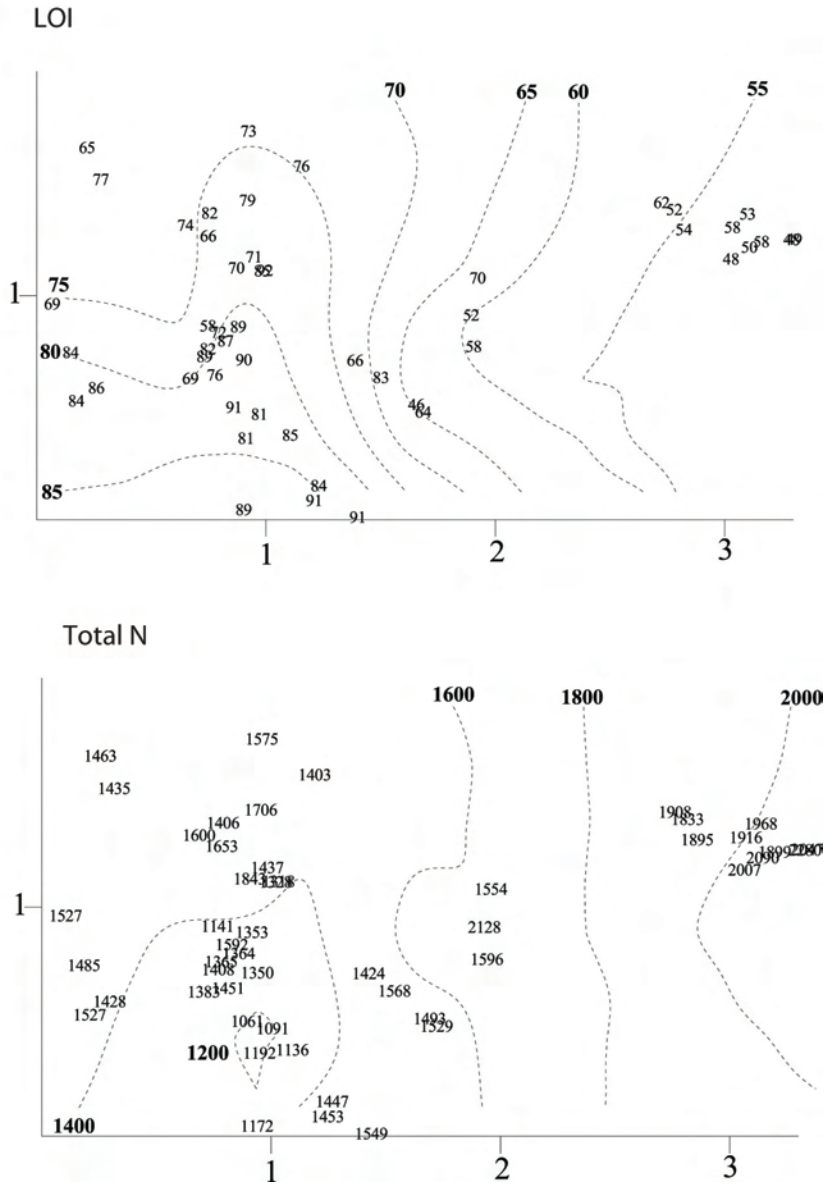

Figs 324-325. Dividalen: isolines for environmental variables in the DCA ordinations of 50 meso plots, axes 1 (horizontal) and 2 (vertical). Values for the environmental variables are plotted onto the meso plots' positions. Scaling in S.D. units. Fig. 324. LOI (R^2 = 0.629). Fig. 325. Total N (R^2 = 0.630). R^2 refers to the coefficient of determination between original and smoothened values as interpolated from the isolines. Names of environmental variables in accordance with Table 2.

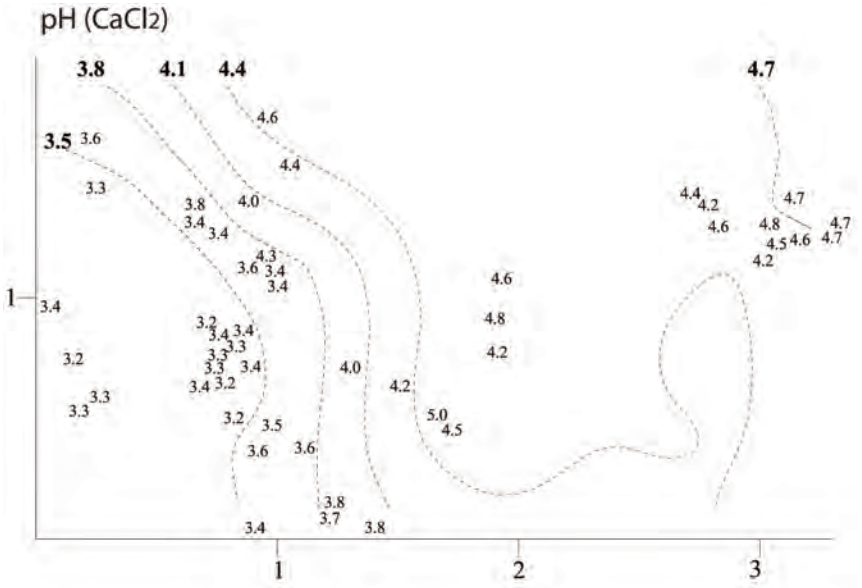

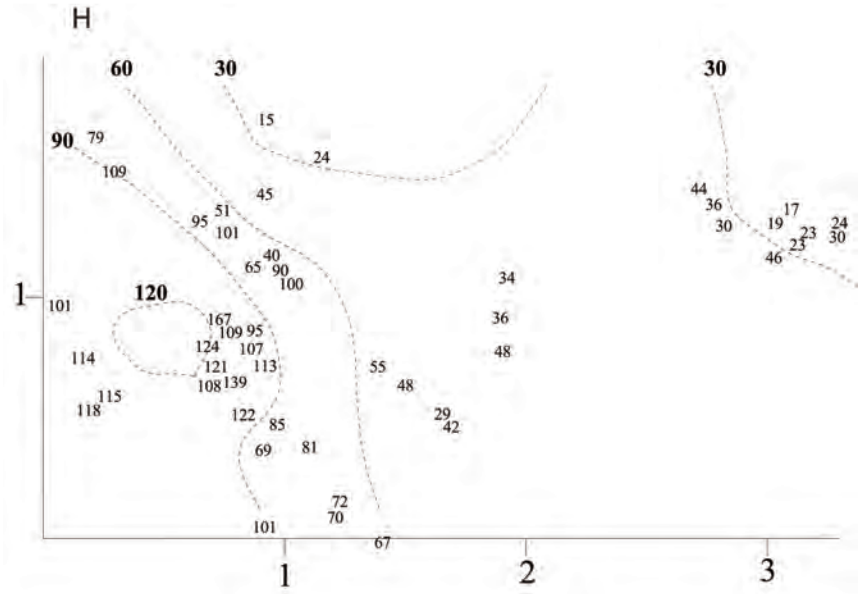

Figs 326-327. Dividalen: isolines for environmental variables in the DCA ordinations of 50 meso plots, axes 1 (horizontal) and 2 (vertical). Values for the environmental variables are plotted onto the meso plots' positions. Scaling in S.D. units. Fig. 326. pH $_{(CaCl2)}$ (R^2 = 0.889). Fig. 327. H (R^2 = 0.899). R^2 refers to the coefficient of determination between original and smoothened values as interpolated from the isolines. Names of environmental variables in accordance with Table 2.

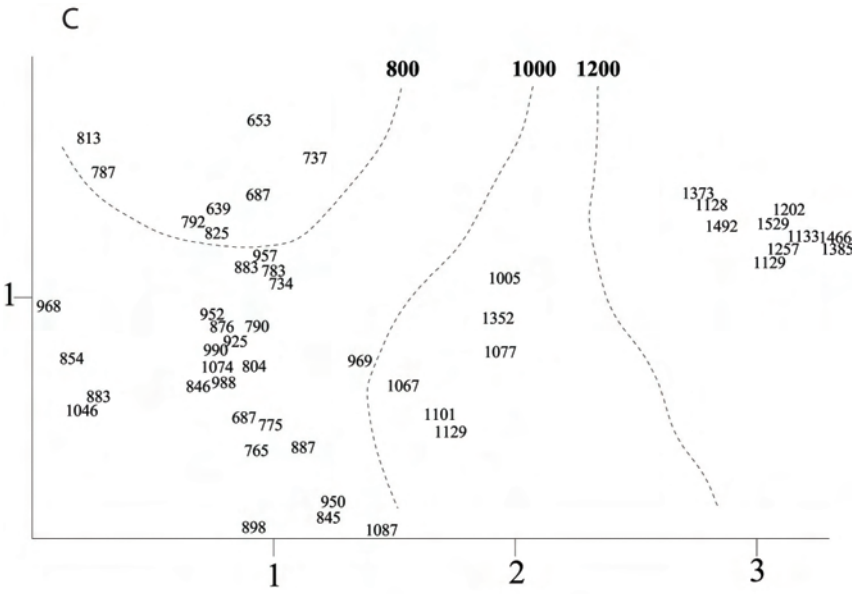

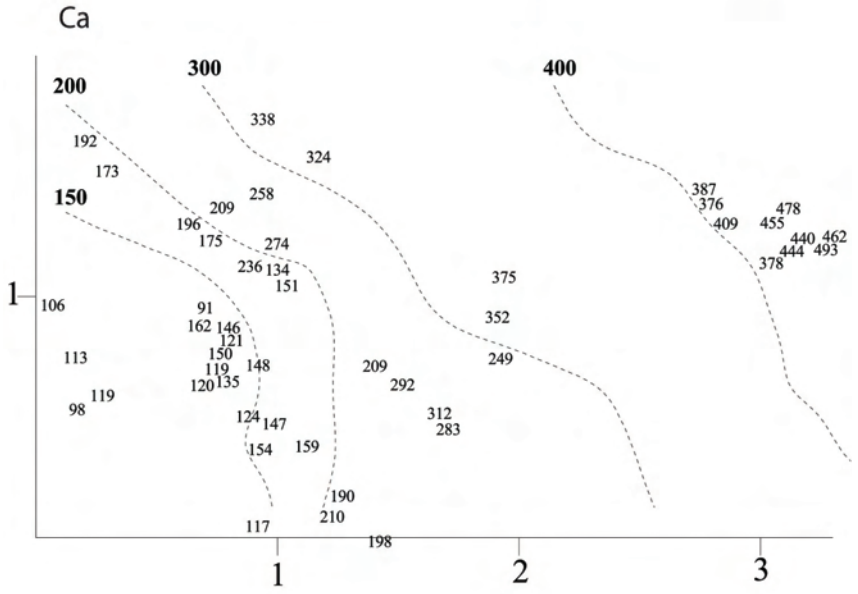

Figs 328-329. Dividalen: isolines for environmental variables in the DCA ordinations of 50 meso plots, axes 1 (horizontal) and 2 (vertical). Values for the environmental variables are plotted onto the meso plots' positions. Scaling in S.D. units. Fig. 328. C (R^2 = 0.832). Fig. 329. Ca (R^2 = 0.895). R^2 refers to the coefficient of determination between original and smoothened values as interpolated from the isolines. Names of environmental variables in accordance with Table 2.

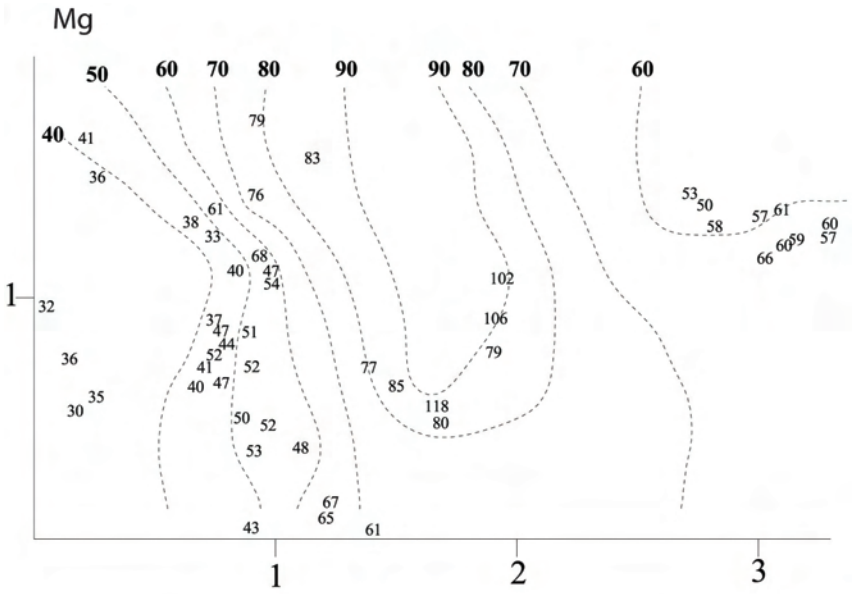

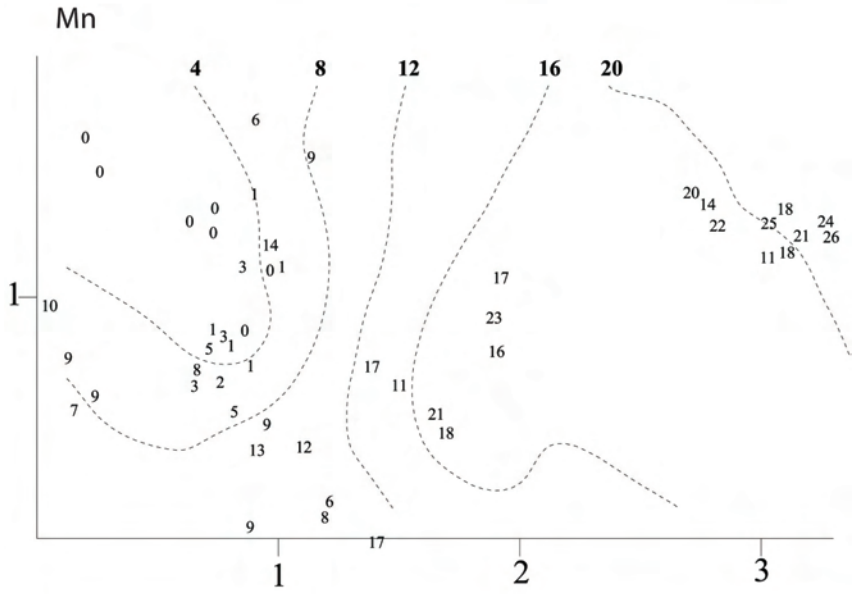

Figs 330-331. Dividalen: isolines for environmental variables in the DCA ordinations of 50 meso plots, axes 1 (horizontal) and 2 (vertical). Values for the environmental variables are plotted onto the meso plots' positions. Scaling in S.D. units. Fig. 330. Mg ($R^2 = 0.821$). Fig. 331. Mn ($R^2 = 0.859$). R^2 refers to the coefficient of determination between original and smoothened values as interpolated from the isolines. Names of environmental variables in accordance with Table 2.

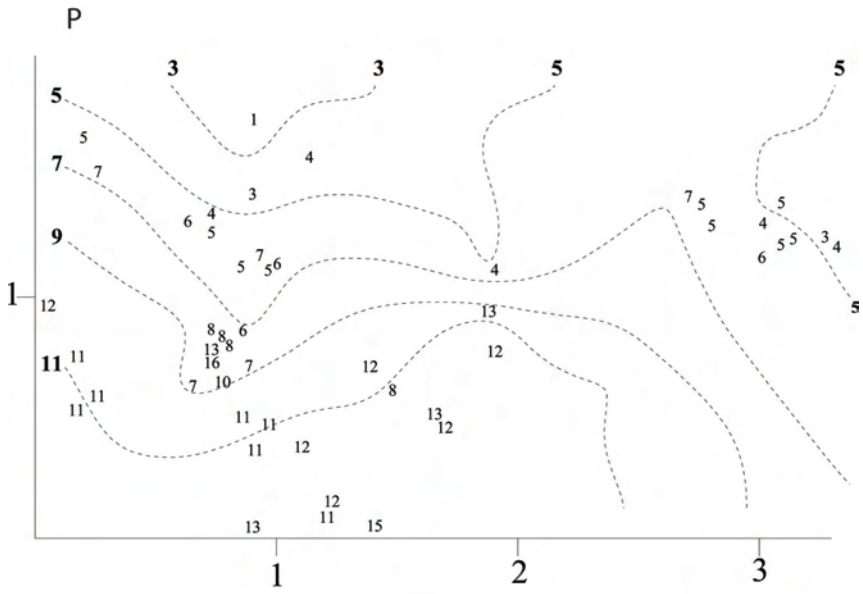

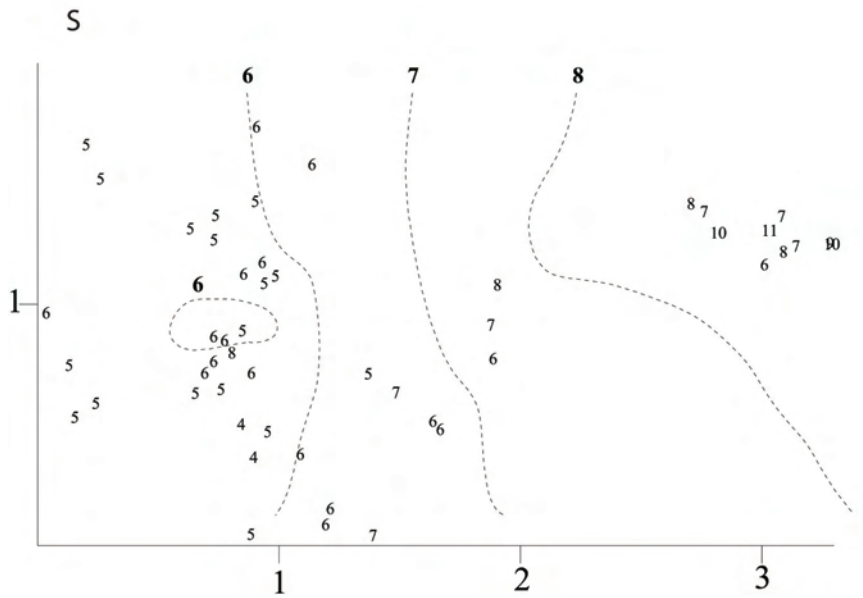

Figs 332-333. Dividalen: isolines for environmental variables in the DCA ordinations of 50 meso plots, axes 1 (horizontal) and 2 (vertical). Values for the environmental variables are plotted onto the meso plots' positions. Scaling in S.D. units. Fig. 332. P (R^2 = 0.830). Fig. 333. S (R^2 = 0.726). R^2 refers to the coefficient of determination between original and smoothened values as interpolated from the isolines. Names of environmental variables in accordance with Table 2.

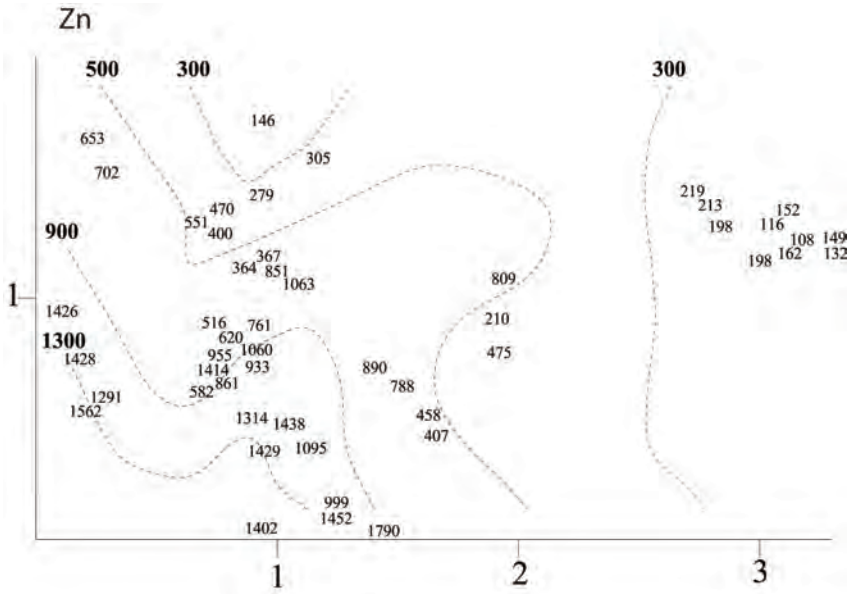

Fig. 334. Dividalen: isolines for environmental variables in the DCA ordinations of 50 meso plots, axes 1 (horizontal) and 2 (vertical). Values for the environmental variables are plotted onto the meso plots' positions. Scaling in S.D. units. Fig. 334. Zn (R^2 = 0.872). R^2 refers to the coefficient of determination between original and smoothened values as interpolated from the isolines. Names of environmental variables in accordance with Table 2.

Frequent species

A total of 141 species was found within the fifty 1 × 1 m meso plots in the Dividalen reference area: 74 vascular plants, 24 mosses, 18 liverworts and 25 lichens. The most frequent species (the sum of subplot frequencies in brackets) were: *Avenella flexuosa* (755 out of 800), *Vaccinium myrtillus* (602), *Vaccinium vitis-idaea* (519), *Barbilophozia lycopodioides* (496), *Chamaepericlymenum suecicum* (474), *Linnaea borealis* (398), *Anthoxanthum odoratum* (356) and *Pleurozium schreberi* (320).

The distribution of species abundance in the DCA ordination

Out of total 141 recorded species, 71 occurred in five or more of the fifty sample plots. *Vaccinium myrtillus* (Fig. 341), *Vaccinium vitis-idaea* (Fig. 343), *Avenella flexuosa* (Fig. 374) and *Barbilophozia lycopodioides* (Fig. 391) had wide ecological amplitudes along both DCA axes, and they were also highly abundant in most of the sample plots.

Species that occurred mostly on the right side of the diagram and thus had preferences for sites with relatively high values of soil pH, Ca, Mg and S were *Salix phylicifolia* (Fig. 338), *Alchemilla glabra* (Fig. 344), *Cerastium fontanum* (Fig. 345), *Myosotis decumbens* (Fig. 356), *Omalotheca norvegica* (Fig. 357*), Rumex acetosa* (Fig. 363), *Saussurea alpina* (Fig. 364), *Trollius europaeus* (Fig. 368), *Poa alpina* (Fig. 377) and *Mnium spinosum* (Fig. 383).

Species that were restricted to plots with low DCA axis 1 scores, i.e. sites poorer in soil nutrients, e.g. lower pH and lower concentrations of Ca, Mg, Mg and S, were *Betula nana* (Fig. 335*), Pedicularis lapponica* (Fig. 359), *Dicranum scoparium* (Fig. 381), *Cladonia arbuscula* (Fig. 394), *Cladonia bellidiflora* (Fig. 395), *Cladonia chlorophaea* (Fig. 396), *Cladonia ecmocyna* (Fig. 398), *Cladonia furcata* (Fig 399), *Cladonia rangiferina* (Fig. 401), *Cladonia sulphurina* (Fig. 402) and *Peltigera aphthosa* (Fig. 405).

Some species also showed distinct patterns along the second DCA axis, related to differences in altitude (τ = 0.563) and soil extractable P (Tables 19–20). Species with preference for higher altitudes and lower amounts of P (plots with high DCA axis 2 scores) were *Phyllodoce caerulea* (Fig. 340), partly also *Equisetum sylvaticum* (Fig. 347), *Pedicularis lapponica* (Fig 359), *Calamagrostis lapponica* (Fig. 371) and *Nephroma arcticum* (Fig. 404). Examples of species that preferred sites at lower altitudes with higher soil contents of extractable P and Zn were *Gymnocarpium dryopteris* (Fig. 350), *Melampyrum sylvaticum* (Fig. 354), *Orthilia secunda* (Fig. 358), *Luzula pilosa* (Fig. 376) and *Brachythecium salebrosum* (Fig. 379).

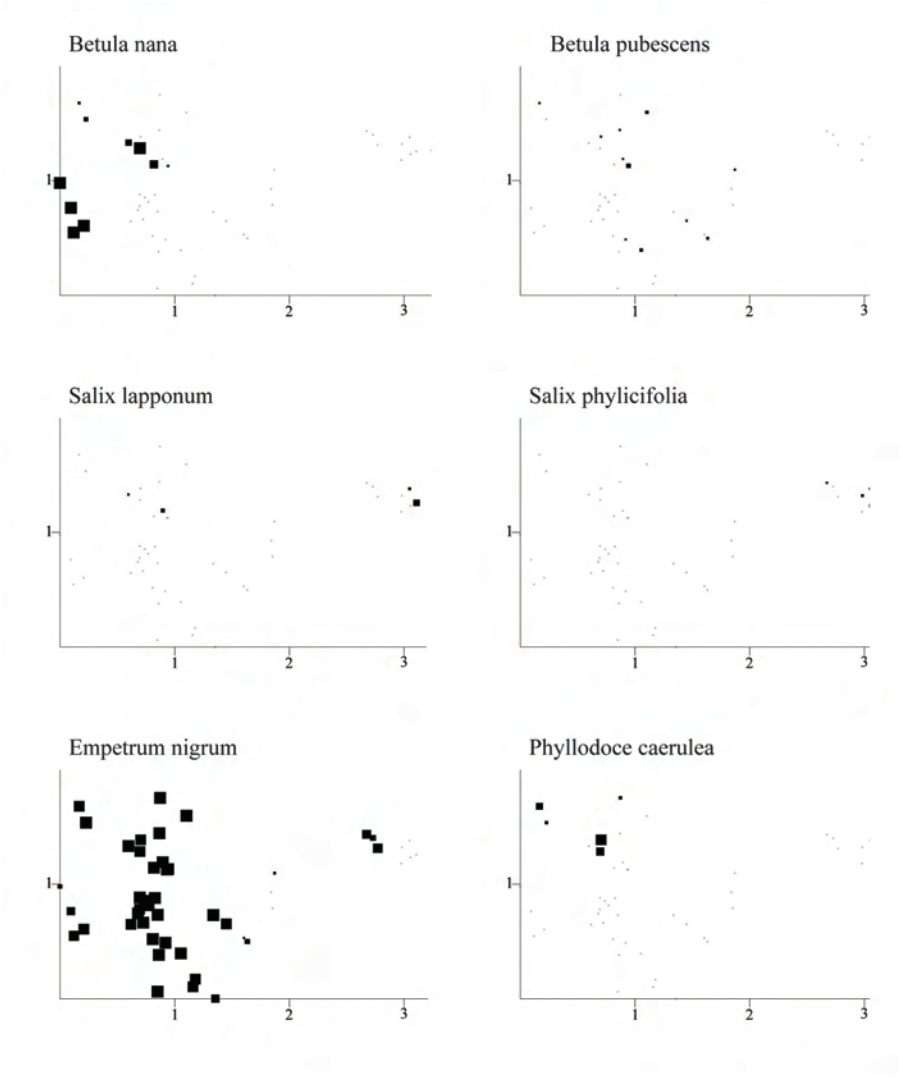

Fig. 335-340. Dividalen: distributions of species abundances in the DCA ordination of 50 sample plots, axes 1 (horizontal) and 2 (vertical). Frequency in subplots for each species in each meso plot proportional to quadrate size. Scaling in S.D. units. Fig. 335. *Betula nana*. Fig. 336. *Betula pubescens*. Fig. 337. *Salix lapponum*. Fig. 338. *Salix phylicifolia*. Fig. 339. *Empetrum nigrum*. Fig. 340. *Phyllodoce caerulea*.

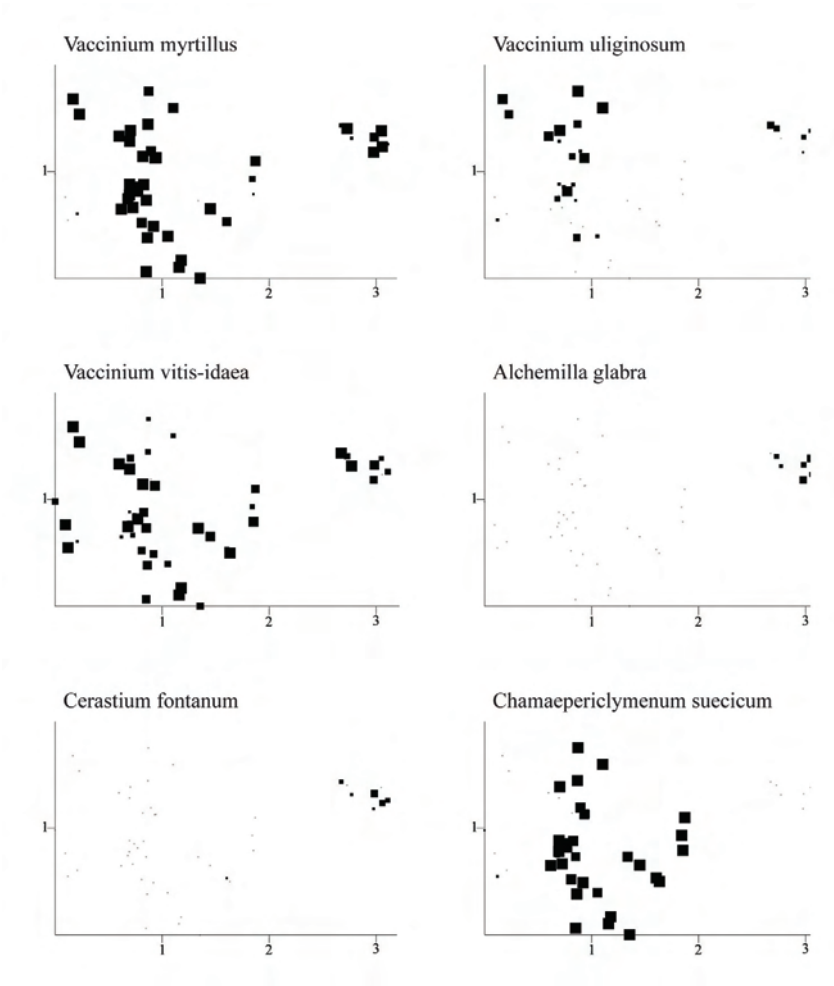

Figs 341-346. Dividalen: distributions of species abundances in the DCA ordination of 50 sample plots, axes 1 (horizontal) and 2 (vertical). Frequency in subplots for each species in each meso plot proportional to quadrate size. Scaling in S.D. units. Fig. 341. *Vaccinium myrtillus*. Fig. 342. *Vaccinium uliginosum*. Fig. 343. *Vaccinium vitis-idaea*. Fig. 344. *Alchemilla glabra*. Fig. 345. *Cerastium fontanum*. Fig. 346. *Chamaepericlymenum suecicum* (syn. *Cornus suecica*).

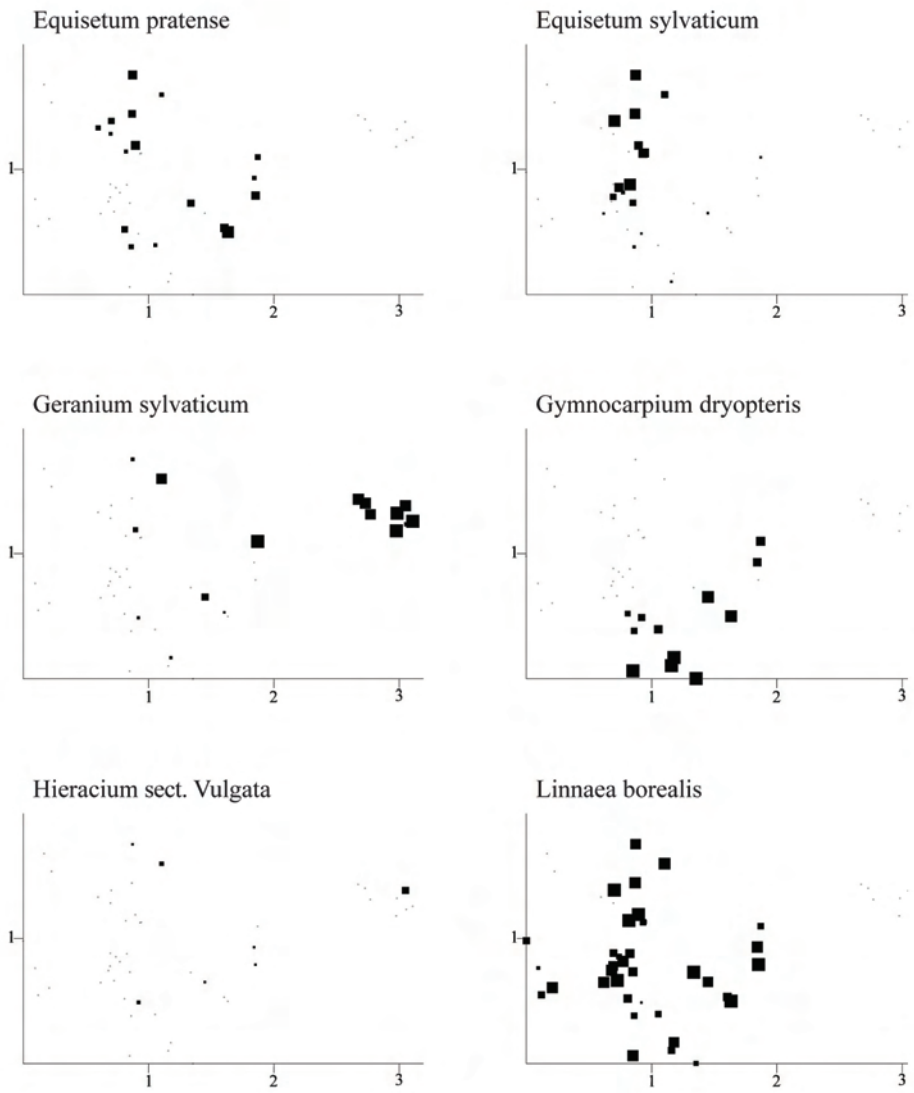

Figs 347-352. Dividalen: distributions of species abundances in the DCA ordination of 50 sample plots, axes 1 (horizontal) and 2 (vertical). Frequency in subplots for each species in each meso plot proportional to quadrate size. Scaling in S.D. units. Fig. 347. *Equisetum pratense*. Fig. 348. *Equisetum*

sylvaticum. Fig. 349. *Geranium sylvaticum*. Fig. 350. *Gymnocarpium dryopteris*. Fig. 351. *Hieracium vulgata*. Fig. 352. *Linnaea borealis*.

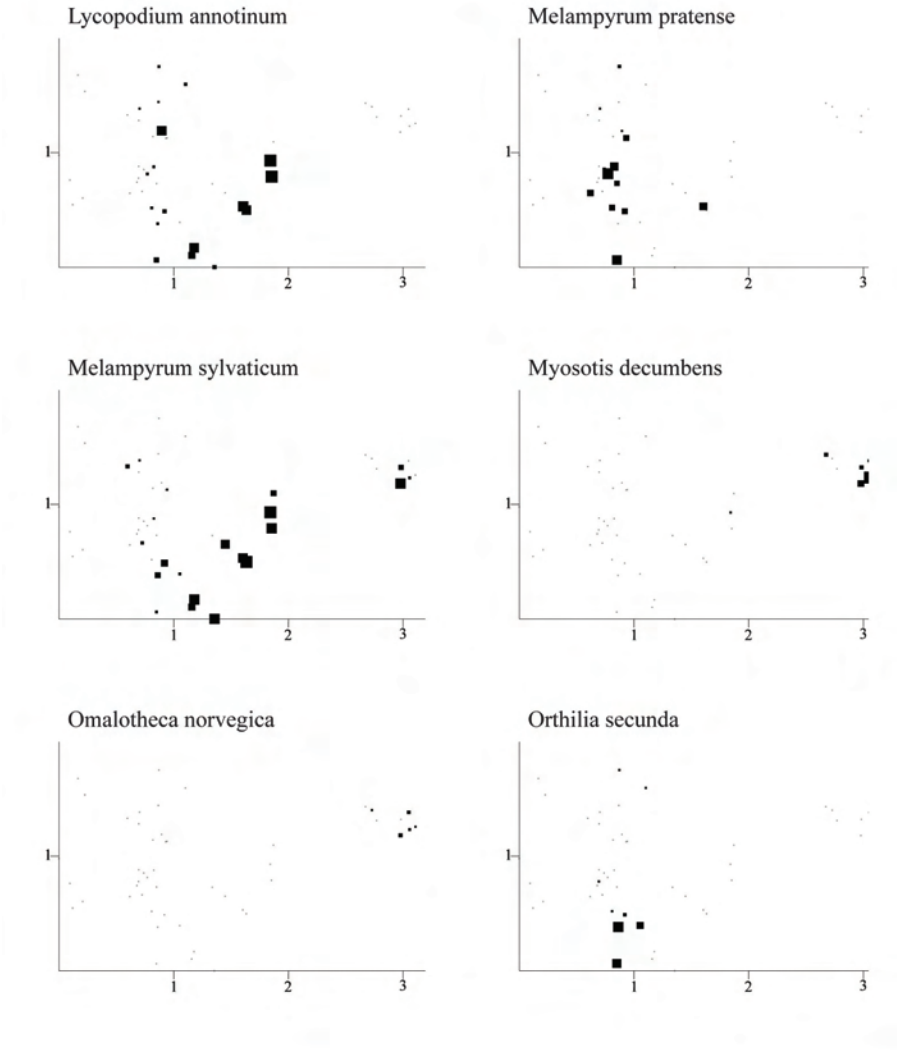

Figs 353-358. Dividalen: distributions of species abundances in the DCA ordination of 50 sample plots, axes 1 (horizontal) and 2 (vertical). Frequency in subplots for each species in each meso plot proportional to quadrate size. Scaling in S.D. units. Fig. 353. *Lycopodium annotinum*. Fig. 354. *Melampyrum pratense.* Fig. 355. *Melampyrum sylvaticum.* Fig. 356. *Myosotis decumbens*. Fig. 357. *Omalotheca norvegica*. Fig. 358. *Orthilia secunda.*

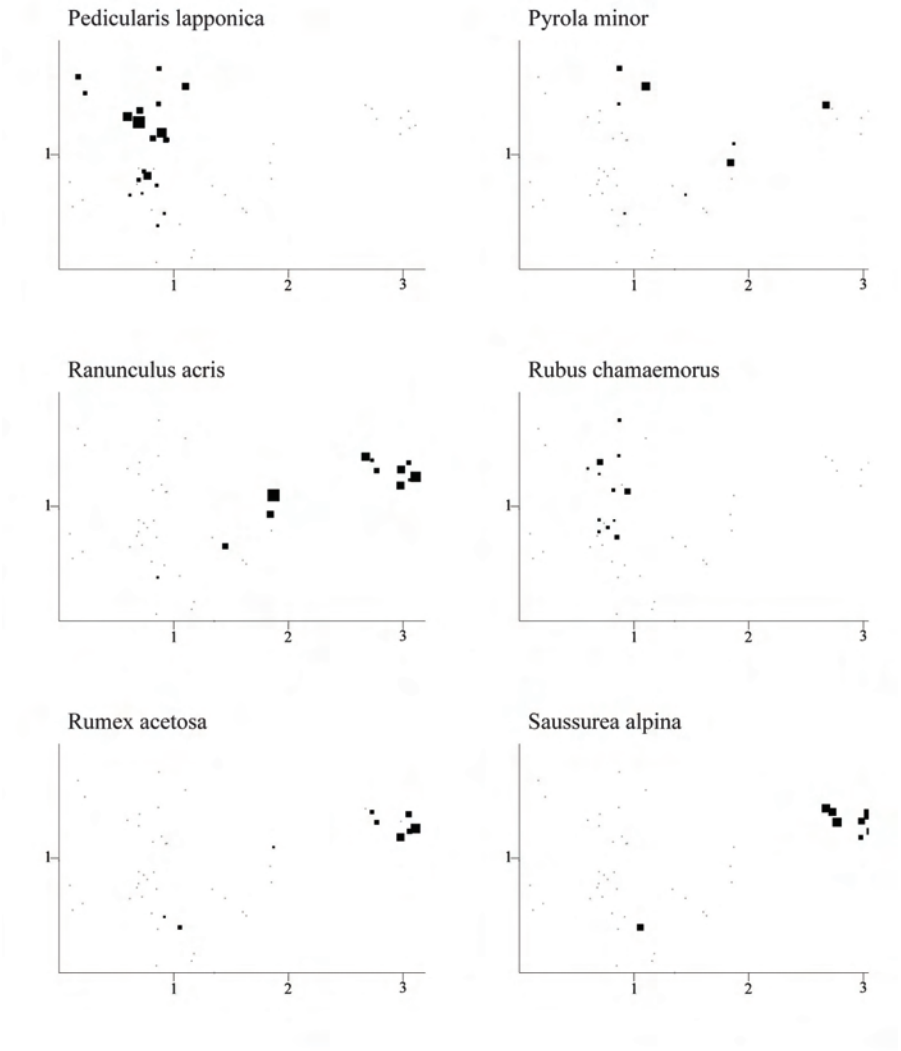

Figs 359-364. Dividalen: distributions of species abundances in the DCA ordination of 50 sample plots, axes 1 (horizontal) and 2 (vertical). Frequency in subplots for each species in each meso plot proportional to quadrate size. Scaling in S.D. units. Fig. 359. *Pedicularis lapponica*. Fig. 360. *Pyrola minor.* Fig. 361. *Ranunculus acris.* Fig. 362. *Rubus chamaemorus*. Fig. 363. *Rumex acetosa.* Fig. 364. *Saussurea alpina*.

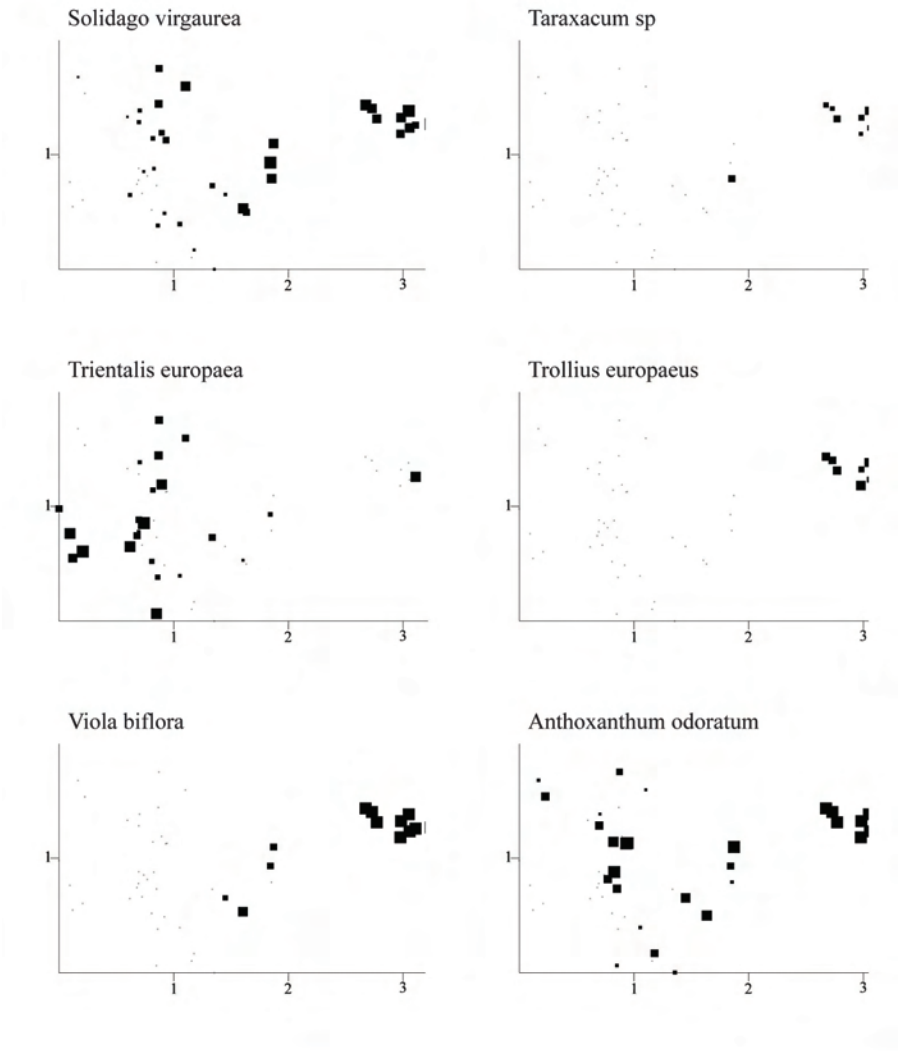

Figs 365-370. Dividalen: distributions of species abundances in the DCA ordination of 50 sample plots, axes 1 (horizontal) and 2 (vertical). Frequency in subplots for each species in each meso plot proportional to quadrate size. Scaling in S.D. units. Fig. 365. *Solidago virgaurea*. Fig. 366. *Taraxacum* sp. Fig. 367. *Trientalis europaea*. Fig. 368. *Trollius europaeus*. Fig. 369. *Viola biflora*. 370. *Anthoxanthum odoratum*.

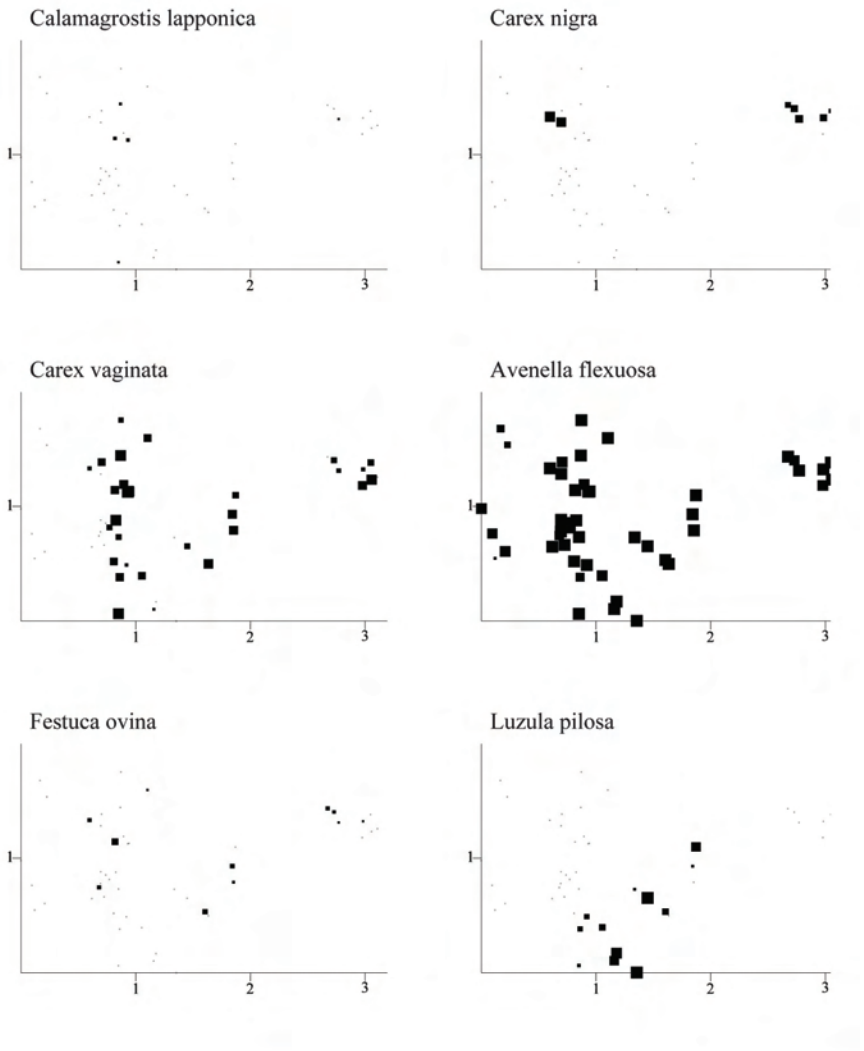

Figs 371-376. Dividalen: distributions of species abundances in the DCA ordination of 50 sample plots, axes 1 (horizontal) and 2 (vertical). Frequency in subplots for each species in each meso plot proportional to quadrate size. Scaling in S.D. units. Fig. 371. *Calamagrostis lapponica*. Fig. 372. *Carex nigra*. 373. *Carex vaginata*. Fig. 374. *Avenella flexuosa* (syn. *Deschampsia flexuosa*). Fig. 375. *Festuca ovina*. Fig. 376. *Luzula pilosa*.

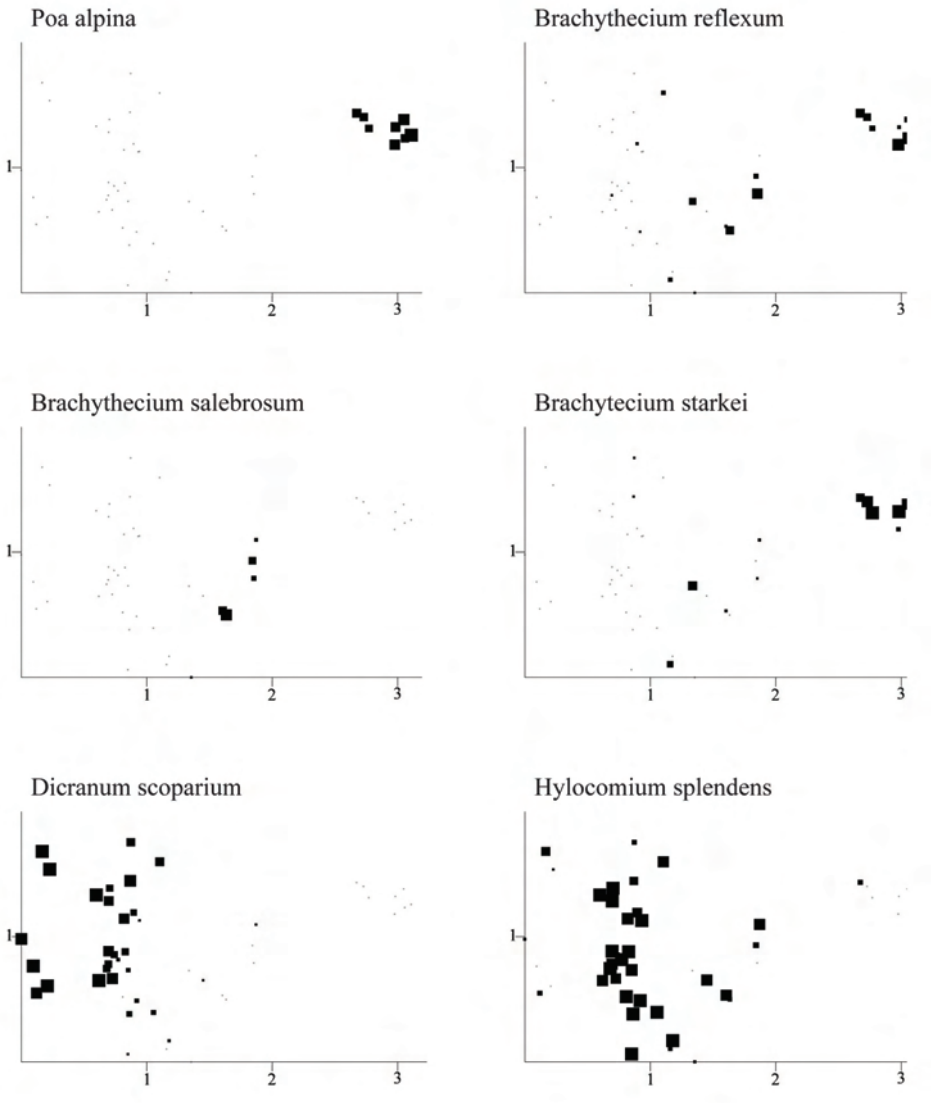

Figs 377-382. Dividalen: distributions of species abundances in the DCA ordination of 50 sample plots, axes 1 (horizontal) and 2 (vertical). Frequency in subplots for each species in each meso plot proportional to quadrate size. Scaling in S.D. units. Fig. 377. *Poa alpina*. Fig. 378. *Brachythecium reflexum.* Fig. 379. *Brachythecium salebrosum.* Fig. 380. *Brachythecium starkei.* Fig. 381. *Dicranum scoparium.* Fig. 382. *Hylocomium splendens.*

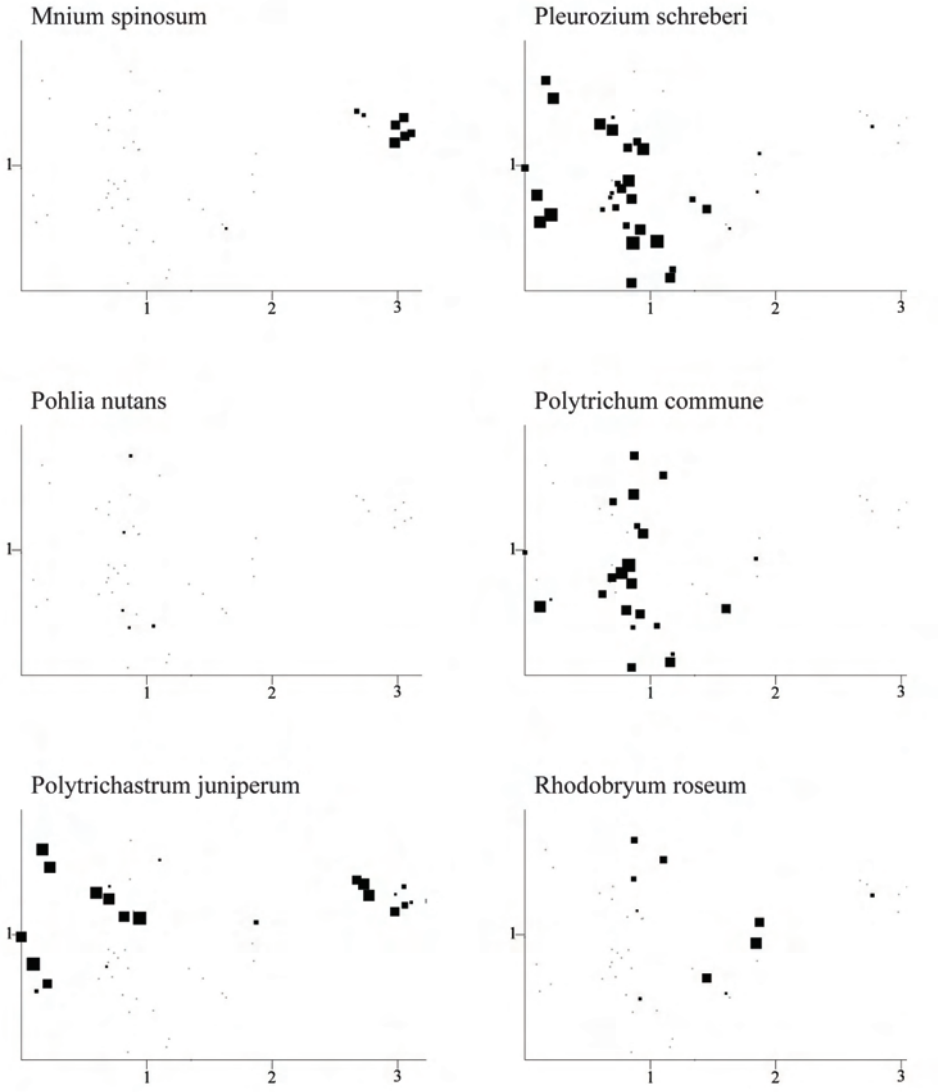

Figs 383-388. Dividalen: distributions of species abundances in the DCA ordination of 50 sample plots, axes 1 (horizontal) and 2 (vertical). Frequency in subplots for each species in each meso plot proportional to quadrate size. Scaling in S.D. units. Fig. 383. *Mnium spinosum.* Fig. 384. *Pleurozium schreberi*. Fig. 385. *Pohlia nutans*. Fig. 386. *Polytrichum commune*. Fig. 387. *Polytrichastrum juniperum*. Fig. 388. *Rhodobryum roseum.*

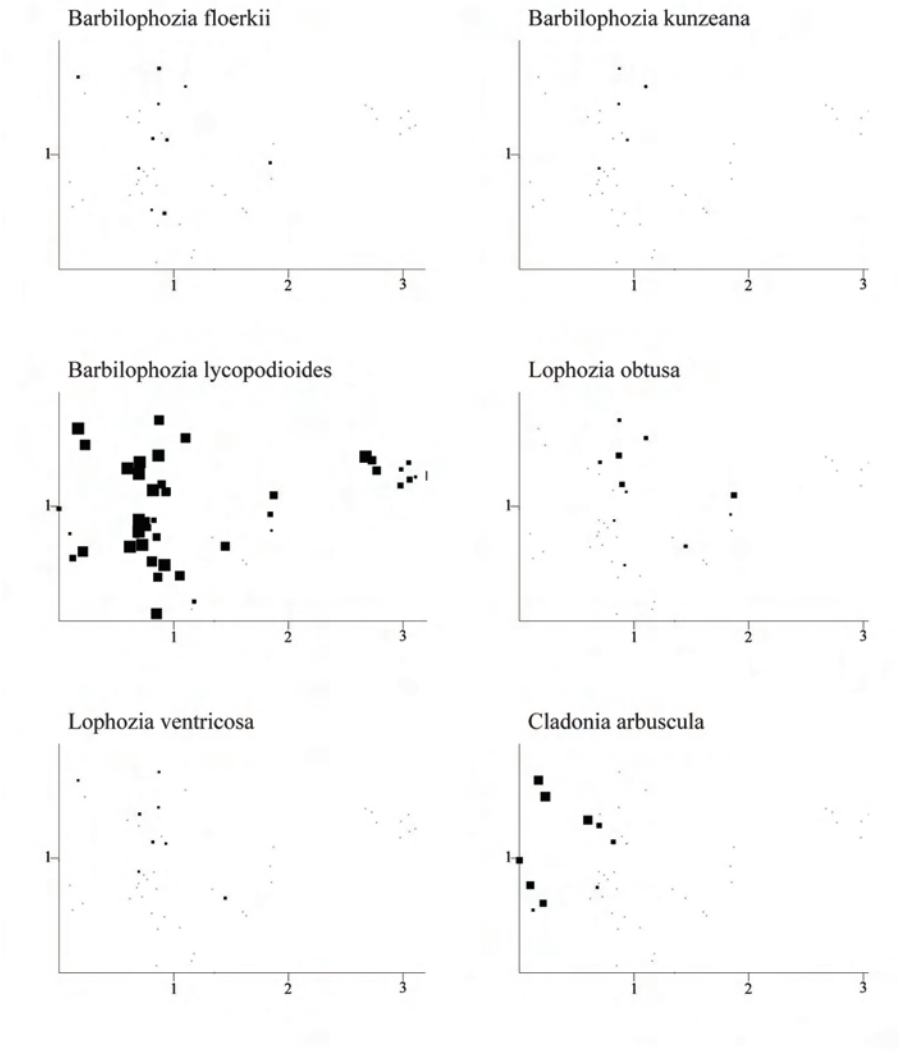

Figs 389-394. Dividalen: distributions of species abundances in the DCA ordination of 50 sample plots, axes 1 (horizontal) and 2 (vertical). Frequency in subplots for each species in each meso plot proportional to quadrate size. Scaling in S.D. units. Fig. 389. *Barbilophozia floerkei*. Fig. 390. *Barbilophozia kunzeana*. Fig. 391. *Barbilophozia lycopodioides*. Fig. 392. *Lophozia obtusa*. Fig. 393. *Lophozia ventricosa*. Fig. 394. *Cladonia arbuscula*.

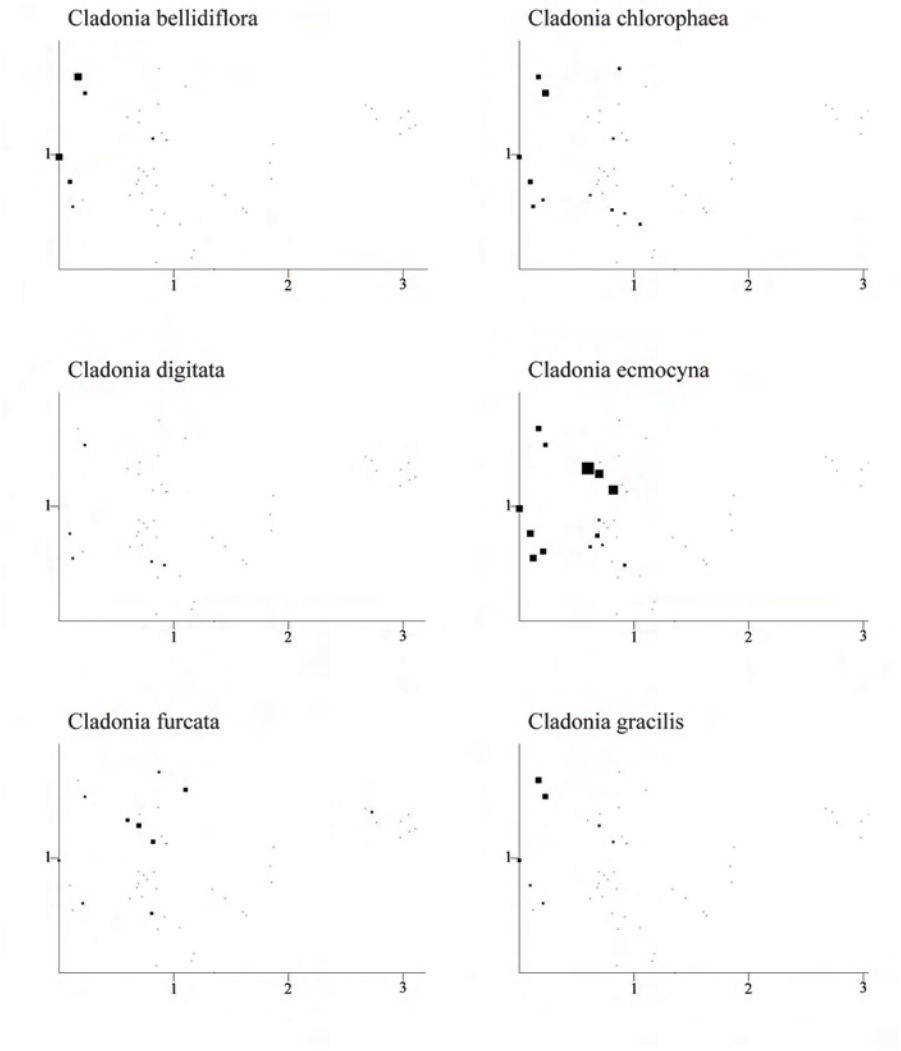

Figs 395-400. Dividalen: distributions of species abundances in the DCA ordination of 50 sample plots, axes 1 (horizontal) and 2 (vertical). Frequency in subplots for each species in each meso plot proportional to quadrate size. Scaling in S.D. units. Fig. 395. *Cladonia bellidiflora*. Fig. 396. *Cladonia chlorophaea*. Fig. 397. *Cladonia digitata*. Fig. 398. *Cladonia ecmocyna.* Fig. 399. *Cladonia furcata.* Fig. 400. *Cladonia gracilis.*

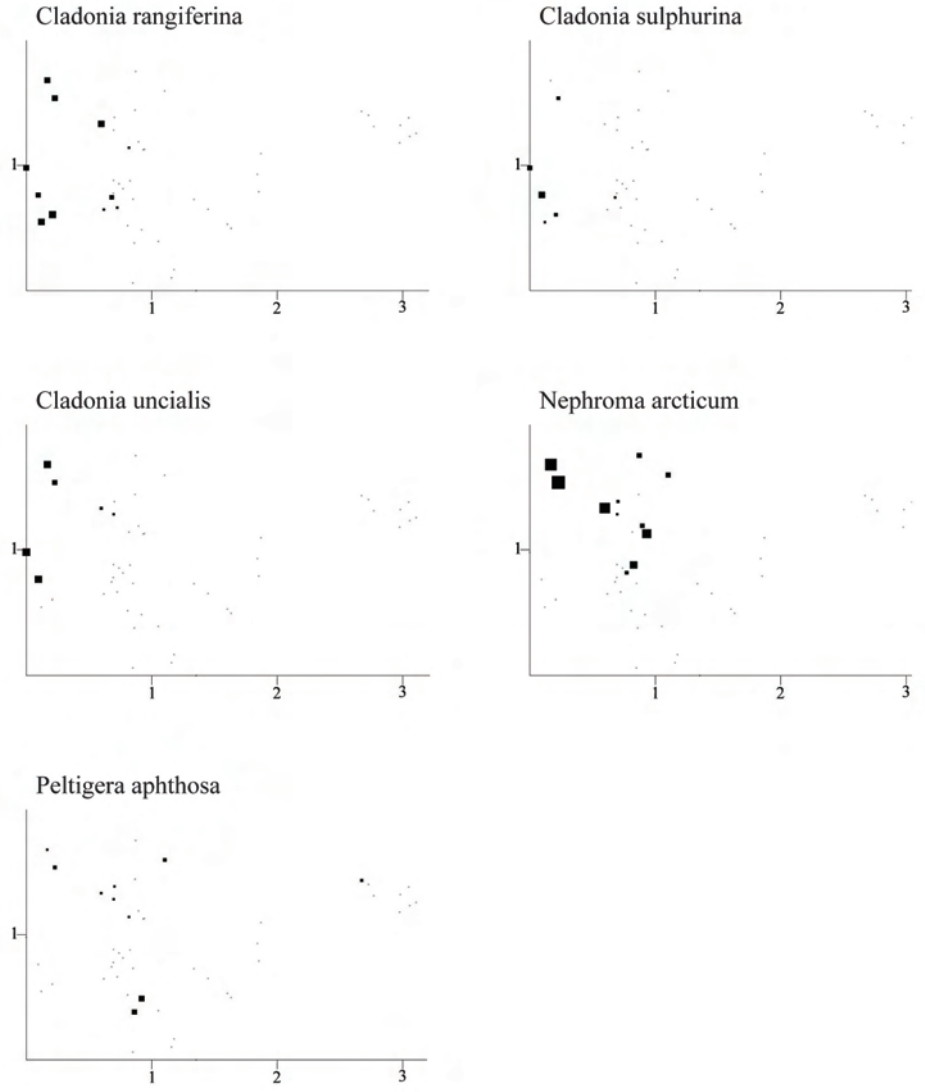

Figs 401-405. Dividalen: distributions of species abundances in the DCA ordination of 50 sample plots, axes 1 (horizontal) and 2 (vertical). Frequency in subplots for each species in each meso plot proportional to quadrate size. Scaling in S.D. units. Fig. 401. *Cladonia rangiferina*. Fig. 402. *Cladonia sulphurina*. Fig. 403. *Cladonia uncialis*. Fig. 404. *Nephroma arcticum.* Fig. 405. *Peltigera aphthosa*.

THE TOTAL DATA SET

Variation in species composition between reference areas

Twenty-one species were restricted to the southermost reference area Lund, located in the middle boreal vegetation zone in the western (O2) vegetation section (Moen 1999). These were *Anemone nemorosa, Blechnum spicant, Carex pilulifera, Danthonia decumbens, Huperzia selago* spp. *selago, Luzula sylvatica, Oreopteris limbosperma, Populus tremula, Pteridium aquilinum, Chiloscyphus coadunatus, Dicranum polysetum, Diplophyllum taxifolium, Hylocomiastrum umbratum, Hypnum cupressiforme, Lepidozia reptans, Leucobryum glaucum, Plagiothecium undulatum, Polytrichastrum formosum, Sphagnum capillifolium and Sphagnum quinquefarium.*

Several species that were common in most of the other reference areas were very rare or totally absent in Lund, such as *Anthoxanthum odoratum, Barbilophozia lycopodioides, Betula nana, Brachythecium reflexum, B. salebrosum, Deschampsia cespitosa, Empetrum nigrum, Geranium sylvaticum, Lophozia obtusa, Polytrichum commune, P. juniperinum, Ranunculus acris, Rhodobryum roseum, Solidago virgaurea* and all lichen species.

The other reference areas, all located in the northern boreal zone, shared a majority of species. However, the Dividalen reference area located in the continental vegetation section, partly on calcaerous bedrock, differed considerable from the others in species composition, as exemplified e.g. by the with occurrence of species such as *Carex lapponica, Cerastium fontanum, Equisetum pratense, Myosotis decumbens, Poa alpina, Saussurea alpina* and *Trollius europaeus.*

Variation in environmental variables between reference areas

Differences among reference areas with respect to range and median values of environmental variables were also found (Table 21). These differences should be interpreted as between area (those included in this study) variation rather than regional biogeographical trends of these variables in Norway. Median soil depth was higher, while the meso plot aspect unfavourability was lower in more northerly situated areas. The median value of loss on ignition was highest in Gutulia and lowest in Møsvatn and Børgefjell. The southernmost reference area, Lund, had the lowest median pH value, while the northernmost area, Dividalen, had the highest value. Lund and Åmotsdalen had the lowest median value of extractable Ca concentrations while the highest value of both of Ca and Mg were found for Dividalen. The median value of extractable Mn was lowest in Lund and highest in Gutulia, while extractable P was highest in Børgefjell and Møsvatn. Lund had the highest soil moisture content and Lund and Gutulia had the highest median value of total N.

Table 21. Statistics for the 31 environmental variables in all six study areas. Min, Med and Max represent minimum, medium and maximum, respectively. The units and names of environmental variables are abbreviated in accordance with Table 2.

Evironmental variables	**Study area** Lund			Møsvatn			Gutulia			Åmotsdalen			Børgefjell			Dividalen		
	Min	Med	Max	Min	Med	Max	Min	Med	Max	Min	Med	Max	Min	Med	Max	Min	Med	Max
Ma Slo	0	12	60	6	15	30	0	9	60	1	7	19	1	9	20	5	14.5	25
Ma Asp	22.5	162.5	177.5	17.5	157.5	175.5	92.5	150.5	176.5	22.5	42.5	112.5	22.5	52.5	107.5	22.5	67.5	121.5
Ma HI	–1.73	–0.18	0.09	–0.58	–0.17	0.26	–1.65	–0.12	0.00	–0.13	0.07	0.25	–0.07	0.06	0.20	–0.05	0.12	0.25
Ma Ter	–2	0	2	–0.78	0.11	0.78	–1	0	2	–1	0	2	–2	0	2	0	0.5	1
Ma Une	1	3	5	0.19	1.07	2.00	0	2	4	0	2	4	1	1.5	4	1	2	3
TBA	0	3	9	0	7	7	2	14	23	0	4	10	0	5	16	0	5	14
Me Slo	0	19	30	3	12	12	0	10	75	0	9	23	0	9	23	2	15	34
Me Asp	0.5	152.5	178.5	75.0	175.0	175.0	33.5	148.0	177.5	0.5	47.5	103.5	4.5	58.5	175.5	17.5	97.5	384.0
Me HI	–0.54	–0.30	0.25	–0.53	–0.17	0.14	–3.63	–0.11	0.61	–0.01	0.11	0.30	–0.15	0.03	0.41	–0.54	0.10	0.49
Me Ter	–1.06	0.00	0.50	–0.56	0.03	0.03	–2.00	0.00	2.00	–0.40	0.00	0.47	–0.56	0.00	0.44	0.00	1.00	2.00
Me Une	0.00	0.75	2.10	0.00	0.61	0.61	1.00	2.00	4.00	0.00	0.58	2.64	0.00	0.78	1.39	0.00	2.00	5.00
Smi	0.0	2.0	18.0	0.0	2.0	2.0	0.0	3.0	62.0	0.0	6.0	30.0	0.0	2.0	16.0	0.0	6.0	65.0
Sme	1.0	16.5	61.0	3.0	16.5	16.5	1.0	10.0	66.0	4.0	24.0	65.0	3.5	18.8	44.0	5.0	37.5	65.0
Sma	11.0	48.0	78.0	8.0	41.5	41.5	3.0	25.0	85.0	15.0	54.5	103.0	20.0	35.5	83.0	45.0	65.0	65.0
Mme	43.9	74.9	83.9	20.8	41.4	78.3	19.7	67.6	82.4	9.40	42.6	73.9	18.4	41.8	79.8	14.2	63.2	83.3
LOI	32.1	73.6	95.0	16.3	48.1	48.1	41.3	85.5	97.8	14.6	68.4	91.3	9.4	51.4	95.2	46.4	73.5	91.8
Total N	1175	1678	2365	1207	1595	1595	1264	1632	2100	1027	1417	2224	1090	1545	2353	1061	1489	2280
pH_{H2O}	3.61	3.90	4.58	3.68	4.17	4.17	3.57	4.23	5.22	3.81	4.27	5.20	3.77	4.10	5.05	3.86	4.35	5.40
pH_{CaCl2}	2.86	3.09	3.82	2.95	3.52	3.52	2.81	3.53	4.88	3.05	3.52	4.70	2.99	3.35	4.56	3.20	3.74	5.03
H	99	154	309	57	104	104	39	96	188	40	110	243	50	100	155	15	70	168
Al	3.67	15.45	110.13	1.46	6.74	6.74	0.48	4.43	30.72	0.92	12.67	73.46	0.95	2.47	22.66	0.95	2.62	17.22
C	405	574	890	549	866	866	508	874	2794	453	823	1358	418	659	1795	639	952	1530
Ca	5.8	57.5	90.6	38.9	102.9	102.9	51.4	98.3	233.5	30.8	76.4	189.1	74.1	105.5	182.1	91.1	197.3	493.2
Fe	0.3	1.1	7.8	0.2	0.7	0.7	0.1	0.3	13.0	0.2	1.1	3.8	0.1	0.2	0.7	0.1	0.5	3.5

K	11.0	18.5	28.5	17.9	37.4	37.4	12.6	33.3	62.4	20.7	35.8	51.3	18.8	37.2	85.4	21.4	32.4	50.8
Mg	4.4	41.2	64.7	11.0	27.4	27.4	6.6	20.4	55.3	19.6	32.5	60.6	33.5	49.5	85.8	30.9	53.5	118.1
Mn	0.1	0.7	2.4	0.7	10.9	10.9	0.4	18.2	97.2	0.4	8.3	74.5	0.4	4.1	70.1	0.6	9.4	26.8
Na	4.9	7.5	17.3	3.7	6.0	6.0	4.7	9.8	15.8	4.4	12.3	20.1	6.6	9.8	14.6	3.3	7.8	18.2
P	0.1	4.2	8.9	1.1	10.4	10.4	0.1	6.4	20.1	0.1	6.8	19.0	3.8	11.2	21.8	1.7	7.7	16.2
S	3.1	5.2	7.7	4.5	6.8	6.8	3.9	7.2	9.8	3.5	5.8	10.4	3.2	5.1	13.1	4.6	6.4	11.2
Zn	191	1470	2287	286	1274	1274	98	761	2152	279	660	2045	407	1175	3342	108	637	1791

DCA ordination of the total data set, all reference areas included

All fifty sample plots from the Lund reference area were clearly separated from sample plots of the other reference areas in the DCA ordination, all restricted to low DCA axis 1 scores (Fig. 406). The other reference areas formed a cluster at medium to high axis 1 scores. Sample plots from Dividalen obtained the highest median score. The sample plots from Lund occupied a narrow interval along DCA axis 2 while sample plots from Møsvatn almost spanned the entire second ordination axis.

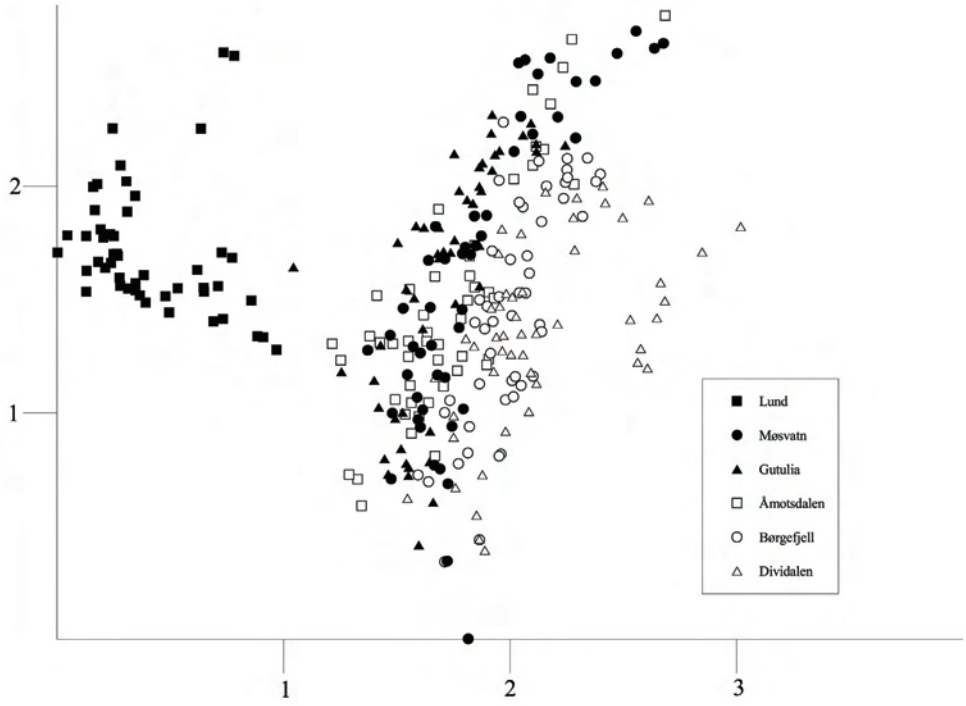

Fig. 406. DCA ordination of the total dataset of 300 meso plots from all reference areas, axes 1 (horizontal) and 2 (vertical). Scaling of axes in S.D. units.

DCA ordination of five reference areas, sample plots from Lund excluded

In a DCA ordination without sample plots from Lund, sample plots from the other reference areas mixed almost completely along DCA axis 1, but less so along DCA axis 2 (Fig. 407). Sample plots from Dividalen obtained the lowest values along the second ordination axis, followed by sample plots from Åmotsdalen, Gutulia, Møsvatn and Børgefjell. Sample plots from Møsvatn were restricted to a small part of the ordination space, DCA axis 2 scores increasing with increasing DCA axis 1 scores (Fig. 407).

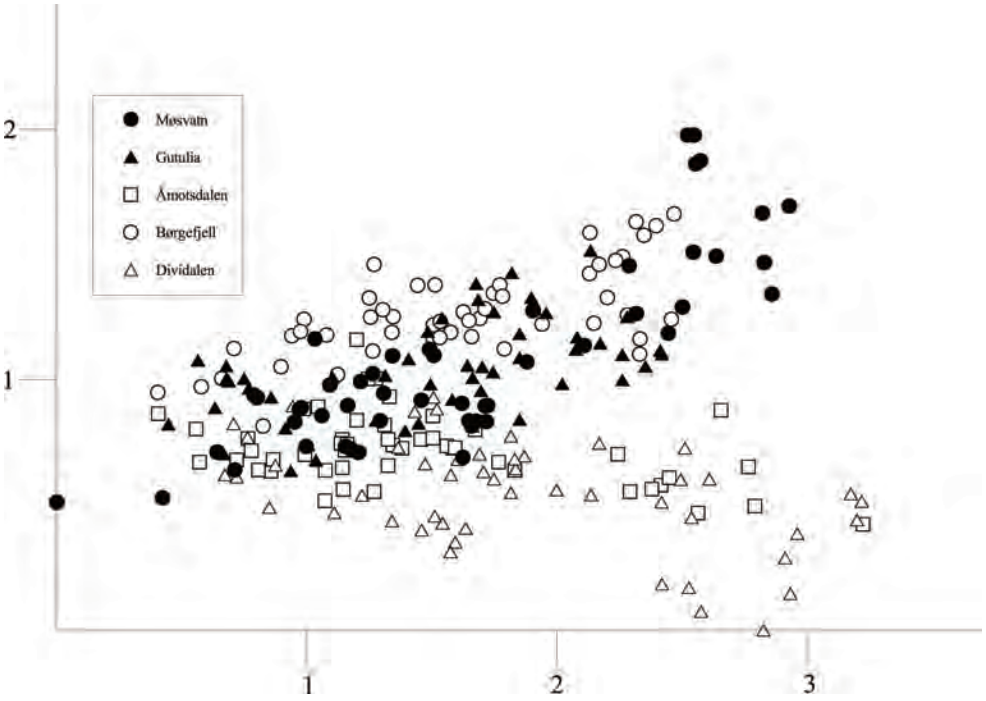

Fig. 407. DCA ordination of 250 meso plots from all reference areas except Lund, axes 1 (horizontal) and 2 (vertical). Scaling of axes in S.D. units.

Correlations between DCA axes (sample plots from Lund excluded) and local and regional climatic/geographical variables

Soil pH and extractable C, Ca, Mn and S concentrations and total N were the variables most strongly positively correlated with DCA axis 1, while exchangeable H and loss on ignition were most strongly negatively correlated, all with $|\tau| > 0.3$ (Table 22). Extractable Mn and S were also strongly correlated with DCA axis 2, as was also effective temperature sum. Latitude was the only variable strongly negatively correlated with DCA axis 2 (Table 23).

Split-plot GLM analysis of relationships between ordination axes and environmental variables

Variation (in plot scores) along DCA axis 1 was partitioned with 4.30 % at the area scale (i.e. between areas), 89.15 % at the macro-plot scale (i.e. between macro plots) and 6.55 % at the (between) meso plot scale within macro plots (Table 22). Along the second ordination axis, 55.21 % of the variation was explained at the between area scale, 36.35 % at the macro-plot scale and 8.44 % at the plot scale (Table 23)

At the area scale, four variables were significantly (at the $\alpha = 0.05$ level) related to DCA 1, while two variables (also at the $\alpha = 0.05$ level) were related to DCA 2. At the macro plot scale level, fifteen environmental variables were significantly related to DCA 1 and twelve variables to DCA 2 (Tables 22 and 23). At the plot scale level, nine environmental variables were significantly related to DCA 1 and four variables to DCA 2 (Tables 22 and 23).

At the area scale, DCA 1 was positively related to the concentration of Al, Na and P and negatively related to meso plot terrain form (at the $\alpha = 0.05$ level). At the macro-plot scale, altitude, macro and meso plot slope, tree basal area, pH and soil concentrations of C, Ca, K, Mn, Na, S and Zn increased significantly along DCA 1 while loss on ignition and exchangeable H decreased. At the plot scale, many of these variables showed the same tendencies. Predictors which were significantly related to DCA 1 at the macro plot but not at the plot scale were macro and meso plot slope, tree basal area and concentrations of K and Na.

The only variables significantly related (at the $\alpha = 0.05$ level) to DCA axis 2 at the area scale (both positively) were the concentrations of Na and P. At the macro-plot scale, DCA 2 was positively related to macro and meso plot aspect unfavourability, meso plot uneveness and soil concentrations of C, K Mn, Na, S and Zn and negatively related to meso plot heat index, minimum soil depth and altitude. At the plot level, DCA 2 was positively significant related to soil concentrations of Mn, S and Zn and negatively related to maximum soil depth (Table 23).

Table 22. The total data set with sample plots from Lund excluded: Split-plot GLM analysis with three levels and Kendall's nonparametric correlation coefficient τ between DCA 1 and 31 environmental variables and 7 regional variables (predictors) in the 50 plots. df_{resid}: degrees of freedom for the residuals; *SS*: total variation; *FVE*: fraction of total variation attributable to a given scale (area, macro plot or plot); SS_{expl}/SS: fraction of the variation attributable to the scale in question, explained by a variable; *r*: model coefficient (only given when significant at the $\alpha = 0.05$ level, otherwise blank); *F*: *F* statistic for test of the hypothesis that $r = 0$ against the two-tailed alternative. * no variation on this scale level. Split-plot GLM relationships significant at level $\alpha = 0.05$, *P*, *F*, *r* and SS_{expl}/SS, and Kendall's nonparametric correlation coefficient $|\tau| \geq 0.30$ are given in bold face. Numbers and abbreviations for names of environmental variables are in accordance with Table 2.

Predictor	Dependent variable = DCA 1 (*SS* = 105.8581)												Correlastion between predictor and DCA 1
	Error level												
	Area $df_{resid} = 3$ $SS_{macro\ plot} = 4.5545$ *FVE* = 0.0430 of *SS*				Macro plot within area $df_{resid} = 44$ $SS_{macro\ plot} = 94.3710$ *FVE* = 0.8915 of *SS*				Plot within macro plot $df_{resid} = 199$ $SS_{plot} = 6.9326$ *FVE* = 0.0655 of *SS*				*Total*
	SS_{expl}/SS_{areat}	*r*	*F*	*P*	$SS_{expl}/SS_{macroplot}$	*r*	*F*	*P*	SS_{expl}/SS_{plot}	*r*	*F*	*P*	τ
Ma Slo	0.2694		1.1061	0.3702	**0.1192**	**1.2737**	**6.0909**	**0.0186**	0.0017		0.3107	0.5780	0.186
Ma Asp	0.0346		0.1074	0.7647	0.0799		4.0130	0.0529	0.0003		0.0530	0.8182	0.140
Ma HI	0.2270		0.8811	0.4172	0.0068		0.3081	0.5824	0.0026		0.4769	0.4908	–0.061
Ma Ter	0.5284		3.3611	0.1641	0.0007		0.0307	0.8619	0.0023		0.4241	0.5159	0.006
Ma Une	0.2774		1.1519	0.3618	0.0126		0.5881	0.4483	0.0023		0.4330	0.5115	–0.032
TBA	0.0001		0.0003	0.9863	**0.3847**	**1.7491**	**27.7050**	**0.0000**	0.0010		0.1858	0.6670	0.292
Me Slo	0.7648		9.7532	0.0524	**0.1103**	**1.5618**	**5.8314**	**0.0211**	0.0031		0.5845	0.4457	0.055
Me Asp	0.0375		0.1169	0.7550	0.0251		1.1606	0.2887	0.0062		1.1655	0.2820	0.066
Me HI	0.2243		0.8674	0.4204	0.0050		0.2230	0.6397	0.0013		0.2391	0.6255	–0.034
Me Ter	**0.8788**	**–1.8439**	**21.7500**	**0.0186**	0.0743		3.6649	0.0638	0.0020		0.3724	0.5426	–0.091
Me Une	0.3404		1.5483	0.3017	0.0060		0.2784	0.6011	0.0108		2.0431	0.1549	–0.016
Smi	0.4208		2.1793	0.2364	0.0431		2.0080	0.1653	0.0022		0.4140	0.5208	–0.087
Sme	0.2838		1.1890	0.3553	0.0120		0.5487	0.4638	0.0051		0.9506	0.3311	–0.046
Sma	0.7477		8.8897	0.0585	0.0001		0.0069	0.9343	0.0177		3.3323	0.0698	–0.072
Mme	0.0836		0.2737	0.6370	0.0394		1.8423	0.1834	0.0160		3.0406	0.0831	–0.038
LOI	0.4422		2.3782	0.2207	**0.5008**	**–1.4731**	**44.0771**	**0.0000**	**0.0331**	**–0.2366**	**6.3761**	**0.0126**	**–0.418**
Total N	0.4030		2.0255	0.2499	**0.5748**	**2.4789**	**67.6840**	**0.0000**	**0.0288**	**0.2658**	**5.5500**	**0.0197**	**0.383**

$pH_{(H2O)}$	0.0496		0.1566	0.7187	**0.7287**	**2.0025**	**114.8530**	**0.0000**	**0.0889**	**0.4606**	**18.0236**	**0.0000**	**0.577**
pH_{CaCl2}	0.0898		0.2961	0.6242	**0.7383**	**1.9931**	**125.2308**	**0.0000**	**0.0858**	**0.4072**	**17.0468**	**0.0001**	**0.591**
H	0.0930		0.3076	0.6178	**0.5646**	**–2.0025**	**57.1259**	**0.0000**	**0.0520**	**–0.2892**	**10.0720**	**0.0018**	**–0.486**
Al	**0.8325**	**3.4700**	**14.9080**	**0.0307**	0.0243		1.1040	0.3006	0.0058		1.0895	0.2982	–0.075
C	0.4148		2.1261	0.2409	**0.4731**	**1.7803**	**38.0929**	**0.0000**	**0.0521**	**0.3462**	**10.3243**	**0.0016**	**0.439**
Ca	0.0204		0.0625	0.8187	**0.5264**	**2.4185**	**47.0737**	**0.0000**	**0.0552**	**0.3513**	**10.8302**	**0.0012**	**0.434**
Fe	0.1319		0.4560	0.5479	0.0152		0.6847	0.4136	0.0000		0.0002	0.9902	–0.055
K	0.2058		0.7774	0.4429	**0.1097**	**0.8832**	**5.5119**	**0.0247**	0.0182		3.5279	0.0622	0.240
Mg	0.0243		0.0746	0.8025	0.0379		1.7451	0.1951	0.0000		0.0060	0.9381	0.110
Mn	0.3495		1.6120	0.2937	**0.5961**	**1.6332**	**68.5629**	**0.0000**	**0.0955**	**0.5316**	**19.5841**	**0.0000**	**0.512**
Na	**0.9046**	**2.7121**	**28.4320**	**0.0129**	**0.2309**	**1.5901**	**14.3091**	**0.0006**	0.0037		0.6906	0.4072	0.296
P	**0.7920**	**3.3161**	**11.4250**	**0.0431**	0.0307		1.4442	0.2375	0.0005		0.0948	0.7586	–0.051
S	0.2726		1.1242	0.3668	**0.6805**	**2.2954**	**91.7113**	**0.0000**	**0.0881**	**0.4394**	**18.0693**	**0.0000**	**0.534**
Zn	0.0173		0.0528	0.8331	**0.1646**	**0.8386**	**8.3288**	**0.0066**	**0.0554**	**0.3276**	**10.8722**	**0.0012**	0.256
Prec.	0.4179		2.1538	0.2385	*	*	*	*	*	*	*	*	–0.083
T	0.2349		0.9210	0.4080	*	*	*	*	*	*	*	*	–0.075
ETS	0.3074		1.3314	0.3321	*	*	*	*	*	*	*	*	–0.053
Tamm's H	0.2351		0.9222	0.4077	*	*	*	*	*	*	*	*	–0.075
Lat.	0.5179		3.2229	0.1705	*	*	*	*	*	*	*	*	0.079
Long.	0.5354		3.4578	0.1599	*	*	*	*	*	*	*	*	0.101
Alt.	0.3303		1.4795	0.3108	**0.0769**	**–0.0078**	**4.2462**	**0.0468**	*	*	*	*	–0.155

Table 23. The total data set with sample plots from Lund excluded: Split-plot GLM analysis with three levels and Kendall's nonparametric correlation coefficient τ between DCA 1 and 31 environmental variables and 7 regional variables (predictors) in the 50 plots. df_{resid}: degrees of freedom for the residuals; *SS*: total variation; *FVE*: fraction of total variation attributable to a given scale (area, macro plot or plot); SS_{expl}/SS: fraction of the variation attributable to the scale in question, explained by a variable; *r*: model coefficient (only given when significant at the $\alpha = 0.05$ level, otherwise blank); *F*: *F* statistic for test of the hypothesis that $r = 0$ against the two-tailed alternative. * no variation on this scale level. Split-plot GLM relationships significant at level $\alpha = 0.05$, *P*, *F*, *r* and SS_{expl}/SS, and Kendall's nonparametric correlation coefficient $|\tau| \geq 0.30$ are given in bold face. Numbers and abbreviations for names of environmental variables are in accordance with Table 2.

Predictor	Dependent variable = DCA 2 (*SS* = 30.1342)												Correlastion between predictor and DCA 2
	Error level												
	Area $df_{resid} = 3$ $SS_{macro\ plot} = 16.6378$ *FVE* = 0.5521 of *SS*				Macro plot within area $df_{resid} = 44$ $SS_{macro\ plot} = 10.9532$ *FVE* = 0.3635 of *SS*				Plot within macro plot $df_{resid} = 199$ $SS_{plot} = 2.5432$ *FVE* = 0.0844 of *SS*				*Total*
	SS_{expl}/SS_{areat}	*r*	*F*	*P*	$SS_{expl}/SS_{macroplot}$	*r*	*F*	*P*	SS_{expl}/SS_{plot}	*r*	*F*	*P*	τ
Ma Slo	0.0874		0.2873	0.6291	0.0475		2.1484	0.1516	0.0003		0.0539	0.8168	0.080
Ma Asp	0.1518		0.5369	0.5168	**0.0979**	**0.4129**	**4.6759**	**0.0375**	0.0063		1.2234	0.2704	0.093
Ma HI	0.0046		0.0137	0.9141	0.0727		3.1697	0.0837	0.0005		0.0981	0.7545	–0.079
Ma Ter	0.0335		0.1041	0.7681	0.0062		0.2436	0.6247	0.0033		0.6443	0.4234	0.028
Ma Une	0.0274		0.0846	0.7900	0.0303		1.1963	0.2815	0.0001		0.0178	0.8940	0.009
TBA	0.2167		0.8302	0.4294	0.0949		4.0427	0.0521	0.0000		0.0049	0.9441	0.070
Me Slo	0.4751		2.7159	0.1979	0.0504		2.1734	0.1494	0.0001		0.0109	0.9168	0.277
Me Asp	0.0221		0.0677	0.8115	**0.1115**	**0.5441**	**5.1980**	**0.0288**	0.0027		0.5201	0.4719	0.061
Me HI	0.0592		0.1889	0.6932	**0.1261**	**–0.5836**	**5.8388**	**0.0210**	0.0001		0.0136	0.9073	–0.097
Me Ter	0.4435		2.3911	0.2198	0.0766		3.2946	0.0781	0.0181		3.5758	0.0605	0.010
Me Une	0.1282		0.4413	0.5540	**0.0987**	**0.3694**	**4.1317**	**0.0497**	0.0003		0.0527	0.8187	0.090
Smi	0.2200		0.8464	0.4254	**0.1174**	**–0.3621**	**5.2485**	**0.0281**	0.0023		0.4472	0.5046	–0.081
Sme	0.7705		10.0720	0.0503	0.0524		2.2229	0.1449	0.0003		0.0627	0.8025	–0.122
Sma	0.4305		2.2675	0.2292	0.0014		0.0552	0.8156	**0.0334**	**–0.1107**	**6.6331**	**0.0109**	0.211
Mme	0.0037		0.0110	0.9230	0.0101		0.3976	0.5325	0.0078		1.5110	0.2208	–0.053
LOI	0.1861		0.6857	0.4683	0.0358		1.4477	0.2370	0.0003		0.0573	0.8111	–0.055
Total N	0.4125		2.1061	0.2426	0.0551		2.2213	0.1451	0.0031		0.6017	0.4391	0.172
$pH_{(H2O)}$	0.0079		0.0240	0.8867	0.0510		2.0731	0.1588	0.0003		0.0574	0.8110	0.081

pH_{CaCl2}	0.0383		0.1194	0.7525	0.0635		2.6144	0.1149	0.0050		0.9723	0.3256	0.086
H	0.0001		0.0004	0.9855	0.0658		2.7068	0.1089	0.0041		0.7987	0.3728	–0.095
Al	0.2152		0.8225	0.4313	0.0005		0.0207	0.8863	0.0024		0.4646	0.4965	–0.050
C	0.0435		0.1366	0.7363	**0.1192**	**0.3367**	**5.2907**	**0.0275**	0.0001		0.0151	0.9023	0.117
Ca	0.3071		1.3300	0.3324	0.0201		0.7950	0.3787	0.0061		1.2042	0.2741	0.037
Fe	0.4521		2.4752	0.2137	0.0150		0.6006	0.4435	0.0008		0.1649	0.6852	0.077
K	0.2058		0.7774	0.4429	**0.1097**	**0.8832**	**5.5119**	**0.0247**	0.0182		3.5279	0.0622	0.240
Mg	0.0243		0.0746	0.8025	0.0379		1.7451	0.1951	0.0000		0.0060	0.9381	0.110
Mn	0.3495		1.6120	0.2937	**0.5961**	**1.6332**	**68.5629**	**0.0000**	**0.0955**	**0.5316**	**19.5841**	**0.0000**	**0.512**
Na	**0.9046**	**2.7121**	**28.4320**	**0.0129**	**0.2309**	**1.5901**	**14.3091**	**0.0006**	0.0037		0.6906	0.4072	0.296
P	**0.7920**	**3.3161**	**11.4250**	**0.0431**	0.0307		1.4442	0.2375	0.0005		0.0948	0.7586	–0.051
S	0.2726		1.1242	0.3668	**0.6805**	**2.2954**	**91.7113**	**0.0000**	**0.0881**	**0.4394**	**18.0693**	**0.0000**	**0.534**
Zn	0.0173		0.0528	0.8331	**0.1646**	**0.8386**	**8.3288**	**0.0066**	**0.0554**	**0.3276**	**10.8722**	**0.0012**	0.256
Prec.	0.4179		2.1538	0.2385	*	*	*	*	*	*	*	*	0.266
T	0.2349		0.9210	0.4080	*	*	*	*	*	*	*	*	–0.065
ETS	0.3074		1.3314	0.3321	*	*	*	*	*	*	*	*	**0.372**
Tamm's H	0.2351		0.9222	0.4077	*	*	*	*	*	*	*	*	–0.065
Lat.	0.5179		3.2229	0.1705	*	*	*	*	*	*	*	*	**–0.311**
Long.	0.5354		3.4578	0.1599	*	*	*	*	*	*	*	*	–0.198
Alt.	0.3303		1.4795	0.3108	**0.0769**	**–0.0078**	**4.2462**	**0.0468**	*	*	*	*	0.062

Partial DCA ordination (sample plots from Lund excluded) with variation due to regional climatic/geographical variables partialled out

The partial DCA with the 7 climatic/geographical variables as covariables (compare Figs 407 and 408) had a shorter first DCA axis (gradient length in S.D. units) while DCA axis 2 had approximately the same gradient length in both ordinations. Plots were largely similarly distributed in the ordination diagrams, but some differences existed. In the partial DCA ordination the Møsvatn plots did not span the entire DCA 1 axis, but were not represented among plots with the highest DCA 1 scores. Sample plots from Gutulia obtained generally higher scores along DCA axis 2 in the partial ordination, mixing with sample plots from Børgefjell. Correlations between corresponding axes in the two DCA ordinations were high; $\tau = 0.743$ for the first and $\tau = 0.605$ for the second axes.

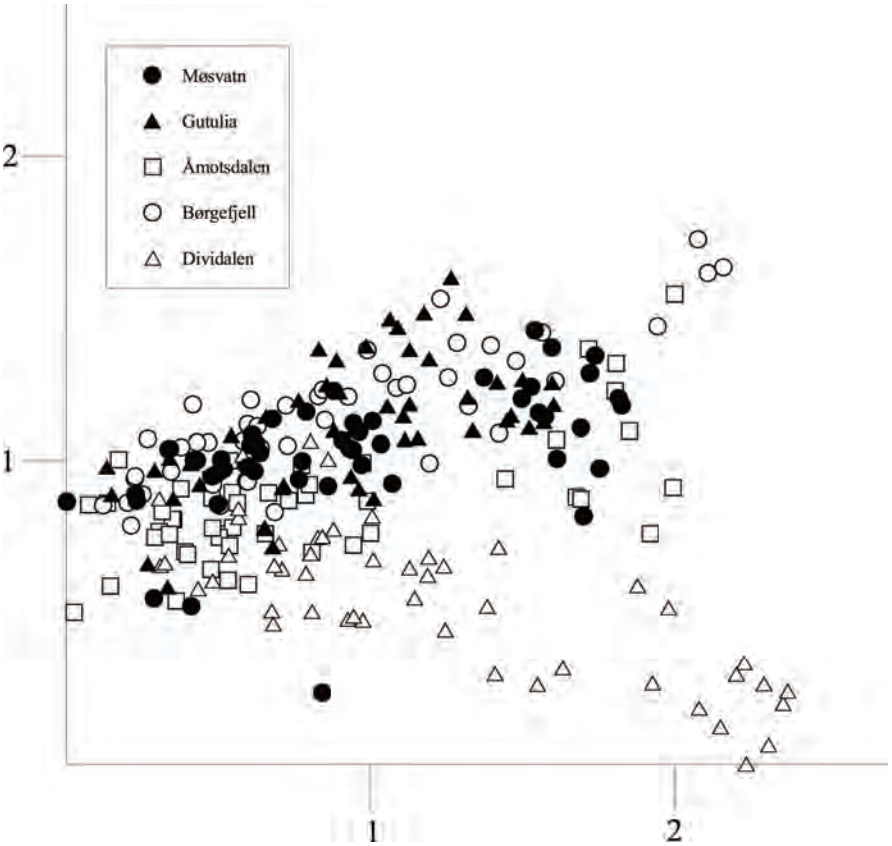

Fig. 408. DCA ordination of 250 meso plots from all reference areas (without Lund), with 7 CCA axes that represent variation exclusively explained by regional climatic/geographical variables as covariables, axes 1 (horizontal) and 2 (vertical). Scaling of axes in S.D. units.

Correlations between partial DCA ordination axes (sample plots from Lund excluded) with variation due to regional climatic/geographical variables partialled out, and local environmental variables

The relationships between partial DCA axes and explanatory variables (Tables 24 and 25) closely resembled those of the ordinary DCA ordination (without covariables; Tables 22 and 23).

Split-plot GLM analysis of relationships between partial ordination axes and environmental variables

Variation (in plot scores) along partial DCA axis 1 was partitioned with 6.16 % at the area scale (i.e. between areas), 83.93 % at the macro-plot scale (i.e. between macro plots) and 9.91 % at the (between) meso plot scale within macro plots (Table 24). Along the second partial ordination axis, 49.62 % of the variation was explained at the between-area scale, 39.63 % at the macro-plot scale and 10.74 % at the plot scale (Table 25).

At the area scale, three variables were significantly (at the $\alpha = 0.05$ level) related to partial DCA axis 1, while no variables (also at the $\alpha = 0.05$ level) were related to partial DCA axis 2. At the macro plot scale level, seventeen environmental variables were significantly related to partial DCA axis 1 and nine variables to partial DCA axis 2 (Tables 24 and 25). At the plot scale level, ten environmental variables were significantly related to partial DCA axis 1 and seven variables to partial DCA axis 2 (Tables 24 and 25).

At the area scale, partial DCA axis 1 was positively related to the concentration of P and negatively related to meso plot slope and terrain form (at the $\alpha = 0.05$ level). At the macro-plot scale, macro and meso plot slope, macro plot aspect unfavourability, tree basal area, pH, Total N and soil concentrations of, C, Ca, K, Mn, Na, S and Zn increased significantly along partial DCA axis 1 while soil moisture, loss on ignition and exchangeable H decreased. At the plot scale, meso plot uneveness, maximum soil depth, pH, Total N and soil concentrations of, C, Ca, K, Mn, and S increased significantly along partial DCA axis 1 while loss on ignition and exchangeable H decreased.

At the area scale, partial DCA axis 2 was not significant related at the $\alpha = 0.05$ level to any of the measured variables. At the macro-plot scale, partial DCA axis 2 was positively related to tree basal area, meso plot slope and soil concentrations of C, K, Mg, Mn and S and negatively related to median soil depth and loss on ignition. At the plot level, partial DCA axis 2 was positively significant related to tree basal area and soil concentrations of Ca, K and Mg and negatively related to maximum soil depth and exchangeable H and extractable Al (Table 25).

Table 24. Partial DCA ordination of the total data set with sample plots from Lund excluded (variation due to 7 regional variables partialled out): Split-plot GLM analysis with three levels and Kendall's nonparametric correlation coefficient τ between DCA 1 and 31 environmental variables and 7 regional variables (predictors) in the 50 plots. df_{resid}: degrees of freedom for the residuals; *SS*: total variation; *FVE*: fraction of total variation attributable to a given scale (area, macro plot or plot); SS_{expl}/SS: fraction of the variation attributable to the scale in question, explained by a variable; *r*: model coefficient (only given when significant at the $\alpha = 0.05$ level, otherwise blank); *F*: *F* statistic for test of the hypothesis that $r = 0$ against the two-tailed alternative. * no variation on this scale level. Split-plot GLM relationships significant at level $\alpha = 0.05$, *P*, *F*, *r* and SS_{expl}/SS, and Kendall's nonparametric correlation coefficient $|\tau| \geq 0.30$ are given in bold face. Numbers and abbreviations for names of environmental variables are in accordance with Table 2.

	Dependent variable = DCA 1 (*SS* = 76.0027)												Correlastion between predictor and DCA 1
	Error level												
Predictor	Area $df_{resid} = 3$ $SS_{macro\ plot} = 4.6835$ *FVE* = 0.0616 of *SS*				Macro plot within area $df_{resid} = 44$ $SS_{macro\ plot} = 63.7860$ *FVE* = 0.8393 of *SS*				Plot within macro plot $df_{resid} = 199$ $SS_{plot} = 7.5332$ *FVE* = 0.0991 of *SS*				*Total*
	SS_{expl}/SS_{areat}	*r*	*F*	*P*	$SS_{expl}/SS_{macroplot}$	*r*	*F*	*P*	SS_{expl}/SS_{plot}	*r*	*F*	*P*	τ
Ma Slo	0.1748		0.6357	0.4835	**0.1859**	**0.9411**	**9.3731**	**0.0042**	0.0160		3.3110	0.0707	0.182
Ma Asp	0.0013		0.0038	0.9550	**0.1153**	**0.7066**	**5.8657**	**0.0208**	0.0000		0.0069	0.9339	0.173
Ma HI	0.1028		0.3436	0.5989	0.0145		0.6697	0.4187	0.0025		0.5112	0.4756	–0.082
Ma Ter	0.5343		3.4419	0.1606	0.0017		0.0767	0.7834	0.0022		0.4384	0.5088	0.006
Ma Une	0.1231		0.4210	0.5627	0.0582		2.8668	0.0993	0.0000		0.0091	0.9243	–0.080
TBA	0.1484		0.5225	0.5220	**0.3873**	**1.5238**	**30.7023**	**0.0000**	0.0010		0.1968	0.6579	**0.316**
Me Slo	**0.8910**	**–0.6985**	**24.5110**	**0.0158**	**0.1864**	**1.3242**	**10.0946**	**0.0031**	0.0003		0.0535	0.8174	0.066
Me Asp	0.0069		0.0209	0.8943	0.0334		1.5595	0.2200	0.0032		0.6541	0.4198	0.074
Me HI	0.3008		1.2909	0.3384	0.0043		0.1970	0.6599	0.0069		1.4051	0.2376	–0.029
Me Ter	**0.9300**	**–1.9236**	**39.8370**	**0.0080**	0.0792		3.8936	0.0564	0.0003		0.0534	0.8175	–0.098
Me Une	0.2155		0.8241	0.4309	0.0283		1.3800	0.2480	**0.0194**	**0.1686**	**4.0661**	**0.0454**	–0.012
Smi	0.6894		6.6573	0.0818	0.0543		2.5834	0.1170	0.0000		0.0025	0.9600	–0.120
Sme	0.5735		4.0342	0.1382	0.0122		0.5717	0.4546	0.0008		0.1693	0.6813	–0.060
Sma	0.6578		5.7674	0.0957	0.0000		0.0000	0.9965	**0.0412**	**0.2481**	**8.6869**	**0.0037**	–0.051
Mme	0.0023		0.0069	0.9389	**0.1009**	**–0.6781**	**4.9710**	**0.0323**	0.0069		1.4050	0.2377	–0.127
LOI	0.2463		0.9804	0.3951	**0.6154**	**–1.3247**	**68.4968**	**0.0000**	**0.2475**	**–0.6853**	**68.3389**	**0.0000**	**–0.486**
Total N	0.7285		8.0474	0.0658	**0.5659**	**2.0267**	**67.3720**	**0.0000**	**0.2544**	**0.7621**	**68.7781**	**0.0000**	**0.388**
$pH_{(H2O)}$	0.0058		0.0175	0.9032	**0.7937**	**1.7398**	**186.8828**	**0.0000**	0.3664	**0.9744**	**114.2144**	**0.0000**	**0.625**

pH_{CaCl2}	0.0004		0.0013	0.9738	**0.7727**	**1.7069**	**181.2997**	**0.0000**	0.4665	**1.1005**	**168.2823**	**0.0000**	**0.627**
H	0.0026		0.0077	0.9355	**0.6493**	**–1.8300**	**96.4307**	**0.0000**	**0.2248**	**–0.6874**	**56.6994**	**0.0000**	**–0.531**
Al	0.6065		4.6245	0.1207	0.0422		1.9859	0.1676	0.0026		0.5191	0.4723	–0.088
C	0.1336		0.4628	0.5451	**0.5099**	**1.5517**	**46.5138**	**0.0000**	**0.0767**	**0.4530**	**17.1988**	**0.0001**	**0.434**
Ca	0.0322		0.0997	0.7729	**0.6113**	**2.1373**	**66.2869**	**0.0000**	**0.1602**	**0.5947**	**37.5110**	**0.0000**	**0.467**
Fe	0.2979		1.2732	0.3413	0.0306		1.4067	0.2436	0.0000		0.0027	0.9586	–0.094
K	0.0221		0.0678	0.8114	**0.1544**	**0.9312**	**8.5041**	**0.0061**	**0.0426**	**0.3235**	**9.0543**	**0.0030**	0.279
Mg	0.0519		0.1643	0.7124	0.0726		3.4594	0.0713	0.0098		1.9923	0.1601	0.168
Mn	0.6840		6.4920	0.0841	**0.6196**	**1.3497**	**74.5841**	**0.0000**	**0.1914**	**0.8164**	**49.0223**	**0.0000**	**0.509**
Na	0.6297		5.1019	0.1091	**0.1882**	**1.1826**	**11.0747**	**0.0021**	0.0106		2.1473	0.1448	0.274
P	**0.9456**	**3.6743**	**52.1360**	**0.0055**	0.0319		1.4823	0.2316	0.0112		2.3320	0.1287	–0.052
S	0.0877		0.2884	0.6285	**0.6838**	**1.9605**	**113.9148**	**0.0000**	**0.0909**	**0.5162**	**20.9260**	**0.0000**	**0.513**
Zn	0.1532		0.5426	0.5147	**0.2756**	**0.9933**	**16.3341**	**0.0003**	0.0168		3.4379	0.0656	0.284

Table 25. Partial DCA ordination of the total data set with sample plots from Lund excluded (variation due to 7 regional variables partialled out): Split-plot GLM analysis with three levels and Kendall's nonparametric correlation coefficient τ between DCA 2 and 31 environmental variables and 7 regional variables (predictors) in the 50 plots. df_{resid}: degrees of freedom for the residuals; *SS*: total variation; *FVE*: fraction of total variation attributable to a given scale (area, macro plot or plot); SS_{expl}/SS: fraction of the variation attributable to the scale in question, explained by a variable; *r*: model coefficient (only given when significant at the $\alpha = 0.05$ level, otherwise blank); *F*: *F* statistic for test of the hypothesis that $r = 0$ against the two-tailed alternative. * no variation on this scale level. Split-plot GLM relationships significant at level $\alpha = 0.05$, *P*, *F*, *r* and SS_{expl}/SS, and Kendall's nonparametric correlation coefficient $|\tau| \geq 0.30$ are given in bold face. Numbers and abbreviations for names of environmental variables are in accordance with Table 2.

	Dependent variable = DCA 2 (*SS* = 23.5077)												Correlastion between predictor and DCA 2
	Error level												
Predictor	Area $df_{resid} = 3$ $SS_{macro\ plot} = 11.6650$ *FVE* = 0.4962 of *SS*				Macro plot within area $df_{resid} = 44$ $SS_{macro\ plot} = 9.3172$ *FVE* = 0.3963 of *SS*				Plot within macro plot $df_{resid} = 199$ $SS_{plot} = 2.5255$ *FVE* = 0.1074 of *SS*				*Total*
	SS_{expl}/SS_{areat}	*r*	*F*	*P*	$SS_{expl}/SS_{macroplot}$	*r*	*F*	*P*	SS_{expl}/SS_{plot}	*r*	*F*	*P*	τ
Ma Slo	0.0057		0.0173	0.9037	0.0521		2.1842	0.1484	0.0006		0.1168	0.7330	0.120
Ma Asp	0.0458		0.1440	0.7296	0.0722		3.1263	0.0858	0.0007		0.1259	0.7232	0.127
Ma HI	0.0172		0.0525	0.8336	0.0007		0.0237	0.8785	0.0016		0.3108	0.5780	–0.005
Ma Ter	0.0023		0.0068	0.9396	0.0093		0.3379	0.5648	0.0023		0.4468	0.5049	0.003
Ma Une	0.1276		0.4388	0.5550	0.0037		0.1345	0.7160	0.0126		2.4372	0.1205	–0.050
TBA	0.0824		0.2693	0.6396	**0.2444**	**0.5453**	**12.5646**	**0.0011**	**0.0256**	**0.0762**	**4.9631**	**0.0273**	0.181
Me Slo	0.6969		6.8973	0.0786	**0.1483**	**0.6719**	**6.9111**	**0.0126**	0.0006		0.1156	0.7343	**0.338**
Me Asp	0.0777		0.2527	0.6498	0.0282		1.0761	0.3067	0.0002		0.0473	0.8281	0.058
Me HI	0.1054		0.3536	0.5939	0.0002		0.0062	0.9376	0.0035		0.6777	0.4116	–0.033
Me Ter	0.7172		7.6095	0.0702	0.0053		0.1933	0.6628	0.0065		1.2493	0.2654	0.022
Me Une	0.0112		0.0341	0.8652	0.0042		0.1519	0.6990	0.0002		0.0302	0.8624	0.006
Smi	0.2906		1.2289	0.3485	0.0855		3.4434	0.0719	0.0093		1.7994	0.1817	–0.102
Sme	0.7224		7.8072	0.0682	**0.1187**	**–0.4301**	**5.1135**	**0.0301**	0.0127		2.4466	0.1198	–0.171
Sma	0.7122		7.4227	0.0723	0.0293		1.1251	0.2961	**0.0271**	**–0.0929**	**5.2595**	**0.0231**	0.176
Mme	0.0624		0.1996	0.6853	0.0246		0.9261	0.3425	0.0101		1.9279	0.1669	–0.161
LOI	0.0171		0.0522	0.8340	**0.1040**	**–0.2816**	**4.4011**	**0.0432**	0.0014		0.2602	0.6107	–0.185
Total N	0.4545		2.5000	0.2120	0.0697		2.7992	0.1032	0.0195		3.7708	0.0539	0.248

$pH_{(H2O)}$	0.0587	0.1871	0.6946	0.0853		3.5993	0.0661	0.0005		0.0867	0.7688	0.187
pH_{CaCl2}	0.1338	0.4633	0.5449	0.0829		3.5067	0.0695	0.0006		0.1107	0.7398	0.187
H	0.0389	0.1215	0.7505	0.0767		3.2103	0.0818	**0.0519**	**–0.1797**	**10.2998**	**0.0016**	–0.181
Al	0.5119	3.1469	0.1742	0.0178		0.6751	0.4169	**0.0210**	**–0.1170**	**4.0898**	**0.0448**	–0.114
C	0.2142	0.8179	0.4325	**0.1546**	**0.4277**	**7.0515**	**0.0118**	0.0000		0.0049	0.9444	0.185
Ca	0.2657	1.0854	0.3741	0.0135		0.5177	0.4766	**0.0556**	**0.2298**	**11.2499**	**0.0010**	0.122
Fe	0.4036	2.0299	0.2494	0.0074		0.2702	0.6065	0.0045		0.8725	0.3517	–0.015
K	0.0828	0.2707	0.6388	**0.3211**	**0.5769**	**18.2208**	**0.0001**	**0.0384**	**0.1241**	**7.4801**	**0.0069**	0.218
Mg	0.0402	0.1258	0.7463	**0.2775**	**0.5639**	**14.6870**	**0.0005**	**0.0502**	**0.2029**	**9.9536**	**0.0019**	0.194
Mn	0.6529	5.6431	0.0980	**0.1271**	**0.3336**	**5.7919**	**0.0215**	0.0023		0.4425	0.5069	0.242
Na	0.2778	1.1541	0.3614	0.0503		1.9153	0.1751	0.0151		2.9059	0.0902	0.049
P	0.2989	1.2789	0.3403	0.0260		0.9755	0.3301	0.0059		1.1209	0.2913	0.033
S	0.0783	0.2549	0.6484	**0.1699**	**0.4769**	**8.0191**	**0.0076**	0.0013		0.2486	0.6188	0.181
Zn	0.5816	4.1694	0.1338	0.0049		0.1793	0.6746	0.0045		0.8608	0.3549	0.050

Distribution of species abundances in the partial DCA ordination (sample plots from Lund excluded) with variation due to regional climatic/geographical variables partialled out

Species more or less restricted to plots with high scores along partial DCA axis 1 (the right side of the ordination diagram), hence showing preference for nutrient-rich sites with high soil pH, were *Bistorta vivipara* (Fig. 415), *Geranium sylvaticum* (Fig. 419), *Ranunculus acris* (Fig. 424), *Rumex acetosa* (Fig. 410), *Solidago virgaurea* (Fig. 427), *Anthoxanthum odoratum* (Fig. 431) and *Brachythecium salebrosum* (Fig. 434). The opposite pattern of distribution in the partial DCA ordination was shown by,species more or less restricted to the left-hand side of the ordination (more nutrient-poor sites) were *Arctostaphylos alpina* (Fig. 410), *Betula nana* (Fig. 409*), Calluna vulgaris* (Fig. 411), *Empetrum nigrum* (Fig. 412), *Cetraria islandica* (Fig. 444), *Cladonia furcata* (Fig. 445) and *Cladonia rangiferina* (Fig. 446).

A few species such as *Vaccinium uliginosum* (Fig. 413) and *Polytrichum juniperum* (Fig. 438) spanned the entire first axis (i.e. the entire gradient related to soil nutrient and base richness represented by variables such as pH, concentrations of Mn, Ca, etc.), but showed a clear preference for plots with low partial DCA axis 2 scores. *Barbilophozia floerkii* (Fig. 443) occurred along the entire first partial DCA axis but were concentrated to high partial DCA axis 2 scores.

The second partial DCA axis separated sample plots with high partial DCA axis 1 scores better than sample plots with low partial DCA axis 1 scores. The sample plots thus occupied a triangle-like area in the space spanned by the two first partial ordination axes (Fig. 407). Species more or less stringly restricted to plots with high partial DCA axis 1 scores (richer in nutrients) and low partial DCA axis 2 scores (characterised by low concentrations of K and total N and low tree densities), were *Bartsia alpina* (Fig. 414), *Cerastium fontanum* (Fig. 416), *Poa alpina* (Fig. 433), *Saussurea alpina* (Fig. 426) *Trollius europaeus* (Fig. 428), *Viola biflora* (Fig. 430) and *Mnium spinosum* (Fig. 436).

Species with high partial DCA scores on both axes were *Cicerbita alpina* (Fig. 417), *Oxalis acetocella* (Fig. 421), *Phegopteris connectilis* (Fig. 422), *Polygonatum verticillatum* (Fig. 423), *Polytrichastrum longisetum* (Fig. 437), *Rhytidiadelphus squarrosus* (Fig. 442) and *Veronica officinalis* (Fig. 429).

Chamaepericlymenum suecicum (Fig. 418) and *Dicranum scoparium* (Fig. 435) had a wide distributions along both partial DCA axes and were only missing in the lower, right part of the diagram.

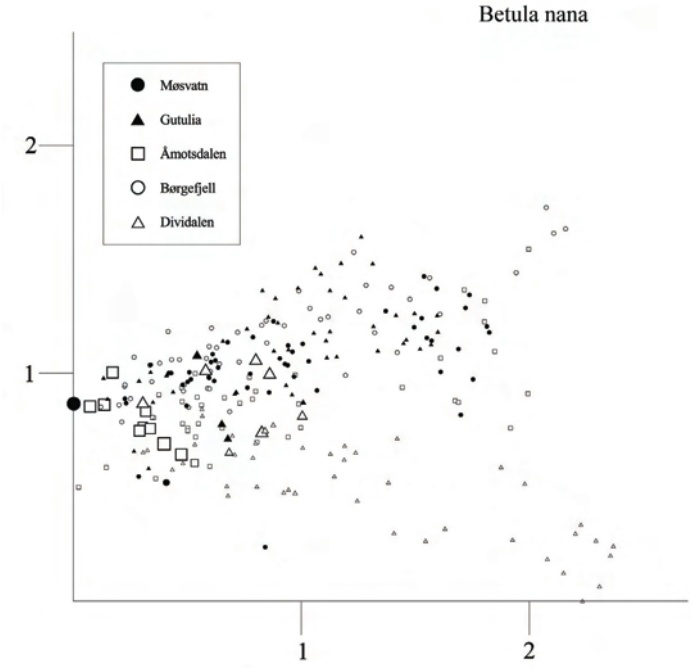

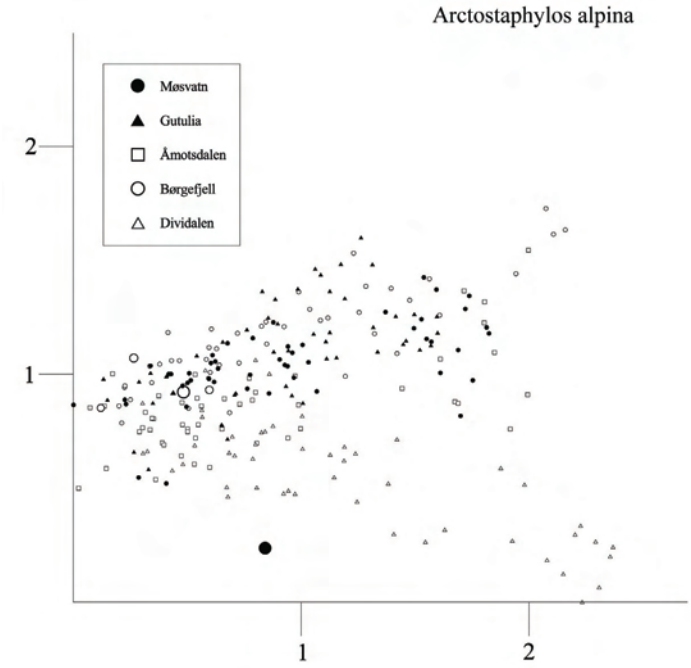

Figs 409-410. The total data set (Lund not included): distributions of species abundances in the DCA ordination of 250 sample plots, axes 1 (horizontal) and 2 (vertical).Frequency in subplots for *Betula nana* (Fig. 409) and *Arctostaphylos alpina* (Fig. 410) in each meso plot proportional to symbol size. Scaling of axes in S.D. units.

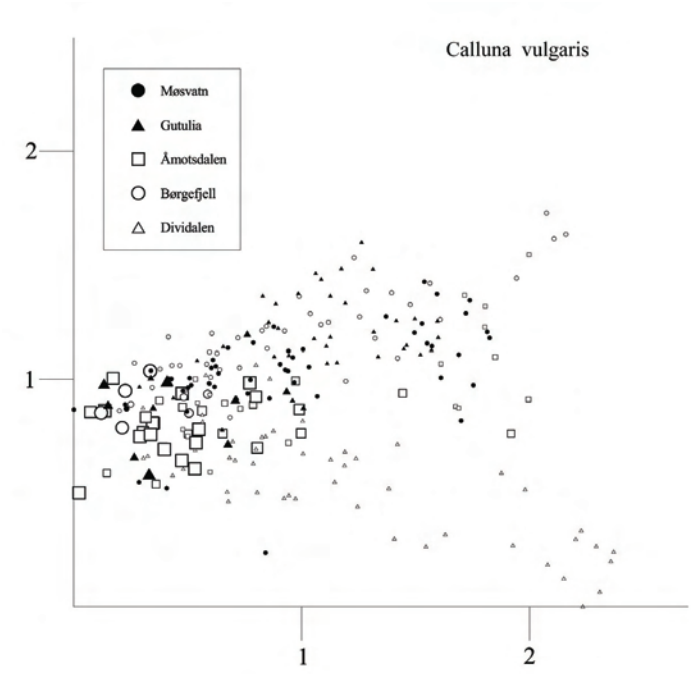

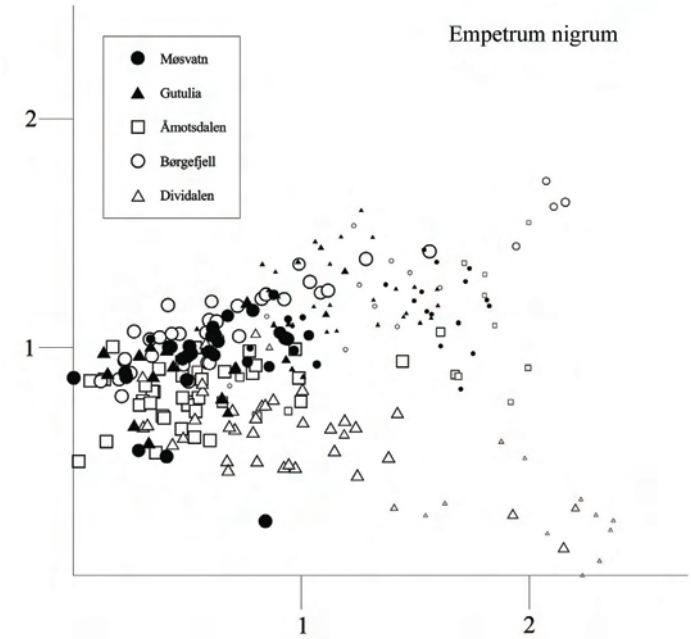

Figs 411-412. The total data set (Lund not included): distributions of species abundances in the DCA ordination of 250 sample plots, axes 1 (horizontal) and 2 (vertical). Frequency in subplots for *Calluna vulgaris* (Fig. 411) and *Empetrum nigrum* (Fig. 412) in each meso plot proportional to symbol size. Scaling in S.D. units.

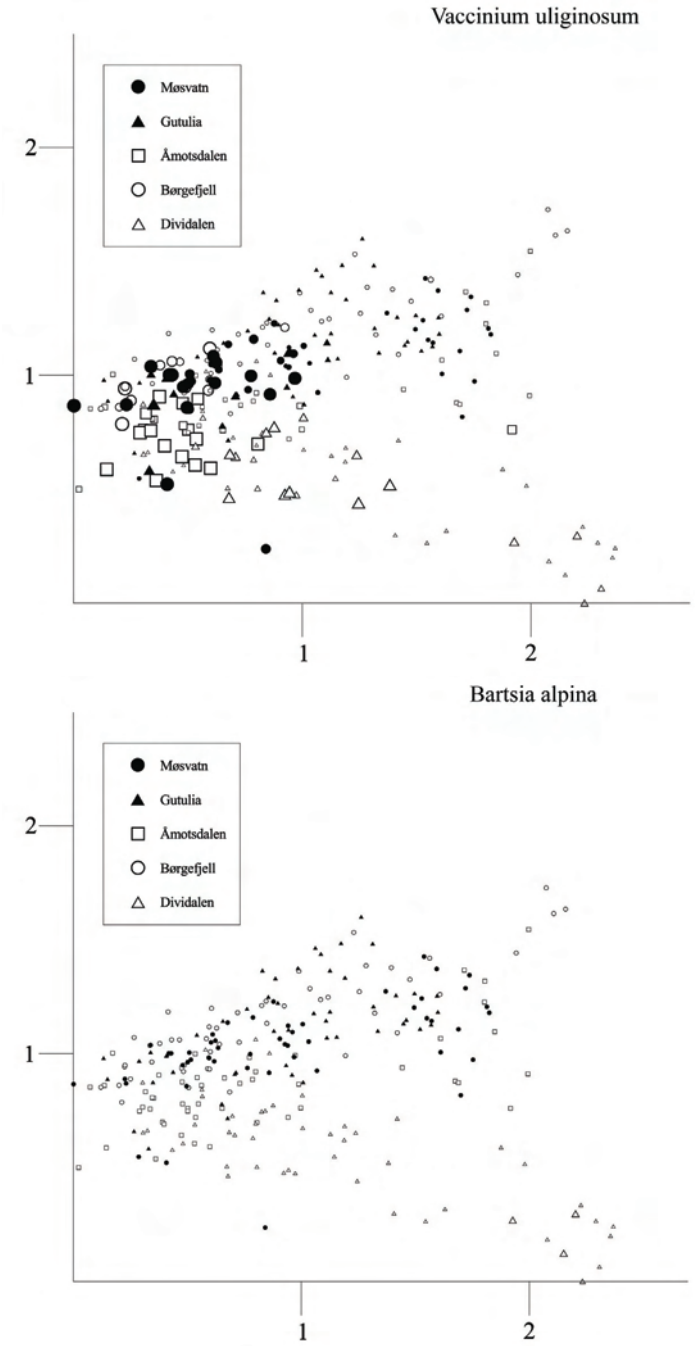

Figs 413-414. The total data set (Lund not included): distributions of species abundances in the DCA ordination of 250 sample plots, axes 1 (horizontal) and 2 (vertical). Frequency in subplots for *Vaccinium uliginosum* (Fig. 413) and *Bartsia alpina* (Fig. 414) in each meso plot proportional to symbol size. Scaling in S.D. units.

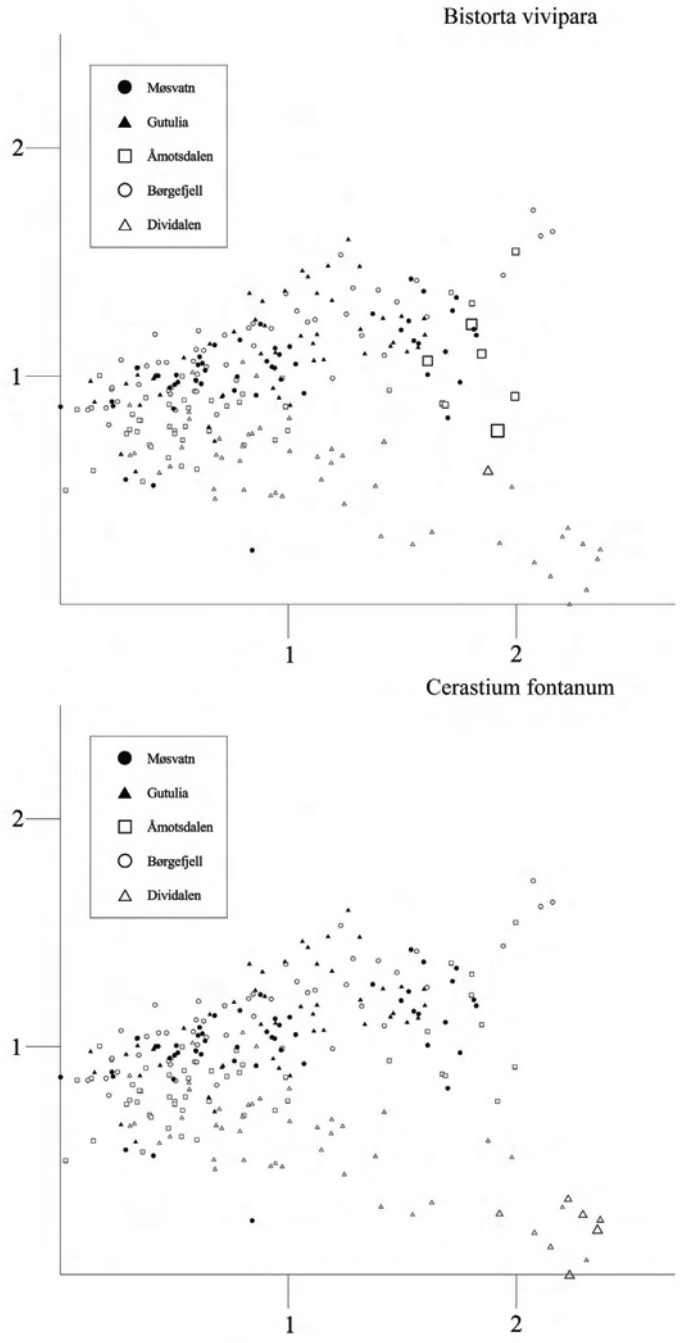

Figs 415-416. The total data set (Lund not included): distributions of species abundances in the DCA ordination of 250 sample plots, axes 1 (horizontal) and 2 (vertical). Frequency in subplots for *Bistorta vivpara* (Fig. 415) and *Cerastium fontanum* (Fig. 416) in each meso plot proportional to symbol size. Scaling in S.D. units.

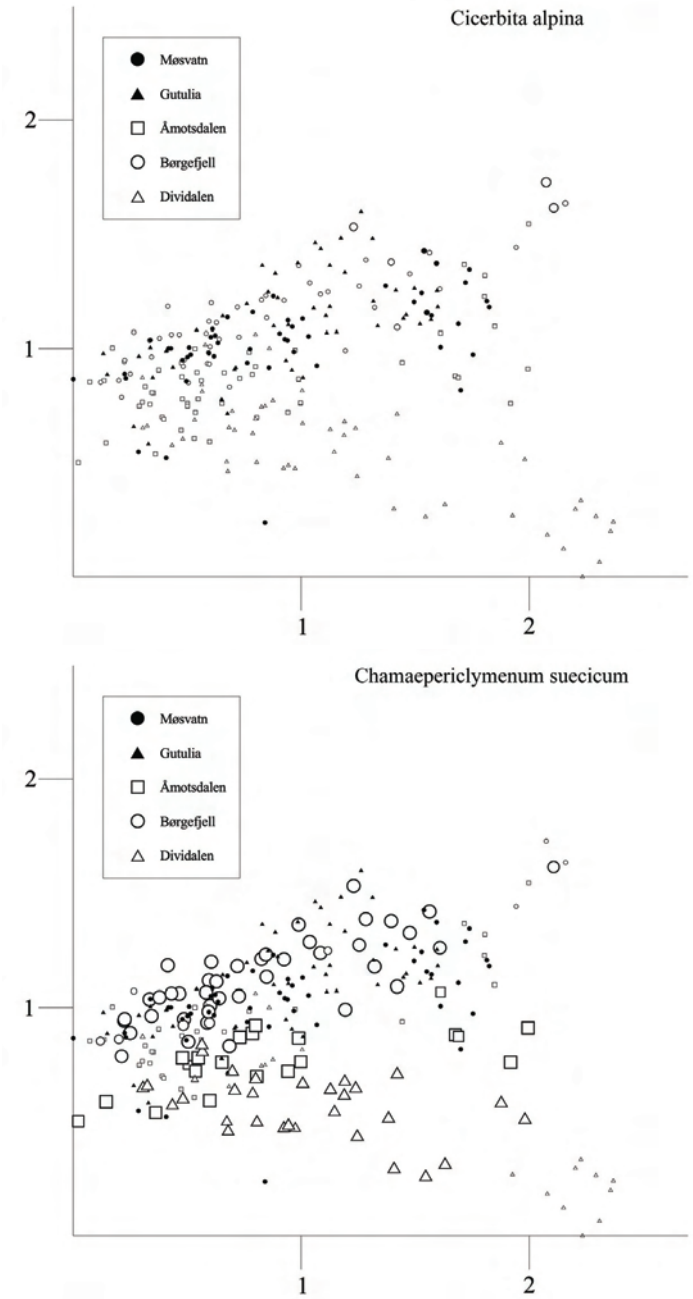

Figs 417-418. The total data set (Lund not included): distributions of species abundances in the DCA ordination of 250 sample plots, axes 1 (horizontal) and 2 (vertical). Frequency in subplots for *Cicerbita alpina* (Fig. 417) and *Chamaepericlymenum suecicum* (Fig. 418) in each meso plot proportional to symbol size. Scaling in S.D. units.

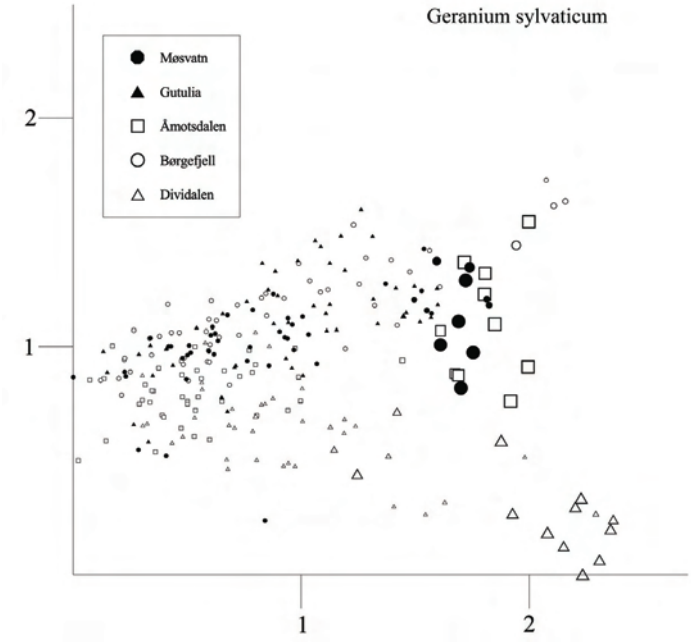

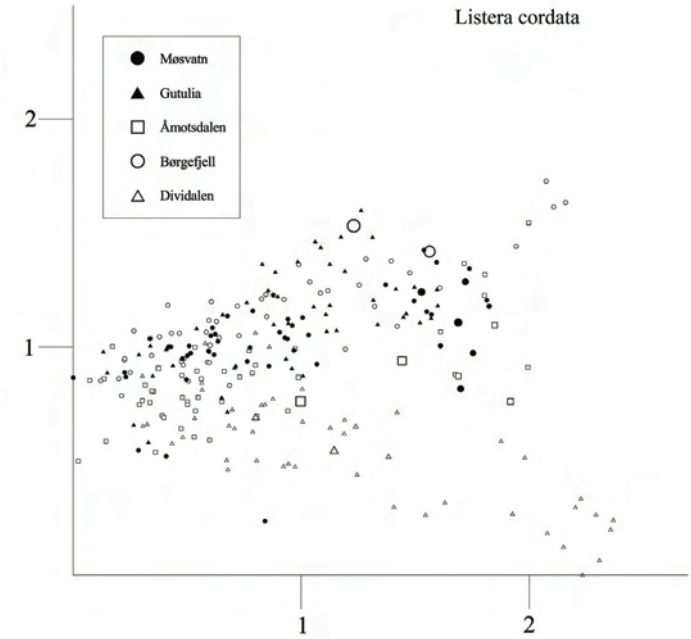

Figs 419-420. The total data set (Lund not included): distributions of species abundances in the DCA ordination of 250 sample plots, axes 1 (horizontal) and 2 (vertical). Frequency in subplots for *Geranium sylvaticum* (Fig. 419) and *Listera cordata* (Fig. 420) in each meso plot proportional to symbol size. Scaling in S.D. units.

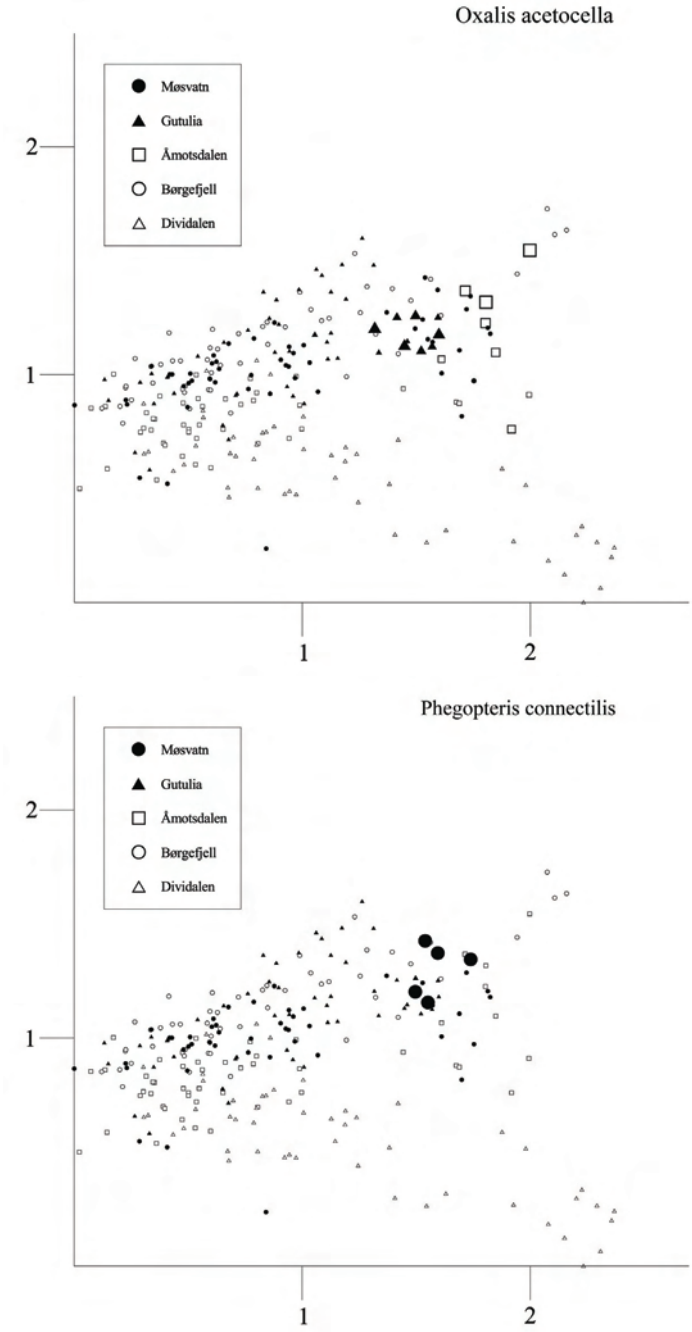

Figs 421-422. The total data set (Lund not included): distributions of species abundances in the DCA ordination of 250 sample plots, axes 1 (horizontal) and 2 (vertical). Frequency in subplots for *Oxalis acetocella* (Fig. 421) and *Phegopteris connectilis* (Fig. 422) in each meso plot proportional to symbol size. Scaling in S.D. units.

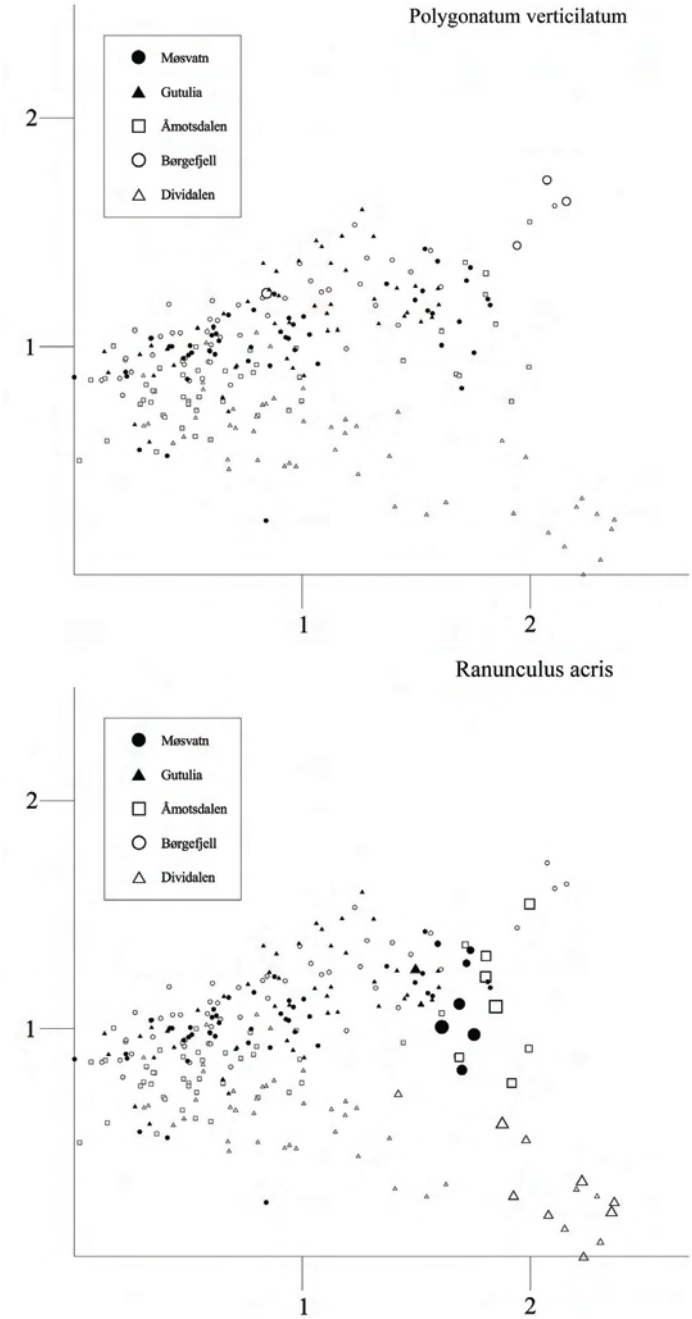

Figs 423-424. The total data set (Lund not included): distributions of species abundances in the DCA ordination of 250 sample plots, axes 1 (horizontal) and 2 (vertical). Frequency in subplots for *Polygonatum verticilatum* (Fig. 423) and *Ranunculus acris* (Fig. 424) in each meso plot proportional to symbol size. Scaling in S.D. units.

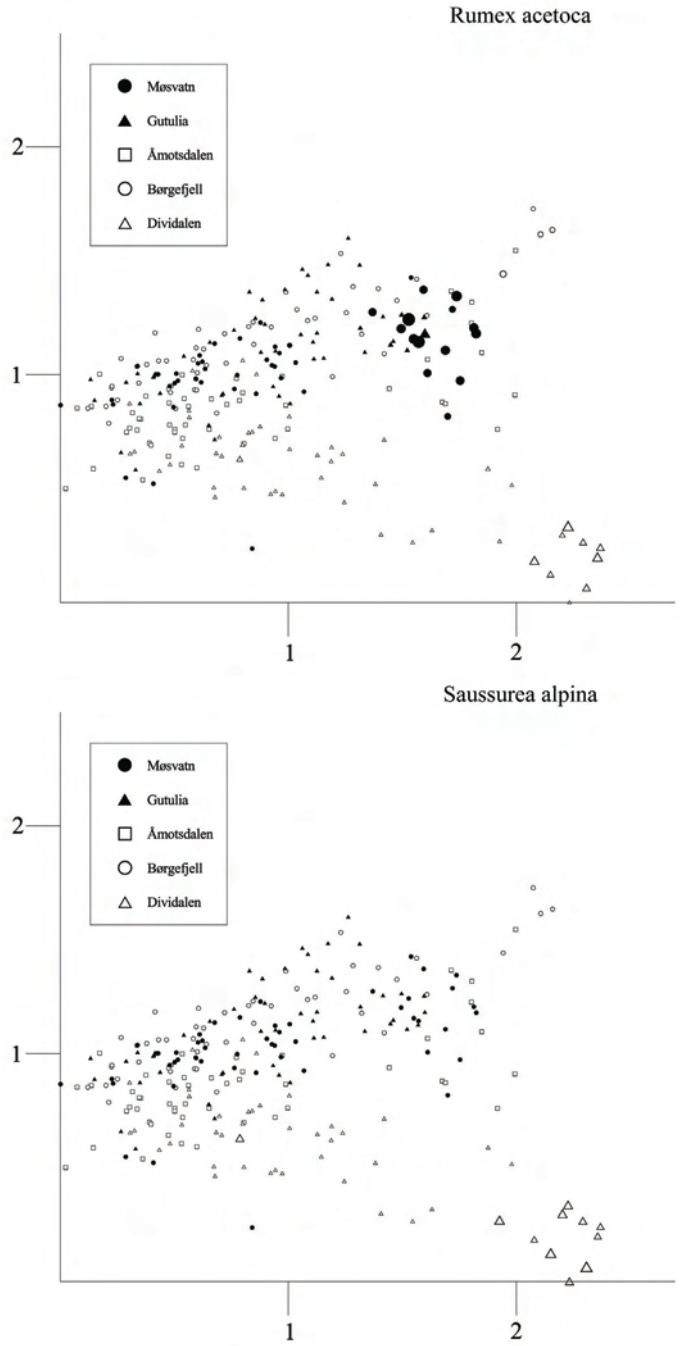

Figs 425-426. The total data set (Lund not included): distributions of species abundances in the DCA ordination of 250 sample plots, axes 1 (horizontal) and 2 (vertical). Frequency in subplots for *Rumex acetosa* (Fig. 425) and *Saussurea alpina* (Fig. 426) in each meso plot proportional to symbol size. Scaling in S.D. units.

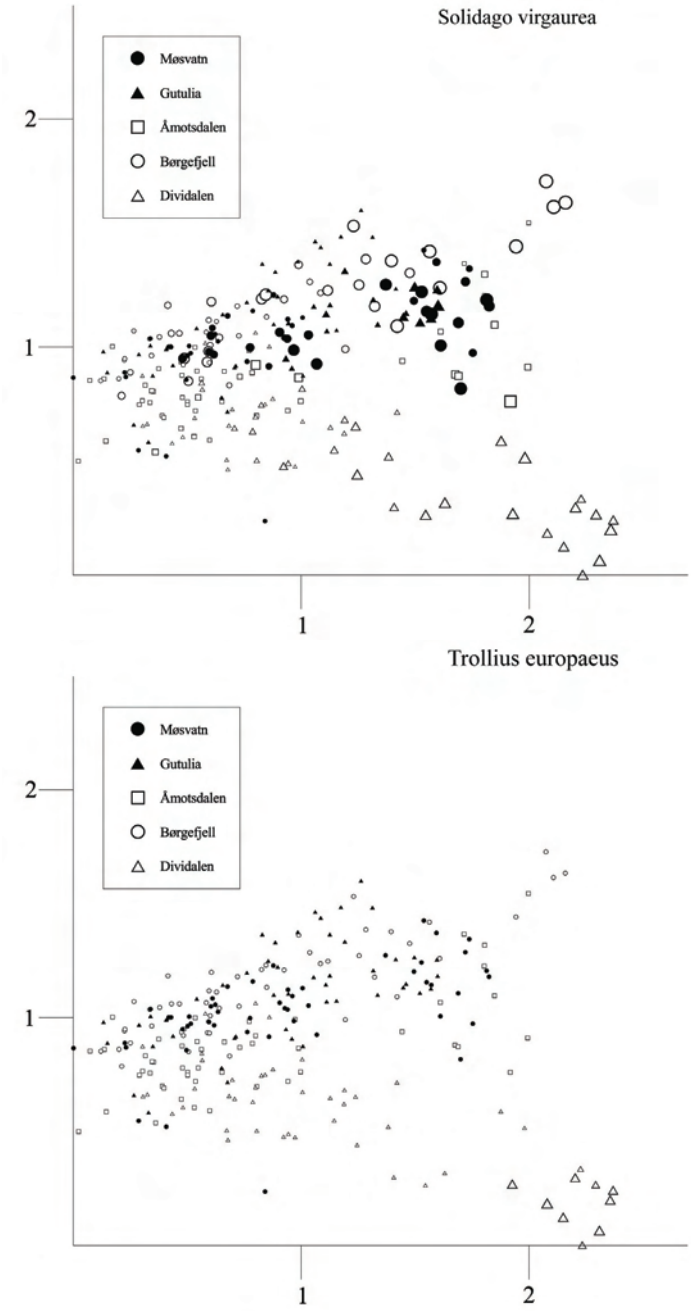

Figs 427-428. The total data set (Lund not included): distributions of species abundances in the DCA ordination of 250 sample plots, axes 1 (horizontal) and 2 (vertical). Frequency in subplots for *Solidago virgaurea* (Fig. 427) and *Trollius europaeus* (Fig. 428) in each meso plot proportional to symbol size. Scaling in S.D. units.

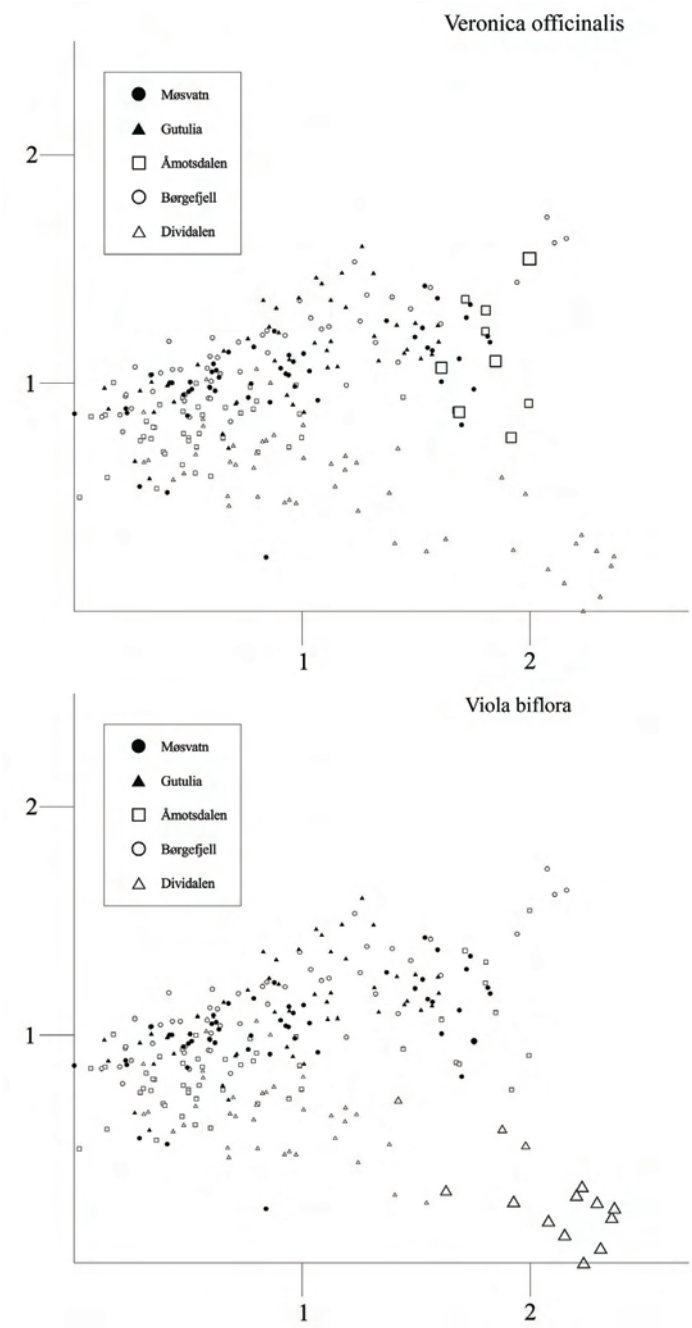

Figs 429-430. The total data set (Lund not included): distributions of species abundances in the DCA ordination of 250 sample plots, axes 1 (horizontal) and 2 (vertical). Frequency in subplots for *Veronica officinalis* (Fig. 429) and *Viola biflora* (Fig. 430) in each meso plot proportional to symbol size. Scaling in S.D. units.

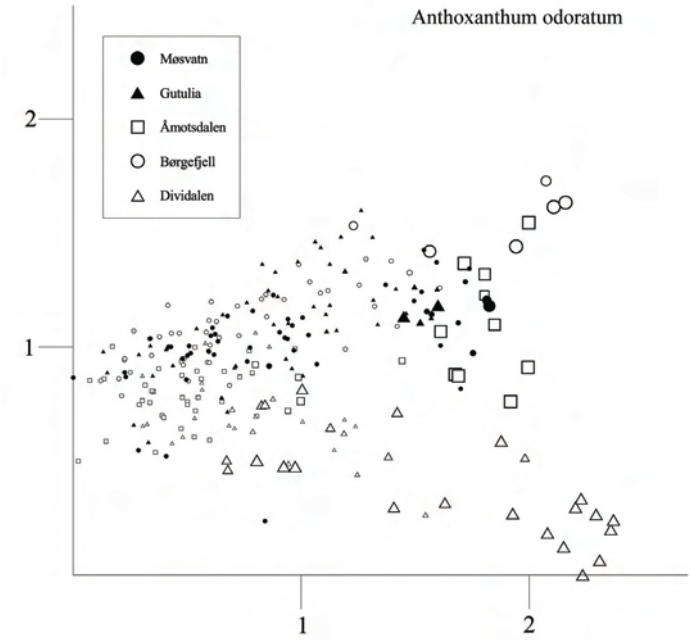

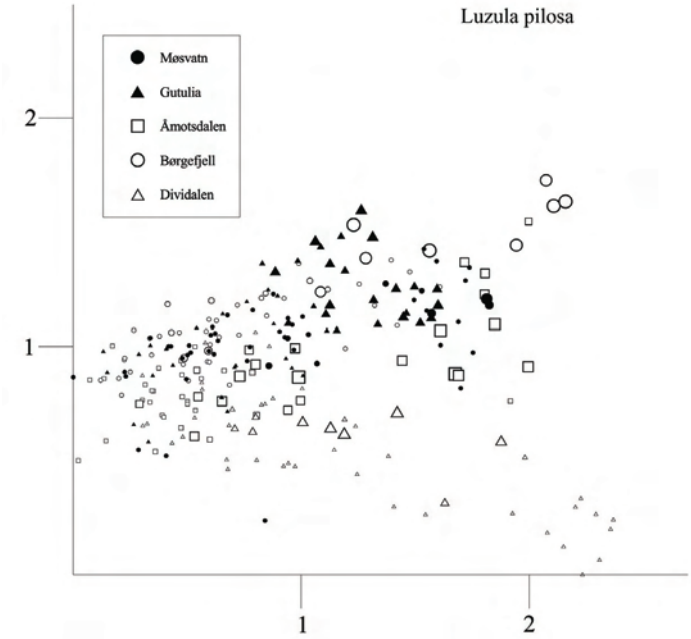

Figs 431-432. The total data set (Lund not included): distributions of species abundances in the DCA ordination of 250 sample plots, axes 1 (horizontal) and 2 (vertical). Frequency in subplots for *Anthoxanthum odoratum* (Fig. 431) and *Luzula pilosa* (Fig. 432) in each meso plot proportional to symbol size. Scaling in S.D. units.

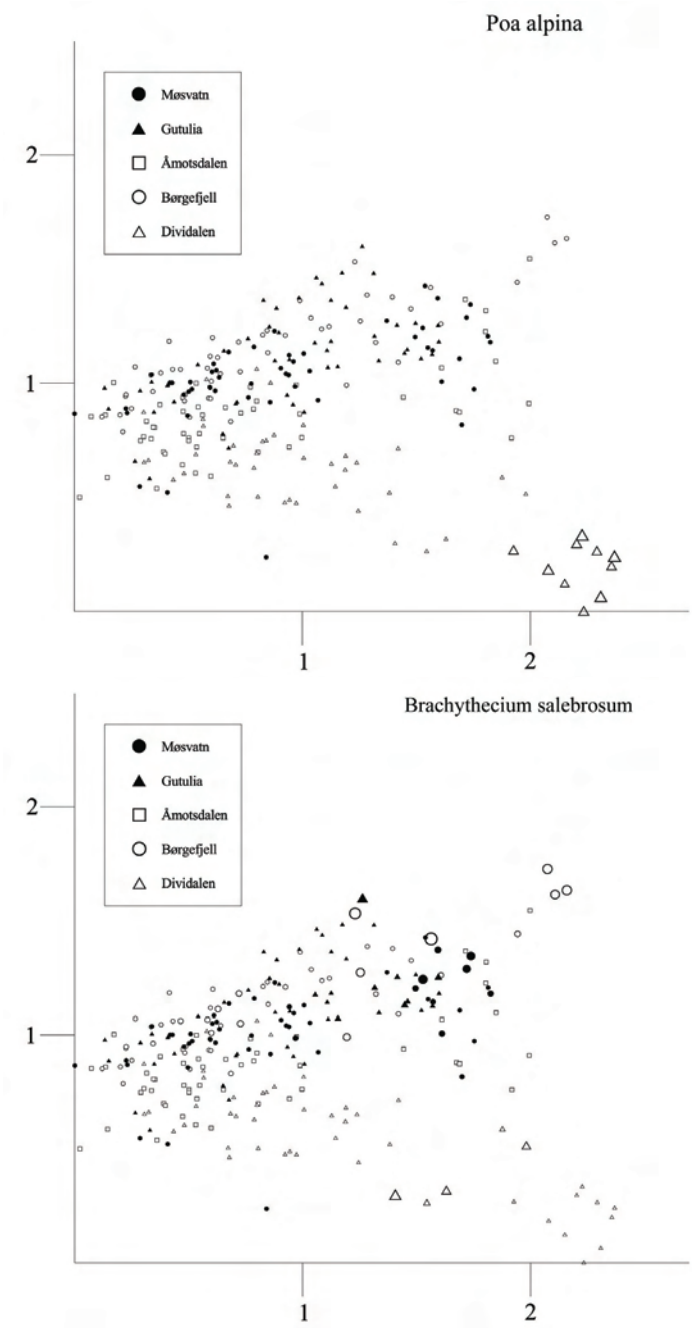

Figs 433-434. The total data set (Lund not included): distributions of species abundances in the DCA ordination of 250 sample plots, axes 1 (horizontal) and 2 (vertical). Frequency in subplots for *Poa alpina* (Fig. 433) and *Brachythecium salebrosum* (Fig. 434) in each meso plot proportional to symbol size. Scaling in S.D. units.

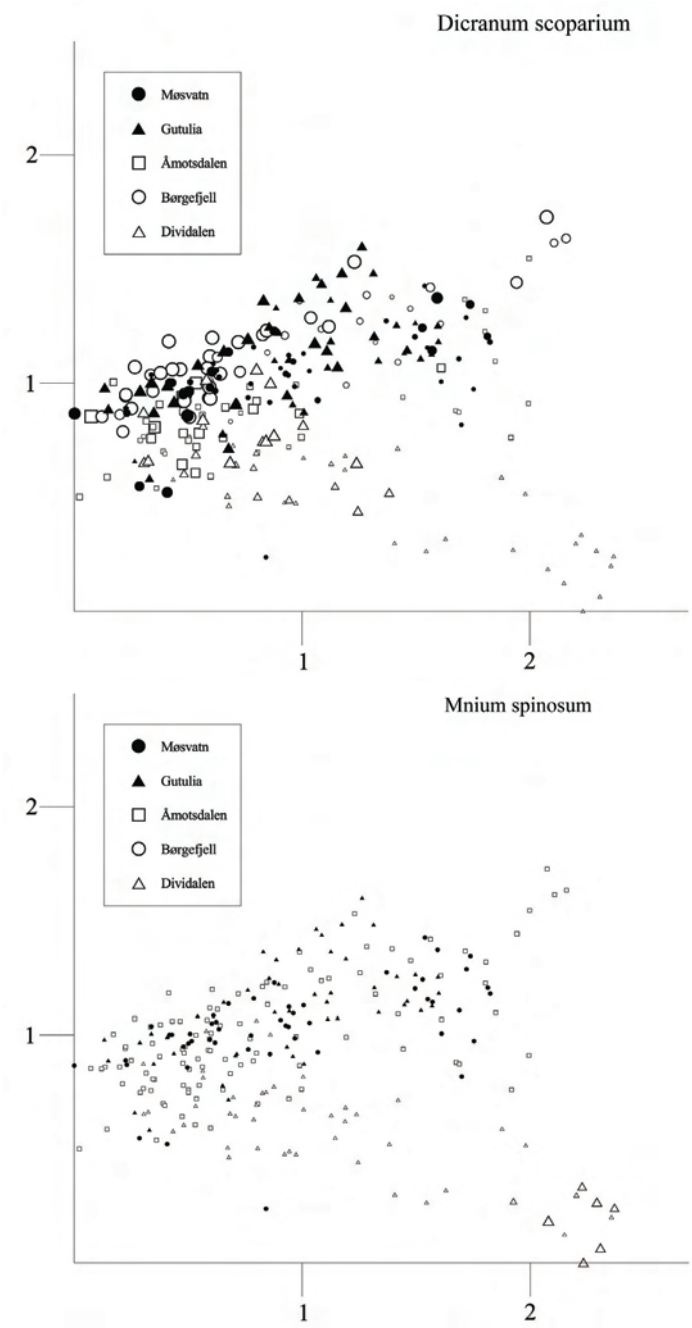

Figs 435-436. The total data set (Lund not included): distributions of species abundances in the DCA ordination of 250 sample plots, axes 1 (horizontal) and 2 (vertical). Frequency in subplots for *Dicranum scoparium* (Fig. 435) and *Mnium spinosum* (Fig. 436) in each meso plot proportional to symbol size. Scaling in S.D. units.

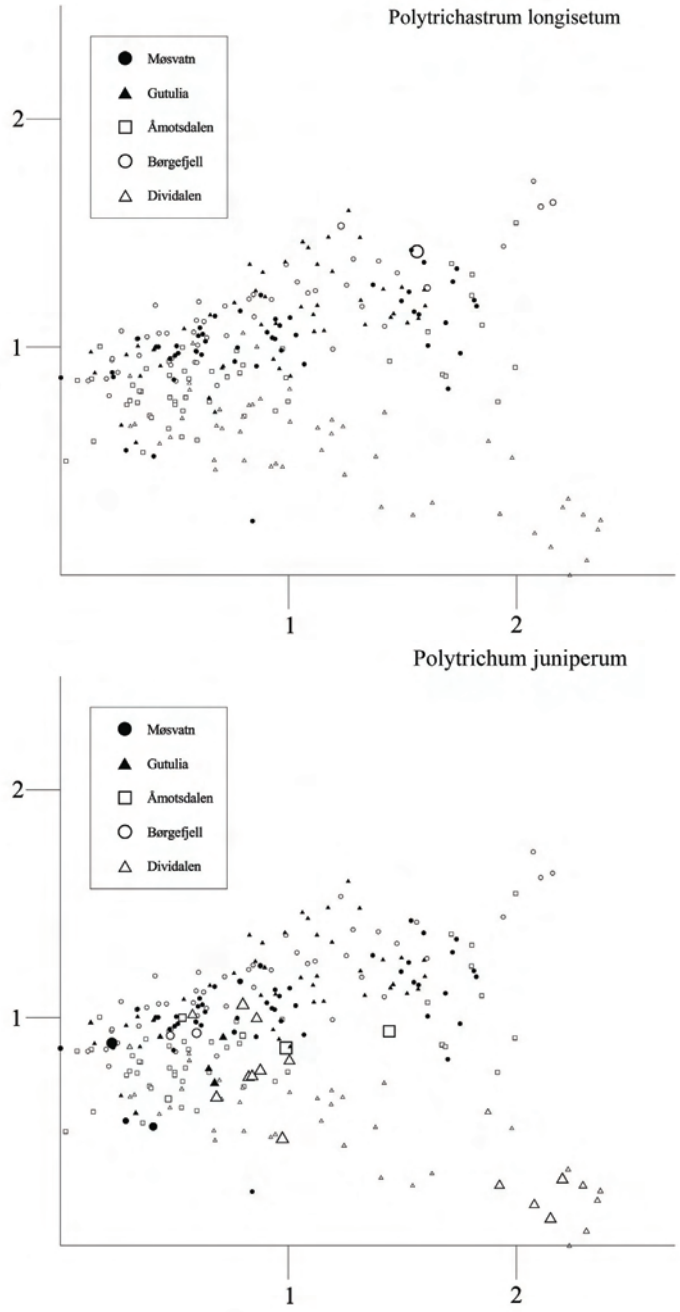

Figs 437-438. The total data set (Lund not included): distributions of species abundances in the DCA ordination of 250 sample plots, axes 1 (horizontal) and 2 (vertical). Frequency in subplots for *Polytrichastrum longisetum* (Fig. 437) *Polytrichum juniperum* (Fig. 438) in each meso plot proportional to symbol size. Scaling in S.D. units.

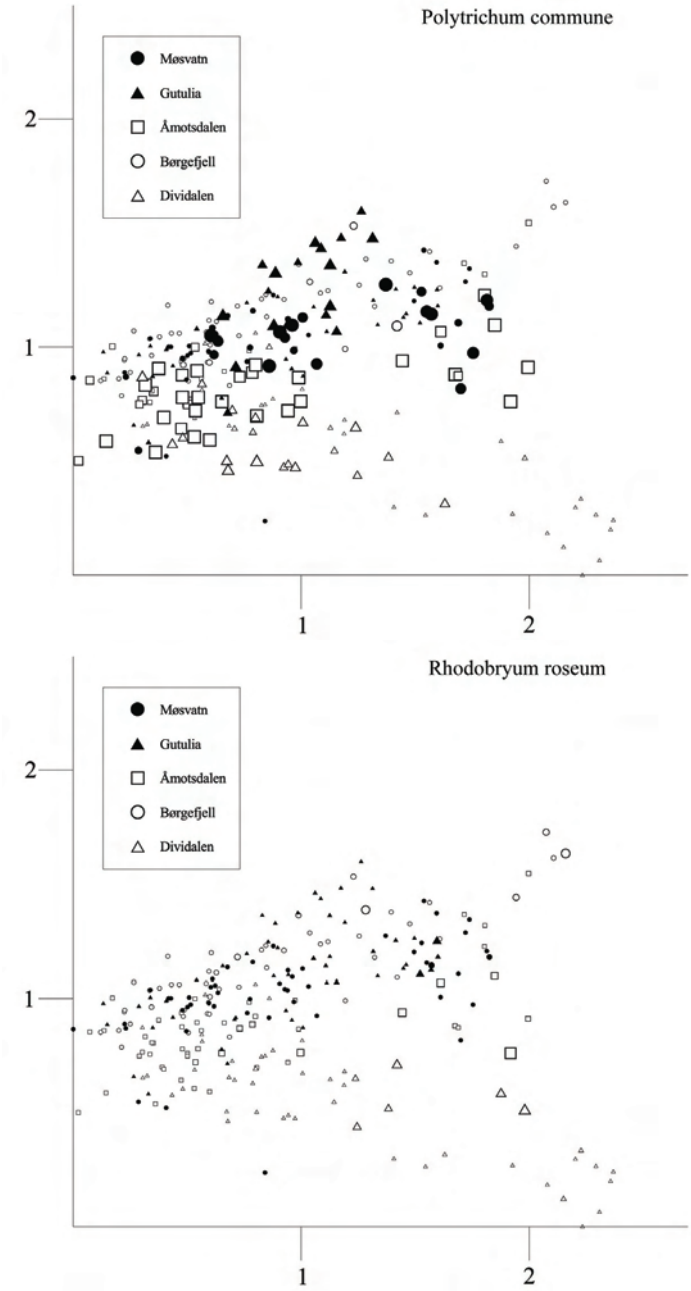

Figs 439-440. The total data set (Lund not included): distributions of species abundances in the DCA ordination of 250 sample plots, axes 1 (horizontal) and 2 (vertical). Frequency in subplots for *Polytrichum commune* (Fig. 439) and *Rhodobryum roseum* (Fig. 440) in each meso plot proportional to symbol size. Scaling in S.D. units.

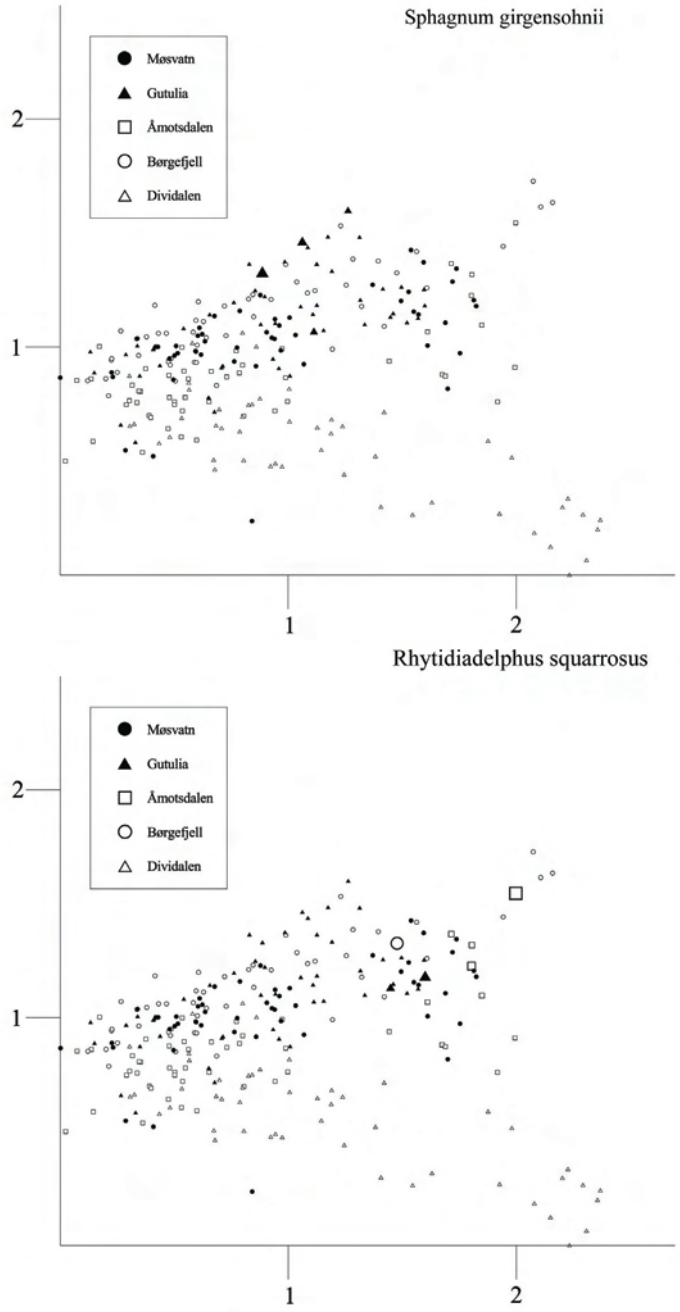

Figs 441-442. The total data set (Lund not included): distributions of species abundances in the DCA ordination of 250 sample plots, axes 1 (horizontal) and 2 (vertical). Frequency in subplots for *Sphagnum girgensohnii* (Fig. 441) and *Rhytidiadelphus squarrosus* (Fig. 442) in each meso plot proportional to symbol size. Scaling in S.D. units.

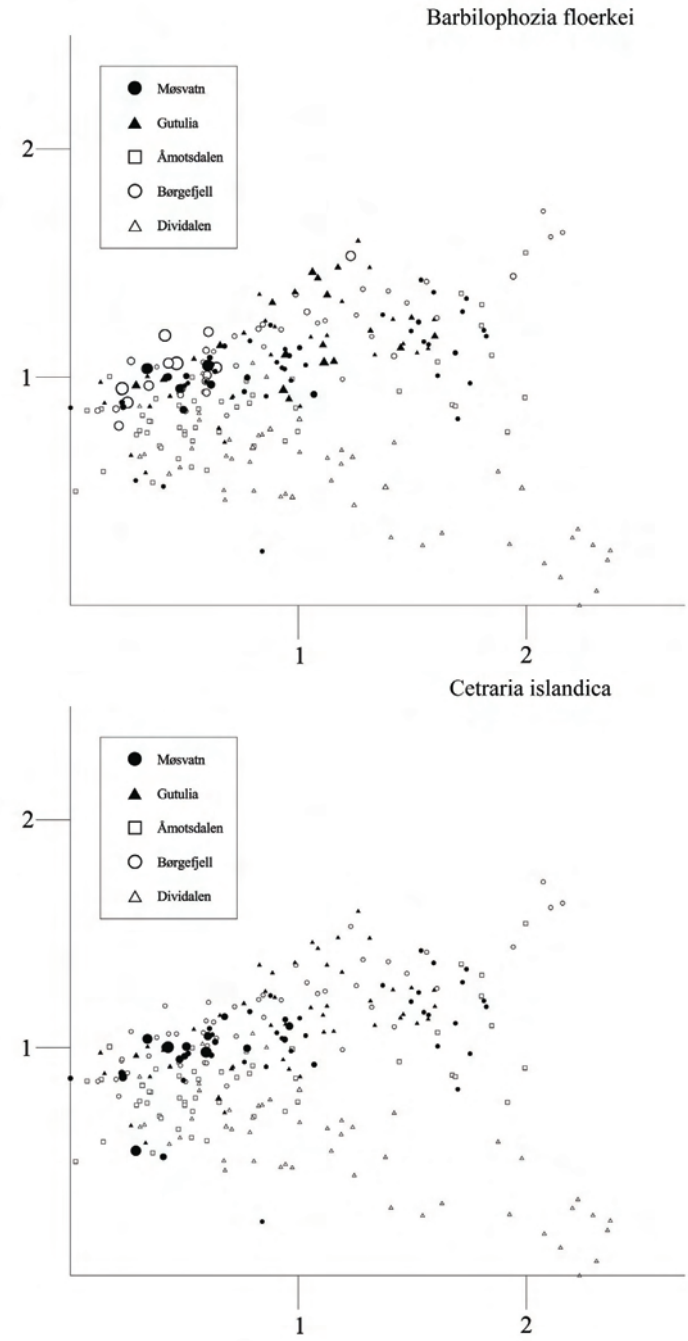

Figs 443-444. The total data set (Lund not included): distributions of species abundances in the DCA ordination of 250 sample plots, axes 1 (horizontal) and 2 (vertical). Frequency in subplots for *Barbilophozia floerkei* (Fig. 443) and *Cetraria islandica* (Fig. 444) in each meso plot proportional to symbol size. Scaling in S.D. units.

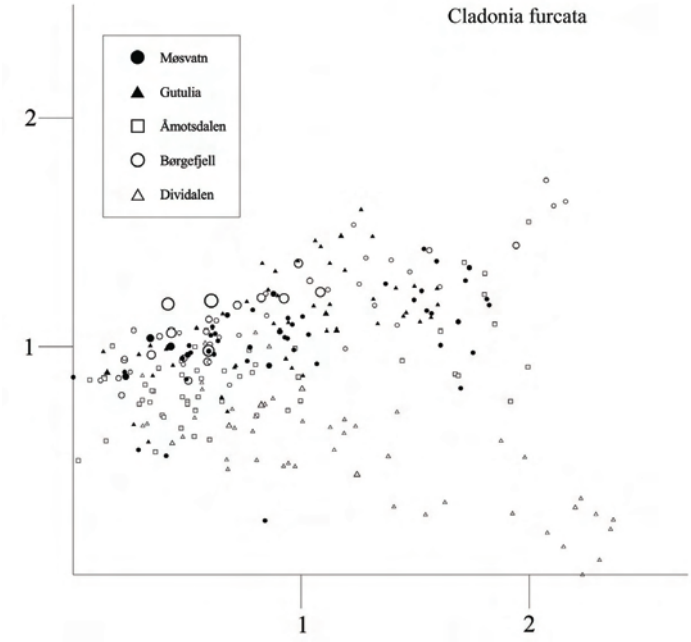

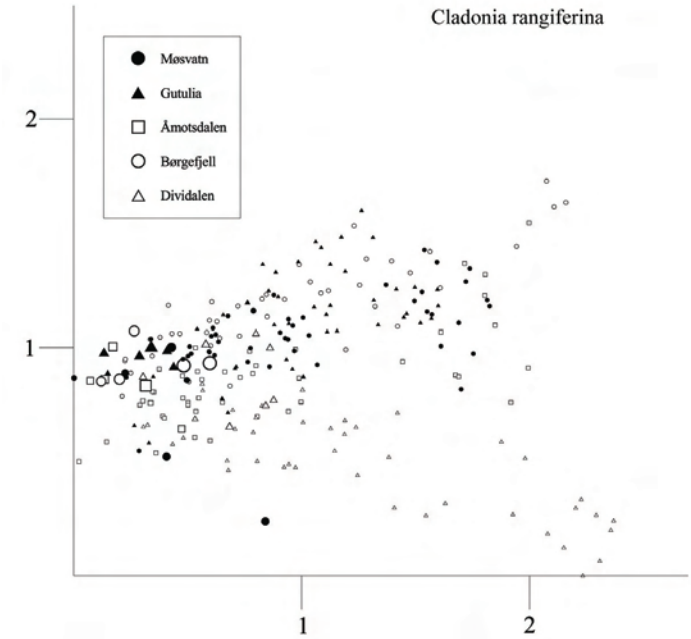

Figs 445-446. The total data set (Lund not included): distributions of species abundances in the DCA ordination of 250 sample plots, axes 1 (horizontal) and 2 (vertical). Frequency in subplots for *Cladonia furcata* (Fig. 445) and *Cladonia rangiferina* (Fig. 446) in each meso plot proportional to symbol size. Scaling in S.D. units.

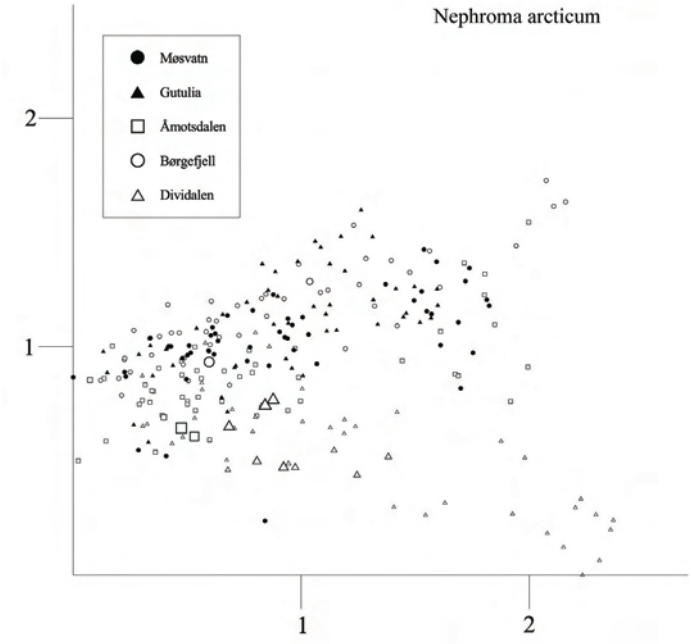

Fig. 447. The total data set (Lund not included): distributions of species abundances in the DCA ordination of 250 sample plots, axes 1 (horizontal) and 2 (vertical). Frequency in subplots for *Nephroma arcticum* in each meso plot proportional to symbol size. Scaling in S.D. units.

DISCUSSION

INTERPRETATION OF MAIN GRADIENTS IN SPECIES COMPOSITION IN EACH REFERENCE AREA

Lund

Sample plots from the Lund reference area span a short gradient in species composition; the gradient length of the first DCA axis is less than 2.5 SD (Fig. 9). The majority of the plots are characterized by species showing low demands for mineral nutrients, such as *Calluna vulgaris* and *Vaccinium* spp. and contain very few herbs (only *Melampyrum pratense*, *Trientalis europaea* and *Maianthemum bifolium* are common). A few plots (to the right in the DCA diagram) are characterized by slightly more nutrient demanding low-fern communities in which *Blechnum spicant*, *Gymnocarpium dryopteris* and *Phegopteris connectilis* occur, and tall fern plant communities with *Dryopteris expansa, Orepoteris limbosperma* and *Pteridium aquilinum* (see Figs 20-56). The relatively species-poor vegetation is probably a result of the acid bedrock (gneiss) of the area, which gives rise to nutrient-poor soils, and the unfavourable north-easterly aspect with low amounts of solar radiation reaching the ground.

Soil pH is by far the environmental variable most strongly related to the main vegetation gradient (DCA axis 1; Table 4). The lowest soil pH values are found in sample plots dominated by *Calluna vulgaris* to the left in the ordination diagram and the highest soil pH values are found in fern communities to the right in the diagram. This confirms our interpretation of the main coenocline (DCA axis 1) as mainly related to the nutrient richness and acid-base status of the soil. Further support from this interpretation comes from the increasing content of total N in soil samples with increasing scores along DCA axis 1.

Fern-dominated plots are found on the steepest slopes, where higher nutrient richness of soils can probably be explained by addition of nutrients by seepage water. However, this coenocline is also positively correlated with aspect unfavourability and negatively correlated with the heat indices, as they face northeast (Fig. 2). The unfavourable local climate of these rather steep northeast-exposed slopes can explain the sparse presence of thermophilous species in these plant communities.

Sample plots dominated by *Vaccinium myrtillus* mostly occur on less steep slopes while plots dominated by *Calluna vulgaris* are situated mainly on flat areas. Thus the variation in species composition in the Lund reference area is mainly caused by complex gradients in soil characteristics and topography-related microclimate. Nevertheless, the variation in species composition (and environmental factors) along these ecoclines is rather restricted.

In most studies of boreal forests soil the concentration of extractable Ca is one of the most important variables explaining variation in species composition, and this element is usually more or less strongly positively correlated with the concentration of extractable Mg and soil pH and negatively correlated with exchangeable H (e.g. Hesselman 1937, Malmstrøm 1949, Kuusipalo 1983b, Taylor et

al. 1987, Aarrestad 2002). The Lund sample plots do, however, follow a different pattern with a negative correlation between concentrations of the base cations Ca and Mg on one hand, and soil pH on the other hand, and a positive correlation between pH and exchangeable H. This result strongly conflicts general soil theories on soil acidity (cf. Schroeder 1984). However, a negative correlation between Ca and pH is also found in oceanic spruce forests by T. Økland (1996), who concludes that in humid areas soil Ca is likely not to contribute to a complex-gradient in soil nutrient concentrations, as is typically the case in less humid areas.

On the other hand, the variation in soil characteristics between the 50 sample plots from the Lund reference area is very small. Thus even small errors in soil sampling and/or chemical analyses, or idiosyncracies of single plots or macro plots, may potentially have strong impact on the outcome of statistical analyses.

The second DCA axis for the Lund plots is significantly correlated with soil moisture, loss on ignition and topographical indices (Table 5). Thus the second main vegetation gradient is probably related to differences in soil moisture, also affected by variation in topography and buildup of humus and peat layers, as exemplified by the distribution of *Sphagnum quinquefarium* in the ordination diagram (Fig. 51).

Most of the floristic variation, represented by DCA axis 1, occurs on the between macro-plot scale (84.49%). The correspondence between the split plot analyses (between macro-plot level) and the Kendall nonparametric correlation coefficients is good. However, even if the variation between plots within macro plots is low, 15.51 %, this is in fact the largest amount of explained variation within macro plots found along DCA axis 1 among the six investigated reference areas. On this most detailed scale, meso plot unevenness together with pH (also the most important variable on the between macro-plot level and the one most strongly correlated with DCA axis 1 according to Kendall's τ) are found to be the most important contributing variables. Also along DCA axis 2, the major fraction of variation along DCA axis 2 (78.76 %) occurs at the between macro-plot level. Along this axis, the best predictor of species composition, revealed by the split-plot tests and by Kendall's τ, is soil moisture.

Møsvatn

In contrast to the Lund area plots from the Møsvatn reference area span a long gradient in species composition; the gradient length of the first DCA axis is 4.5 SD units (Fig. 58). This gradient runs from lichen-dominated plots through bilberry-dominated woodland and small-fern communities to low- and tall herb woodland characterized by species often considered more eutrophic (Fremstad 1997) such as *Cicerbita alpina*, *Geranium sylvaticum, Ranunculus acris, Rumex acetosa* and tall grasses such as *Milium effusum* (Figs 78–125). The main coenocline at Møsvatn represents the longest vegetation gradient in terms of compositional turnover (S.D. units) in any of the six reference areas.

The main vegetation gradient, DCA axis 1, corresponds to a complex soil nutrient richness gradient, along which soil pH and soil nutrient concentrations (C, Ca, K, Mg, Mn, Na, S and total N) increase and loss on ignition and soil exchangeable H decrease (Figs 60-78, Table 7). This demonstrates affinity of plant communities with tall herbs to base-rich and nutrient-rich soils. Along the coenocline related to soil richness also slope and maximum soil depth increase while heat indices decrease. Plots richer in soil nutrients are thus typically situated in steeper north-exposed slopes and receive lower lower solar radiation input than other plots. These relatively steep slopes with soil of high nutrient content also have the highest tree density and probably also the highest tree biomass, as shown by the positive correlation of these variables with tree basal area (Table 7 and Fig. 63). The main compositional gradient mainly reflects variation between macro plots (93.62%). The agreement between results of split-plot analysis and Kendall's τ strengthens the interpretation.

The turnover of species along the first DCA axis also reflects variation normally interpreted as variation from drought-resistant to moisture-demanding vegetation. However, no significant or strong relation between soil moisture (Mme) and this axis is found. This may seem counter-intuitive because steep, northerly exposed plots with tall-herb communities are normally assumed to have higher soil water content due to influx of soil seepage water and lower solar radiation than the exposed ridges and less steep slopes with lichen and bilberry woodland (e. g. Schroeder 1984, Brunet 1991, Stoutjesdijk & Barkman 1992, R. Økland & Eilertsen 1993, Aarrestad 2002). The lack of a clear soil relationship of this main vegetation gradient with soil moisture may, however, be an effect of the bulk soil sampling process or of unknown amounts of precipitation immediately before the soil was sampled, levelling out recorded differences in soil moisture between the plots. Other explanations may also apply, like the 'soil moisture deficiency hypothesis' postulated by R. Økland & Eilertsen (1993) (see later in discussion under the 'The gradient in soil moisture' chapter.

The second vegetation gradient (DCA axis 2) is very short in terms of units of compositional turnover (cf. Fig. 58) and none of the measured variables are strongly related to DCA axis 2; the strongest is macro plot aspect ($\tau = 0.298$) and median soil depth; the latter is significant at the within macro-plot variation level in the split-plot analysis. Meso plots with high DCA 2 scores contain vegetation with high abundances of ferns such as *Phegopteris connectilis* while plots with low DCA 2 scores have a vegetation with indicators of soils richer in nutrients, such as *Geranium sylvaticum* and *Ranunculus acris*. Because of the very small amounts of variation in species composition along DCA axis 2, only separating plots in macro plot 9 from the rest, DCA axis 2 is not likely to represent an ecocline of general validity.

Gutulia

Sample plots in the Gutulia reference area span a shorter gradient in species composition than in the Møsvatn reference area; the gradient length of the first DCA axis is 2.8 SD (Fig. 127). The variation along the first DCA axis runs from species-poor dwarf shrub communities with dominance of

Empetrum nigrum and *Vaccinium* species to slightly more species-rich communities with high abundance of low ferns, grasses and low herbs (Figs 140–196). Gutulia thus lacks tall fern and tall herb communities corresponding to those of the Møsvatn area.

The main vegetation gradient (DCA axis 1) corresponds to a complex soil mineral nutrient and soil base sattus gradient, running from nutrient-poor soils with high organic content in the humus layer and low pH to slightly more nutrient-rich soils with higher pH and lower organic content. This complex soil nutrient gradient is also to some extent related to soil depth, with lower minimum and median soil depths in soils richest in mineral nutrients (Figs 130 and 131). Almost all variation along this axis occurs at the between macro-plot scale level (95.35%). The correspondence between the split plot analysis for this level and Kendall's τ is good.

Only two environmental variables are significantly ($\alpha = 0.05$ level) related to the second DCA ordination axis; both at the macro-plot level at which 77.5% of the variation is explained. This is no more than expected by chance in a multiple-test situation (31 single tests are made at each scale level). In fact, DCA 2 only separates four plots from macro plot 9 and three plots from macro plot 10 from all other plots (these plots obtain high DCA 2 scores). The axis separates lichen-dominated plots with species such as *Cladonia arbuscula, C. bellidiflora, C.cornuta, C. crispata, C. gracilis and C. rangiferina* (Fig. 186, 187, 190, 191, 193,194) with optima at low DCA axis 2 scores from species such as *Rubus chamaemorus* and *Eriophorum vaginatum*. with optima at high DCA axis 2 scores. The high-score plots differ from the rest in having deep soils (Figs 130–131), but no difference in soil moisture was recorded, as suggested by the species compositions of plots occupying contrasting positions along this axis. Like in the Lund area, the lack of a clear soil moisture pattern might be due to errors related to the bulk soil sampling process or precipitation before the soil sampling event, levelling out differences in soil moisture between the plots. There is also a possibility that depth to the ground water table might explain more of this variation in species composition. Because DCA 2 separates small groups of plots only, it may reflect area-specific patterns rather than generally valid ecoclines.

Åmotsdalen

The main vegetation gradient in the Åmotsdalen reference area (DCA axis 1) runs from dwarf-shrub communities dominated by *Betula nana, Calluna vulgaris* and *Empetrum nigrum* and with scattered lichens, to communities dominated by low ferns and herbs, with grasses and a few tall herbs such as *Geranium sylvaticum* and *Ranunculus acris*. The gradient length of the first DCA axis is 3.5 SD (Fig. 198 and Figs 212–248). The magnitude of compositional turnover along DCA axis 1 is somewhat larger than in Lund and Gutulia but smaller than in the Møsvatn reference area.

The main vegetation gradient from dwarf-shrub dominated to herb dominated communities is related to a soil mineral nutrient and base richness gradient, running from low to higher soil pH values and from low to higher concentrations of base cations and total content of nitrogen (Table 13, Figs

200–211). Almost all variation along DCA axis 1 (96.03 %) occurred at the between macro-plot level. Like in the other reference areas, the split plot modelling results accorded well with Kendall's τ correlation coefficients. We conclude that, as in the other reference areas, variaton in soil mineral nutrient availability, is an important structuring factor for the main vegetation gradient.

The variation along the second ordination axis was more evenly split onto the two levels, with 56.03 % between and 43.97 % within macro plots. Only a few variables were significantly related to this axis and the consistency between the results of split-plot analyses and Kendall's τ was low. Soil moisture sorted out by Kendall's τ as relatively strongly related to the axis and indicatively significant ($0.05 < P < 0.10$) at both levels in the split-plot analysis (Table 14). The distributions of species along this axis, e.g. the *Cladonia* species (Figs 257–258) versus species such as *Geranium sylvaticum* and *Ranunculus acris* may suggest that soil moisture, in some way, may be partly responsible for variation along this coenocline. However, the ordination diagram (Fig. 198) also shows that three plots obtain particularly high scores along DCA axis 2 (plots 42, 46 and 38) and one plot (No. 33) obtains low score. This opens for the possibility that DCA axis 2 merely reflects peculiarities of the species compositions of single plots (a noise axis; Gauch 1982).

Børgefjell

The main vegetation gradient in the Børgefjell reference area runs from lichen-dominated dwarf shrub communities (dominance by *Cladonia* spp.; Figs 312–320) to low-herb and fern communities with scattered occurrences of tall ferns (*Dryopteris expansa*) and tall herbs (*Cicerbita alpina*). The main vegetation gradient corresponds to a gradient in soil mineral nutrient richness and base status from sites related to soil pH, base cation concentrations, total content of nitrogen and tree densities (Table 16, Figs 262–273).

Of the variation in vegetation composition along the main ecocline (DCA axis 1), 94.38 % was explained at the between macro-plot scale. Like in the other reference areas, large conformity is found between the split-plot results at the between macro-plot level and the nonparametric Kendall's τ correlation coefficients. Thus, like in the other areas, the mineral nutrient status is regarded as the most important structuring factor for vegetation in Børgefjell.

Of the variation along the second ordination axis, 83.37 % is explained on the between macro-plot level. Soil moisture is a strong predictor of plot score at the between macro-plot scale level, and this variable is also identified as strongly related to the axis by Kendall's τ. Fig. 263 shows that the six plots (plot 40 and all plots in macro plot 9) which are separated along DCA axis 2 by obtaining high scores (see Fig. 260) have lower soil moisture values than the nine plots with high DCA axis 1 scores and low DCA axis 2 scores (macro plot 6 and the remaining plots in macro plot 8). The variation in vegetation along this axis runs from plots dominated by *Dryopteris expansa* (Fig. 284) on moister soil to plots dominated among others by *Polygonatum verticillatum* (Fig. 290) and *Anthoxanthum odoratum* (Fig 293) on slightly drier soils. Both *Dryopteris expansa* and *Polygonatum verticillatum*are

typical of fern dominated, 'flushed' (cf. Malmström 1949, Dahl 1957) vegetation and the segregation along DCA axis 2 in the Børgefjell area may well only reflect idiosyncrasies of the specific macro plots.

Dividalen

The main vegetation gradient in the Dividalen reference area (DCA axis 1) runs from lichen-dominated dwarf-shrub communities with dominance by *Betula nana* (Fig. 335) and *Cladonia* spp. (Figs 394-403) via low fern and herb dominated communities with grasses to communities dominated by tall-herb species such as *Omalotheca norvegica* (Fig. 357), *Saussurea alpina* (Fig. 364) and *Trollius europaeus* (Fig. 368). Dividalen is the reference area in which the highest total number of species (among the areas) is recorded.

The main vegetation gradient corresponds to a complex gradient which reflects soil mineral nutrient and base richness, running from soils poor in mineral nutrients (C, Ca, Mn, Na, S, Zn and total N), high organic content in the humus layer and low pH, to *vice versa*. Almost all variation along this compositional gradient is on the between macro-plot scale level (96.72%). The agreement between results of split-plot analyses and Kendall's τ is good. No terrain variables explain significant amounts of variation along this main ecocline, perhaps because the macro plots are placed along a line transect up a hillside.

Also along DCA axis 2, most of the variation in plot positions (80.94 %) occurs on the between macro-plot level. Soil concentration of P is the strongest predictor (negatively) of plot position on the between macro-plot scale level. Kendall's τ between DCA axis 2 scores and P is also strong. Species typically occurring in plots with low P (high DCA axis 2 scores) are *Phyllodoce caerulea* (Fig. 340), partly also *Equisetum sylvaticum* (Fig. 347), *Pedicularis lapponica* (Fig 359), *Calamagrostis lapponica* (Fig. 371) and *Nephroma arcticum* (Fig. 404). However, variation along this axis also strongly reflects altitudinal differences ($\tau = 0.563$). Dividalen is the only reference area in which the plots span considerable elevational variation (385–615 m a.s.l., see Table 1). We interpret DCA axis 2 as mainly expressing variation in species composition in the study area that results from placement of macro plots along an altitudinal gradient. Temperature-dependent variation in species composition, due to altitudinal (and south-north) variation is one of the main regional ecoclines (Ahti et al. 1968, Pedersen 1990, Moen 1999, Bakkestuen et al. 2008). The variation in P concentrations along this coenocline may or may not represent a general trend or be due to variation within this particular reference area, for reasons so far not known.

MAIN COMPLEX-GRADIENTS IN (MIDDLE AND NORTH) BOREAL BIRCH FORESTS

The gradient in nutrient conditions

The importance of mineral nutrient availability as a main factor structuring vegetation gradients in boreal forests has been emphasized and documented by many authors (e.g. Dahl et al. 1957, Kuusipalo 1985, R. Økland & Bendiksen 1985, Sepponen 1985, Taylor et al. 1987, R. Økland & Eilertsen 1993, T. Økland 1996, R. Økland & Eilertsen 1996, R. Økland et al. 2001). The mineral nutrient and soil base richness complex gradient is thus considered to be the most important complex gradient for the structuring of vegetation in boreal forests. Birch forest ecosystems are expected to differ slightly, but fundamentally, from coniferous forest ecosystems in properties such as the somewhat more favourable chemical composition and/or rates of decomposition of deciduous versus evergreen coniferous litter (Aarrestad 2002, Fjellberg et al. 2007). This influences the rates of soil biological processes (Saetre 1998), physical soil properties such as texture, humus form and moisture retention capacity (Sirén 1955, Green et al. 1993), and the acidity status and availability of essential elements from soils (e.g. Wittich 1961, Saetre et al. 1997, Ewald 2000, Légaré et al. 2001, Qian et al. 2003, Liu et al. 2008). While in coniferous forests input of needle material occurs at more or less constant rates (Saetre 1998) and this material contributes to natural soil acidification, decomposing birch leaves instead contribute to soil improvement (Dimbleby 1952a, 1952b, Gardiner 1968, Miller 1984, Saetre 1998). Neverthless, a comparison of the reference area minimum, median and maximum pH values (Table 21) with those of T. Økland (1996, see Table 35) for monitoring reference areas in spruce forest, reveals no large differences in pH between birch and spruce forest. It should be noted, however, that the selection of reference areas in birch and spruce forests was not made in ways that make possible a *test* of this particular hypothesis.

Soil pH is highly correlated with main compositional gradient in all six areas and always among the three best predictors. Soil pH is thus the parameter which overall best reflects variation along the main vegetation gradient. This is in correspondence with the results obtained in spruce forest where pH contributes to the main coenocline in nine out of ten reference areas and is the variable most strongly correlated with the gradient in six of these (T. Økland 1996). Other studies also find pH to be the best variable in explaining variation along the main vegetation gradient (Sepponen 1985, Lahti & Väisänen 1987, Taylor et al. 1987, R. Økland & Eilertsen 1993, R. Økland et al. 2001, Aarrestad 2002). However, pH mainly structures the vegetation indirectly by influencing the soil fauna and the plant mineral nutrient availability (cf. Glømme 1932, Larcher 2003).

The relative importance of mineral nutrients concentrations and other variables that make up the nutrient complex-gradient are known to vary between different studies and sites. Soil pH, concentrations of nitrogen and exchangeable Ca are usually reported as important in boreal ecosystems (cf. Malmström 1949, Dahl et al. 1967, Kuusipalo 1983b, 1984, 1985, R. Økland & Eilertsen 1993, T. Økland 1996). The six birch forest reference areas show considerable variation with respect to which variables make up the main complex-gradient, although pH and Ca are almost invariably among the most important. The middle boreal and oceanic birch forest in Lund differs strongly from this main

pattern, probably due to the modifying influence of climate, which is very different between Lund and the other reference areas situated in the north boreal zone and in more continental parts of Norway.

Concentrations of S are also correlated with the main vegetation gradient in all areas. Sulphur is, together with P, K, Ca and Mg, defined as one of the macro nutrients which are required in comparatively large amounts (Etherington 1982, Larcher 2003). Plants absorb S in the chemical form of sulphate, although there is some evidence that S-containing amino acids may also be assimilated (Larcher 2003). Sulphur accumulates in leaves and seeds and is an important component of protoplasma and enzymes. In industrial countries significant amounts of sulphur have been added to the soil through the precipitation over the last centuries (Anonymous 2006). H_2S released by waterlogged soils, lake mud and continental shelf sediments also supplies soil with S through natural rainfall, but this is assumed to contribute less than 10 % of the amounts due to industrial pollution (Etherington 1982, Mylona 1993). However, soil concentrations of S are by far not as strong predictors of vegetation gradients in spruce forest (T. Økland 1996) as found in birch forests in our study. The reason for this is still not understood.

Exchangeable concentrations of Ca in soil is highly positively related to the mineral nutrient complex gradient (and thus with pH) in four out of the six areas (Møsvatn, Åmotsdalen, Gutulia and Dividalen). Calcium was also positively related to pH and the main complex-gradient in Børgefjell, but less strongly than in the other four areas. Lund deviated from the other areas by having a negative relationship between Ca and pH and by showing a weak relationship between Ca and all complex-gradients. Most studies of boreal forest vegetation and soils reveal Ca as one of the most important predictors of variation in vegetation along a complex-gradient with soil base status as a central element (cf. Hesselmann 1937, Malmström 1949, Kussipalo 1983b, Taylor et al. 1987, T. Økland 1996). T. Økland (1996) does, however, find that in spruce forests with humid climates Ca and soil moisture co-vary along a different vegetation gradient. Hence T. Økland (1996) suggests that in a humid climate, Ca does not contribute to a 'normal' gradient in soil base status and mineral nutrient concentrations , like is typically the case in less humid areas. The results from birch forests largely agree with these observations. The two areas in which Ca is less strongly related with the main complex-gradient are also the two most humid areas (Lund and Børgefjell). Furthermore, concentrations of Ca are generally lower in Lund than in the other reference areas.

Calcium is essential part of plant cell wall structure which provides for normal transport and retention of other elements and general physical strength of the plant. Ca is believed to balance the effect of alkali salts and organic acids within the plant. Calcium is absorbed as Ca^{2+} ions and exists in a fine balance with magnesium and potassium in plants. Too much of any one of these three elements may cause deficiencies of either the other two (Larcher 2003).

Soil content of total nitrogen is highly related to the main mineral nutrient and soil base richness complex-gradient in four areas (Møsvatn, Åmotsdalen, Børgefjell and Dividalen), to some extent related to this complex-gradient in Gutulia and unrelated to it in Lund. Parallel variation in

nitrogen and soil nutrient status and soil base richness along one main complex-gradient is typically found also in other studies in boreal forests (T. Økland 1996). In all reference areas pH and nitrogen are more or less strongly positively correlated. Nitrogen is usually considered as the most limiting resource in boreal forests (cf. Hesselmann 1937, Malmström 1949, Kussipalo 1984, Tamm 1991). Nitrogen is important for building up new material in plants (Kubin 1983), but also for the microbiological activity in the humus (Olsen 1990), as the microbes need nitrogen for their synthesis of organic matter (Kubin 1983). The strong correlation between total amounts of nitrogen and the main compositional gradient in boreal forests accords with other studies (e.g. T. Økland 1996, R. Økland et al. 2001). This study of birch forests thus lends support to the general notion that the total amount of available nitrogen is important for the species composition and hence a good indicator of the main complex-gradient.

Other elements that are highly correlated with the main complex gradient in all areas (except Lund), are potassium and manganese. These elements are also considered as macronutrients by Larcher (2003); both are important among others in regulation of water physiology of plants.

The gradient in soil moisture

Measured volumetric bulk soil moisture is a significant predictor of vegetation composition turnover in Lund (for the secondmost important ecocline represented by DCA axis 2), and partly also in Børgefjell (also DCA axis 2). These two reference areas are the most oceanic ones among the six areas included in this study. In the other four area no relationship between measured soil moisture and vegetation gradients is found in Møsvatn, Gutulia and Dividalen and a possible, weak, relationship is found in Åmotsdalen (but not at the $\alpha = 0.05$ level). The recorded relationship between measured soil moisture and vegetation gradients in birch forest is thus generally weaker than found in spruce-dominated forests where one of the main coenoclines (DCA 1 or DCA 2) are related to soil moisture in most areas (R. Økland & Eilertsen 1993, T. Økland 1996).

The importance of soil moisture as an important structuring factor in boreal forests is emphazised among others by Carleton & Maycock (1980), Bergeron & Borcard (1983), Kuusipalo (1983a), Lahti & Väisänen (1987), R. Økland & Eilertsen (1993) and T. Økland (1996). On a local scale the soil moisture gradient should in principle be assumed to be independent of the complex gradient in soil mineral nutrients and base status (R. Økland & Eilertsen 1993), but these ecoclines may locally or in part be correlated (Lahti & Väisänen 1987, Carleton 1990, T. Økland 1996). In spruce forest nutrient-rich sites are mainly mostly dry while moist sites almost invariably tend to be poor (T. Økland 1996). This is not in accordance with the results found for the studied birch forest reference areas, and may indicate that this result of T. Økland (1996) does not have general validity, not even for spruce forests.

The weak relationship between measured soil moisture and recorded coenoclines in many of the reference areas may be a result of the way soil moisture is measured. Several authors (R. Økland &

Eilertsen 1993, T. Økland 1996 and R. Økland et. al 2001) have pointed out that species distributions may be related to moisture in several, principally different ways that are not captured by one type of measurement of soil moisture made at one particular time-point. In the background material for the new division of Norway into nature types, Halvorsen et al. (2008), recognise three ecoclines relevant to soil moisture in boreal forests, of which two are related to 'normal' water availability [spring influence, e.g. the difference between *topogenous* paludification, which occurs in small depressions with poor drainage and stagnant water, and *soligenous* paludification, which is favoured by a cold and humid climate and occurs on slopes where the terrain determines the speed and direction of water movement to flushed slopes with fern dominated vegetation, dependent on more constant supply of water, with springs at the end; and water saturation (paludification), which separates sites according to median ('normal') soil moisture]. The relationship between spring influence and water saturation is explained by Halvorsen (2008), among others by the 'water availability triangle' (Halvorsen 2008: Fig. 6). The third ecocline related to soil moisture and water availability is related to risk of extreme drought (R. Økland & Eilertsen 1993, Halvorsen et al. 2008).

The wettest sites (high water saturation) included in this investigation are paludified slopes with high abundance of *Sphagnum* species, such as *S. girgensohnii* and *S. quinquefarium*, and slopes with ferns such as *Phegopteris connectilis* and *Oreopteris limbosperma*. High abundance of *Sphagnum* only occurs in Lund and Gutulia*; S. girgensohnii* are found in Gutulia sample plots 17 and 26–29 and *S. quinquefarium* is abundant in Lund, macro plots 1 and 3–6. Small hepatics like *Cephalozia* and *Calypogeia* spp. in *Sphagnum* carpets, and *Oreopteris limbosperma*, only occurred in Lund (macro plot 7). Furthermore, variation related to risk of extreme drought is likely to be present in several of the areas. Drought-exposed sites are typically richer in *Cladonia* lichens, *Calluna vulgaris* and *Empetrum nigrum*; species that are tyipcal for one end of the *main* coenocline in several of the birch forest reference areas. The lack of any relationship between this variation in species composition and recorded soil moisture in these cases accords with R. Økland & Eilertsen (1993) who postulated the 'soil moisture deficiency hypothesis' to explain this variation, which was not related to among-plot differences in volumetric soil moisture in their study area. Insufficient sampling of variation in species composition related to soil moisture in the reference areas is a probable partial explanation for the poor relationship between coenoclines and soil moisture in some of the reference areas. Furthermore, volumetric bulk soil moisture, as measured in this study, does not only fail to reflect variation along all three moisture-related coenoclines but is also, in itself, vulnerable to variation in weather conditions at and around the time-point sampling takes place.

T. Økland (1996) finds in many spruce reference areas that soil moisture is related to a gradient from within gaps in the forest to sites below trees. Her study reveals drier soil below trees than in gaps between trees, and restriction of several species to the more moist sites in gaps between trees. This variation in soil moisture from below to between trees is explained as an effect of tree canopies (cf. R. Økland & Eilertsen 1993): (1) a strong gradient in throughfall precipitation (low close

to tree stems), caused by canopy interception (C.O Tamm 1953, Beier et al. 1993); (2) stronger water uptake by trees close to stems (cf. Stålfelt 1937b) and large amounts of spruce litter, particularly close to stems, that give rise to a loose and thick humus which dries up rapidly after rainfall, due to a low capacity for retaining moisture (cf. Malmström 1937, Stålfelt 1937b). No such relationships are found in the birch forest reference areas. A likely explanation for this is that the shading effect of the tree layer is less important in birch forests than in spruce forests because the size and density of trees are usually lower in the birch forest. This tendency is likely to be strengthened towards the tree line as the influence of winds increase (R. Økland & Bendiksen 1985).

Disturbance and land use changes

Grazing and trampling by domesticated animals (included domesticated reindeer) have influenced and are still influencing the vegetation in all reference areas, to stringer or lesser extents. The reference areas Gutulia, Børgefjell and Dividalen are constantly influenced by reindeer grazing while Møsvatn and Åmotsdalen are influenced by cattle and sheep grazing. Lund is also to some extent influenced by sheep grazing. The species composition in these areas reflects the grazing (and trampling) pressure, but the extent to which this is the case is difficult to quantify. The most difficult part is to separate effects of grazing by domesticated animals from natural dynamics in the reference areas. An experimental design, with enclosures in which the vegetation was protected from grazing, would have been a valuable reference for such influences. Miles & Kinnairs (1979) have shown that grazing may cause large mortality of birch saplings and that considerable rejuvenation took place in grazer exclosures. One the other hand, Pigott (1983) demonstrates that moderate grazing can promote germination of birch seeds.

Bakkestuen & Erikstad (2002) performed a comparative analysis of aerial photos from 1949 and 1987 in the Møsvatn area, revealing considerably lower summer farm activity in 1989, both in the reference area (birch forest) and in the mountain pasture area close by. Among others, they demonstrate that in 1989 paths were in the process of being overgrown, the forest had grown denser and the openings were smaller and fewer. Such changes in the land use over the last 50–100 years have certainly had, and still have, an impact on the vegetation (cf. Bryn & Daugstad 2001).

MAIN GRADIENTS AND VARIATION IN THE TOTAL DATA SET

Interpretation of main gradients in the total data set

Three different ordinations were performed: one on the total data set, another on the same data set with sample plots from the southernmost reference area Lund excluded, and one partial ordination of the latter data set with variation due to 7 climatic/geographical variables partialled out. In the first of these ordinations all sample plots from Lund split off from the rest of plots along the first ordination axis. This ordination is thus not discussed in further detail here as it merely shows that the vegetation in

Lund differs strongly from that of the other areas, underpinning the importance of variation along the two main regional (climatic) ecoclines; Lund belongs to another vegetation zone and another vegetation section (see Moen 1998).

The new ordination ovtained after removal of sample plots from Lund revealed a first DCA ordination axis along which no segregation of plots from different areas occurred. More that 80 % of the variation in species composition along this axis is explained on the between macro-plot scale level while only approximately 5 % on the between-area scale level. This emphasises that generally applicable local environmental complex-gradients structure variation in vegetation in birch forests (at least within the same vegetation zone).

The corresponding DCA 1 axes in the ordination and in the partial ordination in which variation due to climatic/geographical variables had been partialled out are strongly correlated and correspondingly represent the ecoclines. Such similar patterns are exactly what T. Økland (1996) found in her data from spruce forests. This shows that within a relatively narrow range of vegetation zones and sections, boreal forest vegetation is structured by generally important local complex-gradients, the effect of which is considerably stronger than the effect of geographic distance as such.
Our results show that this local complex-gradient runs from sites with low pH and low content of mineral nutrients (low concentrations of macro nutrients like C, Ca, Mn, S and N) and high loss of ignition to *vice versa*.

The second ordination axis, related to soil concentrations of Mn and S, and with about one half of the variation explained at the between-area scale even in the partial ordination from which the effects of geographic/climated variables had been partialled out, is likely mostly to reflect inevitable variation in species composition between areas large distances apart (cf. Nekola & White 1999).

The proportion of unexplained variation was large. The large size of the data set partly contributes to this because the random variation in a vegetational data set increases with increasing size of a data set (cf. Smith & Urban 1988, R. Økland et. al 1990, R. Økland & Eilertsen 1994 & T. Økland 1996). Vegetational responses to environmental gradients and disturbances that occur at spatial scales below the sample plot size of 1 m^2, like fine-scale topography gradients (R. Økland et al. 2001), also contribute to the unexplained variation (see also R. Økland & Eilertsen 1994). The amount of explained vegetational variation in the total data sets from birch forests is of approximately the same magnitude as found by T. Økland (1996) for spruce forests.

Species with regional variation in response to main complex gradients.

A few species, such as *Gymnocarpium dryopteris* and *Phegopteris connectilis*, show regional variation in response to the main environmental complex gradient underlying the main coenocline (the first ordination axis of the total data set and of separate ordinations of the different reference areas). Most notably, their amplitudes along the main ecocline differs between areas. These species occur on sites with lower pH and lower mineral nutrient concentrations in the humus in sites with a more humid

climate compared to more continental sites, where they reach an optimum on sites with higher pH and higher nutrient concentrations. Correspondence between regional gradients and local environmental gradients has been recognised for a long time. Boyko (1947) refers to this as the geo-ecological law of distribution, which relates to similar concepts such as equivalence of sites (Loucks 1962, Vetaas 1992) and habitat constancy (Walter & Walter 1953, Miehe 1989), or niche constancy (Ferrer-Castán & Vetaas 2003). A species may thus displace its distribution with respect to a measured environmental variable from one climatic region to another, if the measured variable and the condition of primary physiological importance are affected by climate (T. Økland 1996). In spruce forest even more species, like *Anemone nemorosa, Oxalis acetocella, Rubus saxatilis* and *Rhytidiadelphus squarrosus* agg,, have been found to have such a pattern. However, the number of occurrences of these species in birch forest sample plots is too low to allow further discussion of the topic.

Both R. Økland & Bendiksen (1985) and T. Økland (1996) explain this change in optimum by postulating that high soil moisture compensates for lower pH and mineral nutrients contents in the humus layer in a humid climate. This may contradict Boyko's law which says that the amount of nutrients available for these species should be the same on sites where they occur, in the humid reference areas as well as in the more continental. However, in humid climate water flow rates through the humus are higher due to higher precipitation, which is exoected to contribute to higher nutrient supplies and probably also higher turnover rates (Varskog 1995, T. Økland 1996). The access to nutrients may then be higher throughout the year despite the lower pH and nutrients measured at one point in time (see T. Økland 1996). Other explanations may also apply, e.g. that other environmental factors are important in different parts of regional gradients. In that case the premises for Boyko's geo-ecological law are not fulfilled.

COMPARISON WITH VEGETATION CLASSIFICATIONS

The driest and most oligotrophic part of the monitored vegetation can be assigned to the A1b type '*Cladonia-Betula pubescens* ssp. *czerepanovii* subtype' of the '*Cladonia* woodland' in Fremstad (1997). Slightly less 'dryish' vegetation accords with the A2c type, 'Va*ccinium vitis-idaea* - *Empetrum nigrum* coll. subtype' of the '*Vaccinium* woodland'. These types are more or less dominated by lichens and dwarf shrubs, and correspond more or less to the association Cladonio-Betuletum (Nordh.43) K.-Lund 73 and probably to Calamagrostio lapponicae-Pinetum K.-Lund 67 in the northernmost area, Dividalen. Lichen-dominated vegetation is represented in all analysed areas except Lund, and could probably be classified to the drier part of the subxeric topographic moisture series of R. Økland & Bendiksen (1985), due to high abundance of lichens and *Empetrum nigrum* ssp. *hermaphroditum* and the occurrence of *Arctostaphylos alpina*.

A few plots on moist and nutrient-poor soils in Åmotsdalen and Dividalen have a species composition similar to the A3b 'Mountain subtype' of the '*Calluna vulgaris-Vaccinium uliginosum-*

Pinus sylvestris woodland' (Fremstad 1997), comparable with Barbilophozio-Pinetum Br.-Bl. et Siss. 39 em. K.-Lund 67 or the equivalent Empetro hermaphroditi-Betuletum tortuosae Nordh. 43 (Betuletum empetro-cladinosum). Characteristic species are *Betula nana, Calluna vulgaris* and *Vaccinium uliginosum*.

The majority of plots recorded from the monitoring areas represent medium dry and slightly mesic vegetation related to the A4c '*Vaccinium myrtillus-Empetrum nigrum* coll. subtype' of the 'Bilberry woodland' (Fremstad 1997), which occurs in all monitoring areas except Lund. This vegetation is comparable with the Myrtillio-Betuletum tortuosae Nordh. 43 (Betuletum myrtillo-hylocomiosum) K.-Lund 71. A few plots in the more termophilous lower parts of Gutulia, in south-eastern Norway, might also be classified to the A4a '*Vaccinium myrtillus* subtype' of the 'Bilberry woodland' comparable to Eu-Piceetum (Caj. 21) K.-Lund 62, sub-association myrtilletosum K.-Lund 81. This major part of the monitored vegetation definitively belongs to the submesic topographic series of R. H. Økland & Bendiksen (1985), due to the dominance of *Vaccinium myrtillus* and species such as *Maianthemum bifolium*, *Trientalis europaea* and *Solidago virgaurea*.

The vegetation of the south-western, humid area Lund is very different from that of the other monitoring areas, comprising both the A4b '*Vaccinium myrtillus-Cornus suecica* subtype' of the 'Bilberry woodland' and the A7c '*Molinia caerulea* subtype' of the 'Poor grassdominated woodlands' (Fremstad 1997). Less grass-dominated vegetation is comparable with Corno-Betuletum pubescentis Aune 73, probably sub-association myrtilletosum Aune 73, however without *Chamaepericlymenum suecicum*. The major part of the monitored vegetation has a species composition reflecting the submesic topographic-moisture series of R. Økland & Bendiksen (1985). However, grass dominated plant communities (*Molinia caerulea*) and tall fern plant communities (*Orepoteris limbosperma, Dryopteris expansa*) probably correspond to their mesic series.

Vegetation of the submesic series, characterized by small ferns (*Gymnocarpium dryopteris, Phegopteris connectilis*) and herbs (e.g. *Potentilla erecta, Rumes acetosa, Silene dioica, Oxalis acetosella*) occurs in monitoring plots mainly in the Møsvatn, Åmotsdalen, Børgefjell and Dividalen areas. Such more nutrient-rich submesic stands are also represented by a few plots in Gutulia. The vegetation can be assigned to the A5c 'Small fern mountain woodland subtype' of the 'Small fern woodland' (Fremstad 1997), comparable to Eu-Piceetum (Caj. 21) K.-Lund 62, sub-association dryopteridetosum K-Lund 81.

Slightly eutrophic submesic to mesic vegetation is only represented in the Møsvatn and Dividalen areas. The sites richest in mineral nutrients occurred on calcareous rocks in Dividalen. The associated, rather species-rich, vegetation can be assigned to the C2c 'Low herb subtype with scattered tall herbs' of the 'Tall herb, downy birch and Norway spruce forest' (Fremstad 1997), with species comparable with Salicetum geraniosum alpicolum Nordh.43 or Betuletum geraniosum subalpinum Nordh. 43. Characteristic species are *Geranium sylvaticum, Ranunculus acris, Saussurea alpine,*

Pyrola minor, Taraxacum sp. and bryophytes such as *Mnium spinosum, Plagiomnium* ssp. and *Rhodobryum roseum*.

All reference areas have been more or less grazed by domestic animals. In some areas this has probably contributed to a more grass-dominated vegetation, similar to the A7b '*Deschampsia flexuosa* subtype' of the 'Poor, grass-dominated woodland' (Fremstad 1997). It is also possible that the vegetation on some of the herb and grass-dominated plots is partly a result of former scything, thus being comparable with the wooded grassland vegetation types described in Moen (1990) from scythed areas in boreal uplands in central Norway.

CONCLUSION

The main complex environmental gradient, and the variation in vegetation along this gradient, are more or less the same in birch forest areas all over Norway, and also the same as in coniferous forests. Some variation among areas do, however, occur with respect to which environmental variables that contribute to this main complex-gradient. Furthermore, this main ecocline interacts with regional climatic variation. The main complex gradient governing variation in species composition in all six reference areas was the gradient in mineral nutrient status and soil base richness, best expressed by pH and soil concentrations of Ca, K and S. Other contributing variables, like concentrations of Mn, P and total N in soil, vary to some extent in the strength of their relationship with the gradient between reference areas. The middle boreal birch forest of Lund deviate from this pattern, probably due to the climatic differences between this area and the other areas. Tree influence, topographic unfavourability, heat indices, soil moisture and soil depth may locally be related to the main ecocline.

Most of the variation in the vegetation in the studied birch forests occurs at the between macro-plot scale level, leaving small amounts of variation at the between-area and the between-plot within macro-plot scale level.

ACKNOWLEDGEMENTS

TOV, Terrestrial Monitoring of boreal birch forest ecosystems, is funded by the Directorate for Nature Management (DN). We especially want to thank Signe Nybø, our contact in DN, for many encouraging discussions and for important input to this work during many years. Thanks are also due to Else Løbersli (DN) and Ivar Myklebust (formely DN now Artsdatabanken), for many important contributions to TOV from programme initiation until present.

Substantial contributions to vegetation analyses in the field beside the authors have been given by Egil Bendiksen, Ingvar Brattbakk, Anders Often, Ellen Svalheim and Harald Taagvold. We also thank Bodil Wilmann for extensive work with the TOV data base and Erik Framstad, who through his coordinating position in TOV, has contributed in many ways. Special thanks are also given to Eli Fremstad, who was the coordinator of the vegetation studies in TOV during the first years. We are also grateful to Tonje Økland, who prepared the ground for this study through her work on spruce forests. Great thanks are also given to Rune Halvorsen who introduced us to this approach to vegetation ecology in boreal forests. He has also given us valuable input in the planning and writing process of this manuscript. We are also grateful to several previous and present colleagues at our institutes who in several ways have contributed to, or supported, our work. Thanks are also due to many other persons, too many to mention by names, who have contributed in some way, e.g. with logistic or technical support.

REFERENCES

Anderson, D.J., Cooke, R.C., Elkington, T.T. & Read, D.J. 1966. Studies on structure in plant communities. II. The structure of some dwarf-heath and birch-copse communities in Skjaldfannardalur, North-west Iceland. - J. Ecol. 54: 781-793.

Andreassen, K., Clarke, N., Røsberg, I., Timmermann, V. & Aas, W. 2006 Intensiv skogovervåking i 2005. Resultater fra ICP Forests Level 2 flater i Norge. Intensive forest monitoring in 2005. Results from ICP Forests Level 2 plots in Norway. - Viten fra Skog og landskap 04/2006.

Anonymous. 1998. GS+: geostatistics for the environmental sciences Version 2.1. - Gamma Design Software, Plainwell, Mich.

Anonymous. 1999a. ArcView GIS 3.2. - Environmental Systems Research Institute (ESRI) Inc., Redlands, California.

Anonymous 1999b. SPSS®Base 11.0 User's Guide. - SPSS Inc., Chicago.

Anonymous. 2004a. R Version 2.4.1 for Windows. URL: http://cran.r-project.org [The R foundation for statistical computing].

Anonymous. 2004b. R: a language and environment for statistical computing. URL: http://cran.r-project.org. [The R development core team, The R foundation for statistical computing].

Anonymous. 2006. Overvåking av langtransporterte forurensninger 2005 - Sammendragsrapport. - SFT rapport 957/2006, TA-2183/2006.

Abrahamsen, G., Horntvedt, R. & Tveite, B. 1977. Impacts of acid precipitation on coniferous forest ecosystems. - Wat. Air Soil Pollut. 8: 57-73.

Aune, B. 1993. Temperaturnormaler, normalperiode 1961-1990. - DNMI Rapp. 2: 1-63.

Aune, E.I. 1973. Forest vegetation in Hemne, Sør-Trøndelag, Western Central Norway. - K. Norske Vidensk. Selsk. Mus. Miscellanea 12: 1-87.

Auestad, I., Rydgren, K. & Økland, R.H. 2008. Scale-dependence of vegetation - environment relationships in semi-natural grasslands. - J. Veg. Sci. (in press)

Bakkestuen, V., Erikstad, L. & Økland, R.H. 2008. Step-less models for regional environmental variation in Norway. - J. Biogeogr. (in press)

- , Stabbetorp, O.E. & Eilertsen, O. 1999a. Terrestrisk naturovervåking. Vegetasjonsøkologiske undersøkelser av boreal bjørkeskog i Åmotsdalen, Sør-Trøndelag. - Norsk Inst. Naturforsk. Oppdragsmeld. 610: 1-43.

- , Stabbetorp, O. E. & Eilertsen, O. 1999b. Terrestrisk naturovervåking. Vegetasjonsøkologiske undersøkelser av boreal bjørkeskog i Møsvatn-Austfjell, Telemark. - Norsk Inst. Naturforsk. Oppdragsmeld. 611: 1-47.

- & Erikstad L. 2002. Terrestrisk overvåking. Metodeutvikling med fokus på arealdekkende modeller – analyse av detaljerte vegetasjonsdata og regionale miljøvariable. - Norsk Inst. Naturforsk. Oppdragsmelding 759: 1-35.

Bates, J.W. 1992. Mineral nutrient acquisition and rentention by bryophytes. - J. Bryol. 17. 223-240.

Beier, C., Hansen, K. & Gundersen, P. 1993. Spatial variability of throughfall fluxes in a spruce forest. - Environm. Pollution 81: 257-267.

Benum, P. 1958. The flora of Troms fylke. A floristic and phytogeographical survey of the vascular flora of Troms fylke in northern Norway. - Tromsø Mus. Skr. 6: 1-402.

Bergeron, Y. & Bochard, A. 1983. Use of groups in analysis and classification of plant communities in a section of western Quebec. - Vegetatio 56: 45-63.

Borcard, D., Legendre, P. & Drapeau, P. 1992. Partialling out the spatial component of ecological variation. - Ecology 73: 138-157.

Boyko, H. 1947. On the role of plants as quantitative climate indicators and the geo-ecological law of distribution. - J. Ecol. 35: 138-157.

Braak, C.J.F. ter 1986. Canonical correspondence analysis: a new eigenvector technique for multivariate direct gradient analysis. - Ecology 67: 1167-1179.

- 1987a. The analysis of vegetation-environment relationships by canonical correspondence analysis. - Vegetatio 69: 69-77.
- 1987b. CANOCO - a FORTRAN program for canonical community ordination by (partial) (detrended) (canonical) correspondence analysis, principal components analysis and redundancy analysis (version 2.1). - TNO Inst. Appl. Comp. Sci., Stat. Dept. Wageningen, Wageningen.
- & Prentice, I.C. 1988. A theory of gradient analysis. - Adv. ecol. Res. 18: 271-317.
- 1990. Update notes: CANOCO version 3.10. - Agricult. Math. Group, Wageningen.
- & Smilauer, P. 1998. - CANOCO Reference Manual and User's Guide to Canoco for Windows. Software for Canonical Community Ordination (version 4). - Centre for Biometry Wageningen, 1998.
- & Smilauer, P. 2002. - CANOCO Reference Manual and User's Guide to Canoco for Windows. Software for Canonical Community Ordination (version 4.5). - Centre for Biometry Wageningen, 2002.

Brattbakk, I. 1993. Terrestrisk naturovervåking. Vegetasjonsovervåking i Møsvatn-Austfjell. Norsk Inst. Naturforsk. Oppdragsmelding 209: 1-33.

- , Høyland, K., Halvorsen Økland, R., Wilmann, B. & Engen, S. 1991. Terrestrisk naturovervåking. Vegetasjonsovervåking 1990 i Børgefjell og Solhomfjell. - Norsk Inst. Naturforsk. Oppdragsmelding 91: 1-90.

- , Gaare, E., Fremstad Hansen, K. & Wilmann, B. 1992. Terrestrisk naturovervåking. Vegetasjonsovervåking i Åmotsdalen og Lund 1991. - Norsk Inst. Naturforsk. Oppdragsmelding 131: 1-66.

Braun-Blanquet, J. 1928. Pflanzensoziologie. - Springer Verlag, Berlin.

- 1965. Plant sociology: The study of plant communities. - Hafner, London.

Brown, D.H. & Bates, J.W. 1990. Bryophytes and nutrient cycling. - Bot. J. Linn. Soc. 104: 129-147.

Bryn, A. & Daugstad, K. 2001. Summer farming in the subalpine birch forest. In F.E. Wielgolaski (ed.) Nordic mountain birch ecosystem pp. 307-315. - UNESCO Man and Biosphere Series 27.

Carleton, T.J. 1990. Variation in terricolous bryophyte and macrolichen vegetation along primary gradients in Canadian boreal forests. - J. Veg. Sci. 1: 585-594.

- & Maycock, P.F. 1980. Vegetation of the boreal forest south of James Bay: Non-centered component analysis of the vascular flora. - Ecology 61: 1199-1212.

Conover, W.J. 1980. Practical nonparametric statistics. 2nd. ed. - Wiley, New York.

Crawley, M.J. 2002. Statistical Computing: An Introduction to Data Analysis using S-Plus. - John Wiley & Sons. pp. 761.

Dahl, E. 1957. Rondane. Mountain vegetation in South Norway and its relation to the environment. - Skr. Norske Vidensk. Akad. Mat.- Naturv. Kl. 1956: 1-374.

- 1986. Alpine - subalpine plant communities of South Scandinavia. - Phytocoenologia 15: 455-484.

- , Gjems, O. & Kielland-Lund, J. 1967. On the vegetation types of Norwegian conifer forest in relation to the chemical properties of the humus layer. - Meddr norske SkogforsVesen 25: 505-531.

Dargie, T.C.D. 1984. On the integrated interpretation of indirect site ordination: a case study using semi-arid vegetation in south-eastern Spain. - Vegetatio 55: 37-55.

Dierschke, H. 1982. Pflanzensoziologie. Grundlagen und Methoden. - E. Ulmberg Verlag, Stuttgart.

Dimbleby, G.W. 1952a. The root sap of birch on a podsol. - Plant and Soil 4: 141-153.

- 1952b. Soil regeneration on the north-east Yorkshire moors. - J. Ecol. 40: 331-341.

Dons, J.A. & Jorde, K. 1978. Geologisk kart over Norge, berggrunnskart Skien 1 : 250000. - Norges geol. unders. (NGU).

- , Helm, M., & Sigmond, E.M.O. 1990. Frøystaul berggrunnskart 1514 I, 1:50000, foreløpig utgave. - Norges geol. unders. (NGU)

Eilertsen, O. & Pedersen, O. 1989. Virkning av nedveiing og artsfjerning ved DCA-ordinasjon av vegetasjonsøkologiske datasett. - Univ. Trondheim, Vitensk. mus. Rapp. bot. Ser. 1988-1: 5-18.

- Økland, R.H., Økland, T. & Pedersen, O. 1990. Data manipulation and gradient length estimation in DCA ordination. - J.Veg. Sci. 1: 261-270.

- & Brattbakk 1994. Terrestrisk naturovervåking. Vegetasjonsøkologiske undersøkelser av boreal bjørkeskog i Øvre Dividal nasjonalpark. - Norsk Inst. Naturforsk. Oppdragsmelding 286: 1-82.
- & Often, A. 1994. Terrestrisk naturovervåking. Vegetasjonsøkologiske undersøkelser av boreal bjørkeskog i Gutulia nasjonalpark. - Norsk Inst. Naturforsk Oppdragsmelding 285: 1-69.
- & Stabbetorp, O. E. 1997. Terrestrisk naturovervåking. Vegetasjonsøkologiske undersøkelser av boreal bjørkeskog i Børgefjell nasjonalpark. - Norsk Inst. Naturforsk Oppdragsmelding 408: 1-84.
- & Stabbetorp, O. 1997. Terrestisk naturovervåking: Vegetasjonsøkologiske undersøkelser av boreal bjørkeskog i Børgefjell nasjonalpark. Norsk Inst. Naturforsk. Oppdragsrapp. 408: 1-81.

Elkington, T.T. & Jones, B.M.G. 1974. Biomas and primary productivity of birch (Betula pubescens s. lat.) in south-west Greenland. - J. Ecol. 62: 821-830.

Etherington, J.R. 1982. Environment and Plant Ecolgy. - John Wiley & Sons. Chichester. England

Evans, L.S. 1984. Botanical aspects of acidic precipitation. - Bot. Rev. 50: 449-490.

Ewald, J. 2000. The influence of coniferous canopies on understorey vegetation and soils in mountain forests of the northern Calcareous Alps. - Appl. Veg. Sci. 3: 123-134.

Falkengren-Grerup, U. 1986. Soil acidification and vegetation changes in deciduous forest in southern Sweden. - Oecologia 70: 339-347.

Falkengren-Grerup, U. & Lakkenborg-Kristensen, H. 1994. Importance of ammonium and nitrate to the performance of herb-layer species from decidous forests in southern Sweden. - Environm. exp. Bot. 34: 31-38.

Fenstad, G.U., Walløe, L. & Wille, S.Ø. 1977. Three tests for regression compared by stochastic simulation under normal and heavy tailed distribution of errors. - Scand. J. Statist. 4: 31-34.

Ferrer-Castán, D. & Vetaas, O.R. 2003. Floristic variation, chorological types and diversity: do they correspond at broad and local scales? - Divers. Distrib. Vol. 9. Issue 3: 221-235.

Fitje, A. & Strand, L. 1973. Tremålingslære, ed. 2. - Universitetsforlaget, Oslo.

Fjellberg, A., Nygaard, P.H. & Stabbetorp, O.E. 2007. Structural changes in Collembola populations following replanting of birch with spruce in North Norway. *In:* Effects of afforestation on ecosystems, landscape and rural development, pp. 119-125. Proceeding of the AFFORNORD conference, Reykholt, Iceland, June 18-22, 2005. TemaNord 2007/508:

Fremstad, E. & Elven, R. 1987. Enheter for vegetasjonskartlegging i Norge. - Økoforsk Utredning 1, 1987.

- & Sørensen, O.J. 1989. Floristiske og faunistiske undersøkelser i området Frihetsli-Njunis i Målselv. En konsekvensanalyse. - Norsk Inst. Naturforsk.Oppdragsmelding 3: 1-42.
- 1997. Vegetasjonstyper i Norge. - Norsk Inst. Naturforsk.temahefte 12: 1-279.

Framstad, E (ed.) 2008. Natur i endring. Terrestrisk naturovervåking i 2007: Markvegetasjon, epifytter, smågnagere og fugl. - Norsk Inst. Naturforsk. Rapport 362: 1-116 .

Frisvoll, A.A., Elvebakk, A., Flatberg, K.I. & Økland, R.H. 1995. Sjekkliste over norske mosar. Vitskapleg og norsk namneverk. - Norsk Inst. Naturforsk. Temahefte 4: 1-104.

Førland, E.J. 1993. Nedbørsnormaler, normalperiode 1961-1990. - DNMI Rapp. 39: 1-63.

Gardiner, A.S. 1968. The reputatin of birch for soil improvement. A litterature review. - Forestry Commision Research and development Paper 67. HSMO London.

Gauch, H.G. 1982. Multivariate analysis in community Ecology. Cambrigde University Press. Cambrigde.

Gigon, A. & Rorison, I.H. 1972. The response of ecologically distinct plant species to nitrate and to ammonium nitrogen. - J. Ecol. 60: 93-102.

Glømme, H. 1932. Undersøkelser over ulike humustypers amoniakk- og nitratprodusjon samt faktorer som har innflytelse på disse prosesser. - Meddr norske SkogforsVesen 4: 37-328.

Godal, J. B. & Hauge, K. 1964. Gutulia naturpark. Hovedoppgaver i naturvern. - Skogbruksavdelingen, NLH, Ås. Upubl.

Grahn, O. 1977. Macrophyte succession in Swedish lakes caused by deposition of airborne acid substances. - Wat. Air. Soil. Pollut. 7: 295-306.

Green, R.N., Trowbridge, R.L. & Klinka, K. 1993. Towards a taxonomic classification of humus forms. - For. Sci. Monogr. 29: 1-49.

Haapasaari, M. 1998. The oligotrophic heath vegetation of northern Fennoscandia and its zonation. - Acta Bot. Fennica 135: 1-219.

Halvorsen, R. 2008. Begrepsapparat for vanntilgang: vannmetning, kildevannspåvirkning og torvdannelse. Naturtyper i Norge. Bakgrunnsdokument 6 (versjon 0.1): 44–48.

Halvorsen, R., Andersen, T., Blom, H.H., Elvebakk, A., Elven, R., Erikstad, L., Gaarder, G., Moen, A., Mortensen, P.B., Norderhaug, A., Nygaard, K., Thorsnes, T., Ødegaard, F. & Norderhaug, K.M. 2008. Naturtyper i Norge – Lokale basisøkokliner. - Naturtyper i Norge Bakgrunnsdokument 4 (versjon 0.1): 1–79 (www.artsdatabanken.no)

Hämet-Ahti, L. 1963. Zonation of the mountain birch forest in northernmost Fennoscandia. - Annls bot. Soc. zool.-bot. fenn. Vanamo 34: 1-127.

Heikkinen, R. 1991. Multivariate analysis of esker vegetation in southern Häme, S Finland. - Annls bot. Fenn. 28: 201-224.

Hesselman, H. 1926. Studier över barrskogens humustäcke, dess egenskaper och beroende av skogsvården. - Meddn St. SkogsförsAnst. 22: 169-552.

- 1937. Om humustäckets beroende av beståndets ålder och sammansättning i den nordiska granskogen av blåbärsrik *Vaccinium*-typ och dess innverkan på skogen föryngring och tilväxt. - Meddn St. SkogsförsAnst. 30: 529-716.

Hill, M.O. 1979. DECORANA - A FORTRAN program for detrended correspondence analysis and reciprocal averaging. Cornell University, Ithaca. New York, USA.

- & Gauch, H.G.J. 1980. Detrended correspondence analysis: an improvedordination technique. - Vegetatio 42: 47-58.

Hylen, G. & Larsson J.Y. 2007. The condition of Norwegian forests. Results from national surveillance 1989-2006. - Oppdragsrapport fra Skog og landskap 09/2007

Ingelstad, T. 1973. Mineral nutrient requirements of *Vaccinium vitis-idaea* and *Vaccinium myrtillus*. - Physiol. Pl. 29: 239-246.

Kalstad, J. K. 1974. Samene og Dividalen. - In: Vorren, K.-D, pp. 91-98. - Norges nasjonalparker (Øvre Dividal). Luther Forlag, Oslo

Kielland-Lund, J. 1972. Landskap og vegetasjon. - I: Borgos, G. & Elven, R. 1972. - Norges nasjonalparker 4 (Femundsmarka og Gutulia): 72 - 144.

- 1973. A classification of Scandinavian forest for mapping purposes. - IBP i Norden 11: 173-206.
- 1981. Die Waldgesellschaften SO-Norwegians. - Phytocoenologia 9: 53- 250.
- 1994. Syntaxonomy of Norwegian forest vegetation 1993. - Physical Geography 24: 299-310.

Kause, G.H.M., Arndt, U., Brandt, C.J., Bucher, J., Kenk, G. & Matzner, E. 1986. Forest decline in Europe: development and possible causes. - Wat. Air Soil Pollution 31: 647-668.

Krill, A. G. 1987. Snøhetta berggrunnskart 1519 4, 1:50000. Foreløpig utg. – Norges Geol. Unders. (NGU) Upubl.

Krog, H., Østhagen, H. & Tønsberg, T. 1994. Lavflora, 2. utg. Norske busk- og bladlav. - Universitetsforlaget, Oslo.

Kruskal, J.B. 1964a. Multidimensional scaling by optimizing goodness of fit to a nonmetric hypothesis. - Psychometrika 29: 1-27.

- 1964b. Nonmetric multidimensional scaling: a numerical method. - Psychometrika 29: 115-129.
- , Young, F.W. & Seery, J.B. 1973. How to use KYST, a very flexible program to do multidimensional scaling and unfolding. Bell Labs. Murray Hill, New Jersey, unpubl.

Kubin, E. 1983. Nutrients in the soil, ground vegetation and tree layer in an old spruce forest in Northern Finland. - Annls bot. Fenn. 20: 361-390.

Kussipalo, J. 1983a. Distribution of vegetation on mesic forest sites in relation to some characteristics of tree stand and soil fertility. - Silva fenn. 17: 403-418.

- 1983b. Distribution of vegetation on mesic forest sites in relation to some characteristics of the tree stand and soil fertility. - Silva fenn. 17: 403-418.
- 1984. Diversity pattern of the forest understorey vegetation in relation to some site characteristics. -Silva fenn. 18: 121-131.

- 1985. An ecological study of upland forest site classification in southern Finland. - Acta for. fenn. 192: 1-77.
- 1988. Dominance pattern with understorey bryophyte vegetation in southern boreal coniferous forest. In: Barkman, J.J. & Sykora K.V. (eds), pp 111-117. Dependent plant communities. - SPB Acad Publ. The Hague:

Laaksonen, K. 1976. The dependence on mean air temperature upon latitude and altitude in Fennoscandia (1921-1950). – Annls Acad. scient. fenn. Ser. A 3. Geol. Geogr. 119:1-19.

- 1979. Effective temperature sums and durations of the vegetative period in Fennoscandia (1921-1950). - Fennia 157: 2: 171-197.

Lahti, T. & Väisänen, R.A. 1987. Ecological gradients of boreal forests in South Finland: an ordination tests of Cajander's forest site type theory. - Vegetatio 68: 145-156.

Larcher, W. 2003. Physiological Plant Ecolgy. - Springer Verlag. Heidelberg. Germany. 1-513.

Lawesson, J.E., Eilertsen, O., Diekmann, M., Reinikainen, A., Gunnlaugsdottir, E., Fosaa, A.M., Carøe, I., Skov, F., Groom, G., Økland, T., Økland, R., Andersen, P.N., & Bakkestuen, V. 2000. A concept for vegetation studies and monitoring in the Nordic countries. - TemaNord 2000: 517. 1-124

Légaré, S., Bergeron, Y., Leduc, A. & Paré, D. 2001. Comparison of the understory Vegetation in boreal forest types of southwest Quebec. - Can. J. Bot. 79: 1019-1027.

Lid, J. & Lid, D.T. 1994. Norsk flora. 6. Utgåve ved Reidar Elven - Det norske samlaget, Oslo.

Liu, H.Y., Økland, T., Halvorsen, R., Gao, J.X., Liu, Q.R. Eilertsen, O. & Bratli H. 2008. Gradient analyses of forests ground vegetation and its relationships to environmental variables in five subtropical forest areas, S and SW China. - Sommerfeltia (in press).

Løbersli, E. 1989. Terrestrisk naturovervåking i Norge. - Dir. Naturforv. Rapp. 1989: 1-98.

Loucks, O.L. 1962. Ordinating forest communities by means of environmental scalars and phytosociological indices. - Ecological Monographs 32: 137-165.

Malmström, C. 1937. Tönnerssjöhedens försökspark i Halland. Ett bidrag till kännedomen om sydvästra Sveriges skogar, ljunghedar och torvmarker. - Meddn St. SkogsförsAnst. 30: 323-528.

- 1949. Studier över skogstyper och trädslagsfåordelning inom Västerbottens län. - Meddn St. SkogsförsInst. 37: 1-231.

Miehe, G. 1989. Vegetation patterns on Mount Everest as influenced by monsoon and föhn. - Vegetatio 79: 21-32.

Miles, J. 1981. Effect of birch on moorlands. - Institute of Terrestrial Ecology, Cambridge, Great Britain. 1-18.

- Kinnaird, J.W 1979. Grazing: with paticular reference to birch, juniper and Scots pine in the Scottish highlands. - Scottish Forestry 33: 280-289

- & Young, W.F. 1980. The effects on heathland and moorland soils in Scotland and northern England following colonization by birch (*Betula* spp.). - Bull. Ecol. 11: 233-242.

Miller, H.G. 1984. Nutrient cycles in birchwoods. - Proc. Roy. Soc. Edinburgh 85B: 83-96.

Minchin, P.R. 1987. An evaluation of the relative robustness of techniques for ecological ordination. - Vegetatio 69: 89-107.

- 1990. DECODA Version 2.01. - Dept. Biogeogr. Geomorph., Aust. Natn. Univ., Canberra.

Moen, A. 1990. The plant cover of the boreal uplands of central Norway. - Gunneria 63: 1-451. - 1998. Nasjonalatlas for Norge: Vegetasjon. - Statens kartverk, Hønefoss.

Mork, E. & Heiberg, H.H.H. 1937. Om vegetasjonen i Hirkjølen forsøksområde. - Medd. Norske Skogforsøksvesen 19: 615-684, 1 map, 1 pl.

Munch, J. S. 1974. Nordmennene og Dividalen. In: Vorren, K.-D, pp. 99-104. - Norges nasjonalparker (Øvre Dividal). Luther Forlag, Oslo

Mylona, Sophia: Historical development of regional sulphur levels in Europe - Some preliminary results. 1993. - Miljøverndepartementet: Fagrapport nr. 42

Nekola, J.C. & P.S. White. 1999. Distance decay of similarity in biogeography and ecology. J. Biogeogr. 26:867-878

Nordhagen, R. 1928. Die Vegetation und Flora des Sylenegebietes. I. Die Vegetation. - Skr. Norske Vidensk. Akad. Mat. Naturv. Kl. 1927: 1-88.

- 1943. Sikilsdalen og Norges fjellbeiter: en plantesosiologisk monografi. - Bergens museums skrifter; 22, Bergen.

Nystuen, J.P. 1979. Elgå, berggrunnsgeologisk kart 1719 II - M 1:50 000. - Norges geol. unders. (NGU) Unubl.

- & Trømborg, D. 1972. Berggrunn, løsavsetninger og landskapsformer. In: Borgos, G. & Elven, R. 1972, pp. 14-25. - Norges nasjonalparker 4 (Femundsmarka og Gutulia): Luther forlag, Oslo.

Odland, A., Bevanger, K., Fremstad, E., Hanssen, O., Reitan, O. & Aagaard, K. 1992. Fjellskog i Sør-Norge: biologi og forvaltning. - Norsk Inst. Naturforsk. Oppdragsmeld. 123: 1-90.

Ogner, G., Opem, M., Remedios, G., Sjøtveit, G. & Sørlie, B. 1991. The chemical analysis program of the Norwegian Forest Research Institute. - NISK, Ås. Unpubl.

Økland, R.H. 1990. Vegetation ecology: theory, methods and applications with reference to Fennoscandia. - Sommerfeltia Suppl. 1: 1-233.

- 1994. Reanalyse av permanente prøveflater i granskog i overvåkingsområdet Solhomfjell 1993. - Utredn. Dir. Naturforv. 1994: 5: 1-37.

- 1995. Population biology of the clonal moss *Hylocomium splendens* in Norwegian boreal spruce forests. I. Demography. - Journal of Ecology 83: 697-712.

- 2000. Population biology of the clonal moss *Hylocomium splendens* in Norwegian boreal spruce forests. 5. Consequences of the vertical position of individual shoot segments. - Oikos 88: 449-469.
- & Bendiksen, E. 1985. The vegetation of the forest-alpine transition in the Grunningsdalen area, Telemark, SE Norway. - Sommerfeltia 2: 1-224.
- & Eilertsen, O. 1993. Vegetation-environment relationships of boreal coniferous forests in the Solhomfjell area, Gjerstad, S Norway. - Sommerfeltia 16: 1- 254.

  & Eilertsen, O. 1994. Canonical correspondence analysis with variation partitioning: some comments and an application. - J. Veg. Sci. 5: 117-126.
- & Eilertsen, O. 1996. Dynamics of understory vegetation in an old-growth 18 boreal coniferous forest, 1988-1993. - J. Veg. Sci. 7: 747-762.
- , Økland, T & Rydgren, K. 2001. Vegetation-environment relationships of boreal spruce swamp forests in Østmarka Nature Reserve, SE Norway. - Sommerfeltia 29: 1-190.
- Bakkestuen, V. 2004. Fine-scale spatial patterns in populations of the clonal moss *Hylocomium splendens* partly reflect structuring processes in the boreal forest floor. - Oikos. 106: 565-575.

Økland, T. 1988. An ecological approach to the investigation of a beech forest in Vestfold, SE Norway. - Nord. J. Bot. 8: 375-407.
- 1990. Vegetational and ecological monitoring of boreal forests in Norway. I. Rausjømarka in Akershus county, SE Norway. - Sommerfeltia 10: 1-52.
- 1993. Vegetasjonsøkologisk overvåking av barskog i Gutulia nasjonalpark. - Norsk Inst. Jord- Skogkartlegging, Ås. Rapp. 6: 1-76.
- 1996. Vegetation-environment relationships of boreal spruce forest in ten monitoring reference areas in Norway. - Sommerfeltia 22: 1-349.
- , Bakkestuen, V., Økland, R.H. & Eilertsen, O. 2001. Vegetasjonsendringer i Nasjonalt nettverk av flater for intensivovervåking i skog. - Norsk Inst. Jord- Skogkartlegging Rapp. 2001: 1-46.
- , Bakkestuen, V., Økland, R.H. & Eilertsen, O. 2004. Changes in forest understory vegetation in Norway related to long-term soil acidification and climatic change. - J. Veg. Sci. 15: 437-448.

Oksanen, J. 2007. Multivariate analysis of ecological communities in R: vegan tutorial, URL: http://cc.oulu.fi/~jarioksa/opetus/metodi/vegantutor.pdf, pp. 39.

Oksanen, J., Kindt, R., Legendre, P. & O'Hara, B. 2007. Package 'vegan' Version 1.9–13. URL: http://cc.oulu.fi/~jarioksa. -Univ.of Oulu, Oulu, Finland, pp.120.

Olsen, R. 1990. Mikrobielle prosesser i jord sett i forhold til skogens vekst og vitalitet. - Aktuelt Norsk Inst. Skogforsk. 5: 50-61.

Osland, L.M. 1974. Berggrunn. In: Vorren K-D, pp. 15-20. - Norges nasjonalparker (Øvre Dividal). Luther Forlag, Oslo

Palmer, M.W. 1993. Putting things in ever better order: the advantages of canonical correspondence analysis. - Ecology 74. 2215-2230.

Parker, K.C. 1988. Environmental relationships and vegetation associates of columnar cacti in the Sonoran desert. - Vegetatio 78: 125-140.

Pavlidis, T. 1982. Algorithms for graphics and image processing. - Springer-Verlag, Berlin.

Pedersen, O. 1988. Biological data program/PC. Version 1.01. Brukerveiledning. - VegeDataConsult, Oslo.

Pearson, K. 1901. On lines and planes of closest fit to systems of points in space. - Phil. Mag., 6. Ser 2: 559-572.

Peidano, M. & Moreno, G. 1989. The genus Betula (Betulaceae) in the Sistema Centra (Spain). - Willdenowia 18: 343-359.

Pigott, C.D. 1983. Regeneration of oak-birch woodland following exclusion of sheep. - J. Ecol. 71: 629-646.

Ponge, J.-F. & Ferdy, J.-B. 1997. Growth of Fagus sylvatica saplings inan old-growth forests as affected by soil and light conditions. - J. Veg. Sci. 8: 789-796.

Qian, H., Klinka, K., Økland, R.H., Krestov, P. & Kayahara, G.J. 2003. Comparison of species composition and species density of understorey vegetation in the boreal *Picea mariana* and *Populus tremuloides* stands in British Columbia, Canada. - J. Veg. Sci. 14: 173-184.

Reuss, J.O., Cosby, B.J. & Wright, R.E. 1987. Chemical processes governing soil and water acidification. - Nature 329: 27-32.

Rydgren, K. 1994. Low-alpine vegetation in Gutulia National Park, Engerdal, Hedmark, Norway, and its relation to the environment. - Sommerfeltia 21: 1-47.

Saetre, P. 1998. Decomposition, microbial community structure, and earthworm effects along a birch-spruce soil gradient. - Ecology 79: 834-846.

- , Saetre, L.S., Brandtberg, P.-O., Lundkvist, H. & Bengtsson, J. 1997. Ground vegetation composition and heterogeneity in pure Norway spruce and mixed Norway spruce - birch stand. - Can. J. For. Res. 27: 2034-2042.

Scütt, P. & Cowling, E.B. 1985. Waldsterben, a general decline of forest in Central Europe: Symptoms, development and possible causes. - Pl. Dis 69: 548-558.

Sepponen, P. 1985. The ecological classification of sorted soils of varying genesis in northern Finland. - Communtnes Inst. For. Fenn. 129: 1-77.

Sigmond, E.M.O., Gustavson, M. & Roberts, D. 1984. Berggrunnskart over Norge. - Norges geol. unders.. Målestokk 1:1 mill.

Sirén, G. 1955. The development of spruce forest on raw humus sites in northern Finland and its ecology. - Acta for. fenn. 62: 1-408.

Smith, T.M. & Urban, D.L. 1988. Scale and resolution of forest structural pattern. - Vegetatio 74: 143-150.

Sokal, R.R. & Rohlf, F.J. 1995. - Biometry, 3. ed. Freeman, New York.

Sollid, J.L., Carlson, A.B. & Torp, B. 1980a. Trollheimen-Sunndalsfjella-Oppdal. Kvartærgeologiske kart 1:100000. - Univ. Oslo, Geografisk inst. Unpubl.

- , Carlson, A.B. & Torp, B. 1980b. Kvartærgeologiske kart 1:100000. Kort beskrivelse til kartet. - Norsk Geogr. Tidskr. 34: 177-189.

Stabbetorp, O.E., Bakkestuen, V., Eilertsen, O. & Bendiksen, E. 1999. Terrestrisk naturovervåking. Vegetasjonsøkologiske undersøkelser av boreal bjørkeskog i Lund, Rogaland. - Norsk Inst. Naturforsk. Oppdragsmeld. 609: 1-55.

Stålfelt, M.G. 1937a. Der Gasaustauch der Moose. - Planta 27: 30-60.

- 1937b. Die Bedeutung der Vegetation im Wasserhaushalt des Bodens. - Svenska Skogvårdsfören. Tidskr. 35: 161-195.

Tamm, C.O. 1953. Growth, yield and nutrition in carpets of a forest moss (*Hylocomium splendens*). - Meddn St. SkogsforskInst. 43: 1: 1-140.

- 1959. Stuclier over kliinatets huiniclitet i Sverige. - Kungl slrogshogsk slir. 32: 1-49

- 1976. Acid precipitation: biological effects in soil and on forest vegetation. - Ambio 5: 235-238.

- 1991. Nitrogen in terrestrial ecosystems. Questions of productivity, vegetational changes, and ecosystem stability. - Ecol. Stud. 81: 1-116.

Tamm, O. 1959. Studier över klimaets humiditet i Sverige. - K. Skogshögsk. Skr. 32: 1-48.

Taylor, B.R., Carleton, T.J., & Adams, P. 1987. Understorey vegetation change in a Picea mariana chronosequence. - Vegetatio 73: 63-72.

Tonteri, T., Mikkola, K. & Lahti, T. 1990. Compositional gradients in the forest vegetation of Finland. - J. Veg. Sci. 1:691-698.

Tørseth, K. & Semb, A. 1997. Deposition of major inorganic compounds in Norway 1992-1996. - Norsk Inst. Vannforsk. Rapp. 1997: 1-44.

Ulrich, B., Mayer, R. & Khanna, P.K. 1979. Deposition von Luftverunreinigungen und ihre Auswirkungen im Waldekosystem im Solling. - Schr. forst. Fak. Univ. Göttingen 58: 1-291.

Varskog, P. 1995. A study of the chemical composition of Norwegian forest soils with relation to climatic, pedological and edaphic factors. - Dr scient. Thesis, Univ. Trondheim, Trondheim.

Venables, W. & Ripley, B. 2002. Modern Applied Statistics with S-Plus. - Springer, New York, USA.

Vetaas, O.R. 1992. Gradients in field-layer vegetation on an arid misty mountain plateau in the Sudan. - J. Veg. Sci. 3, 527-534.

Vevle, O. 1986. Norske vegetasjonstypar. 3rd ed. - Nistås Forlag, Bø.

Vorren, K.-D. & Engelskjøn, T. 1974. Vegetasjon og flora. - Norges nasjonalparker (Øvre Dividal): 38-69.

Walter, H. & Walter, E. 1953. Einige allgemeine Ergebnisse unserer Forschungsreise nach Südwestafrika 1952/53: Das Gesetz der relativen Standortskonstanz; das Wesen der Pflanzengemeinschaften. - Berichte der Deutschen Botanischen Gesellschaft 66: 228-236.

Wielgolaski, F.E. 1997. Fennoscandian tundra. In: Wielgolaski F.E. (ed.), pp. 227-283. Ecosystems of the world 3. Polar and alpine tundra. - Elsevier, Amsterdam:

Wittich, W. 1961. Der Einfluß der Baumart auf den Bodenzustand. - Allg. Forst-Z. 16: 41-45.

Wittig, R. & Neite, H. 1985. Acid indicators around the trunk base of Fagus sylvatica in limestone and loess beechwoods: distribution pattern and phytosociological problems. - Vegetatio 64: 113-119.

Wold, O. 1989. Botaniske undersøkelser i Gutulia nasjonalpark 1988. - Fylkesmannen i Hedmark, Miljøvernavd. Rapp. 29: 1-32.

Aarrestad P.A. 2002. Vegetation-environment relationships of broad-leaved deciduous forests in Hordaland county, western Norway. - Ilicifolia 3:1-90.

- , Bakkestuen, V., Stabbetorp, O.E. & Wilmann B. 2008. Vegetasjonsøkologiske undersøkelser av boreal bjørkeskog i Møsvatn 2007. In: Framstad, E (ed.) 2008. pp. 16-27. Natur i endring. Terrestrisk naturovervåking i 2007: Markvegetasjon, epifytter, smågnagere og fugl. - NINA Rapport 362:

Aas, Ø. 1989. Skoglige forhold i Gutulia nasjonalpark og i utvidelsesalternativene. - Fylkesmannen i Hedmark, Miljøvernavd. Rapp. 23: 1-41.

Aas, W., Tørseth, K., Solberg, S., Berg, T., Manø, S. & Yttri, K.E. 2002. Overvåking av langtransportert forurenset luft og nedbør. Atmosfærisk tilførsel, 2001. - St. Progm. Forurensn. Overvåking Rapp. 847: 1-156.

Paper 3

This article is removed.

Paper 4

This article is removed.

Paper 5

This article is removed.

Paper 6

sommerfeltia

30

Bendiksen, E., Økland, R.H., Høiland, K., Eilertsen, O. & Bakkestuen, V.

Relationships between macrofungi, plants and environmental factors in boreal coniferous forests in the Solhomfjell area, Gjerstad, S Norway

2004

ISBN 82-7420-044-6

ISSN 0800-6865

Bendiksen, E., Økland, R.H., Høiland, K., Eilertsen, O. & Bakkestuen, V. 2004. Relationships between macrofungi, plants and environmental factors in boreal coniferous forests in the Solhomfjell area, Gjerstad, S Norway. – Sommerfeltia 30: 1-125. Oslo. ISBN 82-7420-044-6. ISSN 0800-6865.

The macrofungal species composition and its relationships to ecological factors and vegetation were investigated in a boreal coniferous forest area. Macrofungi were recorded in 99 16-m^2 macroplots, each divided into 16 subplots of 1 m^2. Presence/absence of each species was recorded in every subplot and frequency in 16 subplots was used as abundance measure. Two 1-m^2 plots within each macro plot had previously been analysed with respect to vascular plants, bryophytes and macrolichens. All plots were provided with measurements of 36 environmental variables. Parallel DCA and two-dimensional LNMDS ordinations of macroplots identified the same two coenocline axes. One more coenocline axis identified by DCA was also possible to interpret ecologically. The first fungal coenocline corresponded to the main coenocline for vegetation, comprising the variation from pine to spruce dominated forests; from ridge via slope to valley bottom. This coenocline is interpreted as the response to two independent complex-gradients: (1) a topography-soil depth complex-gradient in the pine forest, and (2) a complex-gradient in soil nutrient status in the spruce forest. While macro-scale topographic variables were relatively more strongly correlated with the vegetational coenocline, soil pH and nitrogen content were more strongly correlated with the fungal coenocline. It is argued that the soil moisture deficiency hypothesis, i.e. that species differ in drought tolerance, proposed as an explanation for variation along the main vegetational coenocline in pine forests, also applies to pine-forest macrofungi. The responses of macrofungi and plants to edaphic conditions in spruce forest were found to differ in one important respect: while plants common on poor soils are normally present also in richer sites, many macrofungal species were absent or rare there. Reasons for this are discussed. The second coenocline (only identified by DCA), only relevant for the spruce forest, reflected the variation from bryophilous fungal species that avoided sites with dense deciduous litter to saprotrophic species living on incompletely decayed *Populus* and *Betula* litter and ectomycorrhizal fungi associated with deciduous trees. The third coenocline strongly correlated with median soil moisture and also related to fine-scale canopy closure was interpreted as due to a fine-scale paludification gradient. The correspondence between ordination results obtained for fungi and plants demonstrates (1) that distributional patterns of macrofungi and plants within forests to a large extent (but not completely) are caused by the same major environmental complex-gradients and (2) that the same field and analytical methods are applicable to both groups of organisms.

Keywords: Boreal coniferous forests, DCA, Environmental factors, Fungi, Gradient, LNMDS, Macromycetes, Mycorrhiza, Norway, Ordination.

Egil Bendiksen and Vegar Bakkestuen, Norwegian Institute for Nature Research, P.O. Box 736 Sentrum, N-0105 Oslo, Norway; Rune H. Økland, Botanical Museum, Univ. of Oslo, P.O. Box 1172 Blindern, N-0318 Oslo, Norway, and Norwegian Institute of Land Inventory, P.O. Box 115, N-1430 Ås, Norway; Klaus Høiland, Department of Biology, Division of Botany and Plant Physiology, University of Oslo, P.O. Box 1045 Blindern, N-0316 Oslo, Norway; and Odd Eilertsen, Norwegian Institute for Nature Research (present address: Norwegian Institute of Land Inventory).

CONTENTS

INTRODUCTION

Variation in the macrofunga of coniferous forests is partly known from floristical observations and descriptions in floras, partly from studies relating fungi to predefined vegetation types. Fennoscandian works from coniferous forest vegetation based on recording of fruitbodies include among others Østmoe (1979), Bendiksen (1981), Metsänheimo (1982), Mehus (1986), Brandrud (1987), Hintikka (1988), Såstad (1990), Dahlberg (1991), Gulden et al. (1992), Ohenoja (1993), Blomgren (1994), Väre & Ohtonen (1996), and Dahlberg et al. (1997). These studies have been performed within larger plots with none or few measurements of ecological variables. Except for the studies by Såstad (1990) and Väre & Ohtonen (1996), variation in fungal distribution, presence and abundance has not been related to a wide range of potentially important environmental variables.

Knowledge about the responses of living organisms to ecological gradients under natural conditions is increasingly needed as a background for detecting and understanding biotic effects of man-induced environmental changes. In boreal forests, man induces environmental change by several means. Deposition of long-distance airborne pollutants has been most strongly focused for ectomycorrhizal fungi (e.g. Høiland 1993), while modern forestry practices have been especially emphasized in connection with wood-inhabiting corticiaceous and polyporaceous species (Renvall 1995, Bader et al. 1995, Høiland & Bendiksen 1997, Lindblad 1998).

Multivariate gradient analysis has since long been accepted as a standard tool for summarizing vegetation patterns (e.g., Kent & Ballard 1988, R. Økland 1990). From about 1985 there has been a marked increase in the use of these methods in the macrofungal parallel to vegetation ecology. Nevertheless, the field methodology, including sample procedures, of fungal ecological studies has largely remained unaffected.

In Norway, several reference sites for monitoring of vegetation have been established in the boreal zones during the last decade (T. Økland 1990, 1996, R. Økland & Eilertsen 1993, Eilertsen & Often 1994, T. Økland et al. 2001). The Solhomfjell area in S Norway was among the first sites to be established (in 1988; see R. Økland & Eilertsen 1993, 1996, R. Økland 1995a, 1995b). In this area, vegetation-environment relationships have been studied in 200 permanent plots, 1 m^2 each. These plots are situated in groups of two within each of 100 16-m^2 macro plots, in turn distributed on eight transects intended to cover the main variation in vegetation and local environmental factors in the area. This study of relationships between macrofungi, plants and environmental factors is an extension of the study by R. Økland & Eilertsen (1993), in two respects: (1) it is carried out in the same permanent plots, and (2) previous analyses of vegetation and recordings of environmental variables are related to the observed fungal patterns.

The aims of the study are: (1) to find the main gradients in terricolous macrofungal species composition in an area dominated by oligotrophic boreal coniferous forest vegetation and to relate these gradients to environmental complex-gradients; (2) to compare these gradients in macrofungal species composition with gradients in plant species composition; i.e. to test (i) whether gradients in species composition in each of the two groups of organisms are correlated, (ii) in case, test if their relative importance are similar for the two groups, and (iii) discuss the processes behind the observed patterns; and (3) to explore the suitability of gradient analysis techniques (including multivariate methods such as ordination) for use with macrofungi. This study is also designed to form the basis for monitoring of changes in macrofungal species composition, e.g. resulting from deposition of airborne pollutants or climatic change.

THE INVESTIGATION AREA

The investigation area, *c*. 2 km^2, is situated in the Solhomfjell area, Gjerstad, Aust-Agder county, S Norway, 58º58' N, 8º58' E, altitude 350–480 m.a.s.l. (Fig. 1).

GEOLOGY AND GEOMORPHOLOGY

The bedrock belongs to the central-southern Norwegian Precambrian, consisting mainly of gneisses with intrusions of granites and pegmatite (Oftedahl 1980, Sigmond et al. 1984). According to Børset (1979) the area around Svarttjern (the eastern part of the investigation area; Fig. 2) consists of gneissic granites with large pegmatite intrusions, while the Solhomfjell area (the western part of the investigation area) consists of pale granites with numerous pegmatite intrusions and locally a more gneissic structure.

The investigation area is situated in a hilly landscape, with peaks up to 653 m (Solhomfjell), rising from a plateau at 350–400 m, and surrounded by deep valleys at all margins.

Morainic deposits are sparse; the bedrock is covered with morainic deposits in sheltered sites only. Most of the soils have been formed *in situ*. Soils deeper than 50 cm are rarely encountered. Peat

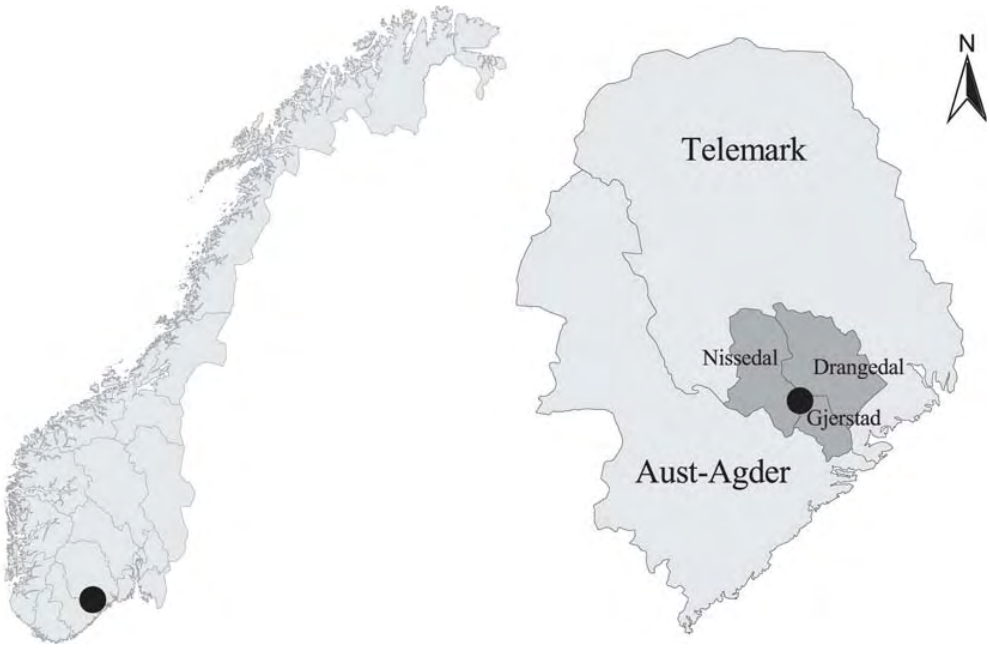

Fig. 1. Maps of Norway (left) and the counties Aust-Agder and Telemark (right) showing the position of the investigation area (dot) close to the border between Gjerstad, Drangedal and Nissedal municipalities. From R. Økland & Eilertsen (1993).

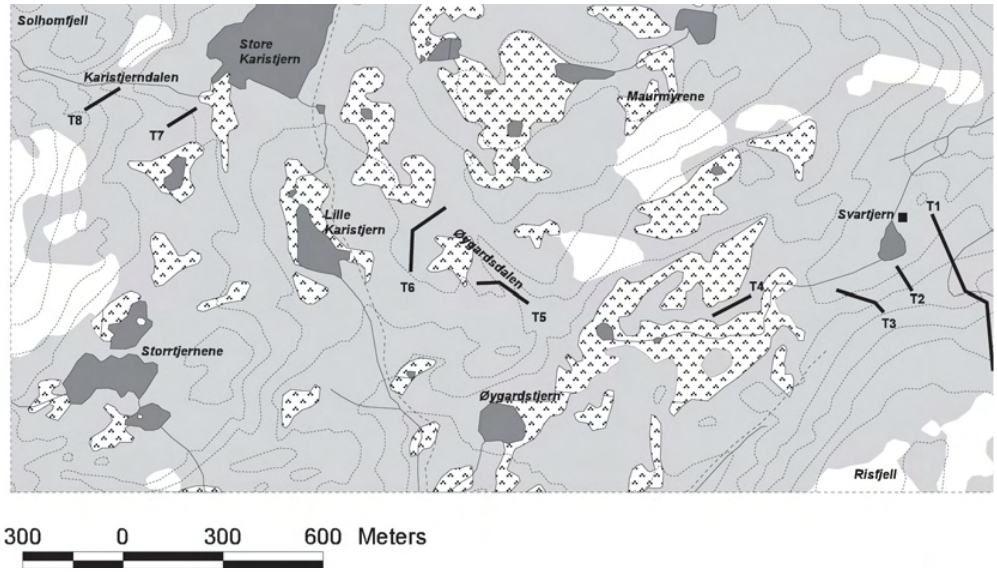

Fig. 2. The investigation area, with transects T1–T8. Contour interval 25 m (reference altitudes: Svarttjern 348 m a.s.l.; Store Karistjern 426 m a.s.l.). Altitudes in m. Heavily shaded – lakes and tarns. Dotted – mires. Lightly shaded – forest. From R. Økland & Eilertsen (1993).

covers extensive areas; narrow sloping fens typically split the forest into smaller stands, dominated by Norway spruce (*Picea abies* (L.) Karst.) and Scots pine (*Pinus sylvestris* L.).

CLIMATE

The climate is suboceanic. The estimated annual mean temperature 1961–90 was 4.2 ºC [data of Aune (1993) from the nearest meteorological station Tveitsund (20 km WNW of the study area, 252 m.a.s.l.), corrected for altitude according to Laaksonen (1976)]. The mean temperature (1961–90) of the warmest and coldest months (July and February) was 14.4 and –5.5 ºC, respectively. Annual mean precipitation (1961–90) at the meteorological station Gjerstad was 1290 mm (Førland 1993); perhaps somewhat higher in the investigation area (R. Økland & Eilertsen 1993).

The main features of climatic *variation* in the study period (1989-91) were as follows (Tab. 1): The 1988/89 winter and the 1989 spring were exceptionally mild: temperature means were above 2.5 ºC all months and a permanent snow cover hardly occurred. Temperatures were close to normals for the rest of the year. The growing season was dry (Tab. 1). Another exceptionally mild and rainy winter (203 mm in February; 4× normal) without stable snow cover followed. April and May 1990 were also mild, but rainfall and temperatures deviated slightly from normals for the rest of the year. Except for the dry spring and summer (only 1 mm in May) and the cold June (Tab. 1), 1991 was close to normals.

FOREST HISTORY AND HUMAN INFLUENCE

The investigation area is protected as a National Nature Reserve (Solhomfjell Forest Reserve), from 1993. The forests in the investigation area have not been commercially exploited [see R. Økland & Eilertsen (1993) for brief summary of conservation history and human activities], and no traces of logging occur. However, the presence of moderate amounts of fallen logs indicates that fallen and standing dead trees have been removed for fuel. Extensive logging has, however, been performed outside the reserve. Trees with fire scars have been observed sporadically but only outside the studied plots. It is likely that the development of vegetation has been continuous for a long time, at least more than one hundred years. Tree ages up to 200 years for Norway spruce and over 350 years for Scots pine have been recorded.

Hafsten (1985) estimated the spruce immigration in the area to have taken place around A.D. 1000).

Annual amounts of acidifying compounds deposited by precipitation (1992 and 1993 averages) were 7.9 kg $N \cdot ha^{-1} \cdot yr^{-1}$ (4.3 kg NO_3-N and 3.6 kg NH_4-N) and 6.4 kg SO_4-$S \cdot ha^{-1} \cdot yr^{-1}$; the annual mean rainwater pH was 4.4 (Tørseth & Røyset 1993, Tørseth & Røstad 1994). The deposition of long distance airborne pollutants is high relative to other parts of Norway (Anonymous 1995).

PHYTO- AND FUNGAL GEOGRAPHY

The area is situated in the southern (and middle) boreal zone [in the terminology of Ahti et al. (1968); see R. Økland & Eilertsen (1993) and Moen (1998)].

Most of the recorded macrofungal species have a wide distribution in the boreal zones of Norway. Five species are, however, southern: *Mycena inclinata* and *Lactarius quietus*, that are associated with *Quercus* spp; *Laccaria amethystina*, which is markedly southern, common in the nemoral and boreonemoral zones and more accidentally present in the southern boreal zone; and *Lactarius camphoratus* and *Amanita virosa*, typical boreonemoral and southern boreal coniferous forest species that decrease markedly from the southern to the middle boreal zone (E. Bendiksen, pers. obs.). *Amanita virosa* is particularly common in the study area.

Tab. 1. Climate in the study period. Data from the meteorological station Tveitsund (Norske meteorologiske Institutt 1988–92) compared with 1961–90 means (Aune 1993, Førland 1993). % – percentage of mean, Δ – difference from mean.

Year	Precipitation						Snow depth	Temperature					
	Year		May–June		May–Sept.		February	Year		May–June		May–Sept.	
	mm	%	mm	%	mm	%	cm	mm	Δ	mm	Δ	mm	Δ
1988	1,329	134	111	74	693	149	53	5.9	0.9	13.4	2.1	13.3	1.0
1989	790	80	44	30	180	39	5	7.1	2.1	11.7	0.5	12.8	0.5
1990	1,157	116	117	79	422	91	4	7.2	2.2	12.5	1.3	12.9	0.6
1991	799	80	90	60	273	59	44	5.9	0.9	9.9	–1.3	12.6	0.3

MATERIAL AND METHODS

The field work was carried out in the years 1988 (recording of plants and environmental variables 1–33), 1989–1991 (recording of fungi), and 1997 (recording of supplementary environmental variables *2 and *3).

THE SAMPLING DESIGN

Eight transects of different lengths were subjectively selected to cover the variation in boreal forest vegetation, as well as the variation in topography, slope, aspect etc., in the investigation area. Every tenth meter along a transect was a potential site for the lower left corner of a macro plot, 16 m^2. Macro plot positions were rejected if they included (1) mires, tarns or elements of ecosystems other than forest, (2) more than 50% naked rock, (3) cliffs higher than 1 m, or (4) boulder stones with diameter larger than 1 m. From the accepted positions, macro plots were drawn at random except for the following restrictions: (1) plot number per transect was to be proportial with transect length, and (2) total plot number was to be 100. The study of fungal species composition was performed in the macro plots. Macro plot No. 20 was heavily disturbed by root uplift early in 1989, and excluded from the study.

Each macro plot was divided into 16 macro subplots, of which two (along opposite margins of the macro plot, in fixed positions) were taken as meso plots (1 m^2). The study of vegetation by R. Økland & Eilertsen (1993) was concentrated to meso plots. Like macro plots, meso plots were rejected and replaced by a neighbouring plot, selected from a fixed priority list, if not meeting a pre-defined set of criteria (see R. Økland & Eilertsen 1993).

All plot corners were permanently marked with subterranean aluminium tubes.

RECORDING OF MACROFUNGI

The term macrofungi is a practical, not a taxonomical concept. The following groups were included: all agarics and boletes (Agaricales, Russulales and Boletales), terricolous Aphyllophorales, gasteromycetes, larger heterobasidiomycetes and ascomycetes. With the exception of *Glomus* sp., which was recorded when seen, hypogeous species were not included in this study. Wood-inhabiting species were included only when emerging from soil-buried wood and/or small wood fragments or twigs up to a diameter of 1 cm. For convenience, we will use the term ‘fungi’ in the meaning ‘macrofungi’ in this paper.

The recorded species are listed in Appendix 1.

The recorded species are divided into ectomycorrhizal and non-mycorrhizal on basis of information in the literature, e.g. Molina et al. (1992) (an exception of the mycorrhizal group is *Glomus* sp., forming VA mycorrhizae). The *Entoloma* species found in this study are considered as

saprotrophs, except for *E. rhodopolium*, which has been shown to be a mycorrhizal species (Modess 1941; cf. also Agerer & Waller 1993).

Presence/absence of all macrofungi was recorded in each macro subplot on four to five occasions between ultimo July or primo August and primo October (always with two visits in September, the optimal season for fruiting) in each of the three years. Recordings were pooled over visiting occasions to give as a result a data matrix with presence/absence data for fungi in macro subplots in the three-year study period. For practical reasons the vernal and late autumnal aspects were excluded. The production of fruitbodies was considered as close to the average in all three years, but with considerable variation within years. The number of fruitbodies was low in extended drought periods such as in late summer 1990, while September and October were moist to fairly moist in all years.

Frequency in subplots (see T. Økland 1988; R. Økland 1990) was calculated for each of the 235 species of fungi in each of the 99 macro plots. The resulting data set is referred to as the *MAF 99* data set.

The number of fungal species per macro plot is referred to as fungal species density, following Magurran (1988) and Grace (1999).

RECORDING OF EXPLANATORY VARIABLES

The term explanatory variable is used, in a collective sense, for the three kinds of variables used in interpretation of variation in fungal species composition: (1) vegetational gradients (gradients in composition of the vegetation), (2) environmental variables, and (3) spatial variables. R. Økland & Eilertsen (1993) give a detailed description of the methods used for recording variables of the first two kinds, and also provide thorough analyses of vegetation-environment relationships. Spatial variables are described by R. Økland & Eilertsen (1994).

Vegetational gradients

Recording of vegetation

Presence/absence (by cover) of *vegetation*, i.e. humus-dwelling vascular plants (the field layer; including lignified species < 80 cm high), bryophytes and lichens (the bottom layer), was recorded in 1988 in each of 16 0.0625 m^2-subplots in each of the 200 meso plots. Frequency in the 16 subplots was used as measure of species abundance. The following data sets analyzed by R. Økland & Eilertsen (1993) were used in the present study:

ME 200 - frequency in subplots data for 171 plant species in 200 meso plots.
MEV 200 - frequency in subplots data for 65 vascular plants species in 200 meso plots.
MEB 200 - frequency in subplots data for 106 bryophyte and lichen species in 200 meso plots.

Vegetational explanatory variables

R. Økland & Eilertsen (1993) found the main compositional gradients in vegetation by ordination. They applied DCA (Detrended Correspondence Analysis; Hill 1979, Hill & Gauch 1980) and LNMDS (Local Non-Metric Multidimensional Scaling; Kruskal 1964a, 1964b, Minchin 1987) in parallel to the ME 200 data set. R. Økland & Eilertsen (1993) interpreted the high similarity of the two-

dimensional solutions obtained by the two methods as strong indications that the main gradient structure in the ME 200 data set had been found (cf. R. Økland 1990, 1996), and that two main coenoclines (Whittaker 1967) exist in forest vegetation in the area. These coenoclines were interpreted ecologically by correlating meso plot scores along axes with the measured environmental variables.

As vegetational explanatory variables, to which patterns of variation in fungal species composition was related, we used meso plot positions along axes of three DCA ordinations [performed by the program CANOCO, Version 2.2 (ter Braak 1987a); species with below-median frequency in the data sets were proportionally downweighted (Eilertsen et al. 1990); detrending by segments and otherwise standard options]:

(1) Ordination of the ME 200 data set, axes 1–4 (*DCAG 1*, *DCAG 2*, *DCAG 3*, *DCAG 4*). The ecocline interpretation of the first two axes (R. Økland & Eilertsen 1993, 1994) was: (i) DCAG 1 was related to topography; running from herb-rich Norway spruce (*Picea abies*) forest on lower slopes and in valleys; via spruce forests on plane to concave slopes, dominated by *Vaccinium myrtillus*; and Scots pine (*Pinus sylvestris*) forests on convex slopes, dominated by ericaceous species; to lichen-rich pine forest on hill tops. Soil nutrient factors are considered important for the differentiation within spruce forest, and soil depth (probably related to risk of extreme drought) within pine forest. (ii) In both forest types, DCAG 2 mostly affected bryophytes and lichens, and was related to fine-scale paludification and canopy closure. Median soil moisture decreased along the axis from interspaces between trees to below trees. DCAG 3 and DCAG 4 were only weakly related to measured environmental variables, and no ecocline interpretation exists for these axes. The set of four DCA ordination axes based upon the ME 200 data set is denoted {D}.

(2) Ordination of the MEV 200 data set, axis 1 (*DCAGV 1*). Axis 1 was the only ecologically interpretable axis in the separate ordination of vascular plants. This axis was strongly correlated with DCAG 1 (Pearson's $r = 0.969$, $P << 0.0001$, $n = 200$; R. Økland & Eilertsen 1993: Tab. 16), and the same ecocline interpretation was therefore valid for both.

(3) Ordination of the MEB 200 data set, axes 1–2 (*DCAGB 1, DCAGB 2)*. These two axes were strongly correlated with the corresponding axes in the ordination of the entire ME 200 data set (axes 1: $r = 0.844$, $P << 0.0001$, $n = 200$; axes 2: $r = 0.811$, $P << 0.0001$, $n = 200$; R. Økland & Eilertsen 1993: Tab. 16), and the same ecocline interpretations were therefore valid.

For all axes, the average of the two meso plot scores was used as macro plot score.

Environmental variables

A total of 33 primary and 3 supplementary environmental variables were recorded (Tab. 2). These can be divided into macro-scale variables, meso-scale variables, and meso-scale humus layer variables. Because the basic sampling unit for the vegetation study was 1 m^2, the influence of trees on the understory was treated among environmental variables; recorded on the macro as well as the meso plot scale.

Tree measurements

The exact positions of stems and canopy perimeters of all trees (> 2 m high) rooted within a 64 m^2 plot having the 16 m^2 macro plot in the centre, and all other trees with canopies covering the macro plot, were mapped. For each tree, the following measurements were made:

Diameter at breast height (1.3 m) was calculated from measurements of stem perimeter in mm.

Height, h, from normal stump height to top, in dm.

Tab. 2. Environmental variables; number, abbreviation, unit of measurement, range of scale, frequency distribution, and transformation applied.

No	Abbrev.	Variable	Unit	Range	Distribution	Transformation
01	MA Slo	Slope	E	0–90	uniform	no
02	MA Auf	Aspect unfavourability		0–200	uniform	no
03	MA Ter	Terrain form		0–5	uniform	no
04	MA Une	Surface unevenness		1–4	uniform	no
05	MA S d	Soil depth		1–4	uniform	no
06	MA Bas	Basal area		0–4	uniform	no
07	MA Can	Canopy cover		0–4	uniform	no
*1	MA Bad	Basal area of deciduous trees		0–4	uniform	no
*2	MA Dli	Deciduous litter cover		0–100	uniform	no
*3	MA Bry	Bryophyte cover		0–100	uniform	no
08	ME Slo	Slope	E	0–90	normal–uniform	no
09	ME Auf	Aspect unfavourability		0–200	uniform	no
10	ME Une	Unevenness		0–4	lognormal	ln (1+x)
11	ME Con	Convexity		–4 – +4	normal	no
12	ME Smi	Soil depth, minimum	cm	0–4	lognormal	ln (1+x)
13	ME Sme	Soil depth, median	cm	0–4	lognormal	ln (1+x)
14	ME Sma	Soil depth, maximum	cm	0–4	lognormal	ln (1+x)
15	ME Lit	Litter index		0–4	lognormal	ln (1+x)
16	ME Bas	Basal area		0–4	uniform	no
17	Mois	Soil moisture	vol. %	0–100	normal	no
18	LI	Loss on ignition	%	0–100	bimodal	no
19	pH_{H_20}	pH, aquous solution		0–14	normal	no
20	pH_{CaCl_2}	pH, measured in $CaCl_2$		0–14	normal	no
21	Ca	Exchangeable Ca	ppm/LI	0–4	lognormal	ln (1+x)
22	Mg	Exchangeable Mg	ppm/LI	0–4	lognormal	ln (1+x)
23	Na	Exchangeable Na	ppm/LI	0–4	lognormal	ln (1+x)
24	K	Exchangeable K	ppm/LI	0–4	lognormal	ln (1+x)
25	H	Exchangeable H	ppm/LI	0–4	± lognormal	ln (1+x)
26	N	Total N	weight %/LI	0–100	± lognormal	ln (1+x)
27	P–AL	Total P	ppm/LI	0–4	lognormal	ln (1+x)
28	Al	Exchangeable Al	ppm/LI	0–4	lognormal	ln (1+x)
29	Fe	Exchangeable Fe	ppm/LI	0–4	lognormal	ln (1+x)
30	Mn	Exchangeable Mn	ppm/LI	0–4	lognormal	ln (1+x)
31	Zn	Exchangeable Zn	ppm/LI	0–4	± lognormal	ln (1+x)
32	P	Exchangeable P	ppm/LI	0–4	lognormal	ln (1+x)
33	S	Exchangeable S	ppm/LI	0–4	± lognormal	ln (1+x)

Height to the crown, h_c, the distance from normal stump height to the point on the stem where the lowest green branch whorl (i.e. the lowest green branch whorl which was separated from the rest of the crown by less than two dry branch whorls) emerged.

Crown area, a, the area of the crown projection, estimated from a map.

Crown cover, b, the projection of living phytomass on the crown area, visually estimated on a percentage scale.

Data for all trees are given in R. Økland & Eilertsen (1993: Appendix 2). Macro plot sketches showing positions of trees as well as special details, are given in R. Økland & Eilertsen (1993: Appendix 3).

Macro-scale variables

The following variables were measured to be representative for the macro plots.

(1) Slope (MA Slo) was measured by a compass (90º scale).

(2) Aspect unfavourability (MA Auf) was recalculated from aspect (measured by a clinometer on a 400º scale) on a linear 0–200 scale, following Dargie (1984), Parker (1988) and Heikkinen (1991): SSW (225º) was considered the most favourable aspect, and given the value 0; NNE (25º) was considered the least favourable aspect and given the value 200. [R. Økland & Eilertsen (1993) refer to this variable partly as Aspect favourability (MA Asf), partly as the Heat index (MA H i). The index does, however, measure aspect *un*favourability (or *coldness*), and has therefore been renamed for clarity.]

(3) Terrain shape (MA Ter) was scored on a six point scale: 0 – valley bottom or concave terrace, 1 – concave valleyside, 2 – plane valleyside, 3 – convex valleyside, 4 – ridge, 5 – hilltop.

(4) Surface unevenness (MA Une) was scored on a four point scale (cf. Rørå et al. 1988): 1 – relatively even (6 terrain roughnesses or less within the 64 m^2 plot enclosing the macro plot; a roughness defined to deviate more than 0.35 m from the surrounding terrain surface), 2 – uneven (7 or more roughnesses), 3 – boulderfield, 4 – coarse, with vertical walls, clefts and cliffs.

(5) Soil depth (MA S d) was scored on a four point scale, based on observations of the surface relief within the 64 m^2 plot (cf. Rørå et al. 1988): 1 – < 25 cm (extensive rock outcrops), 2 – 25–50 cm (localized rock outcrops), 3 – 50–100 cm (no rock outcrops, terrain uneven), 4 – > 100 cm (even surface, glaciofluvial material totally concealing unevennesses of the parent material).

(6) Basal area (MA Bas) was determined by a relascope (Fitje & Strand 1973). Basal area was measured at breast height from the lower left corner of each meso plot, using relascope factor 1. Values for the two meso plots were averaged to give MA Bas. Basal area is an expression of tree density and thus gives information of the light supply to the understory (also see 16 ME Bas).

(7) Canopy cover (MA Can), c, was calculated as the sum-product of the canopy cover (a) and crown area (b) for all trees covering the macro plot (see R. Økland & Eilertsen 1993). The canopy cover index expresses the relative canopy cover in the macro plot, that also takes trees with overlapping crown projections into account.

Three supplementary variables of potential importance for fungi were recorded in all macro plots (*2 and *3 in July 1997):

*(*1) Basal area of deciduous trees (MA Bad)*, derived from 6 MA Bas by only taking deciduous trees into account.

*(*2) Deciduous litter cover (MA Dli)*, was recorded as the percentage of ground covered by deciduous litter.

*(*3) Bryophyte cover (MA Bry)*, was recorded as the percentage of ground covered by bryophytes.

Meso-scale variables

The following variables were measured to be representative for the meso plots.

(8) Slope (ME Slo) was measured by a compass (see 1).

(9) Aspect unfavourability (ME Auf) was calculated from aspect measured by a clinometer (see 2).

(10-11) Microtopographic indices. For each meso plot, indices that express terrain shape at the within-plot scale, *(10) Unevenness (Me Une)* and *(11) Convexity (Me Con)*, were calculated from 16 measurements of the relative heights of the soil surface (see R. Økland & Eilertsen (1993) for details).

(12-14) Soil depth. Soil depth was measured as the maximum distance a steel rod could be driven into the soil. Measurements were made at eight fixed points 25 cm off the egdes of the meso plot; two points along each edge. Three variables were derived: *(12) Soil depth, minimum (ME Smi)*, *(13) Soil depth, median (ME Sme)*, and *(14) Soil depth, maximum (ME Sma)*.

(15) Litter index (ME Lit). The amount of litterfall was estimated from a plot's position relative to all trees covering the plot, and tree characteristics. Trees were considered to be of two kinds: (i) rooted within its crown perimeter ("concentric"); crown then assumed to be conical and gradually tapering, and (ii) rooted outside its crown perimeter ("excentric"); crown assumed to be cylindrical. The amount of litter falling on the plot was considered to be proportional with: (i) crown height ($h - h_c$), (ii) the fraction of the plot lying within the crown perimeter (f), (iii) crown cover (b), and (iv; only relevant for concentric trees) the position of the proximal end of the plot (the end most close to the centre of the stem) relative to the crown perimeter (d_r/d, where d is the length of a line from the stem centre, through the centre of the plot till the crown perimeter, and d_r is the distance along this line from the proximal end of the plot to the crown perimeter). A relative litter index was calculated as follows:

$$l = \Sigma_i [(d_{ri}/d_i) \cdot b_i \cdot f_i \cdot (h - h_{ci})] \qquad \text{stem rooted within crown perimeter,}$$

$$l = \Sigma_i [b_i \cdot f_i \cdot (h_i - h_{ci})] \qquad \text{stem not rooted within crown perimeter;}$$

sums taken over all trees i covering the plot. The litter index is considered a measure of canopy cover.

(16) Basal area (ME Bas) was determined by a relascope (Fitje & Strand 1973). Basal area was measured at breast height from the lower left corner of each meso plot using relascope factor 1 (also see 6 MA Bas).

Meso-scale humus-layer variables

The following variables were measured to be representative for the humus layer (or the upper 5 cm of the humus layer, if thicker).

(17) Soil Moisture (Mois). Samples for determination of soil moisture were collected on 15–16 Oct 1988, after several days without precipitation. These samples probably represented normal (median) moisture conditions (R. Økland & Eilertsen 1993). Two cores, 5 cm high and 98 cm^3 each, were collected just outside the plot (at the lower side of sloping plots). The cores were transferred to plastic bags and kept frozen until analysis. Volumetric soil moisture was determined by weighting the fresh samples, drying the samples at 110 ºC until constant weight, and reweighing.

Samples for chemical and physical analysis were taken on 15–16 Sept 1988. Several (5–10) small samples, 50–100 cm^3 each, were collected and mixed. They were kept frozen for several months. Before analysis at Landbrukets Analysesenter, Ås [procedures according to A.R. Selmer-Olsen (pers. comm.)], the samples were dried at 38 ºC, ground and sifted with 2 mm mesh width.

Exchangeable cations were determined by adding 50 cm^3 1 M NH_4NO_3 solution to 10 g dried soil (cf. Stuanes et al. 1984). The solution was left overnight, filtered, and the sediment washed with 1 M NH_4NO_3 until the volume of extract amounted to 250 cm^3. Element concentrations [*(21) Ca,*

(22) Mg, (23) Na, (24) K, (28) Al, (29) Fe, (30) Mn, (31) Zn, (32) P, and *(33) S*, were determined in the extract by a Jarrell Ash ICAP 1100 instrument.

(18) Loss on ignition (LI) was determined by ashing a sample at 550 ºC in a muffle furnace.

(19) pH, aquous solution (pH_{H_2O}). One part dried sample was mixed with 2.5 parts distilled water and left overnight. pH was measured the next day with an Orion SA 720 meter.

(20) pH, measured in $CaCl_2$ (pH_{CaCl_2}). One part dried sample was mixed with 2.5 parts 0.01 M $CaCl_2$, otherwise as (19).

(25) Exchangeable H [H_3O^+]. 50 ml of the extract was titrated with 0.05 M NaOH until pH = 7.0. The volume of NaOH was corrected for the value used with pure extractant, to obtain the exchangeable acidity.

(26) Total N. Kjeldahl-N was determined by digestion of the dried sample with H_2SO_4, and use of a Se catalyst in a Tecator FIA system.

(27) Total P (P-AL). One part dried sample was mixed with 20 parts of a solution 0.1 M with respect to ammoniumlactate and 0.4 M with respect to acetic acid. pH was adjusted to 3.75. P was determined in the extract by Jarell Ash ICAP 1100.

Transformation of environmental variables

Units of measurement for the 36 environmental variables are shown in Tab. 2. All element concentrations (variables 21–33) were converted from ppm (mg/kg dry sample) to fraction of organic content by multiplication with 100/LI, as recommended by T. Økland (1988).

Frequency distributions for the 33 primary environmental variables over the 200 meso plots were inspected (Tab. 2). The transformation ln (1+x) was applied to more or less lognormally or lograndomly distributed variables. For meso plot variables, the average of transformed values for the two meso plots was used as macro plot value.

The set of 33 transformed primary environmental variables is denoted {E}.

Values for environmental variables 1–33 are given in R. Økland & Eilertsen (1993: Appendix 4). Values for supplementary variables *1–*3 are available from the first author on request.

Spatial variables

In accordance with R. Økland & Eilertsen (1994), UTM grid co-ordinates (five digits for each co-ordinate, accuracy to nearest m) were used as the primary geographical explanatory variables. Co-ordinates for transect end-points were read from maps 1: 5,000, while relative positions of plots within the same transect were taken from field measurements. To allow for recognition of complex spatial trends, seven derived geographical variables were constructed by including all quadratic and cubic combinations of x and y, as suggested by Legendre (1990) and Borcard et al. (1992). The set of nine spatial explanatory variables is denoted {S}.

CLASSIFICATION OF VEGETATION AND DIVISION INTO DATA SUBSETS

Classification

Terricolous macrofungi are ecologically dependent on specific green plants, in different ways. Results so far show high concordance between separate classifications of flora and funga (see Arnolds 1992a).

Furthermore, fungal species seem to segregate along the ecological gradients used for classifying forest (also coniferous forests) into types, (e.g. Haas 1932, Krieglsteiner 1977, Østmoe 1979, Bendiksen 1981). We have therefore based this study on the same assumptions of vegetational and ecological continua as described by R. Økland & Bendiksen (1985) and R. Økland & Eilertsen (1993). Furthermore, we have used the gradient terminology of R. Økland & Eilertsen (1993: 25), and their classification of vegetation into site-types as a basis also for this study of fungi.

A direct gradient approach to classification is appropriate in a continuum (R. Økland & Bendiksen 1985, R. Økland 1989, 1990): a multidimensional gradient pattern is then turned into a reticulate, non-hierarchic classification by division of the gradient axes (Tuomikoski 1942, Webb 1954). Each combination of segments (positions) along the gradients is considered as one *site-type*, which is the basic unit of the classification system. A direct gradient approach to classification requires that the main ecoclines (Whittaker 1960) are known. This is the case for few local areas only (see R. Økland & Eilertsen 1993, T. Økland 1996). R. Økland & Eilertsen (1993) used available general knowledge as basis for their direct gradient approach to classification. They assumed that three local ecoclines were the most important: (1) variation along the topographic moisture complex-gradient (from bilberry-dominated spruce forests to lichen-rich pine forests), composed of several single environmental gradients, (2) variation along a complex-gradient in nutrient status, and (3) fine-scale variation in soil moisture (R. Økland & Bendiksen 1985, Bendiksen & Salvesen 1992). These three ecoclines were subsequently divided into site-types intended to be valid for the Solhomfjell area. Later on, R. Økland & Eilertsen (1993) confirmed the existence of these three important ecoclines by ordination of vegetation and subsequent environmental interpretation. As described in detail on p. 00, the main gradient in vegetation (DCAG 1) was related to topography on a broad scale, but with different important complex-gradients in the spruce and the pine forest: (1) a topography-soil depth complex-gradient in the pine forest, suggested by R. Økland & Eilertsen (1993) to be due to the response of plants to soil moisture deficiency, and (2) a complex-gradient in soil nutrient status in the spruce forest. Furthermore, the second ordination axis (DCAG 2) was interpreted as reflecting (3) fine-scale variation in (median) moisture status, as originally supposed. This confirmation of the ecoclinal structure implies that the site-type classification represents a valid direct gradient approach to classification of vegetation and the environment in the area (see Fig. 3).

In accordance with R. Økland & Eilertsen (1993), the following criteria were used for separation of site-types:

(1) *The topographic moisture gradient* was divided into seven categories, termed *series*. These series intentionally corresponded to the four series distinguished by R. Økland & Bendiksen (1985), considered to be applicable to boreal forest vegetation over S Fennoscandia, and transitions between them: series 1 corresponded to the xeric series of R. Økland & Bendiksen (1985), series 3 to the subxeric series, series 5 to the submesic series, and series 7 to the mesic series. Corresponding types in other classifications of Fennoscandian forest vegetation are given by R. Økland & Eilertsen (1993). Descriptions of vegetation (including vegetation tables) and ecology for each site-type are provided by R. Økland & Eilertsen (1993).

(2) No division of *the complex-gradient in nutrient status* was suggested by R. Økland & Bendiksen (1985), while up to four categories were recognized in the phytosociological classification by Kielland-Lund (1981) and the system of Fremstad (1997). The gradient was divided into four categories: (i) poor forests, negatively characterized, (ii) slightly rich forests, for instance including the 'low fern types', (iii) rich forests, including the poor forms of 'low herb types', and (iv) very rich forests, including the rich forms of 'low herb and tall fern' types.

(3) *The complex-gradient in fine-scale moisture* was divided into two categories; 1 (dry) and 2 (moist).

Every unique combination of positions along the three ecoclines was considered a site-type,

denoted by a three-digit code (see Fig. 3). The first digit indicated the series. In series 5, variation along the nutrient complex-gradient was indicated by a dot followed by a second digit. Variation along this gradient was not found in other series. Variation along the fine-scale moisture gradient was indicated by a hyphen followed by a digit. Examples are 3-2, the moist subxeric site-type; 4-1, the dry subxeric-submesic transitional site-type; and 5.2-2, the moist, slightly rich submesic site-type.

All meso plots were classified to site-type during field work in 1988.

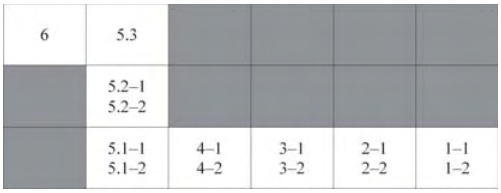

Fig. 3. The classification system adopted in the present study; site-type codes are shown within boxes. The horizontal sequence of types reflects position along the topographic moisture gradient, the vertical sequence reflects position along the complex-gradient in nutrient status. Site-types along the complex-gradient in fine-scale moisture are boxed together; the non-paludified type above, the paludified type below. Shaded boxes indicate site-type combinations not met with in the investigation area. From R. Økland & Eilertsen (1993), redrawn.

Division into data subsets

The 99 macro plots were divided into two subsets, Subset A (spruce forest) with 59 plots and Subset B (pine forest) with 40 plots, on the basis of the average position of meso plot scores along the first axis in the ordination of plant species in the ME 200 data set (see p. 00). This corresponds to the division into Subsets A and B in R. Økland & Eilertsen (1993).

GRADIENT ANALYSIS OF FUNGI

All univariate statistical analyses were made by means of STATGRAPHICS, Version 5.0 (Anonymous 1990).

Ordination

The nature of gradients in fungal species composition

Applied to a matrix of species abundances recorded in sample plots, ordination methods generally extract the main gradients of co-ordinated variation in species composition, coenoclines in the data (e.g. R. Økland 1990). Coenoclines extracted from data sets with observations of fruitbodies represent real structure gradients in the occurrence of fruitbodies of different fungal species while not necessarily gradients in species (mycelia) composition. Fruitbody coenoclines will be gradients in fungal species composition not only if fruitbody and mycelial distributions of all species along all gradients coincide, but also if species' amplitudes (as sterile mycelia) along major complex gradients extend far beyond the limits for fruitbody production, and there are systematic differences between species in abundance distributions along the gradient, e.g. because of differences in survival of mycelia along the gradient. In the latter case, the gradient length of the fruitbody coenoclines will, however, be much higher than of the corresponding species coenoclines (Eilertsen et al. 1990).

During the last decade, new methods for identification of species of below-ground ectomycorrhizal fungal communities have been developed (e.g. Dahlberg 2001, Horton & Bruns 2001). These methods, which comprise morphological descriptions and high-resolution molecular tools for identification of individual mycorrhizae, provide a broader perspective on the nature of gradients in fungal species composition. High abundance in mycorrhizae have been demonstrated for species which never or rarely produce fruitbodies (e.g. Dahlberg & Stenström 1991, Taylor et al. 2000, Horton & Bruns 2001). Furthermore, some typical Agaricales species may be well represented below-ground but rarely occur or lack above-ground in the fruiting period (Mehmann et al. 1995, Gardes & Bruns 1996), but see Laiho (1970) and Agerer (1990). Also the opposite relation occurs; Gardes & Bruns (1996) show that some commonly fruiting species are rare below ground. It has, however, been commented that the strength of correlations between presence above and below ground may be strongly influenced by limitations of methods used for identification of species in the mycorrhiza (Horton & Bruns 2001). As stressed by Dahlberg et al (1997) and Jonsson et al. (1999), below-ground studies are usually based upon sampling of very small areas; thus only a small fraction of all mycorrhizae present within a given area can be analysed. For many taxa, presence below-ground, but absence of fruiting for several years probably occurs because fruiting may require rare combinations of climatical events (cf. Agerer 1985, Ohenoja 1993). Relevant ecological studies on saprotrophs in which abundance above and below ground are compared, are not available. Thus, no methods are currently available that enable complete enumeration of the full fungal species composition within representative areas (like our plots). Until further knowledge has accumulated, gradients identified on the basis of records of fruitbody abundances have to be interpreted with care. With these reservations, we will however for convenience refer to the coenoclines extracted in the present study as gradients in fungal species composition.

Ordination methods

Two ordination methods were applied *in parallel* to extract the main gradients in fungal species composition. Ordination axes may be derived (1) by fitting the abundance data to a statistical model or (2) by the geometric process of finding the low-dimensional plot configuration which distorts the floristic similarities between plots as little as possible (cf. R. Økland 1990). Following the recommendation of R. Økland (1990, 1996) the method of each kind now considered the most appropriate was used: DCA (detrended correspondence analysis) and LNMDS (local non-metric multidimensional scaling) (cf. Kenkel & Orlóci 1986, Minchin 1987, Kent & Ballard 1988, R. Økland 1990, T. Økland 1996, Rydgren 1997). Congruent ordinations by the two methods were considered an indication that the main compositional gradients had been successfully recovered.

Plots with fewer than five species are likely to be inappropriately handled by ordination methods due to low representativity (R. Økland 1990). The *MAF 97* data set, derived from MAF 99 by removal of macro plots 79 and 91 with fewer than 2 species, was therefore used for DCA and LNMDS ordinations. Furthermore, plots Nos 38 and 60 appeared as strong outliers in the DCA ordination of MAF 97 and were removed as well. The new data set, *MAF 95*, was subjected to new ordinations. Separate DCA ordinations were also performed for two subsets of MAF 95; *Subset MAF 58A* with 58 macro plots corresponding to Subset A (spruce forest), and *Subset MAF 37B* with 37 plots corresponding to Subset B (pine forest).

DCA (Hill 1979, Hill & Gauch 1980) of frequency in subplots data was performed by means of CANOCO, Version 3.12 (ter Braak 1987b, 1990), using the following options: proportional downweighting of species with frequency in a data set lower than the median frequency (Eilertsen & Pedersen 1989, Eilertsen et al. 1990), detrending-by-segments (as recommended by Knox (1989), R. Økland (1990) and Eilertsen (1991)), and nonlinear rescaling with standard choice of parameters. In

accordance with recommendations by R. Økland (1999), eigenvalues of DCA ordination axes were reported directly as relative measures of the variation in species composition extracted on the axes, rather than as 'fractions of variation explained' [obtained by division with the total inertia; the sum of eigenvalues for all axes that could be extracted (cf. Greenacre 1984, Borcard et al. 1992)]. All DCA ordinations were completed before the new, dubugged version of Hill's original algorithm (Oksanen & Minchin 1997) was implemented in the CANOCO package. Essential identity of ordination results as obtained from CANOCO, Version 3.12 and the debugged CANOCO, Version ented in the CANOCO package. We made sure that the ordination results were unaffected by bugs, by comparing the ordination axes, one by one, with axes obtained for the same data sets by the debugged CANOCO, Version 4.0 (ter Braak & Šmilauer 1998). In all cases, Kendall's nonparametric (rank) correlation coefficients (Kendall 1938) $|\tau| > 0.98$ were found.

LNMDS (Kruskal 1964a, 1964b, Minchin 1987) of frequency in subplots data was performed by the KYST program (Kruskal et al. 1973) as modified and implemented into the DECODA program package, Version 2.01 (Minchin 1986, 1990). The following options were used: dimensionality = 2, dissimilarity measure = percentage dissimilarity (Bray-Curtis, or Czekanowski measure), standardized by division with species maxima (as recommended by Faith et al. 1987), number of random starting configurations = 100–500, maximum number of iterations = 1000, stress reduction ratio for stopping the iteration procedure (stress is a measure of the correspondence between floristic dissimilarities between plots and inter-plot distances in the ordination diagram) = 0.99999. The solution with the lowest stress was used. The number of starting configurations was initially set to 100, but increased to 500 in the LNMDS ordination of the MAF 97 data set to obtain the minimum stress solution from at least two different starting configurations. The LNMDS axes were linearly rescaled in S.D. units by the nonlinear rescaling procedure of the DECORANA and CANOCO programs (cf. Hill 1979, ter Braak 1987a), by use of rescaled hybrid canonical correspondence analysis (rhCCA; cf. ter Braak 1987b, 1987c), with the original LNMDS scores (one axis in turn) as constraining variables (R. Økland 1990, Eilertsen et al. 1990).

Comparison of ordinations

Axes of different ordinations were subjected to pair-wise comparison using Kendall's nonparametric rank coefficient τ. Kendall's τ was preferred to Pearson's r (cf. Sokal & Rohlf 1995) because it is insensitive to asymmetric frequency distributions and/or inhomogeneous variance distributions. Absolute values of Pearson's r, which was used by R. Økland & Eilertsen (1993), are consistently higher than the absolute values of Kendall's τ, and numerical values for the two correlation coefficients are therefore not directly comparable.

Interpretation of ordination results

Kendall's τ was calculated between ordination axes and all explanatory variables (36 environmental variables and 7 vegetational variables). Although the main emphasis was put on ordinations of the MAF 95 data set, all ordinations were interpreted in order to enable methodological comparisons.

Relationships between environmental variables and between environmental variables and vegetational variables were thoroughly studied by R. Økland & Eilertsen (1993: 35-44).

Variation in species abundance and other properties of the funga along DCA axes

By relating the distribution of a species' abundance to environmentally interpreted ordination diagrams, valuable information of the species' autecology can be obtained (cf. T. Økland 1996). Subplot frequencies for all species occurring in more than 5% of the macro plots were plotted onto macro

plot positions in the DCA ordination diagrams for the MAF 95 data set. Furthermore, DCA axes 1–3 were divided into intervals for which mean frequency and mean subplot frequency was calculated for each species. For all species occurring in more than 5% of the macro plots in the MAF 95 data set, *ranges* along DCA axes 1–3 were also found. For species extending beyond axis ends, range was estimated by assuming symmetric distribution along the axis around the species' optimum (as given by the species score).

Constrained ordination

All analyses were based upon the CCA concept (Canonical Correspondance Analysis; ter Braak 1986, 1987a), performed by means of CANOCO, Version 3.12 (ter Braak 1987b, 1990). Frequency in subplots data for fungi in the MAF 95 data set were used, with proportional downweighting of species with frequency lower than the median frequency (Eilertsen et al. 1990).

Variation explained by single explanatory variables

The variation in species abundances possible to explain by single primary environmental variables was assessed by hybrid CCA, using each explanatory variable in turn as the only constraining variable. Variation is expressed in relative 'inertia units' (IU) as provided by the eigenvalue of the first and only constrained CCA axis. The total inertia of the species-plot matrix was not used for scaling of the explained variation because it is inflated by lack-of-fit-of-data-to-model variation (R. Økland 1999). The hypothesis of non-significant deviation of variation explained by a variable from that explained by a random variable, was tested by the Monte Carlo test in CANOCO (ter Braak 1990), using 199 unrestricted permutations of the constraining variable.

Variation partitioning

The relative importance of the three sets of explanatory variables (vegetational gradients {V}, environmental variables {E}, and spatial variables {S}) for variation in fungal composition was assessed by variation partitioning (Borcard et al. 1992, R. Økland & Eilertsen 1994, R. Økland 1999), generalized from two to three sets of explanatory variables (see R. Økland in press). With two sets of explanatory variables (termed {T} and {U}, respectively), the variation in a data matrix can be partitioned by the following procedure: Denote the variation explained by {T} and {U} T and U, respectively. T is obtained by CCA after forward selection (here: variables with contribution to variation explained significant at the P = 0.01 level were retained) of variables from the set {T} as the sum of all constrained eigenvalues. U is found by a similar procedure. Eliminating variables that do not contribute significantly to explanation of the variation in species abundances gives more realistic estimates of variation explained (Borcard et al. 1992). Furthermore, the variation explained by {T} not shared with {U}, T|U, is found by partial CCA (Borcard et al. 1992), using the significant variables in {U} as covariables and the significant variables in {T} as constraining variables. The remaining components of the variation may then be calculated as follows (cf. R. Økland & Eilertsen 1994: Fig. 1):

$T \cap U$ (shared variation) = $T - T|U$
$U|T$ (variation explained by {U}, not shared by {T}) = $U - T \cap U$
$T \cup U$ = TVE (the total variation explained by the variables; the variation explained by {T, U}) = $T + U - T \cap U$

Due to the additivity of variations explained, i.e. that the total variation explained by {T, U}, T∪U, can be found directly in a CCA with all significant variables in {T} and {U} as constraining variables (R. Økland & Eilertsen 1994), the process is easily generalized to three sets of explanatory variables by applying (partial) CCA to different combinations of sets of significant explanatory variables. The Monte Carlo test (in CANOCO; see ter Braak 1990) was used to assess the significance of each variable upon inclusion in the regression model. Only variables significant at the P = 0.01 level were included.

Relative fractions of variation explained were obtained as percentages of the total variation explained by all three sets of variables (R. Økland 1999).

NOMENCLATURE AND TAXONOMIC NOTES

A list of fungal species with author names is given in Appendix 1. The nomenclature of the orders Agaricales, Russulales and Boletales follows Hansen & Knudsen (1992), with some exceptions and additions: *Armillaria mellea* (Vahl : Fr.) P. Kumm. is used in a collective sense; *Collybia asema* (Fr. : Fr.) P. Kumm. is considered as a species on its own, distinct from *C. butyracea* (Bull. : Fr.) P. Kumm; species of *Cortinarius* (Pers.) Gray treated by Brandrud et al. (1990-97) follow the latter; *Entoloma rhodopolium* (Fr.) P. Kumm. is used in the sense of Noordeloos (1989); *Galerina borealis* A.H. Sm. & Singer in accordance with Smith & Singer (1964); *Galerina calyptrata* P.D. Orton is included in *G. hypnorum* (Schrank : Fr.) Kühner *s. lat.*; *Gymnopilus sapineus* (Fr. : Fr.) Maire is used in the sense of Høiland (1990); *Inocybe subcarpta* Kühner & Boursier is used for the better known name *I. boltonii* R. Heim, here also including *I. soluta* Velen. (= *I. brevispora* Huijsman), cf. Vauras (1992); *Leccinum palustre* M. Korhonen follows Korhonen (1995); *Mycena alcalina* (Fr. : Fr.) P. Kumm. coll. is used as a collective name for *M. stipata* Maas Geest. & Schwöbel and *M. silvaenigrae* Maas Geest. & Schwöbel; *Mycena cineroides* Hintikka is considered as a species of its own, distinct from *M. cinerella* P. Karst.; *M. viscosa* Maire is treated as a distinct species; *Psathyrella* aff. *lutensis* refers to an undetermined species in the subsection *Lutenses* Kits van Wav., following Kits van Waveren (1985).

Camarophyllus (Fr.) P. Kumm. is considered as part of *Hygrocybe* P. Kumm. as in Boertmann (1995), whereas *Xerocomus* Quél. is kept as a separate genus.

Galerina sp. 1 was identified in the field on its strongly orange colour. It does, however, resemble *G. hypnorum* in microscopic and other macroscopic characters and may well turn out to be only a young stage of that species. The other unidentified collections of Agaricales/Boletales, referred to as 'sp.', have only been represented in the material by single fruitbodies or fruitbodies in bad condition. Most probably, these do not belong to any species recognised in the material.

Aphyllophorales s.l., heterobasidiomycetes and gasteromycetes follow Hansen & Knudsen (1997), and ascomycetes follow Hansen & Knudsen (2000).

The nomenclature of vascular plants follows Lid & Lid (1994), and bryophytes follow Frisvoll et al. (1995).

RESULTS

CLASSIFICATION

Thirty-seven of the macro plots were inhomogeneous with respect to site-type, even when the paludification (median soil moisture) gradient (21 macro plots were inhomogeneous with respect to this gradient) was not taken into account. The meso plots in these inhomogeneous plots mostly belonged to neighbouring series along the sequence from 6 to 1, in some cases to neighbouring site-types in series 5. The classification of macro and meso plots to site-types is given in Appendix 2. Subplot frequencies for each species in each plot and species frequencies in the MAF 99 data set are given in Appendices 3–4.

FUNGAL SPECIES DENSITY

Of the totally 235 species found in the 99 macro plots, 122 (52%) were supposed to be mycorrhizal. Tab. 3 shows the fungal species density (average number of species per macro plot in each site-type), totally and separately for mycorrhizal species. Trends were obscured by the low number of macro plots in many site-types, but more reliable figures were obtained by lumping plots near gradient endpoints (bottom rows in Tab. 3). The total number of species increased from *c.* 6 at the xeric end of the topographic moisture gradient (series 1) via 23 in the poor submesic series, to more than 40 in macro plots influenced by flushing (Tab. 3). Only small differences were found between the submesic site-types along the nutrient gradient. The sparse material gives no indication of differences between non-paludified and paludified plots.

The percentage of mycorrhizal species did not vary in a consistent manner between site-types, except for a distinct increase from the subxeric to the xeric site-type (Tab. 3).

ORDINATION

Characteristics of, and comparison between, ordinations of fungi

Characteristics of the ordinations are summarized in Tab. 4.

Ordinations of the MAF 97 data set

DCA. The gradient length of the first DCA axis was 4.86 S.D. units, while the lengths of the subsequent axes were 3.21, 1.95 and 2.23 S.D. units (Tab. 4). The lowest score along DCA 1 was obtained by macro plot 53 (classified to site-type 6), while plot 60 (one meso plot classified to the xeric and one classified to the xeric-subxeric transitional series) occurred at the opposite end of this axis (Figs

Tab. 3. Mean species density (number of species, total and mycorrhizal, per 16-m^2 macro plot), in each site-type. Data for corresponding non-paludified and paludified types are summarised. Macro plots inhomogeneous with respect to other ecoclines (the topographic moisture and nutrient gradients) are left out. The two bottom rows summarise species numbers for macro plots with two meso plots classified to site-types 1 and/or 2, and macro plots with at least one meso plot classified as slightly flushed (site-type 6), respectively.

Site-type		Number of plots			No. of species	No. of mycorrhizal species	% of mycorrhizal species
Code	Name	Total	Non-pal.	Pal.			
1	Xeric	3	2	0	6.3	3.0	47.6
2	Xeric-subxeric transition	2	1	0	12.5	5.5	44.0
3	Subxeric	8	5	1	11.3	3.3	29.2
4	Subxeric-submesic transition	11	6	1	16.4	4.1	25.0
5–1	Poor submesic	22	17	2	23.0	7.3	31.7
5–2	Slightly rich submesic	10	7	3	26.2	10.1	38.5
5–3	Rich submesic	5	5	0	27.4	7.4	27.0
6	Rich slightly flushed	1	–	–	40.0	9.0	22.5
1+2	Widely circumscribed xeric, including xeric-subxeric transition	11	5	0	8.0	3.4	42.5
5+6	Rich, with elements of flush	4	–	–	41.0	12.0	29.3

4–5). The site-types segregated along the axis, making up a sequence from 6, via 5.3 (mainly obtaining scores < 1.0 along this axis), 5.2, 5.1, 4, 3 and 2 to 1. The transition between plots from spruce and pine forest (site-type 4) occurred at *c.* 2.4 S.D. units along this axis. With the exception of plot 60, which occupied an outlying position, the plots made up one continuous cluster, somewhat less dense towards the low-score end of the axis.

Macro plot 38 (representing the slightly rich paludified submesic site-type) occupied an isolated position at the low-score end of DCA 2 (Fig. 4). At the other end of this axis, plots 72 and 73 were found (both representing the poor non-paludified submesic site-type). The spread of plot scores along DCA 2 decreased with increasing DCA-axis 1 score; the two-dimensional point configuration having a characteristic tongue- or trumpet-like shape. The strong concentration of plots near the middle of DCA 2 was reflected in the relative length of the core; small relative to the other axes (Tab. 4).

The end-points with respect to DCA axis 3 were made up by plots 16, 17 and 44 (low-score end), and 21, 95 and 97 (high-score end), respectively. The distribution of plots along DCA 3 was relatively even (Fig. 5), as reflected in the high value for core length (Tab. 4).

LNMDS. The gradient lengths of the LNMDS axes were 4.36 and 3.23 S.D. units, respectively. The macro plots near the ends of DCA-axis 1 also occupied end positions along LNMDS 1 (Fig. 6). The plots were evenly distributed along the axis.

Macro plots 78 and 26 (representing xeric and subxeric, partly paludified site-types), obtained low scores along LNMDS 2. High scores were obtained by plots 63, 49 and 93. Macro plots were relatively evenly distributed also along LNMDS 2 (Fig. 6).

Comparison between DCA and LNMDS ordinations. Rank-ordered plot positions along the first axes of the two ordinations were virtually identical, as evident from the strong correlation in

Tab. 5. The second LNMDS axis was correlated with DCA 2 (but less strongly), as well as with DCA 4.

Ordinations of the MAF 95 data set

DCA. The gradient length of the first DCA axis was 3.81 S.D. units, while the lengths of the subsequent axes were 2.23, 2.24 and 3.15 S.D. units (Tab. 4). DCA 1 had an eigenvalue of 0.471, slightly above

Tab. 4. Summary of ordination results and characteristics of ordination axes. DCA97 and DCA95 – DCA ordinations of the MAF 97 and MAF 95 data sets, respectively; MDS97 and MDS95 – LNMDS ordinations of the same data sets. Total inertia is an expression of the total variation of a data set. For LNMDS, the eigenvalue of first hCCA axis (the hCCA run with the LNMDS scores along one axis as the only constraining variable) is listed. The variation explained relative to a random variable refers to the product n·(variation explained), because 1/n is the expected variation explained by a random variable, when the minimum of the number of species and the number of plots is n. The gradient length is given in S.D. units; of LNMDS axes obtained by hCCA as above. The relative length of core of a gradient is the smallest fraction of the total gradient length that contains at least 90% of the sample plots.

Ordination	Total inertia	Axis	Eigen-value	Var. expl. relative to random variable	Gradient length	Relative length of core of gradient
DCA97	6.240	1	.484	7.53	4.856	.625
		2	.241	3.74	3.211	.384
		3	.166	2.53	1.946	.631
		4	.137	2.14	2.225	.577
MDS97	6.240	1	.452	7.02	4.356	.675
		2	.269*	4.09	3.232	.611
DCA95	5.186	1	.471	8.63	3.805	.761
		2	.182	3.33	2.232	.609
		3	.151	2.76	2.235	.604
		4	.127	2.33	3.154	.314
MDS95	5.186	1	.442	8.09	3.996	.688
		2	.231*	4.23	3.111	.583
DCA58A	3.866	1	.410	6.15	2.782	.820
		2	.183	2.74	1.973	.741
		3	.145	2.18	2.010	.746
		4	.122	1.83	1.922	.572
DCA37B	3.040	1	.294	3.58	2.819	.585
		2	.216	2.70	2.319	.578
		3	.170	2.07	2.656	.327
		4	.115	1.40	1.956	.612

* LNMDS axes 1 and 2 are not orthogonal; the cumulative variation explained by the two LNMDS axes are 0.684 in MDS97 and0.596 in MDS95.

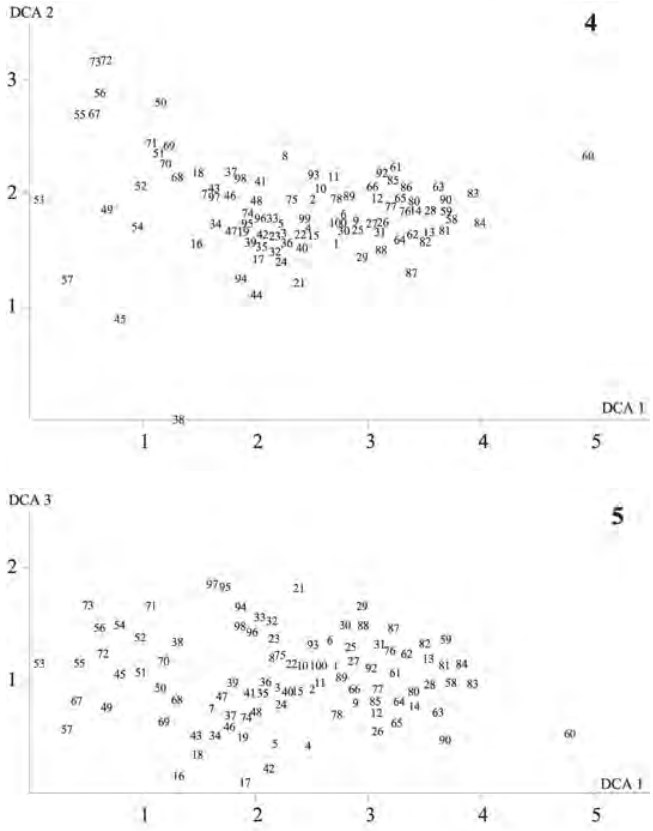

Figs 4–5. DCA ordination of the MAF 97 data set. Axes scaled in S.D. units. Macro plot numbers plotted onto plot positions. Fig. 4. Axes 1 (horizontal) and 2. Fig. 5. Axes 1 (horizontal) and 3.

that of the first DCA axis in the ordination of the MAF 97 data set. The lowest score along DCA 1 was obtained by macro plot 53 (like DCA97 1), while the species-poor plot 84 (one meso plot classified to the xeric and one classified to the xeric-subxeric transitional series) occurred at the opposite end of this axis (Fig. 7). Macro plots classified to site-types 5.3 and 6 mainly obtained scores < 1.0 S.D. units along this axis (Fig. 9). The plots made up one continuous cluster, somewhat less dense towards the low-score end of the axis and with slightly reduced density also at *c.* 2.4 S.D. units along the axis, i.e. at the transition between spruce and pine forest, between Subsets A and B. Only one plot from Subset B obtained a DCA 1 score < 2.40 (No. 93) while only two Subset A plots obtained DCA 1 scores > 2.40 S.D. (Nos 1 and 6).

Several macro plots (16, 17, 44, 45 and 57) obtained low scores along DCA 2, while the high-score end of this axis was occupied by plots 72, 73 and 93 (Fig. 7). Plot scores were relatively evenly distributed along DCA 2, and the range of plot scores along DCA 2 decreased but weakly with increasing DCA-axis 1 score; thus the two-dimensional point configuration in Fig. 7 lacked the tongue-like shape of Fig. 4. No strong concentration of plots occurred near the middle of DCA 2 (cf. the relative length of the core in Tab. 4).

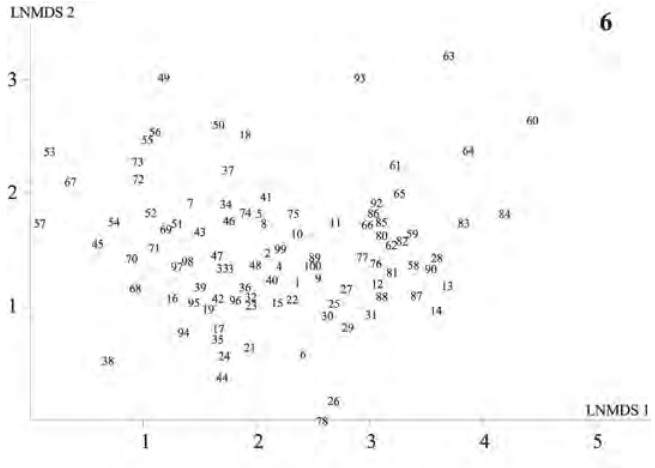

Fig. 6. Two-dimensional LNMDS ordination of the MAF 97 data set, axes 1 (horizontal) and 2. Axes rescaled in S.D. units by means of rhCCA. Macro plot numbers plotted onto plot positions.

The end-points with respect to DCA axis 3 were made up by plots 24 (low-score end) and 41 (high-score end), respectively (Figs 8, 10). The distribution of plots along DCA 3 was relatively even (Fig. 8), as reflected in the high value for core length (Tab. 4).

LNMDS. The gradient lengths of the LNMDS axes were 4.00 and 3.11 S.D. units, respectively. The macro plots near the ends of DCA-axis 1 also occupied end positions along LNMDS 1 (Fig. 11). The plots were evenly distributed along the axis.

Macro plots 78 and 26 obtained low scores along LNMDS 2, while the highest score was obtained by plot 63. The distribution of plots along LNMDS 2 was relatively even (Fig. 11).

Comparison between DCA and LNMDS ordinations. Like the ordinations of the MAF 97 data set, the corresponding first axes in the ordination of the MAF 95 data set were also virtually identical (Tab. 6). The second LNMDS axis was correlated with DCA 3 (but less strongly).

Comparison between the ordinations of the MAF 97 and MAF 95 data sets

The first axes of all four ordinations (two data sets, two methods) were virtually identical ($\tau > 0.85$, see Tab. 7) and clearly represented the main gradient in fungal species composition in forests in the study area. The second axes of the two LNMDS ordinations were also virtually identical ($\tau = 0.870$). However, the second LNMDS axes showed only moderate correspondence with the second axes of the DCA ordinations ($\tau < 0.6$; Tab. 7), and the same applied to the correspondence between second and subsequent DCA axes in the two ordinations. The second LNMDS axes were significantly correlated with both axes 2 and 4 of the DCA ordination of the MAF 97 data set, while being most strongly correlated with axis 3 of the DCA ordination of the MAF 95 data set (Tabs 5–7). The variation along two of the DCA axes (the second and third) in the ordination of the MAF 97 data set was expressed along DCA 2 in the MAF 95 ordination. Furthermore, DCA 4 of MAF 97 was strongly correlated with DCA 3 of MAF 95, and these axes were also correlated with LNMDS 2. Removal of the outlying plot 38 from the MAF 97 data set thus seemed to stabilize the gradient structure extractable by DCA as some of the variation along the outlier-influenced DCA97 2 was removed while some (the part correlated with LNMDS 2) seemed to be retained by the third DCA95 axis (cf. Tab. 7).

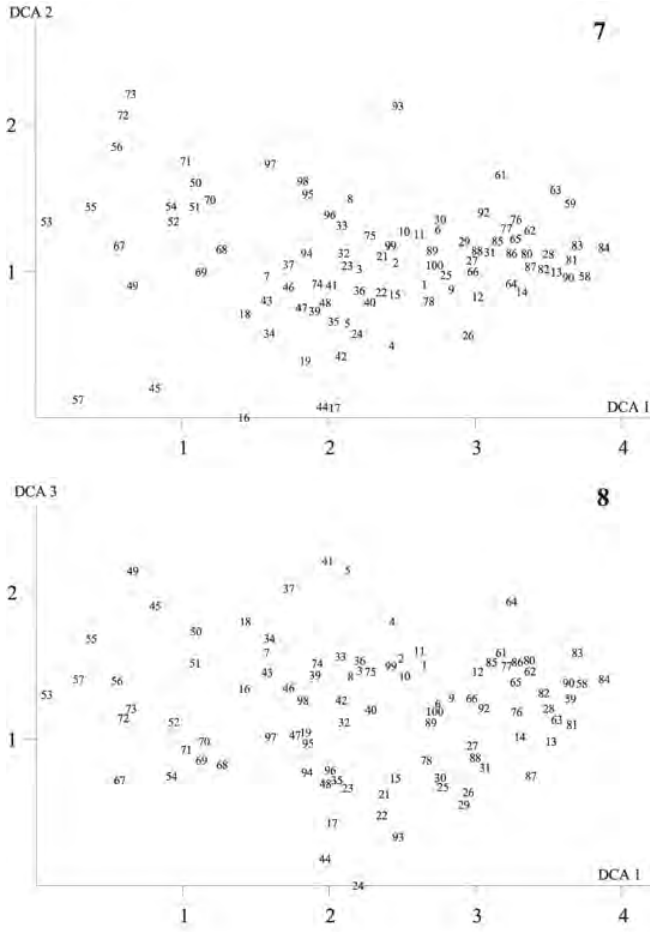

Figs 7–8. DCA ordination of the MAF 95 data set. Axes scaled in S.D. units. Macro plot numbers plotted onto plot positions. Fig. 7. Axes 1 (horizontal) and 2. Fig. 8. Axes 1 (horizontal) and 3.

The ordinations thus lent support to the presence of three gradients in fungal species composition in the area: (1) the main gradient in all ordinations, (2) the gradient expressed by LNMDS 2, DCA97 4 (and partly also DCA97 2) and DCA95 3, and (3) the gradient expressed by DCA95 2 and DCA97 3 (and partly also DCA97 2). Because this gradient structure was most closely reflected by the DCA95 ordination, we focused on this ordination in the subsequent ecological interpretation.

DCA ordinations of data subsets

The MAF 58A subset. The gradient length of the first axis in the separate ordination of macro plots from the spruce forest was 2.78 S.D. units, corresponding to an eigenvalue of 0.410. The sequence of plots along DCA95 1 was almost perfectly recovered; plot 53 obtained the lowest score and plot 6 the highest (Figs 12, 14). Also the sequences of plots along DCA axes 2-3 resembled the sequences

along corresponding DCA95 axes ($\tau > 0.6$; Tab. 8). The ends of axis 2 were occupied by the same plots as in the ordination of the MAF 95 data set, while plot 21 obtained the lowest and plot 5 the highest score along axis 3 (Figs 13, 15). The fourth axes in the two ordinations were also significantly correlated (Tab. 8). The distribution of plots along the first three axes in this ordination was relatively even; this ordination had the highest values for core length encountered for the three first axes in any ordination (see Tab. 4).

The MAF 37B subset. The first axis in the separate ordination of pine-forest plots had a length of 2.82 S.D. units and an eigenvalue of 0.294. It was significantly correlated with the first axis of the DCA95 ordination. Macro-plot 78 (at the transition between the xeric and subxeric series) occupied an isolated position at the low-score end of DCA 1, separated from all other plots by more than 0.6 S.D. units. The xeric plot 63 took a slightly isolated position at the opposite end, where plot 83 (both 63 and 83 close to the xeric-subxeric transition) formed the end of the main point cloud. The bulk of plots obtained DCA 1 scores in the interval 0.6–2.0 (Figs 16, 18). Also DCA axis 2 was influenced by moderate outliers; plot 26 at the low-score end and plots 11 and 61 at the high-score end (Fig. 16). The second DCA37B axis was correlated with the second axis of the DCA95 ordination ($\tau = 0.384$,

Tab. 5. Kendall's rank correlation coefficients τ between macro-plot scores in the ordinations of the MAF 97 data set, with significance probabilities (P). Correlations significant at level $P < 0.0001$ in bold face. n.s. – significance probability less than 0.1.

Axis	MDS97 1		MDS97 2	
	τ	P	τ	P
DCA97 1	**.8594**	**.0000**	–.1095	n.s.
DCA97 2	–.0389	n.s.	**.4841**	**.0000**
DCA97 3	–.0135	n.s.	–.1044	n.s.
DCA97 4	–.0238	n.s.	**.2980**	**.0000**

Tab. 6. Kendall's rank correlation coefficients τ between macro-plot scores in the ordinations of the MAF 95 data set, with significance probabilities (P). Correlations significant at level $P < 0.0001$ in bold face. n.s. – significance probability less than 0.1.

Axis	MDS95 1		MDS95 2	
	τ	P	τ	P
DCA95 1	**.8634**	**.0000**	–.0269	n.s.
DCA95 2	–.0269	n.s.	.2623	.0002
DCA95 3	.0119	n.s.	**.4484**	**.0000**
DCA95 4	–.1884	.0069	–.1792	.0101

Tab. 7. Kendall's rank correlation coefficients τ between macro-plot scores in the ordinations of the MAF 95 and MAF 97 data sets, with significance probabilities (P). Correlations significant at level $P < 0.0001$ in bold face. n.s. – significance probability less than 0.1.

Variable	DCA95 1		DCA95 2		DCA95 3		DCA95 4		MDS95 1		MDS95 2	
	τ	P	τ	P	τ	P	τ	P	τ	P	τ	P
DCA97 1	**.9843**	**.0000**	.0233	n.s.	–.0168	n.s.	–.1669	.0166	**.8692**	**.0000**	–.0578	n.s.
DCA97 2	–.1418	.0418	**.4095**	**.0000**	.1991	.0043	–.1015	n.s.	–.0876	n.s.	**.4699**	**.0000**
DCA97 3	.0262	n.s.	**.5344**	**.0000**	–.2000	.0041	.1897	.0065	.0123	n.s.	–.0762	n.s.
DCA97 4	–.0477	n.s.	–.0636	n.s.	**.6524**	**.0000**	–.1387	.0466	–.0123	n.s.	**.3158**	**.0000**
MDS97 1	**.8534**	**.0000**	.0356	n.s.	.0237	n.s.	–.1949	.0052	**.9775**	**.0000**	.0222	n.s.
MDS97 2	–.1507	.0305	.2540	.0003	**.4517**	**.0000**	–.1893	.0066	–.0795	n.s.	**.8704**	**.0000**

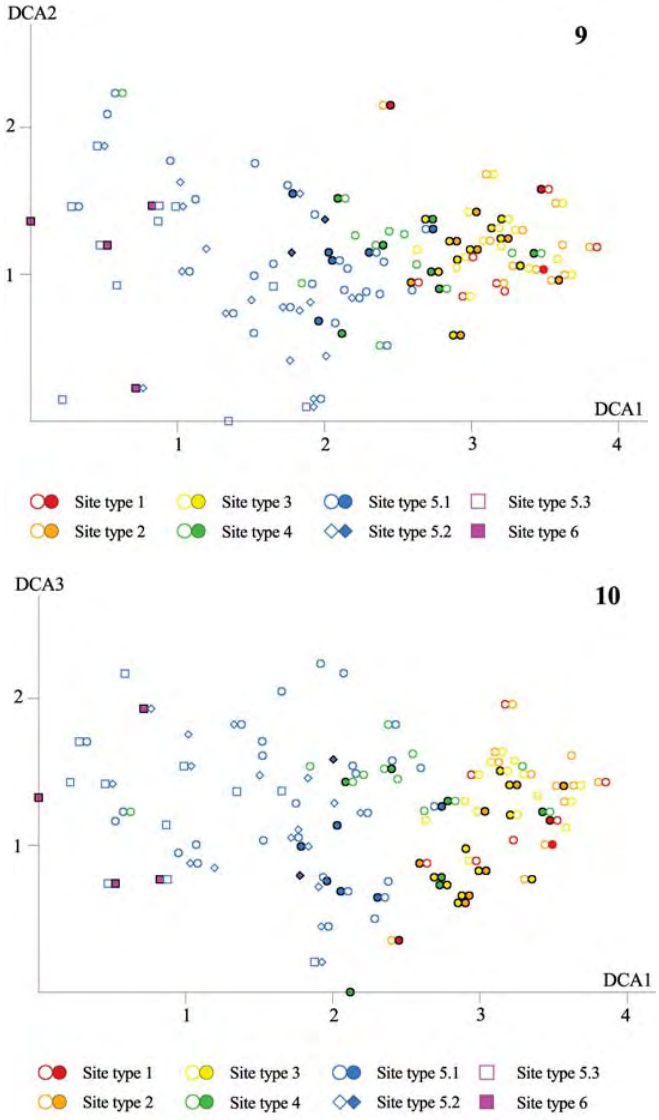

Figs 9–10. DCA ordination of the MAF 95 data set. Axes scaled in S.D. units. Site-type classification of macro plots plotted onto plot positions. Fig. 9. Axes 1 (horizontal) and 2. Fig. 10. Axes 1 (horizontal) and 3. Colour symbols for each actual site-type are shown. Open and filled circle/square represent the non-paludified and the paludified types, respectively. Inhomogeneous plots with respect to paludification are shown by a composite symbol.

P = 0.0009), but even more strongly with DCA95 3 ($\tau = 0.508$, $P < 0.0001$) and DCA95 4 ($\tau = 0.526$, $P < 0.0001$; cf. Tab. 8). The second axis of the pine forest ordination of fungi thus contained elements of the variation expressed along three of the axes of the total data set. The third DCA axis separated

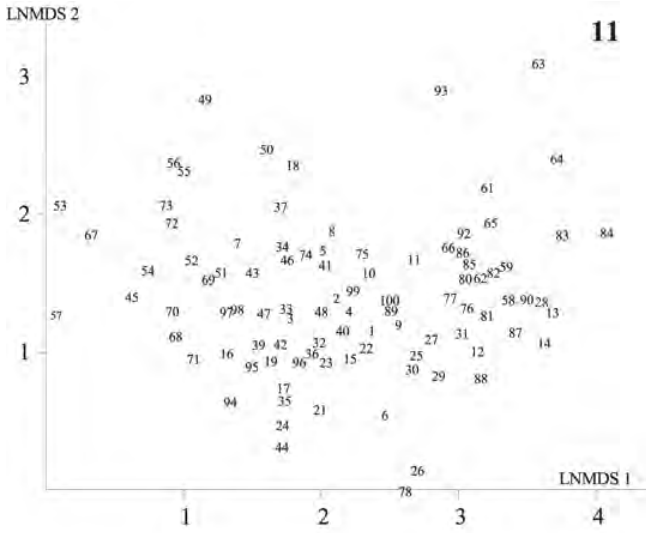

Fig. 11. Two-dimensional LNMDS ordination of the MAF 95 data set, axes 1 (horizontal) and 2. Axes rescaled in S.D. units by means of rhCCA. Macro plot numbers plotted onto plot positions.

plots 93 (score 1.1 S.D. units higher than any other plot) and 84 (score > 0.6 units lower than all other plots), while the bulk of plots occured between 0.65 and 1.55 S.D. units along this axis (Figs 17, 19). This axis was strongly correlated with DCA95 1.

Separate DCA ordinations of data subsets indicated that the gradient structure of fungi in the study area was the result of strong, partly coincident and partly different, gradients in species composition in the spruce and pine forests. The main gradient in fungal composition in the area consisted of the main gradients in either forest type. The secondmost important gradient in the material, DCA95 2, was mainly present in the spruce forest, while the thirdmost important gradient, DCA95 3, occurred as the secondmost important coenocline in the pine forest and the thirdmost important coenocline in the spruce forest.

Relationship between fungal ordinations and vegetational variables

Ordinations of the MAF 95 data set

Macro-plot positions along the first axes of the DCA and LNMDS ordinations of the MAF 95 data set were strongly correlated ($\tau = 0.7$) with averaged meso-plot positions along the first axes of all vegetational ordinations (of the total species composition, and separate ordinations made for the field and bottom layers, see Tab. 9). The correspondence between plot positions along DCA95 1 and positions along corresponding vegetational ordination axes was strong in the spruce forest (Subset A), less strong and significant at the $P < 0.05$ level only for the bottom-layer gradient in the pine forest (Subset B; see Tab. 10). Thus the main gradients in species composition of fungi, vascular plants and cryptogams (bryophytes and lichens) were parallel in the spruce forest, but only partly so in the pine forest.

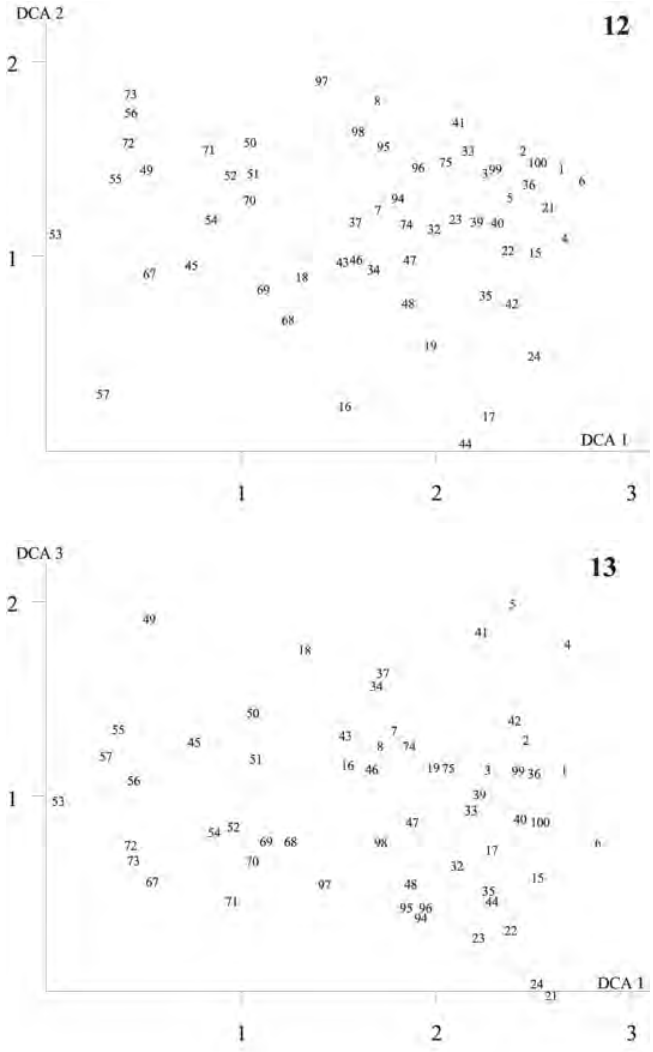

Figs 12–13. DCA ordination of the MAF 58A data set. Axes scaled in S.D. units. Macro plot numbers plotted onto plot positions. Fig. 12. Axes 1 (horizontal) and 2. Fig. 13. Axes 1 (horizontal) and 3.

The second axes in the DCA ordination of the MAF 95 data set was significantly correlated only with the fourth DCA axis in the vegetational ordination ($\tau = 0.370$, $P < 0.0001$; Tab. 9), while the third fungal ordination axis (DCA95 3) and the second LNMDS axis were significantly correlated with the second vegetational DCA ordination axis ($\tau > 0.3$, $P < 0.0001$), both in the ordination of all species and in the separate ordination of species in the bottom layer (DCAG 2 and DCAGB 2, cf. Tab. 9). Thus the secondmost important gradient for the bottom layer (and the vegetation as a whole) corresponded to the thirdmost important gradient in the composition of fungi, while the secondmost important gradient in fungal species composition (at least as indicated by DCA) seemed to have a counterpart in the fourthmost important gradient in vegetation.

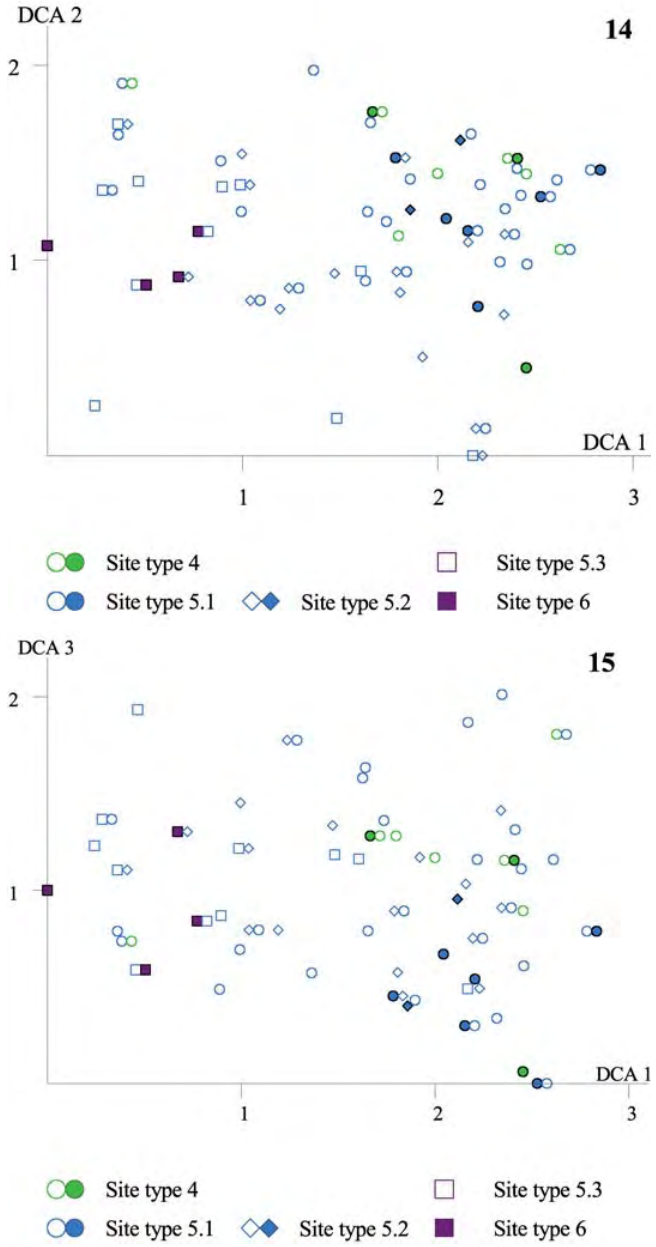

Figs 14–15. DCA ordination of the MAF 58A data set. Axes scaled in S.D. units. Site-type classification of macro plots plotted onto plot positions. Fig. 14. Axes 1 (horizontal) and 2. Fig. 15. Axes 1 (horizontal) and 3. Colour symbols for each actual site-type are shown. Open and filled circle/square represent the non-paludified and the paludified types, respectively. Inhomogeneous plots with respect to paludification are shown by a composite symbol.

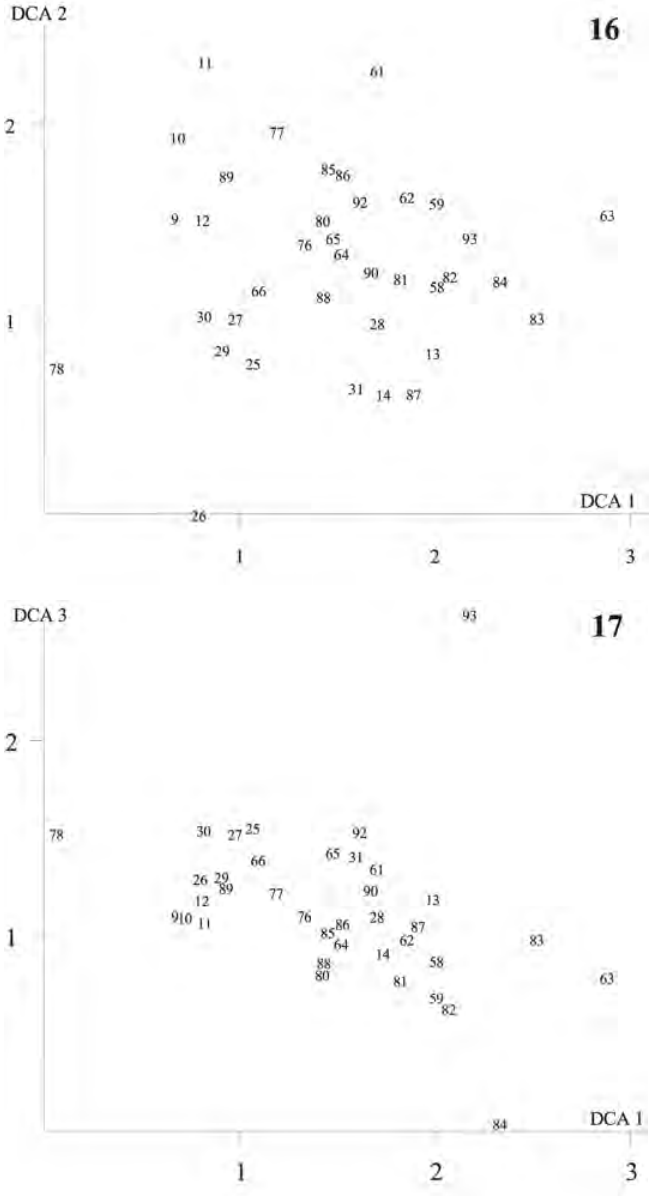

Figs 16–17. DCA ordination of the MAF 37B data set. Axes scaled in S.D. units. Macro plot numbers plotted onto plot positions. Fig. 16. Axes 1 (horizontal) and 2. Fig. 17. Axes 1 (horizontal) and 3.

DCA ordinations of data subsets

The first axis in the DCA ordination of the spruce-forest subset (MAF 58A) was significantly correlated with the first axis of vegetational ordinations (all species groups; see Tab. 11). The second MAF 58A

Tab. 8. Kendall's rank correlation coefficients τ between macro-plot scores in the DCA ordination of the MAF 95 data set and DCA ordinations of the MAF 58A and MAF 37B subsets, with significance probabilities (P). Correlations significant at level P < 0.0001 in bold face. n.s. – significance probability less than 0.1.

Axis	DCA95 1		DCA95 2		DCA95 3		DCA95 4	
	τ	P	τ	P	τ	P	τ	P
DCA58A 1	**.8572**	**.0000**	–.2772	.0021	–.0780	n.s.	–.0920	n.s.
DCA58A 2	.0538	n.s.	**.6185**	**.0000**	.1954	.0303	.2530	.0050
DCA58A 3	–.0986	n.s.	–.1646	.0681	**.7374**	**.0000**	–.2070	.0218
DCA58A 4	.0284	n.s.	–.1005	n.s.	–.1736	.0542	**.3861**	**.0000**
DCA37B 1	**.6396**	**.0000**	.1592	n.s.	.0751	n.s.	.0931	n.s.
DCA37B 2	–.0631	n.s.	.3814	.0009	**.5075**	**.0000**	**.5255**	**.0000**
DCA37B 3	**.4865**	**.0000**	–.0601	n.s.	.2883	.0120	–.1441	n.s.
DCA37B 4	.0721	n.s.	–.2042	.0753	.2462	.0320	–.2102	.0671

axis was also relatively strongly correlated with the first vegetational axis, while the third MAF 58A axis was correlated with DCAG 2, DCAGB 2 and DCAG 3, but at lower significance levels (τ < 0.3; P < 0.02, cf. Tab. 11).

The first three axes of the DCA ordination of the pine forest subset (MAF 37B) was correlated with the corresponding axes of ordinations of vegetation (all τ > 0.3, P < 0.01; Tab. 11). Correlations were much stronger with ordinations of the bottom layer than with the ordination of vascular plants (see Tab. 11).

Interpretation of ordinations by means of environmental variables

Ordinations of the MAF 95 data set

The same 13 environmental variables were strongly correlated (P < 0.0001) with the first axis in the DCA and LNMDS ordinations of the MAF 95 data set (Tab. 12). The highest correlation, τ = –0.601, was obtained between DCA 1 and pH_{CaCl_2}. Five variables had τ values > 0.45 with this axis in both ordinations: macro plot soil depth, pH (2 variables) and Total N (negatively correlated) and total macro-plot terrain shape (positively correlated with DCA 1; indicating transition from valley bottom to convex rigde). Other variables strongly correlated with this axis were slope, deciduous litter cover and basal area, notably of deciduous trees (decreasing along the axis), and loss on ignition (increasing). Except for basal area, macro-plot variables were in most cases more strongly correlated with plot scores than the corresponding meso plot variables (see Tab. 12).

Variables related to topography (such as terrain shape and soil depth) and tree cover were only moderately strongly correlated with this axis in the subsets (cf. Tab. 13), indicating that these variables reflected broad-scale differences between spruce and pine forests. Slope was strongly correlated with DCA 1 only in the pine forest; loss on ignition, soil pH, N and Ca in the spruce forest only.

No variable was strongly correlated with DCA 2 (Tab. 12). Correlations significant at the P < 0.01 level were observed for Mn (τ = –0.237, P = 0.0007), bryophyte cover (τ = –0.231, P = 0.0012), loss on ignition (τ = 0.226, P = 0.0012) and K (τ = –0.224, P = 0.0013). Five more variables were

Tab. 9. Kendall's rank correlation coefficients τ between macro-plot scores in the ordinations of the MAF 95 data set and averaged meso plot scores in DCA ordinations of green plants, with significance probabilities (P). Correlations significant at level P < 0.0001 in bold face. n.s. – significance probability less than 0.1. Numbers and abbreviations for names of environmental variables in accordance with Tab. 2. Ordinations of green plants: DCAG – DCA ordination of the full species composition; DCAGV – DCA ordination of vascular plants; DCAGB – DCA ordination of bryophytes and macrolichens (the bottom layer).

Variable	DCA95 1		DCA95 2		DCA95 3		DCA95 4		MDS95 1		MDS95 2	
	τ	P	τ	P	τ	P	τ	P	τ	P	τ	P
DCAG 1	**.6981**	**.0000**	.1166	.0945	–.0155	n.s.	–.1177	.0914	**.7134**	**.0000**	.0202	n.s.
DCAG 2	–.0528	n.s.	.0912	n.s.	**.3181**	**.0000**	–.1318	.0591	–.0492	n.s.	**.3350**	**.0000**
DCAG 3	–.0871	n.s.	–.1547	.0267	–.0772	n.s.	–.0067	n.s.	–.0602	n.s.	–.0546	n.s.
DCAG 4	.0787	n.s.	**.3695**	**.0000**	.0454	n.s.	–.1026	n.s.	.0729	n.s.	.2822	.0001
DCAGV 1	**.6823**	**.0000**	.1524	.0288	–.0294	n.s.	–.1347	.0533	**.6854**	**.0000**	.0300	n.s.
DCAGB 1	**.6983**	**.0000**	.0821	n.s.	–.0096	n.s.	–.1424	.0412	**.7207**	**.0000**	.0161	n.s.
DCAGB 2	–.1201	.0859	–.0155	n.s.	**.2999**	**.0000**	–.1264	.0707	–.1178	.0920	.2431	.0005

Tab. 10. Kendall's rank correlation coefficients τ between macro-plot scores along the first axis in the DCA ordination of the MAF 95 data set and the first axes in three ordinations of vegetation, with significance probabilities (P), calculated for the whole data set and separately for subsets MAF 58A and MAF 37B. Correlations significant at level P < 0.0001 in bold face. n.s. – significance probability less than 0.1. Explanatory variables derived from ordinations of green plants: DCAG – DCA ordination of the full species composition; DCAGV – DCA ordination of vascular plants; DCAGB – DCA ordination of bryophytes and macrolichens (the bottom layer).

Data set	MAF 95		MAF 58A		MAF 37B	
	τ	P	τ	P	τ	P
DCAG 1	**.6981**	**.0000**	**.5150**	**.0000**	.2239	.0513
DCAGV 1	**.6823**	**.0000**	**.5309**	**.0000**	.0782	n.s.
DCAGB 1	**.6983**	**.0000**	**.4876**	**.0000**	.3012	.0089

Figs 18–19. DCA ordination of the MAF 37B data set. Axes scaled in S.D. units. Site-type classification of macro plots plotted onto plot positions. Fig. 18. Axes 1 (horizontal) and 2. Fig. 19. Axes 1 (horizontal) and 3. Colour symbols for each actual site-type are shown. Open and filled circle/square represent the non-paludified and the paludified types, respectively. Inhomogeneous plots with respect to paludification are shown by a composite symbol.

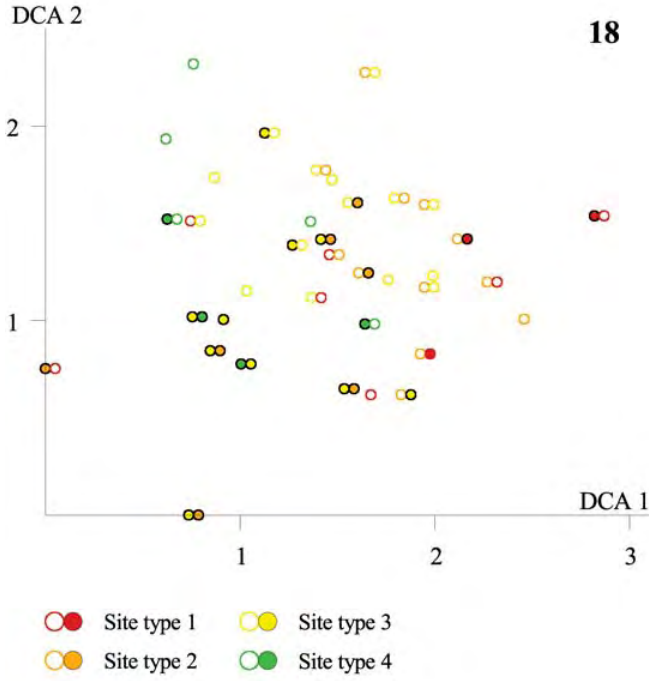
18
DCA 2
DCA 1
1
2
3
Site type 1
Site type 2
Site type 3
Site type 4

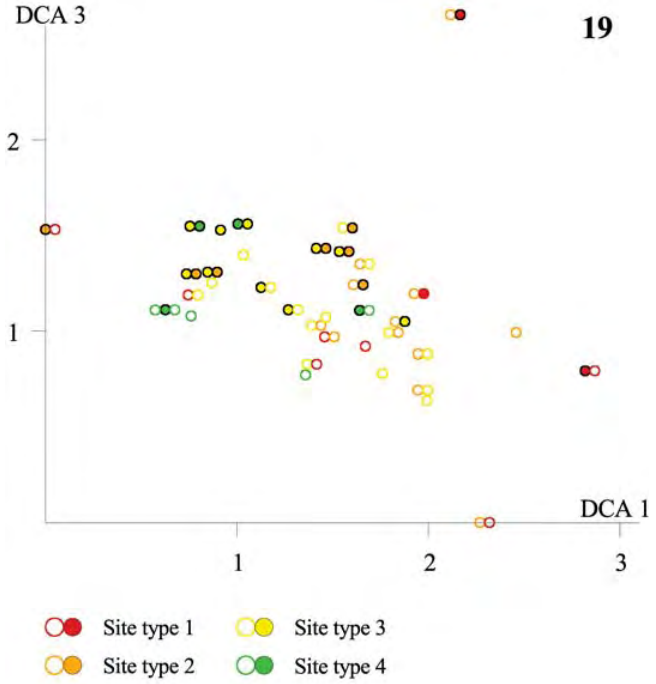
19
DCA 3
DCA 1
1
2
3
Site type 1
Site type 2
Site type 3
Site type 4

correlated with DCA 2 at the $P < 0.05$ level, among them deciduous litter cover ($\tau = 0.151$, $P = 0.037$).

DCA 3 was strongly correlated with one variable, soil moisture, which decreased along the axes ($\tau = –0.465$, cf. Tab. 12). LNMDS 2 was also strongly correlated with soil moisture ($\tau = –0.328$), but even more strongly with bryophyte cover ($\tau = –0.431$, cf. Tab. 12) which was moderately strongly correlated with DCA 3 ($\tau = –0.234$, $P = 0.0011$). Variables related to canopy closure, at the macro- (MA Can) as well as the meso-plot (ME Lit) scales were positively correlated with these axes, most strongly with DCA 3 (Tab. 12). Only four variables; soil moisture, pH, deciduous litter cover and slope, had $\tau > 0.2$ ($P – 0.005$) with DCA 4.

DCA ordination of the spruce-forest subset MAF 58A

The variables strongly correlated with the first axis of fungal species composition in the spruce forest subset were the same that were strongly correlated with DCA95 1 (in this subset): pH, total-N and Ca (all negatively correlated; Tab. 14). Loss on ignition (positively) and bryophyte cover (negatively) were correlated with the second DCA axis at the $P < 0.001$ level. Less strong correlations ($\tau > 0.2$) were noted for deciduous litter cover (positively), Mg and N (both negatively). Soil moisture was strongly negatively correlated with the third DCA axis ($P < 0.0001$, Tab. 14). Other variables correlated with DCA58 3 and with $\tau > 0.25$ were the tree indices (positively correlated; $0.27 \leq \tau$ 0.30, $P < 0.003$), exchangeable acidity (H; negatively) and Ca and Mn (positively).

DCA ordination of the pine-forest subset MAF 37B

Slope was most strongly correlated with the first axis in the ordination of fungi from pine forest ($\tau = –0.363$, $P = 0.002$). Terrain shape was also correlated with this axis (transition from valleyside to convex rigde). Several soil variables, such as Mn, K, S, Na and loss on ignition, and bryophyte cover, were negatively correlated with position along this axis at $P < 0.05$ (Tab. 14). Soil moisture was strongly negatively correlated with DCA 2 ($\tau = –0.542$, $P < 0.0001$). Soil depth (four variables) and tree indices (most strongly at the macro plot scale) were positively correlated with this axis ($\tau > 0.25$), while pH, N, Al and Mn were negatively correlated with DCA 2 at the $P < 0.05$ level. DCA 3 was negatively correlated with pH and slope, and positively correlated with tree variables (Tab. 14).

Variation in species abundances in the DCA ordination of the MAF 95 data set

Characteristics of species responses to the first three DCA axes are summarized in Tab. 15. Differences between mycorrhizal species and saprotrophs with respect to range along these axes are summarized in Figs 20–22. Mycorrhizal fungi generally have much narrower amplitude along the main gradient than was observed for saprotrophs (Fig. 20). More than 50% of the mycorrhizal species had amplitudes < 2 S.D. units, while only 10% of the saprotrophs had such narrow amplitudes. Amplitude > 6 S.D. units was found for no mycorrhizal species but 14% of the saprotrophs. Both groups tended to have wider amplitudes along DCA-axes 2 and 3. For DCA 2, amplitudes were generally wider for the mycorrhizal species (Fig. 21), while for DCA 3 only small differences were found between the two groups (Fig. 22).

Species optima along the first three ordination axes are shown in Figs 23–24 (mycorrhizal species), and Figs 25–26 (saprotrophs). The variation in frequency in subplots for species along the first three ordination axes (species present in above 5% of the plots are shown as Figs 27–188. A wealth of information about the autecology of the species may be deduced from these tables and figures. Here only some points of general interest will be focused.

Tab. 11. Kendall's rank correlation coefficients τ between macro-plot scores in the ordinations of the MAF 95 data subsets (MAF 58A and MAF 37B) and averaged meso-plot scores in DCA ordinations of green plants, with significance probabilities (P). Correlations significant at level P < 0.0001 in bold face. n.s. – significance probability less than 0.1. Numbers and abbreviations for names of environmental variables in accordance with Tab. 2. Ordinations of green plants: DCAG – DCA ordination of the full species composition; DCAGV – DCA ordination of vascular plants; DCAGB – DCA ordination of bryophytes and macrolichens (the bottom layer).

Variable	DCA58 1		DCA58 2		DCA58 3		DCA58 4		DCA37 1		DCA37 2		DCA37 3		DCA37 4	
	τ	P	τ	P	τ	P	τ	P	τ	P	τ	P	τ	P	τ	P
DCAG 1	.4253	.0000	**.2993**	**.0009**	**–.0691**	**n.s.**	**.1151**	**n.s.**	**.3501**	**.0023**	**–.1518**	**n.s.**	**.1247**	**n.s.**	**–.1698**	**n.s.**
DCAG 2	–.1619	.0732	.1959	.0302	.2104	.0199	–.0673	n.s.	.0918	n.s.	.3175	.0058	.3175	.0058	–.2603	.0236
DCAG 3	.0982	n.s.	–.1722	.0567	.2716	.0027	–.2292	.0112	–.0541	n.s.	–.1534	n.s.	–.3820	.0009	–.2075	.0710
DCAG 4	–.3433	.0001	.2193	.0154	–.1221	n.s.	.0930	n.s.	.1402	n.s.	.1944	.0914	–.0347	n.s.	–.1613	n.s.
DCAGV 1	.4268	.0000	**–.2984**	**.0009**	**–.0648**	**n.s.**	**.1156**	**n.s.**	**.1865**	**n.s.**	**–.0692**	**n.s.**	**–.0541**	**n.s.**	**–.0241**	**n.s.**
DCAGB 1	.4294	.0000	**.2017**	**.0255**	**–.0527**	**n.s.**	**.0890**	**n.s.**	**.3916**	**.0007**	**–.1687**	**n.s.**	**.1657**	**n.s.**	**.2048**	**.0752**
DCAGB 2	–.0358	n.s.	.1659	.0670	.2582	.0043	–.0030	n.s.	.0045	n.s.	.3898	.0007	.2814	.0144	.2062	.0731

Tab. 12. Kendall's rank correlation coefficients τ between macro-plot scores in the ordinations of the MAF 95 data set and the 36 environmental variables, with significance probabilities (P). Correlations significant at level P < 0.0001 in bold face. n.s. – significance probability less than 0.1. Numbers and abbreviations for names of environmental variables in accordance with Tab. 2.

Variable	DCA95 1		DCA95 2		DCA95 3		DCA95 4		MDS95 1		MDS95 2	
	τ	P	τ	P	τ	P	τ	P	τ	P	τ	P
01 MA Slo	–.3567	.0000	–.1158	n.s.	–.0633	n.s.	.1733	.0141	–.3635	.0000	–.1930	.0062
02 MA Auf	–.0614	n.s.	.0355	n.s.	–.0776	n.s.	.0709	n.s.	–.0578	n.s.	–.1125	n.s.
03 MA Ter	.5586	.0000	.0986	n.s.	–.0099	n.s.	–.1252	n.s.	.5965	.0000	.0976	n.s.
04 MA Une	–.3261	.0001	–.1317	n.s.	.1349	.0949	.0929	.0148	–.3030	.0002	–.0447	n.s.
05 MA S d	–.5613	.0000	.0282	n.s.	.0537	n.s.	.0517	n.s.	–.5910	.0000	.0274	n.s.
06 MA Bas	–.2494	.0005	–.0953	n.s.	.1599	.0267	–.1436	.0466	–.2335	.0012	.1214	.0923
07 MA Can	–.2775	.0001	.0032	n.s.	.2541	.0003	–.1274	.0692	–.2541	.0003	.2250	.0013
*1 MA Bad	–.4128	.0000	.0732	n.s.	–.0373	n.s.	.1145	n.s.	–.3898	.0000	.0503	n.s.
*2 MA Dli	–.3822	.0000	.1512	.0368	–.0952	n.s.	–.2024	.0052	–.3864	.0000	–.0485	n.s.
*3 MA Bry	.0608	n.s.	–.2314	.0012	–.2339	.0011	–.0470	n.s.	–.0046	n.s.	–.4309	.0000
08 ME Slo	–.3335	.0000	–.0632	n.s.	–.1113	n.s.	.2017	.0041	–.3394	.0000	–.1838	.0088
09 ME Auf	–.0865	n.s.	–.0300	n.s.	–.0725	n.s.	.1002	n.s.	–.0829	n.s.	–.1218	.0845
10 ME Une	–.1358	.0514	–.0177	n.s.	.0067	n.s.	.0659	n.s.	–.1667	.0168	–.1279	.0664
11 ME Con	–.0925	n.s.	–.0387	n.s.	–.0434	n.s.	.1069	n.s.	–.0763	n.s.	–.0023	n.s.
12 ME Smi	.0027	n.s.	.1114	n.s.	–.0378	n.s.	–.0509	n.s.	–.0252	n.s.	.0619	n.s.
13 ME Sme	–.1420	.0418	.1131	n.s.	.0828	n.s.	–.1331	.0566	–.1739	.0127	.0974	n.s.
14 ME Sma	–.2642	.0002	.0708	n.s.	.0885	n.s.	–.0854	n.s.	–.2817	.0001	.0897	n.s.
15 ME Lit	–.2579	.0002	.0244	n.s.	.2426	.0005	–.0481	n.s.	–.2304	.0010	.1891	.0070
16 ME Bas	–.3316	.0000	–.1035	n.s.	.1554	.0273	–.0600	n.s.	–.3157	.0000	.1157	n.s.
17 Mois	–.0587	n.s.	–.0666	n.s.	–.4654	.0000	.2781	.0001	–.0807	n.s.	–.3280	.0000
18 LI	.3829	.0000	.2259	.0012	.0446	n.s.	–.1244	.0744	.3681	.0000	.0175	n.s.
19 pH_{H_2O}	–.5010	.0000	–.0349	n.s.	–.1235	.0877	.2208	.0023	–.4603	.0000	–.0271	n.s.
20 pH_{CaCl_2}	–.6008	.0000	–.0311	n.s.	–.0216	n.s.	.1901	.0082	–.5637	.0000	.0214	n.s.
21 Ca	–.3684	.0000	–.1259	.0708	.1256	.0713	–.0078	n.s.	–.3223	.0000	.1702	.0145
22 Mg	–.2470	.0004	–.1420	.0415	.0813	n.s.	–.0540	n.s.	–.2358	.0007	.0766	n.s.
23 Na	–.0992	n.s.	–.0004	n.s.	–.1158	.0965	.0773	n.s.	–.0835	n.s.	–.0327	n.s.
24 K	–.2551	.0003	–.2244	.0013	.1073	n.s.	.0347	n.s.	–.2573	.0002	–.0488	n.s.
25 H	.3062	.0000	.0869	n.s.	–.2004	.0040	.0249	n.s.	.2887	.0000	–.1622	.0199
26 N	–.5153	.0000	–.0788	n.s.	–.1333	.0558	.1915	.0060	–.4602	.0000	.0188	n.s.
27 P-AL	–.2663	.0001	–.0251	n.s.	–.0347	n.s.	–.0101	n.s.	–.2479	.0004	.0063	n.s.
28 Al	.0903	n.s.	–.1129	n.s.	–.1476	.0341	.1781	.0106	.0791	n.s.	–.2141	.0021
29 Fe	.2004	.0040	–.0681	n.s.	–.1297	.0627	.0159	n.s.	.1758	.0116	–.1935	.0055
30 Mn	–.2569	.0002	–.2370	.0007	.1109	n.s.	.0822	n.s.	–.2385	.0006	.0004	n.s.
31 Zn	–.0311	n.s.	–.1523	.0288	.0625	n.s.	–.0065	n.s.	–.0271	n.s.	–.0336	n.s.
32 P	.0293	n.s.	–.1514	.0297	.0495	n.s.	–.0697	n.s.	.0289	n.s.	–.0914	n.s.
33 S	–.1082	n.s.	–.1429	.0402	.0455	n.s.	.0500	n.s.	–.1050	n.s.	–.0623	n.s.

Ectomycorrhizal fungi

Cortinarius obtusus (Figs 47, 48) was the only very common mycorrhizal species, spanning nearly the whole first axis, and being observed in more than twice as many plots as the secondmost common species. It occurred in most site-types, had a distinct abundance maximum in site-type 5.1 near the middle of the axis, and was absent from the plots with the lowermost DCA 1 scores. These plots mostly had a dense field layer and/or high litterfall, while *C. obtusus* seemed to find its optimum in sites with a dense bryophyte carpet.

A few less frequent species also had very wide amplitudes. *Amanita fulva* (Figs 27, 28, also see Tab. 15) occurred accidentally from site-type 5.2 till the driest plots in series 1, and was one of very few species that fruited during the extremely dry period in August 1990. *Cortinarius scaurus* (Figs 51, 52, Tab. 15) spanned the range from site-types 5.3 to 2.

Several species (many of them with low frequency) were restricted to the low-score end of DCA-axis 1, and to site-types associated with higher nutrient concentrations (5.2, 5.3, and 6). The most frequent among these species were *Hygrophorus pustulatus* (Figs 63, 64) and *Entoloma rhodopolium* (Figs 55, 56), both restricted to DCA 1 < 2.0 S.D. units. *E. rhodopolium* occurred in (fine-scale) paludified sites characterized by low DCA 3 scores, and reached its highest frequency in plot 38 which acted as an outlier in the ordination of the MAF 97 data set and hence was not included in the MAF 95 set.

Many species typical of the 'bilberry-dominated spruce forest' showed concentrations to the middle parts of DCA 1 and site-type 5.1. Examples are *Cortinarius flexipes* (Figs 45, 46), which occurred in 22 of 23 plots classified to series 5 and had a distinct optimum in site-type 5.1; *Amanita virosa* (Figs 29, 30), *Cantharellus tubaeformis* (Figs 31, 32), *Cortinarius albovariegatus* (Figs 33, 34), *C. armeniacus* (Fig. 37, 38), *C. brunneus* (Figs 41, 42), and *Russula emetica* (Figs 89, 90), the latter one almost exclusively confined to series 5, but with a wide amplitude from 5.1 to 5.3.

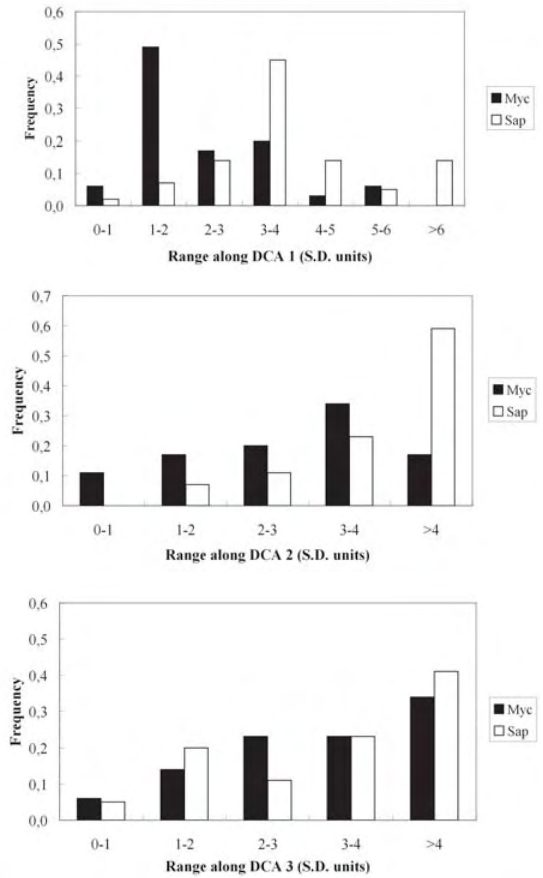

Figs 20–22. Frequency distributions for estimated range along DCAF 95 ordination axes, for ectomycorrhizal and saprotrophic species. Fig. 20. DCA axis 1. Fig. 21. DCA axis 2. Fig. 22. DCA axis 3.

Wider amplitudes towards higher DCA 1 scores (the pine forest) were observed for *Cortinarius biformis* (Figs 39, 40; DCA 1 > *c.* 0.7 S.D.), *Cortinarius stillatitius* (Figs 53, 54; DCA 1 > *c.* 1.5 S.D.), and *Russula vinosa* (Figs 97, 98, 1.9 < DCA 1 < 3.2 S.D.).

Obligate or preferential pine forest species had their main occurrence in plots with high DCA 1 scores. An example is *Lactarius rufus* (Figs 69, 70), with only accidental occurrences in spruce-forest plots. The quantatively most important species with optimum at high DCA 1 scores were *Suillus variegatus* (Figs 99, 100) with a narrow amplitude (2.9 < DCA 1 < 4.5 S.D.; cf. Tab. 15), and *Russula decolorans* (Figs 87, 88) and *R. paludosa* (Figs 91, 92) with a wider amplitudes.

Most of the species mentioned above had wide amplitudes along ordination axes 2 and 3. A limited number of species showed variation in abundance along the second axis. Of these, especially *Leccinum versipelle* (Fig. 77), *Leccinum* sp. (Fig. 79) and *Russula puellaris* (Fig. 93) showed

Tab. 13. Kendall's rank correlation coefficients τ between macro-plot scores along the first axis in the DCA ordination of the MAF 95 data set and 36 environmental variables, with significance probabilities (P). Correlation coefficients are calculated for the whole data set and for subsets MAF 58A and MAF 37B. Correlations significant at level P < 0.0001 in bold face. n.s. – significance probability less than 0.1. Numbers and abbreviations for names of environmental variables in accordance with Tab. 2.

Data set	MAF 95		MAF 58A		MAF 37B	
	τ	P	τ	P	τ	P
01 MA Slo	–.3567	.0000	**.0289**	**n.s.**	**–.2958**	**.0114**
02 MA Auf	–.0614	n.s.	–.0462	n.s.	–.1580	n.s.
03 MA Ter	.5586	.0000	**.1019**	**n.s.**	**.2750**	**.0379**
04 MA Un	–.3261	.0001	–.1497	n.s.	–.0301	n.s.
05 MA S d	–.5613	.0000	**–.2233**	**.0340**	**–.1762**	**n.s.**
06 MA Bas	–.2494	.0005	–.1249	n.s.	.1147	n.s.
07 MA Can	–.2775	.0001	–.1873	.0387	.1548	n.s.
***1 MA BaD**	–.4128	.0000	**–.2550**	**.0064**	**–.0684**	**n.s.**
***2 MA Dli**	–.3822	.0000	**–.2212**	**.0171**	**–.1733**	**n.s.**
*3 MA Bry	.0608	n.s.	.3666	.0001	–.1577	n.s.
08 ME Slo	–.3335	.0000	**–.0843**	**n.s.**	**–.2701**	**.0197**
09 ME Auf	–.0865	n.s.	.0873	n.s.	–.1760	n.s.
10 ME Une	–.1358	.0514	.0000	n.s.	–.0270	n.s.
11 ME Con	–.0925	n.s.	–.0838	n.s.	–.1494	n.s.
12 ME Smi	.0027	n.s.	–.0134	n.s.	–.0075	n.s.
13 ME Sm	–.1420	.0418	–.0709	n.s.	.0376	n.s.
14 ME Sm	–.2642	.0002	–.1343	n.s.	.1566	n.s.
15 ME Lit	–.2579	.0002	–.1511	.0947	.1510	n.s.
16 ME Bas	–.3316	.0000	**–.0974**	**n.s.**	**.1085**	**n.s.**
17 Mois	–.0587	n.s.	–.0472	n.s.	–.0616	n.s.
18 LI	.3829	.0000	**.3311**	**.0002**	**–.1187**	**n.s.**
19 pH_{H_2O}	–.5010	.0000	–.4831	.0000	**–.2419**	**.0451**
20 pH_{CaCl_2}	–.6008	.0000	–.5355	.0000	**–.2883**	**.0174**
21 Ca	–.3684	.0000	–.3769	.0000	**–.0961**	**n.s.**
22 Mg	–.2470	.0004	–.2305	.0106	–.1231	n.s.
23 Na	–.0992	n.s.	–.2111	.0192	–.1982	.0843
24 K	–.2551	.0003	–.0127	n.s.	–.1862	n.s.
25 H	.3062	.0000	**.2220**	**.0138**	**.0841**	**n.s.**
26 N	–.5153	.0000	–.4967	.0000	**–.0601**	**n.s.**
27 P–AL	–.2663	.0001	–.1688	.0613	–.2432	.0341
28 Al	.0903	n.s.	.1918	.0335	–.0360	n.s.
29 Fe	.2004	.0040	.3176	.0004	–.0781	n.s.
30 Mn	–.2569	.0002	–.0502	n.s.	–.1892	.0994
31 Zn	–.0311	n.s.	.1325	n.s.	–.0120	n.s.
32 P	.0293	n.s.	.2874	.0014	–.0360	n.s.
33 S	–.1082	n.s.	.0357	n.s.	–.1622	n.s.

Tab. 14. Kendall's rank correlation coefficients τ between macro-plot scores in the ordinations of the MAF 95 data subsets (MAF 58A and MAF 37B) and the 36 environmental variables, with significance probabilities (P). Correlations significant at level P < 0.0001 in bold face. n.s. – significance probability less than 0.1. Numbers and abbreviations for names of environmental variables in accordance with Tab. 2.

Variable	DCA58 1		DCA58 2		DCA58 3		DCA58 4		DCA37 1		DCA37 2		DCA37 3		DCA37 4	
	τ	P	τ	P	τ	P	τ	P	τ	P	τ	P	τ	P	τ	P
01 MA Slo	.0191	n.s.	–.0301	n.s.	.0031	n.s.	–.0412	n.s.	–.3633	.0019	–.1518	n.s.	–.2100	.0723	–.0812	n.s.
02 MA Auf	–.0669	n.s.	.0109	n.s.	–.0304	n.s.	.0122	n.s.	–.1008	n.s.	.0316	n.s.	–.2002	.0819	–.0376	n.s.
03 MA Ter	.0826	n.s.	.0409	n.s.	.1421	n.s.	–.0975	n.s.	.2950	.0260	–.0080	n.s.	.1435	n.s.	.0598	n.s.
04 MA Une	–.1153	n.s.	–.0120	n.s.	.2230	.0303	.0075	n.s.	–.1504	n.s.	.0602	n.s.	–.0962	n.s.	.1444	n.s.
05 MA S d	–.2638	.0123	.0307	n.s.	–.0696	n.s.	–.0518	n.s.	–.2046	n.s.	.3750	.0065	.1136	n.s.	.0170	n.s.
06 MA Bas	–.0873	n.s.	–.1538	.0985	.2856	.0022	–.1237	n.s.	.0828	n.s.	.2707	.0243	.3313	.0058	–.1561	n.s.
07 MA Can	–.1934	.0328	–.0231	n.s.	.2712	.0028	–.1034	n.s.	.0850	n.s.	.2974	.0103	.2944	.0111	–.1032	n.s.
*1 MA BaD	–.2841	.0024	.0664	n.s.	.0563	n.s.	.0715	n.s.	.0760	n.s.	.1216	n.s.	–.0190	n.s.	–.1292	n.s.
*2 MA Dli	–.2861	.0020	.2124	.0220	–.2399	.0097	–.1587	.0870	–.1896	n.s.	–.1961	n.s.	.2484	.0424	–.0098	n.s.
***3 MA Bry**	.4340	.0000	**–.2457**	**.0080**	**–.2369**	**.0105**	**–.0686**	**n.s.**	**–.2845**	**.0156**	**–.1144**	**n.s.**	**.0990**	**n.s.**	**.2010**	**.0876**
08 ME Slo	–.0623	n.s.	–.0208	n.s.	–.0464	n.s.	–.0257	n.s.	–.2549	.0278	–.1912	.0989	–.2823	.0148	.1051	n.s.
09 ME Auf	.0467	n.s.	.0283	n.s.	–.0418	n.s.	–.0283	n.s.	–.1821	n.s.	–.0425	n.s.	–.1821	n.s.	.0880	n.s.
10 ME Une	.0315	n.s.	–.0327	n.s.	–.0036	n.s.	–.0303	n.s.	–.0931	n.s.	.1111	n.s.	–.0420	n.s.	.0841	n.s.
11 ME Con	–.0826	n.s.	.0656	n.s.	–.0328	n.s.	–.0790	n.s.	–.1253	n.s.	–.1374	n.s.	–.0589	n.s.	.1585	n.s.
12 ME Smi	–.0645	n.s.	.0997	n.s.	–.1946	.0318	.2226	.0140	–.0376	n.s.	.2724	.0179	.1008	n.s.	–.0436	n.s.
13 ME Sme	–.1121	n.s.	.1376	n.s.	–.0709	n.s.	–.0055	n.s.	–.0977	n.s.	.3171	.0058	.1007	n.s.	–.0105	n.s.
14 ME Sma	–.1622	.0722	.0718	n.s.	–.0533	n.s.	–.0278	n.s.	.0211	n.s.	.2982	.0096	.1536	n.s.	.0181	n.s.
15 ME Lit	–.1644	.0690	.0297	n.s.	.2725	.0026	–.1110	n.s.	.0870	n.s.	.2456	.0345	.1968	.0903	–.0015	n.s.
16 ME Bas	–.0680	n.s.	–.1158	n.s.	.2997	.0010	–.0741	n.s.	.1391	n.s.	.2032	.0812	.2583	.0267	–.1513	n.s.
17 Mois	**.0097**	**n.s.**	**–.1865**	**.0388**	–.4214	.0000	**.0920**	**n.s.**	**.0646**	**n.s.**	–.5424	.0000	**–.2299**	**.0454**	**–.0406**	**n.s.**
18 LI	.2318	.0102	.3142	.0005	–.1047	n.s.	.1265	n.s.	–.2329	.0426	.1818	n.s.	–.0947	n.s.	–.0015	n.s.
19 pH_{H2O}	–.4451	.0000	**–.1171**	**n.s.**	**.0057**	**n.s.**	**.0298**	**n.s.**	**–.1842**	**n.s.**	**–.3444**	**.0043**	**–.3220**	**.0077**	**–.1682**	**n.s.**
20 pH_{CaCl2}	–.5106	.0000	**–.0772**	**n.s.**	**.1096**	**n.s.**	**–.0224**	**n.s.**	**–.2206**	**.0688**	**–.2689**	**.0265**	**–.2303**	**.0575**	**–.1176**	**n.s.**
21 Ca	–.3600	.0001	–.1881	.0370	.2644	.0034	–.1869	.0382	–.1562	n.s.	–.1021	n.s.	–.0571	n.s.	.0390	n.s.
22 Mg	–.2039	.0238	–.2184	.0155	.1397	n.s.	–.1373	n.s.	–.2012	.0797	.0090	n.s.	–.0480	n.s.	.0480	n.s.
23 Na	–.2039	.0238	–.1095	n.s.	–.0127	n.s.	.0272	n.s.	–.2643	.0213	–.2042	.0753	–.2012	.0797	–.0691	n.s.
24 K	.0381	n.s.	–.1531	.0897	.2414	.0074	–.0139	n.s.	–.2763	.0161	–.0841	n.s.	–.1231	n.s.	–.0450	n.s.
25 H	.2172	.0160	.0841	n.s.	–.3345	.0002	.1748	.0525	.1862	n.s.	–.1081	n.s.	–.0631	n.s.	–.1832	n.s.
26 N	–.4580	.0000	**–.2063**	**.0222**	**–.0466**	**n.s.**	**–.1204**	**n.s.**	**.0901**	**n.s.**	**–.3243**	**.0047**	**–.1171**	**n.s.**	**.0691**	**n.s.**
27 P–AL	–.1785	.0478	–.0817	n.s.	.0079	n.s.	–.2329	.0098	–.1892	.0994	.0330	n.s.	.1081	n.s.	–.0541	n.s.
28 Al	.2063	.0222	–.0623	n.s.	–.1567	.0823	.1446	n.s.	–.0360	n.s.	–.2462	.0320	–.0931	n.s.	.0270	n.s.
29 Fe	.3418	.0002	–.0284	n.s.	–.1034	n.s.	–.0321	n.s.	–.0060	n.s.	–.0480	n.s.	–.0751	n.s.	.0631	n.s.
30 Mn	–.0430	n.s.	–.1349	n.s.	.3055	.0007	–.1797	.0463	–.3393	.0031	–.2553	.0262	–.0661	n.s.	.0781	n.s.
31 Zn	.1155	n.s.	–.0514	n.s.	.0986	n.s.	–.1567	.0823	–.1802	n.s.	–.0300	n.s.	.1291	n.s.	.2553	.0262
32 P	.2753	.0023	–.0272	n.s.	.0744	n.s.	–.1397	n.s.	–.2162	.0597	–.0120	n.s.	.2012	.0797	.1532	n.s.
33 S	.0236	n.s.	–.0563	n.s.	.1373	n.s.	–.0841	n.s.	–.2643	.0213	–.0961	n.s.	–.0270	n.s.	.1652	n.s.

Tab. 15. Characteristics of ectomycorrhizal species in the MAF 95 data set: range and species score (estimate for optimum; in bold face) with respect to the first three DCA axes; total frequency, and frequency and mean subplot frequency (given as exponent) in each interval along each axis.

Species	Range and score with respect to DCA axis			Tot.	DCA 1								DCA 2					DCA 3				
DCA axis/interval	DCA 1	DCA 2	DCA 3		-0.6	-1.1	-1.7	-2.1	-2.5	-2.9	-3.3	>3.3	-0.6	-0.95	-1.25	-1.6	>1.6	-0.7	-1.1	-1.45	-1.8	>1.8
n				95	8	8	9	19	13	11	16	11	11	21	33	21	9	9	24	29	25	8
Amanita fulva	0.5-**0.76**-1.9(-3.5)	(0.1-)1.5→**2.73**	**-0.54**←1.5	7^{2}	13^{3}	25^{2}	11^{1}	5^{1}	8^{2}	·	·	9^{1}	9^{1}	5^{1}	3^{2}	10^{2}	22^{3}	22^{2}	8^{2}	7^{2}	4^{1}	·
Amanita virosa	1.5-**2.25**-2.7	0.5→**2.25**	0.7→**3.63**	17^{2}	·	·	11^{3}	37^{2}	38^{1}	27^{1}	·	·	9^{1}	24^{2}	18^{1}	10^{1}	22^{3}	11^{1}	13^{2}	10^{1}	28^{1}	25^{5}
Cantharellus tubaeformis	1.0-**2.28**-2.7(-3.2)	0.5-**1.54**-1.6	0.8→**2.91**	13^{2}	·	25^{2}	11^{1}	16^{3}	31^{2}	9^{3}	6^{1}	·	9^{2}	19^{2}	9^{4}	14^{2}	11^{1}	·	13^{2}	10^{2}	16^{2}	25^{3}
Cortinarius albovariegatus	(0.7-)1.8-**1.97**-2.6	0.2-**0.56**-1.5	(0.6-)1.0→**2.94**	15^{2}	·	25^{1}	·	37^{2}	31^{2}	9^{1}	·	·	27^{1}	24^{2}	9^{1}	14^{1}	·	11^{1}	8^{1}	10^{2}	24^{2}	25^{1}
Cortinarius anomalus	0.6-**0.72**-1.9(-2.6)	(-**0.07**←0.2-)0.9→	0.8-**2.15**→	8^{2}	13^{1}	25^{3}	·	21^{2}	·	9^{1}	·	·	9^{4}	5^{1}	3^{4}	14^{1}	22^{2}	·	13^{2}	10^{2}	4^{1}	13^{4}
Cortinarius armeniacus	1.2-**2.28**-2.7	0.4-**2.14**→	(0.8-)1.3→**2.93**	9^{1}	·	·	22^{1}	21^{1}	15^{1}	9^{2}	·	·	9^{1}	5^{1}	12^{1}	10^{2}	11^{1}	·	4^{1}	10^{1}	16^{1}	13^{1}
Cortinarius biformis	0.7-**2.69**→	←**1.58**→	0.8→**2.83**	12^{1}	·	13^{1}	11^{1}	21^{1}	15^{1}	9^{4}	6^{1}	9^{1}	9^{1}	10^{3}	9^{1}	19^{1}	11^{2}	·	8^{1}	7^{2}	20^{2}	25^{1}
Cortinarius brunneus	(0.6-)1.8-**1.94**-2.7	0.4-**2.06**→	0.5-1.5(-**1.66**)	11^{2}	13^{1}	·	·	37^{2}	8^{2}	9^{1}	·	·	18^{1}	10^{3}	3^{1}	19^{2}	11^{1}	22^{2}	17^{1}	7^{1}	8^{4}	·
Cortinarius casimiri	(0.7-)**0.96**-2.3	←**0.08**-1.3(-1.8)	0.5-**0.70**→	8^{2}	·	13^{3}	11^{5}	21^{1}	15^{1}	·	·	·	18^{2}	10^{1}	6^{1}	5^{1}	11^{5}	22^{1}	17^{2}	·	4^{1}	13^{3}
Cortinarius flexipes	0.9-**1.87**-2.4	←**0.69**→	**-0.24**← →	24^{2}	·	50^{2}	44^{1}	47^{2}	46^{3}	·	·	·	36^{1}	43^{3}	15^{3}	14^{1}	22^{1}	44^{5}	38^{2}	10^{1}	24^{2}	13^{1}
Cortinarius obtusus	0.7-**2.67**→	←**2.08**→	← →**2.35**	61^{3}	·	100^{2}	67^{3}	79^{3}	69^{5}	55^{3}	56^{2}	45^{2}	55^{2}	57^{2}	55^{3}	81^{4}	56^{5}	44^{1}	42^{4}	55^{3}	84^{3}	88^{2}
Cortinarius pluvius	**1.69**-2.1	0.9→**2.41**	1.0→**3.09**	5^{1}	·	·	11^{1}	16^{1}	8^{1}	·	·	·	·	10^{2}	3^{1}	5^{1}	11^{1}	·	4^{1}	3^{1}	8^{2}	13^{1}
Cortinarius scaurus	1.3→**4.04**	←**0.23**-1.5	0.7-1.6(-**2.10**)	9^{1}	·	·	22^{1}	5^{1}	8^{1}	9^{1}	6^{1}	27^{2}	9^{1}	5^{1}	18^{2}	5^{1}	·	·	8^{1}	10^{2}	16^{1}	·
Cortinarius stillatitius	1.5-**3.61**→	**-0.13**←1.0(-1.3)	(0.8-)1.1→**2.36**	9^{1}	·	·	11^{1}	16^{1}	8^{1}	18^{1}	·	18^{2}	27^{1}	14^{1}	6^{2}	5^{1}	·	·	8^{1}	14^{1}	8^{1}	13^{1}
Entoloma rhodopolium	←**0.38**-1.9	**-0.98**←1.1(-1.5)	**-0.04**←1.4(-1.9)	6^{1}	13^{2}	25^{1}	·	16^{1}	·	·	·	·	27^{1}	5^{1}	3^{2}	5^{1}	·	11^{1}	13^{1}	3^{2}	·	13^{1}
Glomus sp.	0.6-**1.25**-2.2	0.4-**1.83**(→?)	←**1.09**→	11^{1}	13^{1}	13^{1}	11^{1}	26^{1}	15^{2}	·	·	·	18^{1}	5^{1}	6^{2}	14^{1}	22^{1}	11^{1}	21^{1}	3^{1}	8^{2}	13^{1}
Hygrophorus olivaceoalbus	0.5-**0.86**-2.3	**-0.70**←1.2(-1.8)	**-0.32**←1.5	14^{2}	13^{4}	13^{1}	33^{2}	37^{1}	8^{1}	·	·	·	36^{2}	14^{1}	12^{2}	5^{1}	11^{1}	33^{2}	25^{2}	10^{2}	4^{1}	·
Hygrophorus pustulatus	←**0.51**-2.0	(0.2-)0.8→**2.23**	0.8→**2.34**	12^{2}	38^{2}	38^{3}	22^{1}	16^{4}	·	·	·	·	9^{2}	14^{1}	3^{2}	24^{4}	11^{1}	·	8^{4}	14^{2}	12^{3}	25^{2}
Laccaria amethystina	←**0.08**-1.5	(←?)**0.18**-1.5	1.0-**1.44**-1.9	5^{1}	13^{1}	38^{1}	11^{2}	·	·	·	·	·	9^{1}	5^{2}	·	14^{1}	·	·	4^{1}	7^{2}	4^{2}	13^{1}
Lactarius camphoratus	0.5-**0.64**-2.7	(0.2-)0.8-**1.31**→	**-0.38**← →	13^{2}	25^{4}	25^{2}	22^{3}	21^{1}	8^{4}	9^{1}	·	·	9^{1}	19^{2}	9^{4}	14^{1}	11^{1}	·	29^{3}	10^{1}	4^{1}	13^{1}
Lactarius rufus	(1.1-)2.9→**3.92**	0.6-1.5(-**1.96**)	0.7-1.6(-**2.44**)	6^{2}	·	13^{1}	·	5^{4}	·	9^{1}	6^{1}	18^{3}	9^{1}	5^{1}	9^{2}	5^{4}	·	11^{1}	8^{1}	7^{3}	4^{4}	·
Lactarius theiogalus	1.1-**1.22**-2.3	**-0.86**←1.0	**-1.42**←1.4	7^{5}	·	13^{10}	11^{2}	16^{4}	15^{5}	·	·	·	45^{4}	5^{3}	3^{10}	·	·	44^{4}	8^{7}	3^{2}	·	·
Lactarius vietus	0.5-**0.80**-2.0	0.7-**1.76**→	(**0.16**-)0.8-1.6	5^{3}	13^{4}	13^{1}	11^{1}	11^{4}	·	·	·	·	·	14^{3}	3^{1}	·	11^{4}	·	8^{4}	3^{4}	8^{1}	·
Leccinum palustre	(0.5-)2.3-3.2(-**3.46**)	0.9-**1.67**→	0.6-**1.12**→	9^{2}	13^{1}	·	11^{1}	·	15^{1}	18^{2}	19^{2}	·	·	5^{1}	18^{2}	·	22^{1}	22^{1}	8^{2}	10^{2}	4^{1}	13^{1}
Leccinum versipelle	(0.6-)2.4-**2.98**-3.2	1.2→**3.52**	←**1.19**-1.6	6^{1}	13^{2}	·	·	·	8^{1}	·	25^{1}	·	·	·	6^{1}	5^{1}	33^{2}	11^{1}	·	10^{1}	8^{2}	·
Leccinum sp.	1.7-**3.61**→	1.1→**3.03**	**-0.67**←1.3	5^{1}	·	·	·	11^{1}	8^{1}	·	6^{1}	9^{2}	·	·	6^{2}	5^{1}	22^{1}	11^{1}	13^{1}	3^{1}	·	·
Rozites caperatus	1.5-**2.63**-3.6	0.7-1.6(-**2.37**)	(0.8-)1.3→**2.49**	7^{1}	·	·	22^{1}	16^{1}	·	9^{1}	·	9^{1}	·	10^{1}	6^{1}	10^{2}	11^{1}	·	4^{1}	14^{1}	4^{1}	13^{1}
Russula aquosa	1.1-**1.35**-2.7	0.4-**1.55**-1.8	**-0.30**←1.5	8^{1}	·	13^{2}	33^{1}	5^{2}	15^{1}	9^{1}	·	·	18^{2}	10^{1}	6^{1}	5^{2}	11^{1}	11^{1}	21^{1}	3^{2}	4^{1}	·
Russula betularum	0.9-**1.60**-2.3	**-0.55**←1.4	**-2.37**←1.1	5^{2}	·	25^{1}	·	5^{1}	15^{3}	·	·	·	18^{3}	5^{1}	3^{1}	5^{1}	·	33^{2}	4^{1}	3^{1}	·	·
Russula decolorans	2.8→**4.79**	(**0.81**-)0.9-1.7	0.8-**0.84**-1.5	23^{3}	·	·	·	·	·	9^{1}	69^{2}	91^{4}	·	10^{2}	45^{3}	19^{2}	11^{1}	·	21^{3}	38^{2}	24^{3}	·
Russula emetica	0.9-**1.36**-2.4	← →**2.41**	0.4-**0.60**-1.6	16^{2}	·	38^{1}	33^{1}	37^{2}	15^{2}	·	·	·	18^{1}	19^{2}	6^{2}	24^{1}	22^{3}	11^{1}	29^{1}	17^{2}	8^{1}	·
Russula paludosa	(0.7-)2.1→**4.30**	(0.2-)1.0-**1.47**-1.6	0.6-**1.43**→	16^{3}	·	13^{2}	·	5^{6}	·	27^{2}	13^{3}	73^{3}	9^{2}	·	30^{3}	19^{5}	·	11^{1}	8^{3}	28^{4}	12^{1}	13^{2}
Russula puellaris	1.2-**1.29**-1.8(-2.4)	1.1→**3.84**	**-0.59**←1.0	5^{1}	·	·	22^{1}	11^{1}	8^{1}	·	·	·	·	·	6^{1}	5^{1}	22^{1}	11^{1}	17^{1}	·	·	·
Russula rhodopoda	←**1.54**-2.6	0.7-**0.94**-1.5	1.2→**3.18**	14^{2}	25^{2}	·	22^{1}	21^{1}	31^{3}	9^{1}	·	·	·	43^{2}	6^{1}	10^{2}	·	·	·	14^{2}	20^{2}	50^{1}
Russula vinosa	1.9-**3.17**-3.2(→?)	**-0.23**←1.5	(0.4-)0.8→**3.16**	14^{3}	·	·	·	26^{3}	31^{4}	18^{3}	13^{2}	·	27^{6}	29^{2}	6^{2}	10^{2}	·	11^{1}	8^{2}	14^{3}	12^{2}	38^{5}
Suillus variegatus	2.9→**4.42**	1.0-**1.28**-1.4	1.0-**2.20**→	5^{1}	·	·	·	·	·	·	19^{1}	18^{2}	·	·	12^{2}	5^{1}	·	·	4^{2}	10^{1}	4^{2}	·

Tab. 16. Characteristics of saprotrophic species in the MAF 95 data set: range and species score (estimate for optimum; in bold face) with respect to the first three DCA axes; total frequency, and frequency and mean subplot frequency (given as exponent) in each interval along each axis.

Species	Range and score with respect to DCA axis			Tot.	DCA 1								DCA 2					DCA 3				
DCA axis/interval	DCA 1	DCA 2	DCA 3		-0.6	-1.1	-1.7	-2.1	-2.5	-2.9	-3.3	>3.3	-0.6	-0.95	-1.25	-1.6	>1.6	-0.7	-1.1	-1.45	-1.8	>1.8
n				95	8	8	9	19	13	11	16	11	11	21	33	21	9	9	24	29	25	8
Baeospora myosura	←**0.63**→	←**0.00**→	(**0.32**-)0.7-1.8	15^{2}	38^{3}	25^{3}	22^{1}	5^{1}	31^{2}	·	6^{1}	9^{1}	27^{2}	10^{3}	15^{1}	10^{3}	22^{2}	·	21^{2}	14^{2}	16^{1}	13^{1}
Calocera viscosa	0.5-**1.32**-2.9	←**1.50**→	←**0.50**-1.6	19^{1}	13^{2}	25^{2}	44^{1}	32^{1}	23^{1}	18^{2}	·	·	27^{2}	19^{2}	9^{1}	24^{1}	33^{1}	33^{2}	25^{1}	10^{2}	24^{1}	·
Clavariadelphus junceus	**-0.56**←1.1(-1.5)	← →**2.28**	0.7-**1.20**→	18^{7}	100^{10}	100^{6}	11^{1}	·	·	·	·	·	18^{6}	5^{1}	6^{1}	29^{7}	67^{9}	·	25^{7}	21^{10}	12^{5}	25^{3}
Collybia arrata	0.5-**2.41**→	← →**2.24**	0.7-**0.78**→	16^{2}	13^{1}	13^{1}	44^{2}	16^{2}	·	9^{1}	19^{2}	18^{2}	9^{1}	14^{2}	12^{1}	19^{2}	33^{2}	·	21^{2}	17^{2}	16^{1}	13^{1}
Collybia dryophila	0.5-**0.76**-0.9(-1.7)	(**0.48**-)0.6→	(**0.56**-)0.7→	6^{1}	25^{1}	13^{2}	·	5^{1}	·	9^{1}	6^{1}	·	9^{1}	10^{1}	3^{1}	5^{2}	11^{1}	11^{1}	8^{1}	7^{2}	·	13^{1}
Collybia tuberosa	0.5-**3.08**→	←**1.86**→	←**0.80**→	64^{2}	63^{2}	25^{3}	89^{2}	79^{2}	62^{2}	36^{3}	63^{3}	82^{2}	45^{2}	62^{2}	82^{2}	43^{3}	78^{4}	56^{2}	67^{3}	72^{3}	56^{2}	63^{1}
Cystoderma jasonis	1.0-**2.68**→	**-0.12**←1.6	←**0.16**→	38^{2}	·	25^{2}	33^{2}	63^{3}	54^{2}	55^{2}	25^{2}	18^{1}	73^{3}	43^{2}	39^{2}	24^{2}	11^{1}	67^{3}	42^{2}	41^{2}	24^{2}	25^{2}
Entoloma cetratum	1.1-**2.86**→	**-0.26**←1.5	←**0.05**-1.5	16^{1}	·	13^{1}	22^{1}	32^{1}	·	18^{1}	19^{1}	9^{1}	18^{2}	19^{1}	18^{1}	14^{1}	·	33^{1}	17^{1}	17^{1}	12^{1}	·
Galerina atkinsoniana	←**2.64**→	←**0.38**→	←**0.74**→	71^{2}	13^{1}	63^{2}	67^{2}	89^{3}	92^{3}	100^{2}	75^{1}	27^{2}	82^{3}	86^{2}	67^{2}	67^{2}	44^{4}	100^{2}	83^{2}	48^{3}	76^{2}	63^{2}
Galerina hypnorum	←**2.62**→	←**0.38**→	←**0.39**→	84^{5}	50^{2}	100^{2}	89^{4}	95^{7}	92^{9}	91^{6}	75^{3}	73^{3}	100^{6}	81^{6}	88^{5}	71^{4}	89^{3}	100^{7}	96^{6}	79^{5}	80^{4}	63^{4}
Galerina marginata	**-0.88**←1.0	1.2→**2.73**	0.7-**1.27**-1.7	6^{1}	63^{1}	13^{1}	·	·	·	·	·	·	·	·	3^{1}	10^{2}	33^{1}	·	8^{1}	10^{1}	4^{2}	·
Galerina mniophila	(0.5-)1.3-**2.22**-2.9	**-0.48**←1.5	**-0.35**← →	23^{2}	13^{1}	·	11^{4}	47^{3}	46^{3}	36^{1}	6^{1}	·	64^{3}	24^{3}	21^{2}	14^{1}	·	44^{3}	33^{2}	24^{2}	8^{2}	13^{1}
Galerina sp.1	(1.2-)1.8-**3.45**→	←**0.02**-1.4	**-0.25**← →	25^{2}	·	·	11^{1}	37^{2}	46^{2}	45^{3}	6^{1}	36^{2}	45^{2}	29^{2}	30^{2}	14^{2}	·	56^{3}	29^{2}	21^{2}	16^{2}	25^{1}
Galerina sp.2	1.2-**1.74**-1.9(-3.2)	**-0.59**←0.9(-1.2)	←**0.30**-1.4(-1.7)	8^{1}	·	·	33^{1}	16^{2}	·	9^{1}	6^{1}	·	36^{2}	10^{1}	3^{1}	5^{2}	·	11^{1}	17^{2}	7^{2}	4^{1}	·
Gymnopilus sapineus	1.1-**3.20**→	0.8-1.6(-**2.13**)	0.8-**0.96**→	13^{1}	·	13^{1}	22^{1}	11^{1}	8^{1}	27^{1}	6^{1}	18^{1}	·	5^{1}	18^{1}	19^{1}	11^{1}	·	21^{1}	14^{1}	8^{1}	13^{1}
Heyderia abietis	(1.8-)2.4→**3.94**	0.9-1.5(-**2.00**)	(**0.85**-)0.9-1.5	9^{1}	·	·	·	5^{1}	8^{1}	27^{1}	13^{1}	18^{1}	·	5^{1}	6^{2}	29^{1}	·	·	8^{1}	17^{1}	8^{1}	·
Marasmius androsaceus	← →**3.81**	←**1.16**→	←**1.78**→	85^{6}	50^{1}	38^{1}	78^{3}	89^{3}	92^{8}	100^{7}	100^{9}	100^{8}	64^{4}	100^{5}	88^{8}	90^{7}	56^{3}	89^{4}	79^{4}	90^{7}	88^{8}	75^{5}
Marasmius epiphyllus	**-0.02**←2.4	0.7→**3.27**	0.7→**2.42**	22^{3}	88^{6}	50^{3}	33^{2}	26^{2}	15^{1}	·	·	·	·	14^{2}	9^{2}	38^{2}	78^{6}	·	17^{2}	24^{6}	24^{2}	50^{2}
Micromphale perforans	←**1.49**-2.6	←**0.01**-1.8	← →**2.92**	38^{4}	50^{2}	38^{2}	67^{6}	74^{3}	62^{5}	9^{1}	·	·	55^{5}	57^{4}	27^{4}	29^{2}	33^{2}	22^{3}	38^{2}	24^{2}	48^{5}	75^{5}
Mycena alcalina coll.	**-0.07**←1.1(-2.6)	1.2→**2.41**	**-0.20**→1.5	7^{1}	38^{2}	25^{2}	·	·	8^{1}	9^{1}	·	·	·	·	6^{2}	19^{2}	11^{1}	·	13^{2}	10^{1}	4^{1}	·
Mycena amicta	**-0.18**←1.3	**-0.42**←1.5	**-0.49**←1.4	5^{1}	25^{2}	13^{2}	22^{1}	·	·	·	·	·	18^{1}	·	6^{2}	5^{2}	·	·	13^{2}	7^{1}	·	·
Mycena cinerella	0.5-**1.08**-2.9	← →**2.25**	0.7-**1.10**-1.9	16^{3}	25^{1}	25^{3}	11^{9}	32^{3}	15^{3}	9^{1}	6^{1}	·	9^{4}	10^{1}	15^{3}	19^{3}	33^{4}	11^{1}	29^{4}	10^{2}	12^{2}	13^{4}
Mycena cineroides	←**0.91**-3.2	←**0.86**→	←**1.76**→	52^{4}	63^{4}	100^{4}	78^{6}	74^{4}	62^{2}	27^{1}	25^{1}	·	73^{4}	52^{4}	39^{4}	52^{3}	67^{6}	22^{2}	63^{4}	59^{3}	44^{4}	50^{4}
Mycena epipterygia	←**0.43**-2.1(-2.6)	**-0.36**← →	←**0.25**→	14^{1}	50^{1}	63^{1}	·	16^{2}	·	9^{2}	·	·	18^{3}	14^{1}	6^{2}	19^{2}	22^{1}	11^{3}	13^{1}	17^{2}	8^{1}	25^{1}
Mycena filopes	←**0.11**-1.9	**-0.50**←1.4	**-0.18**←1.5	9^{1}	38^{2}	13^{1}	22^{1}	16^{1}	·	·	·	·	27^{1}	10^{1}	6^{3}	10^{1}	·	11^{1}	8^{3}	14^{1}	8^{1}	·
Mycena flavoalba	←**0.78**-2.6	←**1.90**→	←**2.00**→	33^{2}	75^{2}	63^{2}	78^{3}	37^{2}	38^{1}	9^{1}	·	·	36^{1}	29^{3}	24^{2}	38^{2}	56^{2}	11^{1}	25^{2}	34^{2}	44^{2}	38^{2}
Mycena galericulata	←**0.66**-2.3(-2.6)	←**1.35**→	←**0.06**→	20^{2}	50^{2}	38^{2}	33^{3}	32^{1}	8^{1}	·	·	18^{1}	27^{1}	24^{1}	15^{2}	24^{1}	11^{4}	22^{1}	38^{2}	14^{2}	8^{2}	25^{1}
Mycena galopus	←**2.10**→	←**0.72**→	←**0.22**→	71^{5}	50^{3}	75^{4}	89^{4}	100^{7}	92^{6}	82^{3}	44^{3}	18^{7}	91^{5}	76^{5}	64^{5}	71^{4}	56^{5}	89^{7}	83^{6}	62^{4}	60^{3}	75^{3}
Mycena longiseta	←**0.79**-2.7	← →**2.82**	←**0.08**-1.6	23^{2}	38^{2}	50^{3}	44^{4}	26^{2}	38^{1}	9^{2}	·	·	27^{1}	5^{1}	18^{2}	38^{3}	44^{4}	22^{1}	38^{3}	21^{2}	20^{1}	·
Mycena metata	←**0.75**-3.4	←**0.20**→	←**2.01**→	58^{4}	100^{6}	88^{6}	89^{7}	79^{3}	62^{3}	36^{2}	25^{1}	9^{1}	91^{5}	62^{4}	42^{4}	57^{4}	67^{4}	56^{1}	54^{5}	59^{4}	56^{5}	75^{5}
Mycena pura	**-0.16**←1.7	←**1.61**→	(**0.14**-)0.7-1.4	7^{1}	38^{2}	25^{1}	22^{1}	·	·	·	·	·	9^{1}	5^{1}	6^{2}	5^{1}	22^{2}	·	8^{2}	17^{1}	·	·
Mycena rorida	←**2.42**→	←**2.01**→	←**0.65**→	80^{7}	50^{4}	100^{6}	78^{4}	84^{9}	100^{9}	91^{9}	88^{4}	36^{2}	73^{4}	76^{6}	76^{7}	90^{8}	89^{8}	78^{8}	83^{9}	79^{6}	92^{6}	38^{3}
Mycena rosella	←**0.81**-2.6	**-0.25**→1.5	0.8-**2.04**→	14^{1}	13^{1}	38^{2}	22^{2}	21^{1}	15^{1}	9^{1}	·	·	27^{2}	14^{1}	6^{1}	24^{1}	·	·	13^{2}	10^{1}	16^{1}	38^{1}
Mycena rubromarginata	0.6-**1.82**-3.4	←**1.15**-1.6	←**2.49**→	26^{1}	13^{1}	50^{1}	33^{1}	37^{1}	38^{2}	18^{2}	13^{1}	9^{1}	36^{1}	38^{1}	24^{2}	19^{1}	11^{3}	11^{2}	21^{1}	21^{2}	28^{2}	75^{1}
Mycena sanguinolenta	0.5-**1.22**-2.4(-3.4)	←→**2.28**	(0.0-)0.8→**2.39**	24^{2}	25^{3}	38^{2}	33^{1}	32^{3}	54^{2}	·	6^{1}	9^{1}	18^{2}	29^{1}	24^{2}	14^{2}	44^{4}	33^{2}	29^{2}	24^{2}	16^{2}	25^{1}
Mycena septentrionalis	←**1.56**-3.6(→?)	←**0.57**→	← →**2.70**	62^{5}	63^{3}	88^{5}	78^{9}	79^{5}	69^{4}	64^{4}	50^{3}	9^{1}	64^{6}	76^{4}	48^{5}	71^{4}	56^{5}	33^{3}	42^{4}	55^{4}	92^{5}	88^{7}
Mycena stylobates	0.6-**0.98**-2.3	0.6-**1.34**-1.8	0.7-**2.09**→	8^{1}	13^{1}	13^{1}	22^{2}	16^{1}	8^{1}	·	·	·	9^{2}	14^{1}	3^{1}	10^{1}	11^{1}	·	17^{1}	·	12^{1}	13^{1}
Mycena viridimarginata	(0.2-**1.06**-)1.9-2.3	**-0.62**←1.4	**-0.54**←0.8(-1.4)	5^{1}	13^{1}	·	·	16^{1}	8^{1}	·	·	·	18^{1}	5^{1}	3^{1}	5^{1}	·	22^{1}	8^{1}	3^{1}	·	·
Mycena vulgaris	**-0.18**→2.0	←**1.51**→	0.7-**1.06**→	17^{2}	63^{3}	50^{1}	56^{1}	11^{1}	·	·	·	·	27^{1}	10^{2}	12^{2}	24^{2}	22^{2}	·	17^{2}	17^{2}	16^{1}	38^{1}
Strobilurus esculentus	←**1.00**-2.6	←**0.02**→	←**1.26**→	49^{4}	75^{2}	88^{4}	89^{6}	84^{4}	69^{3}	9^{1}	·	·	82^{5}	62^{4}	33^{4}	38^{4}	67^{2}	67^{3}	54^{4}	38^{4}	48^{4}	63^{4}
Typhula erythropus	**-0.63**→1.3	**-1.09**←1.8	0.9→**2.63**	12^{7}	50^{10}	75^{4}	11^{11}	·	·	·	·	·	27^{14}	5^{3}	3^{2}	24^{5}	11^{2}	·	13^{2}	14^{12}	8^{3}	25^{9}
Typhula phaecorrhiza	**-0.59**←1.1	(0.2-)0.9-**1.82**→	0.9→**2.36**	9^{3}	50^{4}	63^{2}	·	·	·	·	·	·	9^{1}	5^{2}	3^{1}	24^{3}	11^{7}	·	13^{2}	10^{3}	4^{6}	25^{2}
Typhula setipes	←**0.14**-2.3	(0.1-)0.8→**2.95**	0.5-**0.75**→	25^{10}	100^{11}	88^{11}	22^{14}	32^{9}	8^{1}	·	·	·	9^{1}	10^{2}	15^{9}	43^{12}	78^{13}	11^{1}	46^{10}	28^{12}	12^{12}	13^{3}

concentrations to plots with high DCA 2 scores and *Lactarius theiogalus* (Fig. 71) and to a lesser degree *Cortinarius albovariegatus* (Fig. 33) to low-score plots. Most typical pine-forest species were absent from plots with high DCA 2 scores. Species with decreasing abundance along the third axis were, among others, *Cortinarius flexipes* (Fig. 46), *Hygrophorus olivaceoalbus* (Fig. 62), and *Russula betularum* (Fig. 86), while the abundances of *Russula rhodophoda* (Fig. 96) and *Russula vinosa* (Fig. 98) increased along this axis.

Saprotrophs

Several saprotrophic species were very common, spanning most of the first DCA axis (see Tab. 16): *Galerina atkinsoniana* (Figs 119, 120), *G. hypnorum* (Figs 121, 122), *Marasmius androsaceus* (Figs 135, 136), *Mycena galopus* (Figs 157, 158), *M. rorida* (Figs 165, 166), and *M. septentrionalis* (Figs 173, 174). *Marasmius androsaceus* had its optimum displaced towards the pine-forest end of DCA 1 because of high occurrence in *Calluna*-dominated vegetation. The other species had quantitative optima near the middle of the axis. Other species with wide amplitude but somewhat lower frequencies include *Cystoderma jasonis* and *Mycena sanguinolenta*.

Species restricted to special substrates had wide amplitudes with respect to DCA 1 [e.g. *Calocera viscosa* (Figs 103, 104) and *Mycena rubromarginata* (Figs 169, 170) which were found on small pieces of wood, and *Collybia tuberosa* (Figs 111, 112) which grew on dead agaric fruitbodies] if their preferred substrate was present in all forest types. An alternative case is represented by *Strobilurus esculentus* (Figs 181, 182), which was restricted to spruce cones. This species was very common at low DCA 1 scores while stopped abruptly at 2.6 S.D. units along DCA 1 and was thus restricted to plots classified to series 4-6.

Very common species with wide amplitudes but with a limit towards high DCA 1 scores, were *Mycena metata* which was restricted to plots with DCA 1 < 3.4 S.D. units (Figs 161, 162), *M. cineroides* (DCA 1 < 3.2 S.D., cf. Figs 147, 148), and *M. rosella* (Figs 167, 168; DCA 1 < 2.6 S.D.). These Mycena species fruited in rainy periods late in the autumn. Similar distributions along DCA 1 but with lower frequencies were observed for *M. flavoalba* (Figs 153, 154) and *M. longiseta* (Figs 159, 160).

Several species were largely restricted to plots with low DCA 1 scores (series 5 and 6). Examples are *Mycena pura* (Figs 163, 164, DCA < 1.7 S.D. units) and *M. vulgaris* (Figs 179, 180, DCA 1 < 2.0 S.D.), the wood-inhabiting species *Galerina marginata* (Figs 123, 124, DCA 1 < 1.0 S.D.), and the litter-decomposing species *Clavariadelphus junceus* (Figs 105, 106, DCA 1 < 1.1(–1.5) S.D.) and *Marasmius epiphyllus* (Figs 137, 138, DCA 1 < 2.4 S.D. units). Few saprotrophs had narrow or intermediately narrow amplitudes along DCA 1 and optimum in site type 5.1. Exceptions were *Micromphale perforans* (Figs 139, 140, DCA 1 < 2.6 S.D.), which grew on spruce needles, and *Galerina mniophila* (Figs 125, 126, r = (0.5–)1.3–2.9).

Only a few infrequent species were restricted to plots with high DCA 1 scores. Of these, especially *Collybia putilla* and *Mycena clavicularis* seemed to have distinct optima in dry pine forests.

Two of the three *Typhula* species, *T. phacorrhiza* (Figs 185, 186) and the very common and highly abundant *T. setipes* (Figs 187, 188), had restricted distributions along DCA 1 as well as DCA 2. These species were concentrated to plots with high DCA 2 scores while DCA 1 scores were low (< 2.3 S.D. and < 1.1 S.D., respectively). A similar pattern was shared by *Clavariadelphus junceus* (Figs 105, 106) and *Marasmius epiphyllus* (Figs 137, 138), which increased markedly along DCA 2 and occurred in plots with DCA 1 scores below 1.1 (–1.5) and 2.4, respectively. Restriction to low DCA 1 and high DCA 2 scores were observed for *Galerina marginata* (Figs 123, 124), a wood-inhabitant with low frequency in our material. The third *Typhula* species, *T. erythropus* (Figs 183, 184), resembled its congeners with respect to amplitude along DCA 1, but had a different distribution along DCA-axis 2.

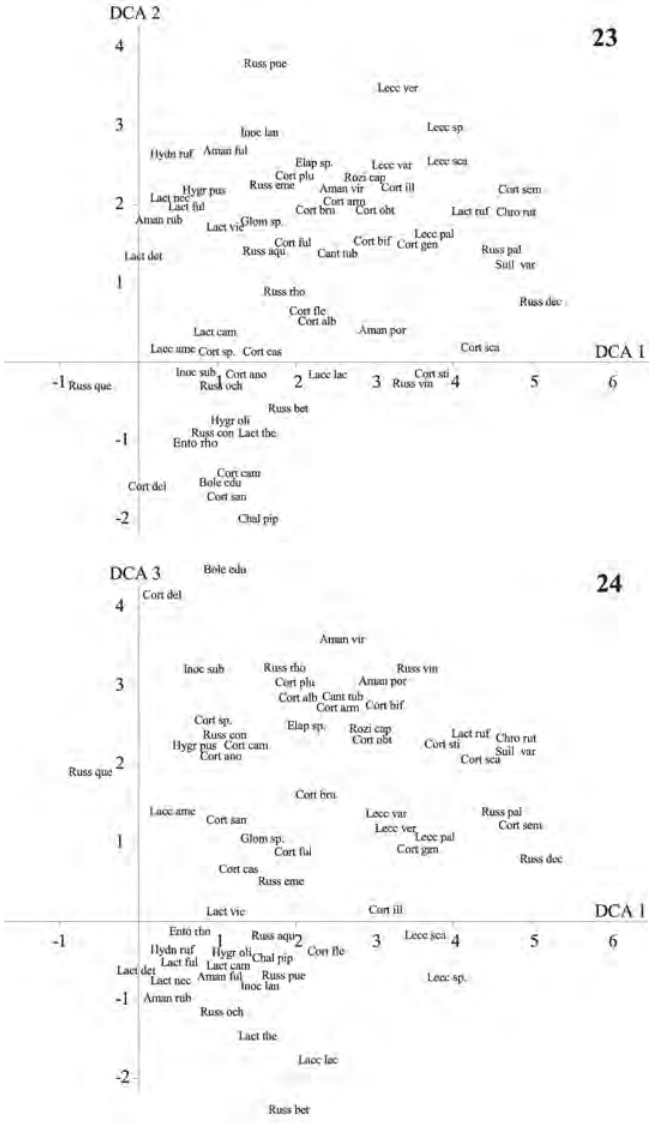

Figs 23–24. DCA ordination of the MAF 95 data set; species optima for ectomycorrhizal species along axes scaled in S.D. units. Fig. 23. Axes 1 (horizontal) and 2. Fig. 24. Axes 1 (horizontal) and 3. Species names are abbreviated in accordance with Appendix 1. Species present in only one or two macro plots are excluded.

A group of species with decreasing abundances along DCA 2 was represented by *Cystoderma jasonis* (Fig. 113), *Galerina* sp.1 (Fig. 127), *G.* sp.2 (Fig. 129), *G. mniophila* (Fig. 125), and *Mycena rubromarginata* (Fig. 169). All of these species were also scarce or lacking at very low DCA 1 scores.

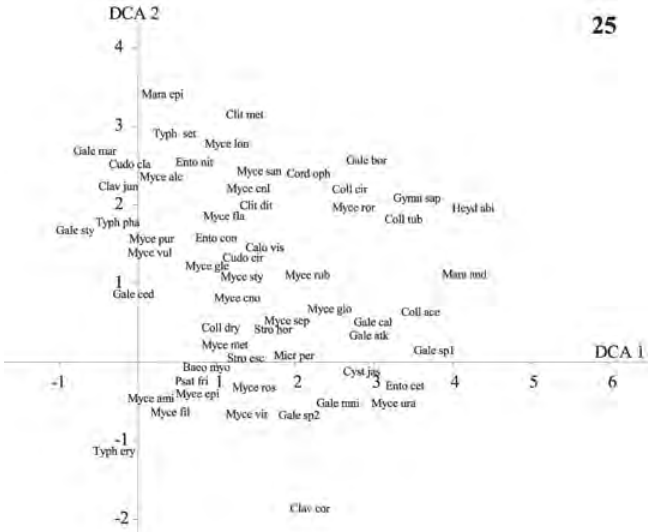

Figs 25–26. DCA ordination of the MAF 95 data set; species optima for saprotrophic species along axes scaled in S.D. units. Fig. 25. Axes 1 (horizontal) and 2. Fig. 26. Axes 1 (horizontal) and 3. Species names are abbreviated in accordance with Appendix 1. Species present in only one or two macro plots are excluded.

Examples of species that decreased along the third axis are *Entoloma cetratum* (Fig. 116), *Mycena galopus* (Fig. 158) and *G. mniophila* (Fig. 126), while *Marasmius epiphyllus* (Fig. 138), *Micromphale perforans* (Fig. 140), *Mycena septentrionalis* (Fig. 174), *Typhula erythropus* (Fig. 184), and *T. phaecorrhiza* (Fig. 186) increased along that axis.

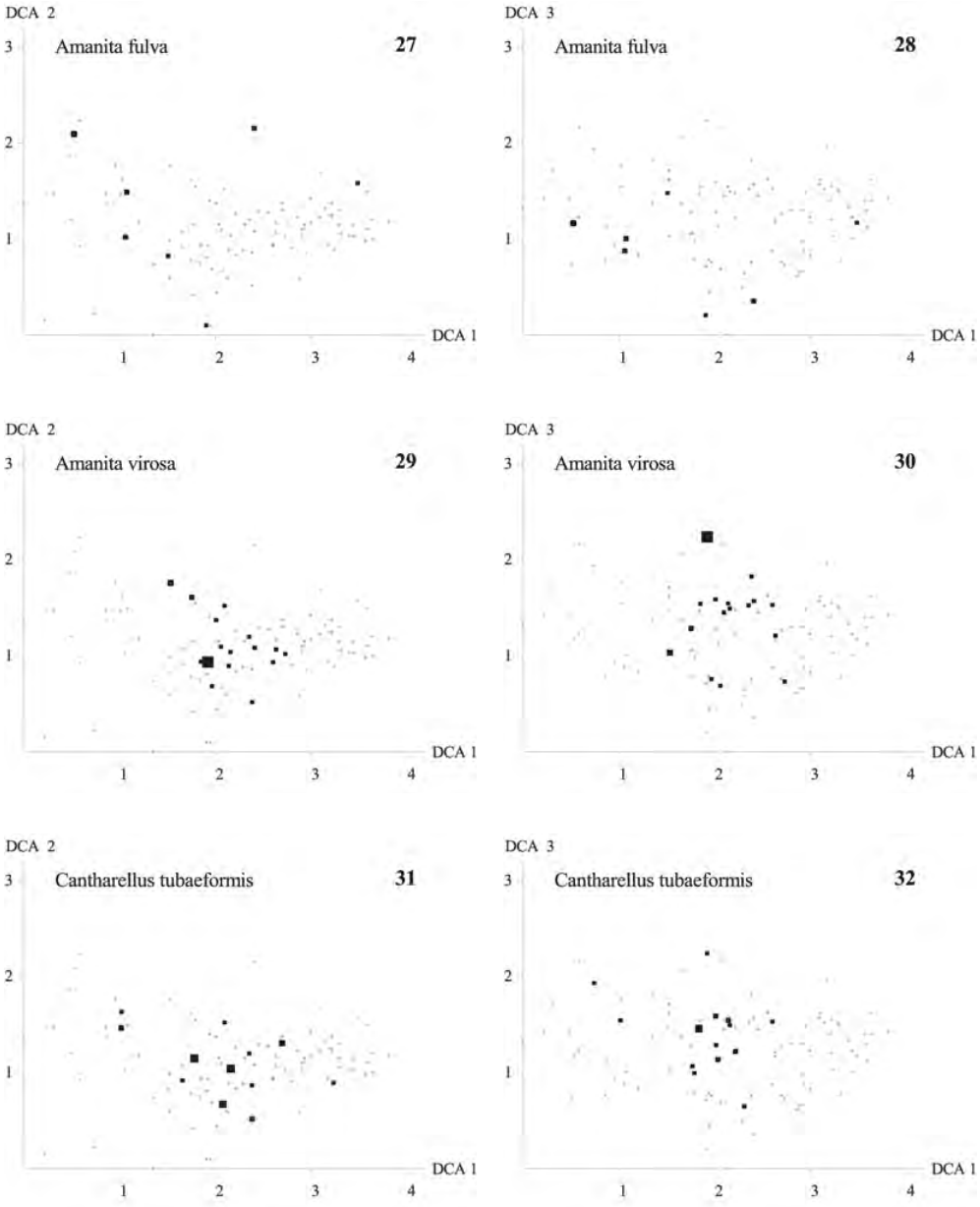

Figs 27–32. DCA ordination of the MAF 95 data set, axes 1 and 2 (left) and 1 and 3 (right). Frequency in subplots for actual species in macro plots plotted onto the macro plot positions. Scaling of axes in S.D. units. Small circle – absent. Square – present; area of square proportional to frequency in subplots. Figs 27–28. *Amanita fulva*, Figs 29–30. *Amanita virosa*, Figs 31–32. *Cantharellus tubaeformis*.

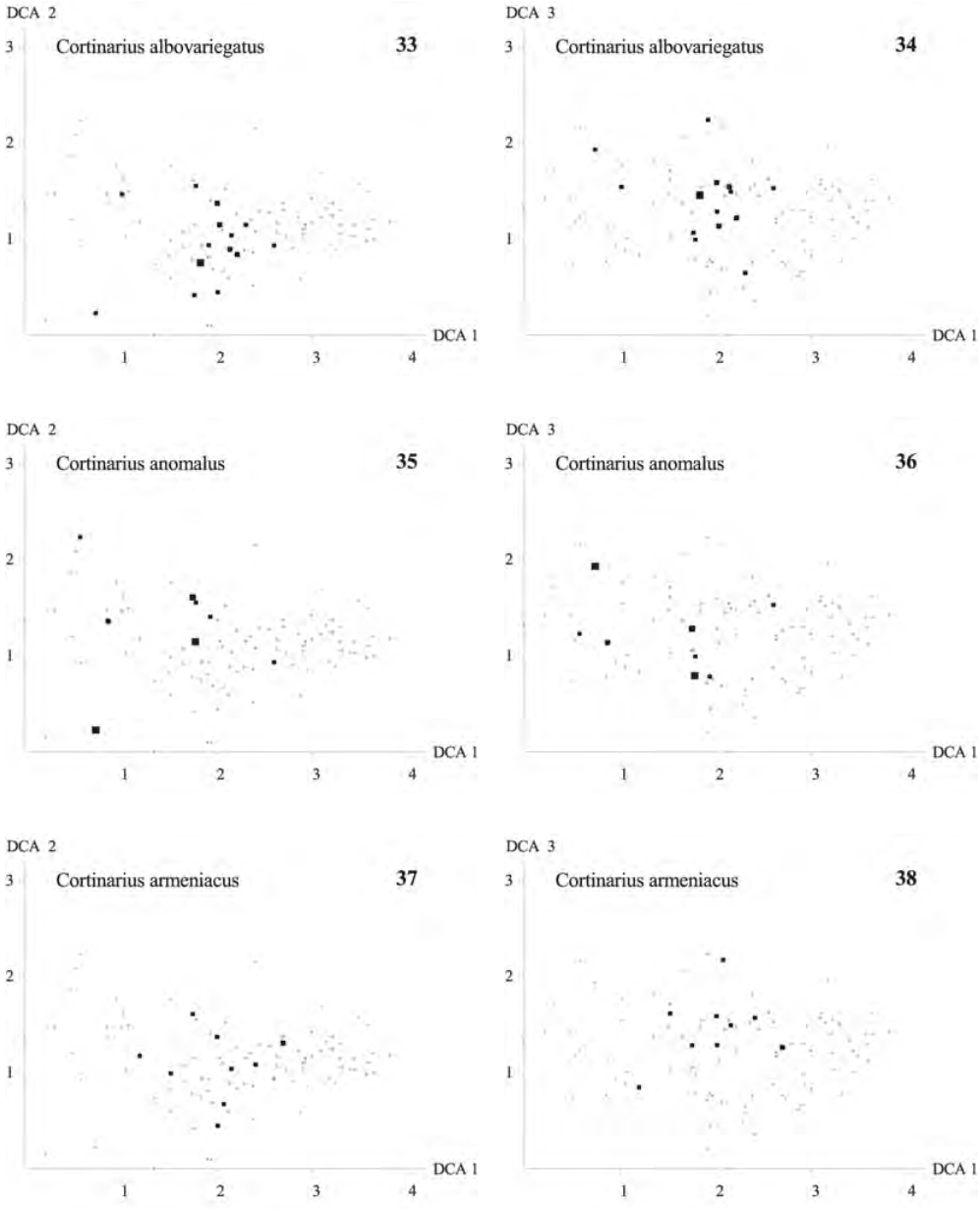

Figs 33–38. DCA ordination of the MAF 95 data set, axes 1 and 2 (left) and 1 and 3 (right). Frequency in subplots for actual species in macro plots plotted onto the macro plot positions. Scaling of axes in S.D. units. Small circle – absent. Square – present; area of square proportional to frequency in subplots. Figs 33–34. *Cortinarius albovariegatus*, Figs 35–36. *Cortinarius anomalus*, Figs 37–38. *Cortinarius armeniacus*.

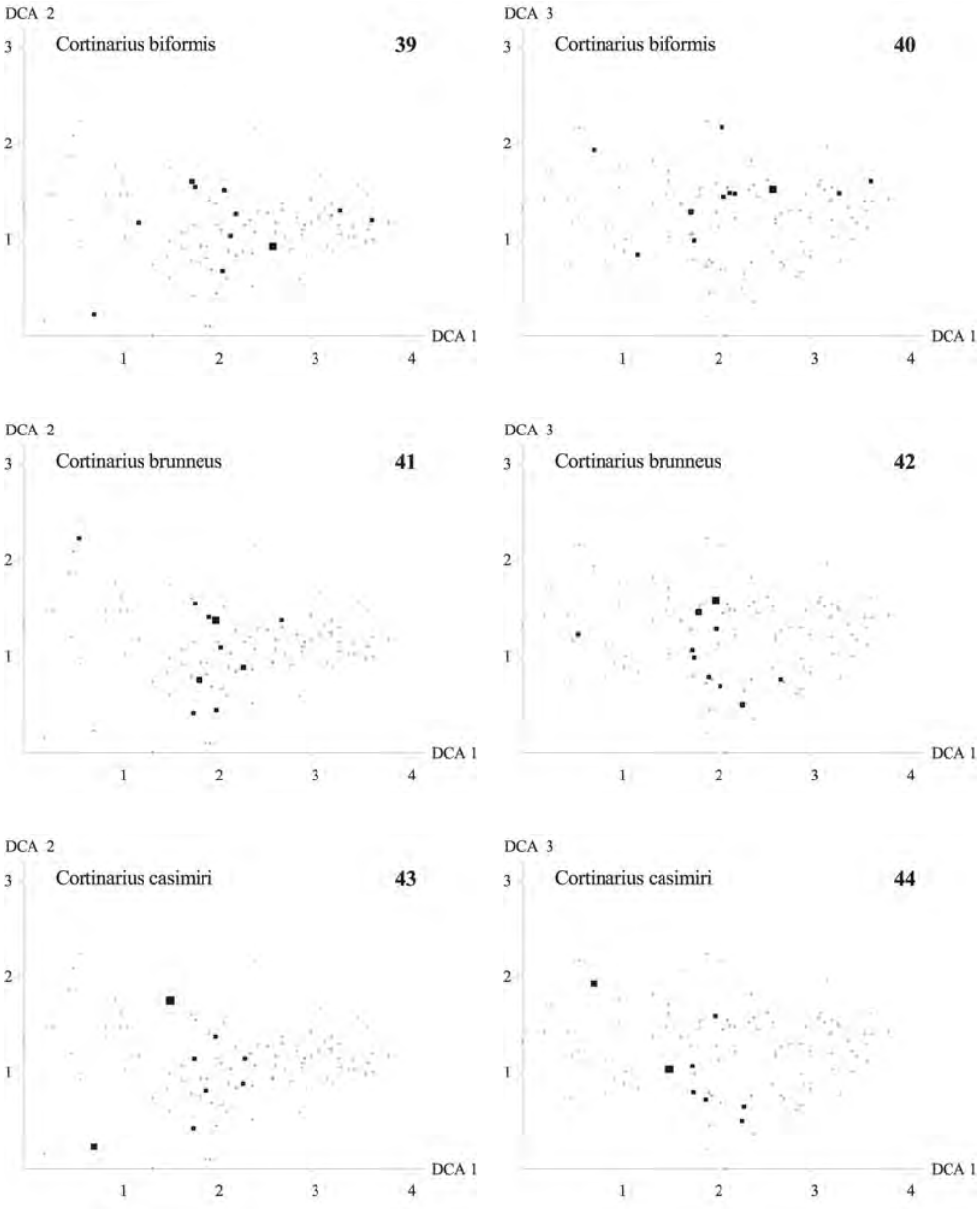

Figs 39–44. DCA ordination of the MAF 95 data set, axes 1 and 2 (left) and 1 and 3 (right). Frequency in subplots for actual species in macro plots plotted onto the macro plot positions. Scaling of axes in S.D. units. Small circle – absent. Square – present; area of square proportional to frequency in subplots. Figs 39–40. *Cortinarius biformis*, Figs 41–42. *Cortinarius brunneus*, Figs 43–44. *Cortinarius casimiri*.

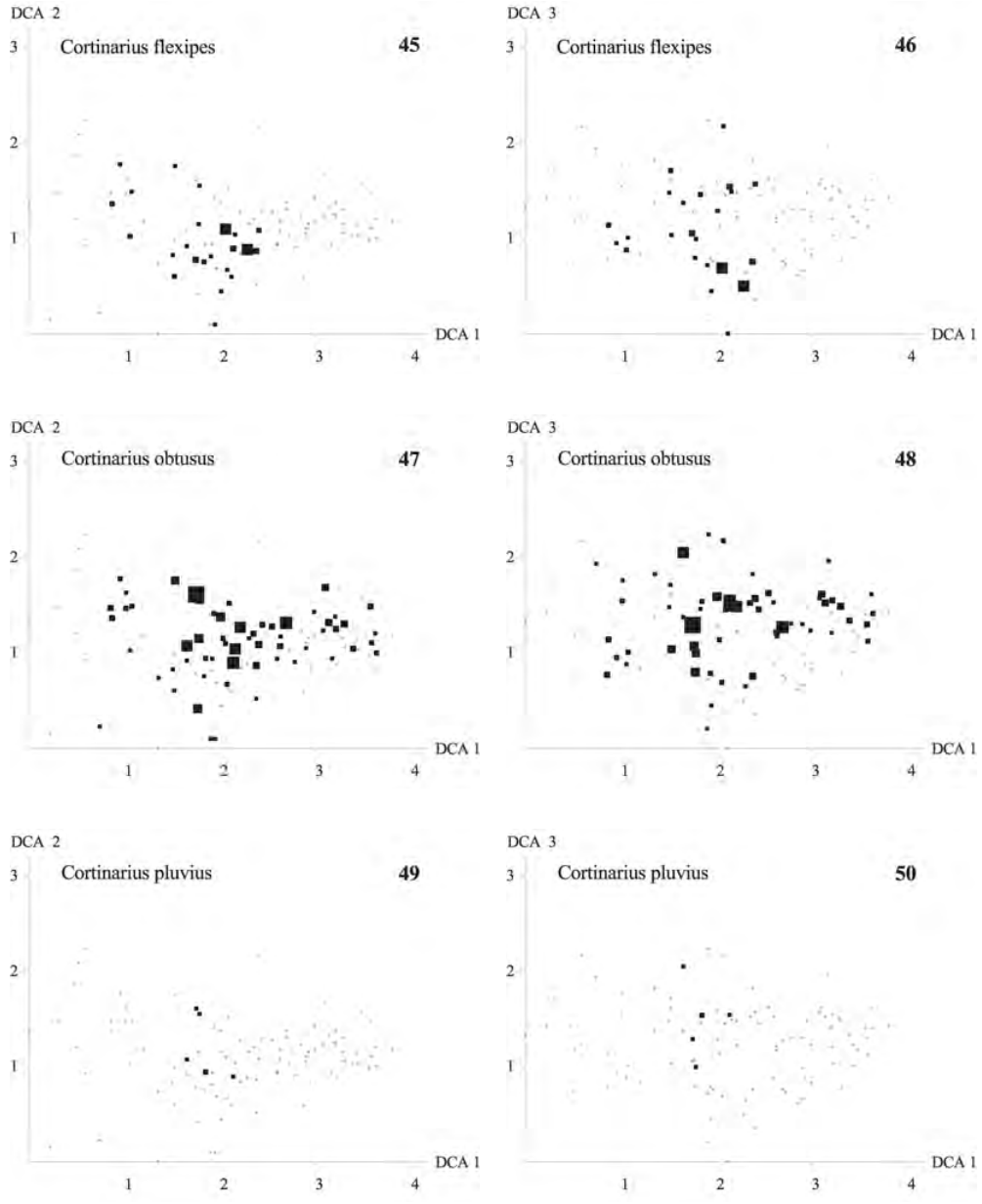

Figs 45–50. DCA ordination of the MAF 95 data set, axes 1 and 2 (left) and 1 and 3 (right). Frequency in subplots for actual species in macro plots plotted onto the macro plot positions. Scaling of axes in S.D. units. Small circle – absent. Square – present; area of square proportional to frequency in subplots. Figs 45–46. *Cortinarius flexipes*, Figs 47–48. *Cortinarius obtusus*, Figs 49–50. *Cortinarius pluvius*.

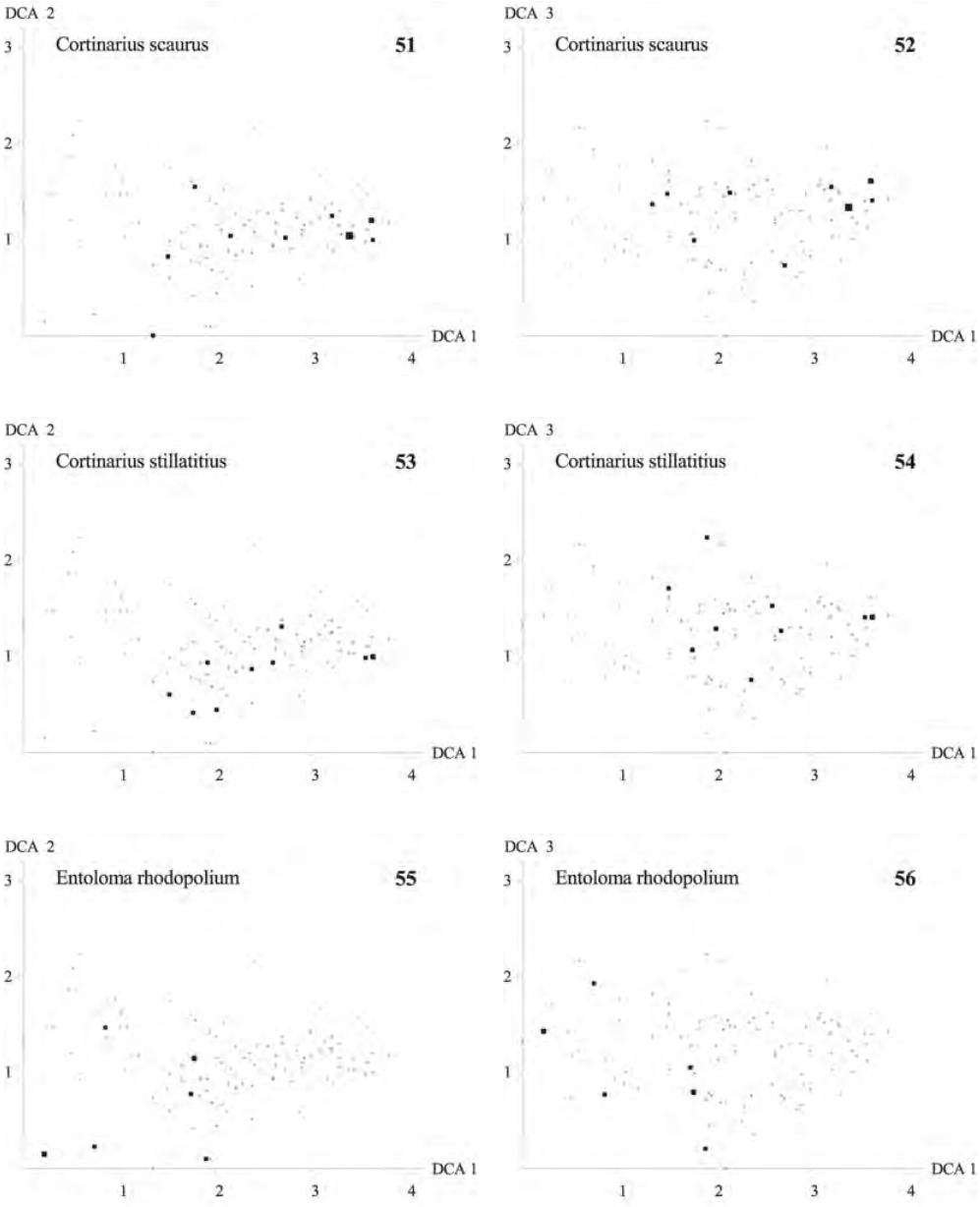

Figs 51–56. DCA ordination of the MAF 95 data set, axes 1 and 2 (left) and 1 and 3 (right). Frequency in subplots for actual species in macro plots plotted onto the macro plot positions. Scaling of axes in S.D. units. Small circle – absent. Square – present; area of square proportional to frequency in subplots. Figs 51–52. *Cortinarius scaurus*, Figs 53–54. *Cortinarius stillatitius*, Figs 55–56. *Entoloma rhodopolium*.

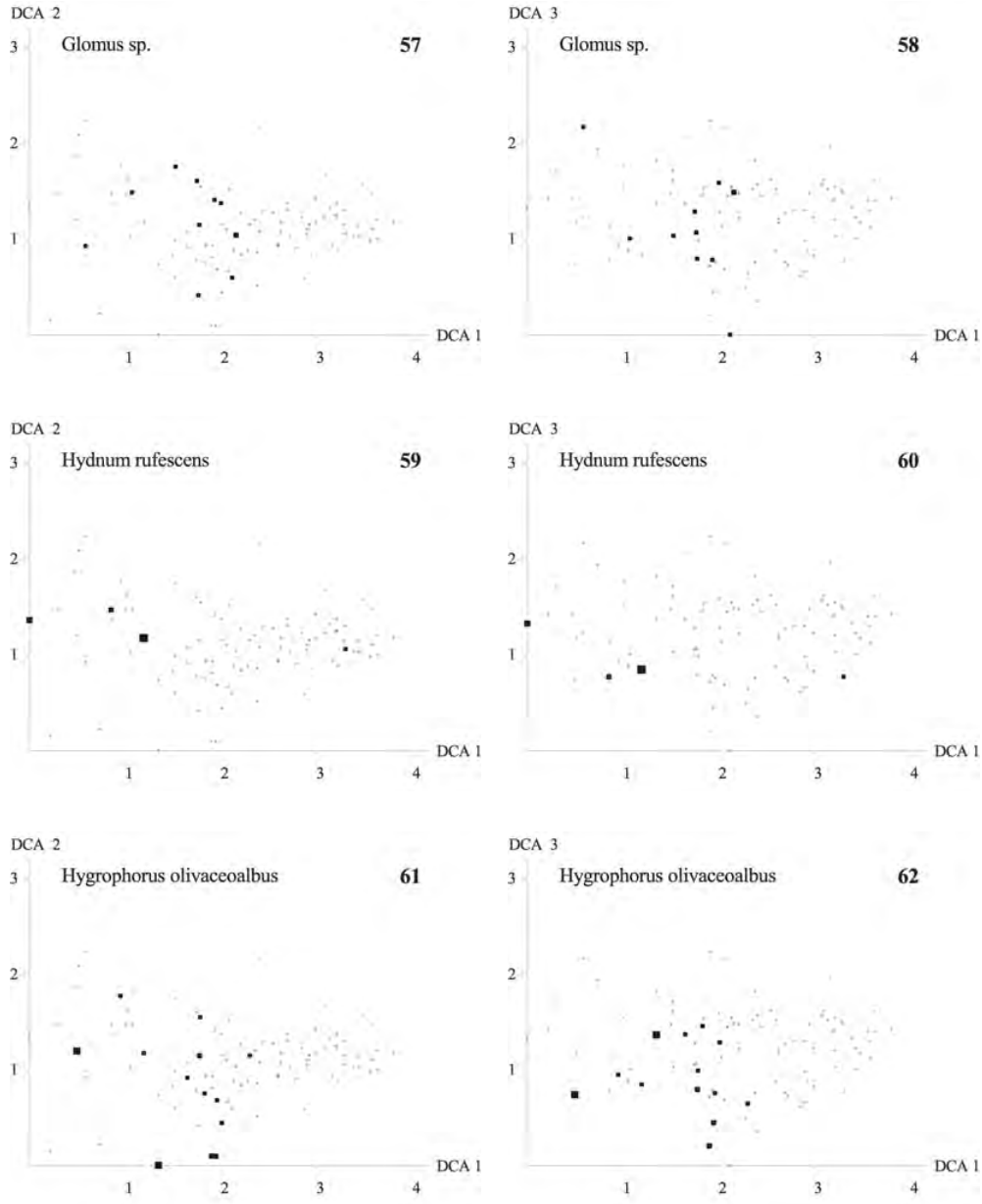

Figs 57–62. DCA ordination of the MAF 95 data set, axes 1 and 2 (left) and 1 and 3 (right). Frequency in subplots for actual species in macro plots plotted onto the macro plot positions. Scaling of axes in S.D. units. Small circle – absent. Square – present; area of square proportional to frequency in subplots. Figs 57–58. *Glomus sp.*, Figs 59–60. *Hydnum rufescens*, Figs 61–62. *Hygrophorus olivaceoalbus*.

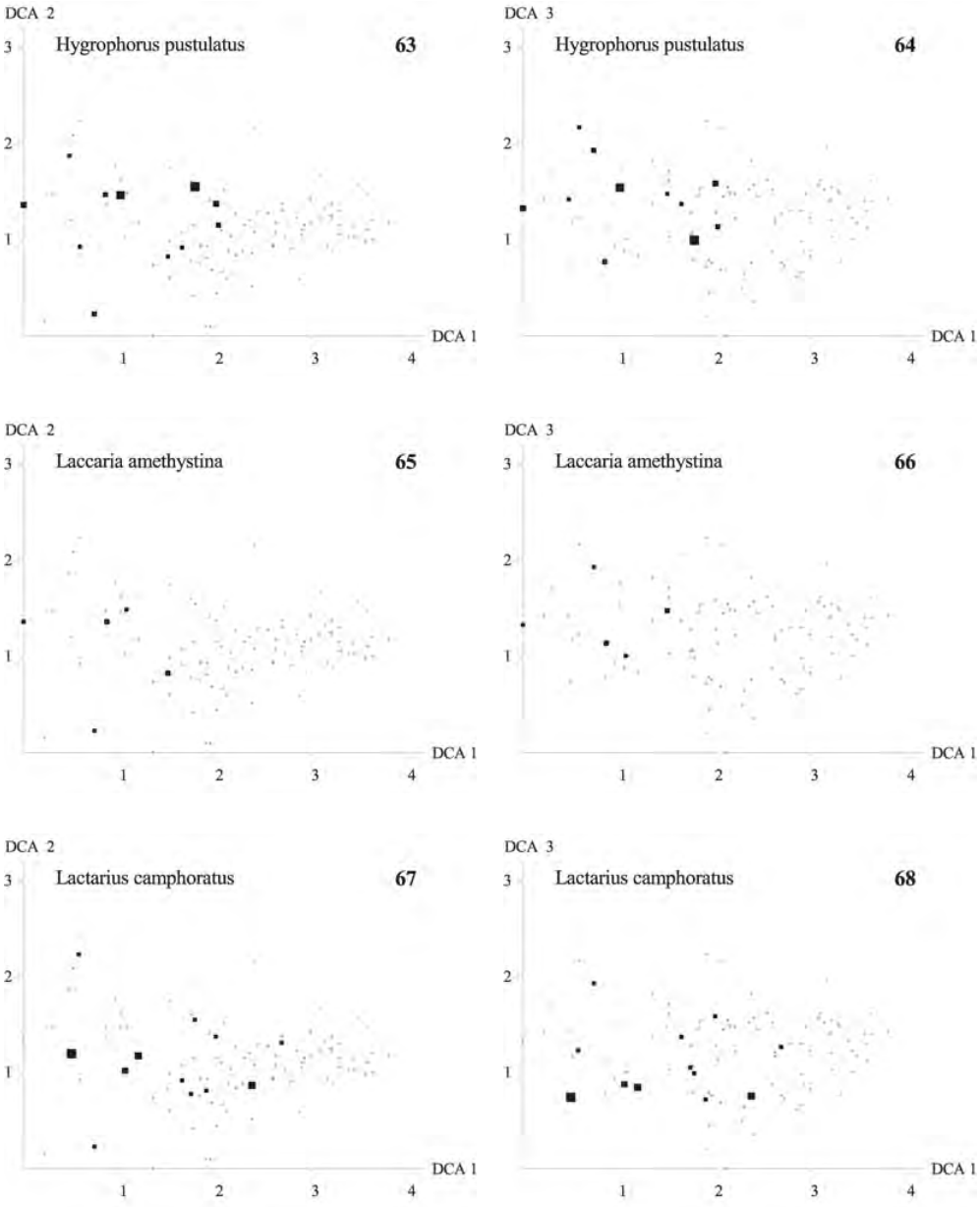

Figs 63–68. DCA ordination of the MAF 95 data set, axes 1 and 2 (left) and 1 and 3 (right). Frequency in subplots for actual species in macro plots plotted onto the macro plot positions. Scaling of axes in S.D. units. Small circle – absent. Square – present; area of square proportional to frequency in subplots. Figs 63–64. *Hygrophorus pustulatus*, Figs 65–66. *Laccaria amethystina*, Figs 67–68. *Lactarius camphoratus*.

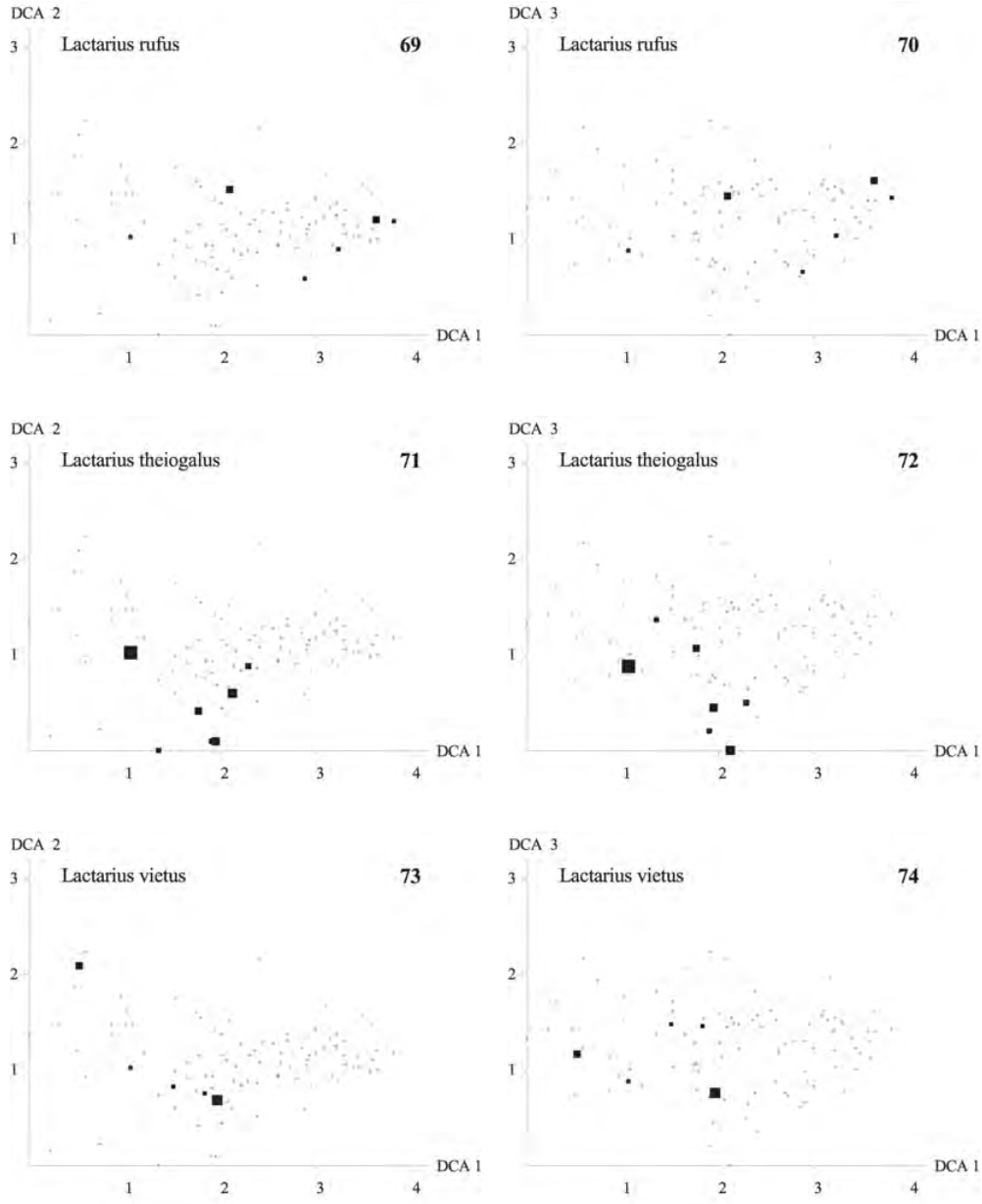

Figs 69–74. DCA ordination of the MAF 95 data set, axes 1 and 2 (left) and 1 and 3 (right). Frequency in subplots for actual species in macro plots plotted onto the macro plot positions. Scaling of axes in S.D. units. Small circle – absent. Square – present; area of square proportional to frequency in subplots. Figs 69–70. *Lactarius rufus*, Figs 71–72. *Lactarius theiogalus*, Figs 73–74. *Lactarius vietus*.

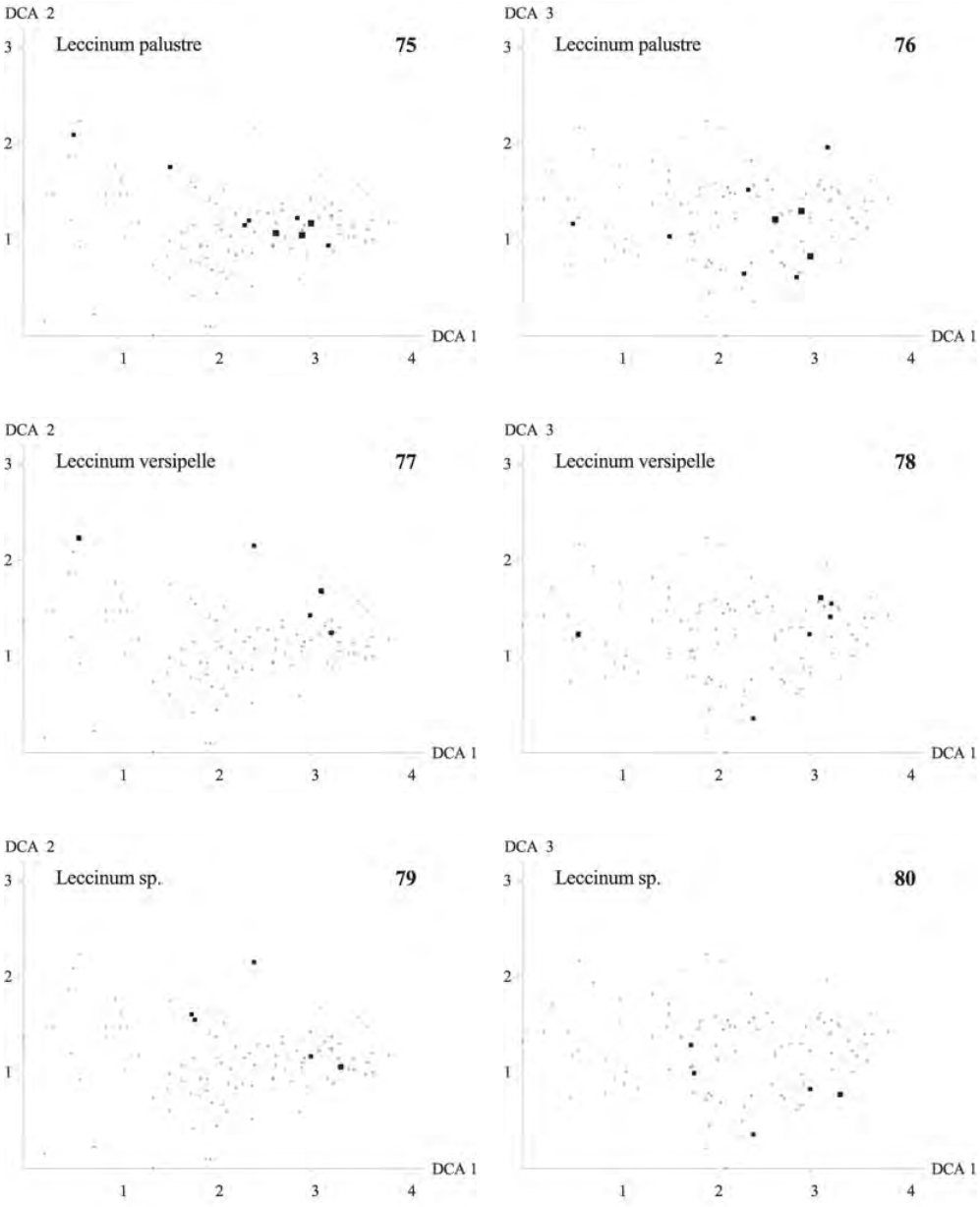

Figs 75–80. DCA ordination of the MAF 95 data set, axes 1 and 2 (left) and 1 and 3 (right). Frequency in subplots for actual species in macro plots plotted onto the macro plot positions. Scaling of axes in S.D. units. Small circle – absent. Square – present; area of square proportional to frequency in subplots. Figs 75–76. *Leccinum palustre*, Figs 77–78. *Leccinum versipelle*, Figs 79–80. *Leccinum* sp..

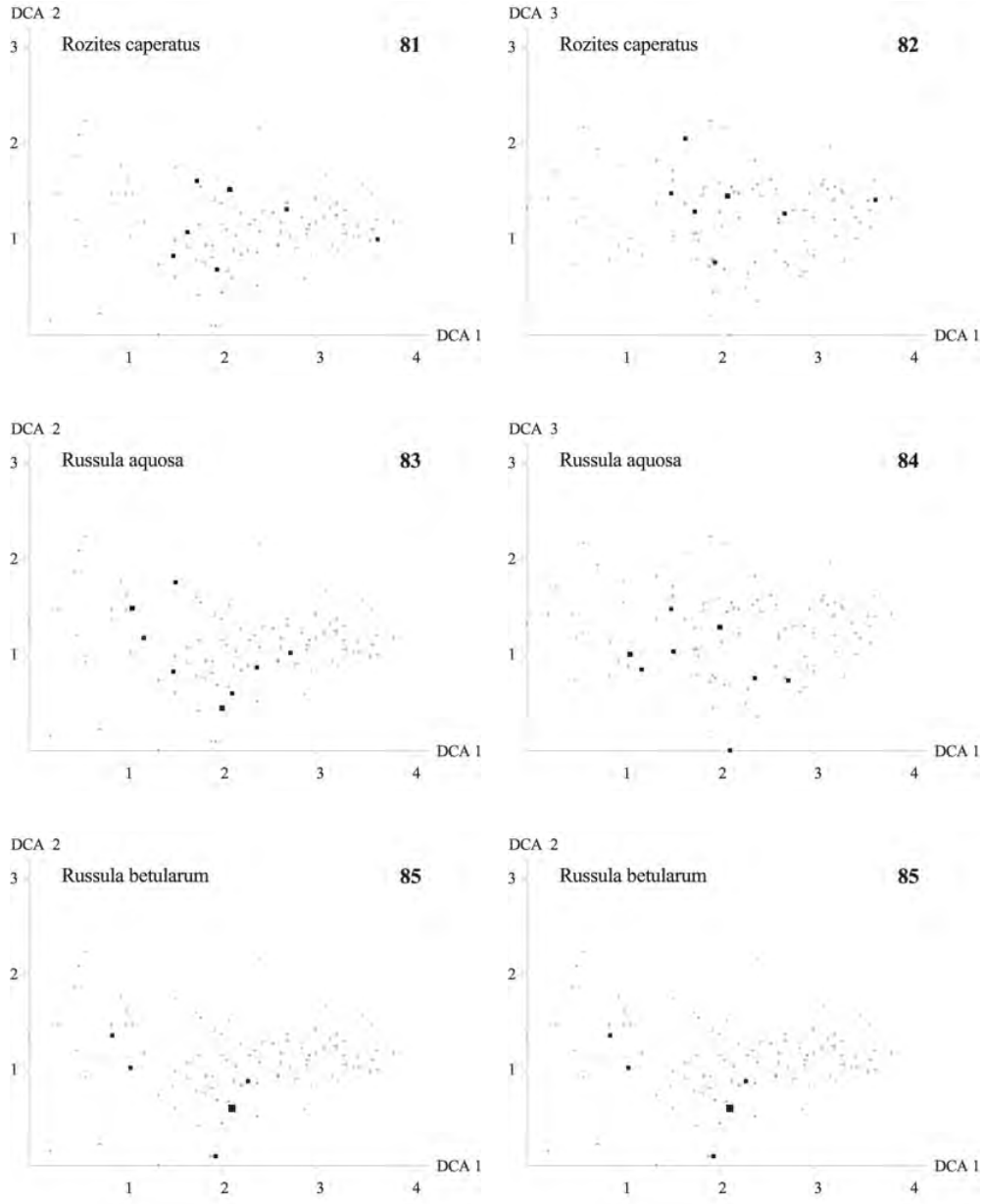

Figs 81–86. DCA ordination of the MAF 95 data set, axes 1 and 2 (left) and 1 and 3 (right). Frequency in subplots for actual species in macro plots plotted onto the macro plot positions. Scaling of axes in S.D. units. Small circle – absent. Square – present; area of square proportional to frequency in subplots. Figs 81–82. *Rozites caperatus*, Figs 83–84. *Russula aquosa*, Figs 85–86. *Russula betularum*.

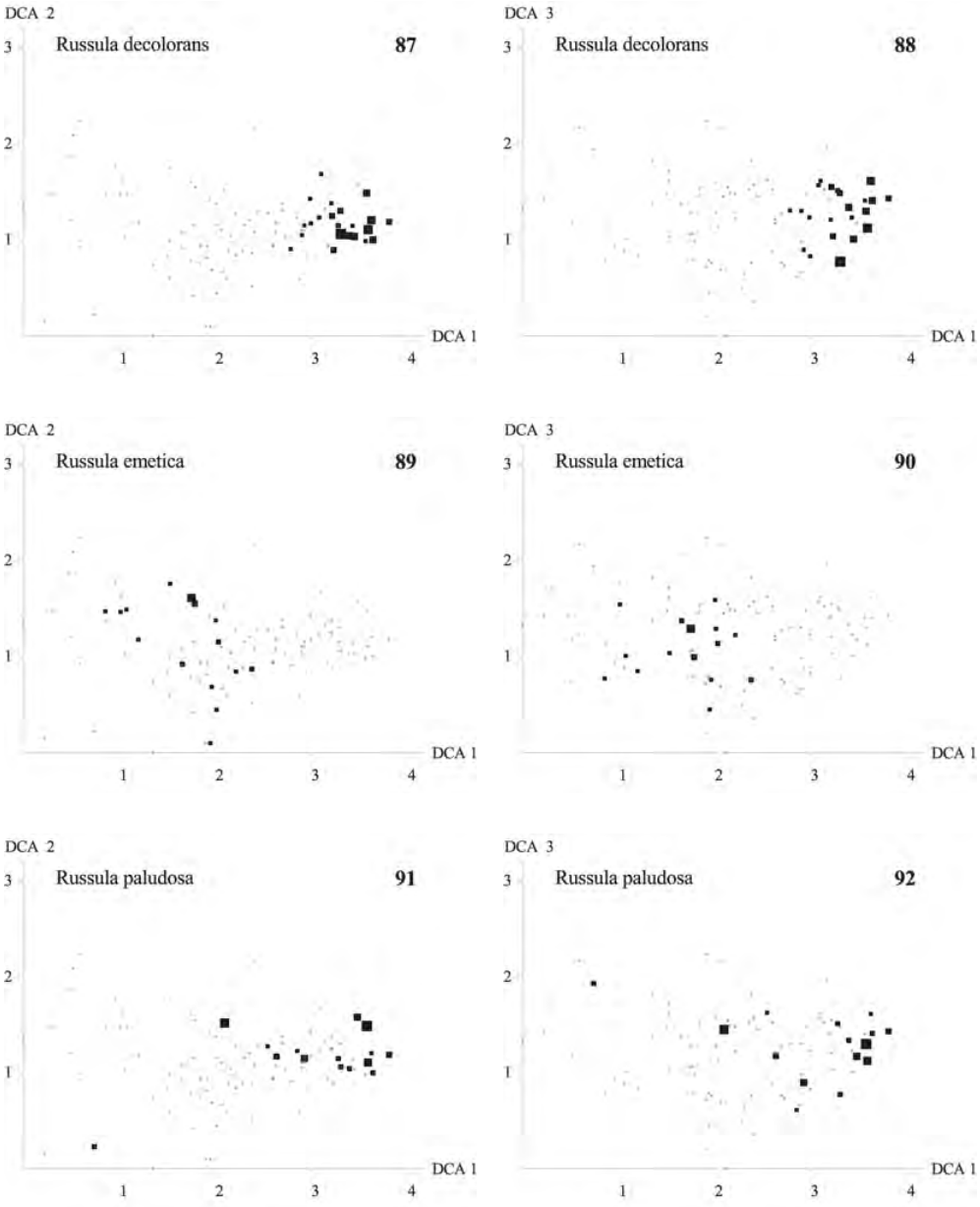

Figs 87–92. DCA ordination of the MAF 95 data set, axes 1 and 2 (left) and 1 and 3 (right). Frequency in subplots for actual species in macro plots plotted onto the macro plot positions. Scaling of axes in S.D. units. Small circle – absent. Square – present; area of square proportional to frequency in subplots. Figs 87–88. *Russula decolorans*, Figs 89–90. *Russula emetica*, Figs 91–92. *Russula paludosa*.

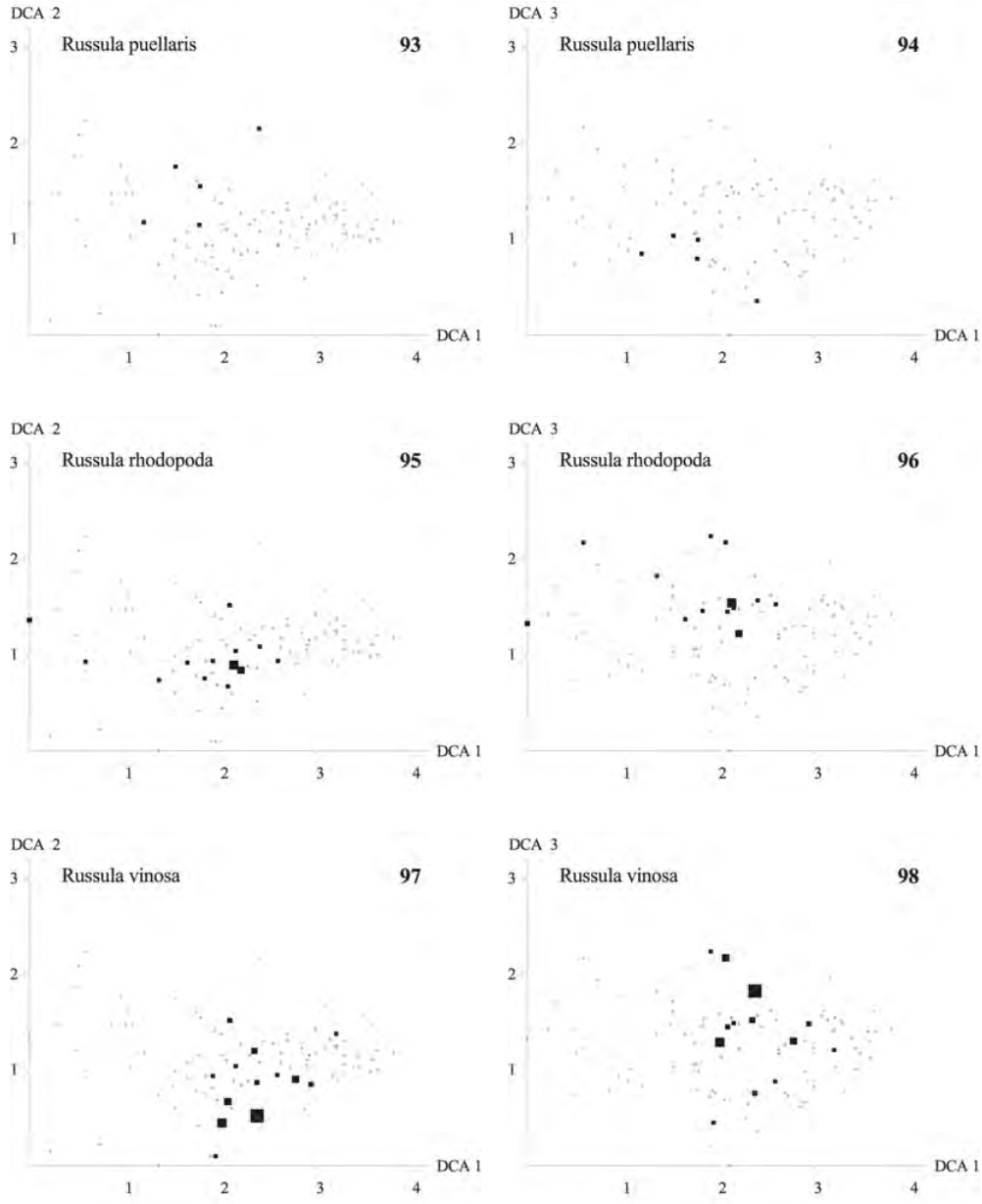

Figs 93–98. DCA ordination of the MAF 95 data set, axes 1 and 2 (left) and 1 and 3 (right). Frequency in subplots for actual species in macro plots plotted onto the macro plot positions. Scaling of axes in S.D. units. Small circle – absent. Square – present; area of square proportional to frequency in subplots. Figs 93–94. *Russula puellaris*, Figs 95–96. *Russula rhodopoda*, Figs 97–98. *Russula vinosa*.

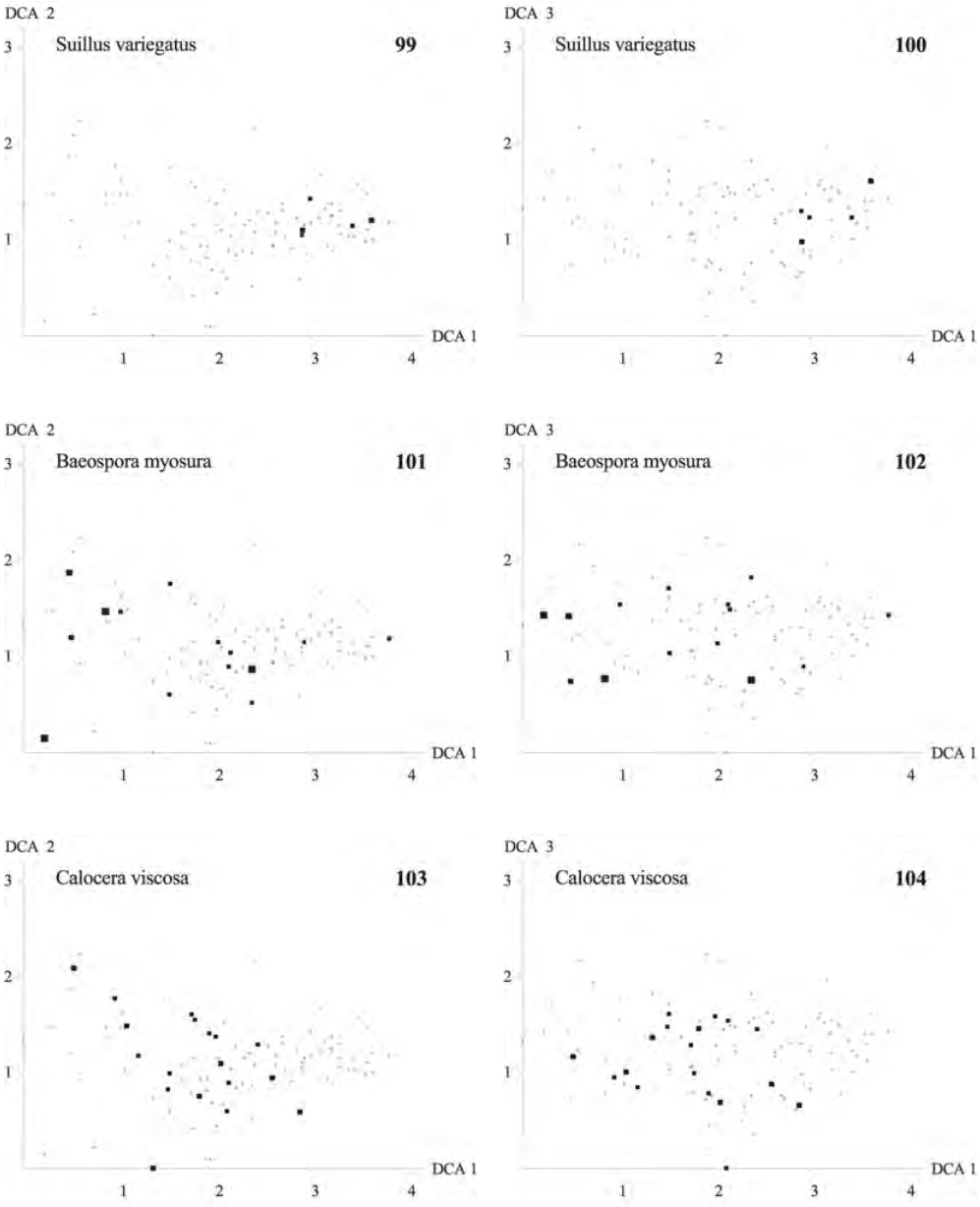

Figs 99–104. DCA ordination of the MAF 95 data set, axes 1 and 2 (left) and 1 and 3 (right). Frequency in subplots for actual species in macro plots plotted onto the macro plot positions. Scaling of axes in S.D. units. Small circle – absent. Square – present; area of square proportional to frequency in subplots. Figs 99–100. *Suillus variegatus*, Figs 101–102. *Baeospora myosura*, Figs 103–104. *Calocera viscosa*.

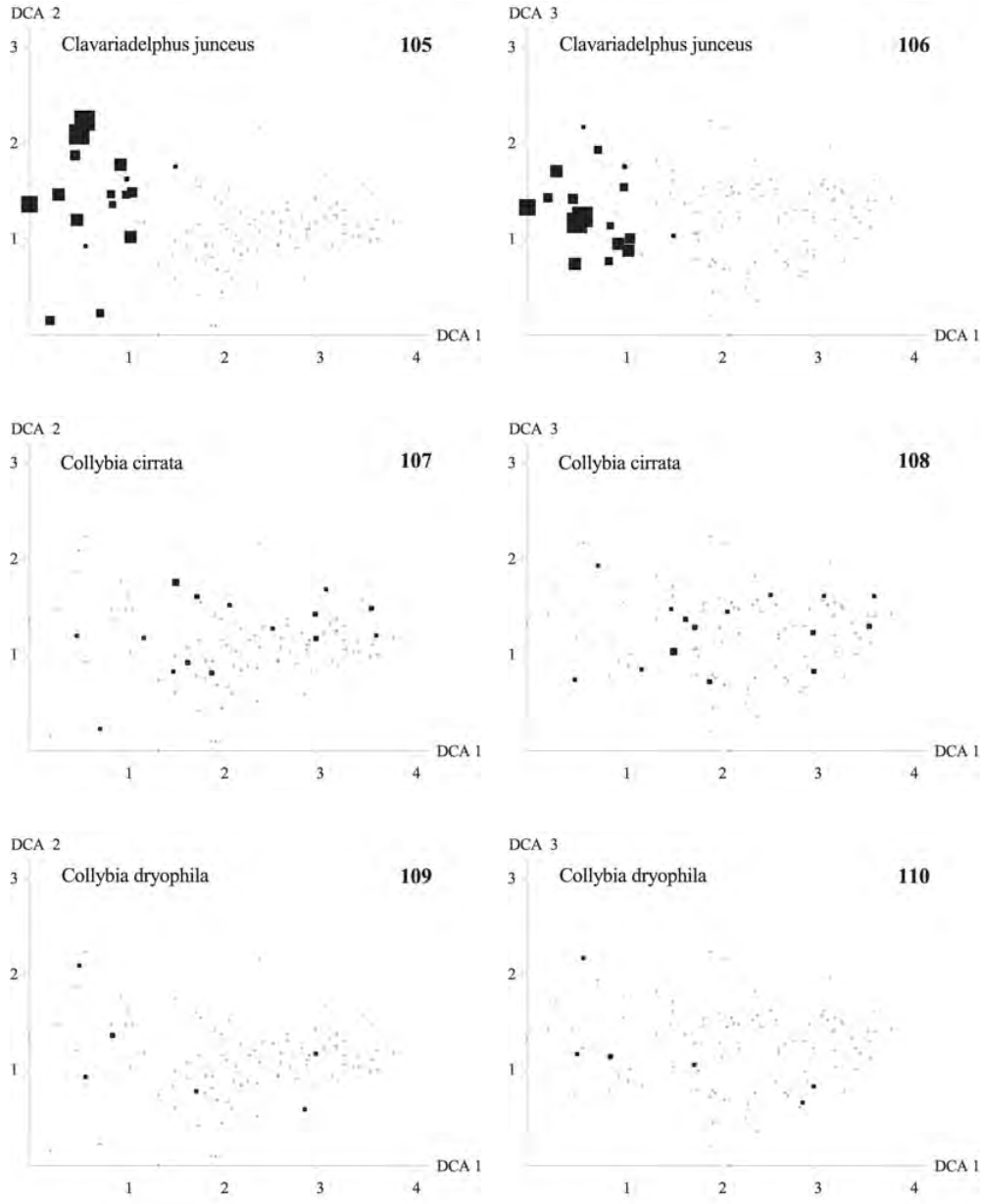

Figs 105–110. DCA ordination of the MAF 95 data set, axes 1 and 2 (left) and 1 and 3 (right). Frequency in subplots for actual species in macro plots plotted onto the macro plot positions. Scaling of axes in S.D. units. Small circle – absent. Square – present; area of square proportional to frequency in subplots. Figs 105–106. *Clavariadelphus junceus*, Figs 107–108. *Collybia cirrata*, Figs 109–110. *Collybia dryophila*.

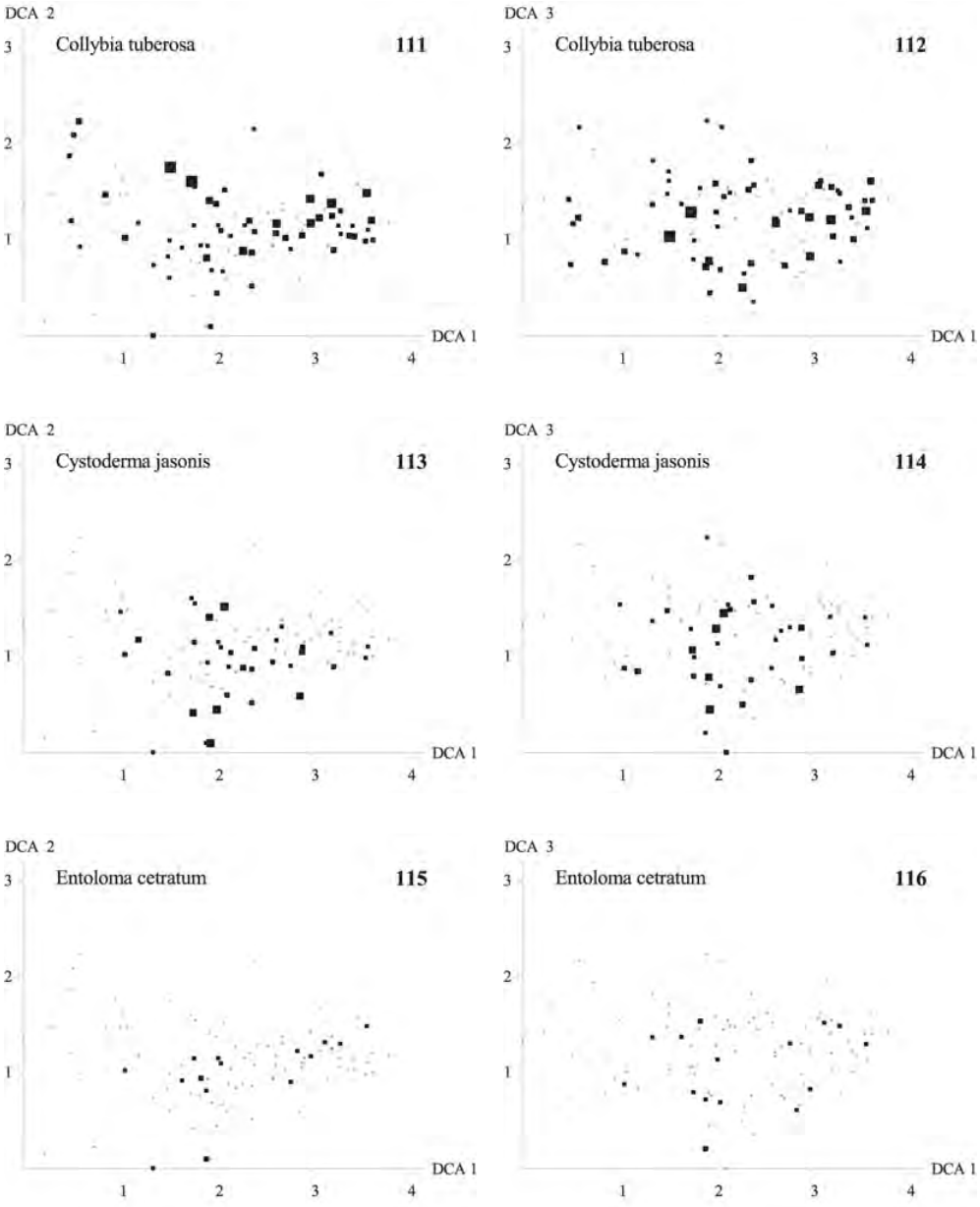

Figs 111–116. DCA ordination of the MAF 95 data set, axes 1 and 2 (left) and 1 and 3 (right). Frequency in subplots for actual species in macro plots plotted onto the macro plot positions. Scaling of axes in S.D. units. Small circle – absent. Square – present; area of square proportional to frequency in subplots. Figs 111–112. *Collybia tuberosa*, Figs 113–114. *Cystoderma jasonis*, Figs 115–116. *Entoloma cetratum*.

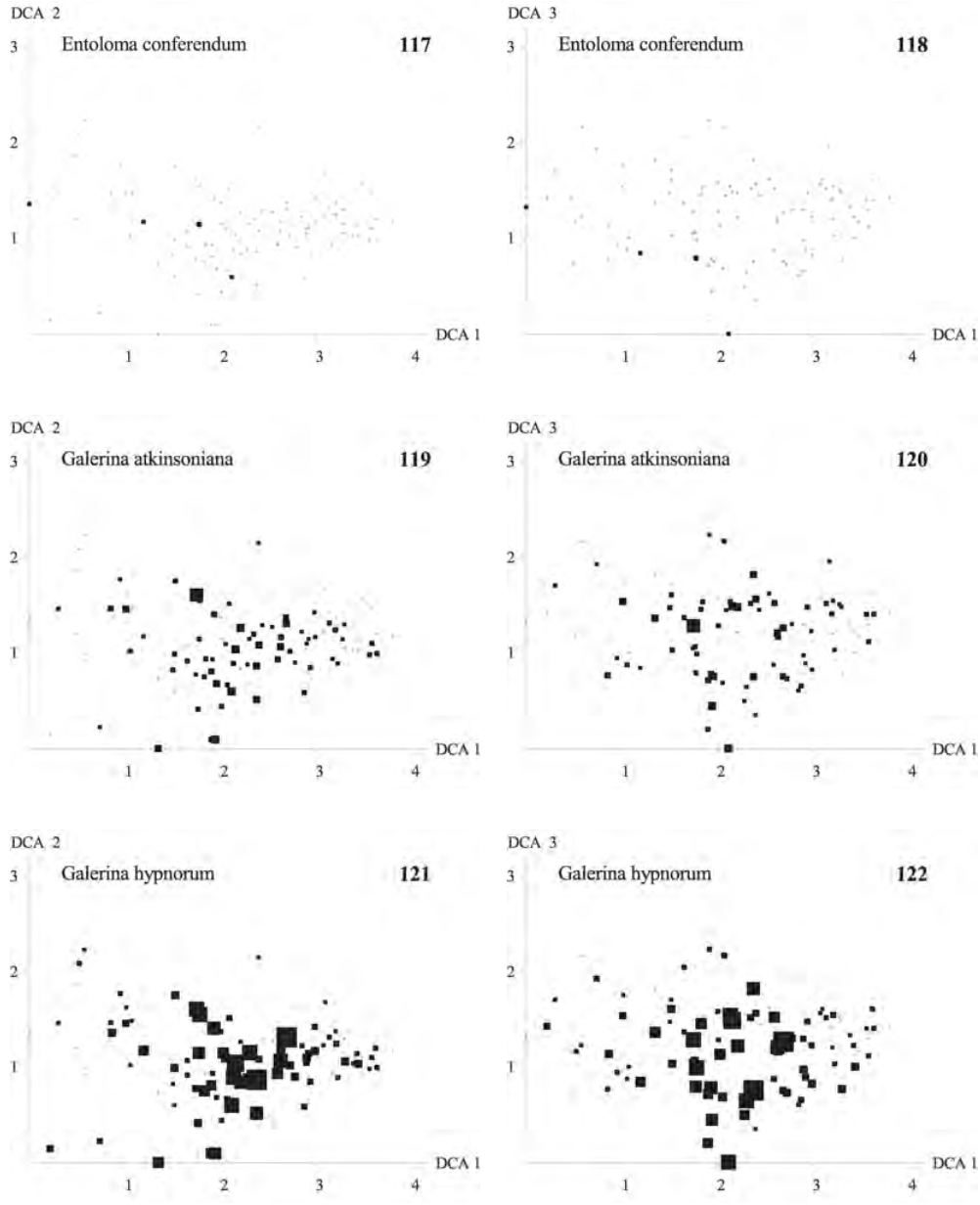

Figs 117–122. DCA ordination of the MAF 95 data set, axes 1 and 2 (left) and 1 and 3 (right). Frequency in subplots for actual species in macro plots plotted onto the macro plot positions. Scaling of axes in S.D. units. Small circle – absent. Square – present; area of square proportional to frequency in subplots. Figs 117–118. *Entoloma conferendum*, Figs 119–120. *Galerina atkinsoniana*, Figs 121–122. *Galerina hypnorum*.

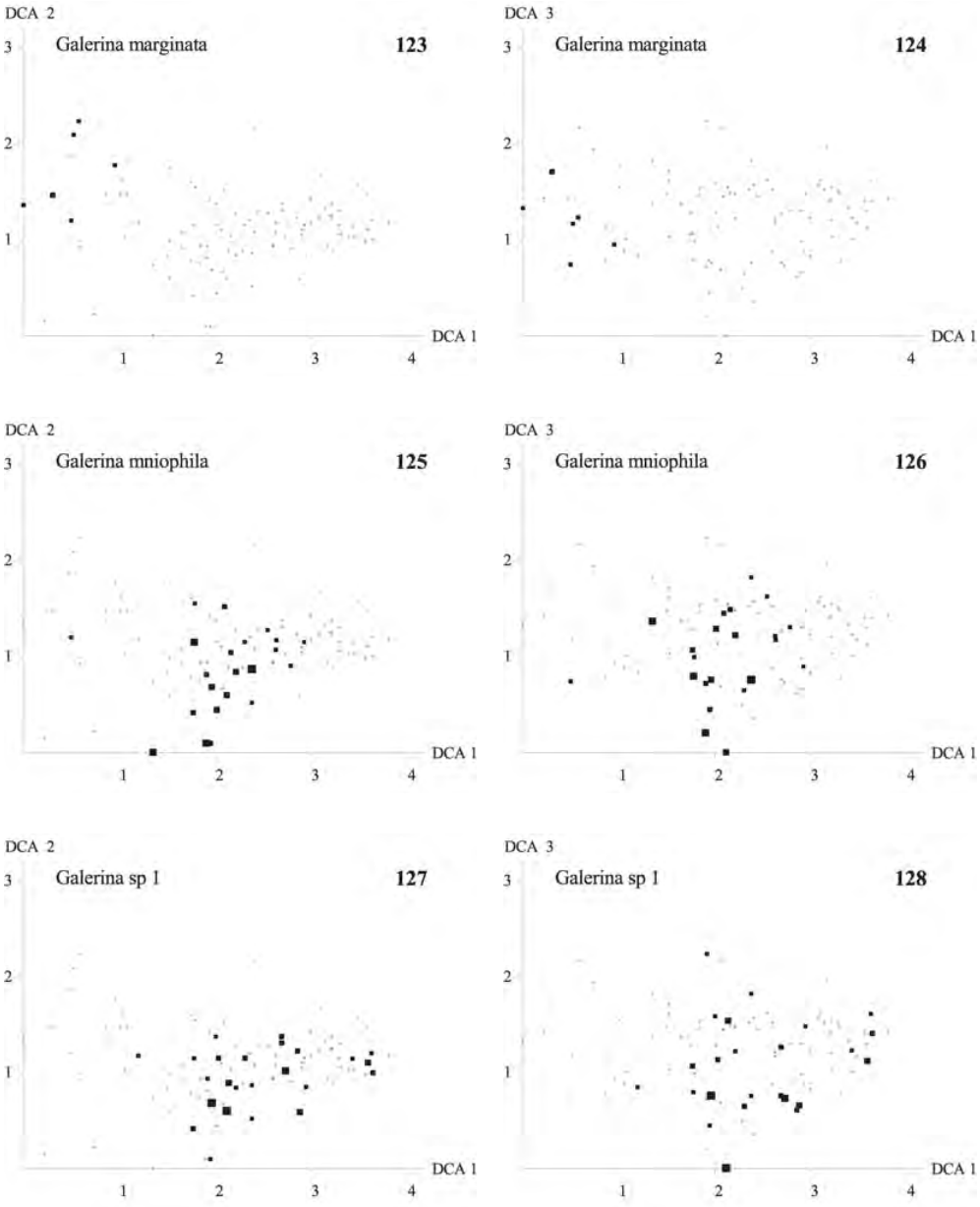

Figs 123–128. DCA ordination of the MAF 95 data set, axes 1 and 2 (left) and 1 and 3 (right). Frequency in subplots for actual species in macro plots plotted onto the macro plot positions. Scaling of axes in S.D. units. Small circle – absent. Square – present; area of square proportional to frequency in subplots. Figs 123–124. *Galerina marginata*, Figs 125–126. *Galerina mniophila*, Figs 127–128. *Galerina* sp 1.

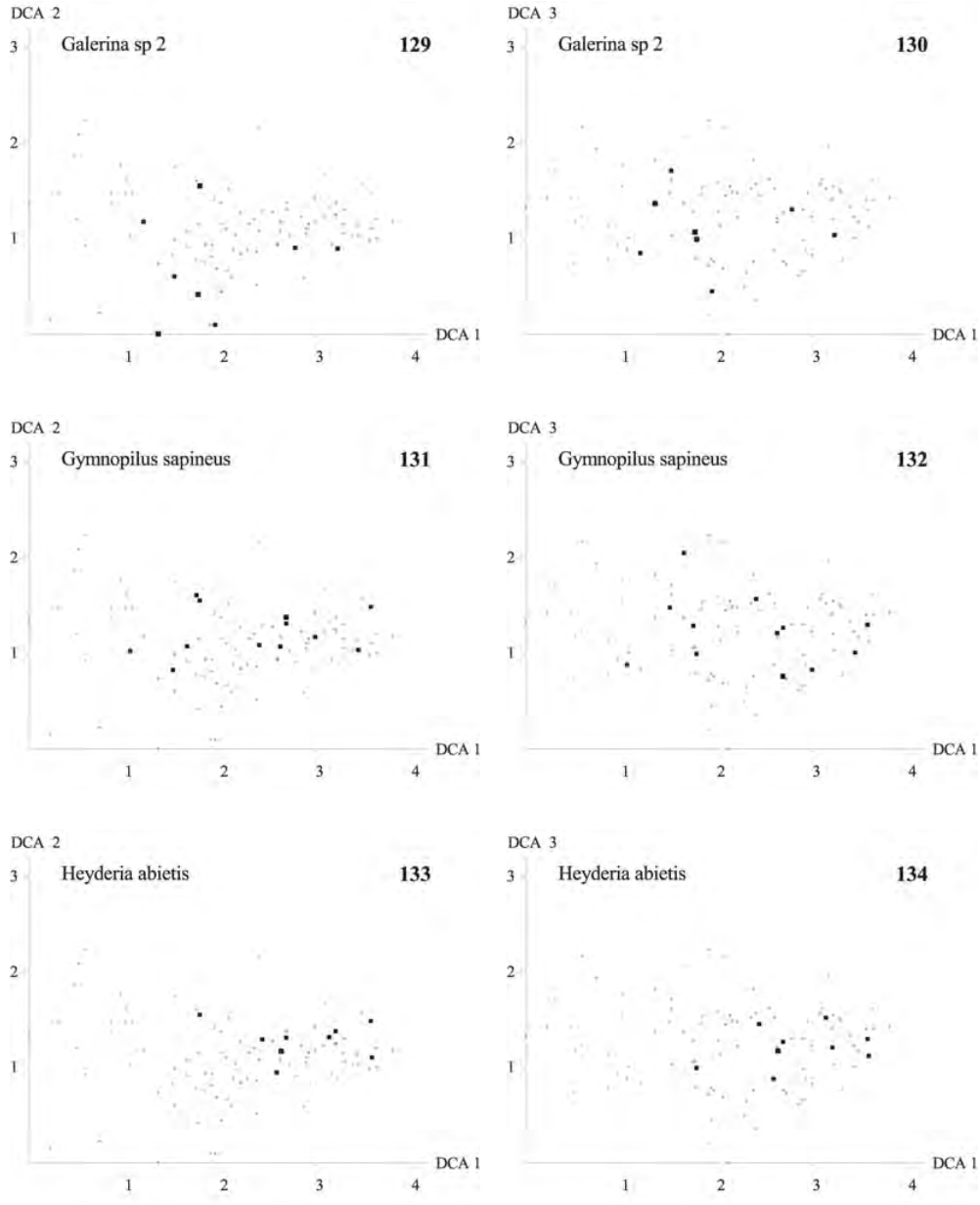

Figs 129–134. DCA ordination of the MAF 95 data set, axes 1 and 2 (left) and 1 and 3 (right). Frequency in subplots for actual species in macro plots plotted onto the macro plot positions. Scaling of axes in S.D. units. Small circle – absent. Square – present; area of square proportional to frequency in subplots. Figs 129–130. G*alerina sp 2*, Figs 131–132. *Gymnopilus sapineus*, Figs 133–134. *Heyderia abietis*.

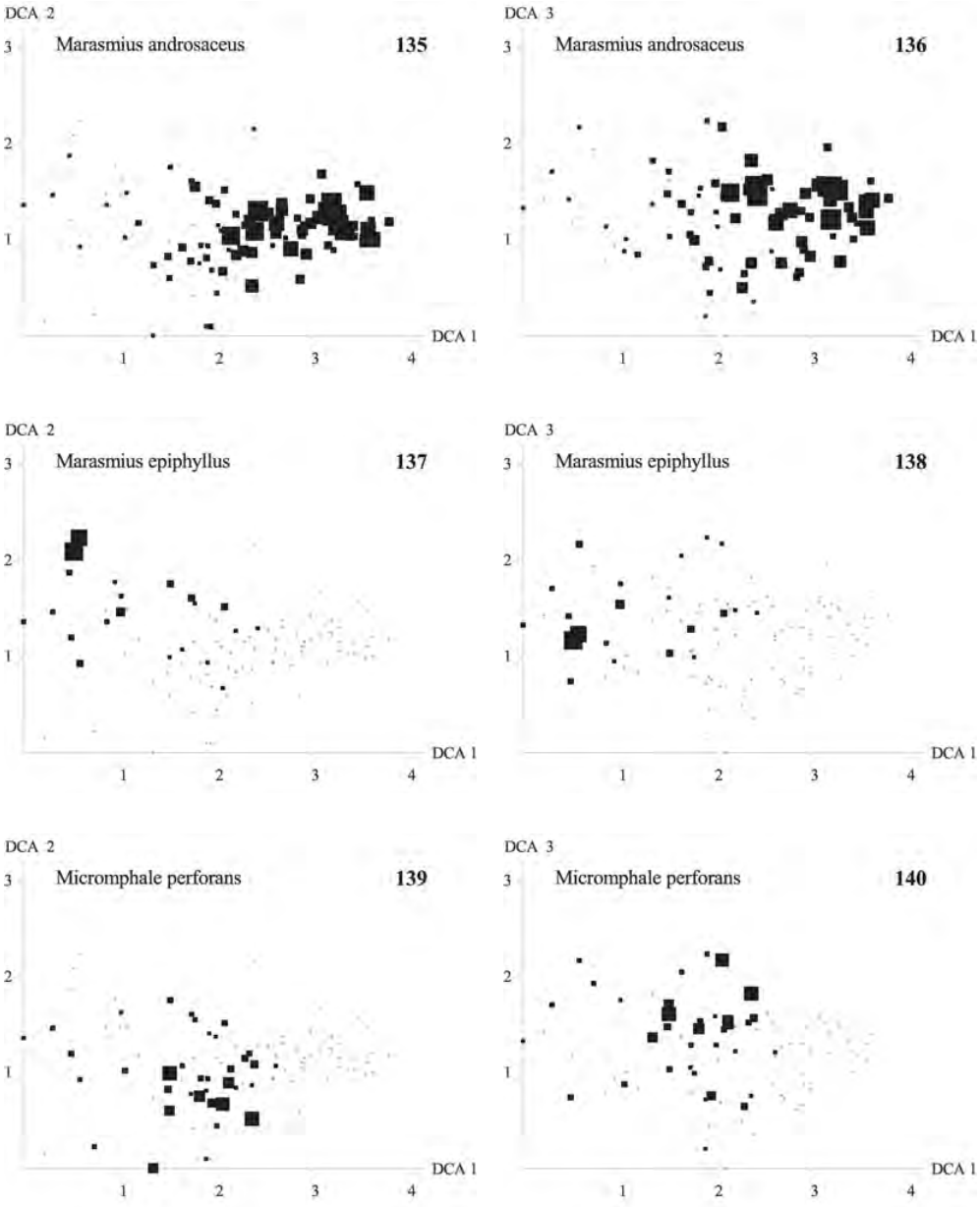

Figs 135–140. DCA ordination of the MAF 95 data set, axes 1 and 2 (left) and 1 and 3 (right). Frequency in subplots for actual species in macro plots plotted onto the macro plot positions. Scaling of axes in S.D. units. Small circle – absent. Square – present; area of square proportional to frequency in subplots. Figs 135–136. *Marasmius androsaceus*, Figs 137–138. *Marasmius epiphyllus*, Figs 139–140. *Micromphale perforans*.

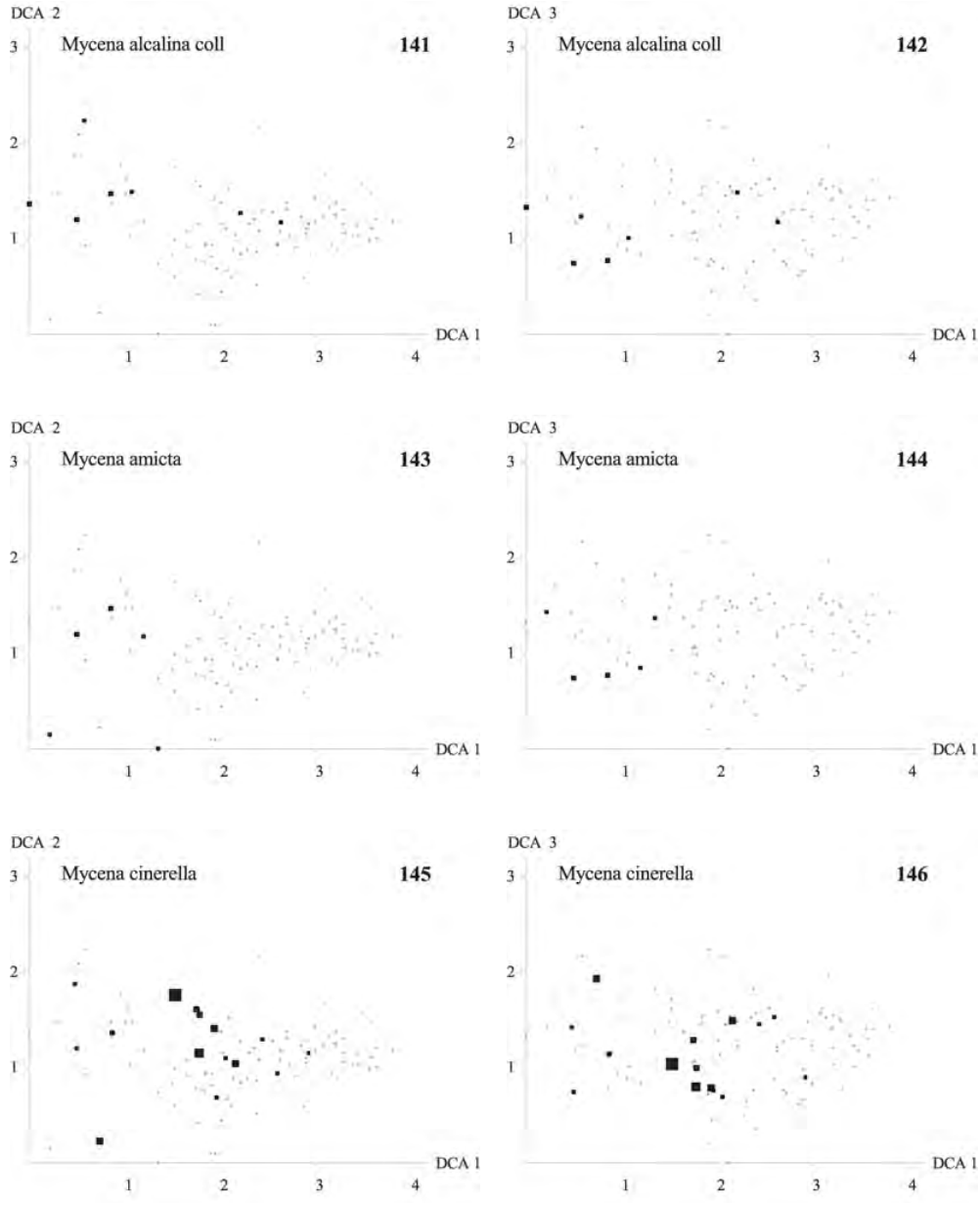

Figs 141–146. DCA ordination of the MAF 95 data set, axes 1 and 2 (left) and 1 and 3 (right). Frequency in subplots for actual species in macro plots plotted onto the macro plot positions. Scaling of axes in S.D. units. Small circle – absent. Square – present; area of square proportional to frequency in subplots. Figs 141–142. *Mycena alcalina* coll., Figs 143–144. *Mycena amicta*, Figs 145–146. *Mycena cinerella*.

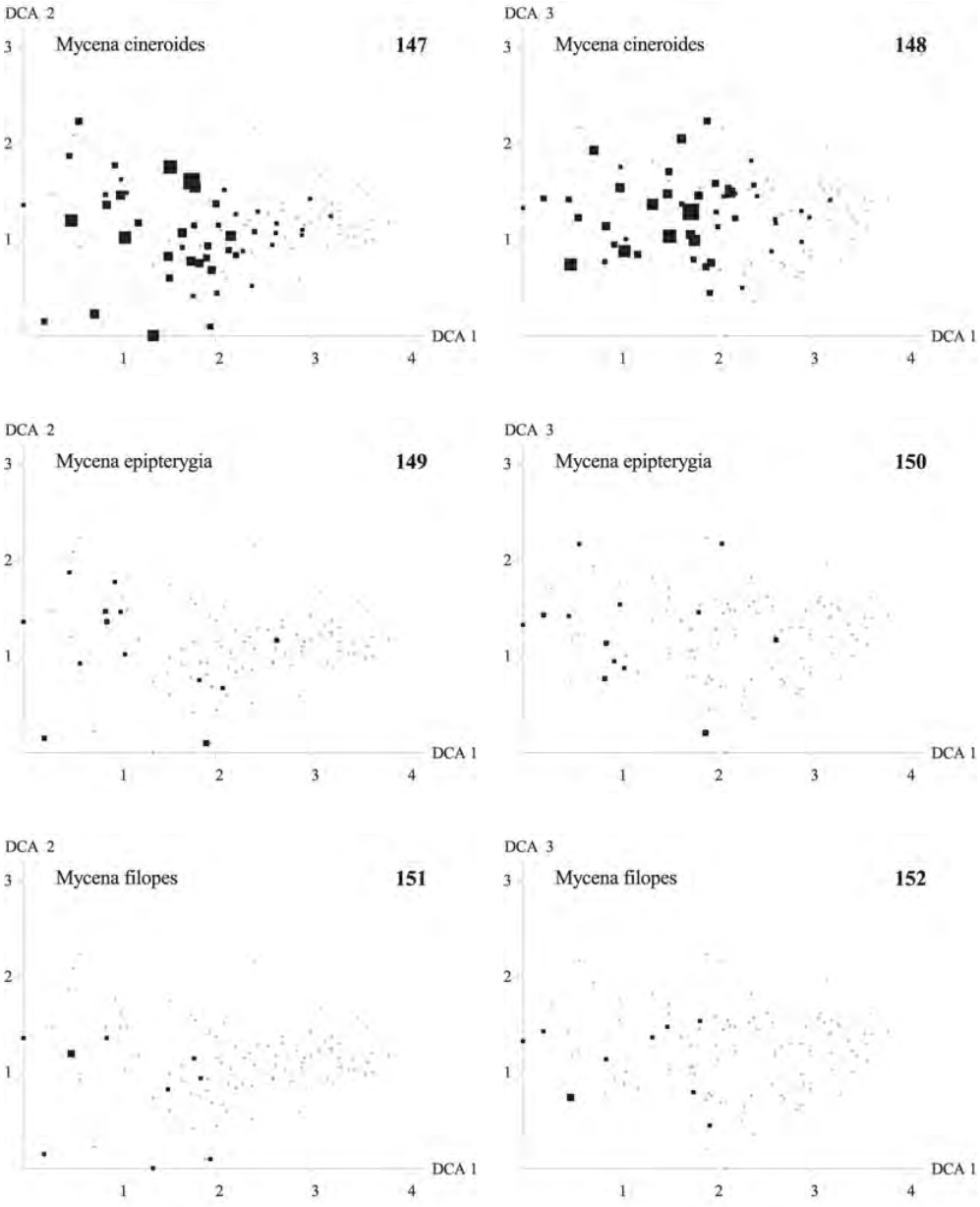

Figs 147–152. DCA ordination of the MAF 95 data set, axes 1 and 2 (left) and 1 and 3 (right). Frequency in subplots for actual species in macro plots plotted onto the macro plot positions. Scaling of axes in S.D. units. Small circle – absent. Square – present; area of square proportional to frequency in subplots. Figs 147–148. *Mycena cineroides*, Figs 149–150. *Mycena epipterygia*, Figs 151–152. *Mycena filopes*.

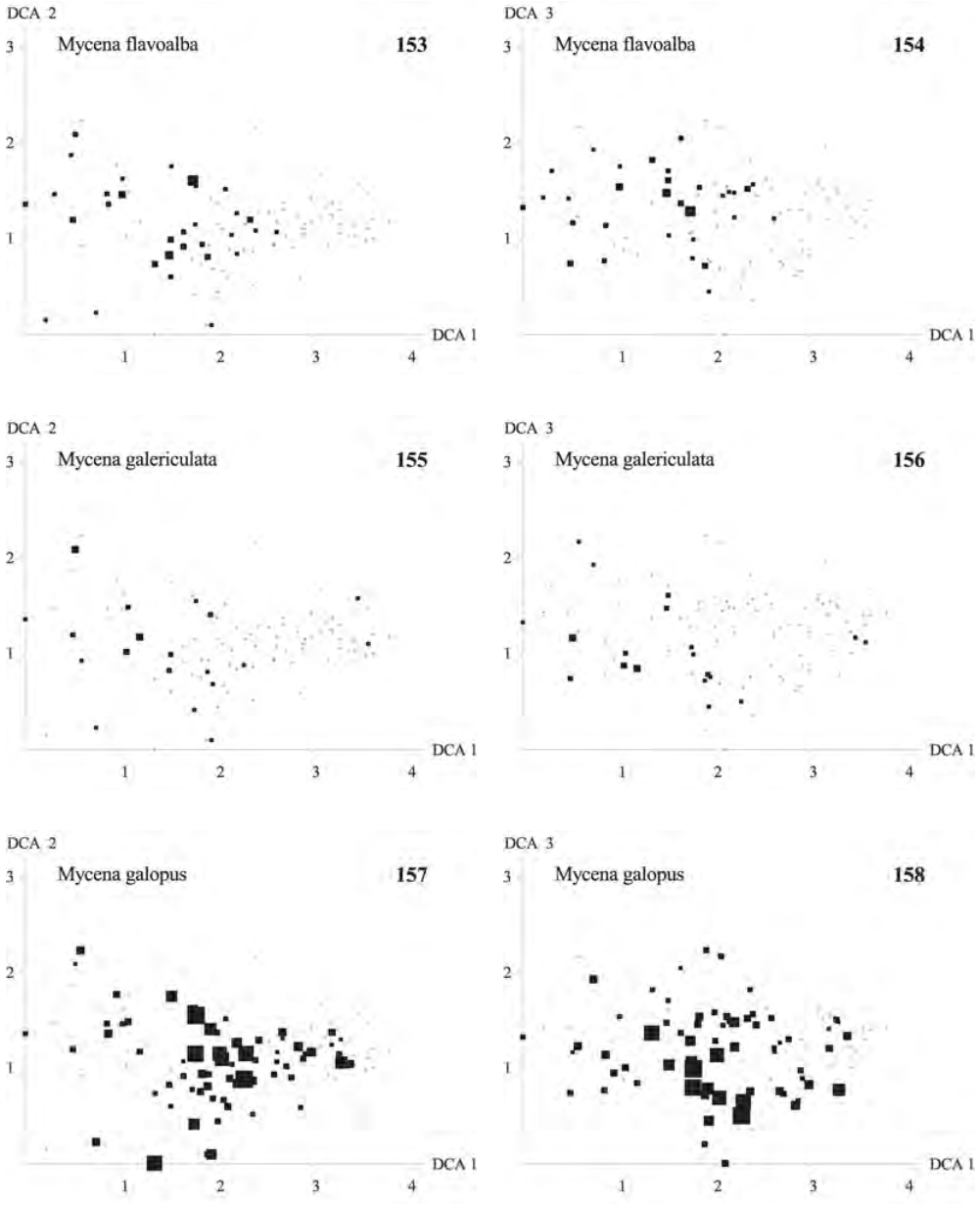

Figs 153–158. DCA ordination of the MAF 95 data set, axes 1 and 2 (left) and 1 and 3 (right). Frequency in subplots for actual species in macro plots plotted onto the macro plot positions. Scaling of axes in S.D. units. Small circle – absent. Square – present; area of square proportional to frequency in subplots. Figs 153–154. *Mycena flavoalba*, Figs 155–156. *Mycena galericulata*, Figs 157–158. *Mycena galopus*.

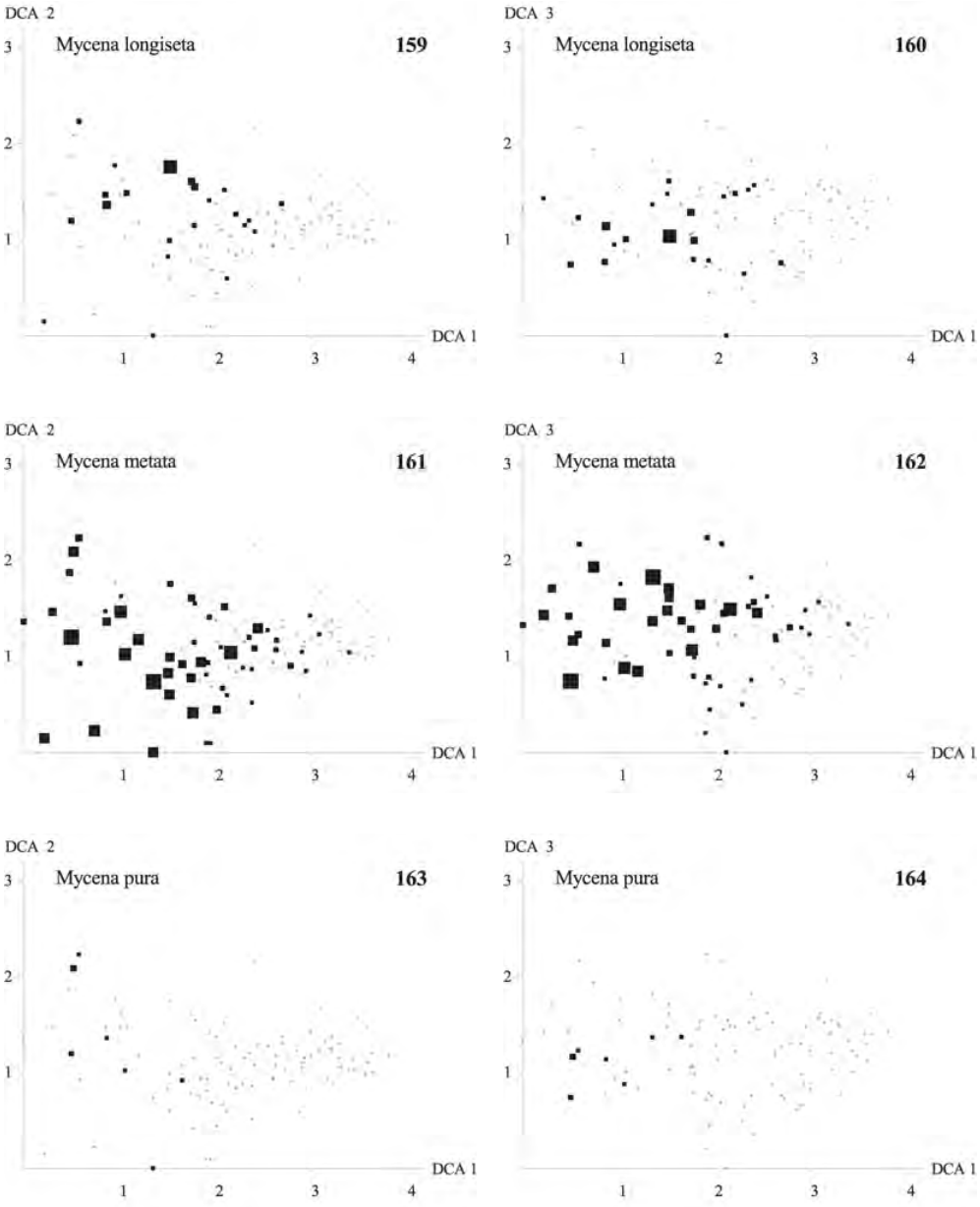

Figs 159–164. DCA ordination of the MAF 95 data set, axes 1 and 2 (left) and 1 and 3 (right). Frequency in subplots for actual species in macro plots plotted onto the macro plot positions. Scaling of axes in S.D. units. Small circle – absent. Square – present; area of square proportional to frequency in subplots. Figs 159–160. *Mycena longiseta*, Figs 161–162. *Mycena metata*, Figs 163–164. *Mycena pura*.

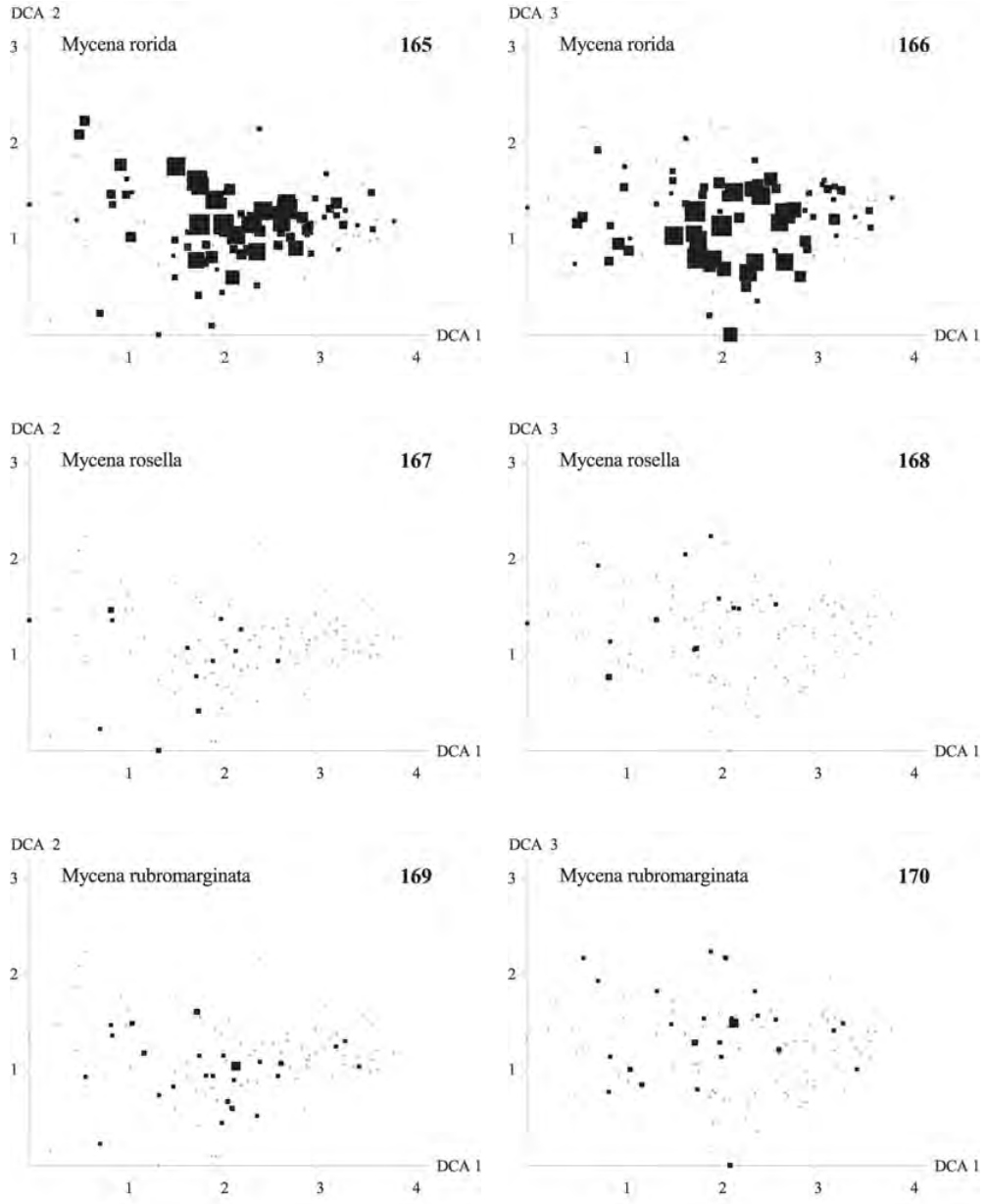

Figs 165–170. DCA ordination of the MAF 95 data set, axes 1 and 2 (left) and 1 and 3 (right). Frequency in subplots for actual species in macro plots plotted onto the macro plot positions. Scaling of axes in S.D. units. Small circle – absent. Square – present; area of square proportional to frequency in subplots. Figs 165–166. *Mycena rorida*, Figs 167–168. *Mycena rosella*, Figs 169–170. *Mycena rubromarginata*.

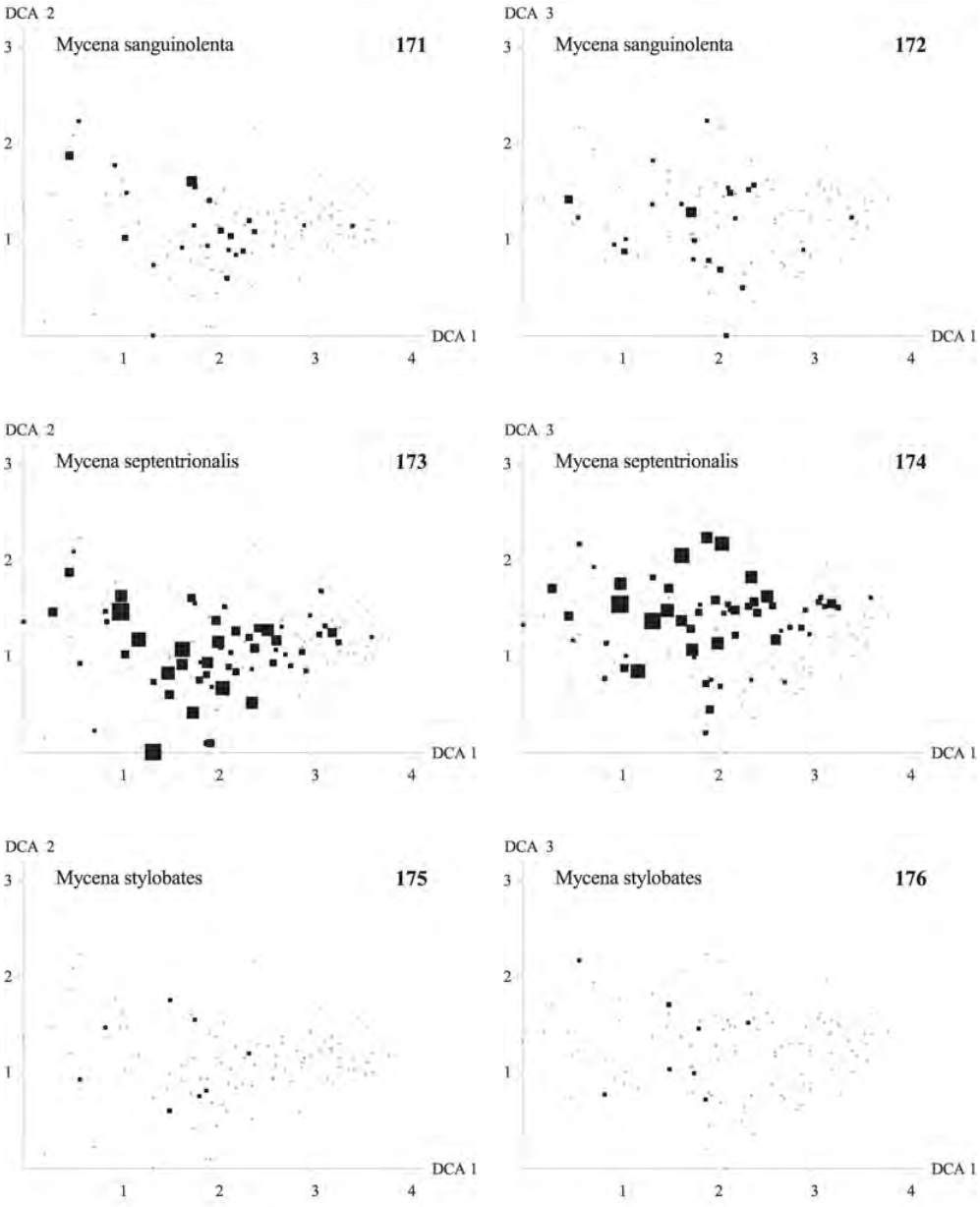

Figs 171–176. DCA ordination of the MAF 95 data set, axes 1 and 2 (left) and 1 and 3 (right). Frequency in subplots for actual species in macro plots plotted onto the macro plot positions. Scaling of axes in S.D. units. Small circle – absent. Square – present; area of square proportional to frequency in subplots. Figs 171–172. *Mycena sanguinolenta*, Figs 173–174. *Mycena septentrionalis*, Figs 175–176. *Mycena stylobates*.

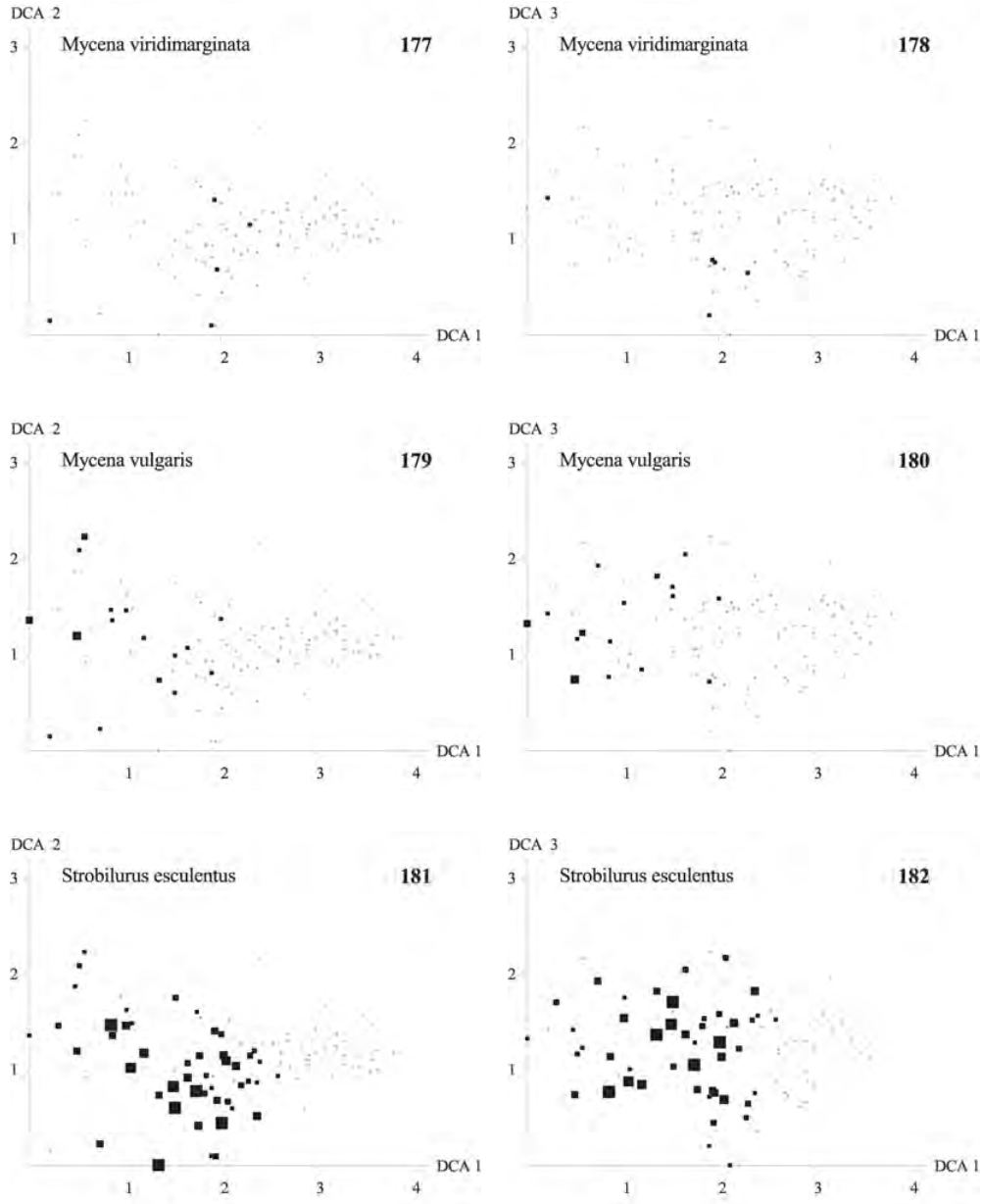

Figs 177–182. DCA ordination of the MAF 95 data set, axes 1 and 2 (left) and 1 and 3 (right). Frequency in subplots for actual species in macro plots plotted onto the macro plot positions. Scaling of axes in S.D. units. Small circle – absent. Square – present; area of square proportional to frequency in subplots. Figs 177–178. *Mycena viridimarginata*, Figs 179–180. *Mycena vulgaris*, Figs 181–182. *Strobilurus esculentus*.

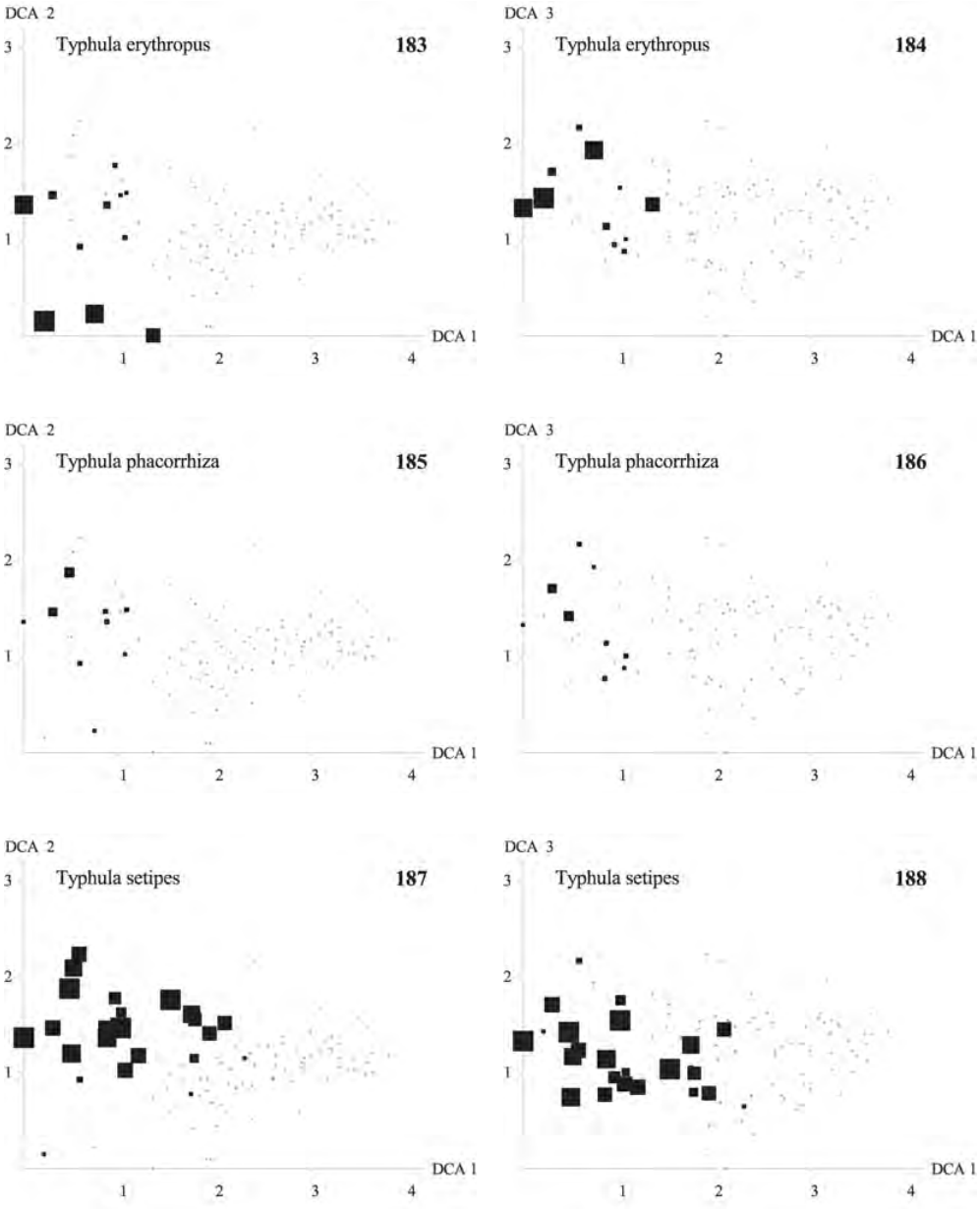

Figs 183–188. DCA ordination of the MAF 95 data set, axes 1 and 2 (left) and 1 and 3 (right). Frequency in subplots for actual species in macro plots plotted onto the macro plot positions. Scaling of axes in S.D. units. Small circle – absent. Square – present; area of square proportional to frequency in subplots. Figs 183–184. *Typhula erythropus*, Figs 185–186. *Typhula phacorrhiza*, Figs 187–188. *Typhula setipes*.

CONSTRAINED ORDINATION

Variation explained by single explanatory variables

Tab. 17 shows that the variation in fungal species abundances in the MAF 95 data set explained by the main vegetational gradient [DCAG 1; 0.38 IU (inertia units)] was not much lower than the variation explained by the main gradient in fungal species composition (0.47 IU; cf. Tab. 4). Relatively high amounts of variation were also explained by the second and fourth vegetational gradients (Tab. 17).

The largest amounts of variation explained by single primary environmental variables were noted for pH_{CaCl_2} (0.32 IU), N (0.30 IU), loss on ignition and terrain shape (0.23 IU), and soil depth at macro scale (0.22 IU). Soil moisture explained an amount of variation in fungal species abundances amounting to 0.12 IU only. Spatial variables explained 0.11 IU or less, i.e. below 2.5× the variation expected to be explained by a random variable (which is n^{-1}; where n is the number of plots; see Tab. 4).

Tab. 17. Variation (VE) in the MAF 95 data set explained by each explanatory variable (in inertia units, IU), as determined by hCCA using the variable in question as the only constraining variable. Significance (P) of each variable determined by a Monte Carlo permutation test; 199 permutations. Explanatory variable sets: E – environmental variables; S – spatial variables; D – DCA ordination axes based on vascular plants, bryophytes and macrolichens.

Set	Variable	VE	P	Set	Variable	VE	P
D	01 DCAG 1	0.38	.005	S	06 xy^2	0.11	.005
E	20 pH_{CaCl_2}	0.32	.005	E	16 ME Rel	0.11	.005
E	26 N	0.30	.005	S	02 y	0.11	.005
E	19 pH_{H_20}	0.27	.005	S	08 xy	0.11	.005
E	18 LI	0.23	.005	S	07 x^2	0.11	.005
E	3 MA Ter	0.23	.005	E	32 P	0.11	.005
E	5 MA SD	0.22	.005	S	09 y^2	0.11	.005
E	25 H	0.20	.005	E	28 Al	0.10	.005
E	21 Ca	0.18	.005	S	04 y^3	0.10	.005
E	30 Mn	0.16	.005	E	14 ME Sma	0.10	.010
D	02 DCAG 2	0.14	.005	D	03 DCAG 3	0.10	.005
E	01 MA Slo	0.14	.005	S	01 x	0.10	.010
D	04 DCAG 4	0.13	.005	E	23 Na	0.10	.005
E	22 Mg	0.13	.005	E	04 MA Une	0.09	.020
E	08 ME Slo	0.13	.005	E	06 MA Rel	0.09	.010
E	27 P	0.12	.005	E	13 ME Sme	0.09	.015
E	07 MA Lig	0.12	.005	E	12 ME Smi	0.09	.005
E	15 ME Lit	0.12	.005	E	33 S	0.08	.020
E	17 Mois	0.12	.005	E	09 ME Auf	0.08	.020
S	05 x^2y	0.11	.005	E	10 ME Une	0.08	.040
E	24 K	0.11	.005	E	02 MA Auf	0.07	.040
S	03 x^3	0.11	.005	E	31 Zn	0.07	n.s.
E	29 Fe	0.11	.005	E	11 ME Con	0.04	n.s.

Tab. 18. Partitioning the variation in the MAF 95 data set onto three sets of explanatory variables; {E} – the set of 33 environmental variables; {S} – the set of 9 spatial variables, and {V} – the set of 4 vegetational variables (DCA axes based on the ME 200 data set including vascular plants, bryophytes and macrolichens). Notation (explained by reference to data sets {E} and {S}): E∪S – total variation explained by {E} and {S}; E∩S – variation shared between {E} and {S}; E|S – variation explained by E, not shared with S. Variation explained (VE) is given in inertia units (IU), and as percentage of the total variation explained by all three sets of variables, TVE (in this case, E∪S∪V = 1.791 IU, which amounts to 34.54 % of the total inertia). TVE is the sum of seven components of explained variation, as shown by boldface letters. The number of variables in each set retained by forward selection (P # 0.01) is given in brackets.

Data set	VE	VE, % of TVE	Component	VE	VE, % of TVE
E (8)	1.061	59.2	E|(S∪V)	0.573	32.0
			(E∩S)|V	0.047	2.6
			(E∩V)|S	0.201	11.2
			E∩S∩V	0.240	13.4
S (7)	0.742	41.4	S|(E∪V)	0.431	24.1
			(E∩S)|V	0.047	2.6
			(S∩V)|E	0.023	1.3
			E∩S∩V	0.0463	13.4
V (4)	0.740	41.3	V|(E∪S)	0.0532	15.4
			(E∩V)|S	0.0388	11.2
			(S∩V)|E	0.0044	1.3
			E∩S∩V	0.0463	13.4
E∪S	1.515				
E∪V	1.360				
S∪V	1.218				
E∪S∪V	1.791				

Variation partitioning

The fraction of the total variation in fungal species composition in the MAF 95 data set (total inertia) explained by significant primary explanatory variables was 34.5% (= TVE; Tab. 18). The eight significant environmental variables {E} explained 59.2% of TVE while the seven significant spatial variables {S} and the four significant vegetational variables {V} explained 41.4 and 41.3% of TVE, respectively. Variation unique to one set of variables made the largest contributions to TVE (32.0, 24.1 and 15.4% of TVE for {E}, {S}, and {V}, respectively), followed by the variation shared among all three variable groups (13.4%) and the non-spatial variation shared between environmental and vegetational variables (11.2%; Tab. 18). The contributions by the remaining two (out of seven) variation components, shared between {S} and only one other set, were negligible.

While only 37% of the variation explained by {V} was not shared with other data sets, 55-58% of the variation explained by environmental and spatial variables was uniquely explained by these sets. As much as 60% of the variation explained by vegetational variables was shared with the environmental variable set {E}.

DISCUSSION

ENVIRONMENTAL INTERPRETATION OF GRADIENTS IN FUNGAL SPECIES COMPOSITION

The main gradient and its relation to broad-scale topography and soil nutrient content

Relationships with environmental variables in spruce and pine forests

The results of fungal ordinations point to the existence of one major gradient in species composition that closely corresponds to the main gradient in vegetation identified by R. Økland & Eilertsen (1993). The main fungal and vegetational gradients are correlated with the same environmental variables [compare Tab. 12 with R. Økland & Eilertsen (1993): Tab. 11] although macro-scale terrain variables are relatively more strongly correlated with the vegetational gradient while soil pH and nitrogen content are more strongly correlated with the fungal gradient [even after differences in absolute values between Pearson's r (used by R. Økland & Eilertsen 1993) and Kendall's τ have been taken into account]. Thus the conclusion of R. Økland & Eilertsen (1993) that the variation from pine to spruce dominated forests depends *primarily* on a macro-scale topographic (ridge-slope-valley) gradient appears to hold true also for fungi.

R. Økland & Eilertsen (1993) suggest, from the different patterns of correlations between ordination scores and environmental variables within spruce and pine forests, that different complex-gradients are responsible for the differentiation of vegetation within these two main forest types; that a nutrient complex-gradient is most important in spruce forest, while topography and soil depth are the most important factors in pine forest. Correlations between environmental variables and fungal ordination axes, calculated separately for spruce and pine forests, resemble those of vegetational coenoclines. However, the significant correlation of this coenocline with pH also in the pine forest (while correlations with soil depth are less strong) open for the possibility that the main gradient in fungal species composition is related to a complex-gradient in soil nutrients in both forest types. On the other hand, the strong relationship of the main gradient with terrain variables may well indicate that factors related to topography contribute *independently* to explain variation along the main gradient in the pine forest. Variation in spruce and pine forests will therefore be discussed separately.

Spruce forest: the complex-gradient in nutrient status

Except for some differences in the variables' rank order (variables ranked by correlation with ordination score), correlation patterns for fungi and plants in spruce forest (Subset A) are closely similar, with pH_{CaCl_2} and nitrogen concentration as the variables most strongly (negatively) correlated with the main gradient for both groups and calcium concentrations (negatively) and loss on ignition (positively) as other important correlated variables. As for vegetation (R. Økland & Eilertsen 1993, 1994), variation along the main fungal coenocline in the spruce forest is mainly related to the nutrient status of the humus layer. Factors controlling the nutrient status of the humus layer are discussed by R. Økland & Eilertsen (1993).

Soil pH is the most frequently focused single factor affecting the composition of the funga. For instance, Bohus (1984) arranged fungi from deciduous forests in a system of pH-classes. The restricted pH-amplitudes of many species and the high compositional turnover from acid to basic coniferous

forest soils are stressed in several mycological studies (e.g. Haas 1932, Šmarda 1973, Krieglsteiner 1977, Østmoe 1979, Bendiksen 1980, 1981, Metsänheimo 1982, Salo 1993). Differences between species in physiological optima along pH gradients are also demonstrated in pure cultures (Melin 1924, Modess 1941, Norkrans 1950, Theodorou & Bowen 1969, Hung & Trappe 1983). Furthermore, high importance of soil acidity to macrofungi is demonstrated by the decrease in number of mycorrhizal root-tips in soils subjected to experimental acidification (Reich et al. 1985, 1986, Blaschke 1986, Dighton et al. 1986, Göbl 1986, Dighton & Skeffington 1987, Entry et al. 1987, Keane & Manning 1987, Dighton 1988). However, Høiland & Jenssen (1994) and Agerer et al. (1998) showed in experiments with acidified irrigation of coniferous forests that acid rain does not necessarily adversely affect the number of fruitbodies of all ectomycorrhizal fungi; for some species the abundance increased in response to acidification.

Although saprotrophic fungal species on average occupy broader intervals along the main coenocline than mycorrhizal species (see p. 38), both groups differentiate along the main gradient. Culture studies demonstrate that the litter-decomposing ability of saprotrophs is pH-dependent and differs among species. For instance, Hintikka (1960) demonstrate poor ability of some coniferous forest species of *Mycena* with ecological pH optima of 4–5 to decompose substrates with pH > 6.0. Other *Mycena* species first grew very slowly, while growth rates increased later on due to the species' ability to acidify their immediate surroundings. Hintikka's observations suggest that saprotrophic species respond to a nutrient gradient because of pH-dependent, interspecific differences in decomposing ability. Competition between decomposers, a probable result for species with ecological ranges that are considerably narrower than physiological tolerances, further increase the compositional turnover along a coenocline. If, however, the range spanned by fruitbodies is narrower than the species' total range, the observed β-diversity exceeds the β-diversity of the fungal *species*.

Even if pH is more strongly correlated with the main fungal gradient than any other measured variable, it cannot be concluded that pH is the *cause* of the differentiation along the gradient. Other variables, alone or in combination, may be important as well.

Soil nitrogen. High importance of nitrogen concentrations in the humus layer, secondmost strongly correlated with the main fungal coenocline in our study, accords with results of many studies, especially of mycorrhizal fungi. Reduction of species number, fruitbody production and/or number of mycorrhiza types are normal effects of experimental fertilization and nitrogen addition (see, among others, Menge & Grand 1978, Ritter & Tölle 1978, Wästerlund 1982, Shubin 1988, Ohenoja 1989, Rühling & Tyler 1991, Termorshuizen & Ket 1991, Arnebrant & Söderström 1992, Termorshuizen 1993, Brandrud 1995, Wiklund et al. 1995, Brandrud & Timmermann 1998, Peter et al. 2001).

Abundance decrease or extinction, as observed over parts of Europe for several mycorrhizal species in the 20th century (see Fellner 1993, Høiland 1993), are often attributed to high atmospheric loads of nitrogen (Arnolds 1988, 1991, Termorshuizen & Schaffers 1987, 1991, Taylor et al. 2000).

Macrofungal species may differ in their response to nitrogen fertilisation because they differ in ability to utilise chemically different nitrogen sources (cf. Ohenoja 1989): not only nitrate and ammonium, but also organic nitrogen which can be utilised by several mycorrhizal species (cf. Lundeberg 1970) in the forms of soluble amino acids, peptides and soluble proteins (Abuzinadah & Read 1986a, 1988). Organic nitrogen may be made accessible to vascular plants by mycorrhiza (Abuzinadah et al. 1986, Abuzinadah & Read 1986b, 1989a, 1989b), but direct uptake of amino acids has also been demonstrated for vascular plants (Chapin et al. 1993, Kielland 1994, Raab et al. 1996, Nordin et al. 2001). When nitrogen may be utilized in many (most?) chemical forms, concentrations of specific forms of nitrogen such as ammonium ions are ecologically inadequate as measures of nitrogen supply (Abuzinadah et al. 1986). This may explain why total nitrogen is strongly correlated with vegetational gradients in forests, as demonstrated for instance by R. Økland & Eilertsen (1993) and T. Økland (1996), and with the main fungal gradient in this study.

Tyler (1985, 1989a, 1989b) demonstrates that abundances of most species of macrofungi in South Swedish deciduous forests (quantified as fruitbody numbers in large plots) may be modelled as a response to edaphic factors, notably base saturation and organic matter content of the humus layer. Hansen (1988a, 1988b) adds soil nitrogen content, which is positively related to base saturation and negatively related to organic matter content, and point to soil pH as important on mor sites and nitrogen mineralisation rate and leaf litter quality on mull sites. The similarity with factors correlated with the main fungal coenocline in the Solhomfjell area is striking, even though the areas differ in climate, the range of variation in important environmental factors and vegetation. This indicates that a main gradient associated with soil nutrient status may be important for fungi in most boreal (and nemoral?) forests. The results of Hansen (1988a, 1988b) may also be interpreted as an indication that concentrations of some heavy metals not measured by us, such as cadmium, influence fungal species abundances under normal field conditions, and hence gradients in fungal species composition.

Loss on ignition, a factor significantly correlated with the main fungal gradient, and other important factors as pH and nitrogen (cf. Økland & Eilertsen 1993, Fig. 5), may also represent independent, ecologically important properties of the humus. Mor and mull soils differ strongly in many physical properties (Green et al. 1993), and Tyler (1989a) points out that, apart from the inorganic soil chemical differences, differences in the organo-chemical properties of the litter and humus may be of importance for the species composition of macrofungi (cf. Romell 1935).

Calcium concentrations are also correlated with plot positions along the main coenocline, in accordance with the results of liming experiments in which negative effects similar to those resulting from nitrogen fertilization are often observed (cf. Kuyper 1989). One example is provided by Eilertsen et al. (1997a), who observe reduced abundance of the saprotrophs *Galerina atkinsoniana* and *Mycena sanguinolenta* in coniferous forests close to the Solhomfjell area after addition of dolomite lime in small concentrations (cf. Eilertsen et al. 1997b). Kuyper (1989) suggests that soil calcium concentrations affect fungi via effects on nitrogen mineralisation and nitrification. This parallels the hypothesis forwarded for natural forest soils, that Ca is the primary environmental variable limiting nitrogen mineralisation rates in humus (Hesselman 1926, Dahl et al. 1967) which has not, however, general validity (T. Økland 1996). The correlation of calcium concentrations with position along the main gradient may thus indicate correlations of both with a third, causal factor. However, a primary role of Ca (and/or Mg) is supported by the experimental liming study of Jonsson et al. (1999). Comparing controls with plots added delomite in low and high quantities, Jonsson et al. (1999) found that the number of root tips per metre root length was significantly lower in the control than in both of the dolomite treatments. This result was taken as an indication that the calcium concentrations as such was more important for the development of fine roots than the resulting pH, since the mean pH in the control and low dolomite plots was 4.1 and 4.0, respectively, whereas the mean pH in the high dolomite plots was 5.5.

Soil *phosphorus* concentrations are not correlated with the main fungal gradient even though phosphorus is physiologically important to macrofungi; the phosphorus content of mycorrhizal and saprotrophic fungi average 5.7 and 11.1 per cent of their dry weight, respectively (Miller & Laursen 1978). Similar results were found for plants in the same plots by R. Økland & Eilertsen (1993). Results of experimental studies in which phosphorus is supplied are not unambiguous: while phosphorus is considered the growth-limiting element for *Mycena galopus* (Frankland et al. 1978), increase as well as decrease depending on species and site conditions is reported by Kuyper (1989).

The closely parallel responses of fungi and plants to edaphic conditions has one important exception: plants, even those common on poor soil (site-type 5.1) are normally present also in richer sites (R. Økland & Eilertsen 1993) while many fungal species are absent or very rare there (see Figs 27-188). R. Økland & Eilertsen (1993) interpret the presence of vascular plants typical of poor sites

also in richer sites as an indication of low importance of competition among established vascular plants along the gradient. These differences between organisms open for different mechanisms as important for species' responses to the nutrient gradient in the two groups, e.g. in one of the following ways (or a combination): (1) The competition among macrofungal species (between the mycelia of different fungal species (cf. Lindahl et al. 2002) as well as with plants, for water and soil nutrients) is more intense than between plants. The mechanisms behind the patterns of distribution of macrofungal species will, however, remain obscure until all species present in a plot as mycelium can be confidently recorded, considering both time and space. (2) Absence of many fungal species from the richer part of the gradient due to physiological reasons; by avoidance of soils with high pH or high concentrations of nitrogen and/or other elements. (3) Responses to other environmental variables such as bryophyte cover, or other variables.

Pine forest: relative importance of factors related to topography and nutrients

While pH and concentrations of soil nutrients such as nitrogen, alone or in combination, appear to be responsible for the distribution of fungal species along the main gradient in spruce forest, environmental interpretation of the main gradient in pine forest is more difficult due to several, less strong correlations: with pH, AL-extractable phosphorus concentrations, terrain shape and slope (see Tab. 13), and with vascular plant coenoclines (cf. Tab. 10). Along the main vegetational gradient in pine forest, pH does not show systematic variation, nitrogen concentrations *increase*, terrain shape varies from convex slopes to ridge tops and soil depth decreases significantly (R. Økland & Eilertsen 1993). At least three explanations of the main fungal coenocline (from poor spruce forest to pine forest) may accord with these patterns: (1) that the nutrient complex-gradient extends into pine forest, (2) that topographic factors are decisive, e.g. via a gradient in soil moisture deficiency, as hypothesized for the corresponding plant coenocline by R. Økland & Eilertsen (1993), and (3) that other causes are in operation.

Data comparable to ours, viz. on the variation in fungal occurrence and abundance from bilberry-dominated spruce forest to lichen-dominated pine forest, are not available. Furthermore, the small range of variation in nutrient conditions in our material reduces the relevance of results from fertilisation studies. A natural starting point for further discussions is therefore the applicability of the soil moisture deficiency hypothesis to macrofungi.

The soil moisture deficiency hypothesis implies that, in rain-free periods, a drought front more rapidly penetrates the humus layer towards lichen-rich pine forests, partly due to more shallow soils, partly for topographic reasons, resulting in longer duration of low moisture availability. Topographic position, soil depth, median particle size and the decomposition rate are often mentioned as important factors varying along this gradient (R. Økland & Eilertsen 1993). Soil moisture deficiency probably affects cryptogams and vascular plants via different mechanisms. While the main vegetational coenocline (DCAG 1) is strongly correlated with soil depth [the most strongly correlated topographic variable, cf. R. Økland & Eilertsen (1993): Tab. 11] in the Solhomfjell area mainly because the main bottom-layer coenocline is strongly correlated with soil depth (R. Økland & Eilertsen 1993: Tab. 17), the vascular plant coenocline is not more strongly correlated with topographic factors than the fungal gradient. R. Økland & Eilertsen (1993) hypothesise that the variation in species composition in the bottom layer is indirectly related to soil moisture deficiency, via the decreasing cover of (and shelter from direct insolation by) the uppermost layers. This interpretation rests upon the assumption that ectohydric and poikilohydric organisms (such as most bryophytes and lichens) have poor capacity for uptake of water directly from the soil and is supported by physiological evidence such as the intolerance of dominant forest bryophytes to direct sun (e.g. Busby et al. 1978; see discussion by R. Økland & Eilertsen 1993). Recent studies do, however, indicate a much stronger dependence of

bryophytes on the soil than previously assumed, both for supply of water and for dissolved nutrients (T. Økland et al. 1999; also see Lewis Smith 1978, Brown & Bates 1990, van Tooren et al. 1990). Most likely, there is a close relationship between cumulative distribution curves for topsoil moisture (duration of soil moisture levels above a given level) and the length of the period a cryptogamic species is hydrated and thus actively photosynthesising; which is considered to be the most important single factor for the growth of forest bryophytes (R. Økland 1997).

The results of this study lead us to hypothesize that the soil moisture deficiency hypothesis may apply also to fungi. Like vascular plant roots, including mycorrhizal roots (cf. Kivenheimo 1947), fungal mycelia have highest density in the humus or upper mineral soil layers, for some species even concentrated to the uppermost litter sublayer (cf. Shantz & Piemeisel 1917, Mikola & Laiho 1962, Mikola et al. 1966, Pirozynski 1968, Harvey et al. 1976, Newell 1984). This suggests that soil-dwelling fungi are subjected to the same constraints on moisture supply from the soil as bryophytes and lichens. The mobility of fungal mycelia may, however, be comparable to that of vascular plant roots, much higher than that of bryophytes and lichens (R. Økland 1995c, 1995e, Dix & Webster 1995). Duddridge et al. (1980) found, by use of tritiated water, that mycorrhizal rhizomorphs have the ability to absorb water and facilitate its transport over long ecological distances and that mycorrhizal species differ in capacity to produce rhizomorphs. Correspondingly, Boddy (1999) infer that the extensive rhizomorphs (including cords) of many saprotrophs are likely to be important for transport of water (and nutrients). Some physiological evidence with relevance for applicability of the soil moisture deficiency hypothesis to fungi exists, for some ecological groups. The minimum water potentials required for growth under controlled conditions vary considerably between the nine leaf-litter decomposing fungi reviewed by Dix (1984), and between the nine wood- and litter-decay species studied by Koske & Tessier (1986). Variation among species in growth rates under low water potentials is also demonstrated for wood-inhabiting fungi in the experiments by Boddy (1983) and Griffith & Boddy (1991); some species growing on twigs are found to survive dry periods with soil moisture levels far below the normal limit for growth (cf. Loman 1965). Laboratory experiments on different ectomycorrhizal fungal species demonstrate interspecific differences in the ability of mycelia to grow in substrates with low water potentials (Uhlig 1972, Mexal & Reid 1973, Theodorou 1978, Coleman & Bledsoe 1989). In the North American study by Coleman & Bledsoe (1989) pine forest species as *Suillus luteus* and *S. granulatus* are shown to have high growth rates by low water potentials, as is the case also for *Boletus edulis*, which was found accidentally in dry pine forest in the present study. On the other hand, the low tolerance of *Hebeloma crustuliniforme*, a species typical for moister forest types, for dry soils is, however, shared by *Lactarius rufus*, known as a typical dry pine-forest species. The possibility that genetic population properties different from those occurring in North Europe are encountered in that study does, however, limit its value for direct comparisons. The American authors do not find any correlation between their results and the aridity of the collection sites, measured crudely as annual precipitation. They do, however, find that the most drought-resistant species also have maximum growth rates under higher water-deficiency stress than less resistant species. Furthermore, Uhlig (1972) finds for six tested ectomycorrhizal species a good ability to survive at much lower water potentials than needed for growth. Several studies in different kinds of dry forests demonstrate that *Cenococcum geophilum* has a high share of the total mycorrhiza (Worsley & Hacskaylo 1959, Meyer 1964, Vogt et al. 1981, Dahlberg et al. 1997). The hyphae of this species are highly specialized to dry conditions (e.g. Pigott 1982). Moser (1964, 1993) recognises one group of species with large fruitbodies, morphologically adaptated to dry sites such as pine forests. This group is exemplified by some *Russula* and *Lactarius* species which have slow development of primordia and fruitbodies with low transpiration rate, among others because of small surface area compared to the volume. The existence of such adaptations may indicate that the soil moisture deficiency hypothesis also applies to fungi.

Our results may indicate that similar differences exist between species of soil- and litter-dwelling saprotrophs and mycorrhizal fungi in coniferous forests, with respect to ability for growth and survival. Observations in the study area during the dry period in August 1990 suggest adaptation to fruiting of several mycorrhizal species in pine forest under dry conditions. Most of the very few fruitbodies observed during this period were observed in dry pine-forest plots. This was especially the case for species with large fruitbodies, such as *Russula paludosa* and *R. decolorans*, which obviously have high demands on water supply for development. Another species commonly observed as fruiting was *Amanita fulva*, which may be adapted to dry conditions by its rather broad and dense gills that may assist in keeping air humidity high in the spore-producing region (cf. Moser 1964). Furthermore, the volva may protect against water loss in young stages.

Most saprotrophic fungal species show declining abundance towards the dry end of the gradient (see Figs 101–188 and Tab. 16), their limits, based upon fruitbodies, are, however, not very sharp. This is exemplified by bryophilous species such as *Galerina hypnorum*, *G. atkinsoniana*, *Mycena galopus* and *M. septentrionalis*; for which the presence of their preferred substrate seems to be more important than the risk of drought. A plausible explanation is the higher potential of most saprotrophs compared with most mycorrhizal species to initiate fruitbody formation by rapid swelling of primordia after rain because of the smaller fruitbodies of the former. Furthermore, species with small fruitbodies may more efficiently utilize small paludified patches. A noticeable adaptation to drought endurance is seen in *Marasmius androsaceus*, a ubiquitous species with particularly high abundance in dry pine forests, which possesses drought-resistant rhizomorphs and fruitbodies with high ability to revive when rain follows drought. For instance, *M. androsaceus* is the only abundant saprotroph in dense *Calluna*-dominated vegetation. Only two of the recorded saprotrophs seem to be more or less confined to dry pine forest: *Collybia putilla*, that grows among pine needles and is observed once in series 1, and *Mycena clavicularis*, for which three of four recordings are made in pine forest.

For mycorrhizal fungi, the picture is somewhat more complicated. The dependence or preference of many species for either spruce or pine as their mycorrhizal partner contributes strongly to the main fungal coenocline. Such species have more or less sharp limits for fruitbody production that coincide with the border between pine and spruce forests. Possible influences by environmental factors such as soil moisture conditions can in these cases not easily be separated from the mycorrhizal factor. Furthermore, the uncertainty remains that fruitbody production does not necessarily occur throughout a species' whole range of occurrence as mycelium. For several fungal species that produce fruitbodies exclusively in association with one specific host, Molina & Trappe (1982) demonstrate ability to form well-developed ectomycorrhizae with one or more other hosts in culture. This opens for the possibility that typical spruce-forest species (especially those with known ability to form associations also with pine), are present as sterile mycorrhizal partners of pine in drier site-types. Observations of each of the typical species of submesic sites (series 5), *Boletus edulis*, *Hydnum rufescens*, and *Cantharellus tubaeformis*, once in pine forest support the hypothesis that species have wider tolerances towards the dry pine forest as mycelia than indicated by the occurrence of fruitbodies. Incidental fruiting in drier sites is likely to be favoured by suitable combinations of climatic factors.

Many species typically associated with spruce may associate with pine in locally favourable, e.g. moister, sites (e.g. Metsänheimo 1982, Väre et al. 1996) This is true for most *Cortinarius* species recorded in this study (E. Bendiksen, pers. obs.), which are present in the poor bilberry-dominated spruce forest (site-type 5.1) and in some regions also in more or less subxeric pine forest sites (corresponding to series 4 and 3), cf. Høiland (1986), Såstad (1990), and Såstad & Jenssen (1993). Their failure to follow the mycorrhizal host to the dry end of its range strongly indicates restriction by soil moisture deficiency.

Many pine-associated species are not restricted to well-drained soils, as they also occur in bog pine forest (cf. Kalamees 1979). Some typical pine mycorrhizal species have also been observed in

forests totally devoid of pines, e.g. *Russula paludosa* and *R. decolorans* [sparse in bilberry-dominated spruce forest (site-type 5.1); E. Bendiksen, pers. obs. in SE Norway], and *Lactarius rufus* [having a wide ecological amplitude that includes pure *Picea* and *Betula* forests (E. Bendiksen, pers. obs.), but with distinct preference for pine forests where it may be highly abundant]. These species seem to have preferences for *Pinus* as mycorrhizal host. Competitive interactions may contribute to their low abundance in spruce forest. Some species, e.g. *Chroogomphus rutilus*, *Cortinarius mucosus*, and *Suillus variegatus*, are obligate or almost obligate pine mycorrhizal species. Other species restricted to the pine forest in this material, but also growing in *Picea*-forest (without *Pinus*) elsewhere, are *Cortinarius lux-nymphae*, *C. semisanguineus*, and *C. mucifluus* (cf. Bendiksen 1981, Høiland 1984, Bendiksen et al. 1993).

Species density (number per plot) decreases for saprotrophs and mycorrhizal species (cf. Tab. 3) [like for vascular plants (cf. R. Økland & Eilertsen 1993, 1996)] towards the dry end of the gradient, indicating that the ecological demands of most fungi are decreasingly well satisfied from poor bilberry-dominated spruce forest to dry pine forests.

R. Økland & Eilertsen (1993) observe relatively sharp limits for many vascular plants along the main coenocline towards the pine forest, and note that these limits contribute considerably to high compositional turnover along the coenocline.

The stronger overlap between site-types in the ordinations of fungi than in ordinations of plants, and the lower compositional turnover along the main fungal gradient (lower gradient length), are likely to be caused by the generally more ubiquitous nature of fungi: contrary to spruce forest vascular plants and mosses like *Maianthemum bifolium*, *Trientalis europaea*, *Hylocomiastrum umbratum* and *Rhytidiadelphus loreus* many fungal species with optima in poor bilberry-dominated spruce forest (site-type 5.1) also occur in the driest pine forests (series 1 and 2).

The significant correlation in pine forest between plot position along the gradient and pH (and AL-extractable phosphorus concentrations) indicates that soil acidity and/or soil nutrient availability may be a third factor contributing to the coenocline, in addition to soil moisture deficiency and the shift from spruce to pine as mycorrhizal host. However, while high importance of soil nutrient factors for the observed shifts in species composition in the pine forest is hardly supported by external evidence, numerous counter-arguments exist: (1) The incidental occurrence of fruitbodies of species with a distinct optimum in spruce forests in pine forest as well, lending support to soil moisture deficiency as an important factor for regulation of fruiting. (2) Restriction of species with well-defined limits towards poorer sites to spruce forest (e.g. *Hygrophorus pustulatus* and *Entoloma rhodopolium*; neither of which are observed in plots classified to the poor submesic site-type, 5.1) while no such examples are known from the pine forest. (3) The paradox that pine-forest plots along comparable first axes in ordinations of fungi and plants are so similar (see Tab. 10) if due to completely different causes. (4) The correlation of the gradient with pH may result from correlations of both with slope and terrain shape. In that case, soil moisture deficiency may be the decisive factor while correlations with pH (and nutrient concentrations) are without causal ecological significance.

One reason why spruce and pine forest subsets overlap along the first fungal ordination axes while a moderate discontinuity is observed in ordinations of vegetation may be that soil moisture deficiency influences plants and fungi in different ways. Thus the fungal ordination does not provide evidence for existence of a point along the gradient like that claimed by R. Økland & Eilertsen (1993) for plants [near the transition between spruce and pine forest in series 4, cf. R. Økland & Eilertsen (1993): Fig. 137], where duration (probability) of soil moisture below a critical level takes over for soil nutrient status as the important complex-gradient. One possibility is that fungi have higher demands for moisture than plants, thus being influenced by soil moisture deficiency even in spruce forest, perhaps along the entire main fungal coenocline. However, this interpretation is not supported by correlations between topographical variables and the main gradient in the spruce forest.

We conclude that increasing soil moisture deficiency is likely to restrict the occurrence and fruiting of several species of fungi towards dry pine forests, and that the main gradient in fungal species composition is accentuated by the preference of mycorrhizal species for either spruce or pine as their main mycorrhizal symbiont.

Spruce forests: a gradient in cover by deciduous litter and bryophytes?

A second fungal coenocline, relevant for spruce forest only, is expressed along the second axis in the ordination of the F95 data set, the third axis in ordination of the F97 data set, and the second axis in a separate ordination of spruce-forest plots. This coenocline is correlated with the fourth axis for vegetation, which R. Økland & Eilertsen (1993) found not to be ecologically interpretable. No ecological variable is correlated with this coenocline at the $P < 0.0001$ level and, with the exception of bryophyte cover, all variables correlated with this coenocline at the $P < 0.025$ level are more strongly correlated with the main coenocline. We hypothesize that this coenocline is due to variation along a complex-gradient in spruce forest from high bryophyte cover and low cover of deciduous litter (notably *Betula* and *Populus*) to low bryophyte cover and high litter cover. Support for this interpretation comes from: (1) The positive correlation with deciduous litter cover ($\tau = 0.1512$, $P = 0.0368$) and the negative correlation with bryophyte cover ($\tau = -0.2314$, $P = 0.0012$). (2) The optima of fungal species associated with deciduous trees at high DCA 2 scores (cf. Fig. 23, 25), viz. the mycorrhizal *Cortinarius armillatus*, *C. raphanoides*, *Lactarius glyciosmus*, *Lactarius vietus*, *Leccinum* spp., and *Tricholoma fulvum*, and the leaf-decaying saprotrophs *Clavariadelphus junceus*, and *Collybia confluens*, *Marasmius epiphyllus*, *Typhula setipes*, and *T. phacorrhiza* (of which several are, however, poorly represented in our materal). (3) The optima of bryophilous species that avoid sites with dense litter at low DCA 2 scores, viz. *Cortinarius albovariegatus*, *Cystoderma jasonis*, *Galerina* sp.1, and *G. mniophila* (for the strong decrease in abundance of *Lactarius theiogalus* along this axis, see p. 00). (4) The negative characterization of plots with high score along this axis by lack of bryophilous fungi. (5) The almost complete absence of deciduous *trees* in pine forests, explaining the lack of variation along this coenocline there. Both *Populus tremula* (cf. Johansson 1996) and *Betula* spp. have wide amplitudes with respect to climatic and local environmental factors, but prefer moist, fertile sites.

Betula and *Populus* provide suitable substrates for fungi, by formation of ectomycorrhizae and by shedding leaves which form a persistent, compact mat. Incompletely decayed *Betula* and *Populus* litter, soaked with water for longer periods, is an important substrate for saprotrophs that fruit in late autumn. Most *Typhula* species have high abundance in plots with high DCA 2 scores and are particularly abundant on this kind of substrate (*T. erythropus* differs by having a low optimum along this axis, probably because of high abundance in the species-rich plots Nos 45 and 57, which occupy outlier positions along this axis). *Quercus* leaves share the properties of *Betula* and *Populus*, but oak is too sparse in the area to be of quantitative importance. Litter produced by the common *Sorbus aucuparia* decay rapidly and hence lacks the qualities of *Betula* and *Populus*.

Few large (or several smaller) deciduous trees may be sufficient to impact moss cover negatively, because shoots of most bryophyte species are unable to survive recurrent burial under large deciduous leaves (R. Økland 1995d, 2000). The negative impact on bryophyte cover increases with increasing leaf size and with increasing decomposition time (cf. Kujala 1926, Tamm 1953, During & Verschuren 1988, R. Økland 1995c); *Populus* litter is thus more detrimental to bryophytes than *Betula* litter (R. Økland, pers. obs.). Large spruce trees negatively impact the moss cover below the crown beacuse of high litterfall, reduced amounts of throughfall precipitation compared to below deciduous trees (cf. Lukkala 1942, Päivänen 1966, Mahendrappa & Kingston 1982) and lowered incident light.

Loss on ignition is positively correlated with position along the coenocline, most likely because litterfall and the thickness of the organic topsoil layer increases along the gradient. A probable reason for the lack of correlation between this coenocline and tree variables is the wind-mediated dispersal of leaves over a large area around each tree, in ways not adequately reflected in indices neither at the 1-m^2 nor at the 16-m^2 scales. The relatively weak relationship between deciduous litter cover and this coenocline indicates that ample litter supply may be one among several factors which make up a complex-gradient. Large deciduous trees occur in, or close to, plots in transects 5 and 8 with high DCA-2 score. These plots differ with respect to aspect, altitude and other local conditions. Presence of large deciduous trees in spruce forest largely reflects forest history and successional state (cf. Hytteborn et al. 1991).

Most saprotrophic species have wider ranges than mycorrhizal species along this coenocline (cf. Fig. 21); perhaps because the number of specialists for dense leaf mats is low (see above), perhaps because sites of this kind occur patchily on scales considerably finer than the plot site of 16 m^2. Specific niches related to factors that vary on scales finer than the plot size are likely to be undetected by multivariate analyses, because within-plot variation is treated as noise (Gauch 1982a, 1982b, Wiens 1989). Patterns of mycorrhizal species may be more adequately represented because they are more broad-scaled, and because they are likely to be accentuated by the restricted distributions of several mycorrhizal host tree species along the gradient.

Pine and spruce forests: the fine-scale paludification gradient

A third fungal coenocline occurs in all ordinations and all subsets – as the third axis in DCA ordinations of F95 and the spruce forest subset F58A, and the second axis in DCA ordinations of F97, the pine forest subset F37B and both LNMDS ordinations. This fungal coenocline is strongly correlated with the second axis in the ordination of vegetation, interpreted by R. Økland & Eilertsen (1993) as 'the response to a complex-gradient consisting of more or less parallel gradients in soil moisture, fine-scale canopy closure (under trees – between trees gradient), soil depth and exchangeable amounts of Al and Fe'. R. Økland & Eilertsen (1993) interpret this vegetational gradient as a fine-scale gradient because it is reflected primarily in the composition of the bottom layer. Furthermore, they stress the difference between this fine-scale paludification gradient which reflects variation in the normal, or median, soil moisture conditions and the soil moisture deficiency gradient (reflecting variation in the danger and duration of extreme drought, see p. 81). R. Økland & Eilertsen (1993) discuss how fine-scale paludifications of different kinds are related to ecological conditions.

This fungal coenocline is most strongly correlated with the corresponding axis in the ordination of cryptogams, perhaps indicating that fungi (fruitbody production) responds to paludification in the same way as bryophytes and lichens, and on the same scale. Strong support for interpretation of this fungal coenocline (like corresponding plant coenoclines) as the response to fine-scale paludification comes from the correlations with soil moisture (which decreases along the gradient). Furthermore, the coenocline is moderately correlated with several tree indices and also weakly correlated with the concentration of extractable aluminium, which decrease along the gradient. In pine forest, plot scores are also moderately strongly correlated with soil depth (increasing) and pH and nitrogen concentrations (decreasing along the gradient). The shift of this coenocline from the second to the third axis in the ordinations suggests that its importance is comparable to the coenocline related to deciduous litter and bryophyte cover.

In the separate ordination of the pine forest subset MAF37B, the second axis, which is most strongly correlated with soil moisture (cf. Tab. 14), is strongly correlated both with the second and third (and fourth) axes in the ordination of MAF95 (cf. Tab. 8). This indicates that in pine forest one

fungal coenocline is the response to a complex gradient made up by deciduous litter and bryophyte cover and variation in fine-scale paludification, running from moist moss-covered (often with *Sphagnum*) to dry litter-covered ground.

Fungi are well known to respond to the fine-scale paludification gradient, e.g. by the frequent reference in mycoecological studies and floras to 'association with *Sphagnum*'. Both mycorrhizal fungi (e.g., *C. flexipes*, *Hygrophorus olivaceoalbus*) and saprotrophs (e.g., *Mycena galopus*) that seem to find their optima in *Sphagnum*-dominated patches have low scores along the ordination axes representing this coenocline. The great water-holding capacity of *Sphagnum* is probably the most important single factor, although saprotrophs may also respond to *Sphagnum* as a substrate. It is not yet known if the different species' mycelia segregate along this gradient or if this coenocline merely reflects specific requirements for fruiting.

Mycorrhizal and saprotrophic species have comparable ranges along this coenocline (Fig. 22). A majority of species in both of the major groups have wide ranges along this coenocline, indicating that species of moist sites are able to grow drier sites as well, while the number of specialist species is low. Conversely, many species typical of the dry end of this coenocline, e.g. *Mycena septentrionalis* which is able to grow in needle beds under dense spruce canopies, may thrive in locally moist sites. Species with special adaptations to paludified sites first appear in sites with a permanently high subsoil water table, such as swamps and mires (see Arnolds 1992b).

Aluminium concentrations are invariably less strongly correlated with the fungal coenocline than with the corresponding plant coenocline, even after differences in absolute values between correlation coefficients are taken into account. Aluminium concentration explains a low fraction of variation in species abundances in tests by single-variable CCA (cf. Tab. 17), indicating that its correlation with the coenocline results because both are correlated with median soil moisture. R. Økland & Eilertsen (1993) ascribe the positive correlations between a vegetation coenocline and Al and Fe concentrations and (median) soil moisture to accumulation of these elements higher in the soil profile in sites where leakage is counteracted by high water supply rates, high content of median soil moisture, and upward capillary movement of water in *Sphagnum* stands.

As discussed for the corresponding vegetational coenocline by R. Økland & Eilertsen (1993), the correlation of this coenocline with (spruce) canopy closure and tree influence indices may indicate a causal relationship. Spruce (and pine) canopies efficiently intercept precipitation, and dense spruce needle litter has low water retention capacity (cf. R. Økland & Eilertsen 1993, T. Økland 1996). Both of these factors will tend to increase the range of soil moisture variation. Needle beds are particularly well developed under vigourous spruce trees with low height to the crown. Many saprotrophs that are able to decompose spruce needles are equally common in moss-rich plots as in needle beds, but some (e.g. *Micromphale perforans* and *M. septentrionalis*) that increase in abundance with increasing plot score along this axes appear to profit from large amounts of substrate available for decomposition. *Mycena septentrionalis* is for many needle-bed dominated plots represented in almost every subplot. Several saprotrophs that grow on deciduous litter, e.g. *Marasmius epiphyllus*, *Typhula erythropus* and *T. phaecorrhiza*, increase in abundance towards the dry end of this gradient. The high correlation of the second axis in the LNMDS ordination of F95 and significant correlations of the second and third axes in the corresponding DCA ordination with bryophyte cover reflects this element of variation in common between the second and third fungal coenoclines, from bryophyte-rich, paludified sites poor in litter to litter-rich, drier sites. Species with peak abundance in needle-bed sites may benefit from lower intensity of competition – with vascular plants, bryophytes and lichens which suffer from adverse moisture conditions, litterfall and strong shade, and other fungi which are negatively affected by the dryness of the substrate. These species normally produce fruitbodies late in the autumn when moisture conditions are more favourable also in litter-bed sites (high amounts of precipitation, low temperatures and low evaporation rates). An important exception to late fruiting is *Marasmius*

androsaceus with its specialized rhizomorphs, which gives this species access to different substrates over a wide area (Lehmann & Hudson 1977, Holmer & Stenlid 1991). Despite of its great ability to grow in dry places this ubiquistic species does not show any clear trend along the third axis (Tab. 16).

FACTORS DETERMINING VARIATION IN FUNGAL ABUNDANCE

The fraction of variation in fungal species abundances in 16-m^2 plots which could be explained by significant environmental variables, 20.5%, is considerably lower than reported by R. Økland & Eilertsen (1994) for plants in 1-m^2 plots (36.5% for vascular plants, 25.1% for cryptogams). R. Økland & Eilertsen (1994) find that the fraction of variation explained by environmental variables at the 0.0625-m^2 plot scale is considerably lower than at the 1-m^2 scale, and attribute this difference to the change of dominant process from environmental control at the broader scale to control by interspecific interaction, clonal processes and random events at the finer scale. The fine-scaled patterns of variation in factors like soil moisture and deciduous litter cover indicate that the difference between fungi and plants in variation explained is likely to be due to a combination of two factors: (1) high amount of within-plot variation in important environmental factors at the 16-m^2 plot scale, and (2) high importance also of factors not included among the measured variables for fruiting of fungi, such as climate, litter quality and quantity, and mycorrhizal partner. However, the inappropriateness of total inertia as a measure of the total variation in species composition (R. Økland 1999), even for data sets that are collected in comparable ways, precludes firm conclusions to be drawn from these figures.

The fraction of the total explained variation in fungal abundance explained by spatial variables is comparable with that reported for plants by R. Økland & Eilertsen (1994). A relatively large fraction of spatial variation, 61%, is not shared with environmental variables. Strictly spatial variation may be due to (1) causes that are stochastic functions of geographic distance, such as clonal growth, aggregated dispersal and mortality, and common (fine-scale disturbance) history, and (2) variation along geographically structured, not measured environmental variables (Borcard et al. 1992, Legendre 1993, R. Økland & Eilertsen 1993). All of these processes are highly important for fungi. For instance, several fungal species have aggregated distribution patterns, e.g. *Lactarius theiogalus* and *Russula puellaris*. The abundance of the former decrease strongly along the second DCA axis in the ordination of the F95 data set, even if *Lactarius theiogalus* seems unaffected by the factors considered important for variation along this coenocline. Localised dispersal patterns may explain why five of the seven plots in which it occurs in our material are from the middle part of transect 1. Similarly, four of the six occurrences of *Russula puellaris* are from southwest of Lake Karistjern; three in adjacent submesic plots from transect 8 and the fourth in the nearest plot in the neighbouring transect 7, in dry pine forest (a most unusual habitat for this species in Scandinavia; E. Bendiksen, pers. obs.). Dispersal, both of spores which fall at higher density and also may have a higher chance of successful establishment close to an earlier established fruiting mycelium (cf. Kallio 1970, Nordén & Larsson 2000), and of mycelia, will contribute to strictly spatial variation in abundance. Both kinds of dispersal are likely to operate on scales where variation is reflected as spatial variation in our data set. Dahlberg & Stenlid (1990) and Dahlberg (1997) demonstrate clonal diameters up to 30 and 27 m, respectively, for *Suillus bovinus* and *S. variegatus*, by somatic incompatibility pairings of isolates, and find mycelial spread to be more important than spore dispersal in areas with low disturbance.

Positions of plots in which we have studied fungi along the four plant ordination axes (vegetational coenoclines) explained the same amount of variation in fungal species abundance as

spatial variables. Forty percent of this variation was strictly due to these vegetational variables, indicating that the species composition of plants is a good predictor of fungal species composition, in part explaining variation in fungal species composition other than the variation explained by environmental variables. Most likely this is because plants (notably bryophytes) often respond to the same, complex sets of environmental conditions as fungi. A consequence of this result is that forest typifications based upon plants are likely to have relevance for fungi as well (cf. Pirk 1948, Barkman 1987).

COMMENTS ON FIELD METHODOLOGY AND INTEGRATED APPROACHES TO MACROFUNGI AND PLANTS

The results obtained by the approach adopted in this study, notably the use of a systematic sampling design as basis for multivariate analyses of patterns, show that this is a powerful approach for elucidating the ecology of fungi. The evaluations of sampling designs by R. Økland & Eilertsen (1993), and of ordination methods by R. Økland & Eilertsen (1993) and T. Økland (1996), both indicating a slight preference for DCA over LNMDS, are also supported by this study.

Since a general discussion of problems related to methodology in studies of macrofungal occurrence patterns will be provided in another study (E. Bendiksen, in prep.), among others with reference to the present study, we will restrict ourselves here to one methodological problem: the choice of plot size. Viewed in the light of our results, the 16-m^2 plot appears as an acceptable compromise; good arguments exist for smaller as well as larger plots . The 16-m^2 plot is too large to represent variation along fine-scaled gradients such as the deciduous litter and paludification/median soil moisture gradients – *c.* 50% of the 16-m^2 plots are inhomogeneous with respect to site-type. However, the nested plot design used in the present study also opens for autecological and other studies based upon 1584 1-m^2 plots (cf. Austin 1981, R. Økland & Eilertsen 1993). A plot size of 1 m^2 may be particularly well suited for saprotrophs, sometimes associated with very local substrates, while the occurrence of mycorrhizal fungi is mostly determined by factors operating on a broader scale (cf. placement of trees).

GENERAL CONCLUSIONS

The closely corresponding results obtained by use of parallel DCA and LNMDS ordinations of fungal abundance data, and the parallel between fungal and vegetational coenoclines, demonstrate (1) that distributional patterns of terricolous macrofungi and plants within forests to a large extent are caused by the same major environmental complex-gradients and (2) that the same field and analytical methods are applicable to both groups of organisms.

Just like the corresponding study of plants in the same plots has provided a valuable basis for studying vegetation dynamics over short time-spans (R. Økland 1995d, R. Økland & Eilertsen 1996, T. Økland et al. 2001), this study should provide a good starting-point for studies of changes in the funga with time; natural and due to man-induced environmental change. The high species richness of the macrofunga, also at oligotrophic sites, and that fact that this funga represents two major and

several minor ecological life-form types, make macrofungi important as indicators of environmental change. Furthermore, an integrated study where many groups of organisms are studied in the same permanent plots opens for new insights of many kinds.

ACKNOWLEDGEMENTS

The present study was financially supported by the TVLF (Supplies and Effects of Long-Distance Airborne Pollutants) programme of The Norwegian Research Council. Additional financial support has been obtained from Norwegian Institute for Nature Research.

Thanks are due to The Directorate of State Forests, Grenland (and later Sørlandet) district, for free use of the old log cabin at 'Den svarte tjønna', our base camp, to Katriina Bendiksen and Arnodd Håpnes for participation in field work, and to the Botanical Museums in Oslo and Oulu (Finland), for providing the first author with good working facilities during important phases of the work.

REFERENCES

Abuzinadah, R.A., Finlay, R.D. & Read, D.J. 1986. The role of proteins in the nitrogen nutrition of ectomycorrhizal plants. II. Utilisation of protein by mycorrhizal plants of Pinus contorta. – New Phytol. 103: 495-506.

Abuzinadah, R.A. & Read, D.J. 1986a. The role of proteins in the nitrogen nutrition of ectomycorrhizal plants. I. Utilization of peptides and proteins by ectomycorrhizal fungi. – New Phytol. 103: 481-493.

Abuzinadah, R.A. & Read, D.J. 1986b. The role of proteins in the nitrogen nutrition of ectomycorrhizal plants. III. Protein utilisation by *Betula*, *Picea* and *Pinus* in mycorrhizal association with Hebeloma crustuliniforme. – New Phytol. 103: 507-514.

Abuzinadah, R.A. & Read, D.J. 1988. Amino acids as nitrogen sources for ectomycorrhizal fungi: utilisation of individual amino acids. – Trans. br. mycol. Soc. 91: 473-479.

Abuzinadah, R.A. & Read, D.J. 1989a. The role of ectomycorrhizal fungi in the nitrogen nutrition of ectomycorrhizal plants. IV. The utilisation of peptides by birch (*Betula pendula* Roth.) infected with different mycorrhizal fungi. – New Phytol. 112: 55-60.

Abuzinadah, R.A. & Read, D.J. 1989b. The role of proteins in the nitrogen nutrition of ectomycorrhizal plants. V. Nitrogen transfer in birch (*Betula pendula*) grown in association with mycorrhizal and non mycorrhizal fungi. – New Phytol. 112: 61-68.

Agerer, R. 1985. Zur Ökologie der Mykorrhizapilze. – Biblthca mycol. 97: 1-160.

Agerer, R. 1990. Gibt es Eine Korrelation zwischen Anzahl der Ektomykorrhizen und Häufigkeit ihrer Fruchtkörper? – Z. Mykol. 56: 155-158.

Agerer, R., Taylor, A.F.S. & Treu, R. 1998. Effects of acid irrigation and liming on the production of fruit bodies by ectomycorrhizal fungi. – Pl. Soil 199: 83-89.

Agerer, R. & Waller, K. 1993. Mycorrhizae of *Entoloma saepium*: parasitism or symbiosis? – Mycorrhiza 3: 145-154.

Ahti, T., Hämet-Ahti, L. & Jalas, J. 1968. Vegetation zones and their sections in northwestern Europe. – Annls bot. fenn. 5: 169-211.

Anonymous, 1990. STATGRAPHICS, Version 5. – Manugistics, Inc., Rockville, Maryland.

Anonymous, 1995. Overvåking av langtransportert forurenset luft og nedbør. Årsrapport 1994. – St. Progm Forurensningsovervåking Rapp. 628: 1-282.

Arnebrant, K. & Söderström, B. 1992. Effects of different fertilizer treatments on ectomycorrhizal colonisation potential in two Scots pine forests in Sweden. – For. Ecol. Mgmt 53: 77-89.

Arnolds, E. 1988. The changing macromycete flora of the Netherlands. – Trans. br. mycol. Soc. 90: 391-406.

Arnolds, E. 1991. Decline of ectomycorrhizal fungi in Europe. – Agric. Ecosyst. Environ. 35: 209-244.

Arnolds, E. 1992a. The analysis and classification of fungal communities with special reference to macrofungi. – In: Winterhoff, W. (ed.), Fungi in vegetation science. Kluwer, Dordrecht, pp. 7-47.

Arnolds, E. 1992b. Macrofungal communities outside forests. – In: Winterhoff, W. (ed.), Fungi in vegetation science. Kluwer, Dordrecht, pp. 113-149.

Aune, B. 1993. Temperaturnormaler, normalperiode 1961-1990. – Norske Meteorol. Inst. Rapp. Klima 1993: 2: 1-63.

Austin, M.P. 1981. Permanent quadrats: an interface for theory and practice. – Vegetatio 46-47: 1-10.

Bader, P., Jansson, S. & Jonsson, B.G. 1995. Wood-inhabiting fungi and substratum decline in selectively logged boreal spruce forest. – Biol. Conserv. 72: 355-362.

Barkman, J.J. 1987. Methods and results of mycocoenological research in the Netherlands. – In: Pacioni, G. (ed.), Studies on fungal communities, Univ. l'Aquila, Italy, pp. 7-38.

Bendiksen, E. 1980. *Cortinarius*, underslekter *Leprocybe*, *Sericeocybe*, *Myxacium* og *Telamonia* i forskjellige suksesjonsstadier av granskogssamfunn i Lunner, Oppland. – Cand. scient Thesis, Univ. Oslo, unpubl.

Bendiksen, E. 1981. Mykorrhizasopp i forskjellige suksesjonssstadier av granskogssamfunn i Lunner, Oppland. – K. norske Vidensk. Selsk. Mus. Rapp. bot. Ser. 1981: 5: 246-258.

Bendiksen, E., Bendiksen, K. & Brandrud, T.E. 1993. *Cortinarius* subgenus *Myxacium* section *Colliniti* (Agaricales) i Fennoscandia, with special emphasis on the Arctic-alpine zones. – Sommerfeltia 19: 1-37.

Bendiksen, E. & Salvesen, P.H. 1992. Flora og vegetasjon på Røverkollen. Forslag til vern av Ravnkollen, Røverkollen og Bånkallåsen. – Oslo kommune, Etat for miljørettet helsevern, Oslo.

Blaschke, H. 1986. Einfluss von saurer Beregnung und Kalkung auf die Biomasse und Mykorrhizierung der Feinwurzeln von Fichten. – Forstw. Cbl. 105: 324-329.

Blomgren, M. 1994. Studier av storsvampfloran i bestånd' av tall och contortatall. – Sver. LantbrUniv. Instn skoglig Landskapsvård Rapp. 57: 1-136.

Boddy, L. 1983. Effect of temperature and water potential on growth rate of wood-rotting basidiomycetes. – Trans. br. mycol. Soc. 80: 141-149.

Boddy, L. 1999. Saprotrophic cord-forming fungi: meeting the challenge of heterogeneous environments. – Mycologia 91: 13-32.

Børset, O. 1979. Inventering av skogreservater på statens grunn. – NF-Rapp. (Inst. Naturforvaltning, Norg. Landbrukshøgskole) 1979: 3: 1-451.

Boertmann, D. 1995. The genus *Hygrocybe*. (Fungi of Northern Europe - Vol. 1). – Svampetryk, Greve.

Bohus, G. 1984. Studies on the pH requirement of soil-inhabiting mushrooms: the R-spectra of mushroom assemblages in deciduous forest communities. – Acta bot. hung. 30: 155-171.

Borcard, D., Legendre, P. & Drapeau, P. 1992. Partialling out the spatial component of ecological variation. – Ecology 73: 1045-1055.

Brandrud, T.E. 1987. Mycorrhizal fungi in 30 years old, oligotrophic spruce (*Picea abies*) plantation in SE Norway. A one-year permanent plot study. – Agarica 8: 48-58.

Brandrud, T.E. 1995. The effects of experimental nitrogen addition on the ectomycorrhizal fungus flora in an oligotrophic spruce forest at Gårdsjön, Sweden. – For. Ecol. Mgmt 71: 111-122.

Brandrud, T.E., Lindström, H., Marklund, H., Melot, J. & Muskos, S. 1990-97. *Cortinarius*, flora photographica (English version). Vols 1–4. – Cortinarius HB, Härnösand.

Brandrud, T.E. & Timmermann, V. 1998. Ectomycorrhizal fungi in the NITREX site at Gårdsjön, Sweden; below and above-ground responses to experimentally-changed nitrogen inputs 1990-1995. – For. Ecol. Mgmt 101: 207-214.

Brown, D.H. & Bates, J.W. 1990. Bryophytes and nutrient cycling. – Bot. J. Linn. Soc. 104: 129-147.

Busby, J.R., Bliss, L.C. & Hamilton, C.D. 1978. Microclimate control of growth rates and habitats of the boreal forest mosses, *Tomentypnum nitens* and *Hylocomium splendens*. – Ecol. Monogr. 48: 95-110.

Chapin, F. S. III, Moilanen, L. & Kielland, K. 1993. Preferential use of organic nitrogen for growth by a nonmycorrhizal arctic sedge. – Nature 361: 150-153.

Coleman, M.D. & Bledsoe, C.S. 1989. Pure culture response of ectomycorrhizal fungi to imposed water stress. – Can. J. Bot. 67: 29-39.

Dahl, E., Gjems, O. & Kielland-Lund, J. Jr. 1967. On the vegetation types of Norwegian conifer forests in relation to the chemical properties of the humus layer. – Meddr Norske SkogforsVesen 23: 504-531.

Dahlberg, A. 1991. Dynamics of ectomycorrhizal fungi in a Swedish coniferous forest: a five year survey of epigeous sporocarps. – In: Dahlberg, A. Ectomycorrhiza in coniferous forest: structure and dynamics of populations and communities. Swed. Univ. Agric. Sci., Dept. For. Mycol. Pathol., Uppsala, pp. 1: 1-26.

Dahlberg, A. 1997. Population ecology of *Suillus variegatus* in old Swedish Scots pine forests. – Mycol. Res. 101: 47-54.

Dahlberg, A. 2001. Community ecology of ectomycorrhizal fungi: an advancing interdisciplinary field. – New Phytol. 150: 555-562.

Dahlberg, A., Jonsson, L. & Nylund, J.-E. 1997. Species diversity and distribution of biomass above and below ground among ectomycorrizal fungi in an old-growth Norway spruce forest in south Sweden. – Can. J. Bot. 75: 1323-1335.

Dahlberg, A. & Stenlid, J. 1990. Population structure and dynamics in *Suillus bovinus* as indicated by spatial distribution of fungal clones. – New Phytol. 115: 487-493.

Dahlberg, A. & Stenström, E. 1991. Dynamic changes in nursery and indigenous mycorrhiza of *Pinus sylvestris* seedlings planted out in forests and clearcuts. – Pl. Soil: 136: 73-86.

Dargie, T.C.D. 1984. On the integrated interpretation of indirect site ordinations: a case study using semi-arid vegetation in south-eastern Spain. – Vegetatio 55: 37-55.

Dighton, J. 1988. Some effects of acid rain on mycorrhizas of Scots pine and potential consequences for forest nutrition. – Comm. Eur. Commun. Air Pollut. Res. Rep. 12: 104-111.

Dighton, J. & Skeffington, R.A. 1987. Effects of artificial acid precipitation on mycorrhizas of Scots pine seedlings. – New Phytol. 107: 191-202.

Dighton, J., Skeffington, R.A., & Brown, K.A. 1986. The effects of sulphuric acid (pH 3) on roots and mycorrhizas of *Pinus sylvestris*. – In: Gianinazzi-Pearson, V. & Pearson, S. (eds.), Physiological and genetical aspects of mycorrhizae. Proc. 1st Eur. Symp. Mycorrh., Dijon 1985, Paris, pp. 739-743.

Dix, N.J. 1984. Minimum water potentials for growth of some litter-decomposing agarics and other basidiomycetes. – Trans. br. mycol. Soc. 83: 152-153.

Dix, N.J. & Webster, J. 1995. Fungal ecology. – Chapman & Hall, London.

Duddridge, J.A., Malibari, A. & Read, D.J. 1980. Structure and function of mycorrhizal rhizomorphs with special reference to their role in water transport. – Nature 287: 834-836.

During, H.J. & Verschuren, G.A.C.M. 1988. Influence of the tree canopy on terrestrial bryophyte communities: microclimate and chemistry of throughfall. – In: Barkman, J.J. & Sýkora, K.V. (eds.), Dependent plant communities, SPB Acad. Publ., The Hague, pp. 99-110.

Eilertsen, O. 1991. Vegetation patterns and structuring processes in coastal shell-beds at Akerøya, Hvaler, SE Norway. – Sommerfeltia 12: 1-90.

Eilertsen, O, Økland, R.H., Økland, T. & Pedersen, O. 1990. Data manipulation and gradient length estimation in DCA ordination. – J. Veg. Sci. 1: 261-270.

Eilertsen, O. & Often, A. 1994. Terrestrisk naturovervåking. Vegetasjonsøkologiske undersøkelser av boreal bjørkeskog i Gutulia nasjonalpark. – Norsk Inst. Naturforsk. Oppdragsmeld. 285: 1-69.

Eilertsen, O. & Pedersen, O. 1989. Virkning av nedveiing og artsfjerning ved DCA-ordinasjon av vegetasjonsøkologiske datasett. – Univ. Trondheim VitenskMus. Rapp. bot. Ser. 1988: 1: 5-18.

Eilertsen, O., Stabbetorp, O.E. & Bendiksen, E. 1997a. Vegetasjonsundersøkelser. – Akt. Skogforsk 1997: 5: 17-20.

Eilertsen, O., Stabbetorp, O.E., Aarrestad, P.A. & Bendiksen, E. 1997b. Counteractions against

acidification in forest ecosystems: Vegetation dynamics in a forested catchment after dolomite application in Gjerstad, S Norway. – BIOGEOMON '97, J. Conf. Abstr. 2: 167.
Entry, J.A., Cromack, K., Jr., Stafford, S.G. & Castellano, M.A. 1987. The effect of pH and aluminium concentration on ectomycorrhizal formation in *Abies balsamea*. – Can. J. For. Res. 17: 865-871.
Faith, D. P., Minchin, P. R. & Belbin, L. 1987. Compositional dissimilarity as a robust measure of ecological distance. – Vegetatio 69: 57-68.
Fellner, R. 1993. Air polution and mycorrhizal fungi in central Europe. – In: Pegler, D.N., Boddy, L., Ing, B. & Kirk, P.M. (eds.), Fungi of Europe: investigation, recording and conservation. Royal Botanic Gardens, Kew, pp. 239-250.
Fitje, A. & Strand, L. 1973. Tremålingslære, ed. 2. – Universitetsforlaget, Oslo.
Førland, E.J. 1993. Nedbørnormaler normalperiode 1961-1990. – Norske meteorol. Inst. Rapp. Klima 1993: 39: 1-63.
Frankland, J.C., Lindley, D.K. & Swift, M.J. 1978. A comparison of two methods for the estimation of mycelial biomass in leaf litter. – Soil Biol. Biochem. 10: 323-333.
Fremstad, E. 1997. Vegetasjonstyper i Norge. – Norsk Inst. Naturforsk. Temahefte 12: 1-279.
Frisvoll, A.A., Elvebakk, A., Flatberg, K.I. & Økland, R.H. 1995. Sjekkliste over norske mosar. – Norsk Inst. Naturforsk. Temahefte 4: 1-104.
Gardes, M. & Bruns, T.D. 1996. Community structure of ectomycorrhizal fungi in a *Pinus muricata* forest: above and below-ground views. – Can. J. Bot. 74: 1572-1583.
Gauch, H.G., Jr. 1982a. Multivariate analysis in community ecology. – Camb. Stud. Ecol. 1: 1-298.
Gauch, H.G., Jr. 1982b. Noise reduction by eigenvector ordinations. – Ecology 63: 1643-1649.
Göbl, F. 1986. Wirkung simulierter saurer Niederschläge auf Bödem und Fichtenjungpflanzen im Gefässversuch. III. Mykorrhizauntersuchungen. – Centbl. Ges. Forstwesen 103: 89-107.
Grace, J. B. 1999. The factors controlling species density in herbaceous plant communities: an assessment. – Perspect. Pl. Ecol. Syst. 2: 1-28.
Green, R. N., Trowbridge, R. L. & Klinka, K. 1993. Towards a taxonomic classification of humus forms. – For. Sci. Monogr. 29: 1-49.
Greenacre, M.J. 1984. Theory and applications of correspondence analysis. – Academic Press, London.
Griffith, G.S. & Boddy, L. 1991. Fungal decomposition of attached angiosperm twigs. III. Effect of water potential and temperature on fungal growth, survival and decay of wood. – New Phytol. 117: 259-269.
Gulden, G., Høiland, K., Bendiksen, K., Brandrud, T.E., Foss, B.S., Jenssen, H.B. & Laber, D. 1992. Macromycetes and air pollution. Mycocoenological studies in three oligotrophic spruce forests in Europe. – Biblthca mycol. 144: 1-81.
Haas, H. 1932. Die bodenbewohnenden Grosspilze in den Waldformationen einiger Gebiete von Württemberg. – Beih. Bot. Centbl. Abt. II 50: 35-134.
Hafsten, U. 1985. The immigration and spread of spruce forest in Norway, traced by biostratigraphical studies and radiocarbon datings. A preliminary report. – Norsk geogr. Tidsskr. 39: 99-108.
Hansen, L. & Knudsen, H. (eds) 1992. Nordic macromycetes. Vol. 2. Polyporales, Boletales, Agaricales, Russulales. – Nordsvamp, Copenhagen.
Hansen, L. & Knudsen, H. (eds) 1997. Nordic macromycetes. Vol. 3. Heterobasidioid, aphyllophoroid and gastromycetoid basidiomycetes. – Nordsvamp, Copenhagen.
Hansen, L. & Knudsen, H. (eds) 2000. Nordic macromycetes. Vol. 1. Ascomycetes. – Nordsvamp, Copenhagen.
Hansen, P.A. 1988a. Prediction of macrofungal occurrence in Swedish beech forests from soil and litter variable models. – Vegetatio 78: 31-44.
Hansen, P.A.1988b. The quantitative occurrence of macrofungal species in Sweedish beech forests

in relation to soil physico-chemical properties. – In: Hansen, P.A. Statistical modelling of soil macrofungal relationships in South Swedish beech forests. Fil. dr. Thesis, Dept of Ecology, Univ. Lund, Sweden, pp. 4: 1-19.

Harvey, A.E., Larsen, M.J. & Jurgensen, M.F. 1976. Distribution of ectomycorrhizae in a mature Douglas-fir/larch forest soil in Western Montana. – For. Sci. 22: 393-398.

Heikkinen, R. 1991. Multivariate analysis of esker vegetation in southern Häme, S Finland. – Annls bot. fenn. 28: 201-224.

Hesselman, H. 1926. Studier över barrskogens humustäcke, dess egenskaper ock beroende av skogsvården. – Meddn St. SkogsförsAnst. 22: 169-552.

Hill, M.O. 1979. DECORANA . A Fortran program for detrended correspondence analysis and reciprocal averaging. – Cornell Univ., Ithaca, New York.

Hill, M.O. & Gauch,, H.G. 1980. Detrended correspondence analysis: an improved ordination technique. – Vegetatio 42: 47-58.

Hintikka, V. 1960. Das Verhalten einige *Mycena*-Arten zum pH sowie deren Einfluss auf die Azidität der Humusschicht der Wälder. – Karstenia 5: 107-121.

Hintikka, V. 1988. On the macromycete flora in oligotrophic pine forests of different ages in South Finland. – Acta bot. fenn. 136: 89-94.

Høiland, K. 1984. *Cortinarius* subgenus *Dermocybe*. – Opera Bot. 71: 1-113.

Høiland, K. 1986. Storsoppfloraens reaksjon overfor forsuring, med spesiell vekt på mykorrhiza-soppene. Undersøkelse foretatt i Norsk institutt for skogforsknings forskningsfelter i Åmli, Aust-Agder. – Miljøverndepartementet, Rapp. T-671: 1-62.

Høiland, K. 1990. The genus *Gymnopilus* in Norway. – Mycotaxon 39: 257-279.

Høiland, K. 1993. Pollution, a great disaster to mycorrhiza? – Agarica 12: 65-88.

Høiland, K. & Bendiksen, E. 1997. Biodiversity of wood-inhabiting fungi in a boreal coniferous forest in Sør-Trøndelag County, Central Norway. – Nord. J. Bot. 16: 643-659.

Høiland, K. & Jenssen, H.B. 1994. Ground vegetation: mycoflora. – Ecol. Stud. 104: 230-238.

Holmer, L. & Stenlid, J. 1991. Population structure and mating system in *Marasmius androsaceus* Fr. – New Phytol. 119: 307-314.

Horton, T.R. & Bruns, T.D. 2001. The molecular revolution in ectomycorrhizal ecology: peeking into the black-box. – Molec. Ecol. 10: 1855-1871.

Hung, L.-L. & Trappe, J.M. 1983. Growth variation between and within species of ectomycorrhizal fungi in response to pH in vitrio. – Mycologia 75: 234-241.

Hytteborn, H., Liu, Q. & Verwijst, T. 1991. Natural disturbance and gap dynamics in a Swedish boreal spruce forest. – In: Nakagoshi, N. & Golley, F.B. (eds), Coniferous forest ecology from an international perspective. SPB Acad. Publ., The Hague, pp. 93-108.

Johansson, T. 1996. Site index curves for European aspen (*Populus tremula* L.) growing on forest land of different soils in Sweden. – Silva fenn. 30: 437-458.

Jonsson, T., Kokalj, S., Finlay, R. & Erland, S. 1999. Ectomycorrhizal community structure in a limed spruce forest. – Mycol. Res. 103: 501-508.

Kalamees, K. 1979. The composition and seasonal dynamics of the fungal cover on mineral soil. – Scripta mycol. 9: 5-70.

Kallio, T. 1970. Aerial distribution of the root-rot fungus *Fomes annosum* (Fr.) Cooke in Finland. – Acta for. fenn.107: 1-55.

Keane, K.D. & Manning, W.J. 1987. Effects of ozone and simulated rain and ozone and sulfur dioxide on mycorhizal formation in paper birch and white pine. – In: Perrey, R., Harrison, R.M., Bell, J.N.B. & Lester, J.N. (eds.), Acid rain, scientific and technical advances. Selper, London, pp. 608-613.

Kendall, M.G. 1938. A new measure of rank correlation. – Biometrika 30: 81-93.

Kenkel, N.C. & Orlóci, L. 1986. Applying metric and nonmetric multidimensional scaling to ecological studies: some new results. – Ecology 67: 919-928.
Kent, M. & Ballard, J. 1988. Trends and problems in the application of classification and ordination methods in plant ecology. – Vegetatio 78: 109-124.
Kielland, K. 1994. Amino acid absorption by arctic plants: implication for plant nutrient and nitrogen cycling. – Ecology 75: 2373-2383.
Kielland-Lund, J. 1981. Die Waldgesellschaften SO-Norwegens. – Phytocoenologia 9: 53-250.
Kits van Waveren, E. 1985. The Dutch, French, and British species of *Psathyrella*. – Persoonia Suppl. 2: 1-300.
Kivenheimo, V.J. 1947. Untersuchungen über die Wurzelsysteme der Samenpflanzen in der Bodenvegetation der Wälder Finnlands. – Annls bot. Soc. zool.-bot. fenn. Vanamo 22: 2: 1-181.
Knox, R.G. 1989. Effects of detrending and rescaling on correspondence analysis: solution stability and accuracy. – Vegetatio 83: 129-136.
Korhonen, M. 1995. New boletoid fungi in the genus *Leccinum* from Fennoscandia. – Karstenia 35: 53-66.
Koske, R.E. & Tessier, B. 1986. Growth of some wood and litter-decay basidiomycetes at reduced water potential. – Trans. br. mycol. Soc. 86: 156-158.
Krieglsteiner, G.J. 1977. Die Makromyzeten der Tannen-Mischwälder des Inneren Schwäbisch-Fränkischen Waldes (Ostwürttemberg) mit besonderer Berücksichtigung des Welzheimer Waldes. – Lempp, Schwäbisch Gmünd.
Kruskal, J.B. 1964a. Multidimensional scaling by optimizing goodness of fit to a nonmetric hypothesis. – Psychometrika 29: 1-27.
Kruskal, J.B. 1964b. Nonmetric multidimensional scaling: a numerical method. – Psychometrika 29: 115-129.
Kruskal, J.B., Young, F.W. & Seery, J.B. 1973. How to use KYST, a very flexible program to do multidimensioanl scaling an unfolding. – Bell Labs, Murray Hill, New Jersey, unpubl.
Kujala, V. 1926. Untersuchungen über die Waldvegetation in Süd- und Mittelfinnland. I. Zur Kenntnis des ökologisch-biologischen Charakters der Waldpflanzenarten unter spezieller Berücksichtigung der Bildung von Pflanzenvereinen. B. Laubmoose. – Communtnes Inst. Quaest. for. finl. 10: 2: 1-59.
Kuyper, T.W. 1989. Auswirkungen der Walddüngung auf die Mykoflora. – Beitr. Kenntn. Pilze Mitteleur. 5: 5-20.
Laaksonen, K. 1976. The dependence on mean air temperatures upon latitude and altitude in Fennoscandia (1921–1950). – Annls Acad. scient. fenn. Ser. A 3 Geol. Geogr. 119: 1-19.
Laiho, O. 1970. *Paxillus involutus* as a mycorrhizal symbiont of forest trees. – Acta for. fenn. 106: 1-72.
Legendre, P. 1990. Quantitative methods and biogeographic analysis. – NATO ASI Ser. Ser. G Ecol. Sci. 22: 9-34.
Legendre, P. 1993. Spatial autocorrelation: trouble or new paradigm? – Ecology 74: 1659-1673.
Lehmann, P.F. & Hudson, H.J. 1977. The fungal succession on normal and urea-treated pine needles. – Trans. br. mycol. Soc. 68: 221-228.
Lewis Smith, R.I. 1978. Summer and winter concentrations of sodium, potassium and calcium in some maritime Antarctic cryptogams. – J. Ecol. 66: 891-909.
Lid , J. & Lid, D.T. 1994. Norsk flora, ed. 6. – Norske Samlaget, Oslo.
Lindahl, B.O., Taylor, A.F.S. & Finlay, R.D. 2002. Defining nutritional constraints on carbon cycling in boreal forests – towards a less “phytocentric” perspective. – Pl. Soil 242: 123-135.
Lindblad, I. 1998. Wood-inhabiting fungi on fallen logs of Norway spruce: relations to forest

management and substrate quality. – Nord. J. Bot. 18: 243-255.
Loman, A.A. 1965. The lethal effect of periodic high temperatures on certain lodgepole pine slash decaying besidiomycetes. – Can. J. Bot. 43: 334-338.
Lukkala, O.J. 1942. Sateen mittauksia erilaissa metsiköissä. – Acta for. fenn. 50: 23: 1-13. (Deutsches Ref.: Niederschlagsmessungen in verschiedenartigen Beständen)
Lundeberg, G. 1970. Utilisation of various nitrogen sources, in particular bound soil nitrogen, by mycorrhizal fungi. – Stud. for. suec. 79: 1-95.
Magurran, A.E. 1988. Ecological diversity and its measurement. – Croom Helm, London.
Mahendrappa, K.D. & Kingston, D.G.O. 1982. Prediction of throughfall quantities under different forest stands. – Can. J. For. Res. 12: 474-481.
Mehmann, B., Egli, S., Braus, G.H. & Brunner, I. 1995. Coincidence between molecular or morphologically classified ectomycorrhizal morphotypes and fruitbodies in a spruce forest. – In: Stocchi, V., Bonfante, P. & Nuti, M. (eds.), Biotechnology of ectomycorrhizae, Plenum, New York, pp. 229-239.
Mehus, H. 1986. Fruit body production of macrofungi in some North Norwegian forest types. – Nord. J. Bot. 6: 679-702.
Melin, E. 1924. Über den Einfluss der Wasserstoffionenkonzentration auf die Virulenz der Wurzelpilze von Kiefer und Fichte. – Bot. Not. 1924: 38-48.
Menge, J.A. & Grand, L.F. 1978. Effect of fertilization on production of epigeous basidiocarps by mycorrhizal fungi in loblolly pine plantations. – Can. J. Bot. 56: 2357-2362.
Metsänheimo, K. 1982. Luoteis-Lapin syyssienisadosta ja -lajistosta vuosina 1976-78. – Pro gradu Thesis, Bot. Mus, Univ. Oulu, unpubl.
Mexal, J. & Reid, P.P. 1973. The growth of selected mycorrhizal fungi in response to induced water stress. – Can. J. Bot. 51: 1579-1588.
Meyer, F.H. 1964. The role of the fungus *Cenococcum graniforme* (Sow.) Ferd. et Winge in the formation of mor. – In: Jongerius, J. (ed.), Soil micromorphology, Elsevier, Amsterdam, pp. 23-31.
Mikola, P., Hahl, J. & Torniainen, E. 1966. Vertical distribution of mycorrhizae in pine forests with spruce undergrowth – Annls bot. fenn. 3: 406-409.
Mikola, P. & Laiho, O. 1962. Mycorrhizal relations in the raw humus layer of northern spruce forests. – Communtnes Inst. for. fenn. 55: 1-13.
Miller, O.K. & Laursen, G.A. 1978. Ecto- and endomycorrhizae of arctic plants at Barrow, Alaska. – In: Thieszen, L. (ed.), Vegetation and production ecology of an Alaskan arctic tundra, Springer, New York, pp. 229-237.
Minchin, P.R. 1986. How to use ECOPAK: an ecological database system. – CSIRO Inst. biol. Res. Div. Wat. Land Res. techn. Mem. 86: 6: 1-138.
Minchin, P.R. 1987. An evaluation of the relative robustness of techniques for ecological ordination. – Vegetatio 69: 89-107.
Minchin, P.R. 1990. DECODA Version 2.01. – Dept. Biogeogr. Geomorph., Aust. natn. Univ., Canberra.
Modess, O. 1941. Zur Kenntnis der Mykorrhizabildner von Kiefer und Fichte. – Symb. bot. upsal. 5: 11: 1-147.
Moen, A. 1998. Nasjonalatlas for Norge: Vegetasjon. – Hønefoss, Statens Kartverk.
Molina, R., Massicotte, H. & Trappe, J.M. 1992. Specificity phenomena in mycorrhizal symbiosis: Community-ecological consequences and practical implications. – In: Allen, M.J. (ed.), Mycorrhizal functioning. An integrative plant-fungal process, Chapman & Hall, New York, pp. 357-423.
Molina, R. & Trappe, J.M. 1982. Patterns of ectomycorrhizal host specificity and potential among Pacific Northwest conifers and fungi. – For. Sci. 28: 423-458.

Moser, M. 1964. Transpirationsschutz bei höheren Pilzen. – Schweiz. Z. Pilzk. 42: 50-54.
Moser, M. 1993. Fungal growth and fructification under stress conditions. – Ukr. bot. J. 50(3): 5-11.
Newell, K. 1984. Interaction between two decomposer basidiomycetes and a collembolan under sitka spruce: distribution, abundance and selective grazing. – Soil Biol. Biochem. 16: 227-233.
Noordeloos, M.E. 1989. Bemerkungen über die Sektion *Rhodopolia* in Mitteleuropa. – Beitr. Kenntn. Pilze Mitteleur. 5: 41-50.
Nordén, B. & Larsson, K.-H. 2000. Basidiospore dispersal in the old-growth forest fungus Phlebia centrifuga (Basidiomycetes). – Nord. J. Bot. 20: 215-219.
Nordin, A., Högberg, P. & Näsholm, T. 2001. Soil nitrogen form and plant nitrogen uptake along a boreal forest productivity gradient. – Oecologia 129: 125-132.
Norkrans, B. 1950. Studies in growth and cellulolytic enzymes of *Tricholoma*, with special reference to mycorrhiza formation. – Symb. bot. upsal. 11: 1: 1-126.
Økland, R.H. 1989. A phytoecological study of the mire Northern Kisselbergmosen, SE Norway. I. Introduction, flora, vegetation and ecological conditions. – Sommerfeltia 8: 1-172.
Økland, R.H. 1990. Vegetation ecology: theory, methods and applications with reference to Fennoscandia. – Sommerfeltia Suppl. 1: 1-233.
Økland, R.H. 1995a. Changes in the occurrence and abundance of plant species in a Norwegian boreal coniferous forest, 1988-1993. – Nord. J. Bot. 15: 415-438.
Økland, R.H. 1995b. Boreal coniferous forest vegetation in the Solhomfjell area, S Norway: structure, dynamics and change, with particular reference to effects of long distance airborne pollution. – Sommerfeltia Suppl. 6: 1-33.
Økland, R.H. 1995c. Persistence of vascular plants in a Norwegian boreal coniferous forest. – Ecography 18: 3-14.
Økland, R.H. 1995d. Population biology of the clonal moss *Hylocomium splendens* in Norwegian boreal spruce forests. I. Demography. – J. Ecol. 83: 697-712.
Økland, R.H. 1995e. Bryophyte and lichen persistence patterns in a Norwegian boreal coniferous forest. – Lindbergia 19: 50-62.
Økland, R.H. 1996. Are ordination and constrained ordination alternative or complementary strategies in general ecological studies? – J. Veg. Sci. 7: 289-292.
Økland, R.H. 1997. Population biology of the clonal moss *Hylocomium splendens* in Norwegian boreal spruce forests. III. Six-year demographic variation in two areas. – Lindbergia 22: 49-68.
Økland, R.H. 1999. On the variation explained by ordination and constrained ordination axes. – J. Veg. Sci. 10: 131-136.
Økland, R.H. 2000. Population biology of the clonal moss *Hylocomium splendens* in Norwegian boreal spruce forests. 5. Consequences of the vertical position of individual shoot segments. – Oikos 88: 449-469.
Økland, R.H. 2003. Partitioning the variation in a sample-by-species data matrix on *n* sets of explanatory variables. – J. Veg. Sci. 14: 693-700.
Økland, R.H. & Bendiksen, E. 1985. The vegetation of the forest-alpine transition in the Grunningsdalen area, Telemark, SE Norway. – Sommerfeltia 2: 1-224.
Økland, R.H. & Eilertsen, O. 1993. Vegetation - environment relationships of boreal coniferous forests in the Solhomfjell area, Gjerstad, S Norway. – Sommerfeltia 16: 1-254.
Økland, R.H. & Eilertsen, O. 1994. Canonical correspondence analysis with variation partitioning: some comments and an application. – J. Veg. Sci. 5: 117-126.
Økland, R.H. & Eilertsen, O. 1996. Dynamics of understory vegetation in a Norwegian old-growth boreal coniferous forest, during a six-year period. – J. Veg. Sci. 7: 747-762.

Økland, T. 1988. An ecological approach to the investigation of a beech forest in Vestfold, SE. Norway. – Nord. J. Bot. 8: 375-407.

Økland, T. 1990. Vegetational and ecological monitoring of boreal forests in Norway. I. Rausjømarka in Akershus county, SE Norway. – Sommerfeltia 10: 1-52.

Økland, T. 1996. Vegetation-environment relationships of boreal spruce forests in ten monitoring reference areas in Norway. – Sommerfeltia 22: 1-349.

Økland, T., Bakkestuen, V., Økland, R. H. & Eilertsen, O. 2001. Vegetasjonsendringer i Nasjonalt nettverk av flater for intensivovervåking i skog. – Norsk Inst. Jord- Skogkartlegging Rapp. 2001: 8: 1-46.

Økland, T., Økland, R. H. & Steinnes, E. 1999. Element concentrations in the boreal forest moss *Hylocomium splendens*: variation related to gradients in vegetation and local environmental factors. – Pl. Soil 209: 71-83.

Østmoe, K. 1979. Økologiske og sosiologiske undersøkelser av storsopper i barskogssamfunn i Ås (Cladonio-Pinetum, Eu-Piceetum myrtilletosum, Melico-Piceetum typicum og Eu-Piceetum athyrietosum). – Cand. real. Thesis, Univ. Oslo, unpubl.

Oftedahl, C. 1980. Geology of Norway. – Norg. geol. Unders. 356: 3-114.

Ohenoja, E. 1989. Forest fertilization and fruiting body production in fungi. – Atti Centro Stud. Fl. mediterr. 7: 233-252.

Ohenoja, E. 1993. Effect of weather conditions on the larger fungi at different forest sites in Northern Finland in 1976-1988. – Acta Univ. Oulu. A 243: 1-69.

Oksanen, J. & Minchin, P. R. 1997. Instability of ordination results under changes in input data order: explanations and remedies. – J. Veg. Sci. 8: 447-454.

Päivänen, J. 1966. Sateen jakaantuminen erilaisissa metsiköissä. – Silva fenn. 119: 3: 1-37. (Eng. summ.: The distribution of rainfall in different types of forest stands)

Parker, K.C. 1988. Environmental relationships and vegetation associates of columnar cacti in the northern Sonoran desert. – Vegetatio 78: 125-140.

Peter, M., Ayer, F. & Egli, S. 2001. Nitrogen addition in a Norway spruce stand altered macromycete sporocarp production and below-ground ectomycorrhizal species composition. – New Phytol. 149: 311-325.

Pigott, C.D. 1982. Survival of mycorrhiza formed by *Cenococcum geophilum* Fr. in dry soils. – New Phytol. 92: 513-517.

Pirk, W. 1948. Zur Soziologie der Pilze im Querceto-Carpinetum. – Z. Pilzk. N.F. 1: 11-20.

Pirozynski, K.A. 1968. Geographical distribution of fungi. – In: Ainsworth, G.C. & Sussman, A.S. (eds.), The fungi. An advanced treatise. Volume III. The fungal population. Acad. Press, New York, pp. 487-504.

Raab, T. K., Lipson, D. A. & Monson, R. K. 1996. Nonmykorrhizal uptake of amino acids by roots of the alpine sedge *Kobresia myosuroides*: implications for the alpine nitrogen cycle. – Oecologia 108: 488-494.

Reich, P.B., Schoettle, A.W., Stroo, H.F. & Amundson, R.G. 1986. Acid rain and ozone influence mycorrhizal infection in tree seedlings. – J. Air Pollut. Control Assoc. 36: 724-726.

Reich, P.B., Schoettle, A.W., Stroo, H.F., Troiano, J. Amundson, R.G. 1985. Effects of O_3, SO_2, and acidic rain on mycorrhizal infection in northern red oak seedlings. – Can. J. Bot. 63: 2049-2055.

Renvall, P. 1995. Community dynamics of wood-rotting Basidiomycetes on decomposing conifer trunks in northern Finland. – Karstenia 35: 1-51.

Ritter, G. & Tölle, H. 1978. Stickstoffdüngung in Kiefernbeständen und ihre Wirkung auf Mykorrhizabildung und Fruktifikation der Symbiosepilze. – Beitr. Forstw. 12: 162-166.

Rørå, A, Kvamme, H., Larsson, J.Y., Nyborg, Å. & Økland, T. 1988. Rapport 1988. Program

'Overvåking av skogens sunnhetstilstand'. – Norsk Inst. Jord- Skogkartlegging, Ås.
Romell, L.G. 1935. Ecological problems of the humus layer in the forest. – Corn. Univ. agr. Exp. Stn Mem. 170: 1-28.
Rühling, Å. & Tyler, G. 1991. Effects of simulated nitrogen deposition to the forest floor on the macrofungal flora of a beech forest. – Ambio 20: 261-263.
Rydgren, K. 1997. Vegetation-environment relationships of old-growth spruce forest vegetation in Østmarka Nature Reserve, SE Norway, and comparison of three ordination methods. – Nord. J. Bot. 16: 421-439.
Såstad, S.M. 1990. The macrofungal flora in two stands of *Pinus sylvestris* forest in Snåsa, Central Norway, a mycocoenological approach. – Cand. scient. Thesis, Univ. Trondheim, unpubl.
Såstad, S. & Jenssen, H.B. 1993. Interpretation of regional differences in the fungal biota as effects of atmospheric pollution. – Mycol. Res. 97: 1451-1458.
Salo, K. 1993. The composition and structure of macrofungus communities in boreal upland type forests and peatlands in North Karelia, Finland. – Karstenia 33: 61-99.
Shantz, H.L. & Piemeisel, R.L. 1917. Fungus fairy rings in Eastern Colorado and their effect on vegetation. – J. agric. Res. 11: 191-245.
Shubin, V.I. 1988. Influence of fertilizers on the fruiting of forest mushrooms. – Acta bot. fenn. 136: 85-87.
Sigmond, E.M.O., Gustavson, M. & Roberts, D. 1984. Berggrunnskart over Norge. 1:1 000 000. – Norg. geol. Unders., Trondheim.
Šmarda, F. 1973. Die Pilzgesellschaften einiger Fichtenwälder Mährens. – Acta Sci. Nat. Brno: 7: 8: 1-44.
Smith, A.H. & Singer, R. 1964. A monograph of the genus *Galerina* Earle. – Hafner, New York.
Sokal, R.R. & Rohlf, F.J. 1995. Biometry, ed. 3. – Freeman, New York.
Stuanes A., Ogner, G. & Opem, M. 1984. Ammonium nitrate as extractant for soil exchangeable acidity and aluminium. – Communs Soil Sci. Pl. Anal. 15: 773-778.
Tamm, C.O. 1953. Growth, yield and nutrition in carpets of a forest moss (*Hylocomium splendens*). – Meddn St. SkogsforskInst. 43: 1: 1-140.
Taylor, A.F.S., Martin, F. & Read, D.J. 2000. Fungal diversity in ectomycorrhizal communities of Norway spruce [Picea abies (L.) Karst.] and beech (Fagus sylvatica L.) along north-south transects in Europe. – Ecol. Stud. 142: 343-365.
ter Braak, C.J.F. 1986. Canonical correspondence analysis: a new eigenvector technique for multivariate direct gradient analysis. – Ecology 67: 1167-1179.
ter Braak, C.J.F. 1987a. The analysis of vegetation-environment relationships by canonical correspondence analysis. – Vegetatio 69: 69-77.
ter Braak, C.J.F. 1987b. Ordination. – In: Jongman, R.H.G., ter Braak, C.J.F. & van Tongeren, O.F.R. (eds.), Data analysis in community and landscape ecology, Pudoc, Wageningen, pp. 91-173.
ter Braak, C.J.F. 1987c. CANOCO – a FORTRAN program for canonical community ordination by (partial)(detrended)(canonical) correspondence analysis, principal components analysis and redundancy analysis (version 2.1). – TNO Inst. appl. Comp. Sci., Stat. Dept. Wageningen, Wageningen.
ter Braak, C.J.F. 1990. Update notes: CANOCO version 3.10. – Agricult. Math. Group, Wageningen.
ter Braak, C.J.F. & Šmilauer, P. 1998. CANOCO reference manual and user's guide to Canoco for Windows: software for canonical community ordination (version 4). – Ithaca, N.Y., Microcomputer Power.
Termorshuizen, A.J. 1993. The influence of nitrogen fertilisers on ectomycorrhizas and their fungal carpophores in young stands of *Pinus sylvestris*. – For. Ecol. Mgmt 57: 179-189.
Termorshuizen, A.J. & Ket, P.C. 1991. Effects of ammonium and nitrate on mycorrhizal seedlings of

Pinus sylvestris. – Eur. J. For. Pathol. 21: 404-413.
Termorshuizen, A.J. & Schaffers, A.P. 1987. Occurrence of carpophores of ectomycorrhizal fungi in selected stands of *Pinus sylvestris* in the Netherlands in relation to stand vitality and air pollution. – Pl. Soil 104: 209-217.
Theodorou, C. 1978. Soil moisture and the mycorrhizal association of *Pinus radiata* D. Don. – Soil Biol. Biochem. 10: 33-37.
Theodorou, C. & Bowen, G.D. 1969. The influence of pH and nitrate on mycorrhizal association of *Pinus radiata* D.Don. – Austr. J. Bot. 17: 59-67.
Tørseth, K. & Røstad, A. 1994. Program for terrestrisk naturovervåking. Overvåking av nedbørkjemi i tilknytning til feltforskningsområdene, 1993. – Norsk Inst. Luftforsk. Oppdragsrapp. 1994: 25: 1-71.
Tørseth, K. & Røyset, O. 1993. Program for terrestrisk naturovervåking. Overvåking av nedbørkjemi i Ualand, Solhomfjell, Møsvatn, Åmotsdalen og Børgefjell, 1992. – Norsk Inst. Luftforsk. Oppdragsrapp. 1993: 13: 1-62.
Tuomikoski, R. 1942. Untersuchungen über die Untervegetation der Bruchmoore in Ostfinnland. I. Zur Methodik der pflanzensoziologischen Systematik. – Annls bot. Soc. zool.-bot. fenn. Vanamo 17: 1: 1-203.
Tyler, G. 1985. Macrofungal flora of Swedish beech forest related to soil organic matter and acidity characteristics. – For. Ecol. Mgmt 10: 13-29.
Tyler, G. 1989a. Edaphical distribution patterns of macrofungal species in deciduous forest of South Sweden. – Acta oecol. 10: 309-326.
Tyler, G. 1989b. Edaphical distribution and sporophore dynamics of macrofungi in hornbeam (*Carpinus betulus* L.) stands of south Sweden. – Nova Hedwigia 49: 239-253.
Uhlig, S.K. 1972. Untersuchungen zur Trockenresistenz mykorrhizabildender Pilze. – ZentBl. Bakteriol. Parasitenkde Infektionskrankheiten Hygiene. 2. Abt. 127: 117-216.
van Tooren, B.F., van Dam, D. & During, H.J. 1990. The relative importance of precipitation and soil as sources of nutrients for *Calliergonella cuspidata* in chalk grassland. – Funct. Ecol. 4: 101-107.
Väre, H. & Ohtonen, R. 1996. Site quality and macrofungal community structures. – Acta Univ. oulu. A 275: 5: 1-15.
Väre, H., Ohenoja, E. & Ohtonen, R. 1996. Macrofungi of oligotrophic Scots pine forests in northern Finland. – Karstenia 36: 1-18.
Vauras, J. 1992. Suomen risakkaiden (*Inocybe*, Agaricales) systematiikasta ja ekoloiasta. – Phil. lic. Thesis, Univ. Åbo, unpubl.
Vogt, K.A., Edmonds, R.L. & Grier, C.C. 1981. Dynamics of ectomycorrhizae in *Abies amabilis* stands: The role of *Cenococcum graniforme*. – Holarct. Ecol. 4: 167-173.
Wästerlund, I. 1982. Försvinner tallens mykorrhizasvampar vid gödsling? – Svensk bot. Tidskr. 76: 411-417.
Webb, D.A. 1954. Is the classification of plant communities either possible or desireable? – Bot. Tidsskr. 51: 362-370.
Whittaker, R.H. 1960. Vegetation of the Siskiyou Mountains, Oregon and California. – Ecol. Monogr. 30: 279-338.
Whittaker, R.H. 1967. Gradient analysis of vegetation. – Biol. Rev. Camb. phil. Soc. 42: 207-264.
Wiens, J.A. 1989. Spatial scaling in ecology. – Funct. Ecol. 3: 385-398.
Wiklund, K., Nilsson, L.-O. & Jacobsson, S. 1995. Effect of irrigation, fertilization, and artificial drought on basidioma production in a Norway spruce stand. – Can. J. Bot. 73: 200-208.
Worsley, J.F. & Hacskaylo, E. 1959. The effect of available soil moisture on the mycorrhizal association of Virginia pine. – For. Sci. 5: 267-268.

APPENDICES

Appendix 1. Full list of species recorded in the investigation area, sorted in (supposed) mycorrhizal and non-mycorrhizal species, respectively. Abbreviations are shown for species occurring in = 5% of the macro plots, for which optima along DCA ordination axes are shown in Figs. 23-26.

Abbr.		Species
		Albatrellus ovinus (Schaeff. : Fr.) Kotl. & Pouzar
Aman	ful	Amanita fulva (Schaeff.) Pers.
		Amanita muscaria (L. : Fr.) Hook.
Aman	por	Amanita porphyria (Alb. & Schwein. : Fr.) Mlady
		Amanita regalis (Fr.) Michael
Aman	rub	Amanita rubescens (Pers. : Fr.) Gray
Aman	vir	Amanita virosa (Fr.) Bertillon
		Bankera fuligineoalba (J.C. Schmidt : Fr.) Pouzar
Bole	edu	Boletus edulis Bull. : Fr.
		Cantharellus cibarius Fr.
Cant	tub	Cantharellus tubaeformis (Bull. : Fr.) Fr.
Chal	pip	Chalciporus piperatus (Bull. : Fr.) Bat.
Chro	rut	Chroogomphus rutilus (Schaeff. : Fr.) O.K. Miller
Cort	alb	Cortinarius albovariegatus (Velen.) Melot
		Cortinarius angelesianus A.H. Sm.
Cort	ano	Cortinarius anomalus (Fr. : Fr.) Fr.
Cort	arm	Cortinarius armeniacus (Schaeff. : Fr.) Fr.
		Cortinarius armillatus (Fr. : Fr.) Fr.
		Cortinarius badiovinaceus M.M. Moser
		Cortinarius balteatus (Fr.) Fr.
Cort	bif	Cortinarius biformis Fr.
Cort	bru	Cortinarius brunneus (Pers. : Fr.) Fr.
Cort	cam	Cortinarius camphoratus Fr.
Cort	cas	Cortinarius casimiri (Velen.) Huijsman
		Cortinarius collinitus (Sow. : Fr.) Gray
		Cortinarius croceus (Schaeff.) Gray
		Cortinarius decipiens (Pers. : Fr.) Fr.
Cort	del	Cortinarius delibutus Fr.
		Cortinarius evernius (Fr. : Fr.) Fr.
		Cortinarius fervidus P.D. Orton
Cort	fle	Cortinarius flexipes (Pers.: Fr.) Fr.
Cort	ful	Cortinarius fulvescens Fr.
Cort	gen	Cortinarius gentilis (Fr.) Fr.
Cort	ill	Cortinarius illuminus Fr.
		Cortinarius limonius (Fr. : Fr.) Fr.
		Cortinarius lux-nymphae Melot
		Cortinarius mucifluus Fr.

Appendix 1 (cont.)

		Cortinarius mucosus (Bull.) Kickx
Cort	obt	Cortinarius obtusus (Fr. : Fr.) Fr.
Cort	plu	Cortinarius pluvius (Fr. : Fr.) Fr.
		Cortinarius purpurascens Fr.
		Cortinarius cf. quarciticus H. Lindstr.
		Cortinarius raphanoides (Pers. : Fr.) Fr.
		Cortinarius rubellus Cooke
Cort	san	Cortinarius sanguineus (Wulfen in Jacq. : Fr.) Fr.
		Cortinarius saturninus (Fr.) Fr.
Cort	sca	Cortinarius scaurus (Fr. : Fr.) Fr.
Cort	sem	Cortinarius semisanguineus (Fr. : Fr.) Fr.
Cort	sti	Cortinarius stillatitius Fr.
		Cortinarius subtortus (Pers. : Fr.) Fr.
		Cortinarius tortuosus (Fr. : Fr.) Fr.
		Cortinarius traganus (Fr. : Fr.) Fr.
		Cortinarius turmalis Fr.
		Cortinarius varius (Schaeff. : Fr.) Fr.
		Cortinarius violaceus (L. : Fr.) Gray
Cort	sp.	Cortinarius sp.
Elap	sp.	Elaphomyces sp.
Ento	rho	Entoloma rhodopolium (Fr.) P. Kumm.
Glom	sp	Glomus sp.
		Hebeloma remyi Bruchet ex Quadraccia
Hydn	ruf	Hydnum rufescens Schaeff. : Fr.
		Hygrophorus camarophyllus (Alb. & Schwein. : Fr.) Dumèe, Grandjean & Maire
Hygr	oli	Hygrophorus olivaceoalbus (Fr. : Fr.) Fr.
Hygr	pus	Hygrophorus pustulatus (Pers. : Fr.) Fr.
		Hygrophorus tephroleucus (Fr.) Fr.
		Inocybe cincinnata (Fr.) Quél.
		Inocybe geophylla (Sow. : Fr.) P. Kumm.
Inoc	lan	Inocybe lanuginosa (Bull. : Fr.) P. Kumm.
		Inocybe mixtilis Britzelm.
		Inocybe napipes J.E. Lange
		Inocybe nitidiuscula (Britzelm.) Sacc.
Inoc	rel	Inocybe relicina (Fr.) Quél.
Inoc	sub	Inocybe subcarpta Kühner & Boursier
Lacc	ame	Laccaria amethystina Cooke
Lacc	lacc	Laccaria laccata (Scop. : Fr.) Berk. & Broome
Lact	cam	Lactarius camphoratus (Bull. : Fr.) Fr.
Lact	det	Lactarius deterrimus Gröger
Lact	ful	Lactarius fuliginosus (Fr. : Fr.) Fr.
		Lactarius glyciosmus (Fr. : Fr.) Fr.
		Lactarius mammosus (Fr. ex Weinm.) Fr.
		Lactarius mitissimus (Fr.) Fr.
Lact	nec	Lactarius necator (Bull. : Fr.) P. Karst.
		Lactarius quietus (Fr. : Fr.) Fr.

Appendix 1 (cont.)

Lact	ruf	Lactarius rufus (Scop. : Fr.) Fr.
		Lactarius sphagneti (Fr.) Neuhoff
Lact	the	Lactarius theiogalus (Bull. : Fr.) Gray ss. Neuhoff
		Lactarius trivialis (Fr. : Fr.) Fr.
Lact	vie	Lactarius vietus (Fr.) Fr.
		Leccinum aurantiacum (Bull.) Gray
		Leccinum niveum (Fr.) Rauschert
Lecc	pal	Leccinum palustre M. Korhonen
Lecc	sca	Leccinum scabrum (Bull. : Fr.) Gray
Lecc	var	Leccinum variicolor Watling
Lecc	ver	Leccinum versipelle (Fr.) Snell
Lecc	sp.	Leccinum sp.
		Paxillus involutus (Batsch : Fr.) Fr.
Rozi	cap	Rozites caperatus (Pers. : Fr.) P. Karst.
		Russula adusta Fr.
Russ	aqu	Russula aquosa Leclair
		Russula atrorubens Quél.
Russ	bet	Russula betularum Hora
Russ	con	Russula consobrina (Fr. : Fr.) Fr.
Russ	dec	Russula decolorans (Fr.) Fr.
		Russula elaeodes (Bres.) Bon
Russ	eme	Russula emetica (Schaeff. : Fr) Pers.
		Russula fragilis (Pers. : Fr.) Fr.
		Russula laricina Velen.
		Russula lutea (Huds. : Fr.) Gray
Russ	och	Russula ochroleuca Pers.
Russ	pal	Russula paludosa Britzelm.
Russ	pue	Russula puellaris Fr.
Russ	que	Russula queletii Fr.
Russ	rho	Russula rhodopoda Zwára
		Russula vesca Fr.
Russ	vin	Russula vinosa Lindbl.
		Russula xerampelina (Schaeff.) Fr.
Suil	var	Suillus variegatus (Schwein. : Fr.) Kuntze
		Thelephora palmata Scop. : Fr.
		Tricholoma fulvum (DC. : Fr.) Sacc.
		Tricholoma saponaceum (Fr. : Fr.) P. Kumm.
		Tylopilus felleus (Bull. : Fr.) P. Karst.
		Xerocomus subtomentosus (L. : Fr.) Quél.
		Agrocybe erebia (Fr. : Fr.) Kühn.
		Armillaria mellea (Vahl : Fr.) P. Kumm. coll.
Baeo	myo	Baeospora myosura (Fr. : Fr.) Singer
Calo	vis	Calocera viscosa (Pers. : Fr.) Fr.
Clav	junc	Clavariadelphus junceus (Alb. & Schwein. : Fr.) Corner
Clav	cor	Clavulina coralloides (L. : Fr.) J. Schröt.
		Clitocybe candicans (Pers. : Fr.) P. Kumm.

Appendix 1 (cont.)

		Clitocybe diatreta (Fr. : Fr.) P. Kumm.
Clit	dit	Clitocybe ditopus (Fr. : Fr.) Gill.
Clit	met	Clitocybe metachroa (Fr.) P. Kumm.
Coll	ace	Collybia acervata (Fr.) P. Kumm.
		Collybia asema (Fr. : Fr.) P. Kumm.
Coll	cir	Collybia cirrata (Pers.) P. Kumm.
		Collybia confluens (Pers. : Fr.) P. Kumm.
		Collybia cookei (Bres.) J.D. Arnold
Coll	dry	Collybia dryophila (Bull. : Fr.) P. Kumm.
		Collybia putilla (Fr. : Fr.) Sing.
Coll	tub	Collybia tuberosa (Bull. : Fr.) P. Kumm.
		Conocybe striipes (Cooke) S. Lundell
		Conocybe sulcatipes (Peck) Kühner
Cord	oph	Cordyceps ophioglossoides (Ehrh. ex Pers. : Fr.) Fr.
Cudo	cir	Cudonia circinans (Pers. : Fr.) Fr.
		Cudonia confusa Bres.
Cudo	cla	Cudoniella clavus (Alb. & Schwein. : Fr.) Dennis
		Cystoderma carcharias (Pers.) Konrad & Maubl.
		Cystoderma fallax A.H. Sm. & Singer
Cyst	jas	Cystoderma jasonis (Cooke & Massee) Harmaja
Ento	cetr	Entoloma cetratum (Fr. : Fr.) M.M. Moser
Ento	con	Entoloma conferendum (Britzelm.) Noordel.
		Entoloma juncinum (Kühner & Romagn.) Noordel.
Ento	nit	Entoloma nitidum (Quél.) Quél.
		Entoloma rhodocylix (Lasch : Fr.) M.M. Moser
		Entoloma turbidum (Fr.) Quél.
		Fayodia gracilipes (Britzelm.) Bresinsky & Stangl
		Flammulina subincarnatus (Joss. & Kühner) Watling
		Galerina allospora A.H. Sm. & Singer
Gale	atk	Galerina atkinsoniana A.H. Sm.
Gale	bad	Galerina badipes (Fr.) Kühner
Gale	bor	Galerina borealis A.H. Sm. & Singer
Gale	hyp	Galerina hypnorum (Schrank : Fr.) Kühner ss. lat.
Gale	mar	Galerina marginata (Batsch) Kühner
Gale	mni	Galerina mniophila (Lasch) Kühner
		Galerina pumila (Pers. : Fr.) Singer
Gale	sty	Galerina stylifera (Atk.) A.H. Sm. & Singer
		Galerina triscopa (Fr.) Kühner
		Galerina unicolor (Vahl : Fr) Singer
Gale	sp1	Galerina sp.1
Gale	sp2	Galerina sp.2
Gymn	sap	Gymnopilus sapineus (Fr. : Fr.) Maire
		Hemimycena delectabilis (Peck) Singer
Heyd	abi	Heyderia abietis (Fr.) Link
		Hygrocybe virginea (Wulfen. : Fr.) P.D. Orton & Watling var. fuscescens (Bres.) Arnolds

Appendix 1 (cont.)

		Hygrophoropsis aurantiaca (Wulfen. : Fr.) J. Schröt.
		Hypholoma capnoides (Fr.) P. Kumm.
		Hypholoma marginatum (Pers. : Fr.) J. Schröt.
		Hypholoma polytrichii (Fr. : Fr.) Singer
		Lycoperdon nigrescens (Pers. : Pers.) Pers.
		Lyophyllum rancidum (Fr.) Singer
		Lyophyllum semitale (Fr.) Kühner
Mara	and	Marasmius androsaceus (L. : Fr.) Fr.
		Marasmius bulliardii Quél. f. acicola (S. Lundell) Noordel.
Mara	epi	Marasmius epiphyllus (Pers. : Fr.) Fr.
Micr	per	Micromphale perforans (Hoffm. : Fr.) Gray
Myce	alc	Mycena alcalina (Fr. : Fr.) P. Kumm. coll.
Myce	ami	Mycena amicta (Fr.) Quél.
		Mycena aurantiomarginata (Fr.) Quél.
Myce	cnl	Mycena cinerella P. Karst.
Myce	cno	Mycena cineroides Hintikka
		Mycena clavicularis (Fr.) Gill.
Myce	epi	Mycena epipterygia (Scop. : Fr.) Gray
Myce	fil	Mycena filopes (Bull. : Fr.) P. Kumm.
Myce	fla	Mycena flavoalba (Fr.) Quél.
		Mycena floridula (Fr.) P. Karst
Myce	gle	Mycena galericulata (Scop. : Fr.) Gray
Myce	glo	Mycena galopus (Pers. : Fr.) P. Kumm.
		Mycena haematopus (Pers. : Fr.) P. Kumm.
		Mycena inclinata (Fr.) Quél.
Myce	lon	Mycena longiseta Höhn.
		Mycena maculata P. Karst.
		Mycena megaspora Kauffman
Myce	met	Mycena metata (Fr.) P. Kumm.
		Mycena oregonensis A.H. Sm.
Myce	pur	Mycena pura (Pers. : Fr.) P. Kumm.
Myce	ror	Mycena rorida (Fr. : Fr.) Quél.
Myce	ros	Mycena rosella (Fr.) P. Kumm.
Myce	rub	Mycena rubromarginata (Fr. : Fr.) P. Kumm.
Myce	san	Mycena sanguinolenta (Alb. & Schwein. : Fr.) P. Kumm.
Myce	sep	Mycena septentrionalis Maas Geest.
		Mycena speirea (Fr. : Fr.) Gill.
Myce	sty	Mycena stylobates (Pers. : Fr.) P. Kumm.
Myce	ura	Mycena urania (Fr. : Fr.) Quél.
Myce	vir	Mycena viridimarginata P. Karst.
		Mycena viscosa Maire
Myce	vul	Mycena vulgaris (Pers. : Fr.) P. Kumm.
		Mycocalia sp.
		Omphalina oniscus (Fr. : Fr.) Quél.
		Pholiota lubrica (Pers. : Fr.) Singer
		Pholiota mixta (Fr.) Singer

Appendix 1 (cont.)

		Pholiota scamba (Fr. : Fr.) M.M. Moser
Psat	fri	Psathyrella friesii Kits van Wav.
		Psathyrella aff. lutensis (Romagn.) Bon
		Psilocybe inquilina (Fr. : Fr.) Bres.
Stor	esc	Strobilurus esculentus (Wulfen. : Fr.) Singer
Stor	hor	Stropharia hornemannii (Fr. : Fr.) S. Lundell
		Tubaria confragosa (Fr.) Kühner
		Tubaria conspersa (Pers. : Fr.) Fayod
Typh	ery	Typhula erythropus (Pers. : Fr.) Fr.
Typh	pha	Typhula phacorrhiza (Reichard : Fr.) Fr.
Typh	set	Typhula setipes (Grev.) Berthier
		Xeromphalina campanella (Batsch : Fr.) Kühner & Maire
		Xeromphalina cornui (Quél.) J. Favre
		Xylaria filiformis (Alb. & Schwein. : Fr.) Fr.

Appendix 2. Classification of macro plots to site-type: position along the topographic moisture and nutrient status gradients. Position of two meso plots along the fine-scale moisture gradient (1 – dry; 2 ! moist) indicated as exponents (all 5.3 and 6 plots are dry). Macro sample plots inhomogeneous with respect to the former two gradients are listed below the table, with site-type classification of its two meso plots in brackets.

Site-type	n	Plots
1	3	14^{11}, 63^{21}, 79^{11}
2	3	83^{11}, 85^{11}, 90^{12}
3	9	27^{22}, 65^{22}, 66^{11}, 76^{21}, 77^{21}, 81^{11}, 82^{11}, 86^{11}, 89^{11}
4	11	8^{21}, 9^{21}, 10^{11}, 11^{11}, 24^{22}, 28^{21}, 74^{11}, 75^{11}, 80^{11}, 99^{12}, 100^{11}
5.1	22	1^{11}, 2^{11}, 3^{11}, 5^{11}, 6^{12}, 7^{11}, 15^{11}, 21^{21}, 22^{11}, 23^{21}, 32^{22}, 34^{11}, 35^{22}, 36^{11}, 37^{11}, 41^{11}, 70^{11}, 71^{11}, 72^{11}, 96^{11}, 97^{11}, 98^{11}
5.2	10	19^{11}, 33^{22}, 38^{22}, 39^{11}, 42^{11}, 43^{11}, 48^{11}, 50^{11}, 68^{11}, 94^{22}
5.3	5	16, 46, 49, 52, 57
6	1	53

Inhomogeneous plots:

4 (4–1, 5.1–1), 12 (1–1, 3–1), 13 (2–1, 1–2), 17 (5.2–1, 5.1–1), 18 (5.2–1, 5.1–1), 25 (4–2, 3–2), 26 (3–2, 2–2), 29 (3–2, 2–2), 30 (3–2, 4–2), 31 (3–2, 2–2), 40 (5.2–1, 5.1–1), 44 (5.3, 5.2–1), 45 (6, 5.2–1), 47 (5.2–1, 5.1–1), 51 (5.3, 5.2–1), 54 (6, 5.3), 55 (5.3, 5.1–1), 56 (5.3, 5.2–1), 58 (2–1, 3–1), 59 (2–1, 3–1), 60 (2–2, 1–1), 61 (2–1, 3–1), 62 (3–1, 2–1), 64 (1–1, 2–1), 67 (6, 5.3), 69 (5.2–1, 5.1–1), 73 (5.1–1, 4–1), 78 (2–2, 1–1), 84 (2–1, 1–1), 87 (2–1, 3–2), 88 (3–1, 1–1), 91 (3–1, 1–1), 92 (3–1, 2–2), 93 (2–1, 1–2), 95 (5.1–2, 5.2–1)

Appendix 3. Mycorrhizal fungi recorded in the 99 macroplots. Species quantity is given as subplot frequency.

Sample plot	1	2	3	4	5	6	7	8	9	10	11	12	13	14	15	16	17	18	19	21	22	23	24	25
Albatrellus ovinus	0	0	0	0	0	2	0	0	0	0	0	0	0	0	0	0	0	0	0	0	0	0	0	0
Amanita fulva	0	0	0	0	0	0	0	0	0	0	0	0	0	0	0	0	0	0	0	0	0	0	0	0
Amanita muscaria	0	0	0	0	0	0	0	0	0	0	0	0	0	0	0	0	0	0	0	0	0	0	0	0
Amanita porphyria	0	2	0	0	1	0	0	0	0	0	0	0	0	0	0	0	0	0	0	0	0	0	0	0
Amanita regalis	0	0	0	0	0	0	0	0	0	0	0	0	0	0	0	1	0	1	0	0	0	0	0	0
Amanita rubescens	0	0	0	0	0	0	0	0	0	0	0	0	0	0	0	0	0	0	1	0	0	0	0	0
Amanita virosa	1	1	1	1	0	0	0	1	0	0	0	0	0	0	0	0	0	0	0	0	0	1	0	1
Bankera fuligineoalba	0	0	0	0	0	0	0	0	0	0	0	0	0	0	0	0	0	0	0	0	0	0	0	0
Boletus edulis	0	0	0	0	0	0	0	0	0	0	0	0	0	0	0	0	0	0	0	0	0	0	0	0
Cantharellus cibarius	0	0	0	1	0	0	0	0	0	0	0	0	0	0	0	0	0	0	0	0	0	0	0	0
Cantharellus tubaeformis	0	0	5	2	4	3	0	1	0	0	0	0	0	1	1	0	0	0	0	0	0	0	0	0
Chalciporus piperatus	0	0	0	0	0	0	0	0	0	0	0	0	0	0	0	2	5	0	1	0	0	0	0	0
Chroogomphus rutilus	0	0	0	0	0	0	0	0	0	0	0	0	0	0	0	0	0	0	0	0	0	0	0	0
Cortinarius albovariegatus	1	0	1	0	0	0	0	0	0	0	0	0	0	0	0	0	0	0	1	1	0	0	0	0
Cortinarius angelesianus	0	1	0	0	0	0	0	0	0	0	0	0	0	0	0	0	0	0	0	0	0	0	0	0
Cortinarius anomalus	1	0	0	0	0	0	0	0	0	0	0	0	0	0	0	0	0	0	0	0	0	0	0	0
Cortinarius armeniacus	0	1	1	0	1	2	1	0	0	0	0	0	0	0	0	0	0	0	0	0	0	0	0	0
Cortinarius armillatus	0	0	0	0	0	0	0	0	0	0	0	0	0	0	0	0	0	0	0	0	0	0	0	0
Cortinarius badiovinaceus	0	0	0	0	0	1	0	0	0	0	0	0	0	0	0	0	0	0	0	0	0	0	0	0
Cortinarius balteatus	0	0	0	0	0	0	0	0	0	0	0	0	0	0	0	0	0	0	0	0	0	0	0	0
Cortinarius biformis	4	0	1	0	1	0	0	1	0	0	0	0	0	0	0	0	0	0	0	0	0	0	0	0
Cortinarius brunneus	0	0	0	0	0	0	0	0	0	0	0	0	0	0	0	0	0	0	1	0	2	1	0	0
Cortinarius camphoratus	0	0	0	0	0	0	0	0	0	0	0	0	0	0	0	10	0	0	0	0	0	0	0	0
Cortinarius casimiri	0	0	0	0	0	0	0	0	0	0	0	0	0	0	0	0	0	0	1	1	1	0	0	0
Cortinarius collinitus	0	0	1	0	0	0	0	0	0	0	0	0	0	0	0	0	0	0	0	0	0	0	0	0
Cortinarius croceus	0	0	0	0	0	0	0	0	1	0	0	0	0	0	0	0	0	0	0	0	0	0	0	0
Cortinarius decipiens	3	0	0	0	0	0	0	0	0	0	0	0	0	0	0	0	0	0	1	0	0	0	0	0
Cortinarius delibutus	0	0	0	0	0	0	0	0	0	0	0	0	0	0	0	0	0	0	0	0	0	0	0	0
Cortinarius evernius	0	0	0	0	0	0	0	0	0	0	0	0	0	0	0	0	0	0	0	2	0	0	0	0
Cortinarius fervidus	0	0	0	0	0	0	0	0	0	0	0	0	0	0	0	0	0	0	0	0	0	0	0	0
Cortinarius flexipes	0	2	1	0	1	0	0	0	0	0	0	0	0	0	3	0	1	0	0	0	8	8	1	0
Cortinarius fulvescens	0	0	1	0	0	0	0	0	1	0	0	0	0	0	0	0	0	0	0	0	0	0	0	0
Cortinarius gentilis	0	1	1	0	0	0	0	0	0	0	0	0	0	0	0	0	0	0	0	1	0	0	0	0
Cortinarius illuminus	0	0	0	0	0	1	0	0	0	0	0	0	0	0	1	0	0	0	0	0	0	0	0	0
Cortinarius limonius	0	0	0	0	0	0	0	0	0	0	0	0	0	0	2	0	0	0	0	0	0	0	0	0
Cortinarius lux-nymphae	0	0	0	0	0	0	0	0	0	0	0	0	0	0	0	0	0	0	0	0	0	0	0	0
Cortinarius mucifluus	0	0	0	0	0	0	0	0	0	0	0	0	0	0	0	0	0	0	0	0	0	0	0	0
Cortinarius mucosus	0	0	0	0	0	0	0	0	0	0	0	2	0	0	0	0	0	0	0	0	0	0	0	0
Cortinarius obtusus	1	4	8	1	2	9	0	2	1	3	3	0	0	0	4	0	1	1	6	1	0	2	0	0
Cortinarius pluvius	0	0	0	0	0	0	0	0	0	0	0	0	0	0	0	0	0	0	0	0	0	0	0	0
Cortinarius purpurascens	0	0	0	0	0	0	0	0	0	0	0	0	0	0	0	0	0	0	0	0	0	0	0	0
Cortinarius cf. quarciticus	0	0	0	0	0	0	0	0	0	0	0	0	0	0	0	0	0	0	0	0	0	0	0	0
Cortinarius raphanoides	0	0	0	0	0	0	0	0	0	0	0	0	0	0	0	0	0	0	0	0	0	0	0	0
Cortinarius rubellus	0	0	0	0	0	0	0	0	0	0	0	0	0	0	0	0	0	0	0	0	0	0	0	0
Cortinarius sanguineus	0	0	0	0	0	0	0	0	0	0	0	0	0	0	0	4	0	0	1	0	0	0	0	0
Cortinarius saturninus	0	0	0	0	0	0	0	0	0	0	0	0	0	0	0	0	0	0	0	0	0	0	0	0
Cortinarius scaurus	0	0	1	0	0	0	0	0	0	0	0	0	0	0	0	1	0	0	0	0	0	0	0	1
Cortinarius semisanguineus	0	0	0	0	0	0	0	0	0	0	0	0	0	0	0	0	0	0	0	0	0	0	0	0
Cortinarius stillatitius	1	0	0	0	0	1	0	0	0	0	0	0	0	0	1	0	0	0	1	0	0	0	0	0
Cortinarius subtortus	0	0	0	0	0	0	0	0	0	0	0	0	0	0	0	0	0	0	0	0	0	0	0	0
Cortinarius tortuosus	0	0	0	0	0	0	0	0	0	0	0	0	0	0	0	0	0	0	0	0	0	0	0	0
Cortinarius traganus	0	0	0	0	0	0	0	0	0	0	0	0	0	0	0	0	0	0	0	0	0	0	0	0
Cortinarius turmalis	0	0	0	0	0	0	0	0	0	0	0	0	1	0	0	0	0	0	0	0	0	0	0	0
Cortinarius varius	0	0	0	0	1	0	0	0	0	0	0	0	0	0	0	0	0	0	0	0	0	0	0	0
Cortinarius violaceus	0	0	0	0	0	0	0	0	0	0	0	0	0	0	0	0	0	0	0	0	0	0	0	0
Cortinarius sp.	0	0	0	0	0	0	0	0	0	0	0	0	0	0	0	0	0	0	0	0	0	0	0	0
Elaphomyces sp.	0	0	0	0	0	2	1	0	0	0	0	0	0	0	0	0	0	0	0	0	0	0	0	0
Entoloma rhodopolium	0	0	0	0	0	0	0	0	0	0	0	0	0	0	0	0	0	0	0	0	0	0	0	0
Glomus sp.	0	0	2	0	0	0	0	0	0	0	0	0	0	0	0	0	0	0	1	0	0	0	1	0
Hebeloma remyi	0	0	0	0	0	0	0	0	0	0	0	0	0	0	0	0	0	0	0	0	0	0	0	0
Hydnum rufescens	0	0	0	0	0	0	0	0	0	0	0	0	0	0	0	0	0	0	0	0	0	0	0	0
Hygrophorus camarophyllus	0	0	0	0	0	0	0	0	0	1	0	0	0	0	0	0	0	0	0	0	0	0	0	0
Hygrophorus olivaceoalbus	0	0	0	0	0	0	0	0	0	0	0	0	0	0	0	4	2	0	0	1	0	0	0	0
Hygrophorus pustulatus	0	0	0	0	0	0	0	0	0	0	0	0	0	0	0	0	0	0	0	0	0	0	0	0
Hygrophorus tephroleucus	0	0	0	0	0	0	0	0	0	0	0	0	0	0	0	0	0	0	0	0	0	0	0	0
Inocybe cincinnata	0	0	0	0	0	0	0	0	0	0	0	0	0	0	0	0	0	0	0	0	0	0	0	0
Inocybe geophylla	0	0	0	0	0	0	0	0	0	0	0	0	0	0	0	0	0	0	0	0	0	0	0	0
Inocybe lanuginosa	0	0	0	0	0	0	0	0	0	0	0	0	0	0	0	0	0	0	0	2	0	0	0	0
Inocybe mixtilis	0	0	0	0	0	0	0	0	0	0	0	0	0	0	0	0	0	0	0	0	0	0	0	0
Inocybe napipes	0	0	0	0	0	0	0	0	0	0	0	0	0	0	0	0	0	0	0	0	0	0	0	0
Inocybe nitidiuscula	0	0	0	0	0	0	0	0	0	0	0	0	0	0	0	0	0	0	0	0	0	0	0	0
Inocybe relicina	0	0	0	0	0	0	0	0	0	0	0	0	0	0	0	0	0	0	0	0	0	0	0	0
Inocybe subcarpta	0	0	0	0	0	0	0	0	0	0	0	0	0	0	0	0	0	0	0	0	0	0	0	0

Appendix 3 (continued).

Sample plot	26	27	28	29	30	31	32	33	34	35	36	37	38	39	40	41	42	43	44	45	46	47	48	49	50
Albatrellus ovinus	0	0	0	0	0	0	0	0	0	0	0	0	0	1	0	0	0	0	0	0	0	0	0	0	0
Amanita fulva	0	0	0	0	0	0	0	0	0	0	0	0	0	0	0	0	0	1	1	0	0	0	0	0	0
Amanita muscaria	0	0	0	0	0	0	0	0	0	0	0	0	0	0	0	0	0	0	0	1	0	0	0	0	0
Amanita porphyria	0	0	0	0	0	0	0	0	0	0	0	0	0	0	0	0	0	0	0	0	0	1	0	0	0
Amanita regalis	0	0	0	0	0	0	0	0	0	0	0	0	0	0	0	0	0	0	0	0	0	0	0	0	0
Amanita rubescens	0	0	0	0	0	0	0	0	0	0	0	0	0	0	0	0	0	0	0	0	0	0	0	0	0
Amanita virosa	0	0	0	0	0	0	0	1	0	1	1	0	0	0	0	8	0	0	0	0	0	0	0	0	0
Bankera fuligineoalba	0	0	0	0	0	0	0	0	0	0	0	0	0	0	0	0	0	0	0	0	0	0	0	0	0
Boletus edulis	0	0	0	0	0	0	0	0	0	0	0	0	0	0	0	0	0	0	0	1	0	0	0	1	0
Cantharellus cibarius	0	0	0	0	0	0	0	0	0	0	0	0	0	0	0	0	0	0	0	0	0	0	0	0	0
Cantharellus tubaeformis	0	0	0	0	0	0	0	0	0	0	0	0	0	0	0	0	0	0	0	0	1	0	0	0	1
Chalciporus piperatus	0	0	0	0	0	0	0	0	0	0	0	0	0	0	0	0	0	0	0	1	0	0	0	0	0
Chroogomphus rutilus	0	0	0	0	0	0	0	0	0	0	0	0	0	0	0	0	0	0	0	0	0	0	0	0	0
Cortinarius albovariegatus	0	0	0	0	0	0	2	2	0	0	2	0	0	4	2	1	1	0	0	1	0	0	0	0	0
Cortinarius angelesianus	0	0	0	0	0	0	0	0	0	0	0	0	0	0	0	0	0	0	0	0	0	0	0	0	0
Cortinarius anomalus	0	0	0	0	0	0	0	0	0	0	0	0	0	0	0	0	0	0	0	4	0	0	0	0	0
Cortinarius armeniacus	0	0	0	0	0	0	0	1	0	0	0	0	0	0	0	0	1	0	0	0	0	0	0	0	0
Cortinarius armillatus	0	0	0	0	0	0	0	0	0	0	0	0	0	0	0	0	0	0	0	0	0	0	0	0	0
Cortinarius badiovinaceus	0	0	0	0	0	0	0	0	0	0	0	0	0	0	0	0	0	0	0	0	0	0	0	0	0
Cortinarius balteatus	0	0	0	0	0	0	0	0	0	0	0	0	0	0	0	0	0	0	0	1	0	0	0	0	0
Cortinarius biformis	0	0	0	0	0	0	0	0	0	0	0	0	0	0	0	0	0	0	0	1	0	0	0	0	0
Cortinarius brunneus	0	0	0	0	1	0	0	4	0	0	0	0	0	3	0	0	1	0	0	0	0	0	0	0	0
Cortinarius camphoratus	0	0	0	0	0	0	0	0	0	0	0	1	0	0	0	0	0	0	0	0	3	0	1	0	0
Cortinarius casimiri	0	0	0	0	0	0	0	1	0	0	0	0	0	0	0	0	0	0	0	3	0	0	1	0	0
Cortinarius collinitus	0	0	0	0	0	0	0	0	0	0	0	0	0	0	0	0	0	0	0	0	0	0	0	0	0
Cortinarius croceus	0	0	0	0	0	0	0	0	0	0	0	0	0	0	0	0	0	0	0	0	0	0	0	0	0
Cortinarius decipiens	0	0	0	0	0	0	0	0	0	0	0	0	0	0	0	0	0	0	0	0	0	0	0	0	0
Cortinarius delibutus	0	0	0	0	0	0	0	0	0	0	0	0	0	0	0	1	0	0	0	4	0	0	0	0	0
Cortinarius evernius	0	0	0	0	0	0	0	2	0	0	0	0	0	0	0	0	0	0	0	0	0	0	0	0	0
Cortinarius fervidus	0	0	0	0	0	0	0	0	0	0	0	0	0	0	0	0	0	0	0	0	1	0	0	0	0
Cortinarius flexipes	0	0	0	0	0	0	0	0	2	0	3	0	0	2	0	0	1	1	0	0	1	3	1	0	0
Cortinarius fulvescens	0	0	0	0	0	0	0	0	0	0	0	0	0	0	0	0	0	0	0	0	0	0	0	0	0
Cortinarius gentilis	0	0	0	0	0	0	0	0	0	0	0	0	0	0	0	0	0	0	0	0	0	0	0	0	0
Cortinarius illuminus	0	0	0	0	0	0	0	0	0	0	0	0	0	0	0	0	0	0	0	0	0	0	0	0	0
Cortinarius limonius	0	0	0	0	0	0	0	0	0	0	0	0	0	0	0	0	0	0	0	0	0	0	0	0	0
Cortinarius lux-nymphae	1	0	0	0	0	0	0	0	0	0	0	0	0	0	0	0	0	0	0	0	0	0	0	0	0
Cortinarius mucifluus	0	0	0	0	0	0	0	0	0	0	0	0	0	0	0	0	0	0	0	0	0	0	0	0	0
Cortinarius mucosus	0	0	0	0	0	0	0	0	0	0	0	0	0	0	0	0	0	0	0	0	0	0	0	0	0
Cortinarius obtusus	0	0	0	0	0	0	2	6	1	0	9	8	2	1	0	1	0	1	1	1	1	0	0	0	1
Cortinarius pluvius	0	0	0	0	0	0	0	0	0	0	1	1	0	0	0	0	0	0	0	0	0	0	0	0	0
Cortinarius purpurascens	0	0	0	0	1	0	0	0	0	0	0	0	0	0	0	0	0	0	0	0	0	0	0	0	0
Cortinarius cf. quarciticus	0	0	0	0	0	0	0	0	0	0	0	0	0	0	0	0	0	0	0	0	0	0	0	0	0
Cortinarius raphanoides	0	0	0	0	0	0	0	0	0	0	0	0	0	0	0	0	0	0	0	0	0	0	0	0	0
Cortinarius rubellus	0	0	0	0	0	0	0	0	0	0	0	0	0	0	0	0	0	0	0	0	0	0	0	0	0
Cortinarius sanguineus	0	0	0	0	0	0	0	0	0	0	0	0	0	0	0	0	0	0	0	0	0	0	0	0	0
Cortinarius saturninus	0	0	0	0	0	0	0	0	0	0	0	0	0	0	0	0	0	0	0	0	0	0	0	0	0
Cortinarius scaurus	0	0	0	0	0	0	0	0	0	0	0	0	0	0	0	0	0	1	0	0	0	0	0	0	0
Cortinarius semisanguineus	0	0	0	0	0	0	0	0	0	0	0	0	0	0	0	0	0	0	0	0	0	0	0	0	0
Cortinarius stillatitius	0	0	0	0	0	0	0	0	1	0	0	0	0	0	0	1	1	0	0	0	0	0	0	0	0
Cortinarius subtortus	0	0	0	0	0	0	0	0	0	0	0	0	0	0	0	0	0	0	0	0	0	0	0	0	0
Cortinarius tortuosus	2	0	0	0	0	0	0	0	0	0	0	0	0	0	0	0	0	0	0	0	0	0	0	0	0
Cortinarius traganus	0	0	0	0	0	0	0	0	0	0	0	0	0	0	0	0	0	0	0	0	0	0	0	0	0
Cortinarius turmalis	0	0	0	0	0	0	0	0	0	0	0	0	0	0	0	0	0	0	0	0	0	0	0	0	0
Cortinarius varius	0	0	0	0	0	0	0	0	0	0	0	0	0	0	0	0	0	0	0	0	0	0	0	0	0
Cortinarius violaceus	0	0	0	0	0	0	0	0	0	0	0	0	0	0	0	0	0	0	0	0	0	0	0	0	0
Cortinarius sp.	0	0	0	0	0	0	0	0	0	0	0	0	0	0	0	0	0	0	0	1	0	0	0	0	0
Elaphomyces sp.	0	0	0	0	0	0	0	1	0	0	0	0	0	0	0	0	0	0	0	0	0	0	0	0	0
Entoloma rhodopolium	0	0	0	0	0	0	0	0	0	0	0	0	9	0	0	0	0	0	1	1	0	1	0	0	0
Glomus sp.	0	0	0	0	0	0	0	1	0	0	0	0	0	0	0	0	0	0	0	0	0	0	0	1	0
Hebeloma remyi	0	0	0	0	0	0	0	0	0	0	0	0	0	0	0	0	0	0	0	0	0	0	0	0	0
Hydnum rufescens	0	0	0	0	0	0	0	0	0	0	0	0	2	0	0	0	0	0	0	0	0	0	0	0	0
Hygrophorus camarophyllus	0	0	0	0	0	0	0	0	0	0	0	0	0	0	0	0	0	0	0	0	0	0	0	0	0
Hygrophorus olivaceoalbus	0	0	0	0	0	0	0	0	0	1	0	0	0	1	0	0	1	0	2	0	1	0	0	0	0
Hygrophorus pustulatus	0	0	0	0	0	0	2	3	0	0	0	0	2	0	0	0	0	1	0	2	1	0	0	1	0
Hygrophorus tephroleucus	0	0	0	0	0	0	0	0	0	0	0	0	0	0	0	0	0	0	0	0	0	0	0	0	0
Inocybe cincinnata	0	0	0	0	0	0	0	0	0	0	0	0	0	0	0	0	0	0	0	0	0	0	0	0	0
Inocybe geophylla	0	0	0	0	0	0	0	0	0	0	0	0	0	0	0	0	0	0	0	0	0	0	0	1	0
Inocybe lanuginosa	0	0	0	0	0	0	0	0	0	0	0	0	0	0	0	0	0	0	0	0	0	0	0	0	0
Inocybe mixtilis	0	0	0	0	0	0	0	0	0	0	0	0	0	0	0	0	0	0	1	0	0	0	0	0	0
Inocybe napipes	0	0	0	0	0	0	0	0	0	0	0	0	0	0	0	0	0	0	3	0	0	0	0	0	0
Inocybe nitidiuscula	0	0	0	0	0	0	0	0	0	0	0	0	0	0	0	0	0	0	0	5	0	0	0	0	0
Inocybe relicina	0	0	0	0	0	0	0	0	0	0	0	0	2	0	0	0	0	0	0	0	0	0	0	0	0
Inocybe subcarpta	0	0	0	0	0	0	0	0	0	0	0	0	0	0	0	0	0	0	0	0	0	0	0	2	0

Appendix 3 (continued).

Sample plot	51	52	53	54	55	56	57	58	59	60	61	62	63	64	65	66	67	68	69	70	71	72	73	74	75
Albatrellus ovinus	0	0	0	0	0	0	0	0	0	0	0	0	0	0	0	0	0	0	0	0	0	0	0	0	0
Amanita fulva	0	0	0	0	0	0	0	0	0	0	0	0	1	0	0	0	0	0	2	2	0	3	0	0	0
Amanita muscaria	0	0	0	0	0	0	0	0	0	0	0	0	0	0	0	0	0	0	0	0	0	0	0	0	0
Amanita porphyria	0	0	0	0	0	0	0	0	0	0	0	0	0	0	0	0	0	0	0	0	0	0	0	0	0
Amanita regalis	0	0	0	0	0	0	0	0	0	0	0	0	0	0	0	0	0	0	0	0	0	0	0	0	0
Amanita rubescens	0	0	1	3	0	0	0	0	0	0	0	0	0	0	0	0	0	0	0	0	0	0	0	0	0
Amanita virosa	0	0	0	0	0	0	0	0	0	0	0	0	0	0	0	0	0	0	0	0	0	0	0	1	0
Bankera fuligineoalba	0	0	0	0	0	0	0	0	0	0	1	0	0	0	0	0	0	0	0	0	0	0	0	0	0
Boletus edulis	0	0	0	0	0	0	0	0	0	0	0	0	0	1	0	0	0	0	0	0	0	0	0	0	0
Cantharellus cibarius	0	0	0	0	0	0	0	0	0	0	0	0	0	0	0	0	0	0	0	0	0	0	0	0	0
Cantharellus tubaeformis	2	0	0	0	0	0	0	0	0	0	0	0	0	0	0	0	0	0	0	0	0	0	0	0	0
Chalciporus piperatus	0	0	0	0	0	0	0	0	0	0	0	0	0	0	0	0	0	0	0	0	0	0	0	0	0
Chroogomphus rutilus	0	0	0	0	0	0	0	0	0	0	1	0	0	0	0	0	0	0	0	0	0	0	0	0	0
Cortinarius albovariegatus	1	0	0	0	0	0	0	0	0	0	0	0	0	0	0	0	0	0	0	0	0	0	0	0	0
Cortinarius angelesianus	0	0	0	0	0	0	0	0	0	0	0	0	0	0	0	0	0	0	0	0	0	0	0	0	0
Cortinarius anomalus	0	2	0	0	0	0	0	0	0	0	0	0	0	0	0	0	0	0	0	0	0	0	1	0	0
Cortinarius armeniacus	0	0	0	0	0	0	0	0	0	0	0	0	0	0	0	0	0	1	0	0	0	0	0	0	0
Cortinarius armillatus	0	0	0	0	0	0	0	0	0	0	0	0	0	0	0	0	0	0	0	0	0	0	0	0	0
Cortinarius badiovinaceus	0	0	0	0	0	0	0	0	0	0	0	0	0	0	0	0	0	0	0	0	0	0	0	0	0
Cortinarius balteatus	0	0	0	0	0	0	0	0	0	0	0	0	0	0	0	0	0	0	0	0	0	0	0	0	0
Cortinarius biformis	0	0	0	0	0	0	0	0	0	0	0	1	0	0	0	0	0	1	0	0	0	0	0	0	1
Cortinarius brunneus	0	0	0	0	0	0	0	0	0	0	0	0	0	0	0	0	0	0	0	0	0	0	1	0	0
Cortinarius camphoratus	0	0	0	0	0	0	0	0	0	0	0	0	0	0	0	0	0	0	0	0	0	0	0	0	0
Cortinarius casimiri	0	0	0	0	0	0	0	0	0	0	0	0	0	0	0	0	0	0	0	0	0	0	0	0	0
Cortinarius collinitus	0	0	0	0	0	0	0	0	0	0	0	0	0	0	0	0	0	0	0	0	0	0	0	0	0
Cortinarius croceus	0	0	0	0	0	0	0	0	0	0	0	0	0	0	0	0	0	0	0	0	0	0	0	0	0
Cortinarius decipiens	0	0	0	0	0	0	0	0	0	0	0	0	0	0	0	0	0	0	0	0	0	0	0	0	0
Cortinarius delibutus	0	0	1	0	0	0	0	0	0	0	0	0	0	0	0	0	0	0	0	0	0	0	0	0	0
Cortinarius evernius	0	0	0	0	0	0	0	0	0	0	0	0	0	0	0	0	0	0	0	0	0	0	0	0	0
Cortinarius fervidus	0	0	0	0	0	0	0	0	0	0	0	0	0	0	0	0	0	0	0	0	0	0	0	0	0
Cortinarius flexipes	0	2	0	0	0	0	0	0	0	0	0	0	0	0	0	0	0	0	2	1	1	0	0	0	0
Cortinarius fulvescens	0	0	0	1	0	0	0	0	0	0	0	0	0	0	0	0	0	0	0	0	0	0	0	0	0
Cortinarius gentilis	0	0	0	0	0	0	0	0	0	0	0	0	0	0	0	0	0	0	0	0	0	0	0	0	0
Cortinarius illuminus	0	0	0	0	0	0	0	0	0	0	0	0	0	0	0	0	0	0	0	0	0	0	0	0	0
Cortinarius limonius	0	0	0	0	0	0	0	0	0	0	0	0	0	0	0	0	0	0	0	0	0	0	0	0	0
Cortinarius lux-nymphae	0	0	0	0	0	0	0	0	0	0	0	0	0	0	0	0	0	0	0	0	0	0	0	0	0
Cortinarius mucifluus	0	0	0	0	0	0	0	0	0	3	0	0	0	0	0	0	0	0	0	0	0	0	0	0	0
Cortinarius mucosus	0	0	0	0	0	0	0	0	0	0	0	0	0	0	0	0	0	0	0	0	0	0	0	0	0
Cortinarius obtusus	2	3	0	3	0	0	0	2	3	0	4	4	0	1	0	1	0	0	1	2	2	0	0	2	8
Cortinarius pluvius	0	0	0	0	0	0	0	0	0	0	0	0	0	0	0	0	0	0	0	0	0	0	0	2	0
Cortinarius purpurascens	0	0	0	0	0	0	0	0	0	0	0	0	0	0	0	0	0	0	0	0	0	0	0	0	0
Cortinarius cf. quarciticus	0	0	0	0	0	0	0	0	0	0	0	0	0	0	0	0	0	0	0	0	0	0	0	0	0
Cortinarius raphanoides	0	0	0	0	0	0	0	0	0	0	0	0	0	0	0	0	0	0	0	1	0	0	0	0	0
Cortinarius rubellus	0	0	0	0	0	0	0	0	0	0	0	0	0	0	0	0	0	0	0	0	0	0	0	0	0
Cortinarius sanguineus	0	0	0	0	0	0	0	0	0	0	0	0	0	0	0	0	0	0	1	0	0	0	0	0	0
Cortinarius saturninus	0	0	0	0	0	0	1	0	0	0	0	0	0	0	0	0	0	0	0	0	0	0	0	0	0
Cortinarius scaurus	0	0	0	0	0	0	0	1	0	0	0	0	0	0	0	0	0	0	0	0	0	0	0	0	0
Cortinarius semisanguineus	0	0	0	0	0	0	0	0	0	0	0	0	1	0	1	0	0	0	0	0	0	0	0	0	0
Cortinarius stillatitius	0	0	0	0	0	0	0	2	0	0	0	0	0	0	0	0	0	0	0	0	0	0	0	0	0
Cortinarius subtortus	0	0	0	0	0	0	0	0	0	0	0	0	0	0	0	0	0	0	0	0	0	0	0	0	0
Cortinarius tortuosus	1	0	0	0	0	0	0	0	0	0	0	0	0	0	0	0	0	0	0	0	0	0	0	0	0
Cortinarius traganus	0	0	0	0	0	0	0	0	0	0	0	0	0	0	0	0	0	0	0	0	0	0	0	0	0
Cortinarius turmalis	0	0	0	0	0	0	0	0	0	0	0	0	0	0	0	0	0	0	0	0	0	0	0	0	0
Cortinarius varius	0	0	0	0	0	0	0	0	0	0	0	0	0	0	0	0	0	0	0	0	0	0	0	0	0
Cortinarius violaceus	0	0	0	0	1	0	0	0	0	0	0	0	0	0	0	0	0	0	0	0	0	0	0	0	0
Cortinarius sp.	0	0	0	0	0	0	0	0	0	0	0	0	0	0	0	0	0	0	0	0	0	0	0	0	0
Elaphomyces sp.	0	1	0	0	0	0	0	0	0	0	0	0	0	0	0	0	0	0	0	0	0	0	0	0	0
Entoloma rhodopolium	0	0	0	1	0	0	2	0	0	0	0	0	0	0	0	0	0	0	0	0	0	0	0	0	0
Glomus sp.	0	0	0	0	0	0	0	0	0	0	0	0	0	0	0	0	0	0	0	1	0	0	0	0	0
Hebeloma remyi	0	0	0	0	0	0	0	0	0	0	0	0	0	0	0	0	0	0	0	0	0	0	0	0	0
Hydnum rufescens	0	0	3	2	0	0	0	0	0	0	0	0	0	0	0	0	0	5	0	0	0	0	0	0	0
Hygrophorus camarophyllus	0	0	0	0	0	0	0	0	0	0	0	0	0	0	0	0	0	0	0	0	0	0	0	0	0
Hygrophorus olivaceoalbus	0	0	0	0	0	0	0	0	0	0	0	0	0	0	0	0	4	1	0	0	1	0	0	0	0
Hygrophorus pustulatus	5	0	3	2	0	1	0	0	0	0	0	0	0	0	0	0	0	0	0	0	0	0	0	0	0
Hygrophorus tephroleucus	0	0	1	0	0	0	0	0	0	0	0	0	0	0	0	0	0	0	0	0	0	0	0	0	0
Inocybe cincinnata	0	0	2	0	0	0	0	0	0	0	0	0	0	0	0	0	0	0	0	0	0	0	0	0	0
Inocybe geophylla	0	0	0	1	0	0	0	0	0	0	0	0	0	0	0	0	0	0	0	0	0	0	0	0	0
Inocybe lanuginosa	0	0	0	1	0	0	0	0	0	0	0	0	0	0	0	0	0	0	0	0	0	0	0	0	0
Inocybe mixtilis	0	0	0	0	0	0	0	0	0	0	0	0	0	0	0	0	0	0	0	0	0	0	0	0	0
Inocybe napipes	0	0	0	0	0	0	0	0	0	0	0	0	0	0	0	0	0	0	0	0	0	0	0	0	0
Inocybe nitidiuscula	0	0	0	0	0	0	0	0	0	0	0	0	0	0	0	0	0	0	0	0	0	0	0	0	0
Inocybe relicina	0	0	0	0	0	0	0	0	0	0	0	0	0	0	0	0	0	0	0	0	0	0	0	0	0
Inocybe subcarpta	0	0	0	0	0	0	0	0	0	0	0	0	0	0	0	0	0	1	0	0	0	1	0	0	0

Appendix 3 (continued).

Sample plot	76	77	78	79	80	81	82	83	84	85	86	87	88	89	90	91	92	93	94	95	96	97	98	99	100
Albatrellus ovinus	0	0	0	0	0	0	0	0	0	0	0	0	0	0	0	0	0	0	0	0	0	0	0	0	0
Amanita fulva	0	0	0	0	0	0	0	0	0	0	0	0	0	0	0	0	0	2	0	0	0	0	0	0	0
Amanita muscaria	0	0	0	0	0	0	0	0	0	0	0	0	0	0	0	0	0	0	0	0	0	0	0	0	0
Amanita porphyria	0	0	0	0	0	0	0	0	0	0	0	0	0	0	0	0	0	0	0	0	0	0	0	0	0
Amanita regalis	0	0	0	0	0	0	0	0	0	0	0	0	0	0	0	0	0	0	0	0	0	0	0	0	0
Amanita rubescens	0	0	0	0	0	0	0	0	0	0	0	0	0	0	0	0	0	0	0	0	0	0	0	0	0
Amanita virosa	0	0	0	0	0	0	0	0	0	0	0	0	0	0	0	0	0	0	0	0	0	3	2	1	1
Bankera fuligineoalba	0	0	0	0	0	0	0	0	0	0	0	0	0	0	0	0	0	0	0	0	0	0	0	0	0
Boletus edulis	0	0	0	0	0	0	0	0	0	0	0	0	0	0	0	0	0	0	0	0	0	0	0	0	0
Cantharellus cibarius	0	0	0	0	0	0	0	0	0	0	0	0	0	0	0	0	0	0	0	0	0	0	0	0	0
Cantharellus tubaeformis	0	0	0	0	0	0	0	0	0	0	0	0	0	0	0	0	0	0	5	0	0	0	0	1	0
Chalciporus piperatus	0	0	0	0	0	0	0	0	0	0	0	0	0	0	0	0	0	0	0	0	0	0	0	0	0
Chroogomphus rutilus	0	2	0	0	0	0	0	0	0	0	0	0	0	0	1	0	0	0	0	0	0	0	0	0	0
Cortinarius albovariegatus	0	0	0	0	0	0	0	0	0	0	0	0	0	0	0	0	0	0	0	1	0	0	0	0	0
Cortinarius angelesianus	0	0	0	0	0	0	0	0	0	0	0	0	0	0	0	0	0	0	0	0	0	0	0	0	0
Cortinarius anomalus	0	0	0	0	0	0	0	0	0	0	0	0	0	0	0	0	0	0	4	1	1	0	3	0	0
Cortinarius armeniacus	0	0	0	0	0	0	0	0	0	0	0	0	0	0	0	0	0	0	0	0	0	0	1	0	0
Cortinarius armillatus	0	0	0	0	0	0	0	0	0	0	0	0	0	0	0	0	0	0	0	0	0	0	0	1	0
Cortinarius badiovinaceus	0	0	0	0	0	0	0	0	0	0	0	0	0	0	0	0	0	0	0	0	0	0	0	0	0
Cortinarius balteatus	0	0	0	0	0	0	0	0	0	0	0	0	0	0	0	0	0	0	0	0	0	0	0	0	0
Cortinarius biformis	0	0	0	0	0	0	0	1	0	0	0	0	0	0	0	0	0	0	0	1	0	0	2	0	0
Cortinarius brunneus	0	0	0	0	0	0	0	0	0	0	0	0	0	0	0	0	0	0	0	1	1	0	0	0	0
Cortinarius camphoratus	0	0	0	0	0	0	0	0	0	0	0	0	0	0	0	0	0	0	0	0	0	0	0	0	0
Cortinarius casimiri	0	0	0	0	0	0	0	0	0	0	0	0	0	0	0	0	0	0	1	0	0	5	0	0	0
Cortinarius collinitus	0	0	0	0	0	0	0	0	0	0	0	0	0	0	0	0	0	0	0	0	0	0	0	0	0
Cortinarius croceus	0	0	0	0	0	0	0	0	0	0	0	0	0	0	0	0	0	0	0	0	0	0	0	0	0
Cortinarius decipiens	0	0	0	0	0	0	0	0	0	0	0	0	0	0	0	0	0	0	0	0	0	0	0	0	0
Cortinarius delibutus	0	0	0	0	0	0	0	0	0	0	0	0	0	0	0	0	0	0	0	0	0	0	0	0	0
Cortinarius evernius	0	0	0	0	0	0	0	0	0	0	0	0	0	0	0	0	0	0	0	0	0	0	0	0	0
Cortinarius fervidus	0	0	0	0	0	0	0	0	0	0	0	0	0	0	0	0	0	0	0	0	0	0	0	0	0
Cortinarius flexipes	0	0	0	0	0	0	0	0	0	0	0	0	0	0	0	0	0	0	1	1	0	1	0	0	0
Cortinarius fulvescens	0	0	0	0	0	0	0	0	0	0	0	0	0	0	0	0	0	0	0	0	0	0	0	0	0
Cortinarius gentilis	0	0	1	0	0	0	0	0	0	0	0	0	0	0	0	0	0	0	0	0	0	0	0	0	0
Cortinarius illuminus	0	0	0	0	0	0	0	0	0	0	0	0	0	0	0	0	0	0	0	0	0	0	1	0	0
Cortinarius limonius	0	0	0	0	0	0	0	0	0	0	0	0	0	0	0	0	0	0	0	0	0	0	0	0	0
Cortinarius lux-nymphae	0	0	1	0	0	0	0	0	0	0	0	0	0	0	0	0	0	0	0	0	0	0	0	0	0
Cortinarius mucifluus	0	0	0	0	0	0	0	0	0	0	0	0	1	0	0	0	0	0	0	0	0	0	0	0	0
Cortinarius mucosus	0	0	0	0	0	0	0	0	0	0	0	0	0	0	0	0	0	0	0	0	0	0	0	0	0
Cortinarius obtusus	1	4	0	0	0	2	3	1	0	1	3	0	0	1	0	0	1	0	6	5	2	5	13	3	3
Cortinarius pluvius	0	0	0	0	0	0	0	0	0	0	0	0	0	0	0	0	0	0	0	1	0	0	1	0	0
Cortinarius purpurascens	0	0	0	0	0	0	0	0	0	0	0	0	0	0	0	0	0	0	0	1	0	0	0	0	0
Cortinarius cf. quarciticus	1	0	0	0	0	0	0	0	0	0	0	0	0	0	0	0	0	0	0	0	0	0	0	0	0
Cortinarius raphanoides	0	0	0	0	0	0	0	0	0	0	0	0	0	0	0	0	0	0	0	0	0	0	0	0	0
Cortinarius rubellus	0	0	0	0	0	0	0	0	0	0	0	0	0	0	0	0	0	0	1	0	0	0	0	0	0
Cortinarius sanguineus	0	0	0	0	0	0	0	0	0	0	0	0	0	0	0	0	0	0	0	0	0	0	0	0	0
Cortinarius saturninus	0	0	0	0	0	0	0	0	0	0	0	0	0	0	0	0	0	0	0	0	0	0	0	0	0
Cortinarius scaurus	0	0	0	0	0	0	4	2	0	0	1	0	0	0	0	0	0	0	0	1	0	0	0	0	0
Cortinarius semisanguineus	0	0	0	0	0	0	0	0	0	0	1	0	0	0	0	0	1	0	0	0	0	0	0	0	0
Cortinarius stillatitius	0	0	0	0	0	0	0	0	0	0	0	0	0	0	1	0	0	0	0	0	0	0	0	0	0
Cortinarius subtortus	0	0	0	0	0	0	0	0	0	0	0	0	0	0	0	0	0	0	0	0	0	0	10	0	0
Cortinarius tortuosus	0	0	0	0	0	0	0	0	0	0	0	0	0	0	0	0	0	0	0	0	0	0	0	0	0
Cortinarius traganus	0	0	0	0	1	0	0	0	0	0	0	0	0	0	0	0	0	0	0	0	0	0	0	0	0
Cortinarius turmalis	0	0	0	0	0	0	0	0	0	0	0	0	0	0	0	0	0	0	0	0	0	0	0	0	0
Cortinarius varius	0	0	0	0	0	0	0	0	0	0	0	0	0	0	0	0	0	0	0	0	0	0	0	0	0
Cortinarius violaceus	0	0	0	0	0	0	0	0	0	0	0	0	0	0	0	0	0	0	0	0	0	0	0	0	0
Cortinarius sp.	0	0	0	0	0	0	0	0	0	0	0	0	0	0	0	0	0	0	0	0	0	1	1	0	0
Elaphomyces sp.	0	0	0	0	0	0	0	0	0	0	0	0	0	0	0	0	0	0	0	0	0	0	0	0	0
Entoloma rhodopolium	0	0	0	0	0	0	0	0	0	0	0	0	0	0	0	0	0	0	2	0	0	0	0	0	0
Glomus sp.	0	0	0	0	0	0	0	0	0	0	0	0	0	0	0	0	0	0	1	0	1	1	1	0	0
Hebeloma remyi	0	0	0	0	0	0	0	0	0	0	0	0	0	0	0	0	0	0	1	0	0	0	0	0	0
Hydnum rufescens	0	0	0	0	0	0	0	0	0	0	0	1	0	0	0	0	0	0	0	0	0	0	0	0	0
Hygrophorus camarophyllus	0	0	0	0	0	0	0	0	0	0	0	0	0	0	0	0	0	0	0	0	0	0	0	0	0
Hygrophorus olivaceoalbus	0	0	0	0	0	0	0	0	0	0	0	0	0	0	0	0	0	0	2	1	0	0	0	0	0
Hygrophorus pustulatus	0	0	0	0	0	0	0	0	0	0	0	0	0	0	0	0	0	0	0	6	0	0	0	0	0
Hygrophorus tephroleucus	0	0	0	0	0	0	0	0	0	0	0	0	0	0	0	0	0	0	0	0	0	0	0	0	0
Inocybe cincinnata	0	0	0	0	0	0	0	0	0	0	0	0	0	0	0	0	0	0	0	0	0	0	0	0	0
Inocybe geophylla	0	0	0	0	0	0	0	0	0	0	0	0	0	0	0	0	0	0	0	0	0	0	0	0	0
Inocybe lanuginosa	0	0	0	0	0	0	0	0	0	0	0	0	0	0	0	0	0	0	0	0	0	1	0	0	0
Inocybe mixtilis	0	0	0	0	0	0	0	0	0	0	0	0	0	0	0	0	0	0	0	0	0	0	0	0	0
Inocybe napipes	0	0	0	0	0	0	0	0	0	0	0	0	0	0	0	0	0	0	0	0	0	0	0	0	0
Inocybe nitidiuscula	0	0	0	0	0	0	0	0	0	0	0	0	0	0	0	0	0	0	0	0	0	0	0	0	0
Inocybe relicina	0	0	0	0	0	0	0	0	0	0	0	0	0	0	0	0	0	0	1	1	0	0	0	0	0
Inocybe subcarpta	0	0	0	0	0	0	0	1	0	0	0	0	0	0	0	0	0	0	0	0	0	0	0	0	0

Appendix 3 (continued).

Sample plot	1	2	3	4	5	6	7	8	9	10	11	12	13	14	15	16	17	18	19	21	22	23	24	25
Laccaria amethystina	0	0	0	0	0	0	0	0	0	0	0	0	0	0	0	0	0	0	0	0	0	0	0	0
Laccaria laccata	0	0	0	0	0	0	0	0	0	0	0	0	0	0	0	0	0	0	0	0	0	0	1	0
Lactarius camphoratus	0	0	0	0	0	1	0	0	0	0	0	0	0	0	4	0	0	0	0	0	0	0	0	0
Lactarius deterrimus	0	0	0	0	0	1	0	0	0	0	0	0	0	0	0	0	0	0	0	0	0	0	0	0
Lactarius fuliginosus	0	0	0	0	0	0	0	0	0	0	0	0	0	0	0	0	0	0	0	0	0	0	0	0
Lactarius glyciosmus	0	1	0	0	0	0	0	0	0	0	0	0	0	0	0	0	0	0	0	0	0	0	0	0
Lactarius mammosus	0	0	0	0	0	0	0	0	0	0	0	0	0	0	0	0	0	0	0	0	0	0	0	0
Lactarius mitissimus	0	0	0	0	0	0	0	0	0	0	0	0	0	0	0	0	0	0	0	0	0	0	0	0
Lactarius necator	0	0	0	0	0	0	0	0	0	0	0	0	0	0	0	0	0	0	0	0	0	0	0	0
Lactarius quietus	0	0	0	0	0	0	0	0	0	0	0	0	0	0	0	0	0	0	0	0	0	0	0	0
Lactarius rufus	0	0	0	0	0	0	0	4	0	0	0	0	0	1	0	0	0	0	0	0	0	0	0	0
Lactarius sphagneti	0	0	0	0	0	0	0	0	0	0	0	0	0	0	0	0	0	0	0	0	0	0	0	0
Lactarius theiogalus	0	0	0	0	0	0	0	0	0	0	0	0	0	0	0	2	5	0	4	0	3	0	6	0
Lactarius trivialis	0	0	0	0	0	0	0	0	0	0	0	0	0	0	0	0	0	0	0	0	0	0	0	0
Lactarius vietus	0	0	0	0	0	0	0	0	0	0	0	0	0	0	0	0	0	0	0	0	0	0	0	0
Leccinum aurantiacum	0	0	0	0	0	0	0	0	0	0	0	0	0	0	0	0	0	0	0	0	0	0	0	0
Leccinum niveum	0	0	0	0	0	0	0	0	0	0	0	0	0	0	0	0	0	0	0	0	0	0	0	0
Leccinum palustre	0	0	0	0	0	0	0	0	0	0	0	0	0	0	0	0	0	0	0	1	0	0	0	0
Leccinum scabrum	0	0	0	0	0	0	0	0	0	0	0	0	0	0	0	0	0	0	0	0	0	0	0	0
Leccinum variicolor	0	0	0	0	0	0	0	0	0	0	0	0	0	0	0	0	0	0	0	1	0	0	0	0
Leccinum versipelle	0	0	0	0	0	0	0	0	0	0	0	0	0	0	0	0	0	0	0	0	0	0	0	0
Leccinum sp.	0	0	0	0	0	0	0	0	0	0	0	0	0	0	0	0	0	0	0	0	0	0	0	0
Paxillus involutus	0	0	0	0	0	0	0	0	0	0	0	0	0	0	0	0	0	0	0	0	0	0	0	0
Rozites caperatus	0	0	0	0	0	1	0	2	0	0	0	0	0	0	0	0	0	0	0	0	0	0	0	0
Russula adusta	0	0	0	0	0	0	0	0	0	0	0	0	0	0	0	0	0	0	0	0	0	0	0	0
Russula aquosa	0	0	0	0	0	0	0	0	0	0	0	0	0	0	1	0	0	0	0	0	0	0	1	1
Russula atrorubens	0	0	0	0	0	0	0	0	0	0	0	0	0	0	0	0	0	0	0	0	0	0	0	0
Russula betularum	0	0	0	0	0	0	0	0	0	0	0	0	0	0	0	0	1	0	0	0	1	0	4	0
Russula consobrina	0	0	0	0	0	0	0	0	0	0	0	0	0	0	0	0	0	1	2	0	0	0	0	0
Russula decolorans	0	0	0	0	0	0	0	0	1	0	0	0	4	3	0	0	0	0	0	0	0	0	0	0
Russula elaeodes	0	0	0	0	0	0	0	1	0	0	0	0	0	0	0	0	0	0	0	0	0	0	0	0
Russula emetica	0	0	0	0	0	0	0	0	0	0	0	0	0	0	2	0	1	0	0	0	0	0	0	0
Russula fragilis	0	0	0	0	0	0	0	0	0	0	0	0	0	0	0	0	0	0	0	0	0	2	0	0
Russula laricina	0	0	0	0	0	0	0	0	0	0	0	0	0	0	0	0	0	0	0	0	0	0	0	0
Russula lutea	0	0	0	0	0	0	0	0	0	0	0	0	0	0	0	0	0	0	0	0	0	0	0	0
Russula ochroleuca	0	0	0	0	0	0	0	0	0	0	0	0	0	0	0	0	0	0	1	0	0	0	0	0
Russula paludosa	0	0	0	0	0	0	0	6	0	0	1	0	0	0	0	0	0	0	0	0	0	0	0	0
Russula puellaris	0	0	0	0	0	0	0	0	0	0	0	0	0	0	0	0	0	0	0	0	0	0	0	0
Russula queletii	0	0	0	0	0	0	0	0	0	0	0	0	0	0	0	0	0	0	0	0	0	0	0	0
Russula rhodopoda	1	1	1	0	1	0	0	1	0	0	0	0	0	0	0	0	0	1	0	0	0	0	0	0
Russula vesca	0	0	0	0	0	0	0	0	0	0	0	1	0	0	0	0	0	0	0	0	0	0	0	0
Russula vinosa	0	0	1	10	4	0	0	2	4	0	0	2	0	0	2	0	1	0	0	0	0	0	0	0
Russula xerampelina	0	0	0	0	0	0	0	0	0	0	0	0	0	0	0	0	0	0	0	0	0	0	0	0
Suillus variegatus	0	0	0	0	0	0	0	0	0	0	0	0	0	0	0	0	0	0	0	0	0	0	0	0
Thelephora palmata	0	0	0	0	0	0	0	0	0	0	0	0	0	0	0	0	0	0	0	0	0	0	0	0
Tricholoma fulvum	0	0	0	0	0	0	0	0	0	0	0	0	0	0	0	0	0	0	0	0	0	0	0	0
Tricholoma saponaceum	0	0	0	0	0	0	0	0	0	0	0	0	0	0	0	0	0	0	0	0	0	0	0	0
Tylopilus felleus	0	0	0	0	0	0	0	0	0	0	0	0	0	0	0	0	0	1	0	0	0	0	0	0
Xerocomus subtomentosus	0	0	0	0	0	0	0	0	0	0	0	0	0	1	0	3	0	0	0	0	0	0	0	0

Appendix 3 (continued).

Sample plot	26	27	28	29	30	31	32	33	34	35	36	37	38	39	40	41	42	43	44	45	46	47	48	49	50
Laccaria amethystina	0	0	0	0	0	0	0	0	0	0	0	0	0	0	0	0	0	2	0	1	0	0	0	0	0
Laccaria laccata	0	0	0	0	0	0	0	0	0	0	0	0	3	0	0	0	0	0	0	0	0	0	1	0	0
Lactarius camphoratus	0	0	0	0	0	0	0	1	0	0	0	0	0	0	0	0	0	0	0	1	1	1	1	0	0
Lactarius deterrimus	0	0	0	0	0	0	0	0	0	0	0	0	0	0	0	0	0	0	0	0	0	0	0	0	0
Lactarius fuliginosus	0	0	0	0	0	0	0	0	0	0	0	0	0	0	0	0	0	0	0	0	2	0	0	0	0
Lactarius glyciosmus	0	0	0	0	0	0	0	0	0	0	0	0	0	0	0	0	0	0	0	0	0	0	0	0	0
Lactarius mammosus	0	0	0	0	0	0	0	0	0	0	0	0	0	0	0	0	0	0	0	0	0	0	0	0	0
Lactarius mitissimus	0	0	0	0	0	0	0	0	0	0	0	0	0	0	0	0	0	0	0	0	0	0	0	0	0
Lactarius necator	0	0	0	0	0	0	0	0	0	0	0	0	0	0	0	0	0	0	0	0	0	0	0	0	0
Lactarius quietus	0	0	0	0	0	0	0	0	0	0	0	0	0	0	0	0	0	0	0	0	0	0	0	0	0
Lactarius rufus	1	0	0	0	0	0	0	0	0	0	0	0	0	0	0	0	0	0	0	0	0	0	0	0	0
Lactarius sphagneti	0	0	0	0	0	0	0	0	0	0	1	0	0	0	0	0	0	0	0	0	0	1	0	0	0
Lactarius theiogalus	0	0	0	0	0	0	0	0	0	0	0	0	0	0	0	0	0	0	2	0	0	0	0	0	0
Lactarius trivialis	0	0	0	0	0	0	0	0	0	0	0	0	0	0	0	0	0	0	0	0	0	0	0	0	0
Lactarius vietus	0	0	0	0	0	0	0	0	0	7	0	0	0	1	0	0	0	1	0	0	0	0	0	0	0
Leccinum aurantiacum	0	0	0	0	0	0	0	0	0	0	0	0	0	0	0	0	0	0	0	3	0	0	0	0	0
Leccinum niveum	0	0	0	0	0	0	0	0	0	0	0	0	0	0	0	0	0	0	0	0	0	0	0	0	0
Leccinum palustre	0	0	0	1	0	3	0	0	0	0	0	0	0	0	0	0	0	0	0	0	0	0	0	0	0
Leccinum scabrum	0	0	0	2	0	0	0	0	0	0	0	0	0	0	0	0	0	0	0	0	0	0	0	0	0
Leccinum variicolor	0	0	0	0	0	0	0	0	0	0	0	0	2	0	0	0	0	0	0	0	0	0	0	0	0
Leccinum versipelle	0	0	0	0	0	0	0	0	0	0	0	0	0	0	0	0	0	0	0	0	0	0	0	0	0
Leccinum sp.	0	0	0	0	0	1	0	0	0	0	0	0	0	0	0	0	0	0	0	0	0	0	0	0	0
Paxillus involutus	0	0	0	0	0	0	0	0	0	0	0	0	0	0	0	0	0	1	0	0	0	0	0	0	0
Rozites caperatus	0	0	0	0	0	0	0	0	0	1	0	1	0	0	0	0	0	1	0	0	0	0	0	0	0
Russula adusta	0	0	0	0	0	0	0	0	0	0	0	0	0	0	0	0	0	0	0	0	0	0	0	0	0
Russula aquosa	0	0	0	0	0	0	0	0	0	0	0	0	0	0	0	0	2	1	0	0	0	0	0	0	0
Russula atrorubens	0	0	0	0	0	0	0	0	0	0	0	0	0	0	0	0	1	0	0	0	0	0	0	0	0
Russula betularum	0	0	0	0	0	0	0	0	0	0	0	0	0	0	0	0	0	0	0	0	0	0	0	0	0
Russula consobrina	0	0	0	0	0	0	0	0	0	0	0	0	0	0	0	0	0	0	0	0	0	0	0	1	0
Russula decolorans	0	0	1	0	0	1	0	0	0	0	0	0	0	0	0	0	0	0	0	0	0	0	0	0	0
Russula elaeodes	0	0	0	0	0	0	0	0	0	0	0	0	0	0	0	0	0	0	0	0	0	0	0	0	0
Russula emetica	0	0	0	0	0	0	2	1	0	1	0	0	1	0	1	0	1	0	0	0	2	0	0	0	0
Russula fragilis	0	0	0	0	0	0	0	0	0	0	0	0	0	0	0	0	0	0	0	0	0	0	0	0	0
Russula laricina	0	0	0	0	0	0	0	0	0	0	0	0	0	0	0	0	0	0	0	0	0	0	0	0	0
Russula lutea	0	0	0	0	0	0	0	0	0	0	0	0	0	0	0	0	0	0	0	0	0	0	0	0	0
Russula ochroleuca	0	0	0	0	0	0	0	0	0	0	0	0	0	0	0	0	0	0	0	0	0	0	8	0	0
Russula paludosa	0	0	0	1	0	0	0	0	0	0	0	0	0	0	0	0	0	0	0	2	0	0	0	0	0
Russula puellaris	0	0	0	0	0	0	0	0	0	0	0	0	1	0	0	0	0	0	0	0	0	0	0	0	0
Russula queletii	0	0	0	0	0	0	0	0	0	0	0	0	0	0	0	0	0	0	0	1	0	0	0	0	0
Russula rhodopoda	0	0	0	0	0	0	0	0	0	0	6	0	0	1	4	1	0	0	0	0	1	0	0	1	0
Russula vesca	0	0	0	0	0	0	0	0	0	0	0	0	0	0	0	0	0	0	0	0	0	0	0	0	0
Russula vinosa	0	0	0	0	0	0	0	0	0	0	0	0	0	0	0	1	6	0	0	0	0	0	0	0	0
Russula xerampelina	0	0	0	0	0	0	0	0	0	0	0	0	0	0	0	1	0	0	0	0	0	0	0	0	0
Suillus variegatus	0	2	1	0	0	0	0	0	0	0	0	0	0	0	0	0	0	0	0	0	0	0	0	0	0
Thelephora palmata	0	0	0	0	0	0	0	0	0	0	0	0	0	0	0	0	0	0	0	0	0	0	0	0	0
Tricholoma fulvum	0	0	0	0	0	0	0	1	0	0	0	0	0	0	0	0	0	0	0	0	0	0	0	0	0
Tricholoma saponaceum	0	0	0	0	0	0	0	0	0	0	0	0	0	1	0	0	0	0	0	0	0	0	0	0	0
Tylopilus felleus	0	0	0	0	0	0	0	0	0	0	0	0	0	0	0	0	0	0	0	0	0	0	0	0	0
Xerocomus subtomentosus	0	0	0	0	0	0	0	0	0	0	0	0	0	0	0	0	0	0	0	0	0	0	0	0	0

Appendix 3 (continued).

Sample plot	51	52	53	54	55	56	57	58	59	60	61	62	63	64	65	66	67	68	69	70	71	72	73	74	75
Laccaria amethystina	0	2	1	0	0	0	0	0	0	0	0	0	0	0	0	0	0	0	0	1	0	0	0	0	0
Laccaria laccata	0	0	0	0	0	0	0	0	0	0	0	0	0	0	0	0	0	0	0	0	0	0	0	0	0
Lactarius camphoratus	0	0	0	0	0	0	0	0	0	0	0	0	0	0	0	0	6	4	3	0	0	0	1	0	0
Lactarius deterrimus	1	0	0	4	0	0	1	0	0	0	0	0	0	0	0	0	0	0	0	0	0	0	0	0	0
Lactarius fuliginosus	0	2	0	3	0	0	0	0	0	0	0	0	0	0	0	0	0	0	0	0	0	0	0	0	0
Lactarius glyciosmus	0	0	0	0	0	0	0	0	0	0	0	0	0	0	0	0	0	0	0	0	0	0	0	0	0
Lactarius mammosus	0	0	0	0	0	0	0	0	0	0	0	0	1	0	0	0	0	0	0	0	0	0	0	0	0
Lactarius mitissimus	0	0	0	0	0	0	0	0	0	0	0	0	0	0	0	0	0	1	0	0	0	0	0	0	0
Lactarius necator	0	0	0	2	0	0	0	0	0	0	0	0	0	0	0	0	4	7	0	0	0	0	0	0	0
Lactarius quietus	0	0	0	0	0	0	0	0	0	0	0	0	0	0	0	0	1	0	0	0	0	0	0	0	0
Lactarius rufus	0	0	0	0	0	0	0	0	0	8	0	0	0	0	0	0	0	0	1	0	0	0	0	0	0
Lactarius sphagneti	0	0	0	0	0	0	0	0	0	0	0	0	0	0	0	0	0	0	0	0	0	0	0	0	0
Lactarius theiogalus	0	0	0	0	0	0	0	0	0	0	0	0	0	0	0	0	0	0	10	0	0	0	0	0	0
Lactarius trivialis	0	0	0	0	0	0	0	0	0	0	0	0	0	0	0	0	0	0	0	0	0	0	0	0	0
Lactarius vietus	0	0	0	0	0	0	0	0	0	0	0	0	0	0	0	0	0	1	0	0	0	4	0	0	0
Leccinum aurantiacum	0	0	0	0	0	0	0	0	0	0	0	0	0	0	0	0	0	0	0	0	0	0	0	0	0
Leccinum niveum	0	0	0	0	0	0	0	0	0	0	0	0	0	0	0	0	0	0	0	0	0	0	0	0	0
Leccinum palustre	0	0	0	0	0	0	0	0	0	0	0	0	0	1	0	3	0	0	0	0	0	1	0	0	0
Leccinum scabrum	0	0	0	0	0	0	0	0	0	0	0	0	0	0	0	0	0	0	0	0	0	0	0	0	0
Leccinum variicolor	0	0	0	0	0	0	0	0	0	0	0	0	0	0	0	0	0	0	0	0	0	0	0	0	0
Leccinum versipelle	0	0	0	0	0	0	0	0	0	0	2	0	0	0	1	0	0	0	0	0	0	0	2	0	0
Leccinum sp.	0	0	0	0	0	0	0	0	0	0	0	0	0	0	0	0	0	0	0	0	0	0	0	0	0
Paxillus involutus	0	0	0	0	0	0	0	0	0	0	0	0	0	0	0	0	0	0	0	0	0	0	0	0	0
Rozites caperatus	0	0	0	0	0	0	0	1	0	0	0	0	0	0	0	0	0	0	0	0	0	0	0	0	0
Russula adusta	0	0	0	0	0	0	0	0	0	0	0	0	0	0	0	0	0	1	0	0	0	0	0	0	0
Russula aquosa	0	0	0	0	0	0	0	0	0	0	0	0	0	0	0	0	0	1	0	2	0	0	0	0	0
Russula atrorubens	0	0	0	0	0	0	0	0	0	0	0	0	0	0	0	0	0	0	0	0	0	0	0	0	0
Russula betularum	0	1	0	0	0	0	0	0	0	0	0	0	0	0	0	0	0	0	1	0	0	0	0	0	0
Russula consobrina	0	0	0	0	0	0	0	0	0	0	0	0	0	0	0	0	0	0	0	0	0	0	0	0	0
Russula decolorans	0	0	0	0	0	0	0	4	4	0	1	3	0	0	0	1	0	0	0	0	0	0	0	0	0
Russula elaeodes	0	0	0	0	0	0	0	0	0	0	0	0	0	0	0	0	0	0	0	0	1	0	0	0	0
Russula emetica	1	0	0	1	0	0	0	0	0	0	0	0	0	0	0	0	0	1	0	1	0	0	0	0	0
Russula fragilis	0	0	0	0	0	0	0	0	0	0	0	0	0	0	0	0	0	0	1	0	0	0	0	0	0
Russula laricina	0	0	0	1	0	1	0	0	0	0	0	0	0	0	0	0	0	0	0	0	0	0	0	0	0
Russula lutea	0	0	0	0	0	0	0	0	0	0	0	0	0	0	0	0	0	2	0	0	0	0	0	0	0
Russula ochroleuca	0	0	0	0	0	0	0	0	0	0	0	0	0	0	0	0	5	0	0	0	0	0	0	0	0
Russula paludosa	0	0	0	0	0	0	0	2	7	0	0	0	4	0	0	0	0	0	0	0	0	0	0	0	0
Russula puellaris	0	0	0	0	0	0	0	0	0	0	0	0	0	0	0	0	0	1	0	0	0	0	0	0	0
Russula queletii	0	1	2	0	0	0	0	0	0	0	0	0	0	0	0	0	0	0	0	0	0	0	0	0	0
Russula rhodopoda	0	0	2	0	0	0	0	0	0	0	0	0	0	0	0	0	0	0	0	0	0	0	0	0	0
Russula vesca	0	0	0	0	0	0	0	0	0	0	0	0	0	0	0	0	0	0	0	0	0	0	0	0	0
Russula vinosa	0	0	0	0	0	0	0	0	0	0	0	0	0	0	0	0	0	0	0	0	0	0	0	0	0
Russula xerampelina	0	0	0	0	0	0	0	0	0	0	0	0	0	0	0	0	0	0	0	0	0	0	0	0	0
Suillus variegatus	0	0	0	0	0	0	0	0	0	0	0	0	0	0	0	1	0	0	0	0	0	0	0	0	0
Thelephora palmata	0	0	0	0	0	0	1	0	0	0	0	0	0	0	0	0	0	0	0	0	0	0	0	0	0
Tricholoma fulvum	0	0	0	0	0	0	0	0	0	0	0	0	0	0	0	0	0	0	0	0	0	0	0	0	0
Tricholoma saponaceum	0	0	0	0	0	0	0	0	0	0	0	0	0	0	0	0	0	0	0	0	0	0	0	0	0
Tylopilus felleus	0	0	0	0	0	0	0	0	0	0	0	0	0	0	0	0	0	0	0	0	0	0	0	0	0
Xerocomus subtomentosus	0	0	0	0	0	0	0	0	0	0	0	0	0	0	0	0	0	0	0	0	0	0	0	0	0

Appendix 3 (continued).

Sample plot	76	77	78	79	80	81	82	83	84	85	86	87	88	89	90	91	92	93	94	95	96	97	98	99	100
Laccaria amethystina	0	0	0	0	0	0	0	0	0	0	0	0	0	0	0	0	0	0	0	0	0	0	0	0	0
Laccaria laccata	0	0	0	0	0	0	0	0	0	0	0	0	0	0	0	0	0	0	1	0	0	0	0	0	0
Lactarius camphoratus	0	0	0	0	0	0	0	0	0	0	0	0	0	0	0	0	0	0	0	1	0	0	0	0	0
Lactarius deterrimus	0	0	0	0	0	0	0	0	0	0	0	0	0	0	0	0	0	0	0	0	0	0	0	0	0
Lactarius fuliginosus	0	0	0	0	0	0	0	0	0	0	0	0	0	0	0	0	0	0	0	0	0	0	0	0	0
Lactarius glyciosmus	0	0	0	0	0	0	0	0	0	0	0	0	0	0	0	0	0	0	0	0	0	1	0	0	0
Lactarius mammosus	0	0	0	0	0	0	0	0	0	0	0	0	0	0	0	0	0	0	0	0	0	0	0	0	0
Lactarius mitissimus	0	0	0	0	0	0	0	0	0	0	0	0	0	0	0	0	0	0	0	0	0	0	0	0	0
Lactarius necator	0	0	0	0	0	0	0	0	0	0	0	0	0	0	0	0	0	0	0	0	0	0	0	0	0
Lactarius quietus	0	0	0	0	0	0	0	0	0	0	0	0	0	0	0	0	0	0	0	0	0	0	0	0	0
Lactarius rufus	0	0	0	1	0	0	0	4	1	0	0	0	0	0	0	0	0	0	0	0	0	0	0	0	0
Lactarius sphagneti	0	0	0	0	0	0	0	0	0	0	0	0	0	0	0	0	0	0	0	0	0	0	0	0	0
Lactarius theiogalus	0	0	0	0	0	0	0	0	0	0	0	0	0	0	0	0	0	0	0	0	0	0	0	0	0
Lactarius trivialis	0	0	0	0	0	0	0	0	0	0	0	0	0	0	0	0	0	0	0	1	0	0	0	0	0
Lactarius vietus	0	0	0	0	0	0	0	0	0	0	0	0	0	0	0	0	0	0	0	0	0	0	0	0	0
Leccinum aurantiacum	0	0	0	0	0	0	0	0	0	0	0	0	0	0	0	0	0	0	0	0	0	0	0	0	0
Leccinum niveum	0	0	0	0	0	0	0	0	0	0	0	0	0	0	0	0	0	0	1	0	0	0	0	0	0
Leccinum palustre	0	0	0	0	0	0	0	0	0	0	0	0	0	0	0	0	0	0	0	0	0	1	0	1	3
Leccinum scabrum	0	0	0	0	0	0	0	0	0	0	1	0	0	0	0	0	0	0	0	0	0	1	0	0	0
Leccinum variicolor	0	0	0	0	0	0	0	0	0	0	0	0	0	0	0	0	0	0	0	0	1	0	0	2	0
Leccinum versipelle	0	0	0	0	0	0	0	0	0	0	1	0	0	0	0	0	1	1	0	0	0	0	0	0	0
Leccinum sp.	0	0	0	0	0	0	0	0	0	0	0	2	0	0	0	0	0	1	0	1	0	0	1	0	0
Paxillus involutus	0	0	0	0	0	0	0	0	0	0	0	0	0	0	0	0	0	0	0	0	0	0	0	0	0
Rozites caperatus	0	0	0	0	0	0	0	0	0	0	0	0	0	0	0	0	0	0	0	0	0	0	1	0	0
Russula adusta	0	0	0	0	0	0	0	0	0	0	0	0	0	0	0	0	0	0	0	0	0	0	0	0	0
Russula aquosa	0	0	0	0	0	0	0	0	0	0	0	0	0	0	0	0	0	0	0	0	0	1	0	0	0
Russula atrorubens	0	0	0	0	0	0	0	0	0	0	0	0	0	0	0	0	0	0	0	0	0	0	0	0	0
Russula betularum	0	0	0	0	0	0	0	0	0	0	0	0	0	0	0	0	0	0	0	0	0	0	0	0	0
Russula consobrina	0	0	0	0	0	0	0	0	0	0	0	0	0	0	0	0	0	0	0	0	0	0	0	0	0
Russula decolorans	1	0	0	0	2	6	4	5	3	1	3	7	1	0	1	0	1	0	0	0	0	0	0	0	0
Russula elaeodes	0	0	0	0	0	0	0	0	0	0	0	0	0	0	0	0	0	0	0	0	0	0	0	0	0
Russula emetica	0	0	0	0	0	0	0	0	0	0	0	0	0	0	0	0	0	0	0	3	0	1	5	0	0
Russula fragilis	0	0	0	0	0	0	0	0	0	0	0	0	0	0	0	0	0	0	0	0	0	0	0	0	0
Russula laricina	0	0	0	0	0	0	0	0	0	0	0	0	0	0	0	0	0	0	0	0	0	0	0	0	0
Russula lutea	0	0	0	0	0	0	0	0	0	0	0	0	0	0	0	0	0	0	0	0	0	0	0	0	0
Russula ochroleuca	0	0	0	0	0	0	0	0	0	0	0	0	0	0	0	0	0	0	0	0	0	0	0	0	0
Russula paludosa	0	0	0	0	2	5	2	1	3	0	0	2	4	3	0	0	0	0	0	0	0	0	0	0	0
Russula puellaris	0	0	0	0	0	0	0	0	0	0	0	0	0	0	0	0	0	1	1	1	0	1	0	0	0
Russula queletii	0	0	0	0	0	0	0	0	0	0	0	0	0	0	0	0	0	0	0	0	0	0	0	0	0
Russula rhodopoda	0	0	0	0	0	0	0	0	0	0	0	0	0	0	0	0	0	0	0	0	0	0	0	0	0
Russula vesca	0	0	0	0	0	0	0	0	0	0	0	0	0	0	0	0	0	0	0	0	0	1	0	0	0
Russula vinosa	1	0	1	0	0	0	0	0	0	0	0	0	0	0	0	0	0	0	0	0	0	0	0	3	0
Russula xerampelina	0	0	0	0	0	0	0	0	0	0	0	0	0	0	0	0	0	0	0	0	0	0	0	0	0
Suillus variegatus	0	0	0	0	0	0	0	2	0	0	0	0	0	0	0	0	1	0	0	0	0	0	0	0	0
Thelephora palmata	0	0	0	0	0	0	0	0	0	0	0	0	0	0	0	0	0	0	0	0	0	0	0	0	0
Tricholoma fulvum	0	0	0	0	0	0	0	0	0	0	0	0	0	0	0	0	0	0	0	0	0	0	0	0	0
Tricholoma saponaceum	0	0	0	0	0	0	0	0	0	0	0	0	0	0	0	0	0	0	0	0	0	0	0	0	0
Tylopilus felleus	0	0	0	0	0	0	0	0	0	0	0	0	0	0	0	0	0	0	0	0	0	0	0	0	0
Xerocomus subtomentosus	0	0	0	0	0	0	0	0	0	0	0	0	0	0	0	0	0	0	0	0	0	0	0	0	0

Appendix 4. Saprotrophic fungi recorded in the 99 macroplots. Species quantity is given as subplot frequency.

Sample plot	1	2	3	4	5	6	7	8	9	10	11	12	13	14	15	16	17	18	19	21	22	23	24	25
Agrocybe erebia	0	0	0	0	0	0	0	0	0	0	0	0	0	0	0	0	0	0	0	0	0	0	0	0
Armillaria mellea coll.	0	0	0	0	0	0	0	0	0	0	0	0	0	0	0	0	1	0	0	0	0	0	0	0
Baeospora myosura	0	0	1	1	0	0	0	0	0	0	0	0	0	0	4	0	0	0	0	0	0	0	0	0
Calocera viscosa	0	0	0	0	0	0	1	0	0	1	0	0	0	0	0	2	0	0	0	0	0	2	1	0
Clavariadelphus junceus	0	0	0	0	0	0	0	0	0	0	0	0	0	0	0	0	0	0	0	0	0	0	0	0
Clavulina coralloides	0	0	0	0	0	0	0	0	0	0	0	0	0	0	0	0	2	0	0	0	0	0	0	0
Clitocybe candicans	0	0	0	0	0	0	0	0	0	0	0	0	0	0	0	0	0	0	0	0	0	0	0	0
Clitocybe diatreta	0	0	1	0	0	0	0	0	0	0	0	0	0	0	0	0	0	0	0	0	0	0	0	0
Clitocybe ditopus	0	0	0	0	0	0	0	0	0	0	0	0	0	0	0	0	0	0	0	0	0	0	0	0
Clitocybe metachroa	0	0	0	0	0	0	0	0	0	0	0	0	0	0	0	0	0	0	0	0	0	0	0	0
Collybia acervata	0	0	0	1	0	0	0	0	0	0	0	0	0	0	0	0	0	0	0	0	0	0	0	0
Collybia asema	1	0	0	0	0	0	0	0	0	0	0	0	0	0	0	0	0	0	0	0	0	0	0	0
Collybia cirrata	0	0	0	0	0	0	0	1	0	0	1	0	0	0	0	0	0	0	0	0	0	0	0	0
Collybia confluens	0	0	0	0	0	0	0	0	0	0	0	0	0	0	0	0	0	0	0	0	0	0	0	0
Collybia cookei	0	0	0	0	0	0	0	0	0	0	0	0	0	0	0	0	0	0	0	0	0	0	0	0
Collybia dryophila	0	0	0	0	0	0	0	0	0	0	0	0	0	0	0	0	0	0	0	0	0	0	0	0
Collybia putilla	0	0	0	0	0	0	0	0	0	0	0	0	0	1	0	0	0	0	0	0	0	0	0	0
Collybia tuberosa	0	2	1	2	1	0	1	2	1	0	0	0	3	3	3	2	2	1	0	1	5	2	0	3
Conocybe striipes	0	0	0	0	0	0	0	0	0	0	0	0	0	0	0	0	0	0	0	0	0	0	0	0
Conocybe sulcatipes	0	0	0	0	0	0	0	0	0	0	0	0	0	0	0	0	0	0	0	0	0	0	0	0
Cordyceps ophioglossoides	0	0	0	0	0	2	1	0	0	0	0	0	0	0	0	0	0	0	0	0	0	0	0	0
Cudonia circinans	0	0	0	0	0	0	1	0	0	0	0	0	0	0	0	0	0	0	0	0	0	0	0	0
Cudonia confusa	0	0	0	0	0	0	0	0	0	0	0	0	0	0	0	0	0	0	0	0	0	0	0	0
Cudoniella clavus	0	0	0	0	0	0	0	0	0	0	0	0	0	0	0	0	0	0	0	0	0	0	0	0
Cystoderma carcharias	0	0	0	0	0	0	0	0	0	0	0	0	0	0	0	0	0	0	0	0	0	0	0	0
Cystoderma fallax	0	0	0	0	0	0	0	0	0	0	0	0	0	0	0	0	0	0	0	0	0	0	0	0
Cystoderma jasonis	1	2	2	2	0	1	0	5	1	0	0	0	0	2	2	1	5	0	4	0	3	1	2	0
Entoloma cetratum	0	0	0	0	0	0	0	0	1	0	0	0	0	0	0	1	0	0	0	0	0	1	0	0
Entoloma conferendum	0	0	0	0	0	0	0	0	0	0	0	0	0	0	0	0	0	0	0	0	0	0	1	0
Entoloma juncinum	0	0	0	0	0	0	0	0	0	0	0	0	0	0	0	0	0	0	0	0	0	0	0	0
Entoloma nitidum	0	0	0	0	0	0	0	0	0	0	0	0	0	0	0	0	0	0	0	0	0	0	0	0
Entoloma rhodocylix	0	0	0	0	0	0	0	0	0	0	0	0	0	0	0	0	0	0	0	0	0	0	0	0
Entoloma turbidum	0	1	0	0	0	0	0	0	0	0	0	0	0	0	0	0	0	0	0	0	0	0	0	0
Fayodia gracilipes	0	0	0	0	0	0	0	0	0	0	0	0	0	0	0	0	0	0	0	0	0	0	0	0
Flammulaster subincarnatus	0	0	0	0	0	0	0	0	0	0	0	0	0	0	0	0	0	0	0	0	0	0	0	0
Galerina allospora	0	0	0	0	0	0	0	0	0	0	0	0	0	0	0	0	0	0	0	0	0	0	0	0
Galerina atkinsoniana	3	4	5	4	2	4	2	1	1	1	1	2	0	1	4	4	5	0	2	1	1	1	5	2
Galerina badipes	0	0	0	0	0	0	0	0	0	0	0	0	0	0	0	0	0	0	0	0	0	0	0	0
Galerina borealis	0	0	0	0	0	0	0	0	0	0	0	0	0	0	0	0	0	0	0	4	0	1	0	0
Galerina hypnorum	8	4	14	10	3	16	5	3	5	0	0	3	5	2	16	8	9	0	5	12	7	6	12	5
Galerina marginata	0	0	0	0	0	0	0	0	0	0	0	0	0	0	0	0	0	0	0	0	0	0	0	0
Galerina mniophila	0	0	2	1	0	0	0	2	1	0	1	0	0	0	5	4	2	0	2	1	0	0	3	0
Galerina pumila	0	0	0	0	0	0	0	0	0	0	0	0	0	0	0	0	0	0	0	0	0	0	0	0
Galerina stylifera	0	0	0	0	0	0	0	0	0	0	0	0	0	0	0	0	0	0	0	0	0	0	0	0
Galerina triscopa	0	0	0	0	0	0	0	0	0	0	0	0	0	0	0	0	0	0	0	0	0	0	0	0
Galerina unicolor	0	0	0	0	0	0	0	0	0	0	0	0	0	0	0	0	1	0	0	0	0	0	0	0
Galerina sp.1	0	0	0	1	0	2	0	0	0	0	0	1	0	0	1	0	1	0	2	2	0	0	5	4
Galerina sp.2	0	0	0	0	0	0	0	0	1	0	0	0	0	1	0	2	1	0	2	0	0	0	0	0
Gymnopilus sapineus	0	1	0	0	0	1	0	0	0	0	0	0	1	0	0	0	0	0	0	0	0	0	0	0
Hemimycena delectabilis	0	0	0	0	0	0	0	0	0	0	0	0	0	0	0	0	0	0	0	0	0	0	0	0
Heyderia abietis	0	0	0	0	0	1	0	0	0	1	0	0	0	0	0	0	0	0	0	0	0	0	0	0
Hygrocybe virginea var. fuscescens	0	0	0	0	0	0	0	0	0	0	0	0	0	0	0	0	0	0	0	0	0	0	0	0
Hygrophoropsis aurantiaca	0	0	0	0	0	0	0	0	0	0	0	0	0	0	0	1	0	0	0	0	0	0	0	0
Hypholoma capnoides	0	0	0	0	0	0	0	0	0	0	0	0	0	0	0	0	0	0	0	0	0	0	0	0
Hypholoma marginatum	0	0	0	0	0	0	0	0	0	0	0	0	0	0	0	0	0	0	0	3	0	0	0	0
Hypholoma polytrichii	0	0	0	0	0	0	0	0	0	0	0	0	0	0	0	0	3	0	0	0	0	0	0	0
Lycoperdon nigrescens	0	0	0	0	0	0	0	0	0	0	0	0	0	0	0	0	0	0	0	0	0	0	0	0
Lyophyllum rancidum	0	0	0	0	0	0	0	0	0	0	0	0	0	0	0	0	0	0	0	0	0	0	0	0
Lyophyllum semitale	0	0	0	0	0	0	0	0	0	0	0	0	0	0	0	0	0	0	0	0	0	0	0	0
Marasmius androsaceus	11	15	15	10	6	9	0	4	12	16	8	8	4	3	8	1	3	3	0	4	8	1	0	2
Marasmius bulliardii f. acicola	0	0	0	0	0	0	0	0	0	0	0	0	0	0	0	0	0	0	0	0	0	0	0	0
Marasmius epiphyllus	0	0	0	0	1	0	1	4	0	1	0	0	0	0	0	0	0	0	0	0	0	0	0	0
Micromphale perforans	0	5	4	11	10	0	11	3	0	0	0	0	0	0	1	7	0	0	0	4	0	0	0	0
Mycena alcalina coll.	0	0	0	0	0	0	0	0	0	0	0	0	0	0	0	0	0	0	0	0	0	0	0	0
Mycena amicta	0	0	0	0	0	0	0	0	0	0	0	0	0	0	0	1	0	0	0	0	0	0	0	0
Mycena aurantiomarginata	0	0	0	0	0	0	0	0	0	0	0	0	0	0	0	0	0	0	0	0	0	0	0	0
Mycena cinerella	1	0	4	0	0	0	0	0	0	1	0	0	0	0	0	0	0	0	0	0	0	1	0	0
Mycena cineroides	0	2	7	1	0	0	0	1	0	1	0	0	0	0	0	8	3	0	1	0	1	0	0	0
Mycena clavicularis	0	0	0	0	0	0	0	0	0	0	0	0	0	0	0	0	0	0	0	0	0	0	0	0
Mycena epipterygia	0	0	0	0	1	0	0	0	0	0	0	0	0	0	0	0	0	0	0	0	0	0	0	0
Mycena filopes	0	0	0	0	0	0	0	0	0	0	0	0	0	0	0	1	1	0	0	0	0	0	0	0
Mycena flavoalba	0	1	1	0	0	0	3	1	0	0	0	0	0	0	0	0	1	3	0	0	0	0	0	0
Mycena floridula	0	0	0	0	0	0	0	0	0	0	0	0	0	0	0	0	0	0	0	0	0	0	0	0

Appendix 4 (continued).

Sample plot	26	27	28	29	30	31	32	33	34	35	36	37	38	39	40	41	42	43	44	45	46	47	48	49	50
Agrocybe erebia	0	0	0	0	0	0	0	0	0	0	0	0	0	0	0	0	0	0	0	0	0	0	0	0	0
Armillaria mellea coll.	0	0	0	0	0	0	0	0	0	0	0	0	0	0	0	0	0	0	0	1	0	0	0	0	0
Baeospora myosura	0	0	0	0	0	0	1	0	1	0	1	0	0	0	0	0	0	0	0	0	0	0	0	0	0
Calocera viscosa	2	0	0	0	0	0	0	1	0	0	1	0	0	2	0	0	0	1	0	0	0	0	0	0	0
Clavariadelphus junceus	0	0	0	0	0	0	0	0	0	0	0	0	0	0	0	0	0	0	0	5	0	0	0	1	2
Clavulina coralloides	0	0	0	0	0	0	0	0	0	0	0	0	0	0	0	0	0	0	4	0	0	1	0	0	0
Clitocybe candicans	0	0	0	0	0	0	0	0	0	0	0	0	0	0	0	0	0	0	0	0	1	0	0	0	0
Clitocybe diatreta	0	0	0	0	0	0	0	0	0	0	0	0	0	0	0	0	0	0	0	0	0	0	1	0	0
Clitocybe ditopus	0	0	0	0	0	0	0	0	0	0	0	0	0	0	0	0	0	0	1	0	0	0	0	0	0
Clitocybe metachroa	0	0	0	0	0	0	3	0	0	0	0	0	0	0	0	0	0	0	0	0	0	0	0	0	0
Collybia acervata	0	0	0	0	0	0	0	0	0	0	0	0	0	0	0	0	0	0	0	0	0	0	0	0	0
Collybia asema	0	0	0	0	0	0	0	0	0	0	0	0	0	0	0	0	0	0	0	0	0	0	0	0	0
Collybia cirrata	0	0	0	0	0	2	0	0	0	0	0	0	0	0	0	0	0	1	0	1	2	0	2	0	0
Collybia confluens	0	0	0	0	0	0	0	0	0	0	0	0	0	0	0	0	0	0	0	0	0	0	0	0	0
Collybia cookei	0	0	0	0	0	0	0	0	0	0	0	0	0	0	0	0	0	0	0	0	0	0	0	0	0
Collybia dryophila	1	0	0	0	0	1	0	0	0	0	0	0	0	0	0	0	0	0	0	0	0	1	0	1	0
Collybia putilla	0	0	0	0	0	0	0	0	0	0	0	0	0	0	0	0	0	0	0	0	0	0	0	0	0
Collybia tuberosa	0	0	1	0	0	5	1	3	1	1	0	0	0	0	0	1	2	1	0	0	1	0	4	1	0
Conocybe striipes	0	0	0	0	0	0	0	0	0	0	0	0	0	0	0	0	0	0	0	0	0	0	0	0	0
Conocybe sulcatipes	0	0	0	0	0	0	0	0	0	0	0	0	0	0	0	0	0	0	0	0	0	0	0	0	0
Cordyceps ophioglossoides	0	0	0	0	0	0	0	1	0	0	0	0	0	0	0	0	0	0	0	0	0	0	0	0	0
Cudonia circinans	0	0	0	0	0	0	0	0	0	2	0	0	0	0	0	0	0	0	0	0	0	0	0	0	0
Cudonia confusa	0	0	0	0	0	0	0	0	0	0	0	0	0	0	0	0	0	0	0	0	0	0	0	1	0
Cudoniella clavus	0	0	0	0	0	0	0	0	0	0	0	0	0	0	0	0	0	0	0	0	0	0	0	0	0
Cystoderma carcharias	0	0	0	0	0	0	0	0	0	0	0	0	0	0	0	0	0	0	0	1	0	0	0	0	0
Cystoderma fallax	0	0	0	0	0	0	0	0	0	0	0	0	0	0	0	0	0	0	0	0	0	0	0	0	0
Cystoderma jasonis	4	2	0	0	0	0	1	0	0	0	1	0	0	0	0	1	5	2	1	0	0	0	0	0	0
Entoloma cetratum	0	0	0	1	0	1	1	0	0	0	0	0	1	0	0	0	0	0	2	0	1	0	1	0	0
Entoloma conferendum	0	0	0	0	0	0	0	0	0	0	0	0	5	0	0	0	0	0	0	0	0	0	0	0	0
Entoloma juncinum	0	0	0	0	0	0	0	0	0	0	0	0	0	0	0	0	0	0	0	0	0	0	0	0	0
Entoloma nitidum	0	0	0	0	0	0	0	0	0	0	0	0	0	0	0	0	0	0	0	0	1	0	0	0	1
Entoloma rhodocylix	1	0	0	0	0	0	0	0	0	0	0	0	0	0	0	0	0	0	0	0	0	0	0	0	0
Entoloma turbidum	0	0	0	0	0	0	0	0	0	0	0	0	0	0	0	0	0	0	0	0	0	0	0	0	0
Fayodia gracilipes	0	0	0	0	0	0	3	3	0	0	0	0	0	0	0	0	0	0	0	0	0	0	0	0	0
Flammulaster subincarnatus	0	0	0	0	0	0	0	0	0	0	0	0	0	0	0	0	0	0	0	0	0	0	0	0	0
Galerina allospora	0	0	0	0	0	0	0	0	0	0	0	0	0	0	0	0	0	0	0	0	0	0	0	0	0
Galerina atkinsoniana	2	1	0	1	3	1	0	0	0	4	2	0	0	2	0	1	2	2	2	1	2	1	3	0	0
Galerina badipes	0	0	0	0	0	0	0	0	0	0	0	0	0	0	0	0	0	1	0	0	0	0	0	0	0
Galerina borealis	0	0	0	0	0	0	0	0	0	0	0	0	0	0	0	0	0	0	0	0	0	0	0	0	0
Galerina hypnorum	3	5	2	2	4	5	8	2	1	12	12	2	0	8	10	2	2	1	7	3	2	4	7	0	1
Galerina marginata	0	0	0	0	0	0	0	0	0	0	0	0	0	0	0	0	0	0	0	0	0	0	0	0	0
Galerina mniophila	0	0	0	0	0	0	0	0	0	3	0	0	0	0	3	0	3	0	4	0	0	0	2	0	0
Galerina pumila	0	0	0	0	0	0	0	0	0	0	0	0	0	0	0	0	0	0	0	0	0	0	0	0	0
Galerina stylifera	0	0	0	0	0	0	0	0	0	0	0	0	0	0	0	0	0	0	0	0	0	0	0	0	0
Galerina triscopa	0	0	0	0	0	0	0	0	0	0	0	0	0	0	0	0	0	0	0	0	0	0	0	0	0
Galerina unicolor	0	0	0	0	0	0	0	0	0	0	0	0	0	0	0	0	0	0	0	0	0	0	0	0	0
Galerina sp.1	3	0	1	2	2	0	2	1	0	5	3	0	0	0	1	1	0	0	0	0	0	0	0	0	0
Galerina sp.2	0	0	0	0	0	0	0	0	1	0	0	0	0	0	0	0	0	0	0	0	0	0	0	0	0
Gymnopilus sapineus	0	0	0	0	2	1	0	0	0	0	0	1	0	0	0	0	0	1	0	0	0	0	0	0	0
Hemimycena delectabilis	0	0	0	0	0	0	0	0	0	0	0	0	0	0	0	0	0	0	0	0	0	0	0	0	0
Heyderia abietis	0	0	0	0	0	0	0	0	0	0	0	0	0	0	0	0	0	0	0	0	0	0	0	0	0
Hygrocybe virginea var. fuscescens	0	0	0	0	0	0	0	0	0	0	0	0	0	0	0	0	0	0	0	0	0	0	0	0	0
Hygrophoropsis aurantiaca	0	0	0	0	0	0	0	0	0	0	0	0	0	0	0	0	0	0	0	0	0	0	0	0	0
Hypholoma capnoides	0	0	0	0	0	0	0	0	0	0	0	0	0	0	0	0	0	0	0	0	0	0	0	0	0
Hypholoma marginatum	0	0	0	0	0	0	0	0	0	0	0	0	0	0	0	0	0	0	0	0	0	0	0	0	0
Hypholoma polytrichii	0	0	0	0	0	0	0	0	0	0	0	0	0	0	0	0	0	0	0	0	0	0	0	0	0
Lycoperdon nigrescens	0	0	0	0	0	0	0	0	0	0	0	0	0	0	0	0	0	0	0	0	0	1	0	0	0
Lyophyllum rancidum	0	0	0	0	0	0	0	0	0	0	0	0	0	0	0	0	0	0	0	0	1	0	0	0	0
Lyophyllum semitale	0	0	0	0	0	0	0	0	0	0	0	0	0	0	0	0	0	0	0	0	0	0	0	0	0
Marasmius androsaceus	6	8	7	4	8	8	1	5	3	2	1	0	1	1	7	2	2	4	1	0	5	4	4	1	0
Marasmius bulliardii f. acicola	0	0	0	0	0	0	0	0	0	0	0	0	0	0	0	0	0	0	0	8	0	0	0	3	0
Marasmius epiphyllus	0	0	0	0	0	0	0	0	0	0	0	1	0	0	0	1	0	0	0	0	0	0	0	4	2
Micromphale perforans	0	0	0	0	0	0	0	1	7	6	8	2	4	8	1	2	2	4	1	2	0	1	1	2	1
Mycena alcalina coll.	0	0	0	0	0	0	0	0	0	0	0	0	0	0	0	0	0	0	0	0	0	0	0	0	0
Mycena amicta	0	0	0	0	0	0	0	0	0	0	0	0	0	0	0	0	0	0	0	0	0	0	0	0	0
Mycena aurantiomarginata	0	0	0	0	0	0	0	0	0	0	0	0	0	0	0	0	0	0	0	3	0	0	0	0	0
Mycena cinerella	0	0	0	0	0	0	0	0	0	1	0	0	0	0	0	0	0	0	0	4	0	0	0	0	0
Mycena cineroides	0	1	0	0	0	0	2	4	4	5	3	6	0	5	3	4	2	6	0	6	2	6	4	0	1
Mycena clavicularis	0	0	0	0	0	0	0	0	0	0	0	0	0	0	0	0	0	0	0	0	0	0	0	0	0
Mycena epipterygia	0	0	0	0	0	0	0	0	0	0	0	0	0	1	0	0	0	0	3	0	0	0	0	1	0
Mycena filopes	0	0	0	0	0	0	0	0	0	0	0	0	0	0	0	0	0	1	0	0	0	0	0	0	0
Mycena flavoalba	0	0	0	0	0	0	0	0	0	2	0	0	2	0	0	1	0	0	5	0	1	3	0	3	0	1
Mycena floridula	0	0	0	0	0	0	0	0	0	0	0	0	0	0	0	0	0	0	0	0	0	0	0	0	0

Appendix 4 (continued).

Sample plot	51	52	53	54	55	56	57	58	59	60	61	62	63	64	65	66	67	68	69	70	71	72	73	74	75
Agrocybe erebia	0	0	1	0	0	0	0	0	0	0	0	0	0	0	0	0	0	0	0	0	0	0	0	0	0
Armillaria mellea coll.	0	0	0	0	0	0	0	0	0	0	0	0	0	0	0	0	0	0	0	0	0	0	0	0	0
Baeospora myosura	1	0	0	4	0	3	4	0	0	0	0	0	0	0	0	0	2	0	0	0	0	0	0	0	0
Calocera viscosa	0	0	0	0	0	0	0	0	0	0	0	0	0	0	0	0	0	1	0	2	1	2	0	0	0
Clavariadelphus junceus	5	4	13	5	9	7	6	0	0	0	0	0	0	0	0	0	9	0	9	7	9	16	16	0	0
Clavulina coralloides	0	0	0	0	0	0	0	0	0	0	0	0	0	0	0	0	0	0	0	0	0	0	0	0	0
Clitocybe candicans	0	0	0	0	0	0	0	0	0	0	0	0	0	0	0	0	0	0	0	0	0	0	0	0	0
Clitocybe diatreta	0	0	0	0	0	0	0	0	0	0	0	0	0	0	0	0	0	0	0	0	0	0	0	0	0
Clitocybe ditopus	1	0	0	0	0	0	0	0	0	0	0	0	0	0	0	0	0	0	0	0	0	0	0	0	0
Clitocybe metachroa	2	0	0	1	0	0	0	0	0	0	0	0	0	0	0	0	0	0	0	0	0	0	0	0	0
Collybia acervata	0	0	0	0	0	0	0	0	0	0	0	0	0	0	0	0	1	0	0	0	0	0	0	0	2
Collybia asema	0	0	0	0	0	0	0	0	0	0	0	0	0	0	0	0	0	0	0	0	0	0	0	0	0
Collybia cirrata	0	0	0	0	0	0	0	0	2	0	1	0	0	0	0	0	1	1	0	0	0	0	0	0	0
Collybia confluens	0	0	0	2	0	0	0	0	0	0	0	0	0	0	0	0	0	0	0	0	0	0	0	0	0
Collybia cookei	0	0	0	0	0	0	0	0	0	0	0	0	0	0	0	0	0	0	1	0	0	0	0	0	0
Collybia dryophila	0	2	0	0	0	0	0	0	0	0	0	0	0	0	0	0	0	0	0	0	0	1	0	0	0
Collybia putilla	0	0	0	0	0	0	0	0	0	0	0	0	0	0	0	0	0	0	0	0	0	0	0	0	0
Collybia tuberosa	0	0	0	3	0	2	0	2	5	1	2	2	0	0	0	3	2	1	3	0	0	2	3	1	0
Conocybe striipes	0	0	0	0	0	0	0	0	0	0	0	0	0	0	0	0	0	0	1	0	0	0	0	0	0
Conocybe sulcatipes	0	0	0	0	0	0	0	0	0	0	0	0	0	0	0	0	1	0	0	0	0	0	1	0	0
Cordyceps ophioglossoides	0	1	0	0	0	0	0	0	0	0	0	0	0	0	0	0	0	0	0	0	0	0	0	0	0
Cudonia circinans	0	0	0	1	0	0	0	0	0	0	0	0	0	0	0	0	0	0	0	0	0	0	0	0	0
Cudonia confusa	0	0	0	0	0	0	0	0	0	0	0	0	0	0	0	0	0	0	0	0	0	0	0	0	0
Cudoniella clavus	0	0	1	0	0	1	0	0	0	0	0	0	0	0	0	0	1	0	0	0	0	0	0	0	0
Cystoderma carcharias	0	0	1	0	0	0	0	0	0	0	0	0	0	0	0	0	0	0	0	1	0	0	0	0	0
Cystoderma fallax	0	0	1	0	0	0	0	0	0	0	0	0	0	0	0	0	0	0	0	0	0	0	0	0	0
Cystoderma jasonis	1	0	0	0	0	0	0	0	0	0	0	0	0	0	1	3	0	3	2	0	0	0	0	0	0
Entoloma cetratum	0	0	0	0	0	0	0	0	1	0	0	1	0	0	0	0	0	0	1	0	0	0	0	2	0
Entoloma conferendum	0	0	1	0	0	0	0	0	0	0	0	0	0	0	0	0	0	1	0	0	0	0	0	0	0
Entoloma juncinum	0	0	0	0	0	0	0	0	0	0	0	0	0	0	0	0	1	0	0	0	0	0	0	0	0
Entoloma nitidum	0	1	0	1	0	0	0	0	0	0	0	0	0	0	0	0	0	0	0	0	0	0	0	0	0
Entoloma rhodocylix	0	0	0	0	0	0	0	0	0	0	0	0	0	0	0	0	0	0	0	0	0	0	0	0	0
Entoloma turbidum	0	0	0	0	0	0	0	0	0	0	0	0	0	0	0	0	0	0	0	0	0	0	0	0	0
Fayodia gracilipes	0	0	0	0	0	0	0	0	0	0	0	0	0	0	0	0	0	0	0	0	0	0	0	0	0
Flammulaster subincarnatus	0	0	0	0	0	0	0	0	0	0	0	0	0	0	0	0	0	0	0	0	0	0	3	1	0
Galerina allospora	0	0	0	0	0	0	0	0	0	0	0	0	0	0	0	0	0	0	4	0	0	0	0	0	0
Galerina atkinsoniana	4	0	0	3	1	0	0	2	0	0	0	1	0	1	2	0	0	1	2	0	1	0	0	2	5
Galerina badipes	0	0	1	0	0	0	0	0	0	0	0	0	0	0	0	0	1	0	0	0	0	0	0	0	0
Galerina borealis	0	0	0	0	0	0	0	0	0	0	0	0	0	0	0	0	0	0	0	0	0	0	0	0	0
Galerina hypnorum	4	5	0	2	1	0	4	2	0	0	1	0	0	0	0	3	0	7	1	1	2	2	1	0	1
Galerina marginata	0	0	1	0	2	0	0	0	0	0	0	0	0	0	0	0	1	0	0	0	1	1	1	0	0
Galerina mniophila	0	0	0	0	0	0	0	0	0	0	0	0	0	0	0	0	1	0	0	0	0	0	0	0	0
Galerina pumila	0	0	0	0	0	0	0	0	0	0	0	0	0	0	0	0	0	0	0	0	0	0	0	0	0
Galerina stylifera	0	0	3	0	0	0	0	0	0	0	0	0	0	0	0	0	1	0	1	0	0	0	0	0	0
Galerina triscopa	0	0	0	0	0	0	0	0	0	0	0	0	0	0	0	0	1	0	0	0	0	0	0	0	0
Galerina unicolor	0	0	0	0	0	0	0	0	0	0	0	0	0	0	0	0	0	0	0	0	0	0	0	0	0
Galerina sp.1	0	0	0	0	0	0	0	0	2	0	0	0	0	0	0	0	0	1	0	0	0	0	0	0	0
Galerina sp.2	0	0	0	0	0	0	0	0	0	0	0	0	0	0	0	0	0	1	0	0	0	0	0	0	0
Gymnopilus sapineus	0	0	0	0	0	0	0	0	1	0	0	0	0	0	0	0	0	1	0	0	0	0	0	0	0
Hemimycena delectabilis	0	0	3	0	0	0	0	0	0	0	0	0	0	0	0	0	1	0	0	0	0	0	0	0	0
Heyderia abietis	0	0	0	0	0	0	0	0	1	0	0	0	0	0	0	0	0	0	0	0	0	0	0	0	0
Hygrocybe virginea var. fuscescens	0	0	2	0	0	0	0	0	0	0	0	0	0	0	0	0	0	0	0	0	0	0	0	0	0
Hygrophoropsis aurantiaca	0	0	0	0	0	0	0	0	0	0	0	0	0	0	0	0	1	0	0	0	0	0	0	0	0
Hypholoma capnoides	1	0	0	0	0	0	0	0	0	0	0	0	0	0	0	0	0	0	0	0	0	0	0	0	0
Hypholoma marginatum	0	0	0	0	0	0	0	0	0	0	0	0	0	0	0	0	0	0	0	0	0	0	0	0	0
Hypholoma polytrichii	0	0	0	0	0	0	0	0	0	0	0	0	0	0	0	0	0	0	0	0	0	0	0	0	0
Lycoperdon nigrescens	0	0	0	0	0	0	0	0	0	0	0	0	0	0	0	0	0	0	0	0	0	0	0	0	0
Lyophyllum rancidum	0	0	0	1	0	0	0	0	0	0	0	0	0	0	0	0	0	0	0	0	0	0	0	0	0
Lyophyllum semitale	0	0	0	0	0	0	0	0	0	0	1	0	0	0	0	0	0	0	0	0	0	0	0	0	0
Marasmius androsaceus	0	1	1	0	1	1	0	12	12	3	6	9	3	5	10	5	0	3	1	1	0	0	0	2	4
Marasmius bulliardii f. acicola	0	0	0	0	0	0	0	0	0	0	0	0	0	0	0	0	0	0	0	0	0	0	0	0	0
Marasmius epiphyllus	6	2	2	0	2	3	0	0	0	0	0	0	0	0	0	0	3	0	0	0	1	15	13	0	1
Micromphale perforans	0	0	1	0	2	0	0	0	0	0	0	0	0	0	0	0	3	0	3	0	0	0	0	3	0
Mycena alcalina coll.	0	0	2	2	0	0	0	0	0	0	0	0	0	0	0	0	2	0	0	1	0	0	1	0	1
Mycena amicta	0	0	0	2	0	0	1	0	0	0	0	0	0	0	0	0	2	1	0	0	0	0	0	0	0
Mycena aurantiomarginata	0	0	0	1	0	0	0	0	0	0	0	0	0	0	0	0	0	0	0	0	0	0	0	0	0
Mycena cinerella	0	2	0	0	0	1	0	0	0	0	0	0	0	0	0	0	1	0	0	0	0	0	0	0	0
Mycena cineroides	6	5	1	2	0	3	3	0	0	0	0	0	0	0	1	1	9	4	9	1	3	0	4	0	1
Mycena clavicularis	0	0	0	0	0	0	0	0	0	0	0	0	0	0	1	0	0	0	0	0	0	0	0	0	0
Mycena epipterygia	1	2	1	2	0	1	2	0	0	0	0	0	0	0	0	0	0	0	1	0	1	0	0	0	0
Mycena filopes	0	1	1	0	0	0	1	0	0	0	0	0	0	0	0	0	4	0	0	0	0	0	0	1	0
Mycena flavoalba	4	2	2	2	1	1	1	0	0	0	0	0	0	0	0	0	3	0	0	0	0	2	0	2	1
Mycena floridula	0	0	0	0	0	0	0	0	0	0	0	0	0	0	0	0	1	0	0	0	0	0	0	0	0

Appendix 4 (continued).

Sample plot	76	77	78	79	80	81	82	83	84	85	86	87	88	89	90	91	92	93	94	95	96	97	98	99	100
Agrocybe erebia	0	0	0	0	0	0	0	0	0	0	0	0	0	0	0	0	0	0	0	0	0	0	0	0	0
Armillaria mellea coll.	0	0	0	0	0	0	0	0	0	0	0	0	0	0	0	0	0	0	0	0	0	0	0	0	0
Baeospora myosura	0	0	0	0	0	0	0	0	1	0	0	0	1	0	0	0	0	0	0	0	0	1	0	0	0
Calocera viscosa	0	0	2	0	0	0	0	0	0	0	0	0	0	0	0	0	0	0	0	1	1	0	1	0	0
Clavariadelphus junceus	0	0	0	0	0	0	0	0	0	0	0	0	0	0	0	0	0	0	0	0	0	1	0	0	0
Clavulina coralloides	0	0	0	0	0	0	0	0	0	0	0	0	0	0	0	0	0	0	0	0	0	0	0	0	0
Clitocybe candicans	0	0	0	0	0	0	0	0	0	0	0	0	0	0	0	0	0	0	0	0	0	0	0	0	0
Clitocybe diatreta	0	0	0	0	0	0	0	0	0	0	0	0	0	0	0	0	0	0	0	0	0	0	0	0	0
Clitocybe ditopus	0	0	0	0	0	0	0	0	0	0	0	0	0	0	0	0	0	0	0	3	0	0	0	0	0
Clitocybe metachroa	0	0	0	0	0	0	0	0	0	0	0	0	0	0	0	0	0	0	0	4	0	0	0	0	0
Collybia acervata	0	0	0	0	3	0	0	0	0	0	0	0	0	0	0	0	0	0	0	0	0	0	0	0	0
Collybia asema	0	0	0	0	0	0	0	0	0	0	0	0	0	0	0	0	0	0	0	0	0	0	0	0	0
Collybia cirrata	0	0	0	0	0	0	0	1	0	0	0	0	0	0	0	0	2	0	0	0	0	4	2	0	0
Collybia confluens	0	0	0	0	0	0	0	0	0	0	0	0	0	0	0	0	0	0	0	0	0	0	0	0	0
Collybia cookei	0	0	0	0	0	0	0	0	0	0	0	0	0	0	0	0	0	0	0	0	0	0	0	0	0
Collybia dryophila	0	0	0	0	0	0	0	0	0	0	0	0	0	0	0	0	0	0	0	0	0	0	0	0	0
Collybia putilla	0	0	0	0	0	0	0	0	0	0	0	0	0	0	0	0	0	0	0	0	0	0	0	0	0
Collybia tuberosa	6	0	0	0	1	1	3	4	0	4	3	1	0	5	2	0	5	1	1	1	4	8	8	3	3
Conocybe striipes	0	0	0	0	0	0	0	0	0	0	0	0	0	0	0	0	0	0	0	0	0	0	0	0	0
Conocybe sulcatipes	0	0	0	0	0	0	0	0	0	0	0	0	0	0	0	0	0	0	0	0	0	0	0	0	0
Cordyceps ophioglossoides	0	0	0	0	0	0	0	0	0	0	0	0	0	0	0	0	0	0	0	0	0	0	0	0	0
Cudonia circinans	0	0	0	0	0	0	0	0	0	0	0	0	0	0	0	0	0	0	0	0	0	0	0	0	0
Cudonia confusa	0	0	0	0	0	0	0	0	0	0	0	0	0	0	0	0	0	0	0	0	0	0	0	0	0
Cudoniella clavus	0	0	0	0	0	0	0	0	0	0	0	0	0	0	0	0	0	0	0	0	0	0	1	0	0
Cystoderma carcharias	0	0	0	0	0	0	0	0	0	0	0	0	0	0	0	0	0	0	0	0	0	0	0	0	0
Cystoderma fallax	0	0	0	0	0	0	0	0	0	0	0	0	0	0	0	0	0	0	0	0	0	0	0	0	0
Cystoderma jasonis	0	0	1	0	0	1	0	0	0	0	0	0	0	1	1	0	0	0	0	2	1	4	0	1	0	0
Entoloma cetratum	0	1	0	0	0	0	0	0	0	0	0	0	0	0	0	0	0	0	0	1	0	0	0	0	0
Entoloma conferendum	0	0	0	0	0	0	0	0	0	0	0	0	0	0	0	0	0	0	0	2	0	0	0	0	0
Entoloma juncinum	0	0	0	0	0	0	0	0	0	0	0	0	0	0	0	0	0	0	0	0	0	0	0	0	0
Entoloma nitidum	0	0	0	0	0	0	0	0	0	0	0	0	0	0	0	0	0	0	0	0	0	0	0	0	0
Entoloma rhodocylix	0	0	0	0	0	0	0	0	0	0	0	0	0	0	0	0	0	0	0	1	0	0	0	0	0
Entoloma turbidum	0	0	0	0	0	0	0	0	0	0	0	0	0	0	0	0	0	0	0	0	0	0	0	0	0
Fayodia gracilipes	0	0	0	0	0	0	0	0	0	0	0	0	0	0	0	0	0	0	0	0	0	0	0	0	0
Flammulaster subincarnatus	0	0	0	0	0	0	0	0	0	0	0	0	0	0	0	0	0	0	0	0	0	0	0	0	0
Galerina allospora	0	0	0	0	0	0	0	0	0	0	0	0	0	0	0	0	0	0	0	0	0	0	0	0	0
Galerina atkinsoniana	0	2	1	0	1	2	0	0	0	0	1	0	1	3	2	0	1	1	2	2	3	2	10	2	4
Galerina badipes	0	0	0	0	0	0	0	0	0	0	0	0	0	0	0	0	0	0	0	0	0	0	0	0	0
Galerina borealis	0	0	0	0	0	0	0	0	0	0	0	0	0	0	0	0	0	0	0	1	1	0	0	0	0
Galerina hypnorum	1	2	3	0	0	2	1	2	0	1	3	5	4	6	1	2	3	1	9	12	10	5	12	4	11
Galerina marginata	0	0	0	0	0	0	0	0	0	0	0	0	0	0	0	0	0	0	0	0	0	0	0	0	0
Galerina mniophila	0	0	0	0	0	0	0	0	0	0	0	0	1	1	0	0	0	0	4	1	0	0	0	0	1
Galerina pumila	0	0	0	0	0	0	0	2	0	0	0	0	0	0	0	0	0	0	0	0	0	0	0	0	0
Galerina stylifera	0	0	0	0	0	0	0	0	0	0	0	0	0	0	0	0	0	0	0	0	0	0	0	0	0
Galerina triscopa	0	0	0	0	0	0	0	0	0	0	0	0	0	0	0	0	0	0	0	0	0	0	0	0	0
Galerina unicolor	0	0	0	0	0	0	0	0	1	0	0	0	0	0	0	0	0	0	0	0	0	0	0	0	0
Galerina sp.1	0	0	0	0	0	3	0	1	0	0	0	0	0	0	0	0	0	0	1	0	0	0	0	0	0
Galerina sp.2	0	0	0	0	0	0	0	0	0	0	0	0	0	0	0	0	0	0	0	2	0	0	0	0	0
Gymnopilus sapineus	0	0	0	0	0	0	0	0	0	0	0	0	0	0	0	0	0	0	0	1	0	0	1	0	1
Hemimycena delectabilis	0	0	0	0	0	0	0	0	0	0	0	0	0	0	0	0	0	0	0	0	0	0	0	0	0
Heyderia abietis	1	1	1	0	0	1	0	0	0	0	0	0	0	2	0	0	0	0	0	1	0	0	0	0	0
Hygrocybe virginea var. fuscescens	0	0	0	0	0	0	0	0	0	0	0	0	0	0	0	0	0	0	0	0	0	0	0	0	0
Hygrophoropsis aurantiaca	0	0	0	0	0	0	0	0	0	0	0	0	0	0	0	0	0	0	0	0	0	0	0	0	0
Hypholoma capnoides	0	0	0	0	0	0	0	0	0	0	0	0	0	0	0	0	0	0	0	0	0	0	0	0	0
Hypholoma marginatum	0	0	0	0	0	0	0	0	0	0	0	0	0	0	0	0	0	0	0	0	0	0	1	0	0
Hypholoma polytrichii	0	0	0	0	0	0	0	0	0	0	0	0	0	0	0	0	0	0	0	0	0	0	0	0	0
Lycoperdon nigrescens	0	0	0	0	0	0	0	0	0	0	0	0	0	0	0	0	0	0	0	0	0	0	0	0	0
Lyophyllum rancidum	0	0	0	0	0	0	0	0	0	0	0	0	0	0	0	0	0	0	0	0	0	0	0	0	0
Lyophyllum semitale	0	0	0	0	0	0	0	0	0	0	0	0	0	0	0	0	0	0	0	0	0	0	0	0	0
Marasmius androsaceus	16	11	1	0	16	12	7	4	6	10	16	9	5	12	9	7	6	1	0	7	5	2	3	8	8
Marasmius bulliardii f. acicola	0	0	0	0	0	0	0	0	0	0	0	0	0	0	0	0	0	0	0	0	0	0	0	0	0
Marasmius epiphyllus	0	0	0	0	0	0	0	0	0	0	0	0	0	0	0	0	0	0	0	1	0	4	4	0	0
Micromphale perforans	0	0	0	0	0	0	0	0	0	0	0	0	0	0	0	0	0	0	0	2	1	3	2	3	1
Mycena alcalina coll.	0	0	0	0	0	0	0	0	0	0	0	0	0	1	0	0	0	0	0	0	0	0	0	0	0
Mycena amicta	0	0	0	0	0	0	0	0	0	0	0	0	0	0	0	0	0	0	0	0	0	0	0	0	0
Mycena aurantiomarginata	0	0	0	0	0	0	0	0	0	0	0	0	0	0	0	0	0	0	0	0	0	0	0	0	0
Mycena cinerella	0	0	0	0	0	0	0	0	0	0	0	0	1	0	0	0	0	0	6	3	4	9	3	0	0
Mycena cineroides	0	0	1	0	0	0	0	0	0	0	0	0	0	1	0	0	1	0	3	8	0	10	13	0	1
Mycena clavicularis	0	0	0	0	0	0	0	2	0	0	0	0	0	0	0	0	0	0	0	0	0	0	0	0	0
Mycena epipterygia	0	0	0	0	0	0	0	0	0	0	0	0	0	2	0	0	0	0	0	0	0	0	0	0	0
Mycena filopes	0	0	0	0	0	0	0	0	0	0	0	0	0	0	0	0	0	0	1	0	0	0	0	0	0
Mycena flavoalba	0	0	0	0	0	0	0	0	0	0	0	0	0	0	0	0	0	0	1	1	0	1	7	3	1
Mycena floridula	0	0	0	0	0	0	0	0	0	0	0	0	0	0	0	0	0	0	0	0	0	0	0	0	0

Appendix 4 (continued).

Sample plot	1	2	3	4	5	6	7	8	9	10	11	12	13	14	15	16	17	18	19	21	22	23	24	25
Mycena galericulata	0	0	0	0	0	0	2	0	0	0	0	0	0	0	0	0	1	0	1	0	1	0	0	0
Mycena galopus	3	3	2	2	3	1	0	2	3	4	0	0	0	0	5	12	7	2	8	12	14	11	4	3
Mycena haematopus	0	0	0	0	0	0	0	0	0	0	0	0	0	0	0	0	0	0	0	0	0	0	0	0
Mycena inclinata	0	0	0	0	0	0	0	0	0	0	0	0	0	0	0	0	0	0	0	0	0	0	0	0
Mycena longiseta	0	1	0	0	0	0	2	1	0	0	0	0	0	0	0	1	0	0	0	1	0	0	1	0
Mycena maculata	1	0	0	0	0	0	0	0	0	0	0	0	0	0	0	0	0	0	0	0	0	0	0	0
Mycena megaspora	0	0	0	0	0	0	0	0	0	0	0	0	0	0	0	0	0	0	0	0	0	0	0	0
Mycena metata	0	3	10	1	2	0	6	4	3	7	1	1	0	0	1	7	1	12	8	0	1	1	1	0
Mycena oregonensis	0	0	0	0	0	0	0	0	0	0	0	0	0	0	0	0	0	0	0	0	0	0	0	0
Mycena pura	0	0	0	0	0	0	0	0	0	0	0	0	0	0	0	1	0	0	0	0	0	0	0	0
Mycena rorida	6	8	15	3	0	16	4	8	12	15	10	3	0	1	14	2	0	0	4	14	7	11	11	6
Mycena rosella	1	0	1	0	0	0	0	0	0	0	0	0	0	0	0	2	0	0	2	0	0	0	0	0
Mycena rubromarginata	1	1	6	1	2	0	0	0	0	0	0	0	1	0	0	0	0	1	0	0	0	0	2	0
Mycena sanguinolenta	0	2	3	0	0	0	0	0	0	0	0	0	0	0	0	1	0	1	0	0	2	3	2	0
Mycena septentrionalis	4	6	2	9	11	1	0	2	2	5	9	2	0	0	1	13	5	3	9	0	0	2	0	1
Mycena speirea	0	0	0	0	0	0	0	0	0	0	0	0	0	0	0	0	0	0	0	0	0	0	0	0
Mycena stylobates	0	0	0	0	0	0	0	0	0	0	0	0	0	0	0	0	0	0	0	0	0	0	0	0
Mycena urania	0	0	0	0	0	1	0	0	0	0	0	0	0	0	0	1	0	0	0	0	0	0	0	0
Mycena viridimarginata	0	0	0	0	0	0	0	0	0	0	0	0	0	0	0	0	0	0	0	1	0	0	0	0
Mycena viscosa	0	0	0	0	0	0	0	0	0	0	0	0	0	0	0	0	0	0	0	0	0	0	0	0
Mycena vulgaris	0	0	0	0	0	0	1	0	0	0	0	0	0	0	0	0	0	2	0	0	0	0	0	0
Mycocalia sp.	0	0	0	0	0	0	0	0	0	0	0	0	0	0	0	0	0	0	0	0	0	0	0	0
Omphalina oniscus	0	0	0	0	0	0	0	0	0	0	0	0	0	0	0	0	0	0	0	0	0	0	0	0
Pholiota lubrica	0	0	0	0	0	0	0	0	0	0	0	0	0	0	0	0	0	0	0	0	0	0	0	0
Pholiota mixta	0	0	0	0	0	0	0	0	0	0	0	0	0	0	0	0	0	0	0	0	0	0	0	0
Pholiota scamba	0	0	0	0	0	0	0	0	0	0	0	0	0	0	0	0	0	0	0	0	0	0	0	0
Psathyrella Lutenses coll.	0	0	0	0	0	0	0	0	0	0	0	0	0	0	0	0	0	0	0	0	0	0	2	0
Psathyrella friesii	0	0	0	0	0	0	0	0	0	0	0	0	0	0	0	0	1	0	0	0	0	0	0	0
Psilocybe inquilina	0	0	0	0	0	0	0	0	0	0	0	0	0	0	0	0	0	0	0	0	0	0	0	0
Strobilurus esculentus	1	1	5	5	3	0	0	0	0	0	0	0	0	0	1	9	3	4	5	3	2	6	1	0
Stropharia hornemannii	0	0	0	0	0	0	0	0	0	0	0	0	0	0	0	0	0	0	0	0	0	0	3	0
Tubaria confragosa	0	0	0	0	0	0	0	1	0	0	0	0	0	0	0	0	0	0	0	0	0	0	0	0
Tubaria conspersa	0	0	0	0	0	0	0	0	0	0	0	0	0	0	0	0	0	0	0	0	0	0	0	0
Typhula erythropus	0	0	0	0	0	0	0	0	0	0	0	0	0	0	0	11	0	0	0	0	0	0	0	0
Typhula phacorrhiza	0	0	0	0	0	0	0	0	0	0	0	0	0	0	0	0	0	0	0	0	0	0	0	0
Typhula setipes	0	0	0	0	0	0	0	11	0	0	0	0	0	0	0	0	0	0	0	1	0	0	0	0
Xeromphalina campanella	0	0	0	0	0	0	0	0	6	0	0	0	0	0	0	0	0	0	0	0	0	0	0	0
Xeromphalina cornui	0	0	0	0	0	0	0	0	0	0	0	0	0	0	0	0	0	0	0	0	0	0	0	0
Xylaria filiformis	0	0	0	0	0	0	0	0	0	0	0	0	0	0	0	0	0	0	0	0	0	0	0	0

Appendix 4 (continued).

Sample plot	26	27	28	29	30	31	32	33	34	35	36	37	38	39	40	41	42	43	44	45	46	47	48	49	50
Mycena galericulata	0	0	0	0	0	0	0	0	0	1	0	0	1	0	0	0	0	2	0	1	0	0	1	1	0
Mycena galopus	2	3	0	6	5	6	11	3	2	13	4	1	6	4	6	3	3	3	3	5	3	2	5	0	0
Mycena haematopus	0	0	0	0	0	0	0	0	0	0	0	0	0	0	0	0	0	0	0	0	0	0	0	0	0
Mycena inclinata	0	0	0	0	0	0	0	0	0	0	0	0	0	0	0	0	0	0	0	0	0	0	0	0	0
Mycena longiseta	0	0	0	0	2	0	0	0	0	0	0	0	0	0	0	0	0	1	0	0	0	0	0	0	0
Mycena maculata	0	0	0	0	0	0	0	0	0	0	0	0	0	0	0	0	0	0	0	0	0	0	0	0	0
Mycena megaspora	1	0	0	0	0	0	0	0	0	0	0	0	0	0	0	0	0	0	0	0	0	0	0	0	0
Mycena metata	0	0	0	0	0	0	0	0	7	0	0	0	0	0	0	2	5	7	1	8	5	6	1	2	1
Mycena oregonensis	0	0	0	0	0	0	0	0	0	0	0	0	0	0	0	0	0	0	0	0	0	0	0	0	0
Mycena pura	0	0	0	0	0	0	0	0	0	0	0	0	0	0	0	0	0	0	0	0	1	0	0	0	0
Mycena rorida	0	8	1	8	14	0	16	8	3	1	5	2	0	5	7	0	2	1	3	4	4	13	9	0	2
Mycena rosella	0	0	0	0	0	0	0	1	0	0	0	1	0	0	0	1	0	0	0	1	0	1	0	0	0
Mycena rubromarginata	0	0	0	0	0	0	1	0	0	0	1	0	2	0	0	1	1	1	0	1	0	0	0	1	0
Mycena sanguinolenta	0	0	1	0	0	0	0	0	0	0	1	0	0	0	1	1	0	0	0	0	1	0	0	0	0
Mycena septentrionalis	0	0	0	0	0	0	9	6	6	1	3	12	0	4	4	8	0	10	2	1	8	0	4	2	9
Mycena speirea	0	0	0	0	0	0	0	0	0	0	0	0	0	0	0	0	0	0	0	0	0	0	0	0	0
Mycena stylobates	0	0	0	0	0	0	0	0	2	0	0	0	1	1	0	0	0	0	0	0	0	0	1	1	0
Mycena urania	0	0	0	0	0	0	0	0	0	0	0	0	0	0	0	0	0	0	0	0	0	0	0	0	0
Mycena viridimarginata	0	0	0	0	0	0	0	0	0	1	0	0	0	0	0	0	0	0	1	0	0	0	0	0	0
Mycena viscosa	0	0	0	0	0	0	0	0	0	0	0	0	0	0	0	0	0	0	0	0	0	0	0	0	0
Mycena vulgaris	0	0	0	0	0	0	0	1	1	0	0	1	0	0	0	0	0	0	0	1	0	0	1	0	0
Mycocalia sp.	0	0	0	0	0	0	0	0	0	0	0	0	0	0	0	0	0	0	0	0	0	0	0	0	0
Omphalina oniscus	0	0	0	0	0	0	0	0	0	0	0	0	0	0	0	0	0	0	0	0	0	0	0	0	0
Pholiota lubrica	0	0	0	0	0	0	0	0	0	0	0	0	0	0	0	0	0	0	0	0	0	0	0	1	0
Pholiota mixta	0	0	0	0	0	0	0	0	0	0	0	0	0	0	0	0	0	0	0	0	0	0	0	0	0
Pholiota scamba	0	0	0	0	0	0	0	0	0	0	0	0	0	0	0	0	0	0	0	0	0	0	0	0	0
Psathyrella Lutenses coll.	0	0	0	0	0	0	0	0	0	0	0	0	0	0	0	0	0	0	0	0	0	0	0	0	0
Psathyrella friesii	0	0	0	0	0	0	0	0	0	0	0	0	0	0	0	0	0	0	0	0	0	0	0	0	0
Psilocybe inquilina	0	0	0	0	0	0	0	0	0	0	0	0	0	0	0	0	0	0	0	0	0	0	0	0	0
Strobilurus esculentus	0	0	0	0	0	0	5	3	9	4	0	3	7	3	3	0	9	8	1	4	5	9	1	0	1
Stropharia hornemannii	0	0	0	0	0	0	0	1	0	0	0	0	0	0	0	0	0	1	0	0	0	0	0	0	0
Tubaria confragosa	0	0	0	0	0	0	0	0	0	0	0	0	0	0	0	0	0	0	0	0	0	0	0	0	0
Tubaria conspersa	0	0	0	0	0	0	0	0	0	0	0	0	0	0	0	0	0	0	0	0	0	0	0	0	0
Typhula erythropus	0	0	0	0	0	0	0	0	0	0	0	0	0	0	0	0	0	0	0	15	0	0	0	3	0
Typhula phacorrhiza	0	0	0	0	0	0	0	0	0	0	0	0	0	0	0	0	0	0	0	1	0	0	0	2	0
Typhula setipes	0	0	0	0	0	0	0	0	0	0	0	0	0	0	0	0	0	0	0	0	0	1	0	3	7
Xeromphalina campanella	0	0	0	0	0	0	0	0	0	0	0	0	0	0	0	0	0	0	0	0	0	0	0	0	0
Xeromphalina cornui	0	0	0	0	0	0	0	0	0	0	0	0	0	0	0	0	0	0	0	0	0	0	0	0	0
Xylaria filiformis	0	0	0	0	0	0	0	0	0	0	0	0	0	0	0	0	0	0	0	0	0	0	0	0	0

Appendix 4 (continued).

Sample plot	51	52	53	54	55	56	57	58	59	60	61	62	63	64	65	66	67	68	69	70	71	72	73	74	75
Mycena galericulata	0	0	1	0	0	0	0	0	0	0	0	0	1	0	0	0	2	4	3	2	0	4	0	0	0
Mycena galopus	2	5	2	3	0	0	0	0	0	0	0	1	0	0	1	0	3	3	0	4	4	1	5	5	7
Mycena haematopus	0	0	1	0	0	0	0	0	0	0	0	0	0	0	0	0	0	0	0	0	0	0	0	0	0
Mycena inclinata	0	0	0	0	0	0	0	0	0	0	0	0	0	0	0	0	0	2	0	0	0	0	0	0	0
Mycena longiseta	0	5	0	3	0	0	1	0	0	0	0	0	0	0	0	0	3	0	0	3	1	0	2	0	2
Mycena maculata	0	0	0	0	0	0	0	0	0	0	0	0	0	0	0	0	0	0	0	0	0	0	0	0	0
Mycena megaspora	0	0	0	0	0	0	0	0	0	0	0	0	0	0	0	0	0	0	0	0	0	0	0	0	0
Mycena metata	9	5	3	1	5	4	7	0	0	0	0	0	0	0	0	1	12	8	9	10	0	7	4	7	0
Mycena oregonensis	0	0	1	0	0	0	0	0	0	0	0	0	0	0	0	0	0	0	0	0	0	0	0	0	0
Mycena pura	0	1	0	0	0	0	0	0	0	0	0	0	0	0	0	0	2	0	1	0	0	3	1	0	0
Mycena rorida	5	4	1	6	0	0	0	0	4	0	2	2	0	0	2	2	1	0	7	11	9	7	7	5	4
Mycena rosella	0	1	1	3	0	0	0	0	0	0	0	0	0	0	0	0	0	0	0	0	0	0	0	0	1
Mycena rubromarginata	0	1	0	1	0	0	0	0	0	0	0	1	0	0	1	0	0	2	0	2	0	0	0	1	0
Mycena sanguinolenta	0	0	0	0	0	5	0	0	0	0	0	0	0	0	0	0	0	0	3	1	1	0	1	0	0
Mycena septentrionalis	14	2	1	2	6	6	0	0	0	0	2	0	0	0	0	3	0	11	5	1	0	1	0	1	6
Mycena speirea	0	0	0	0	0	0	0	0	0	0	0	0	0	0	0	0	0	0	0	0	0	0	1	0	0
Mycena stylobates	0	0	0	1	0	0	0	0	0	0	0	0	0	0	0	0	0	0	0	0	0	0	0	0	0
Mycena urania	0	0	0	0	0	0	0	0	0	0	0	0	0	0	0	0	0	0	0	0	0	0	0	0	0
Mycena viridimarginata	0	0	0	0	0	0	1	0	0	0	0	0	0	0	0	0	0	0	0	0	0	0	0	0	0
Mycena viscosa	0	0	0	0	0	0	0	0	0	0	0	0	0	0	0	0	0	1	0	0	0	0	0	0	0
Mycena vulgaris	1	1	4	1	0	0	1	0	0	0	0	0	0	0	0	0	5	1	0	0	0	1	3	0	0
Mycocalia sp.	0	0	0	0	0	0	0	0	0	0	0	0	0	0	0	0	0	0	0	0	0	0	0	0	0
Omphalina oniscus	0	0	0	0	0	0	0	0	0	0	0	0	0	0	0	0	0	0	0	0	0	0	0	0	0
Pholiota lubrica	0	0	0	0	0	0	0	0	0	0	0	0	0	0	0	0	4	0	0	0	0	0	0	0	0
Pholiota mixta	0	0	0	0	0	0	0	0	0	1	0	0	0	0	0	0	0	0	0	0	0	0	0	0	0
Pholiota scamba	0	0	0	0	0	0	0	0	0	0	0	0	0	0	0	0	0	2	0	0	0	0	0	0	0
Psathyrella Lutenses coll.	0	0	0	0	0	0	0	0	0	0	0	0	0	0	0	0	0	0	0	0	0	0	0	0	0
Psathyrella friesii	0	0	0	0	0	0	0	0	0	0	0	0	0	0	0	0	1	0	0	2	0	0	0	0	0
Psilocybe inquilina	0	0	0	0	0	0	0	0	0	0	0	0	0	0	0	0	6	0	0	0	0	0	0	0	0
Strobilurus esculentus	5	4	1	9	3	1	0	0	0	0	0	0	0	0	0	0	4	6	7	1	0	2	1	2	0
Stropharia hornemannii	0	0	0	0	0	0	0	0	0	0	0	0	0	0	0	0	0	2	0	0	0	0	0	0	0
Tubaria confragosa	0	0	0	0	0	0	0	0	0	0	0	0	0	0	0	0	0	0	0	0	0	0	0	0	0
Tubaria conspersa	0	0	0	0	0	0	0	0	0	0	0	0	0	0	0	0	0	0	0	0	0	0	4	0	0
Typhula erythropus	1	4	15	0	5	0	16	0	0	0	0	0	0	0	0	0	0	0	2	1	2	0	0	0	0
Typhula phacorrhiza	0	2	1	2	6	7	0	0	0	0	0	0	0	0	0	0	0	0	1	2	0	0	0	0	0
Typhula setipes	16	15	16	11	12	16	1	0	0	0	0	0	0	0	0	0	15	12	12	5	9	14	12	0	0
Xeromphalina campanella	0	0	0	0	0	0	0	0	0	0	0	0	0	0	0	0	0	0	0	0	0	0	0	1	0
Xeromphalina cornui	0	0	0	0	0	0	0	0	0	0	0	0	0	0	0	1	0	0	0	0	0	0	0	0	0
Xylaria filiformis	0	0	0	0	0	0	0	0	0	0	0	0	0	0	0	0	0	0	0	0	0	1	3	0	0

Appendix 4 (continued).

Sample plot	76	77	78	79	80	81	82	83	84	85	86	87	88	89	90	91	92	93	94	95	96	97	98	99	100
Mycena galericulata	0	0	0	0	0	1	0	0	0	0	0	0	0	0	0	0	0	0	0	1	2	0	0	0	0
Mycena galopus	4	0	0	0	3	0	5	0	0	0	0	9	2	1	0	0	0	0	13	14	9	8	7	4	2
Mycena haematopus	0	0	0	0	0	0	0	0	0	0	0	0	0	0	0	0	0	0	0	0	0	0	0	0	0
Mycena inclinata	0	0	0	0	0	0	0	0	0	0	0	0	0	0	0	0	0	0	0	0	0	0	0	0	0
Mycena longiseta	0	0	0	0	0	0	0	0	0	0	0	0	0	0	0	0	0	0	2	4	1	10	4	1	0
Mycena maculata	0	0	0	0	0	0	0	0	0	0	0	0	0	0	0	0	0	0	0	0	0	0	0	0	0
Mycena megaspora	0	0	0	0	0	0	0	0	0	0	0	0	0	0	0	0	0	0	0	0	0	0	0	0	0
Mycena metata	0	0	0	0	0	0	1	0	0	1	0	0	0	2	0	0	1	0	2	1	2	3	4	2	2
Mycena oregonensis	0	0	0	0	0	0	0	0	0	0	0	0	0	0	0	0	0	0	0	0	0	0	0	0	0
Mycena pura	0	0	0	0	0	0	0	0	0	0	0	0	0	0	0	0	0	0	0	0	0	0	0	0	0
Mycena rorida	8	5	2	0	5	3	0	0	1	2	3	0	5	14	0	0	3	2	16	14	15	15	16	12	5
Mycena rosella	0	0	0	0	0	0	0	0	0	0	0	0	0	0	0	0	0	0	0	0	0	0	0	0	0
Mycena rubromarginata	0	0	0	0	0	0	0	0	0	0	0	0	0	0	0	0	0	0	1	0	0	0	3	0	2
Mycena sanguinolenta	0	0	0	0	0	0	0	0	0	0	0	0	1	0	0	0	0	0	1	2	2	0	7	2	0
Mycena septentrionalis	0	2	0	0	3	0	0	1	0	3	6	0	0	7	0	0	1	0	0	1	0	0	5	4	1
Mycena speirea	0	0	0	0	0	0	0	0	0	0	0	0	0	0	0	0	0	0	0	1	0	0	0	0	0
Mycena stylobates	0	0	0	0	0	0	0	0	0	0	0	0	0	0	0	0	0	0	0	1	0	1	0	1	0
Mycena urania	0	0	0	0	0	0	0	0	0	0	0	0	0	0	0	0	0	0	0	0	0	0	0	2	0
Mycena viridimarginata	0	0	0	0	0	0	0	0	0	0	0	0	0	0	0	0	0	0	0	0	1	0	0	0	0
Mycena viscosa	0	0	0	0	0	0	0	0	0	0	0	0	0	0	0	0	0	0	0	0	0	0	0	0	0
Mycena vulgaris	0	0	0	0	0	0	0	0	0	0	0	0	0	0	0	0	0	0	0	0	0	0	0	0	0
Mycocalia sp.	0	0	0	0	0	0	0	0	0	0	0	0	0	0	0	0	0	0	2	0	0	0	0	0	0
Omphalina oniscus	0	0	0	0	0	0	0	0	0	0	0	0	0	0	1	0	0	0	0	0	0	0	0	0	0
Pholiota lubrica	0	0	0	0	0	0	0	0	0	0	0	0	0	0	0	0	0	0	0	0	0	0	0	0	0
Pholiota mixta	0	0	0	0	0	0	0	0	0	0	0	0	0	0	0	0	0	0	0	0	0	0	0	0	0
Pholiota scamba	0	0	0	0	0	0	0	0	0	0	0	0	0	0	0	0	0	0	0	0	0	0	0	0	0
Psathyrella Lutenses coll.	0	0	0	0	0	0	0	0	0	0	0	0	0	0	0	0	0	0	0	0	0	0	0	0	0
Psathyrella friesii	0	0	0	0	0	0	0	0	0	0	0	0	0	0	0	0	0	0	0	0	0	0	0	0	0
Psilocybe inquilina	0	0	0	0	0	0	0	0	0	0	0	0	0	0	0	0	0	0	0	0	0	0	0	0	0
Strobilurus esculentus	0	0	0	0	0	0	0	0	0	0	0	0	0	0	0	0	0	0	4	0	4	3	1	2	0
Stropharia hornemannii	0	0	0	0	0	0	0	0	0	0	0	0	0	0	0	0	0	0	0	0	0	0	0	0	0
Tubaria confragosa	0	0	0	0	0	0	0	0	0	0	0	0	0	0	0	0	0	0	0	0	0	0	0	0	0
Tubaria conspersa	0	0	0	0	0	0	0	0	0	0	0	0	0	0	0	0	0	0	0	0	0	0	0	0	0
Typhula erythropus	0	0	0	0	0	0	0	0	0	0	0	0	0	0	0	0	0	0	0	0	0	0	0	0	0
Typhula phacorrhiza	0	0	0	0	0	0	0	0	0	0	0	0	0	0	0	0	0	0	0	0	0	0	0	0	0
Typhula setipes	0	0	0	0	0	0	0	0	0	0	0	0	0	0	0	0	0	0	6	10	11	16	14	0	0
Xeromphalina campanella	0	0	0	0	0	0	0	0	0	0	0	0	0	0	0	0	0	0	0	0	0	0	0	0	0
Xeromphalina cornui	1	0	0	0	0	0	0	0	0	0	0	0	0	0	0	0	0	0	0	0	0	0	0	0	0
Xylaria filiformis	0	0	0	0	0	0	0	0	0	0	0	0	0	0	0	0	0	0	0	0	0	0	0	0	0

SOMMERFELTIA AND SOMMERFELTIA SUPPLEMENT

Vol. 1. A. Hansen & P. Sunding: Flora of Macaronesia. Checklist of vascular plants. 3. revised edition. 167 pp. NOK 140. (Jan. 1985; out of stock).

Vol. 2. R.H. Økland & E. Bendiksen: The vegetation of the forest-alpine transition in Grunningsdalen, S. Norway. 224 pp. NOK 170. (Nov. 1985).

Vol. 3. T. Halvorsen & L. Borgen: The perennial Macaronesian species of Bubonium (Compositae-Inuleae). 103 pp. NOK 90. (Feb. 1986).

Vol. 4. H.B. Gjærum & P. Sunding: Flora of Macaronesia. Checklist of rust fungi (Uredinales). 42 pp. NOK 50. (Dec. 1986).

Vol. 5. J. Middelborg & J. Mattsson: Crustaceous lichenized species of the Caliciales in Norway. 71 pp. NOK 70. (May 1987).

Vol. 6. L.N. Derrick, A.C. Jermy & A.C. Paul: Checklist of European Pteridophytes. xx + 94 pp. NOK 95. (Jun. 1987).

Vol. 7. L. Malme: Distribution of bryophytes on Fuerteventura and Lanzarote, the Canary Islands. 54 pp. NOK 60. (Mar. 1988).

Vol. 8. R.H. Økland: A phytoecological study of the mire Northern Kisselbergmosen, SE. Norway. I. Introduction, flora, vegetation, and ecological conditions. 172 pp. NOK 140. (Oct. 1989).

Vol. 9. G. Mathiassen: Some corticolous and lignicolous Pyrenomycetes s. lat. (Ascomycetes) on Salix in Troms, N Norway. 100 pp. NOK 85. (Oct. 1989).

Vol. 10. T. Økland: Vegetational and ecological monitoring of boreal forests in Norway. I. Rausjømarka in Akershus county, SE Norway. 52 pp. NOK 55. (June 1990).

Vol. 11. R.H. Økland (ed.): Evolution in higher plants: patterns and processes. Papers and posters presented on a symposium arranged on occasion of the 175th anniversary of the Botanical Garden in Oslo, June 5-8, 1989. 183 pp. NOK 150. (Dec. 1990).

Vol. 12. O. Eilertsen: Vegetation patterns and structuring processes in coastal shell-beds at Akerøya, Hvaler, SE Norway. 90 pp. NOK 85. (June 1991).

Vol. 13. G. Gulden & E.W. Hanssen: Distribution and ecology of stipitate hydnaceous fungi in Norway, with special reference to the question of decline. 58 pp. NOK 110. (Feb. 1992).

Vol. 14. T. Tønsberg: The sorediate and isidiate, corticolous, crustose lichens in Norway. 300 pp. NOK 330. (May 1992).

Vol. 15. J. Holtan-Hartwig: The lichen genus *Peltigera*, exclusive of the *P. canina* group, in Norway. 77 pp. NOK 90. (March 1993).

Vol. 16. R.H. Økland & O. Eilertsen: Vegetation-environment relationships of boreal coniferous forests in the Solhomfjell area, Gjerstad, S Norway. 254 pp. NOK 170. (March 1993).

Vol. 17. A. Hansen & P. Sunding: Flora of Macaronesia. Checklist of vascular plants. 4. revised edition. 295 pp. NOK 250. (May 1993).

Vol. 18. J.F. Ardévol Gonzáles, L. Borgen & P.L. Péres de Paz: Checklist of chromosome numbers counted in Canarian vascular plants. 59 pp. NOK 80. (Sept. 1993).

Vol. 19. E. Bendiksen, K. Bendiksen & T.E. Brandrud: *Cortinarius* subgenus *Myxacium* section *Colliniti* (Agaricales) in Fennoscandia, with special emphasis on the Arctic-alpine zones. 37 pp. NOK 55. (Nov. 1993).

Vol. 20. G. Mathiassen: Corticolous and lignicolous Pyrenomycetes s.lat. (Ascomycetes) on *Salix* along a mid-Scandinavian transect. 180 pp. NOK 180. (Nov. 1993).

Vol. 21. K. Rydgren: Low-alpine vegetation in Gutulia National Park, Engerdal, Hedmark, Norway, and its relation to the environment. 47 pp. NOK 65. (May 1994).

Vol. 22. T. Økland: Vegetation-environment relationships of boreal spruce forests in ten monitoring reference areas in Norway. 349 pp. NOK 230. (May 1996).

Vol. 23. T. Tønsberg, Y. Gauslaa, R. Haugan, H. Holien & E. Timdal: The threatened macrolichens of Norway - 1995. 258 pp. NOK 220. (June 1996).

Vol. 24. C. Brochmann, Ø.H. Rustan, W. Lobin & N. Kilian: The endemic vascular plants of the Cape Verde islands, W Africa. 356 pp. NOK 230. (Dec. 1997).

Vol. 25. A. Skrindo & R.H. Økland: Fertilization effects and vegetation-environment relationships in a boreal pine forest in Åmli, S Norway. 90 pp. NOK 90. (Dec. 1998).

Vol. 26. A. Granmo: Morphotaxonomy and chorology of the genus *Hypoxylon* (Xylariaceae) in Norway. 81 pp. NOK 120. (Sept. 1999).

Vol. 27. A. Granmo, T. Læssøe & T. Schumacher: The genus *Nemania* s.l. (Xylariaceae) in Norden. 96 pp. NOK 135 (Sept. 1999).

Vol. 28. H. Krog: Corticolous macrolichens of low montane rainforests and moist woodlands of eastern Tanzania. 75 pp. NOK 135 (July 2000).

Vol. 29. R.H. Økland, T. Økland & K. Rydgren: Vegetation-environment relationships of boreal spruce swamp forests in Østmarka Nature Reserve, SE Norway. 190 pp. NOK 155 (Sept. 2001).

Vol. 30. E. Bendiksen, R.H. Økland, K. Høiland, O. Eilertsen & V. Bakkestuen: Relationships between macrofungi, plants and environmental factors in boreal coniferous forests in the Solhomfjell area, Gjerstad, S Norway. 125 pp. NOK 140. (Oct. 2004).

Supplement Vol. 1. R.H. Økland: Vegetation ecology: theory, methods and applications with reference to Fennoscandia. 233 pp. NOK 180. (Mar. 1990).

Supplement Vol. 2. R.H. Økland: Studies in SE Fennoscandian mires, with special regard to the use of multivariate techniques and the scaling of ecological gradients. (Dissertation summary). 22 pp. NOK 35. (Dec. 1990).

Supplement Vol. 3. G. Hestmark: To sex, or not to sex... Structures and strategies of reproduction in the family Umbilicariaceae (Lecanorales, Ascomycetes). (Dissertation summary). 47 pp. NOK 55. (Dec. 1991).

Supplement Vol. 4. C. Brochmann: Polyploid evolution in arctic-alpine *Draba* (Brassicaceae). 37 pp. NOK 60. (Nov. 1992).

Supplement Vol. 5. A. Hansen & P. Sunding: Botanical bibliography of the Canary Islands. 116 pp. NOK 130. (May 1994).

Supplement Vol. 6. R.H. Økland: Boreal coniferous forest vegetation in the Solhomfjell area, S Norway: structure, dynamics and change, with particular reference to effects of long distance airborne pollution. 33 pp. NOK 43. (May 1995).

Supplement Vol. 7. K. Rydgren: Fine-scale disturbance in an old-growth boreal forest - patterns and processes. 25 pp. NOK 40. (May 1997).

Paper 7

This article is removed.

Paper 8

This article is removed.

Paper 9

This article is removed.

Paper 10

This article is removed.

Paper 11

This article is removed.